Siderophore piracy of *Burkholderia cenocepacia*

Syakira Mohammed Hussein

A thesis submitted in partial fulfilment of the requirement for the degree of

Doctor of Philosophy

The University of Sheffield
Faculty of Medicine, Dentistry and Health
Department of Infection, Immunity and Cardiovascular Disease
January 2019

بسم الله الرحمن الرحيم

This thesis is dedicated to my beloved late mother
Khatijah Bee Zainul Abidin

Abstract

One of the ways *B. cenocepacia* survives in iron-limited conditions is by sequestering iron using endogenously produced siderophores. A bioinformatic analysis was conducted to determine whether *B. cenocepacia* may encode systems for utilising siderophores secreted by other bacteria (xenosiderophores). The ability of *B. cenocepacia* to also utilise xenosiderophores was analysed using a siderophore-deficient *B. cenocepacia* mutant. The TonB-dependent receptors (TBDRs) involved in transporting such siderophores were investigated by inactivating genes encoding putative TBDRs in *B. cenocepacia.* The requirements of the TonB1 complex for xenosiderophore transport was also investigated. A cytoplasmic membrane protein predicted to be involved in iron transport into the cytosol was also examined.

B. cenocepacia was shown to utilise xenosiderophores containing the commonly used ligands for iron chelation such as the hydroxamate group and the catecholate group, as well as mixed ligand type siderophores exhibiting two hydroxamate groups and a single hydroxycarboxylate ligand. The hydroxamate siderophores identified included hexadentates (ferrichrome, ferricrocin, ferrioxamine B, triacetylfusarinine C), tetradentates (alcaligin and rhodotorulic acid) and the bidentate, cepabactin. Two TBDRs, BCAL0116 and BCAL2281, and one cytoplasmic membrane protein, BCAL0117, were shown to be required for the utilisation of these siderophores except for cepabactin. The catecholate siderophores shown to be utilised included a linear tri-catecholate (dihydroxybenzoylserine (DHBS) trimer), bis-catecholates (azotochelin, DHBS dimer and cepaciachelin) and mono-catecholates (DHBS). One TBDR, BCAM2007, was shown to be solely responsible for the utilisation of azotochelin and likely also, cepaciachelin.

The mixed-ligand siderophores able to benefit *B. cenocepacia* included those containing a combination of hydroxamate and aspartate-type hydroxycarboxylate (malleobactin) or the citrate-type hydroxycarboxylate (schizokinen and arthrobactin) ligands. The ornibactin TBDR, OrbA, and the malleobactin TBDR in *B. thailandensis*, MbaD, were shown to play a role in the utilisation of both siderophores. The utilisation of xenosiderophores identified in this study was demonstrated to require the TonB1 complex. Investigation of xenosiderophore utilisation in this context can potentially serve as a preliminary step in the development of Trojan-horse antibiotics. In addition, the TBDR, BCAM2626, was demonstrated to be the sole TBDR for utilisation of haem by *B. cenocepacia*.

Main Supervisor

Dr Mark S. Thomas

Co supervisor

Dr Jonathan G. Shaw

Department of Infection, Immunity and Cardiovascular Disease
Faculty of Medical school

Internal examiner

Prof Robert K. Poole
Department of Molecular Biology and Biotechnology

External examiner

Prof Simon C. Andrews
University of Reading, UK

Acknowledgements

I would like to express my heartfelt gratitude to my supervisor, Mark Stephen Thomas of his time and effort in guiding, supporting and supervising me all through this research study. Your supervision has made me a better person, - and a better rresearcher. Thank you also to my co-supervisor, Jonathan Shaw. Special thanks to my husband, Tengku Shamsul Bahry Raja Husain for being lovely and supportive throughout my study period. Thanking you for giving me the chance to complete this study. I would like to thank Rob Hanson and Simon Thorpe from the Department of Chemistry for their chromatography and mass spectrometry services and Jessica Willis from the ISCD department for her technical support. Many thanks to all my laboratory colleagues Aaron, Chris, Helena, Jamie, Ruyue, Sayali and Saeedah for their kind support while working in the laboratory Lu103 and also to my office Lu128 colleagues and DDP teachers. To all my beloved family members, friends and acquaintances who shared their tremendous help and support morally, technically, financially, physically and spiritually. Thank you so much. The study period has been fun and interesting with all of you. I would like to thank the Ministry Education of Malaysia and the University of Sheffield for opening a gateway for me to seek knowledge. I also would like to express my deepest thanks to my internal examiner, Professor Robert Poole and external examiner, Professor Simon Andrews. The viva examination has broadened my view of this research. Last, but most importantly, I thank God for these gifts and all the people I came across throughout this study. This thesis is written with His love and with His quote : "We also sent down Iron, with its strength and diverse uses for mankind" Al Hadid (31-26): The iron [verse 25/29:57/114].

List of Abbreviations

ABC	ATP binding cassette
Bcc	Burkholderia cepacia complex
ACP	Acyl carrier protein
ATP	Adenosine triphosphate
BHR	Broad host range
CAA	Casamino acids
CAS	Chrome azurol-S
DMSO	Dimethyl sulfoxide
EDDHA	Ethylenediamine-N,N'-bis (2-hydroxyphenylacetic acid)
EDTA	Ethylenediaminetetraacetic acid
BSA	Bovine serum albumin
BSA	Bovine serum albumin
CF	Cystic fibrosis
CFTR	Cystic fibrosis transmembrane regulator
CGD	Chronic granulamatous disease
CM	Cytoplasmic membrane
cPhe	Chlorophenylalanine
CSIs	Conserved sequence insertions and deletions
CTD	C terminal domain
Da	Dalton
DHBA	Dihydroxybenzoate
DHBS	2,3-dihydroxybenzoyl-L-serine
DMSO	Dimethyl sulfoxide
DNA	Deoxyribonucleic acid
dNTP	deoxyribonucleotide triphosphate
DTPA	Diethylenetriamine pentaacetic acid
EPS	Exopolysaccharide
ESI	Electrospray ionisation
EtBr	Ethidium bromide
$FeCl_3$	Iron chloride
GFP	Green Fluorescent Protein
HCl	Hydroxychloric acid
HDTMA	Hexadecyltrimethylammonium bromide
HPLC	High performance liquid chromatography
HTP	Haem transport protein
IPTG	Isopropyl β-D-1-thiogalactopyranoside
IST	Iso-sensitest
kb	Kilobase
LB	Lysogeny broth
$MgSO_4$	Magnesium sulphate
HO	Haem oxygenase
K_2HPO_4	Potassium hydrogen phosphate
KCl	Potassium chloride
kDa	Kilo dalton
LB	Lysogeny broth
LC-MS	Liquid chromatography–mass spectrometry
LPS	Lipopolysaccharide
M	Molar
m/z	Mass per charge number
M9	Minimal salts agar
mA	Mili ampere

MALDI-TOF	Matrix Assisted Laser Desorption/Ionization-time of flight
MCS	Multiple cloning site
MDR	Multi-drug resistant
MFS	Major facilitator superfamily
MFS	Major Facilitator Superfamily
$MgCl_2$	Magnesium chloride
$MgSO_4$	Magnesium Sulphate
ML	maximum likelihood
MLST	Multi locust sequence typing
mM	Mili molar
$MnCl_2$	Manganese chloride
MOPS	3-N-morpholino propanesulfonic acid
MW	Molecular weight
NAD	Nicotinamide adenine dinucleotide
NaOH	Sodium hydroxide
NBD	Nucleotide binding domain
NCBI	National Center for Biotechnology Information
NEAT	Near transporter
NIS	NRPS-independent siderophore
NO	Nitric oxide
NRPS	Non-ribosomal peptide synthetase
OMP	Outer membrane protein
OD	Optical density
OM	Outer membrane
OMR	Outer membrane receptor
oriT	Origin of transfer
oriV	Origin of replication
PBP	Periplasmic binding protein
PBP	Periplasmic Binding Protein
PCR	Polymerase chain reaction
psi	Pounds per square inch
Rpm	Revolutions per minute
TAE	Tris base-acetate-EDTA
TBDR	TonB-dependent receptor
TE	Tris HCl-EDTA
X-gal	5-bromo-4-chloro-3-indolyl-β-D-galactopyranoside
pmf	Proton motive force
QS	Quorum sensing
RND	Resistance-Nodulation-Division
ROS	Reactive oxygen species
Rpm	Rotation per minute
SBP	Solute Binding Protein
SEM	Standard area of the mean
SOD	Superoxide dismutase
SOE	Splicing overlap extension
sRNA	small noncoding RNA
TBDR	TonB-dependent receptor
TBDT	TonB-dependent transporter
TE	Tris-EDTA
TMD	Transmembrane domain
UPGMA	Unweighted Pair Group Method with Arithmetic Mean
UV	Ultra violet
WT	Wildtype

List of Strain Abbreviations

A. baumanii	*Acinetobacter baumanii*
A. baylyi	*Acinetobacter baylyi*
A. fumigatus	*Aspergillus fumigatus*
A. viridinutans	*Aspergillus viridinutans*
A. xylosoxidans	*Achromobacter xylosoxidans*
B. ambifaria	*Burkholderia ambifaria*
B. anthracis	*Bacillus anthracis*
B. bronchiseptica	*Bordetella bronchiseptica*
B. cenocepacia	*Burkholderia cenocepacia*
B. cepacia	*Burkholderia cepacia*
B. cereus	*Bacillus cereus*
B. contaminans	*Burkholderia contaminans*
B. japonicum	*Bradyrhizobium japonicum*
B. megaterium	*Bacillus megaterium*
B. metalica	*Burkholderia metallica*
B. multivorans	*Burkholderia multivorans*
B. parapertussis	*Bordetella parapertussis*
B. phymatum	*Paraburkholderia phymatum*
B. pseudomallei	*Burkholderia pseudomallei*
B. pyrrocinia	*Burkholderia pyrrocinia*
B. subtilis	*Bacillus subtilis*
B. terrae	*Paraburkholderia terrae*
B. thailandensis	*Burkholderia thailandensis*
B. vietnamiensis	*Burkholderia vietnamiensis*
B. xenovorans	*Burkholderia xenovorans*
C. metallidurans	*Cupriavidus metallidurans*
D. chrysanthemi	*Dickeya chrysanthemi*
D. dadantti	*Dickeya dadantti*
E. coli	*Escherichia coli*
H. influenzae	*Haemophilus influenzae*
H. pylori	*Helicobacter pylori*
M. catarrhailis	*Moraxella catarrhailis*
M. tuberculosis	*Mycobacterium tuberculosis*
N. gonorrhoeae	*Neisseria gonorrhoeae*
N. meningitidis	*Neisseria meningitidis*
P. aeruginosa	*Pseudomonas aeruginosa*
P. chlororaphis	*Pseudomonas chlororaphis*
P. chrysogenum	*Penicillium chrysogenum*
P. fluorescens	*Pseudomonas fluorescens*
P. protegens	*Pseudomonas protegens*
P. syringae	*Pseudomonas syringae*
S. aureus	*Staphylococcus aureus*
S. maltophilia	*Stenotrophomonas maltophilia*
S. marcescens	*Serratia marcescens*
S. pilosus	*Streptomyces pilosus*
S. pneumoniae	*Streptococcus pneumoniae*
S. viridosporus	*Streptomyces viridosporus*
V. cholerae	*Vibrio cholerae*
V. mimicus	*Vibrio mimicus*
Y. enterolitica	*Yersinia enterolitica*
Y. pestis	*Yersinia pestis*

Table of Contents

Abstract iii

Acknowledgements v

List of Abbreviations vi

List of Strain Abbreviations viii

Table of Contents ix

List of Tables xv

List of Figures xvi

Chapter 1 1

Introduction 1

1.1 The role of iron in microorganisms 3

1.2 Iron acquisition mechanisms in bacteria 4

1.3 Siderophore-mediated iron-uptake mechanisms 4

1.3.1 Siderophore and iron-siderophore complexes 4
1.3.2 Classes of siderophore ligands 6
1.3.3 Biosynthesis of siderophores 6
1.3.4 Mechanism of siderophore transport 9
1.3.4.1 Translocation across the cytoplasmic membrane 9
1.3.4.2 Translocation across the outer membrane 14
1.3.5 Mechanism of iron release from iron-siderophore complex 17
1.3.6 Fate of Fe(II) in the cytoplasm 19
1.3.7 Utilisation and transport of xenosiderophores in bacteria 19
1.38 Siderophores as medicinal therapy 21

1.4 Alternative iron uptake mechanisms in bacteria 23

1.4.1 Iron uptake via haem 23
1.4.2 Acquisition of iron from transferrin and lactoferrin 27
1.4.3 Acquisition of iron from ferritin 28
1.4.4 Direct ferrous (II) iron uptake 28

1.5 Regulation of iron uptake 30

1.6 *Burkholderia* species 30

1.6.1 *Burkholderia cepacia* complex (Bcc) 33
1.6.2 Bcc pathogenesis and disease 33
1.6.2.1 Cystic fibrosis 33
1.6.2.2 Chronic granulomatous disease 36
1.6.3 Virulence determinants in Bcc 37
1.6.4 Alternative iron uptake mechanisms and iron regulation in *Bcc* 40
1.6.4.1 Prevalence 41
1.6.5 Siderophore-mediated iron uptake in Bcc 43
1.6.5.1 Ornibactin 43

1.6.5.2 Pyochelin 45
1.6.5.3 Cepaciachelin 48
1.6.5.4 Cepabactin 48
1.6.6 Antibiotic resistance mechanisms of Bcc infection 50

1.7 Hypotheses 51

1.8 Simplified aims of study 52

Chapter 2 53

Materials and Methods 53

2.1 Bacterial strains 55

2.2 Plasmid vectors 55

2.3 Primers 55

2.4 Bacteriological techniques 55

2.4.1 Bacteriological media 55
2.4.1.1 Lysogeny broth (LB) and agar 55
2.4.1.2 Lennox agar 55
2.4.1.3 Minimal salts (M9-glucose) medium and agar 55
2.4.1.4 Iso–Sensitest (IST) broth and agar 65
2.4.1.5 Chrome azurol S (CAS) agar 65
2.4.1.6 King's B broth and agar 66
2.4.1.7 Casamino acids liquid media 66
2.4.1.8 R2A broth and agar 66
2.4.2 Media supplements/solutions preparation 67
2.4.3 Maintenance of bacterial strains 68
2.4.3.1 Glycerol stocks 68
2.4.4: Techniques for plasmid DNA transfer 69
2.4.4.1 Transformation of *E. coli* cells 69
2.4.4.2 Conjugation of plasmid DNA into *B. cenocepacia* 70
2.4.4.3 Chromosomal mutagenesis of *B. cenocepacia* 70

2.5: Techniques for DNA purification and analysis 71

2.5.1: PCR techniques 71
2.5.1.1 PCR regime 71
2.5.2 Genomic DNA template preparation 72
2.5.2.1 Colony picking 72
2.5.3 Purification of plasmid DNA 72
2.5.4 Purification of DNA fragments 73
2.5.5 Restriction digestion techniques 73
2.5.6 DNA ligation techniques 73
2.5.7 Agarose gel DNA electrophoresis 74
2.5.8 DNA gel extraction 74
2.5.9 DNA Sequencing 75

2.6 Xenosiderophore utilisation bioassay 75

2.6.1 Disc diffusion assay 75
2.6.2 Liquid growth stimulation bioassay 76

2.7 HPLC purification and liquid chromatography mass spectrometry (LC-MS) analysis 76

2.8 Statistical analyses 77

Chapter 3 79

3.1 Rationale 81

3.2 Identification of putative TBDRs in *B. cenocepacia* 81

3.3 Phylogenetic analysis of putative TBDRs 84

3.4 Genomic context of TBDR genes 112

3.5 Investigation of putative TBDRs in other *Burkholderia* species 113

3.6 Identification of TonB systems in *B. cenocepacia* 119

3.7 Bioinformatic Identification of putative cytoplasmic membrane transport systems for metal chelates in *B. cenocepacia.* 122

3.8 Discussion 125

Chapter 4 127

4.1 Rationale 129

4.2 Construction and characterisation of markerless *B. cenocepacia* Δ*pobA* mutants 129

4.2.1 Allelic replacement using pEX18TpTer-*pheS* 129
4.2.2 Construction of pEX18TpTer-*pheS*-Δ*pobA* 131
4.2.3 Construction of *B. cenocepacia* Δ*pobA* mutants 131
4.2.4 Phenotypic analysis of *B. cenocepacia* Δ*pobA* mutants 134
4.2.4.1 Optimisation of liquid growth stimulation assay 134

4.3 Identification of hydroxamate xenosiderophores utilised by *B. cenocepacia* 138

4.3.1 Screening of hydroxamate xenosiderophore utilisation by disc diffusion assays 138
4.3.2 Utilisation of hydroxamate siderophores by *B. cenocepacia* in liquid medium 140
4.3.2.1 Growth stimulation assay of the hydroxamate siderophores in liquid medium 143

4.4 Identification of a specific TBDR for hydroxamate xenosiderophores 143

4.4.1 Generation of H111ΔpobA-BCAL0116::TpTer 146
4.4.2 Analysis of the role of the BCAL0116 TBDR in utilisation of hydroxamate siderophores. 148
4.4.3 Bioinformatic search of an additional hydroxamate TBDR 148
4.4.4 Analysis of the role of the BCAL2281 TBDR in utilisation of hydroxamate siderophores 150
4.4.4.1 Construction of pEX18TpTer-*pheS*-BCAL2281 and pEX18TpTer-*pheS*-ΔBCAL2281 150
4.4.4.2 Screening of cepabactin and ferrichrome utilisation by H111ΔpobAΔBCAL2281 150
4.4.4.3 Screening of cepabactin and ferrichrome utilisation by the H111ΔpobAΔBCAL2281-BCAL0116::TpTer mutant 152

4.5 Complementation of the BCAL0116 and BCAL2281 TBDR mutants 152

4.5.1 Construction of complementation plasmids, pSRKKm-BCAL0116 and pSRKKm-BCAL2281 154
4.5.2 Complementation analysis of hydroxamate siderophore TBDR mutants using disc diffusion assay 154
4.5.3 Effect of inactivation of BCAL0116 and BCAL2281 on growth of *B. cenocepacia* promoted by hydroxamate siderophores in liquid medium 159
4.5.4 Complementation analysis of the hydroxamate siderophore TBDR mutants using the liquid growth stimulation assay 159

4.6 Role of the TonB1 system in utilisation of hydroxamate siderophores 160

4.6.1 Effect of an *exbB1* null allele on the ability of *B. cenocepacia* to utilise hydroxamate siderophores 160

4.7 Identification of the inner membrane transport system for hydroxamate siderophore uptake 164

4.7.1 Construction of pEX18TpTer-*pheS*-Cm-SceI-ΔBCAL0117 164
4.7.2 Generation of a *B. cenocepacia* ΔBCAL0117 mutant 165
4.7.3 Screening of hydroxamate siderophore utilisation by H111ΔpobAΔBCAL0117 167
4.7.4 Complementation of the ΔBCAL0117 mutant 167
4.7.4.1 Construction of pSRKKm-BCAL0117 170
4.7.4.2 Complementation of H111ΔpobAΔBCAL0117 by pSRKKm-BCAL0117 170
4.7.5 Liquid growth stimulation assay of the ΔBCAL0117 mutant and its complementation 170

4.8 Albomycin sensitivity assay of *B. cenocepacia* H111 173

4.8.1 Screening of *B. cenocepacia* H111 for albomycin sensitivity 173

4.9 Discussion 176

4.9.1 Utilisation of hydroxamates as *B. cenocepacia* xenosiderophores 176
4.9.2 TBDRs for hydroxamate xenosiderophore utilisation 184
4.9.3 Role of the TonB1 complex in hydroxamate xenosiderophore transport 184
4.9.4 Identification of a putative inner membrane transporter for hydroxamate siderophores in *B. cenocepacia* 186
4.9.5 Albomycin toxicity study 188

Chapter 5 191

5.1 Rationale 193

5.2 Screening of the utilisation of catecholate siderophores present in bacterial supernatants 193

5.2.1 Screening of fimsbactin utilisation by *B. cenocepacia* using *A. baylyi* culture supernatants 193
5.2.2 Screening of enterobactin utilisation by *B. cenocepacia* using *E. coli* culture supernatants 194
5.2.3 Screening of siderophore utilisation by *B. cenocepacia* using *B. subtilis* bacterial supernatants 195
5.2.4 Screening of siderophore utilisation by *B. cenocepacia* using *B. ambifaria* bacterial supernatants 195
5.2.5 *B. cenocepacia* utilisation of siderophores present in *S. marcescens* Db10 culture supernatants 195
5.2.5.1 Analysis of siderophores produced by *S. marcescens* Db10 199

5.3 Investigation of the utilisation of purified catecholate siderophores by *B. cenocepacia* 200

5.3.1 Screening for the utilisation of yersiniabactin by *B. cenocepacia* 200
5.3.2 Investigation of the utilisation of azotochelin and vibriobactin by *B. cenocepacia* 206
5.3.3 Analysis of purified enterobactin and bacillibactin utilisation by *B. cenocepacia* 206
5.3.4 Analysis of the ability of *B. cenocepacia* to utilise DHBS derivatives as xenosiderophores 206

5.4 Identification of the TBDR for catecholate siderophore utilisation in *B. cenocepacia* 208

5.4.1 Screening TBDR mutants for defects in catecholate siderophore utilisation 208
5.4.2 Construction of a *B. cenocepacia* BCAM2007 mutant 210
5.4.2.1 Construction of pEX18TpTer-*pheS*-Cm-SceI-ΔBCAM2007 210
5.4.2.2 Generation of H111ΔpobA ΔBCAM2007 by allelic replacement 211
5.4.3 Analysis of catecholate siderophore utilisation by H111ΔpobAΔBCAM2007 211
5.4.4 Complementation of H111ΔpobAΔBCAM2007 213
5.4.4.1 Construction of the complementation plasmid 213

5.4.4.2 Complementation of H111ΔpobAΔBCAM2007 by pBBR1MCS-BCAM2007 216

5.5 Investigation of the role of BCAM2007 in cepaciachelin utilisation 216

5.6 Investigation of the role of BCAM1187 in DHBS utilisation 219

5.6.1 Generation of H111ΔpobA-BCAM1187::TpTer and H111ΔpobAΔBCAM2007-BCAM1187::TpTer 219
5.6.2 Analysis of the role of BCAM1187 in disc diffusion and liquid growth stimulation assays..... 222

5.7 Role of the *B. cenocepacia* TonB1 system in utilisation of catecholate siderophores..... 222

5.7.1 Analysis of catecholate siderophores utilisation by a B. cenocepacia *exbB1* mutant 222

5.8 Investigation of the role of BCAL0117 in utilisation of catecholate siderophores..... 222

5.9 Discussion 223

5.9.1 Utilisation of catecholate siderophores by *B. cenocepacia* 223
5.9.2 Transport of catecholate siderophores by *B. cenocepacia* 229

Chapter 6 237

6.1 Rationale..... 239

6.2 Screening for utilisation of hydroxcarboxylate siderophores by *B. cenocepacia* 239

6.3 Screening for utilisation of hydroxamate-hydroxycarboxylate siderophores by *B. cenocepacia*..... 239

6.3.1 Screening for utilisation of malleobactin 241
6.3.1.1 Confirming *B. thailandensis* mutant characteristics 244
6.3.1.2 Generation of H111ΔpobAΔfptA..... 247
6.3.1.3 Phenotypic characterisation of H111ΔpobAΔfptA and H111ΔC3ΔpobAΔfptA..... 250
6.3.1.4 Analysis of malleobactin utilisation by the H111ΔpobAΔfptA mutant 250
6.3.2 Analysis of the ability of *B. cenocepacia* to utilise phymabactin 250
6.3.2.1 Analysis of the ability of culture supernatants of *B. phymatum* and *B. terrae* to support growth of *B. cenocepacia* Δ*pobA* under iron limiting conditions..... 250
6.3.2.2 Construction of *B. phymatum* and *B. terrae* phymabactin mutants..... 252
6.3.3 Analysis of the ability of *B. cenocepacia* to utilise schizokinen, arthrobactin and aerobactin ... 253

6.4 Identification of a TBDR for hydroxycarboxylate-hydroxamate siderophores 257

6.4.1 Construction of pBBR-*orbA* and allelic replacement vector pSHAFT2-*orbA*::TpTer..... 259
6.4.2 Generation of H111ΔpobA-orbA::TpTer and H111ΔC3ΔpobA-orbA::TpTer 262
6.4.3 Analysis of malleobactin utilisation by H111ΔpobA-orbA::TpTer and H111ΔC3ΔpobA-orbA::TpTer 262
6.4.4 Screening of phymabactin utilisation by H111ΔpobA-orbA::TpTer 264

6.5 Complementation of the *orbA* mutant 264

6.5.1 Construction of pSRKKm-*fmtA* 264
6.5.2 Complementation analysis of the malleobactin utilisation phenotype of the *B. cenocepacia orbA* mutant 267

6.6 Screening for the TBDR for citrate-type hydroxycarboxylate-hydroxamate siderophores arthrobactin and schizokinen 267

6.6.1 Generation of double and triple TBDR mutants..... 269
6.6.2 Analysis on the utilisation of arthrobactin and schizokinen by *B. cenocepacia*..... 273

6.7 Investigation of the utilisation of catecholate-hydroxamate siderophores by *B. cenocepacia*..... 275

6.8 Investigation of utilisation of phenolate siderophores *by B. cenocepacia* 275

6.9 Role of the TonB1 system in utilisation of mixed hydroxamate-hydroxycarboxylate siderophores 277

6.10 Investigation into the role of the BCAL0117 hydroxamate siderophore inner membrane transport system in utilisation of hydroxamate-hydroxycarboxylate mixed type siderophores 277

6.11 Discussion 277

6.11.1 Utilisation of mixed ligand siderophores containing hydroxycarboxylate groups 277
6.11.2 The role of the TonB1 system and BCAL0117 hydroxamate siderophore inner membrane transport system in utilisation of hydroxamate-hydroxycarboxylate mixed type siderophores 284
6.11.3 Non-utilised siderophores 284

Chapter 7 287

Identification and characterisation of the *B. cenocepacia* outer membrane haem transport system 287

7.1 Rationale 289

7.2 Identification of the TBDR for haem utilisation 289

7.2.1 Generation of a markerless *B. cenocepacia* H111 ΔBCAM2626 mutant 289

7.3 Haem growth induction assay with *B. cenocepacia* H111ΔBCAM2626 mutant 291

7.4 Confirming the role of the gene product of BCAM2626 as the haem receptor protein 291

7.4.1 Construction of pBBR1-*huvA* 294
7.4.2 Complementation of a *B. cenocepacia* haem receptor mutant 294

7.5 Analysis of haem utilisation in *B. cenocepacia* by liquid growth stimulation assay 294

7.5.1 Generation of *B. cenocepacia* H111-orbA::TpTer and H111ΔfptA TBDR mutants 294
7.5.2 Generation of *B. cenocepacia* H111ΔhuvA-orbA::TpTer, H111ΔfptAΔhuvA and H111ΔfptA-orbA::TpTer mutants 297
7.5.3 Generation of a *B. cenocepacia* ΔfptAΔhuvA-orbA::TpTer triple TBDR mutant 297
7.5.4 Phenotype confirmation of mutants 297
7.5.5 Growth stimulation assay of *huvA*, *orbA* and *fptA* mutants in liquid medium 297

7.6 Discussion 300

7.6.1 Growth curve studies 300

Chapter 8 305

8.1 Conclusion 307

8.2 Limitations 313

8.3 Future work 313

Appendices 316

APPENDIX 1 316

APPENDIX 2 317

Bibliography 318

List of Tables

CHAPTER 1

Table 1.1 List of Bcc members 35

CHAPTER 2

Table 2.1 Bacterial strains used in this study 56
Table 2.2 Plasmids used in this study 61
Table 2.3 Oligonucleotides used in this study 63
Table 2.4 Antibiotics used for bacterial selection 68
Table 2.5 Components for GoTaq G2 Flexi DNA polymerase 71
Table 2.6 Components of restriction digestion 73
Table 2.7 Components for a typical ligation (1:1) 74
Table 2.8 Sources of Purified Siderophores used 76

CHAPTER 3

Table 3.1 List of putative TBDRs present in *B. cenocepacia* J2315 and H111 strains 85
Table 3.2 Identification of conserved domains in putative TBDRs present in *B. cenocepacia* J2315 and H111 strains 86
Table 3.3 List of putative TBDRs in representative *Burkholderia* species from the Bcc, *Pseudomallei* and *Xenovorans* group (*Paraburkholderia*) arranged according to bioinformatic homology. The colour code indicates the location of the TBDR gene loci on the chromosome 116
Table 3.4 Putative cytoplasmic membrane transporters for iron in *B. cenocepacia* J2315 and H111 124

CHAPTER 4

Table 4.1 Ability of hydroxamate siderophores to promote growth of *B. cenocepacia*[a] under iron restriction conditions[b] 145
Table 4.2 Analysis of the role of BCAL0116 and BCAL2281 in siderophore utilisation by disc diffusion assay 163
Table 4.3 Analysis of the role of BCAL0117 in hydroxamate siderophore utilisation[a] 175
Table 4.4 Producers of hydroxamate xenosiderophores utilised by *B. cenocepacia* H111 178

CHAPTER 6

Table 6.1 Degree of fluorescence of *B. thailandensis* and its mutant derivatives under UV light 245

CHAPTER 8

Table 8.1 Siderophores tested for utilisation by *B. cenocepacia* H111 strain 309
Table 8.2 Xenosiderophores utilised by *P. aeruginosa* identified or confirmed in this study[a] 310
Table 8.3 List of TBDR function in *B. cenocepacia* J2315 and H111 strains[a] 310

List of Figures

CHAPTER 1

Figure 1.1: The common siderophore ligands with examples 7
Figure 1.2: Ribbon model of the Type II ABC transport system, $BtuC_2D_2$ 10
Figure 1.3: Schematic diagram showing the mechanism of ferric siderophore transport in Gram-positive bacteria 12
Figure 1.4: A ribbon model of the TBDR FhuA for transporting ferrichrome in *E. coli* 15
Figure 1.5: Diagram of a TBDR and the TonB complex involved in ferric siderophore transport in Gram-negative bacteria 18
Figure 1.6: Diagram showing the mechanism of ferric-siderophore transport in Gram-negative bacteria 20
Figure 1.7: Ribbon model of a haemophore, HasR, interacting with the HasA TBDR in *S. marcescens* 25
Figure 1.8: Diagram of haemoglobin and haem uptake by Gram-negative bacteria..... 26
Figure 1.9: Diagram showing the TonB-independent uptake of Fe(II) in Gram-negative bacteria by FeoABC, YfeABCD, EfeU(O/M)B and FtrABCD 31
Figure 1.10: Classification scheme for *Burkholderia* species 34
Figure 1.11: The molecular structures of siderophores produced by Bcc members 44
Figure 1.12: The monomer precursors in the biosynthesis of the ornibactin molecule 46
Figure 1.13: Diagram showing the proposed mechanism of ferric-ornibactin transport in *Burkholderia* species 46
Figure 1.14: Structure of the ferric-pyochelin complex 47
Figure 1.15: The precursors in the biosynthesis of the cepaciachelin molecule 49
Figure 1.16: Diagram showing the proposed mechanism of ferric-cepaciachelin transport in *Burkholderia* species 49

CHAPTER 3

Figure 3.1: Alignment of *E.coli* BtuB and the putative *B. cenocepacia* TBDR, BCAM1593/I35_RS23700 87
Figure 3.2: Alignment of OprC of *P. aeruginosa* and the putative *B. cenocepacia* TBDR, BCAM0948/I35_RS20820 88
Figure 3.3: Alignment of CntO and the putative TBDR, BCAS0360/I35_RS31880 89
Figure 3.4: Alignment of ZnuD and the putative TBDR, BCAM1571/I35_RS23575 90
Figure 3.5: Alignment of PiuA and the putative TBDR, BCAM2007/I35_RS25625..... 91
Figure 3.6: Alignment of PA2911 and the putative TBDRs, BCAL1345/I35_RS06170 and BCAM0491/I35_RS06170 92
Figure 3.7: Alignment of putative TBDRs in *B. cenocepacia* J2315 99
Figure 3.8: Alignment of putative TBDRs in *B. cenocepacia* H111 106
Figure 3.9: Rooted UPGMA phylogenetic tree of TBDRs from *B. cenocepacia* J2315..... 108
Figure 3.10: Maximum likelihood phylogenetic tree of TBDRs from *B. cenocepacia* J2315..... 109
Figure 3.11: Rooted UPGMA phylogenetic tree of TBDRs from *B. cenocepacia* H111 110
Figure 3.12: Maximum likelihood phylogenetic tree of TBDRs from *B. cenocepacia* H111..... 111
Figure 3.13: Gene organisations of all TBDR gene loci in *B. cenocepacia* H111 115
Figure 3.14: Genomic context of TonB complexes in *B. cenocepacia*..... 121

CHAPTER 4

Figure 4.1: Molecular structures of hydroxamate siderophores investigated in this study 130
Figure 4.2: Gel electrophoresis of putative pEX18TpTer-*pheS*-Δ*pobA* plasmid clones 133
Figure 4.3: Integration of pEX18TpTer-*pheS*-Δ*pobA* into the *B. cenocepacia* 133
Figure 4.4: PCR screening candidate of *B. cenocepacia* Δ*pobA* mutants..... 135
Figure 4.5: Construction of pEX18TpTer-*pheS*-Δ*pobA* and mechanism of allelic replacement in *B. cenocepacia* 136
Figure 4.6: Phenotypic confirmation of the *B. cenocepacia* siderophore-deficient *pobA* mutant..... 137
Figure 4.7: Iron chelators 137
Figure 4.8: Optimisation of DTPA concentrations for establishing iron starvation conditions for *B. cenocepacia* in liquid culture..... 139
Figure 4.9: Growth promotion of H111ΔpobA by ferrichrome, ferrioxamine B, and TAFC under iron limiting conditions..... 141
Figure 4.10: Analysis of alcaligin, cepabactin, coprogen and rhodotorulic acid utilisation by *B. cenocepacia* using the disc diffusion assay 142
Figure 4.11: Growth curves of *B. cenocepacia* H111ΔpobA mutant in iron-depleted medium supplemented with different xenosiderophores 144
Figure 4.12: PCR screening of candidate H111ΔpobA-BCAL0116::TpTer mutants..... 147
Figure 4.13: Screening of hydroxamate siderophore utilisation by *B. cenocepacia* TBDR mutants..... 149
Figure 4.14: Gel electrophoresis of candidate H111ΔpobAΔBCAL2281 plasmids..... 151
Figure 4.15: Construction of pEX18TpTer-*pheS*-ΔBCAL2281 151
Figure 4.16: Screening of hydroxamate siderophore utilisation by *B. cenocepacia* TBDR mutants..... 153
Figure 4.17: Gel electrophoresis analysis of BCAL0116 amplification for construction of pSRKKm-BCAL0116 complementation plasmid 155
Figure 4.18: Diagrammatic representation of the construction of complementation plasmid pSRKKm-BCAL0116..... 156
Figure 4.19: Complementation analysis of the BCAL0116 and BCAL2281 TBDR mutants using the disc diffusion assay 158
Figure 4.20: Growth curves of *B. cenocepacia* H111 hydroxamate siderophore TBDR mutants in the presence and absence of ferrioxamine B and cepabactin in iron depleted medium and complementation analysis for ferrioxamine B 161
Figure 4.21: Effect of inactivation of the BCAL0116 and BCAL2281 TBDRs on ferrichrome-stimulated growth of *B. cenocepacia* in iron-limited broth culture 162
Figure 4.22: Amplification of BCAL0117/I35_RS00625 and generation of pEX18TpTer-*pheS*-Cm-SceI-ΔBCAL0117 166
Figure 4.23: Construction of *B. cenocepacia* Δ*pobA*ΔBCAL0117 168
Figure 4.24: Effect of inactivation of the BCAL0117 gene on hydroxamate siderophore utilisation by *B. cenocepacia* H111 169
Figure 4.25: Construction of pSRKKm-BCAL0117..... 171
Figure 4.26: Complementation analysis of a *B. cenocepacia* BCAL0117 mutant for hydroxamate siderophore utilisation 172
Figure 4.27: Growth of *B. cenocepacia* H111ΔpobAΔBCAL0117 in iron-depleted medium supplemented with ferrichrome and ferrioxamine B..... 174
Figure 4.28: Albomycin sensitivity assay..... 177
Figure 4.29: Molecular structure of ferrioxamine E..... 183
Figure 4.30: Ball and stick model of iron-hydroxamate xenosiderophore complex utilised by *B. cenocepacia* H111 183
Figure 4.31: Amino acid sequence alignment of BCAL0116/I35_RS00620 and BCAL2281/I35_RS11045 from *B. cenocepacia* H111..... 185

Figure 4.32: Prediction of transmembrane helices in BCAL0117/I35_RS00625 and related inner membrane proteins 187
Figure 4.33: Alignment of BCAL0117/I35_RS00625 with related inner membrane transport proteins 189

CHAPTER 5

Figure 5.1: Molecular structures of some catecholate siderophores screened for utilisation by *B. cenocepacia* 196
Figure 5.2: Screening of catecholate siderophore using disc diffusion assays 197
Figure 5.3: Enterobactin biosynthesis pathway 198
Figure 5.4: Screening of siderophore utilisation from supernatants of *S. marcescens* Db10 201
Figure 5.5: Molecular structures of siderophores detected in supernatants of *S. marcescens* Db10 202
Figure 5.6: HPLC chromatogram of *S. marcescens* Db10 supernatant in iron-limiting conditions 203
Figure 5.7: Mass spectra of compounds present in *S. marcescens* Db10 supernatant following growth in M9-glucose medium 204
Figure 5.8: Mass spectra of compounds present in *S. marcescens* Db10 supernatant following growth in M9-glucose medium containing 2,2'-bipyridyl 205
Figure 5.9: Analysis of catecholate siderophore utilisation by *B. cenocepacia* using the disc diffusion assay 207
Figure 5.10: Growth curves of *B. cenocepacia* H111ΔpobA in iron-depleted medium supplemented with catecholate siderophores 209
Figure 5.11: Construction of pEX18TpTer-*pheS*-Cm-SceI-ΔBCAM2007 and generation of H111ΔpobA ΔBCAM2007 212
Figure 5.12: Effect of inactivation of BCAM2007 on catecholate siderophore utilisation 214
Figure 5.13: Growth curves of *B. cenocepacia* H111ΔpobAΔBCAM2007 in iron-depleted medium supplemented with azotochelin and the DHBS derivatives 215
Figure 5.14: PCR screening of *E. coli* JM83 transformants containing candidate BCAM2007 complementation plasmids 217
Figure 5.15: Complementation of the ΔBCAM2007 mutant for catecholate siderophore utilisation 218
Figure 5.16: Generation of H111ΔpobAΔBCAM2007-orbA::TpTer mutants 220
Figure 5.17: Role of BCAM2007 in cepaciachelin utilisation by *B. cenocepacia* 220
Figure 5.18: Generation of *B. cenocepacia* BCAM1187 mutants 221
Figure 5.19: Molecular structures of the DHBS derivatives siderophores tested in this study 225
Figure 5.20: Molecular structures of bis- and tris- catecholate siderophores 228
Figure 5.21: Amino acid sequence alignments and phylogenetic tree of catecholate TBDRs in *P. aeruginosa* and *B. cenocepacia* 231
Figure 5.22: Crystal structure of PiuA of *P. aeruginosa* 232
Figure 5.23: Molecular structures of catecholate/hydroxypyridone siderophore-antibiotic conjugates 235

CHAPTER 6

Figure 6.1: Chemical structures of the hydroxycarboxylate siderophores investigated in this study..... 240
Figure 6.2: Analysis of a hydroxycarboxylate (rhizoferrin) utilisation by *B. cenocepacia* using the disc diffusion assay 240
Figure 6.3: Chemical structures of citrate hydroxamate siderophores used in this investigation 242
Figure 6.4: Ability of *B. thailandensis* culture supernatants to promote growth of siderophore deficient *B. cenocepacia* under iron-limiting conditions..... 243
Figure 6.5: CAS agar plate of streaked *B. thailandensis* E264 and its mutant derivatives..... 243
Figure 6.6: Screening *pchE* and *mbaB* alleles in *B. thailandensis* E264 wild type and mutant strains 246
Figure 6.7: Confirmation of growth promotion of siderophore deficient *B. cenocepacia* with *B. thailandensis pchE*::tet mutant derivative under iron-limiting conditions 248
Figure 6.8: Diagram showing construction of pEX18TpTer-*pheS*-Δ*fptA* 248
Figure 6.9: Construction of pEX18TpTer-*pheS*-Δ*fptA* and generation of H111ΔpobAΔfptA 249
Figure 6.10: Demonstration of malleobactin utilisation by *B. cenocepacia* 251
Figure 6.11: Growth stimulation of siderophore-deficient B*. cenocepacia* by *B. phymatum* and *B. terrae* under iron limiting conditions 254
Figure 6.12: Construction of H111-orbI::Tp, and *B. phymatum* and *B. terrae phmA*::Tp mutants..... 254
Figure 6.13: CAS agar analysis of H111-orbI::Tp, and *B. phymatum* and *B. terrae phmA*::Tp mutants... 254
Figure 6.14: Analysis of schizokinen and aerobactin utilisation by *B. cenocepacia* 255
Figure 6.15: Growth curves of *B. cenocepacia* H111ΔpobA in iron-depleted medium supplemented with arthrobactin and schizokinen 256
Figure 6.16: Alignment of OrbA TBDR in *B. cenocepacia* and the OrbA TBDR homologues..... 258
Figure 6.17: Construction of pBBR1-*orbA*::TpTer 260
Figure 6.18: Construction of pSHAFT2-*orbA*::TpTer..... 261
Figure 6.19: Construction of pBBR1-*orbA* and pBBR1-*orbA*::TpTer 263
Figure 6.20: Generation of H111ΔpobA-*orbA*::TpTer 263
Figure 6.21: Analysis of utilisation of malleobactin by *orbA* TBDR mutant 265
Figure 6.22: Analysis of the utilisation of ornibactin by a siderophore-deficient *B. thailandensis* mutant 266
Figure 6.23: Analysis of the utilisation of phymabactin by disc diffusion assay 266
Figure 6.24: Construction of pSRKKm-*fmtA* 268
Figure 6.25: Complementation of a *B. cenocepacia orbA* mutant by *orbA* and *fmtA* in *trans* 268
Figure 6.26: Confirmation of H111ΔpobA-BCAL1371::TpTer-BCAM2439::Cm genotype..... 270
Figure 6.27: Screening of candidate H111ΔpobA-BCAL1709::TpTer, H111ΔpobA-BCAL1709::TpTer-BCAM0499::Cm, H111ΔC3ΔpobA-BCAL1709::TpTer and H111ΔpobA-BCAL0491::TpTer mutants 272
Figure 6.28: Screening of candidate *B. cenocepacia* H111ΔC3ΔpobA-BCAL1371::Tp and H111ΔC3ΔpobA- BCAM2349::Cm-BCAL1371::TpTer mutants 274
Figure 6.29: Effect of TBDR inactivation on utilisation of arthrobactin and schizokinen by *B. cenocepacia* 276
Figure 6.30: The molecular structures of some siderophores tested for utilisation by *B. cenocepacia* . 278
Figure 6.31: Analysis of nicotianamine utilisation by *B. cenocepacia*..... 278
Figure 6.32: Analysis of arthrobactin utilisation by a *B. cenocepacia* BCAL0117 mutant..... 279
Figure 6.33: The molecular structures of malleobactin and ornibactin..... 281
Figure 6.34: Diagrammatic representation of the predicted domain organisation of the two NRPSs encoded in the ornibactin, malleobactin and phymabactin siderophore biosynthetic gene clusters in *B. cenocepacia*, *B. thailandensis*, *B. xenovorans* and *B. phymatum* 282
Figure 6.35: The molecular structures of the fimsbactins 286

CHAPTER 7

Figure 7.1: Molecular structure of haem 290
Figure 7.2: The putative haem uptake gene cluster in *B. cenocepacia.* 290
Figure 7.3: Construction of a plasmid for *B. cenocepacia* BCAM2626 mutant generation 292
Figure 7.4: Generation of *B. cenocepacia* BCAM2626 mutant by allelic replacement 293
Figure 7.5: Haem growth stimulation assay of the ΔBCAM2626 mutant 295
Figure 7.6: Construction of BCAM2626 complementation plasmid 295
Figure 7.7: Complementation analysis of the huvA mutant phenotype 296
Figure 7.8: Generation of double TBDR mutants, H111ΔhuvA-orbA::TpTer and H111ΔfptAΔhuvA 298
Figure 7.9: Generation of the triple TBDR mutant H111ΔhuvAΔfptA-orbA::TpTer 299
Figure 7.10: Confirmation of haem utilisation defect of H111ΔfptAΔhuvA, H111ΔhuvA-orbA::TpTer and H111ΔfptAΔhuvA-orbA::orbA::TpTer 299
Figure 7.11: Haemin optimisation assay and growth of *huvA*, *fptA* and *orbA* single and multiple mutants with and without haemin addition in iron-limiting M9-glucose (CAA) medium containing 1 µM DTPA 301

Chapter 1

Introduction

1.1 The role of iron in microorganisms

Iron is the fourth most abundant element in the earth's crust, after oxygen, silicon and aluminium (Exley, 2009). It is indispensable for the growth and survival of almost all organisms, including microorganisms. There are a few exceptions such as the bacteria *Borrelia burgdorferi* which finds an alternative for iron by using other metals for survival such as manganese (Posey and Gherardini, 2000). Iron is naturally toxic to all living organisms in high concentrations due to the formation of free radicals via Fenton chemistry (Fenton, 1894), hence it is most often needed in small amounts. Though required in small amounts, the role of iron is enormous as it acts as a cofactor and in enzyme catalysis in many pivotal metabolic and regulatory processes. These include iron-sulfur protein or ferredoxin assembly in electron transport systems and in di-iron and mononuclear iron enzymes, such as ribonucleotide reductase and superoxide dismutase which is involved in DNA synthesis and antioxidant defense, respectively (Braun and Hantke, 2011). Iron is a transition metal and can exist in two redox states: the soluble ferrous (Fe^{2+} or Fe(II)) form or insoluble ferric (Fe^{3+} or Fe(III)) oxidation states rendering it as an excellent biocatalyst or electron carrier (Andrews et al., 2003).

Back in the early earth's atmosphere, molecular oxygen was a minor component and iron mainly existed in its ferrous state. Ancient microorganisms may have survived with ferrous rather than ferric ions. Currently, iron mainly exists in the insoluble Fe^{3+} form in the environment due to the presence of atmospheric oxygen (Kasting, 1993; Philpott, 2006). Moreover, the solubility of Fe(III) at neutral pH is relatively low with a ferric ion concentration of 10^{-18} to 10^{-17} M, whereas microorganisms require a concentration of 10^{-7} to 10^{-5} M to achieve optimal growth (Andrews et al., 2003). To overcome this inconvenience, bacteria and fungi have evolved multiple systems to solubilise these iron ions from the surrounding environments to guarantee an ample supply of iron for intracellular use.

In the host environment, iron availability is even more highly limited as it is accommodated in iron-binding host proteins (haemoglobin, haemopexin, transferrin, lactoferrin and ferritin) rendering available free ferric iron to be as low as 10^{-24} M (Raymond et al., 2003). This is particularly to prevent reactive oxygen species (ROS) generation, a reaction that could impose damage on the cell constituents (Cabiscol et al., 2000). The sequestration of iron by the host also serves to restrict the growth of pathogens, implying an innate immunity strategy or iron-targeted nutritional immunity. As most microorganisms are not readily able to take up iron bounded in host proteins, iron comes to be a limiting growth factor. Due to this, microorganisms have adopted advanced and alternative strategies to incorporate host iron into their systems and maintain iron homeostasis. These strategies may also be considered as virulence determinants in each pathogenic microorganism (Caza and Kronstad, 2013).

1.2 Iron acquisition mechanisms in bacteria

Environmental-living microorganisms are able to sequester iron from diverse iron sources such as from minerals in soil and water as part of their survival strategy. In contrast, pathogens can seize iron in their hosts from ferritin, transferrin, lactoferrin, free haem, or haem-containing proteins, such as haemopexin, myoglobin and haemoglobin as survival mechanisms. The ability to sequester iron from these proteins or compounds is termed iron piracy and the uptake of these compounds involves several transport systems (Noinaj et al., 2012).

Gram-positive and Gram-negative bacteria possess distinct mechanisms of acquiring iron due to their membrane organisational structures (Caza and Kronstad, 2013). Gram-negative bacteria possess an outer membrane (OM), in addition to the cytoplasmic membrane (CM), common to all bacteria. Besides offering an additional level of protection to the bacteria, the OM also impedes the uptake of essential nutrients into the cell. Small hydrophilic molecules are able to cross the OM by passive diffusion through transmembrane porins but molecules that are greater than 600 Da or are present at very low concentrations are poorly permeable through porins (Novikova and Solovyeva, 2009). These molecules require energised or active transport systems to translocate them across the OM (Miller and Steinberg, 1977). However, no energy source is available to support this transport (Lugtenberg and Van Alphen, 1983). Gram-positive bacteria generally have a thicker peptidoglycan layer embedded with proteins, carbohydrates and teichoic acids and most importantly, do not have an OM and periplasm, which dictates a slightly different but simpler mechanism to capture iron.

An important way of scavenging iron by microorganisms is by producing and secreting siderophores, low molecular weight compounds that are able to strongly chelate ferric iron (Crosa and Walsh, 2002). This system is useful for survival both in the environment and in the animal or plant host.

This review henceforth, will focus on the features of these siderophores and how Gram-negative and Gram-positive bacteria differ in acquiring iron-siderophore complexes. Gram-positive bacteria will not be evaluated in detail as part of this review as they are not the main focus of this study. The review will also consider alternative iron acquisition mechanisms used by bacterial pathogens, including haem uptake.

1.3 Siderophore-mediated iron-uptake mechanisms

1.3.1 Siderophore and iron-siderophore complexes

Many bacteria and fungi are known to produce one or more of these iron-scavenging compounds at any one time. Hence, there are many different types of siderophores being isolated and studied (Hider and Kong, 2010).

Siderophores are small, ferric iron-chelating molecules generally with a molecular mass of 600 – 1500 Da. The first siderophore isolated was mycobactin from *Mycobacterium johnei* in 1949 (Francis et al., 1949). Since then, more than 500 different siderophores have been recognised from bacteria, fungi and higher plants. Siderophores are produced when iron is scarce or when the intracellular iron concentration in microorganisms drops below a threshold value of approximately 10^{-6} M (Miethke and Marahiel, 2007). Due to their very high affinities for Fe(III), siderophores are able to seize iron ions from iron-binding proteins or oxide hydrate complexes.

The scavenged iron is an element which has two electrons in its outer shell and requires six others to be in a stable state. It therefore forms six covalent bonds with coordinating ligands found in siderophores to establish iron complexes or ferric siderophores. In some cases, a stable hexacoordinate or a hexadentate complex forms a square planar conformation with four donated electrons,while two others are arranged vertically, and an iron atom in the centre forming an octahedral coordination geometry (Barry and Challis, 2009). High affinity siderophores usually provide three bidentate groups to accommodate the six coordination sites of Fe(III) and establish a 1:1 complex. Ferrichrome is a hexadentate siderophore and thereby requires only one molecule to form a hexadentate coordination complex with Fe(III), and therefore is considered a strong siderophore (Zheng and Nolan, 2012). Accordingly, iron secures three molecules of a bidentate siderophore to form a complex or two molecules of a tridentate or tetradentate siderophore to be in a stable octahedral shape. An example of a bidentate siderophore is cepabactin where three molecules of the siderophore form the octahedral complex with ferric ion (Klumpp et al., 2005). Pyochelin is tetradentate whereby two molecules of pyochelin are required to form a complex with the Fe(III) ion (Brandel et al., 2012a). Here one pyochelin molecule provides four ligand atoms to Fe(III) and the other two electrons are donated by another pyochelin molecule, leaving two remaining coordinating groups in a pyochelin molecule occupied by other molecules such as water or hydroxides (Tseng et al., 2006).

These water-soluble octahedral complexes formed between siderophore and Fe(III) (ferric-siderophore complexes) are easily utilised by bacteria. The binding affinity of siderophores for ferric iron can be described by pM values. The pM Fe(III) value is the measure of the negative log of the free iron ion concentration with standard total concentrations of iron and ligand at a pH of 7.4. Higher pM values may indicate greater iron affinity. For example, the pM value for enterobactin is 35.5, ferrioxamine B is 26.6 and rhizoferrin is 20.0. Regardless of having different pM Fe(III) values, the three siderophores exhibit an identical denticity of 6 (Hider and Kong, 2010; Raymond et al., 2015).

Secretion of certain siderophores in the human host can also triggers the production of siderocalin. Siderocalin is an innate immune substance that prevents the ability of siderophores to scavenge iron in the respective host (Clifton et al., 2009; Goyal and Anishetty, 2014). For instance, siderocalin can form complexes with certain catecholate siderophores such as bacillibactin and enterobactin causing them to lose effectiveness (Cendrowski et al., 2004). In some cases, pathogens are able to encounter this situation by secreting siderophores which are resistant to siderocalin termed stealth siderophores (Cescau et al., 2007). An example of a stealth siderophore is petrobactin, secreted by *Bacillus anthracis.* In addition to petrobactin, *B. anthracis* also produces bacillibactin, and petrobactin seems to counter the loss of effectiveness of bacillibactin and maintains pathogenicity to human hosts (Abergel et al., 2006).

1.3.2 Classes of siderophore ligands

There are three common bidentate ligand types found in siderophores: hydroxamates, catecholates and α-hydroxycarboxylates. Less common are bidentate ligands that contain the phenolate group (Crichton and Boelaert, 2001) (Figure 1.1). The common component of all these ligands is oxygen. The hydroxamate group consists of a carbonyl group that is on an adjacent carbon to an N-hydroxyl group. The oxygen ion from the carbonyl group and the adjacent oxygen ion bonded to the nitrogen atom both take part in chelating ferric ion. Hydroxamate-type siderophores include ferrioxamine B, triacetylfusarinine C and ferrichrome (Figure 1.1A). Catecholates are comprised of an aromatic ring backbone with two hydroxyl groups on adjacent carbons of the ring, while phenolates have one hydroxyl group. Although the phenolate group is actually monodentate, in the siderophore it is usually linked to a heterocyclic ring containing an electron donor atom to produce a bidentate ligand as in pyochelin, mycobactin and yersiniabactin (Cox and Graham, 1979). The catecholate groups are usually linked to the rest of the siderophore molecule by an amide group which is important for the function of the catechol. Examples of siderophores with a catecholate backbone are the widely researched, enterobactin (Crichton and Boelaert, 2001) and bacillibactin (Nakano et al., 1992) (Figure 1.1B). These catecholates chelate ferric ions via their hydroxyl groups. The other ligand, the α-hydroxycarboxylate class, contains a carboxylic acid group and a hydroxyl on the adjacent carbon atom as exemplified by rhizoferrin (Figure 1.1D). In addition, there are also mixed ligand siderophores which involve combination of ligands in the same siderophore molecule. For example, ornibactin exhibits both hydroxycarboxylate and hydroxamate groups on a peptide backbone (Stephan et al., 1993; Thomas, 2007).

1.3.3 Biosynthesis of siderophores

The biosynthesis of siderophores involves the activity of two main pathways, the non-ribosomal peptide synthetase (NRPS) and the NRPS-independent siderophore (NIS) synthetase pathways (Barry and Challis, 2009). Examples of siderophores synthesised via NRPS enzymes include pyochelin, yersiniabactin, vibriobactin, ornibactin and enterobactin.

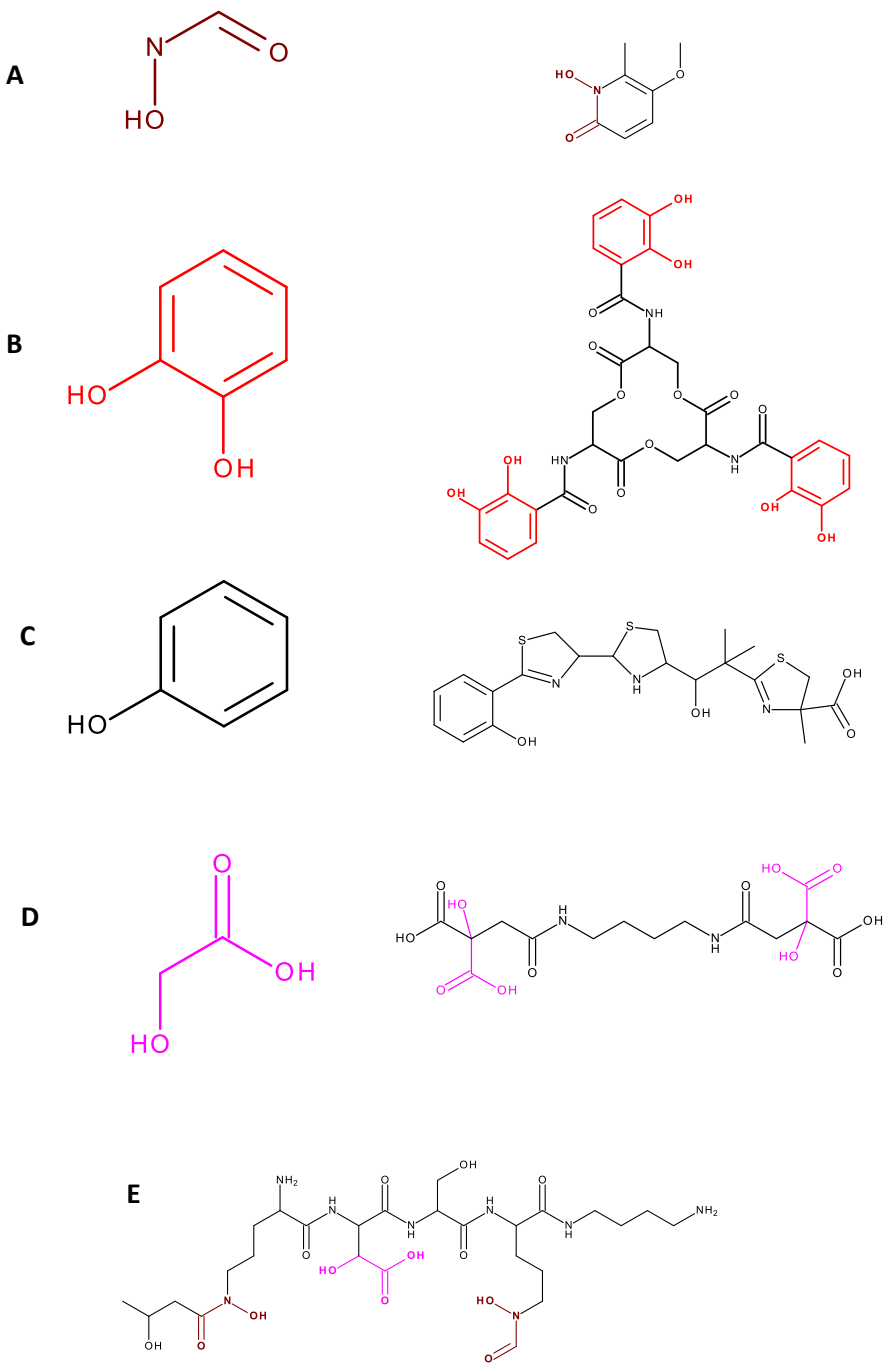

Figure 1.1: The common siderophore ligands with examples
The ligands commonly found in siderophores. (A) hydroxamate-cepabactin containing one hydroxamate ligand, (B) catecholate-enterobactin containing three catecholate ligands, (C) phenolate-yersiniabactin containing one phenolate ligand and (D) α-hydroxycarboxylate-rhizoferrin containing two α-hydroxycarboxylate ligands. (E) mixed ligand-ornibactin containing one α-hydroxycarboxylate and two hydroxamate ligands. Structures were produced using Accelrys 4.2.

Siderophores comprised of non-ribosomal-synthesised peptide analogues often contain non-canonical amino acids combined with other functional ligands. For example, some siderophores are 'capped' at the N-terminal end with an aromatic constituent such as salicylic acid as in the case of pyochelin or yersiniabactin (Gehring et al., 1998).

NRPSs are large multimodular enzymes where each module is comprised of a minimum of three domains, the adenylation or activation (A) domain, the thiolation or peptidyl carrier protein (PCP) domain and the condensation (C) domain. These domains are generally present in the order of A-PCP-C. In the case where one of the siderophore building blocks is not an amino acid, the PCP domain is substituted with an aryl carrier protein (ArCP) domain. Each module takes part in incorporating one aryl or amino acid unit sequentially in the formation of the siderophore molecule via thiol-based intermediates (Thomas, 2007).

The highly selective A domain is involved in substrate recognition and activation. The PCP domain is a site for cofactor binding to which substrate and intermediates are subsequently covalently bound. The C domain catalyses peptide bond formation between two intermediates or precursors by a condensation reaction. By analysing the A domains, the substrates for the peptide formation can often be predicted. The termination or thioesterase (TE) domain is typically situated at the C-terminus of the NRPS assembly line and is responsible for the release of the mature siderophore (Marahiel and Essen, 2009; Marahiel, 2016). Activation of the PCP or the ArCP domain of NRPSs involves an enzyme monomer named phosphopantetheinyltransferase (PPTase).

Prior to siderophore formation, the PPTase modifies the PCP/ArCP domain by catalysing the transfer of the 4' phosphopantetheine prosthetic group (P-pant) from coenzyme A to a conserved serine residue found in a phosphopantetheinylation site within the PCP/ArCP domain. This allows the formation of a flexible thiol-terminated 4'-phosphopantetheine to which the peptide intermediates and precursors attach via a thioester bond and gain access to the catalytic reaction centres within the NRPS module for the formation of the siderophore molecule (Gerc et al., 2014; Beld et al., 2014). PPTase enzymes are further divided into three families: the Sfp-type family, the AcpS-type family and another that is involved in the fatty acid and polyketide synthesis. The AcpS family is also involved in the biosynthesis of fatty acids including lipid A, phospholipids and lipoic acid. The Sfp family is principally responsible for the activation of the NRPSs for siderophore production (Copp and Neilan, 2006; Asghar et al., 2011).

The other important class of siderophore is biosynthesised independently of NRPSs, through the NIS synthetase biosynthetic pathways. NIS enzymes commonly function in the biosynthesis of the hydroxycarboxylate and also mixed ligand siderophores, specifically involving condensing citric acid as a hydroxycarboxylate ligand donor.

There are so far five classes of the NIS characterised: the A, A', B, C and C' enzymes. Many siderophores require more than one NIS enzyme for their biosynthesis. An example of an NIS siderophore is aerobactin which is produced by *Escherichia coli* (Challis, 2005), and also by several other bacteria such as *Aerobacter aerogenes* (McDougall and Neilands, 1984), *Vibrio mimicus* (Moon et al., 2004) and *Escherichia fergusonni* (Šmajs et al., 2003). Several NIS siderophores, such as aerobactin, achromobactin, petrobactin and rhizoferrin, contain a citrate moiety. Most NIS enzymes have been characterised from bacteria and also archaea. Rhizoferrin is the only fungal NIS whose synthesis been characterised to date, where the mechanism of action is the same as that of the bacterial NIS enzymes (Carroll and Moore, 2018).

1.3.4 Mechanism of siderophore transport

1.3.4.1 Translocation across the cytoplasmic membrane

Both Gram-negative and Gram-positive bacteria possess ATP-binding cassette (ABC) transporters to translocate substances through the cytoplasmic membrane. The highly-conserved ABC transporter is part of a large family of transport proteins which span the entire CM and are powered by ATP hydrolysis. ABC transporters are among the largest protein superfamilies and have been categorised into seven distinct types. Three of the transporter types function as importers (Types I, II and III) and two are exporters (Types IV and V). Type VI functions as extractors while Type VII are mostly efflux pumps releasing toxic substances such as antibiotics or drugs (Thomas and Tampé, 2018).

Type I and II importers are only found in bacteria while type III are found in archaea and plants. The bacterial importers commonly require a substrate binding protein to transfer the substrate to the ABC transporters. Type I transporters are commonly involved in importing sugars such as maltose. Translocation of other nutrients such as iron commonly use the Type II system. An example of a type II ABC transport system is the $BtuC_2D_2$ system responsible for transporting vitamin B_{12} into the bacterial cytoplasm (Korkhov et al., 2012) (Figure 1.2). In this review emphasis will be on the bacterial importers particularly the type II system ABC transporter.

The basic components of all types of ABC transporters are the presence of two transmembrane domains (TMDs) and two nucleotide binding proteins (NBDs). The TMDs are the translocation permease proteins while the NBDs take part in binding and hydrolysing ATP. The TMDs and the NBDs in the bacterial importers are usually a separate polypeptide chains and do not possess the feature of the bacterial exporters in which both domains are fused together. Bacterial ABC transporters are commonly assembled from up to four separate protein subunits (Locher et al., 2002; Miethke and Marahiel, 2007) and possess a wide range of substrate specificities (Fath and Kolter, 1993).

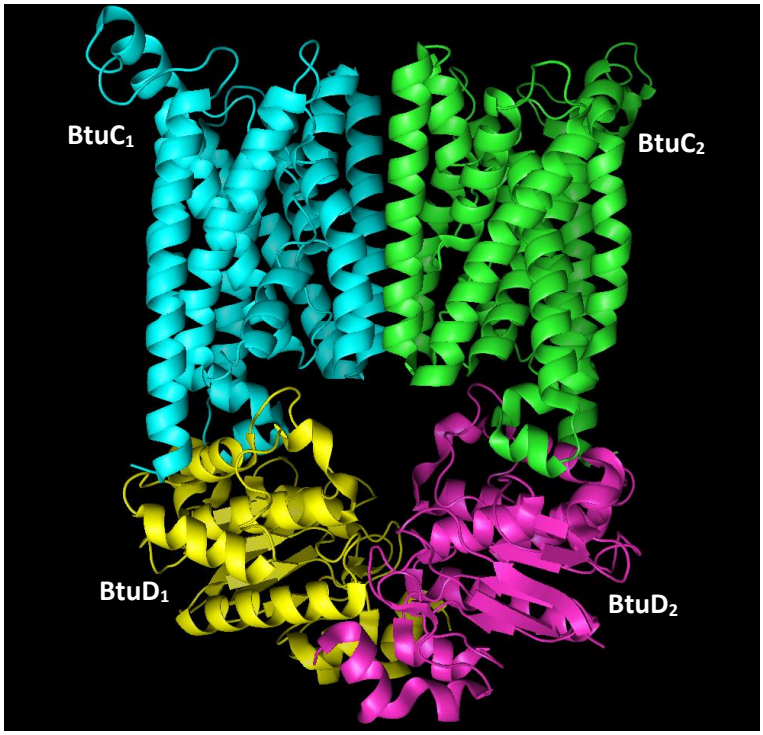

Figure 1.2: Ribbon model of the Type II ABC transport system, $BtuC_2D_2$
An example of a Type II ABC transporter, $BtuC_2D_2$ (PDB ID: 1L7V) (Locher et al., 2002), responsible for transporting vitamin B_{12} into the bacterial cytoplasm. $BtuC_2D_2$ possesses 16 TMDs (blue and green) in total. The NBD subunits are depicted in yellow and pink. Type II system ABC transporters are known to transport iron-siderophore complexes. Illustration was performed with Swiss Model and PyMOL.

In most cases, bacterial ABC exporters possess TMDs and NBDs which are fused forming two domains while the eukaryotic exporters have the four domains fused together in a single polypeptide. TMDs undergo conformational changes when induced by the NBDs which are activated by binding and hydrolysis of ATP. Non-covalent interaction causes TMDs to undergo outward facing conformations ready to accept substrates from their cognate binding proteins such as the lipoprotein solute-binding proteins (SBPs) or the periplasmic binding protein (PBPs).

The ferric siderophore forms a complex with the PBP or SBP and interacts with the permease upon transfer of the substrate (Hollenstein et al., 2007). In Gram-positive bacteria, ferric siderophore complexes bind to SBPs which act as a substrate receptor on the outer surface of the cytoplasmic membrane (CM). The iron complex is translocated into the bacterial cytoplasm via the ABC transporter present on the CM (Figure 1.3). In Gram-negative bacteria, once the substrate passes the OM, it will bind to the PBPs which transfer the substrate to the permease component of the ABC transporter. By including the PBP or the SBP, these ABC transporters are therefore comprised of 5 domains (Schalk and Guillon, 2013). When the NBDs release ADP and the inorganic phosphate following ATP hydrolysis, the permease transporters flip back into an inward-facing position and releases substrates into the cytoplasm. The NBDs are insensitive to substrate and therefore translocation of substrates into the bacterial cytoplasm are ATP-driven. The Type II system ABC transporter binds substrate with a higher affinity and possesses a different TMD from the Type I system but both types possess the same NBD. Moreover, Type II import substances that are present at a very low concentration and contrasts with the Type I transporter which transports substrates in abundance (Schalk and Guillon, 2013).

The common ABC transporter consists of one subunit of PBP, two subunits of identical permeases and two subunits of the NBDs as found in *E. coli,* $FepBC_2D_2$, which is involved in translocating enterobactin (Shea and McIntosh, 1991). In this case, FepB is a PBP, FepC is the permease and FepD is the NBD or ATPase. In some cases, the permease domains are fused into one polypeptide chain as seen with $FhuDBC_2$ which transports hydroxamate siderophores in *E. coli* (Mademidis and Köster, 1998) or there may be two distinct permeases, as seen with $VctPDGC_2$ transporting vibriobactin in *Vibrio cholerae* (Wyckoff and Payne, 2011). In the first case, FhuD is a PBP, FhuB is a permease and FhuC is the NBD or ATPase, whereas in the second case in *V. cholerae*, VctP is the PBP, VctD and VctG are the two permeases and VctC is the NBD or ATPase. In *Yersinia pestis*, the ABC transporter, YbtPQ, which transports yersiniabactin, does not include a PBP and possesses two identical polypeptides, YbtP and YbtQ, which act as heterodimers containing an N-terminal permease and a C-terminal ATPase in each protein (Perry and Fetherston, 2011). Similarly for the ABC transporter, IrtAB, in which IrtA and IrtB act as heterodimers in *Mycobacterium tuberculosis* (Ryndak et al., 2010).

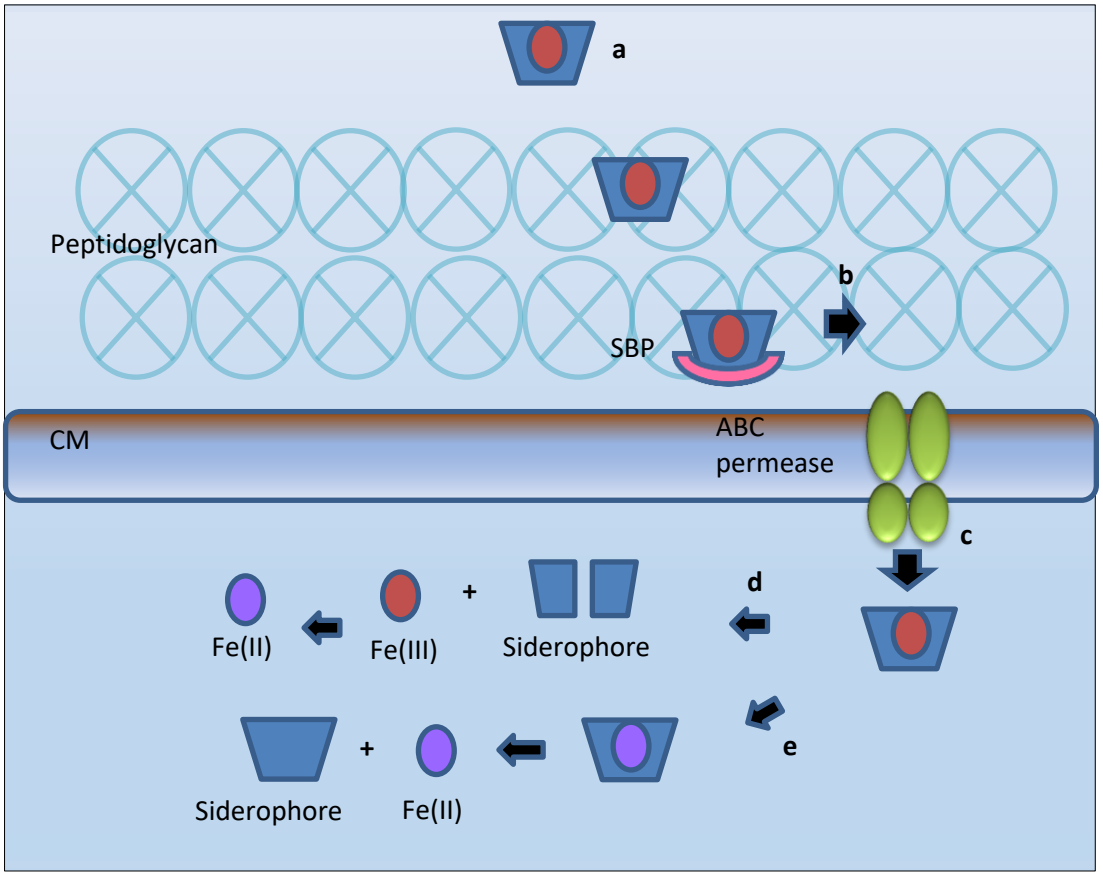

Figure 1.3: Schematic diagram showing the mechanism of ferric siderophore transport in Gram-positive bacteria

a. In Gram-positive bacteria, the ferric-siderophore passes through the peptidoglycan and binds to a lipoprotein SBP. **b.** The SBP transfers the ferric siderophore to the ABC transporter for transport into the cytoplasm. **c.** The ferric siderophore is translocated into the bacterial cytoplasm via the ABC permease. **d.** Siderophore is degraded by hydrolase to release the Fe(III). The Fe(III) is then reduced to Fe(II) by a reductase for use in the cell. **e.** Alternatively, Fe(III) in the ferric-siderophore complex is directly reduced to Fe(II) prior to being released into the bacterial cytosol, leaving the siderophore intact.

Pyoverdine is transported in *Pseudomonas aeruginosa* via the ABC transporter complex, $FpvCFD_2E_2$ and FpvWXYZ. In this case, FpvD and FpvE are the permease and the NBD components, respectively (Schalk and Guillon, 2013; Ganne et al., 2017). FpvC and FpvF exhibit two distinct PBPs, whereby FpvC has a higher affinity for iron and FpvF has a higher affinity for the iron-complex. The existence of two PBPs may to a limited extent, be involved in the release of iron from pyoverdine in the periplasmic domain of *P. aeruginosa* alongside FpvGHJK or FpvWXYZ proteins (Brillet et al., 2012; Ganne et al., 2017; Gao et al., 2018b).

Cytoplasmic transporters are traditionally divided into those that transport substances down a concentration gradient and those acting against the gradients, which are the active transporters. Uniporters transport substances down the concentration gradient by allowing conformational changes of the transport protein. The active transporters are divided into primary transporters which utilise metabolic energy sources such as ATP for transport and secondary transporters which are driven by electrochemical gradients via proton or sodium ions. Secondary transporters are sorted into the symporters and antiporters, which transport two molecules in the same and opposite direction, respectively. The ABC transporters of iron complexes are commonly categorised as the primary transporters (Henderson et al., 2019).

Other cytoplasmic membrane proteins reported to be involved in translocating iron complexes are the single subunit permeases which may be considered as secondary transporters driven by electrochemical proton gradients. Examples of single subunit permeases involved in iron-complex transport are the RhtX which transports rhizobactin in *Sinorhizobium meliloti*, FptX and FiuB which transport pyochelin and ferrichrome in *P. aeruginosa,* respectively (Cuív et al., 2004; Hannauer et al., 2010a).

The gene expressing these permeases are usually proximal to the iron related genes and no PBPs and ATPase genes or genes expressing ABC transporters were seen near to the permease gene involving proton motive force (pmf) energy (Cuív et al., 2004). The mechanism of the translocation using these permeases therefore has not been fully elucidated. The transfer of the iron complex to the permease may be direct or it may occur by diffusion in the periplasm. The permeases are reported similar to permeases which are pmf dependent such as the AmpG permease involved in cell wall recycling and induction of β-lactamases (Cheng and Park, 2002). However, the use of pmf has not been demonstrated with the ferric siderophore transport permeases (Schalk and Guillon, 2013).

1.3.4.2 Translocation across the outer membrane

1.3.4.2.1 TonB-dependent receptors

Gram-positive and Gram-negative bacteria have fairly different ferric siderophore transport systems due to the difference in their cell envelopes. Gram-negative bacteria have a double-layer membrane structure (Silhavy et al., 2010) and require more complex mechanisms to import the ferric siderophores. They therefore have an additional transport system to translocate iron across the OM. Thus, in Gram-negative bacteria, ferric siderophores are initially recognised by transporters located on the outer membrane, which are dependent on the TonB complex for an active transport energy. They are therefore known as TonB dependent receptors (TBDRs). TonB dependent transport systems are comprised of the TBDR and the cytoplasmic membrane-anchored TonB complex. These TBDRs are specific to particular ferric siderophores or a group of structurally related siderophores (Noinaj et al., 2010). TBDRs are also involves in the uptake of other metal chelate complexes such as the cobalamin-vitamin B_{12}, haem and nickel chelates. TBDRs have also been observed to be parasitised by unrelated molecules such as bacteriocins and bacteriophages (Schauer et al., 2008).

For most siderophores produced, the corresponding TBDRs in each Gram-negative bacterium are named according to the specific siderophore they are able to transport. For example, in *E. coli* the TBDR is named as FhuA, abbreviated from ferric hydroxamate uptake and was designated as such because it could internalise the hydroxamate-type siderophore ferrichrome (Locher et al., 1998). The receptor FptA refers to ferric-pyochelin transport in *P. aeruginosa*. PupA and PupB (Pseudobactin uptake protein) are pseudobactin (pyoverdine) receptors in *Pseudomonas putida.* Additionally, FauA (Ferric alcaligin uptake) is a receptor for alcaligin in *Bordetella* species, and FpvA, a ferric pyoverdine receptor in *P. aeruginosa* (Caza and Kronstad, 2013).

TBDRs are composed of a 22-stranded β-barrel which spans the OM and resembles a pore. A globular plug domain which is conserved for most transporters, is folded in the barrel interior and resides within the pore. A loop of the TBDR protein extends into the extracellular space and detects a specific substrate such as an iron source or a ferric siderophore at the extracellular side of the membrane. An example of a crystal structure of a TBDR, FhuA from *E. coli* is shown in Figure 1.4. The ferric siderophore is transported through the TBDR upon energy-based interaction with the TonB complex (Noinaj et al., 2010).

1.3.4.2.2 The TonB complex

The TonB complex is comprised of three CM proteins (TonB-ExbB-ExbD). Most Gram-negative bacteria possess a single TonB protein but there can be additional orthologues. Some bacteria are reported to have up to nine *tonB* genes (Chu et al., 2007), although a few have none.

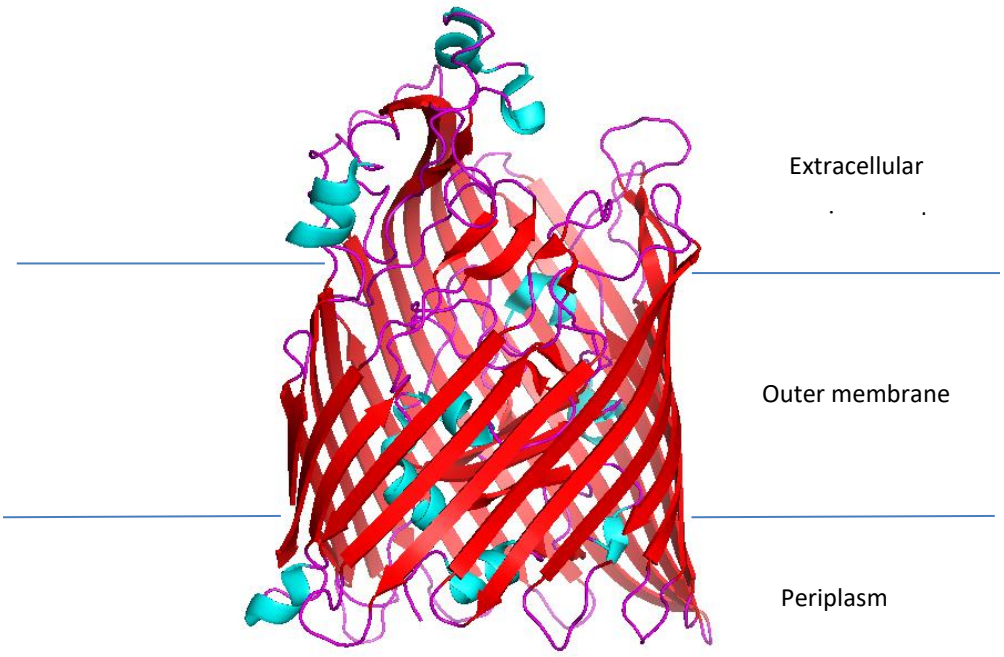

Figure 1.4: A ribbon model of the TBDR FhuA for transporting ferrichrome in *E. coli*
Side view of a hydroxamate TBDR, FhuA (PDB ID: 2GRX) of *E. coli* (Pawelek et al., 2006). α-helices are shown in blue, β-strands are shown in red and loops are in magenta. Structure is depicted using Swissmodel and PyMol.

The TonB complex is composed of three domains: a short N-terminal cytoplasmic domain, a transmembrane domain (TMD) and a periplasmic C-terminal domain (CTD) (Köhler et al., 2010). However, the largest region of the protein is the proline-rich periplasmic linker that connects the TMD to the 90 residue CTD (Chu et al., 2007). The important part of the protein, the CTD is most well studied and has recently been shown to be involved in lowering the energy barrier for ferricsiderophore uptake (Oeemig et al., 2018).

A recent study on the crystal structure of ExbB reveals a composition of six ExbB subunits (Maki-Yonekura et al., 2018), composed of 26 kDa monomers. Each of the monomers traverses the CM three times, with the largest part of the protein present in the cytoplasm (Kampfenkel and Braun, 1993; Celia et al., 2016). Similarly, ExbD is comprised of three 17.8 kDa monomers (Maki-Yonekura et al., 2018) which contain a single transmembrane region at the N-terminus and a larger part of the protein extending into the periplasmic domain (Kampfenkel and Braun, 1992; Garcia-Herrero et al., 2007). This section was recently suggested to exist as three small rod like structures which fits into the ExbB hexamer channel (Maki-Yonekura et al., 2018).

Two mechanisms were proposed for the energy conversion by ExbBD to facilitate substrate translocation into the periplasmic space via the TBDR: the energy transduction mechanism and the recently proposed, energy transition mechanism (Maki-Yonekura et al., 2018).

In the energy transduction mechanism, the TonB complex is proposed to use the pmf of the periplasmic space through the interaction of the ExbB and ExbD proteins. Protons from the periplasmic domain facilitate a rotational force of the ExbD helices within the ExbB ring and form a cation-selective proton channel through which they harness the pmf for energy production to energise TonB (Celia et al., 2016). ExbD interacts with the TonB protein through its periplasmic domain and transduces the pmf energy to TonB. TonB that has undergone conformational change then transduces the energy to the TBDR by linking the structurally conserved CTD of TonB to a conserved region at the N-terminus of the TBDR plug domain called the TonB box. The TonB box is a hydrophobic five to seven amino acid regions located in the periplasm. The binding of TonB CTD to the TBDR TonB box forms an extended β-sheet and induces conformational changes to the TBDR. This energy coupling interaction regulates the opening of the pore within the TBDR by movement of the plug domain. The mechanism therefore facilitates active transport of substrates across the OM and release of the substrate into the periplasmic space (Schauer et al., 2008; Krewulak and Vogel, 2011; Celia et al., 2016).

In the energy transition mechanism, a high concentration of hydronium ions in the cytoplasm allows protonation of the acidic residues within the ExbBD component and causes electrostatic repulsion among the subunits. This causes one ExbB and two ExbD subunits to be repelled from the ExbB hexamer ring and forms a denser packing pentamer ring with only one ExbD subunit. A denser packing pentamer ring prevents excessive proton influx thereby lowering the pmf and hindering the transport of substrates through the TBDR. The ExbBD channel is therefore controlled by joining and removing of the ExbBD subunits (Maki-Yonekura et al., 2018). Both proposed mechanisms involve six subunits of the ExbB protein and three subunits of the ExbD protein as shown in Figure 1.5.

1.3.5 Mechanism of iron release from iron-siderophore complex

Upon internalisation, the iron ion is released from the siderophore into the bacterial cytoplasm by one of several mechanisms. One mechanism involves intracellular ferric-siderophore reductases, as for instance, occurs for the ferric-ferrichrome complex in *E. coli*, in which ferrichrome is reduced by the reductase enzyme FhuF in the bacterial cytoplasm (Fontecave et al., 1994; Matzanke et al., 2004) (Figure 1.6). The acetylated-ferrichrome is recycled into the extracellular medium by an unknown mechanism. The ferric-ferrichrome complex in *P. aeruginosa* was suggested to undergo the same pathway as in *E. coli* (Hannauer et al., 2010a). However, the reductase enzyme responsible for the process in *P. aeruginosa* has not been elucidated. The apo-ferrichrome in *P. aeruginosa* then undergoes acetylation by an acetyltransferase, FiuC, to decrease its affinity for iron in the cytoplasm before it is recycled into the extracellular medium by an unknown mechanism. Diacetylated-ferrichrome upon release then forms a complex with another Fe (III) ion (Hannauer et al., 2010b).

Siderophore-bound Fe(III) could also undergo reduction to Fe(II), catalysed by the reductases that are found extracellularly or membrane-bound in certain pathogens, as an alternative to being transported into the cytoplasm as a chelated complex (Caza and Kronstad, 2013). Specifically, in the case of the siderophore pyoverdine, iron is removed in the periplasm by the reduction pathway prior to being internalised into the bacterial cytosol. A suggested reduction mechanism included the participation of PBPs and a reductase, FpvG alongside FpvHJK proteins and the product of the recently reported operon, *fpvWXYZ* (Gao et al., 2018b; Ganne et al., 2017). The iron-free pyoverdine is then re-exported (Brillet et al., 2012). Recycled pyoverdine is described to be exported across the outer membrane via the same efflux pump by which the newly synthesized mature siderophores are exported (Hannauer et al., 2010b; Yeterian et al., 2010).

Alternatively, the siderophore may be degraded by ferric-siderophore hydrolases in the cytoplasm prior to release of Fe(III) such as occurs with the siderophore enterobactin. Enterobactin is hydrolysed in *E. coli* by the Fes enzyme at its ester bonds (Lin et al., 2005; Miethke and Marahiel, 2007).

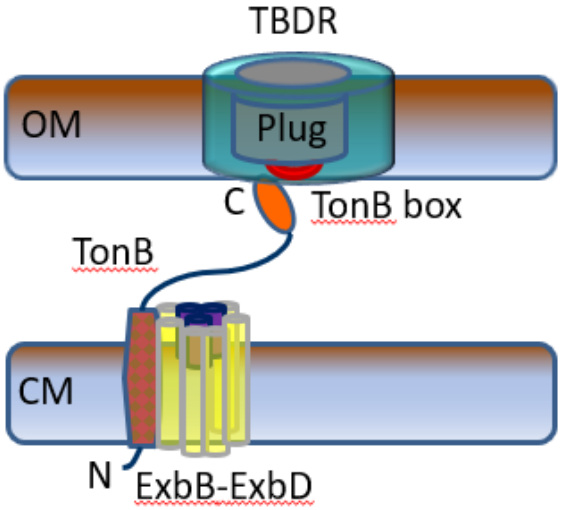

Figure 1.5: Diagram of a TBDR and the TonB complex involved in ferric siderophore transport in Gram-negative bacteria

The TBDR (teal) with an inner plug domain (grey) which resembles a pore is located in the OM. The TonB complex is comprised of a TonB protein (blue-spotted brown) and the ExbB-ExbD protein subunits. The TonB protein consists of a periplasmic linker connecting a C-terminal domain (CTD) (orange) to the TMD and an N-terminal domain (NTD) localised in the bacterial cytoplasm. The ExbB protein subunits form a hexamer ring (yellow) with three ExbD protein subunits (purple) within the ring. The structure of TonB complex, particularly the ExbBD protein, is drawn according to predictions proposed by Celia et al., (2016) and Maki-Yonekura et al., (2018). Translocation of the ferric siderophore complex across the OM occurs when the CTD of the TonB protein interacts with the TonB box (red) of the TBDR N-terminal plug domain.

Similarly, the siderophore bacillibactin is hydrolysed by the esterase BesA in *Bacillus* spp. (Abergel et al., 2009) (Figure 1.6). Another siderophore that undergoes hydrolysis is salmochelin in *E. coli*. The siderophore is cleaved by a periplasmic hydrolase, IroE, at its ester bond and the byproduct of the cleavage, a linear trimer, is then cleaved again in the cytoplasm by IroD into a dimer, monomer or the 2',3-dihydroxybenzoylserine (DHBS) (Zhu et al., 2005). Another model reported the hydrolysis of salmochelin in the periplasm by IroE and the apo-salmochelin is excreted into the extracellular milieu (Lin et al., 2005; Schalk and Guillon, 2013).

1.3.6 Fate of Fe(II) in the cytoplasm

In the cytoplasm, iron is in the Fe(II) form after having been reduced and is utilised by bacteria by incorporating Fe(II) into iron-requiring enzymes or stored in iron storage proteins. It is suggested that Fe(II) is incorporated into chaperones before being assimilated into such proteins to avoid formation of ROS by Fenton reaction. Possible compounds that may act as chaperones include sugar phosphates, citrates and glutathiones. In *E. coli*, iron released from ferrichrome and ferrioxamine B was shown to bind to a sugar phosphate (Böhnke and Matzanke, 1995). Citrates and glutathiones are widely distributed in the cytoplasm and are likely to bind to Fe(II) (Hider and Kong, 2011; Schalk and Guillon, 2013).

1.3.7 Utilisation and transport of xenosiderophores in bacteria

Bacterial species encode TBDRs to take up ferric siderophore complexes derived both from endogenous siderophores and also from siderophores secreted by other bacteria or fungi. These exogenous siderophores are termed xenosiderophores and the ability of other microorganisms to exploit these siderophores is termed siderophore piracy. The means of using xenosiderophores is an advantage to microorganisms as it increases their ability to survive in an iron-limited environment by allowing them access to additional iron sources available in polymicrobial surroundings. This saves the metabolic energy used for synthesising their own endogenous siderophore for survival (Schalk and Guillon, 2013).

Kümmerli and coworkers (2009) demonstrated an increase in siderophore production when siderophore producers co-exist with microorganisms which exploit their siderophores (Kümmerli et al., 2009). Similarly, Tyrell and colleagues demonstrated that siderophore production increases in *B. cenocepacia* in response to a co-colonised environment to allow it to compete for iron, as an example, in a chronic respiratory infection, where *P. aeruginosa* plays a part in co-colonising (Tyrrell et al., 2015). It has also been suggested that the marine bacterium, *Shewanella algae* selectively produces a chimeric siderophore that inhibits the siderophore piracy of a competitor organism, in this case the *Vibrio alginolyticus* (Szamosvári et al., 2018). In view of these interspecies interactions, each bacterial species generally employs their own high-affinity system for iron uptake (Matzanke et al., 1997).

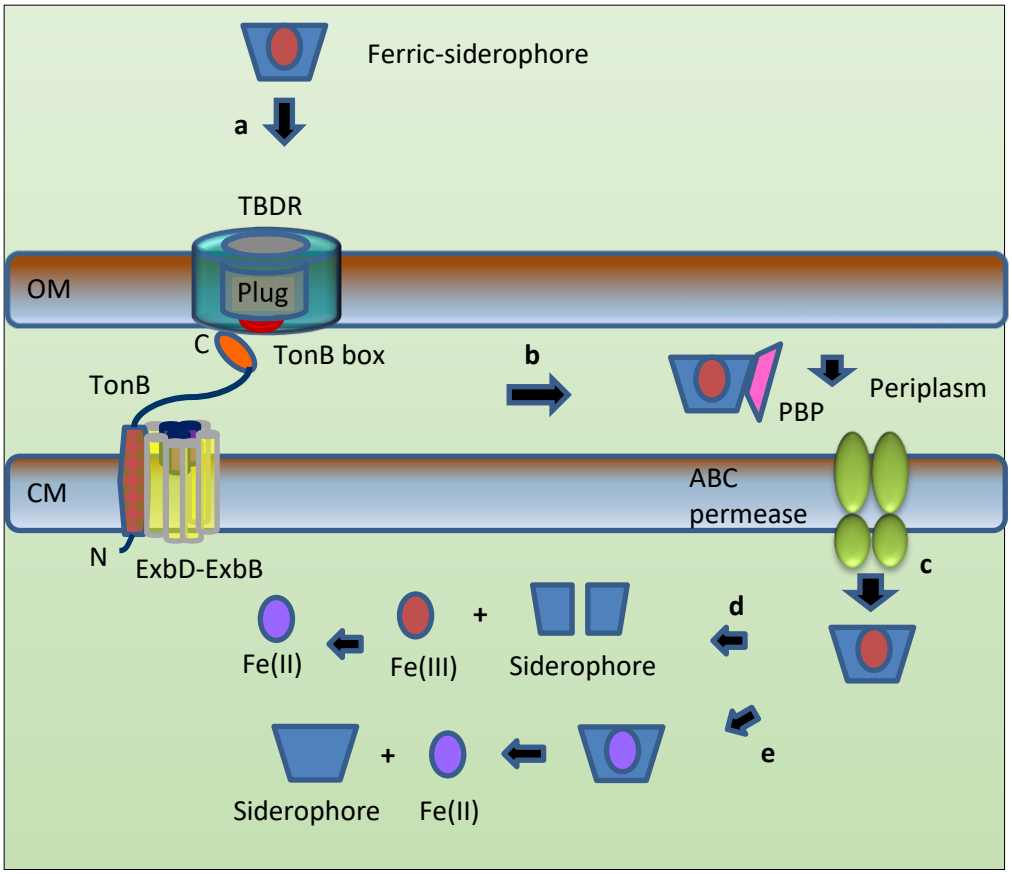

Figure 1.6: Diagram showing the mechanism of ferric-siderophore transport in Gram-negative bacteria **a.** In Gram-negative bacteria, a ferric-siderophore is transported through the TBDR barrel via the plug domain facilitated by the pmf energy transduced by the TonB complex. **b.** In the periplasm, the ferric siderophore attaches to a PBP which transfers the complex to the ABC transporter. **c.** Iron is translocated across the cytoplasmic membrane into the cytoplasm. **d.** The siderophore is degraded by a hydrolase to release Fe(III). The Fe(III) is then reduced to Fe(II) by a reductase for use in the cell. e. Alternatively, Fe(III) in the ferric-siderophore complex is directly reduced to Fe(II) prior to being released into the bacterial cytosol, leaving the siderophore intact.

Utilisation of xenosiderophores is generally limited by the need for specific TBDR genes, although the capacity to rapidly evolve TBDRs to adapt to substrate environment has been demonstrated in which just one or two amino acid changes can switch the specificity of a TBDR (Chatterjee and O'Brian, 2018). The authors aligned their studies with those of Noinaj et al. (2010) and concluded that TBDR mutant studies show that small sequence changes are sufficient to allow utilisation of alternative iron chelates.

To date, xenosiderophore utilisation is most well studied in *E. coli* and *P. aeruginosa* (Visca et al., 2002). In *E. coli,* there are at least eight distinctive siderophore-mediated Fe(III) transport systems including an additional system for iron uptake from ferric citrate (FecA) (Crichton and Boelaert, 2001; Raymond et al., 2003; Chatterjee and O'Brian, 2018). A typical commensal *E. coli* only produces the siderophore enterobactin while some pathogenic *E. coli* produce both enterobactin and aerobactin. The presence of many TBDRs highlights the ability of *E. coli* to use xenosiderophores. Each of the seven transport systems recognises a single type of ferric siderophore or closely related siderophores. For instance, the TBDRs FepA (Lundrigan and Kadner, 1986), FhuA (Pawelek et al., 2006), FhuE, FhuF, IroN and IutA, specifically transport enterobactin, ferrichrome, rhodotorulic acid, ferrioxamines, salmochelins and aerobactin, respectively (Guerinot, 1994; Hantke et al., 2003). The TBDRs Fiu and Cir serve as transporters for dihydroxybenzoylserine (DHBS). The FhuE protein, in addition, transports iron using other hydroxamate siderophores, such as coprogen and ferrioxamine B, besides rhodotorulic acid (Hantke, 1983; Hider and Kong, 2010). In this case, several of these TBDRs are responsible for transporting the xenosiderophores. Most of these siderophores are of fungal origin such as coprogen and rhodotorulic acid, which are produced by *Trichoderma* spp. (Lehner et al., 2013) and *Rhodotorula spp.* (Imbert et al., 1995), respectively. Xenosiderophore utilisation in *P. aeruginosa* include the ability of the bacterium to utilise ferrioxamine B by FoxA receptor. Ferrioxamine B transport via FoxA is also reported in *Yersinia entercolitica* (Báumler and Hantke, 1992; Cuív et al., 2007). *Pseudomonas fluorescens* was also found to have a receptor for ferrichrome (Zheng and Nolan, 2012).

Moreover, Matzanke and colleagues demonstrated the ability of mycobacteria to utilise a variety of xenosiderophores (Matzanke et al., 1999). *Neisseria gonorrhoeae,* on the other hand, does not produce endogenous siderophores but is able to utilise xenosiderophores such as enterobactin and salmochelin by having the *fbpABC* operon (Strange et al., 2011). *Bradyrhizobium japonicum* similarly does not synthesise siderophores but expresses TBDR genes for xenosiderophore utilisation (Small et al., 2009).

1.38 Siderophores as medicinal therapy

Development of 'Trojan horse' antibiotics has been emerging in which siderophores are covalently conjugated with an antibiotic moiety. These syntheses are analogous to naturally-occurring 'Trojan horse' antibiotics called sideromycins, such as albomycin (Braun et al., 2009).

Albomycin was first discovered in 1947, where it delivers a natural antibiotic into *E. coli* via the ferric-ferrichrome receptor, FhuA (Ferguson et al., 2000) and FhuD (Clarke et al., 2002). Trojan horse drug delivery systems are therefore a promising control strategy for multidrug resistant (MDR) bacterial pathogens (de Carvalho and Fernandes, 2014). This notion has been implemented as a drug delivery technology by using siderophore uptake pathways (Wencewicz et al., 2013).

The catecholate siderophore, enterobactin conjugated to the broad spectrum antibiotic ciprofloxacin (Ent-Cipro) was shown to be selectively effective to uropathogenic *E. coli* (Neumann et al., 2018). Certain fabrication of siderophore-antibiotic conjugates involves the use of synthetic instead of natural siderophores. Recently, the antibiotic cephalosporin has been conjugated to a synthetic siderophore with a catecholate moiety, named as cefiderocol. The siderophore cephalosporin has been shown to be effective to the enteric bacteria and also to several Gram-negative pathogens such as *P. aeruginosa, Acinetobacter baumannii and Stenotrophomonas maltophilia.* Clinical testing on the efficacy and safety is undergoing using cefiderocol and was reported to show tolerance for use as a new drug specifically for urinary tract infections (Portsmouth et al., 2018) and endocarditis (Edgeworth et al., 2018). A gram-positive antibiotic, daptomycin was shown to be effective against Gram-negative bacteria by linking the antibiotic with a natural siderophore, fimsbactin A and also with other synthetic siderophores containing hydroxamate and catecholate ligands (daptomycin-siderophore mimic conjugates). These conjugates, named as 1 to 6, are reported to be effective against the MDR *A. baumannii* strains (Ghosh et al., 2018).

Efforts are continuing to investigate the effectiveness of conjugating desirable siderophore analogues with antibiotics (mostly β-lactams), to control the blooming of infectious disease (de Carvalho and Fernandes, 2014). Siderophore conjugates would enable antibiotics which have been discontinued due to high resistance of pathogens, for instance by membrane permeability complications, to be newly effective (Silver, 2008). This is carried out by delivering these antibiotics intracellularly to pathogens, particularly the Gram-negatives, as siderophore-antibiotic conjugates through TBDR and and ABC permeases, thereby implying a targeted antibiotic delivery.

Siderophore-antibiotic conjugates can be pathogen-specific or broad spectrum depending on the siderophore used. In the case of pathogen-specific conjugated siderophores, fast diagnosis of pathogens responsible prior to direct-targeted treatment is required compared to broad spectrum antibiotics (Fischbach and Walsh, 2009). Therefore, advancement in developing detection of bacterial pathogens via siderophore-based sensors is ongoing which include the detection via fluorescence characteristics of certain siderophores, i.e. pyoverdine from *P. aeruginosa* (Heo and Hua, 2009; Zheng and Nolan, 2012). Moreover, a biosensor for pyoverdine using combination of nanomaterials has recently been shown to be promising for clinical diagnosis (Cernat et al., 2018).

1.4 Alternative iron uptake mechanisms in bacteria

Bacteria also possess strategies other than releasing siderophores to sequester iron from the environment or their host. Additional pathogen mechanisms for obtaining iron include scavenging iron directly from haem or from haem-containing proteins, from iron storage or iron transport proteins, such as ferritin, transferrin and lactoferrin, and acquiring ferrous ions (Fe^{2+}) by direct uptake. These mechanisms are discussed briefly in this section.

1.4.1 Iron uptake via haem

Haem is a porphyrin ring containing a ferrous iron atom at its centre (ferriprotoporphyrin IX). It is toxic to cells at higher concentrations. In eukaryotes, red blood cells lyse in the presence of free haem. Haem oxidases or haem oxygenases, which catalyse the degradation of haem, primarily protect cells from toxicity in mammals. However, in bacteria, haem degradation primarily functions in iron acquisition due to the liberation of free iron (Fe^{2+}) (Choby and Skaar, 2016). Most of the available iron in host organisms is secured in the haem-bound state within haemoproteins such as haemoglobin and myoglobin, and most bacteria that infect vertebrate tissues have systems dedicated to the acquisition of haem as a source of iron. Gram-negative and Gram-positive bacterial species have relatively similar mechanisms for haem (or haemin when the iron is oxidised) uptake; the difference principally involves the location of cell surface haem receptors. Gram-negative bacteria employ TBDRs and translocations via the periplasm, while the haem receptors for Gram-positive bacteria are located on the cytoplasmic membrane. Haemoprotein receptors can also be cell-wall embedded in Gram-positive bacteria.

In most cases, the binding and transport of haem in Gram-negative bacteria is relatively similar to the siderophore-mediated uptake mechanism. TBDRs or the haem-binding proteins (HBPs) located in the outer membrane are able to acquire haem directly from haemoproteins. In the periplasmic space, the haem binds to a haem transport protein, HTP, and is delivered to the ABC transporters. The haem is then transported to the cytoplasm facilitated by these ATP-dependent permeases. As iron cannot be released from haem, this molecule is then degraded by bacterial haem oxygenases (HOs), resulting in release of free iron. Alternatively, the haem can be recycled (Anzaldi and Skaar, 2010). There are several identified TBDRs that transport haem in Gram-negative pathogens and many more putative receptors in genomic database (Runyen-Janecky, 2013). Examples are HutA, HutR and HutX in *V. cholerae* and ChuX in *E. coli.*

Haem uptake systems in Gram-negative bacteria are encoded by similar haem uptake operons *(hmuRSTUV*) and have been characterised in several bacterial pathogens such as *V. cholerae* (*hutABCD*) (Su et al., 2015) and *P. aeruginosa* (*phuRSTUVW*) (Smith and Wilks, 2015). They are also present in Gram-positive bacteria such as *Bacillus cereus* (Khalil et al., 2015).

Regulatory proteins such as HemP, Fur (Ferric uptake regulator) and IscR (Iron-sulfur coordinating regulator) are reported to be involved in regulating haem uptake in iron-replete and iron-limiting conditions.

Alternatively, some Gram-negative and a few Gram-positive bacterial species are also able to capture haem by secreting haemophores. Haemophores belongs to a class of secreted proteins that have a high-affinity for haem. They bind to free haem or haem-containing proteins and deliver them to bacterial cells through binding with the haemophore receptors (Cescau et al., 2007). Haemophores can also be found as surface receptors. Both types of haemophores employ TBDRs and ABC transporters to convey haem to the cytoplasm (Wandersman and Delepelaire, 2012).

HxuA (Haemopexin utilisation protein A) from *Haemophilus influenzae* is an example of a 100 kDa haemophore that binds and forms complexes with haemopexin, a plasma protein that transports and recycles haem (Hanson et al., 1992). HxuA can be found free or anchored to the outer membrane. The complex formed triggers release of haem from haemopexin, making it available to be transported via the HxuC haem TBDR into the bacterial cytosol (Zambolin et al., 2016).

One of the most studied haemophores is HasA (haem acquisition system) first identified in *Serratia marcescens*. HasA is a 19 kDa monomer secreted by the Type I secretion system (T1SS) (Létoffé et al., 1994), one of the six major secretion systems in Gram–negative bacteria (Silverman et al., 2012). HasA captures haem from haemopexin, myoglobin and haemoglobins of diverse mammalian species such as human and bovine irrespective of the haem redox status, Fe (III) or Fe (II) (Wandersman and Delepelaire, 2004; Wandersman and Delepelaire, 2012). Upon capture, HasA delivers haem to the HasR TBDR on the outer membrane (Izadi-Pruneyre et al., 2006). A crystal structure of the HasA-HasR complex from *S. marcescens* is shown in Figure 1.7. The HasA/HasR system has been reported in pathogens such as *P. aeruginosa*, *V. cholerae* and *Y. pestis* (Ochsner et al., 2000; Rossi et al., 2001). The mechanisms of haemophore-dependent and -independent haem transport in Gram-negative bacteria are illustrated in Figure 1.8.

In Gram-positive bacteria, the iron surface determinant system (Isd) is prominently involved in importing haem into the bacterial cytosol. Most Gram-positive bacteria possess Isd with one or more near transporter (NEAT) domains anchored to the cell surface that bind and acquire haem either directly or from host haemoglobin. In some bacteria, studies have shown whereby extracted haem is transported through the bacterial cell wall via an Isd protein cascade and is relocated from one NEAT domain to another until it reaches the cytoplasmic membrane. Transportation of haem via the NEAT domains does not require energy.

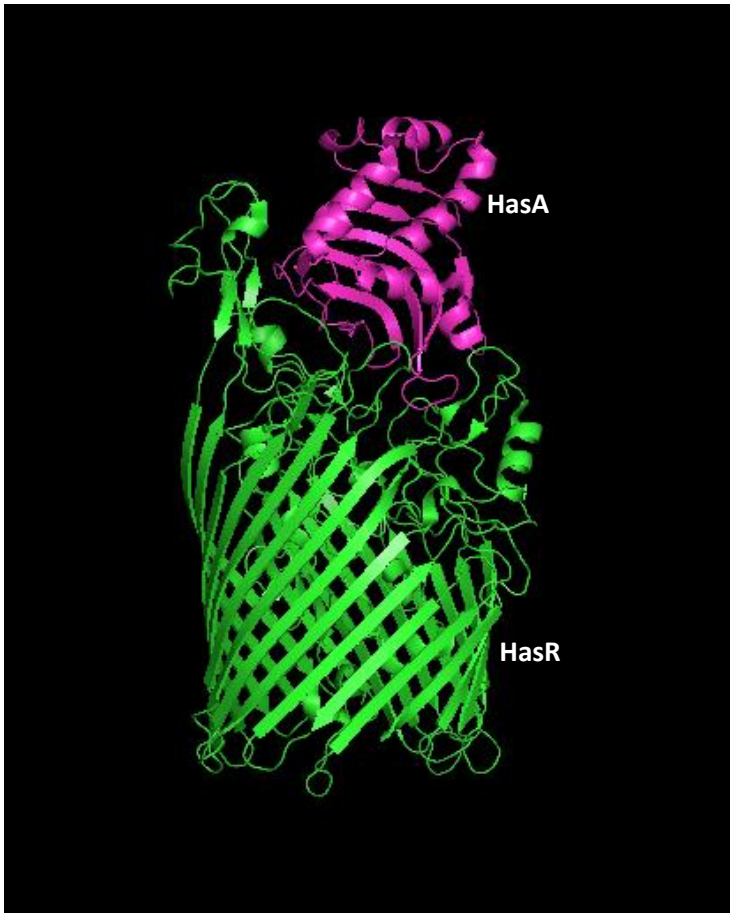

Figure 1.7: Ribbon model of a haemophore, HasR, interacting with the HasA TBDR in *S. marcescens*
A ribbon structure showing the HasA haemophore in *S. marcescens* (pink) bound to HasR (green) (PDB ID: 3CSL) used for haem uptake. Structure is depicted using Swissmodel and PyMol.

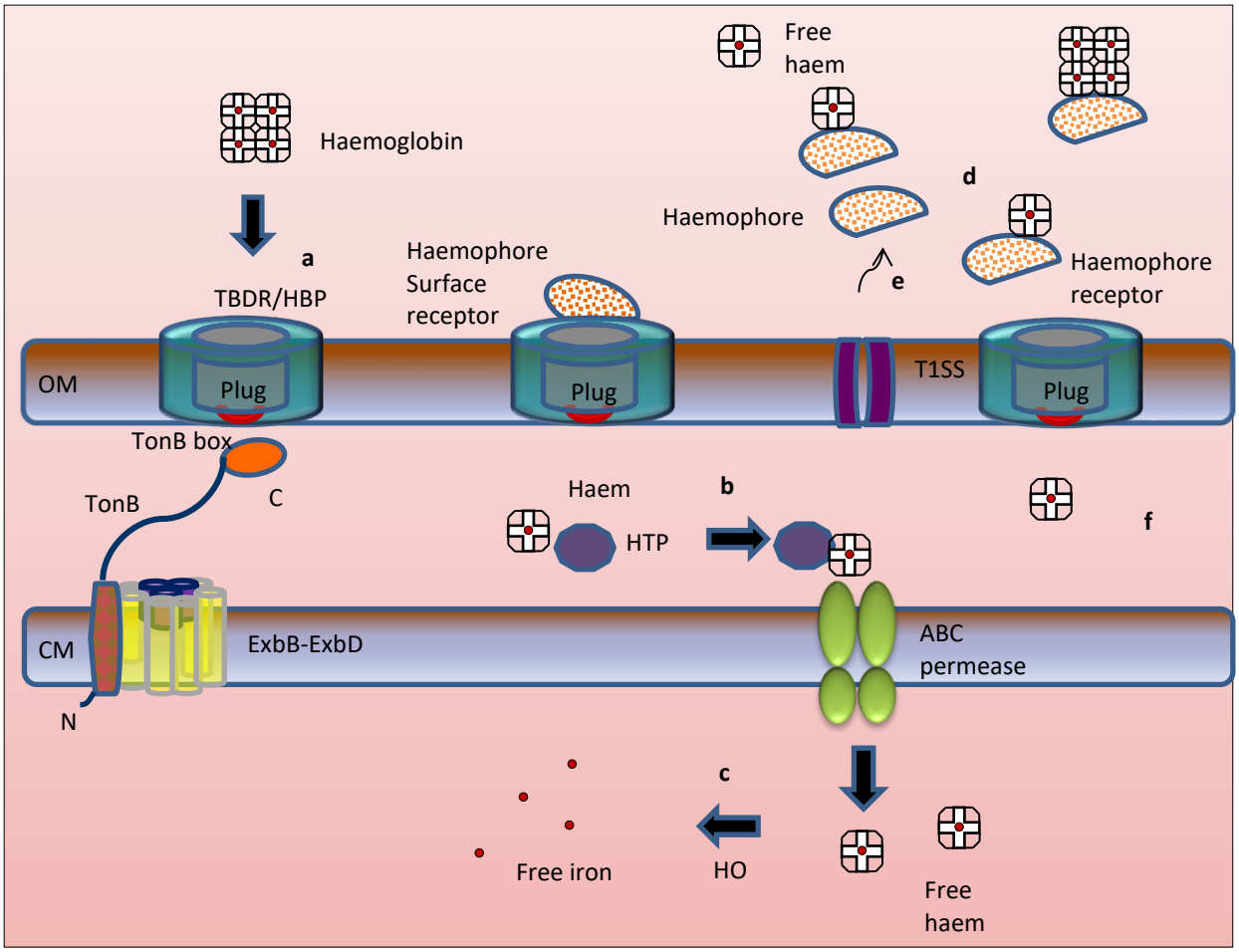

Figure 1.8: Diagram of haemoglobin and haem uptake by Gram-negative bacteria
a. Haem is captured from haemoglobin by HBP (a haem-specific TBDR or a haemophore-specific TBDR such as HasR) in the OM and is internalised into the periplasmic domain with energy transduced by the TonB system. **b.** The free haem attaches to HTP in the periplasm and is transported via an ABC permease to the cytoplasm. **c.** The haem is then degraded by haem oxygenases (HO) and iron is released inside the bacterial cell. **d.** Alternatively, haemophores (such as HasA) are secreted and attach to free haem and haem-containing proteins outside the cell. Haem-bound haemophore then binds to the haemophore receptor (a TBDR such as HasR) located on the OM and the haem is transported into the periplasm. Haemophores may also be found attached to the OM surface and act as receptors. **e**. These haemophores are secreted by the T1SS. **f.** refer to b.

ABC transporters take part in importing haem into the cytoplasm and similarly, haem is then degraded by the oxygenase-type enzymes (Caza and Kronstad, 2013). *Staphylococcus aureus* is an example of a pathogen with NEAT receptors on the cell surface (Grigg et al., 2007). In addition, *B. anthracis* is reported to secrete NEAT proteins into its supernatant to acquire haem (Honsa et al., 2011).

1.4.2 Acquisition of iron from transferrin and lactoferrin

Transferrin is an 80 kDa secreted protein found in the plasma of vertebrate host organisms. It is produced in liver and is exuded into the bloodstream to transport ferric ions to host tissues. It is also found in the pancreas, bone marrow and brain. Lactoferrin is a member of the transferrin family that can sequester iron even in a highly acidic environment such as in infected tissues. It is secreted by the exocrine glands and can be found in milk, respiratory fluids, bile, saliva and other secretions (Lambert, 2012). Both transferrin and lactoferrin are monomeric glycoproteins consisting of two similar lobes for iron-binding such that both proteins bind to two Fe(III) ions per monomer. Transferrin is predominantly an iron-transporter while lactoferrin is classed as an innate defence protein which binds iron (Baker and Baker, 2004).

A number of Gram-negative bacteria species such as *N. gonorrhoeae* and *Neisseria meningitidis* possess a bipartite transferrin binding protein system (TbpA-TbpB or Tbp1-Tbp2) located in the OM (Cornelissen et al., 1992). TbpA is a β-barrel TBDR and TbpB is also a barrel with a two-lobe (N- and C- lobe) lipoprotein that is anchored in the extracellular side of the bacterial OM by its lipid moiety (Ronpirin et al., 2001). Both TbpA and TbpB are able to bind to apo-transferrin and holo-transferrin with different affinities. The function of TbpA is more efficient in the presence of its co-receptor, TbpB. TbpB takes the role of capturing the transferrin by forming a complex and delivers it to TbpA. TbpAs are capable of extracting iron from transferrin and transport them across the outer membrane (Strange et al., 2011). The ferric ions in the periplasm bind to the PBPs, FbpA and are transported into the cytoplasm via the ABC transporter, FbpBC, in which the FbpB acts as the permease and the FbpC as the NBDs (Adhikari et al., 1996).

Iron acquisition from lactoferrin involves the lactoferrin binding proteins Lbp1 and Lbp2, (also termed LbpAB). Lactoferrin is captured by a lipoprotein anchored to the OM (Lbp2) and is transferred to the TBDR (Lbp1) in a similar manner to TbpA and TbpB (Schryvers et al., 1998). LbpB is highly similar to TbpB but possesses charged amino acid clusters in its C-lobe that are not present in TbpB (Chan et al., 2018).

Iron bound to transferrin and lactoferrin could also be released by binding of these proteins to host catecholamine stress hormones, principally dopamine, epinephrine and norepinephrine (O'Donnell et al., 2006). Host catecholamines which bind to transferrin and lactoferrin form complexes directly with the Fe(III) and subsequently reduce Fe(III) to Fe(II) which is then freed from transferrin (Sandrini et al., 2010).

Free iron may then be taken up by bacterial pathogens either directly or via other iron uptake mechanisms such as siderophores. Several pathogens possess TBDRs that directly recognise iron-catecholamine complexes, for instance the BfrA, BfrD and BfrE catecholamine receptors in the respiratory opportunistic pathogen, *Bordetella bronchiseptica* (Armstrong et al., 2012; Caza and Kronstad, 2013).

Acquiring iron from these host glycoproteins is classed as a direct iron uptake mechanism and this requires specific receptors or binding proteins. Composition of iron sources may vary in different hosts, and pathogens that employ direct mechanisms may have difficulty in surviving. Therefore, indirect iron uptake mechanisms such as production of haemophores and siderophores are more prevalent in pathogens (Miethke and Marahiel, 2007).

1.4.3 Acquisition of iron from ferritin

Ferritin is a large, nearly spherical intracellular iron storage protein, with a size of nearly 500 kDa. It can bind up to 4,500 Fe(III) atoms, and is a significantly rich source of iron for pathogens (Hoare et al., 1975). It is a non-haem iron-containing protein commonly found in host organisms or in other eukaryotes as a means of sequestering and maintaining iron homeostasis in the host (Sheldon and Heinrichs, 2015). Few pathogens have been demonstrated to be able to utilise ferritin, one of which is the Gram-negative diplococcus *N. meningitidis.* It has been shown that *N. meningitidis* can trigger rapid degradation of ferritin during the course of an infection (Larson et al., 2004).

1.4.4 Direct ferrous (II) iron uptake

An alternative iron uptake strategy, besides capturing iron from host proteins, involves a direct intake of soluble Fe(II). Soluble Fe(II) predominates over Fe(III) under anaerobic conditions and low pH, a state which favours Fe(II) stability, and so ferrous iron transport generally involves pathogens growing anaerobically, in low pH and in microaerophilic conditions. No OM protein has been identified in the ferrous iron transport system, whereby transport of soluble ferrous iron only involves the typical porins and is independent of TonB. In several Gram-negative pathogens, Fe(II) can diffuse freely through porins in the OM and is transported into the bacterial cytoplasm though a specific transporter found in the inner membrane.

One of those systems is the ferrous iron transport (FeoABC) system found in *E. coli* (Kammler et al., 1993) and other pathogens including *V. cholerae* and the microaerophile *Helicobacter pylori* (Velayudhan et al., 2000). FeoA is a small, ~8.0 kDa cytoplasmic protein that associates with FeoB. FeoB is a ~80 kDa transmembrane protein with a high-affinity for Fe(II) which acts as a permease for transport of the metal into the cell. The N-terminal cytoplasmic domain of FeoB may involve in GTP binding and hydrolysis for transport energy support (Cartron et al., 2006). FeoC is a small ~8.0 kDa protein which interacts with the cytoplasmic domain of FeoB (Weaver et al., 2013) and was predicted to regulate the *feoB* gene expression

(Cartron et al., 2006). Two mechanisms were proposed in Fe(II) transport via FeoB protein in which the protein may form a channel or exist in a trimeric structure and form a pore (Seyedmohammad et al., 2016; Sestok et al., 2018). Other examples of ferrous iron transport systems which involve ABC transporters are the SitABCD (Salmonella iron transporter) in *Salmonella typhimurium* (Janakiraman and Slauch, 2000), SstABCD transporter in *S. aureus* (Beasley et al., 2011) and YfeABCD systems in *Y. pestis* (Bearden and Perry, 1999). Here, YfeA is a PBP, YfeC and YfeD are two permease subunits located in the cytoplasmic membrane and YfeB acts as the ATPase for energy support (Fetherston et al., 2010).

The widely conserved EfeUOB (elemental ferrous iron uptake) iron transporter system is found in Gram-negative pathogens such as *E. coli* (Cao et al., 2007) and in Gram-positive bacteria such as *Bacillus subtilis* (Miethke et al., 2013). In *Pseudomonas syringae*, the transporter is termed the EfeUMB system as the protein EfeM is found instead of EfeO. The EfeU(O/M)B system has a dual mechanism for iron acquisition where it allows Fe(II) and Fe(III) transport and occurs in both aerobic and anaerobic conditions. EfeU is an iron permease membrane protein, whereas EfeB is a periplasmically located Fe(II) iron peroxidase protein, which disposes excess electrons released from ferroxidation of Fe(II). EfeO is also a periplasmic Fe(III) binding protein which delivers Fe(III) to EfeU. The homologue of EfeO, EfeM, is a periplasmic Fe(II) binding protein and also has a role as a ferroxidase, taking part in oxidising Fe(II) to Fe(III). The structures of EfeO and EfeM are distinct but they have a similar function in the EfeU(O/M)B system. The N-terminal region of the EfeO protein consists of a cupredoxin-like domain and the C-terminal region is involved in metal-binding, while in EfeM, the cupredoxin domain is absent leaving only the C-terminal domain of the protein (Rajasekaran et al., 2010a). Briefly, Fe(II) binds to EfeB, where it is subsequently oxidised by the copper centre of the cupredoxin domain to Fe(III). EfeB accepts electrons from the ferroxidase reaction and disposes of these electrons by combining them with a peroxide (Rajasekaran et al., 2010b). Fe(III) is transferred to the ferric ion binding protein, EfeO, and is delivered to the membrane permease EfeU. The Fe(III) ion is then transported across the cytoplasmic membrane into the cell by EfeU (Große et al., 2006; Cao et al., 2007).

The FtrABCD system found in *Bordetella spp.* (Brickman and Armstrong, 2012) and *Brucella abortus* (Elhassanny et al., 2013) also involves internalisation of Fe(II) following its oxidation to Fe(III) and is similar to the EfeU(O/M)B system. The FtrABCD system consists of FtrA, FtrB, FtrC and FtrD proteins, and the mechanism involves Fe(II) being internalised by the OM porin channels whereupon it binds to a homodimeric FtrA, a Fe(II) binding protein in the periplasm. FtrB then oxidises Fe(II) to Fe(III) via the copper within its cupredoxin-like domain and the Fe(III) is subsequently transferred to the FtrC permease for transport across the cytoplasmic membrane.

Electrons liberated from ferrioxidation activity are transferred to a ferrodoxin, FtrD, in the cytoplasm where they are passed to an electron acceptor, and at the same so reoxidising the ferroxidase centre of FtrB (Brickman and Armstrong, 2012; Elhassanny et al., 2013). Several pathogens possess more than one ferrous uptake system such as in *Y. pestis* which has YfeABCD, FeoABC and EfeUOB systems (Perry et al., 2015). An illustration of iron uptake via by FeoABC, YfeABCD, EfeU(O/M)B and FtrABCD is depicted in Figure 1.9.

1.5 Regulation of iron uptake

Iron uptake is tightly regulated by the ferric uptake regulator (Fur) protein. To maintain iron homeostasis, Fur acts as a transcriptional repressor for genes involved in iron uptake when the intracellular iron concentration is sufficient. Fur is a low molecular weight protein monomer (~17 kDa) and has an affinity for intracellular ferrous ions, which act as a cofactor (co-repressor). Fur is divided into two domains, the N-terminal DNA-binding domain and C-terminal domain that binds to one Fe^{2+} per subunit to form Fur-Fe^{2+} dimer complexes (Escolar et al., 1999). Fur-Fe^{2+} dimer binds to an AT-rich operator sequence known as the Fur box, located at the promoters for iron acquisition genes. The Fur box is comprised of at least three repeats of the hexameric GATAAT base sequence. Multiple Fur-Fe^{2+} dimers can bind with DNA at one time by occupying positions outside the Fur box regions. In iron starvation conditions, Fur protein or apo-Fur, detaches from the Fur box, allowing the transcription and expression of the genes involved in iron uptake (Bagg and Neilands, 1987; Andrews et al., 2003; Carpenter et al., 2009; Fillat, 2014; Seo et al., 2014).

Fur is a highly conserved protein and is expressed by most Gram-negative bacteria. The protein belongs to a FUR family of metalloregulators involved in the regulation of Zn^{2+}, Mg^{2+} and Ni^{2+} uptake, among others. In *E. coli*, the Fur regulator regulates at least 90 genes involved in metabolism and virulence including genes related to iron uptake, storage and efflux mechanisms (Deng et al., 2015). In some cases, Fur regulates the transcription of an ECF sigma factor gene which, in turn, activates transcription of endogenous siderophore biosynthesis and iron uptake genes, including xenosiderophore uptake (TBDR and ABC transporter encoding genes) (Wilson and Lamont, 2000; Latorre et al., 2018; Endicott et al., 2017). Additionally, DtxR, IdeR and IscR are other iron-related transcription regulators similar to Fur, and some are found in the Gram-positive bacteria (Gold et al., 2001; Merchant and Spatafora, 2014; Schwartz et al., 2001).

1.6 *Burkholderia* species

The genus *Burkholderia* was first reported by Walter H. Burkholder in 1942 as pathogens of carnations and onions. Back then, he named these pathogens as *Pseudomonas caryophylli* and *Pseudomonas alliicola,* respectively (Burkholder, 1942).

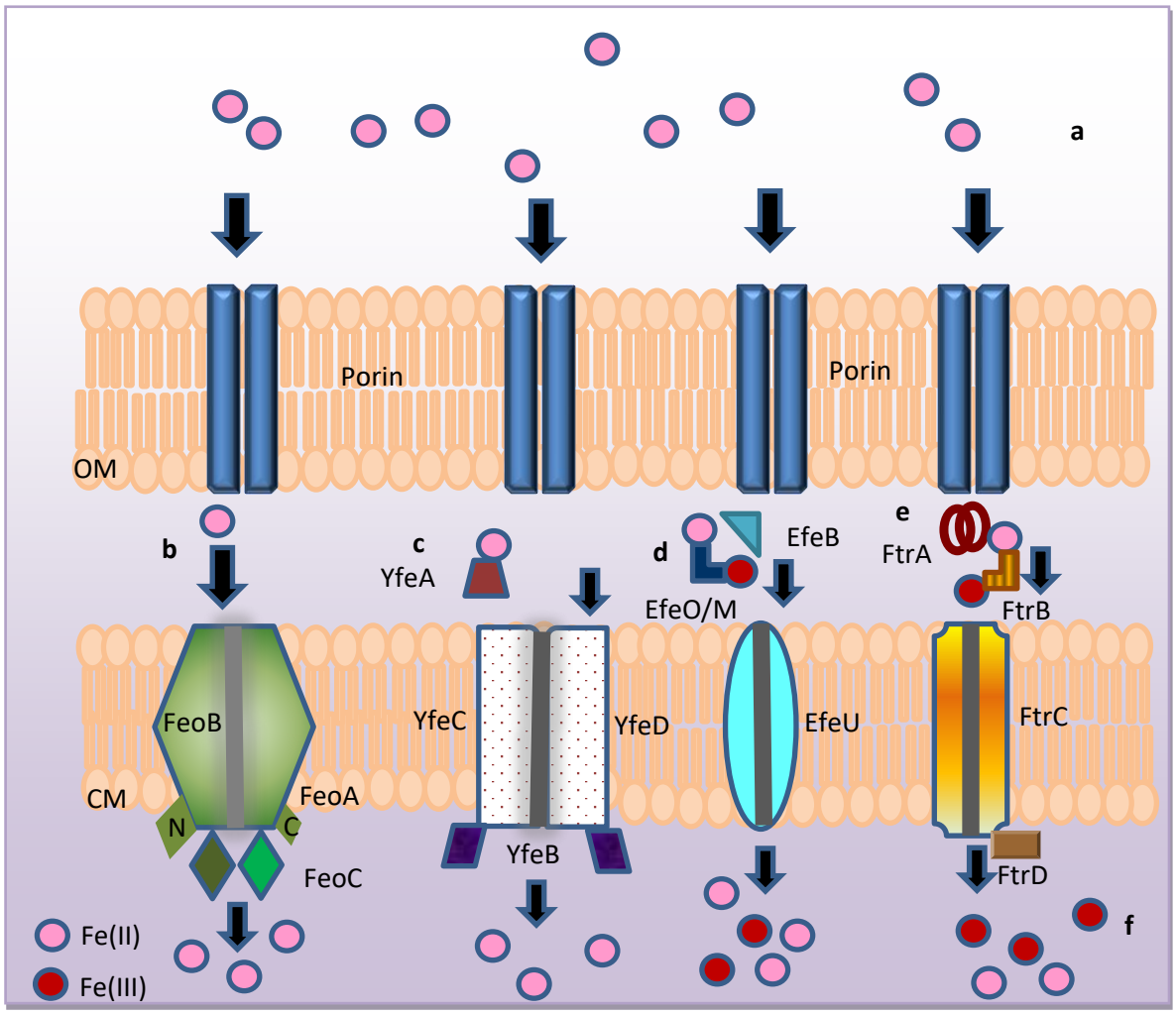

Figure 1.9: Diagram showing the TonB-independent uptake of Fe(II) in Gram-negative bacteria by FeoABC, YfeABCD, EfeU(O/M)B and FtrABCD

a. Fe(II) is internalised into the bacterial periplasm via porins. **b.** In Feo system, Fe(II) is directly transported into the cytoplasm via the FeoB permease. **c.** In YfeABCD system, Fe(II) binds with the PBP, YfeA, in the periplasm and is transported into the cytoplasm by a permease composed of YfeC and YfeD using ATP energy hydrolysed by YfeB. **d.** In the EfeU(O/M)B system, Fe(II) binds to periplasmic EfeO/M and is oxidised to Fe(III). EfeB takes the excess electrons released during the ferrioxidation process. Fe(III) and also Fe(II) are then transported into the cytoplasm through the EfeU permease. **e.** In the FtrABCD system, Fe(II) binds to periplasmic FtrA, and an adjacent FtrB oxidises Fe(II) to Fe(III). Only Fe(III) is transported into the bacterial cytoplasm via the FtrC permease. **f.** Iron in the form of Fe(II) or Fe(II) is released into the bacterial cytosol. FtrD is an electron acceptor of ferrioxidase activity. Note that EfeU has a higher affinity to transport Fe(II) and FtrC can transport both Fe(II) and Fe(III) into the bacterial cytoplasm.

In 1950, Burkholder reported another pathogen which is involved in causing sour skin in onions, later identified as a human pathogen, named as *Pseudomonas cepacia* (Burkholder, 1950; Gilardi, 1972). In 1992, a division of the *Pseudomonas* genus comprising of seven species was proposed to be renamed as the new genus *Burkholderia* on the basis of phenotypic characteristics, 16S rRNA sequences, cellular lipid, DNA–DNA homology values and fatty acid composition (Palleroni et al., 1973; Yabuuchi et al., 1992). The genus *Burkholderia* is taxonomically located within the phylum *Proteobacteriaceae*, in the β-proteobacterial subphylum (Class), the order *Burkholderiales* and the family *Burkholderiaceae* (Parte, 2018).

The *Burkholderia* genus constitutes a large group with exceptional metabolic diversity and biochemical characteristics. Nearly 100 species have been isolated, many of which are of clinical or environmental importance (Suárez-Moreno et al., 2012; Smet et al., 2015). Members of this genus have relatively large (7-9 Mb) GC-rich (>66 %) genomes comprised of multiple circular chromosomes (Parke and Gurian-Sherman, 2001). This feature explains the ability of the *Burkholderia* species to possess diverse morphology and occupy a wide range of ecological niches and having nutritionally versatile traits.
They are ubiquitous in the environment, particularly in soil, water and also in association with plants and fungi (Compant et al., 2008). In keeping with their ability to endure in different niches and conditions, findings proved that the outer membrane receptors (OMRs) of *Burkholderia* species show diversity in expression during adaptation to new environments (Liu et al., 2015).

While some *Burkholderia* species are plant pathogens, others are beneficial by promoting plant growth via nitrogen fixation. Some species are also reported to inhibit growth of other plant pathogens and have the capability to control plant hormone levels (Coenye and Vandamme, 2003; Kai et al., 2007). The opportunistic and clinically pertinent species are further subdivided into two groups, the *Burkholderia cepacia* complex and the *Burkholderia pseudomallei* group. The *B. cepacia* complex is capable of causing bacteraemia and severe respiratory tract infections (LiPuma, 2005) while *B. pseudomallei* can cause glanders and melioidosis disease. *B. pseudomallei* is usually found in soil and surface water mainly in regions of southeast Asia and northern Australia (Mark et al., 2011; Limmathurotsakul et al., 2016).

In 2014, Sawana and colleagues divided the genus into two separate genera: the clinically-important group of *Burkholderia* species are grouped with the phytopathogens in one genus (Clade I) and another group which mostly contain environmentally-important species is characterised as Clade II and was called the new genus *Paraburkholderia.* The phylogenomic analysis by molecular markers using conserved sequence insertions and deletions (CSIs) further subdivided Clade I into three subgroups: Clade Ia contains the Bcc species; Clade Ib includes *B. pseudomallei* and closely related species; and Clade 1c comprises the plant pathogens. Clade II, (*Paraburkholderia*) is also subdivided into Clade IIa and Clade IIb on grounds of genetic divergence (Sawana et al., 2014).

The *Paraburkholderia* spp. are isolated from different ecological niches, including from human and environmental isolates. In 2016, several species of the genus *Burkholderia* (i.e *Burkholderia udeis*) and *Paraburkholderia* (i.e *Paraburkholderia grimmiae*) were redesignated to a new genus named *Caballeronia (*i.e *Caballeronia udeis and Caballeronia grimmiae,* respectively*)* (Dobritsa and Samadpour, 2016). Prior to the subdivision of *Burkholderia* spp. into *Paraburkholderia* spp., the genus *Burkholderia* was divided into four groups, set apart by the previous phylogenetic study via the 16S rRNA. There are the Bcc and the pseudomallei, xenovorans and the environmental groups (Tayeb et al., 2008) (Figure 1.10). The environmental group was further categorised into the SBE (stinkbug-associated beneficial and environmental) and PBE (plant-associated beneficial and environmental) group (Takeshita et al., 2015).

1.6.1 *Burkholderia cepacia* complex (Bcc)

The Bcc group is currently comprised of 24 genetically distinct species that include *B. cenocepacia*, *Burkholderia ambifaria*, *Burkholderia cepacia*, *Burkholderia vietnamiensis*, *Burkholderia dolosa*, *Burkholderia multivorans*, *Burkholderia pyrrocinia*, *Burkholderia ubonensis* and *Burkholderia pseudomultivorans* (Peeters et al., 2013) (Table 1.1). Bcc members are generally found in soil, water and in association with plants, similar to other *Burkholderia* species. A few of the Bcc isolates have been exploited for various purposes including as biological control, in bioremediation and as plant growth stimulation. However, since a number of the Bcc are involved in human infections; extensive practise of biotechnological applications are restricted (Coenye and Vandamme, 2003).

1.6.2 Bcc pathogenesis and disease

Species from the Bcc are mostly pathogenic and are manifest from asymptomatic colonisation of respiratory airways to severe respiratory tract infections in immunocompromised individuals, mainly in patients with cystic fibrosis (CF) and chronic granulomatous disease (CGD) (LiPuma, 2005).

1.6.2.1 Cystic fibrosis

CF disease is a life-limiting recessive autosomal genetic disorder which affects 1/2500 live births in Caucasians. The disease commonly affects people in Europe, USA and the UK (Frost et al., 2018). CF is characterised by a dysfunctional chloride ion transporter called the cystic fibrosis transmembrane regulator (CFTR) protein, which is present in the epithelial cell membranes. CFTR plays a role in regulating fluids in the body including the airways and intestines (Riordan et al., 1989; Cheng et al., 1990).

Although most organs are affected, the defect of CFTR brings a higher risk to the respiratory tract, particularly the lungs of CF patients causing high mucus viscosity and reduced clearance aggravated by a lack of airway surface liquid.

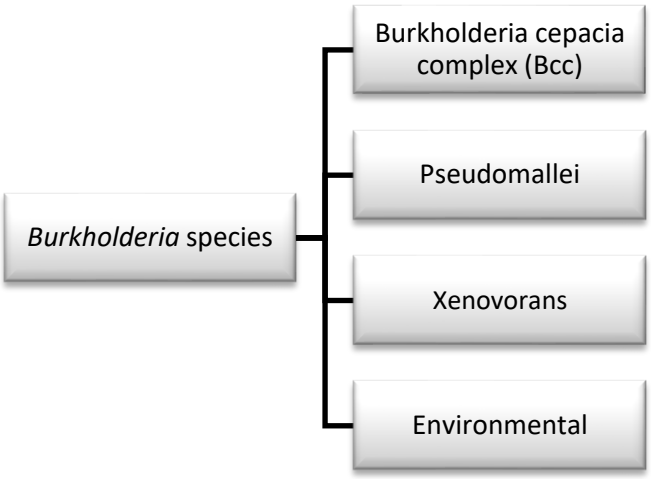

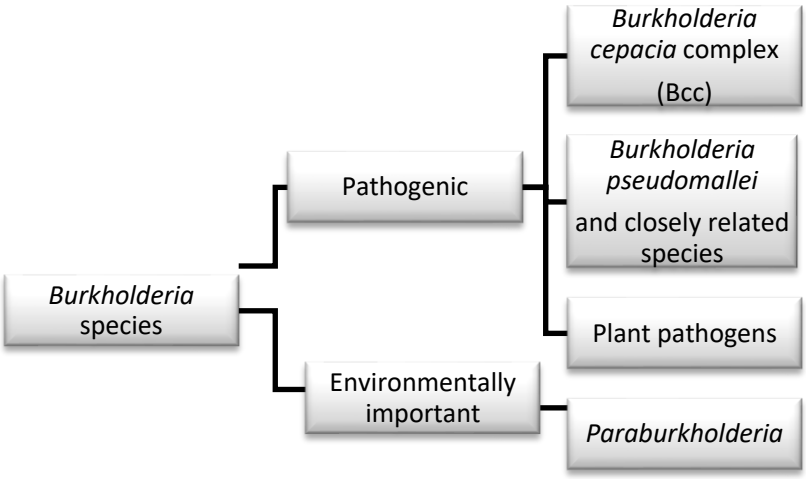

Figure 1.10: Classification scheme for *Burkholderia* species
Diagram showing the group division of the *Burkholderia* species by Mahenthiralingam et al., (2005) and Sawana et al., (2014).

Table 1.1 List of Bcc members

Species	Former name (Genomovar)	Origin[ab]	References
Burkholderia alpina	-	Mexico[ab]	(Weber and King, 2017)
Burkholderia ambifaria	VII	Trinidad[a] USA[b]	(Coenye et al., 2001b)
Burkholderia anthina	VIII	USA	(Vandamme et al., 2002)
Burkholderia arboris	-	USA[ab]	(Vanlaere et al., 2008)
Burkholderia cenocepacia	III	UK[ab]	(Coenye and Vandamme, 2003)
Burkholderia cepacia	I	USA[a]	(Yabuuchi et al., 1992) (Ballard et al., 1970)
Burkholderia contaminans	-	Spain[ab]	(Berriatua et al., 2001)
Burkholderia diffusa	-	USA[ab]	(Vanlaere et al., 2008)
Burkholderia dolosa	VI	USA[ab]	(Vermis et al., 2004)
Burkholderia lata	-	Trinidad[ab]	(Vanlaere et al., 2009)
Burkholderia latens	-	Italy[ab]	(Vanlaere et al., 2008)
Burkholderia metallica	-	USA[ab]	(Vanlaere et al., 2008)
Burkholderia multivorans	II	Belgium[b]	(Vandamme et al., 1997a)
Burkholderia paludis	-	Malaysia[ab]	(Ong et al., 2016)
Burkholderia pseudomultivorans	-	USA[b]	(Peeters et al., 2013)
Burkholderia pyrrocinia	IX	Unknown	(Vandamme et al., 2002)
Burkholderia puraquae	-	Argentina[ab]	(Martina et al., 2018)
Burkholderia seminalis	-	USA[ab]	(Vanlaere et al., 2008)
Burkholderia stabilis	IV	UK[a]	(Vandamme et al., 2000)
Burkholderia stagnalis	-	USA[a]	(Smet et al., 2015)
Burkholderia territorii	-	Australia[ab]	(Smet et al., 2015)
Burkholderia ubonensis	-	Thailand[ab]	(Vanlaere et al., 2008)
Burkholderia vietnamiensis	V	Vietnam[ab]	Gillis et al., 1995
Burkholderia xenovorans	-	USA[ab]	Goris et al ., 2004

[a]firstly recovered
[b]referring to type strain

This leads to chronic bacterial infection in both the upper and lower respiratory airways as a result of impaired clearance of pathogens. The chronic airways inflammation is associated with progressive deterioration in respiratory function (McCarron et al., 2018).

1.6.2.1.1 Microbiome of CF

A complex variety of microorganisms are demonstrated to colonise the CF lung, 87 genera overall in the largest study which include significant fungal communities (Coburn et al., 2015; Huang and LiPuma, 2016). A large study over a wide age range of CF patients reported the core CF microbiome to consist of five genera: *Streptococcus*, *Prevotella*, *Rothia*, *Veillonella* and *Actinomyces*. CF-associated pathogens such as *P. aeruginosa, S. aureus, H. influenzae, Stenotrophomonas maltophilia, Streptococcus pneumoniae, Moraxella catarrharlis, Achromobacter* spp., *Bordetella* spp., *Aspergillus* spp., non-tuberculous mycobacterium and also multiple Bcc members were less prevalent than the core group, but notably tended to dominate when present (LiPuma, 2010; Coburn et al., 2015; Kapnadak et al., 2016). As a result, many species are involved in colonizing lungs with CF, rendering CF as a polymicrobial disease.

The CF microbiome generally evolves with age, with reduced diversity of the bacterial community in older patients, where both the species of *Pseudomonas* and the Bcc members come to dominate (Fodor et al., 2012; Coburn et al., 2015; Huang and LiPuma, 2016). The main cause of bacterial respiratory infections in CF patients are therefore reported to be *P. aeruginosa* (~40 %) whereas the Bcc members contribute to less than 5% of cases of the disease (O'Toole, 2018; Frost et al., 2018). Bcc members therefore contribute a smaller percentage of respiratory infections in CF and non-CF patients. Infection by the Bcc members, although in a small percentage, is associated with severe respiratory symptoms and is a major challenge to treat (Scoffone et al., 2017). Chronic infections by Bcc in CF patients importantly contribute to the complexity of the disease, with progressive damage to pulmonary tissue, leading to respiratory failure and mortality.

The Bcc species are clinically challenging pathogens in CF because they are difficult to identify, highly resistant to antibiotics and also have the ability to spread easily between CF individuals. Although colonisation by one Bcc species was considered the norm in infected patients, newer techniques show co-infections with different Bcc species and infection with different strains of the same species (Drevinek and Mahenthiralingam, 2010; Teri et al., 2018).

1.6.2.2 Chronic granulomatous disease

In the 1960s, chronic granulomatous disease (CGD) was known as a disease of phagocytes (Nathan et al., 1969). CGD is a genetic disease causing the function of phagocytes to be defective in respiratory burst. This is because the reduced nicotinamide dinucleotide phosphate (NADPH) oxidase system is disrupted

due to a defect in any of four subunits present in NADPH oxidase (Kobayashi et al., 2004). The NADPH oxidase system plays a central role in the host defence mechanism. It is responsible in generating microbiocidal superoxides anion radicals in phagolysosomes by transferring electrons from NADPH to oxygen molecules in response to phagocytosis. This consequently generate more toxic antimicrobial ROS intermediates including hydrogen peroxide (H_2O_2) via the enzyme superoxide dismutase (SOD), hydroxyl anions (OH^-), hypohalous acid and peroxynitrite anions ($ONOO^-$) (Segal et al., 2000). Peroxynitrite anions are formed by a rapid reaction between nitric oxide (NO) present in the phagocyte vacuoles and superoxide anion. Nitric oxide can also be converted into inflammatory oxidants NO_2Cl and nitric oxide radicals ($.NO_2$) in the phagocytic vacuoles via nitric oxide synthase (Rosenzweig, 2008; McLean et al., 2010).

In GCD individuals, the defective activities of the NADPH complex interrupt these defence mechanisms. These causes masses of immune cells to aggregate and develop abnormal tissue granulomas and inflammatory complications that obstruct vital organs, rendering CGD patients more susceptible to bacterial and fungal infections (Panday et al., 2015). The presence of cationic transporters such as Nramp1, may exacerbate the effect of these toxic compounds on invading microbes, causing more damage to the host (Karupiah et al., 2000).

CGD patients are notably susceptible to pulmonary pathogens including *S. aureus*, the Bcc members, *Serratia* spp., *Norcardia* spp., *M. tuberculosis* and also fungi such as members of the *Aspergillus* genus (Bennett et al., 2018). *Burkholderia* spp. particularly *B. cenocepacia* is commonly isolated from the lungs of patients with CGD together with *Aspergillus* spp. and *Serratia* spp. Several of the mentioned pathogens may cause sepsis and pulmonary complications such as pneumonia, and both are major causes of death in chronic CGD patients (Marciano et al., 2014; Bennett et al., 2018).

1.6.3 Virulence determinants in Bcc

Bcc members, particularly *B. cenocepacia*, have multiple virulence determinants that underlie their clinical notoriety. Among the virulence factors are as below.

The main virulence factor in Bcc is most probably the universal **oxidative stress response**, exhibited in response to ROS. Among protective enzymes released by the bacterium are catalases, peroxidases and superoxide dismutase. In addition, pyomelanin pigments secreted by some Bcc members have been shown to act against oxidative stress (Drevinek et al., 2008). The **exopolysaccharide (EPS)** cepacian is composed of branched acylated heptasaccharide repeats with various sugars (d-glucose, d-rhamnose, d-mannose, d-galactose, and d-glucuronic acid, at a ratio of 1:1:1:3:1) (Cescutti et al., 2000).

EPS are demonstrated to be able to inhibit and interfere with the function of neutrophils and the production of ROS in infected hosts. The polysaccharide is also involved in the formation of a thick and mature biofilm, adherence and antibiotic resistance (Conway et al., 2004; Sousa et al., 2007).

Biofilms allow persistent infection by Bcc members and are considered a common trait of pathogens. Bcc members are able to form biofilms on biotic and abiotic surfaces and this trait increases resistance of the members to antimicrobials and antibiotics. Genes involved in biofilm formation are upregulated during the infection process in response to host immunity to intensify virulence (Sass et al., 2015). The **lipopolysaccharide (LPS)** of the Bcc members is important in causing infection and contributes to a strong immune response in the host which can cause cell damage (Bamford et al., 2007; Uehlinger et al., 2009). The constituents of the LPS in some Bcc are different from other Gram-negative bacteria in that they possess fewer phosphate groups and consist of an unusual sugar (i.e substitution of Kdo residue (deoxy-D-manno-octulosonic acid) with a Kdo analogue, D-glycero-D-talooctulosonic acid (Ko)) within the inner core of its existing short chain of sugar residues (oligosaccharide). The existence of this unusual sugar lowers the anionic charge of the Bcc cell surface and makes binding of cationic antimicrobial peptides less effective, which promotes antimicrobial resistance (Loutet et al., 2006; Ortega et al., 2009).

The **quorum sensing** (QS) system is a cell to cell communication system that responds to released chemical signals. There are at least two types of QS system employed by the Bcc members involving the release of N-acyl-homoserine lactone (AHL) and cis-2-dodecenoic acid (BDSF) signal molecules. In *B. cenocepacia*, the system is involved in regulating swarming motility and also in regulating biofilm formations (Huber et al., 2001). It also regulates the expression of other virulence factors such as toxin-antitoxin (TA) production (Schmid et al., 2012; Van Acker et al., 2014), extracellular protein secretion and also the biosynthesis of siderophores by the pathogen (Lewenza et al., 1999; Venturi et al., 2004). Bcc members are reported to be able to respond to their own QS molecules (Ryan et al., 2009) and to those of other pathogens such as *P. aeruginosa,* thus allowing inter-species communication in a co-infection environment (Lutter et al., 2001; Eberl, 2006). The QS system is recently demonstrated to be modulated by a two-component system, RqpSR (Regulating Quorum sensing and Pathogenicity (Cui et al., 2018).

Besides having a role as transcription regulators, **alternative sigma factors** also contribute to the virulence of Bcc members. One of these alternative sigma factors, the RpoN (σ^{54}) has a role in motility, biofilm and EPS formation, and also in metabolic adaptation by nitrogen metabolism (Flannagan and Valvano, 2008; Lardi et al., 2015). Another example is the alternative sigma factor, RpoE (σ^{E}), which besides mediating virulence, is involved in gene activation in response to environmental stress and allows the Bcc members to survive in adverse conditions such as in high temperatures or osmolarity (Flannagan and Valvano, 2008;

Silva et al., 2018). Both RpoN (Saldías et al., 2008)) and RpoE (Flannagan and Valvano, 2008) were reported to be involved in intracellular trafficking and survival within infected macrophages.

Protein secretion systems are also reported to have a significant role in the virulence of Bcc members. There are six types of secretion systems described in the Bcc. Type I secretion systems (T1SS) are involved in secreting proteins with haemolytic activity in the Bcc strains (Christine C et al., 2002). T2SS is described in *B. cenocepacia* and is involved in secreting two zinc metalloproteases, ZmpA and ZmpB, which play a role in the virulence of the bacterium (Kooi et al., 2005; Kooi et al., 2006). T3SS is involved in evasion of the host immune system (Tomich et al., 2003). There are two types of T4SS been described in *B. cenocepacia*, T4SS-1, encoded on a plasmid and T4SS-2, encoded on the bacterial chromosome. T4SS-1 is reported to participate in the virulence of *B. cenocepacia* in onions and intracellular survival in phagocytes (Sajjan et al., 2008) and the role of T4SS-2 is under investigation (O'Grady et al., 2011). Four Type V secretion systems (T5SS) are encoded within the genome of *B. cenocepacia.* Two of the systems secrete protein containing pertactin and another two, transport protein containing haemagglutinin repeats reported to involve in bacterial adhesions (Leitão et al., 2017). T6SS is involved in puncturing and injecting bacterial effectors into target cell membranes for virulence (Schwarz et al., 2014).

Among **extracellular proteins** secreted by the Bcc members are the haemolysins, adhesins, lipases, and proteases (Kooi and Sokol, 2009; Thomson and Dennis, 2012). These extracellular proteins have a role in intracellular invasion by interacting with the epithelial cells and causes proteolytic effect to the extracellular matrix of the host (Mullen et al., 2007; Mil-Homens and Fialho, 2012). In addition, serine proteases have been documented to be involved in sequestration of iron by ferritin (Whitby et al., 2006).

Other virulence factors include surface appendages such as the **cable pili** and **flagella** that take part in motility, cell adhesion and invasion in the lung tissues (McClean and Callaghan, 2009; Drevinek et al., 2008). A *B. cenocepacia* mutant lacking a functional flagellum results in a non-virulent strain (Urban et al., 2004). The cable pili contribute to the ability to enter and survive within host cells and are mostly found in epidemic strains, particularly *B. cenocepacia* (Chung et al., 2003). Extensive descriptions of the virulence determinants in Bcc members are described and reviewed by and Loutet and Valvano (2010) and Sousa et al. (2017).

One of the most extensively studied virulence factors in pathogens in an iron restricted environment is **siderophore-mediated** uptake. Siderophore-mediated iron uptake is employed by many pathogens to acquire iron from the host (Butt and Thomas, 2017). Bcc members synthesise and release siderophores in iron-limited conditions as a survival strategy in infections of the human host. Bcc members are also capable of acquiring iron by other mechanisms as previously discussed.

The **iron uptake strategies** are considered as virulence factors in Bcc members, particularly in competing for iron held by host proteins (Zughaier and Cornelis, 2018). Iron uptake strategies in Bcc are discussed in the next section.

1.6.4 Alternative iron uptake mechanisms and iron regulation in *Bcc*

A few *B. cenocepacia* and *B. pseudomallei* strains have been experimentally confirmed to utilise external haemin (Whitby et al., 2006; Thomas, 2007; Tyrrell et al., 2015). Gene cluster encoding a haem uptake system have been identified in chromosome 2 of most Bcc members as demonstrated in *B. cenocepacia* and also the *B. pseudomallei* genome (with the exception of *B. vietnamiensis*), indicating the use of this nutrient by the Bcc (Shalom et al., 2007; Konings et al., 2013; Butt and Thomas, 2017). As in other pathogens, Fur and HemP are demonstrated to be involved in regulating the haem uptake operon in *Burkholderia* species. HemP particularly has been reported to bind to haemin and exhibit multiple regulatory roles in the haem uptake of *B. multivorans.* The protein has been shown to activate the *hmuRSTUV* operon in *B. multivorans* by binding to the promoter region upstream of the operon which encodes the proteins for haemin uptake (Sato et al., 2017).

A complete ferrous iron uptake, *feoABC,* gene cluster has not been identified in the genomes of the Bcc members (Butt and Thomas, 2017). In severe infection of CF patients, the availability of iron changes from predominantly ferric to ferrous ions. This is due to the reduced oxygen tension in lungs of such patients and also the hypoxic effect of biofilms formed by pathogens (Hunter et al., 2013). To take advantage of the abundance of ferrous ions in later stages of CF disease, the Bcc members are predicted utilise the FtrABCD system.

B. cenocepacia is reported to possesses the FtrABCD system that internalises Fe(II) and Fe(III) as substrates (Mathew et al., 2014; Butt and Thomas, 2017). In addition to ferrous ions, increased levels of ferritin observed in the lungs of CF patients may play a role as an iron source in some Bcc members (Stites et al., 1999; Whitby et al., 2006).

An investigation by Whitby and colleagues demonstrated that *B. cenocepacia* is able to utilise ferritin as an iron source and the mechanism involves a serine protease secreted by the bacterium (Whitby et al., 2006). While lactoferrin levels are reported to increase in CF patients (Valenti et al., 2011), transferrin levels were not elevated (Stites et al., 1999). In a study conducted by Tyrell and colleagues (2015), *B. cenocepacia* was demonstrated to utilise haemin and ferritin as iron sources, and only use lactoferrin and transferrin when the biosynthesis of siderophore by the pathogen was inactivated (Tyrrell et al., 2015). So far, *B. cenocepacia* is the only Bcc member experimentally documented to ferritin, lactoferrin and transferrin (Whitby et al., 2006; Mathew et al., 2014; Pradenas et al., 2017).

Some clinical isolates of *B. cenocepacia* produce the siderophores ornibactin and pyochelin under iron-limiting conditions (Darling et al., 1998). Studies also showed that pyochelin seems to be a less efficient siderophore compared to ornibactin (Visser et al., 2004). Previous work has indicated that salicylic acid, a precursor of pyochelin, is a siderophore in *B. cenocepacia* (Visca et al., 1993). However, this is no longer thought to be the case as it was shown that salicylate was not an active siderophore in the chrome azurol S (CAS) assay, an assay used to detect siderophore production by orange halo formation around the bacterial colony (Schwyn and Neilands, 1987; Machuca and Milagres, 2003; Asghar et al., 2011).

Production and utilisation of ornibactin in *B. cenocepacia* are shown to be regulated by an ECF sigma factor, OrbS and by the CepR-CepI quorum-sensing system. The expression of OrbS is in turn, regulated by Fur (Agnoli et al., 2006). Fur is also reported to act as a repressor in the acquisition of iron in *B. multivorans* (Yuhara et al., 2008). However, Lowe and colleagues, (2001) demonstrated that the *fur* promoter is not responsive to iron availability in *B. cepacia* (Lowe et al., 2001). In addition, Fur is also reported to be involved in regulating small non-coding regulatory RNAs (sRNAs). At least 167 putative sRNAs are identified in *B. cenocepacia,* however, few are functionally characterised (Pita et al., 2018). A number of these conserved sRNAs (ncS63, Bc_KC_sr1 and Bc_KC_sr2) are shown to be involved in regulating iron homeostasis in *B. cenocepacia* (Sass et al., 2017; Ghosh et al., 2017).

1.6.4.1 Prevalence

Multilocus sequence typing (MLST) which include molecular typing of several housekeeping genes is the standard used for typing Bcc members. Sequencing of *recA* genes and 16S rRNA have so far been commonly used to diagnose Bcc members to the species and genomovar level (Baldwin et al., 2005; Voronina et al., 2018). Other means of identification, such as by MALDI-TOF, that have used to differentiate o ther genus to the species level have not been accurate when applied to the *Burkholderia* (Chien et al., 2018).

Among the Bcc members that cause respiratory infection in CF patients, *B. multivorans* and *B. cenocepacia* interchangeably have the highest prevalence, causing approximately 90 % of Bcc infections, and are associated with rapid decline in lung function (Reik et al., 2005). In fact, *B. cenocepacia* was the most common Bcc species isolated from CF patients since the 1990s (Vandamme et al., 1997b). This is followed by *B. gladioli* (not a Bcc) and *B. vietnamiensis* (Drevinek and Mahenthiralingam, 2010).

Bcc species, particularly *B. cenocepacia* and less commonly *B. multivorans*, are associated with high mortality due to their ability to cause necrotising pneumonia, septicaemia and respiratory failure referred to as 'cepacia syndrome'. 'Cepacia syndrome' is a rare but almost untreatable condition. Other Bcc member, *B. multivorans* and *B. contaminans,* were also reported to be involved in causing 'cepacia syndrome' (Power et al., 2016; Blackburn et al., 2004; Farrell et al., 2018).

CF patients infected with *B. cenocepacia* have been reported to have a shorter survival than other CF patients (Jones et al., 2004) and some studies find *B. cenocepacia* to be associated with an accelerated decline in pulmonary function compared to patients infected with either *B. multivorans* or *P. aeruginosa* (Courtney et al., 2004). In contrast to *B. multivorans* and *P. aeruginosa*, which showed reduced virulence over time of infection, *B. cenocepacia* was seen to be more adaptable in chronic infections by demonstrating increased attachments to host epithelial cells, anti-microbial resistance, tolerance of iron limitation and adaptation to low oxygen conditions. The latter was shown to be due to expression of a gene cluster, referred to as the *lxa* locus (low oxygen adaptation), having a role in adaptation to hypoxic CF lungs (Cullen et al., 2018).

It has been documented that Bcc member species, particularly *B. cenocepacia*, can persist in the lungs and airways of CF patients, years after the first colonisation, but show diverse phenotypes during the course of infection in CF patients due to genetic adaptation and clonal expansion (Coutinho et al., 2011). Besides exhibiting intrinsic resistance to multiple antibiotics, Bcc members are transmissible and cross infections have been documented by *B. cenocepacia* and also *B. cepacia.* With increased prevention strategies such as imposing segregation of Bcc-infected patients from non Bcc-infected patients, Bcc infections in recent years were shown to decline and infections are mostly acquired from the environment (Teri et al., 2018).

Some *B. cenocepacia* strains are highly virulent and are responsible for epidemic outbreaks in CF patients. Based on DNA-DNA hybridisation and *recA* analysis, *B. cenocepacia* can be phylogenetically categorised into four groups, genomovars IIIA to IIID (Vandamme et al., 2003). *B. cenocepacia* strains from the ET12 lineage i.e. J2315, BC7, K56-2, belonging to genomovar IIIA, are highly transmissible and were responsible for epidemic outbreaks in CF patients in Eastern Canada and the UK in the 1990's (Sun et al., 1995; LiPuma, 2010). A study in Milan, Italy, over the course of 10 years (2005-2015) also documented *B. cenocepacia* as the most prevalent species, followed by *B. stabilis* and *B. multivorans* (Teri et al., 2018). Similar prevalence of *B. cenocepacia* was seen in Russia, mostly by the ST709 strain, also from the ET12 lineage, representing up to 90 % of the infections caused by the Bcc (Voronina et al., 2018). The *B. cenocepacia* ET12 lineage is isolated mostly from humans and rarely from the environment.

The human isolates were recently demonstrated to contain more prophages (latent forms of viral bacteriophages) than environmental isolates and studies are ongoing in the investigation on the effect of these phages in virulence (Bodilis et al., 2018). Lung transplants have been implemented in patients with infected dysfunctional lungs. However, some cases have reported less favourable outcomes with patients infected with *B. cenocepacia* and *B. gladioli* (Dupont, 2017; Prabhu and Valchanov, 2017).

1.6.5 Siderophore-mediated iron uptake in Bcc

Bcc members are capable of producing up to four different types of iron-binding siderophores: ornibactin, pyochelin, cepabactin and cepaciachelin (Figure 1.11) (Sokol, 1986; Meyer et al., 1989; Stephan et al., 1993; Barelmann et al., 1996; Thomas, 2007). Ornibactin is proposed to be the primary siderophore produced by Bcc. Several Bcc members produce pyochelin as a secondary siderophore while others produce cepaciachelin as the secondary siderophore. Each of the Bcc endogenous siderophores and their uptake systems are expanded on below.

1.6.5.1 Ornibactin

Ornibactin was firstly isolated from an environmental isolate of *B. vietnamiensis* (Stephan et al., 1993). Since then, it was identified in many clinical and a few environmental isolates of the Bcc members. It seems to be a primary siderophore in most Bcc species (Butt and Thomas, 2017). Ornibactin is a linear tetrapeptide siderophore with a L-ornithine-D-aspartate-L-serine-L-ornithine backbone (Figure 1.11A and Figure 1.12). The N^5-amino group of the N-terminal ornithine is acylated with a β-hydroxy acid (hydroxybutanoic acid, hydroxyhexanoic acid or hydroxyoctanoic acid). These acylations give rise to three different lengths of acyl chains in ornibactin and yield three types of the siderophore having carbon chain lengths of C4, C6 and C8 (Stephan et al., 1993). The N^5-amino group of the amino acid is also hydroxylated. The N^5-amino group in the side chain of the C-terminal ornithine is acylated by formic acid and is hydroxylated. The carboxyl group of the C-terminal ornithine is linked to a molecule of 1,4 diaminobutane (putrescine). The β-carbon of the D-aspartate is also hydroxylated (Thomas, 2007; Butt and Thomas, 2017). Due to these modifications, ornibactin is a hexadentate siderophore, exhibiting three bidentate groups, with two hydroxamate ligands and one α-hydroxycarboxylate ligand (Figure 1.11A).

The biosynthesis and utilisation of ornibactin requires a cluster of 14 genes (*pvdAF-orbABCDEFGHIJKL*). The assembly of ornibactin by the enzyme ornibactin synthetase involves two NRPSs, OrbI and OrbJ (Agnoli et al., 2006). Four predicted PCP domains are present in the two NRPSs: three are found in OrbI for loading ornithine, aspartate and serine and one in OrbJ for ornithine. The tripeptide (L-Orn-D-Asp-L-Serine) formed via OrbI is linked to the C-terminal ornithine by OrbJ. The tetrapeptide is released from the final PCP domain via thioesterase present in the terminal domain of the same NRPS with an addition of a putrescine at the carboxyl end of the tetrapeptide (Agnoli et al., 2006; Asghar et al., 2011).

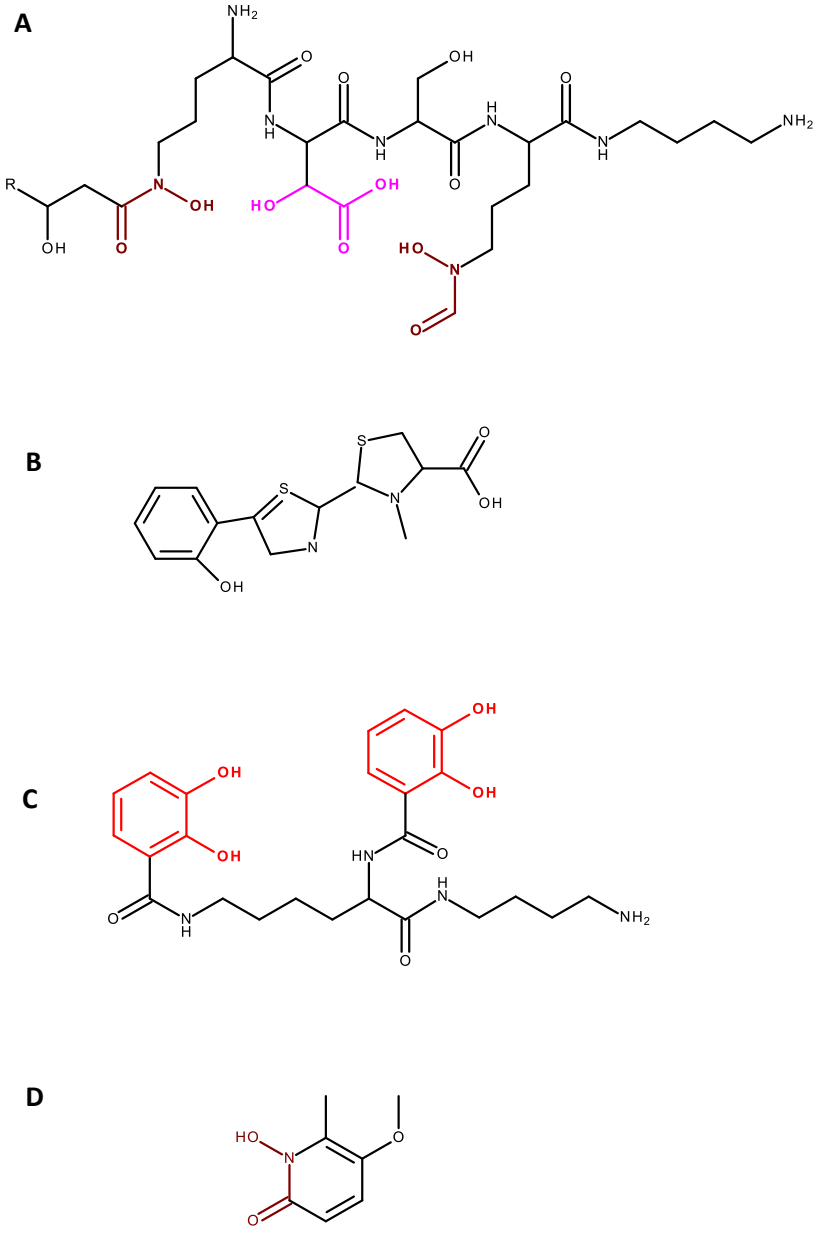

Figure 1.11: The molecular structures of siderophores produced by Bcc members
Chemical structures of (A) ornibactin, R= C1, C3 or C5, (B) pyochelin, (C) cepaciachelin and (D) cepabactin. The hydroxamate ligands are depicted in brown red, the catecholate ligands are depicted in red and the hydroxycarboxylate ligands are depicted in pink. Chemical structures were depicted using Accelrys Draw 4.2.

Exogenous ferric-ornibactin is transported into the periplasmic domain via the TBDR OrbA (Sokol et al., 2000; Shalom et al., 2007; Thomas, 2007). The putative PBP (OrbB) is proposed to transfer ferric ornibactin complexes to the ABC permease comprised of OrbC and OrbD for translocation into the cytosol. A reductase enzymes (OrbF) is proposed to take part in reducing the iron atom in the complex to Fe(II) which is then released from ornibactin (Agnoli et al., 2006) (Figure 1.13).

1.6.5.2 Pyochelin

Pyochelin was isolated from *P. aeruginosa* and characterised in the early 1980s by Cox and co-workers. The siderophore is a secondary siderophore in *P. aeruginosa* and some Bcc members and is usually produced in chronic or severe infections (Sokol, 1986). It is commonly produced in small amounts or not at all in some Bcc clinical isolates including *B. cenocepacia*. Pyochelin binds to Fe^{3+} by a stoichiometry of 2:1 at a relatively low affinity (Tseng et al., 2006) (Figure 1.11B and Figure 1.14).

Other than iron, it is also able to chelate Ag(I), Al(III), Cd(II), Co(II), Cr(II), Cu(II), Co(II), Eu(III), Ga(III), Hg(II), Mn(II), Mo(VI), Ni(II), Pb(II), Sn(II), Tb(III), Tl)I), V(IV) and V(V) Zn(II). However, it only been shown to transport Ga(III), Co(II), Mo(VI) and Ni(II) at a much lower rate than iron (Visca et al., 1992; Baysse et al., 2000; Braud et al., 2009; Brandel et al., 2012b). The siderophore gives out a yellow-green fluorescent colour in UV light and impart a red brown colour when forming a complex with iron (ferripyochelin) at a pH of 2.5. The iron-free pyochelin is unstable to light and is highly labile in solution (Cox and Graham, 1979; Cox et al., 1981).

Pyochelin may exist in two stereoisomer forms, pyochelin I and pyochelin II. It is synthesised from salicylate acid by successive addition and cyclisation of two molecules of cysteine involving two NRPSs (PchE and PchF). The pyochelin biosynthesis gene cluster is comprised of two divergent operons of *pchDCBA* and *pchEFGHI*. These genes are reported to be regulated by the Fur protein, the product of the *pchR* gene and also by sulphur availability (Thomas, 2007). The structural biology concerning the NRPSs assembly entailed in pyochelin biosynthesis has recently been described (Ronnebaum and Lamb, 2018). Based on studies on the analogous system in *P. aeruginosa*, both stereoisomer forms of pyochelin are proposed to be transported into the cytosol of the Bcc members by the TBDR FptA and a single subunit cytoplasmic transporter, FptX (Cuív et al., 2004).

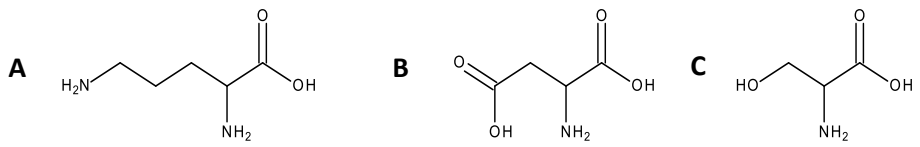

Figure 1.12: The monomer precursors in the biosynthesis of the ornibactin molecule
The structure of ornibactin is composed of two molecules of (A) L-ornithine, one molecule of (B) D-aspartic acid and one molecule of (C) L-serine.

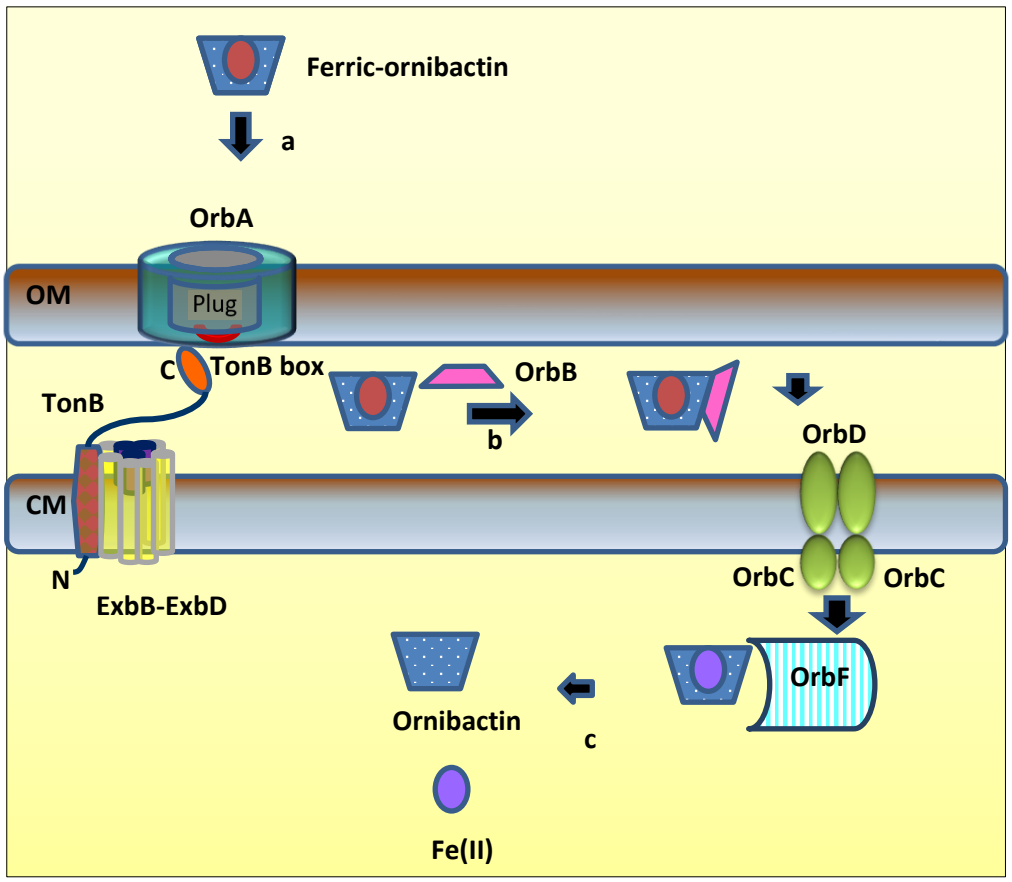

Figure 1.13: Diagram showing the proposed mechanism of ferric-ornibactin transport in *Burkholderia* species
a. Ferric-ornibactin enters the TBDR β-barrel and attaches to the plug domain (grey). **b.** In the periplasm, ferric ornibactin attaches to the periplasmic binding protein OrbB which brings it to the OrbD and OrbC components of the ABC transporter for internalisation into the cytoplasm. **c.** Iron is released from cytoplasmically located ferric ornibactin after iron atom in the complex is directly reduced to Fe(II) by reductase OrbF.

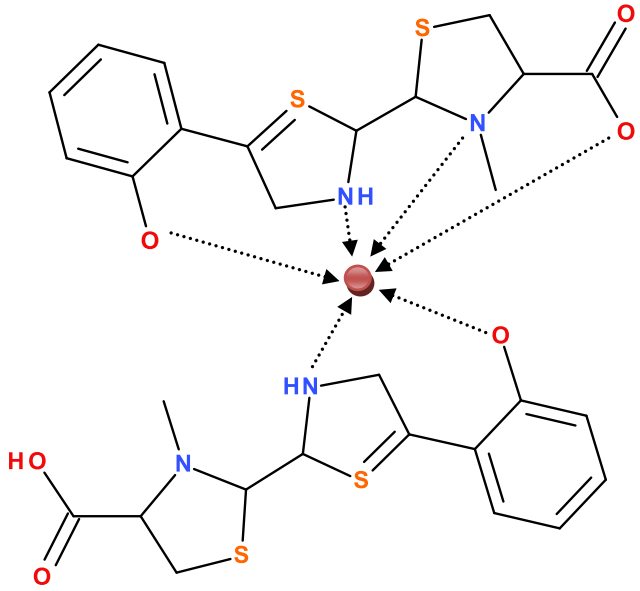

Figure 1.14: Structure of the ferric-pyochelin complex
The ferric-pyochelin complex involves two molecules of pyochelin and one Fe(III) atom (pink red) with a stoichiometry of 2:1 pyochelin-Fe(III) complex (Tseng et al., 2006). Sulfur atoms are depicted in orange, oxygen atoms in red and nitrogen in blue. Chemical structures are illustrated by Accelrys Draw 4.2.

1.6.5.3 Cepaciachelin

Cepaciachelin is a 789 Da bis-catecholate peptide siderophore with a scientific name of 1-N-[2-N',6-N'-di(2,3-dihydroxybenzoyl)-L-lysyl]-1,4-diaminobutane (Barelmann et al., 1996). The structure of cepaciachelin is comprised of four building blocks (Figure 1.11C and Figure 1.15), where a lysine molecule is bonded by an amide linkage to two molecules of 2,3-di-hydroxybenzoic acid (2,3-DHBA) and is also conjugated to a molecule of putrescine (diaminobutane) on its α-carboxyl group. Cepaciachelin was initially isolated from *B. cepacia* PHP7 (LMG11351) obtained from the soil rhizosphere but is presently identified as *B. ambifaria* AMMD (Gillis et al., 1995; Barelmann et al., 1996). By *in silico* analyses of the genomes of Bcc members, cepaciachelin has been predicted to be produced by several other Bcc members, such as *B. metallica*, *B. stagnalis* and *B. pyrrocinia* (Butt and Thomas, 2017). The biosynthetic genes of cepaciachelin were identified as being in a cluster as with most siderophores (Pupin et al., 2016; Esmaeel et al., 2016).

The cluster is found in the large chromosome of *B. ambifaria* and is predicted to encode two NRPSs, constituting one A domain for the building of the precursor di-hydroxybenzoic acid (DHBA) and a C-A-TE domain module (CpcA and CpcC). Synthesised cepaciachelin is predicted to be exported into the extracellular milieu via CpcH. Other proteins encoded by the cepaciachelin biosynthetic gene cluster include a TBDR gene (CpcG), a predicted PBP (CpcF) and cytoplasmic membrane ABC transporter (CpcFIJ) (Esmaeel et al., 2016; Butt and Thomas, 2017) (Figure 1.16). Additionally, although cepaciachelin is described as a siderophore, the role of cepaciachelin in Bcc members has not been fully determined.

1.6.5.4 Cepabactin

Cepabactin, with a scientific name of 1-hydroxy-5 methoxy-6-methyl 1 (1H)-pyridone is a heterocyclic hydroxamate siderophore (Figure 1.11D). It is also categorised as a hydroxypyridone. Thus, it can be said that cepabactin is in a position between a hydroxamate and a catecholate. Cepabactin was initially isolated from the *P. cepacia* strain ATCC25416 from onion, and from a soil isolate strain ATCC17759 (Meyer et al., 1989). These now are named as *B. cepacia* strains. Other clinical CF isolates of Bcc have been screened for cepabactin production and less than 15 % show the production of this siderophore (Darling et al., 1998) and, so far only *B. cepacia* has been demonstrated to produce cepabactin (Meyer, 1992). As the biosynthetic genes for cepabactin have not been identified, it is not possible to predict other cepabactin producers by bioinformatic analysis (Butt and Thomas, 2017).

Cepabactin has been demonstrated to act as a siderophore in iron-limited condition by liquid growth stimulation assays and by forming an orange complex with Fe^{3+} ions (Meyer et al., 1989).

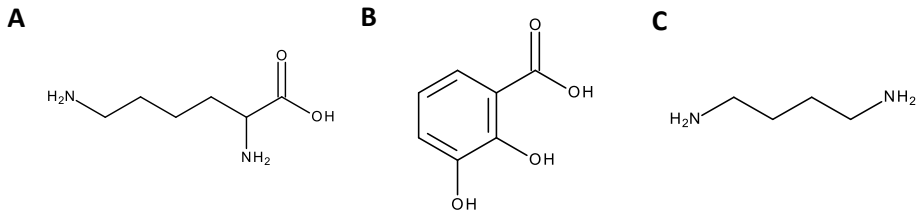

Figure 1.15: The precursors in the biosynthesis of the cepaciachelin molecule
The structure of cepaciachelin is composed of one molecule of (A) lysine, two molecules of (B) 2,3-di-hydroxybenzoic acid (2,3-DHBA) and one molecule of (C) putrescine. The structure of cepaciachelin is shown in Figure 1.11.

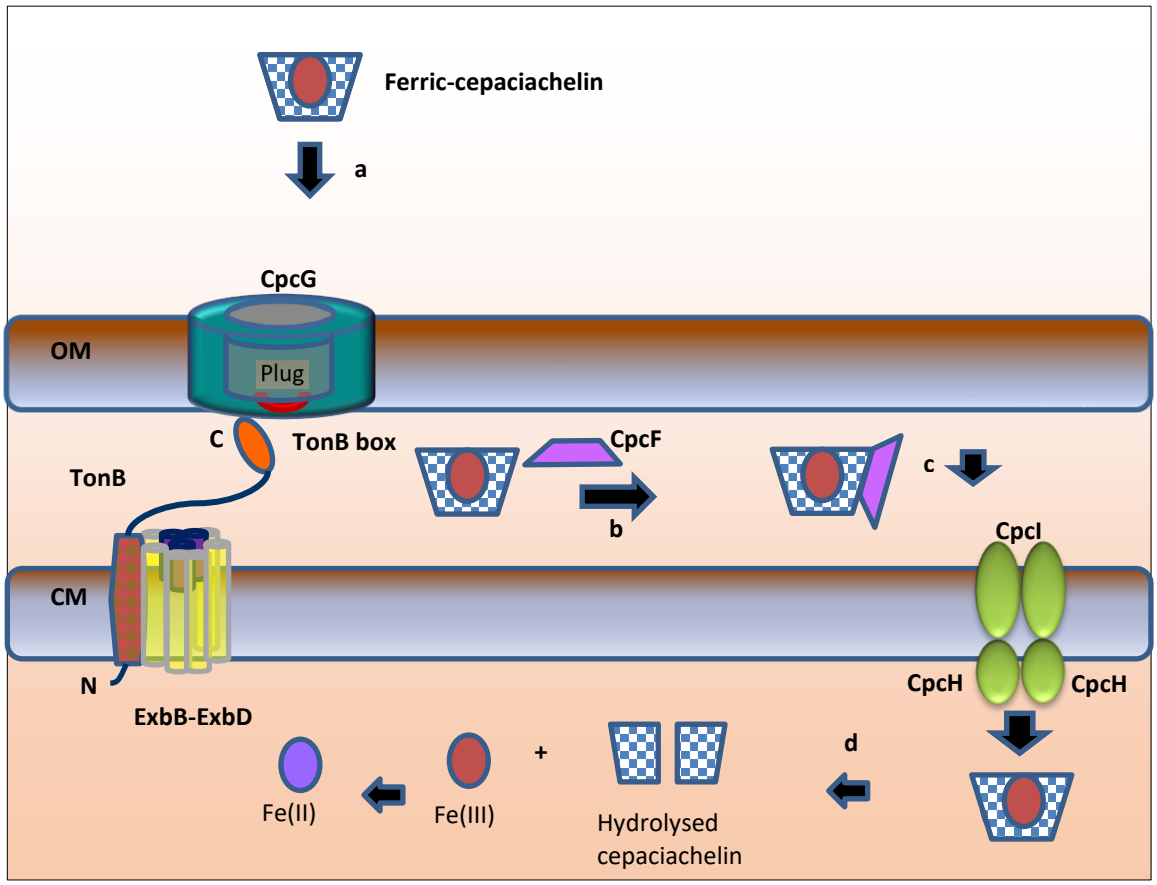

Figure 1.16: Diagram showing the proposed mechanism of ferric-cepaciachelin transport in *Burkholderia* species
a. Ferric-cepaciachelin is translocated into the periplasmic domain through the plug domain (grey) present within the TBDR β-barrel (teal), CpcG. Internalisation of the cepaciachelin complex is facilitated by the energy transduced by the TonB complex. **b.** In the periplasm, ferric-cepaciachelin attaches to the periplasmic binding protein, CpcF (pink) which transfers the complex to the ABC transporter CpcIJ (green). **c.** The ferric-cepaciachelin is transported into the bacterial cytoplasm through the ATP-driven CpcIJ transporter. **d.** Cepaciachelin is predicted to be hydrolysed by an unknown mechanism releasing Fe(III) **e.** Fe(III) is reduced to Fe(II) by an unknown reductase.

Klumpp and colleagues (2005) showed that cepabactin, acting as a bidentate siderophore, forms an octahedral complex with Fe^{3+} with a stoichiometry of 3:1, whereby three cepabactin molecules are required to provide six electrons to the ferric ion. As *B. cepacia* produces pyochelin, Klump and coworkers also demonstrated a combination of cepabactin and pyochelin achieving an octahedral Fe(III) complex with ratio of 1:1:1. In this case the pyochelin provides two bidentate ligands and cepabactin provides one (Klumpp et al., 2005). Studies have also demonstrated that cepabactin and siderocalin are able to form stable complexes. By forming complexes with cepabactin, it may demonstrate the ability of the host to prevent cepabactin from sequestering iron and this can render the cepabactin producers less pathogenic to respective host (Goyal and Anishetty, 2014). So far, the TBDR for cepabactin has not been reported in any pathogens documented to be able to utilise the siderophore.

1.6.6 Antibiotic resistance mechanisms of Bcc infection

Bcc members are highly resistant to commonly used antibiotics due to their intrinsic and acquired resistance traits. They are increasingly resistant to many classes of antibiotics: fluoroquinolones (ciprofloxacin), polymyxin (colistin), β-lactams (cephalosporin), aminoglycosides (amikacin) and chloramphenicol (Chien et al., 2018). Their unique LPS with reduced charges limits binding of the polymyxins. Several Bcc members express β-lactamase enzymes such as PenA, PenB, AmpC beta lactamases and carbapenemases, and so are able to inactivate several classes (A, B, C and D) of the β-lactamase-antibiotics. Several enzymes in resistant Bcc members are altered such as the DNA gyrase and dihydrofolate reductase rendering certain antibiotics less effective, such as the trimethoprim-based antibiotics. Other causes of resistance include porin mutations, changes in cell permeability, alteration of antibiotic targets, antibiotic modifying or degrading enzymes, efflux pumps and *in vivo* biofilm formations (Rajendran et al., 2010; Sousa et al., 2011). Whilst the RND (resistance-nodulation-division) superfamily is only found in Gram-negative bacteria, the efflux systems of the other four families: MFS (major facilitator superfamily), ABC, SMR (small multidrug resistance) and MATE (multidrug and toxic compound extrusion) are commonly found in both Gram-positive and Gram-negative bacteria (Poole, 2007; Sun et al., 2014). These pumps are efficient in generating multi-drug resistant (MDR) phenotypes in Bcc members. There are also cases of potential antibiotics being effective *in vitro* but not clinically effective in eradicating bacteraemia caused by the Bcc members, indicating complex host-related mechanisms of resistance (Buroni et al., 2014).

First-line options of antibiotics against Gram-negative pathogens such as vancomycin, meropenem and ceftazidime are increasingly less useful against the Bcc members. Moreover, high doses of these antibiotics may also lead to drug intolerance in patients. Combinations of drugs have also been implemented as therapies to allow a more effective synergistic effect. A drug combination of a cephalosporin and a non beta-lactam beta-lactamase inhibitor, ceftazidime-avibactam has recently been

demonstrated to be effective in eradicating a bacteraemia caused by *B. contaminans* (Tamma et al., 2018) and demonstrated a high *in vitro* susceptibility to *B. cenocepacia* (Van Dalem et al., 2018). Additionally, the Bcc members also exhibit increased resistance to disinfectants and are commonly isolated from hospital environments, which contributes to nosocomial infections (Shukla et al., 2018). On the whole, treating Bcc infected patients is an enduring challenge and developing treatment strategies for Bcc infection have been ongoing due to their emerging antibiotic resistance traits.

Other ways to develop antimicrobial therapies is by identifying the essential genes involved in the Bcc members. Determining these essential genes may allow the development of anti-microbial drug targets (Higgins et al., 2017). An example of essential genes recently recognised in the *Burkholderia* spp. is the genes of the Mla pathways mainly responsible in maintaining the barrier function of the outer membrane. A lesion in the pathway allows some *Burkholderia* spp. to be sensitive to antibiotics effective against Gram-positive species and the host innate immune system, although this was not observed in *E. coli* and *P. aeruginosa*. The pathway therefore may be involved in the intrinsic resistance of the *Burkholderia* spp. and could be targeted for antimicrobial therapies (Bernier et al., 2018). Moreover, as the production of siderophores is an important virulence determinant in pathogens, characterisation of the genes responsible for their biosynthesis, secretion and uptake can be a target to control infections by the Bcc species (Asghar et al., 2011).

1.7 Hypotheses

In this study, attention is focused on the Bcc members with emphasis on *Burkholderia cenocepacia*, which is also one of the most common causes of Bcc infection. *B. cenocepacia* is known to produce the siderophores pyochelin and ornibactin when its surrounding iron sources are scarce. Research shows that many pathogens are able to use siderophores secreted by other bacteria (xenosiderophores) as additional iron sources. It is therefore hypothesised that *Burkholderia* species have the same feature, although there is little information regarding siderophore piracy in these species. A recent preliminary study carried out in our laboratory has shown that *B. cenocepacia* can use two tri-bidentate hydroxamate ligand containing siderophores (ferrioxamine and ferrichrome) as iron chelators (Sofoluwe and Thomas, unpublished results). This observation was the stimulus for one aim of this project: to investigate additional siderophores that *Burkholderia* species could take advantage of as an iron source, including xenosiderophores harbouring other iron-binding ligands (catecholate and hydroxycarboxylate).

As *B. cenocepacia* is highly resistant to antibiotics, identifying additional usable xenosiderophores may contribute to the development of broader spectrum 'Trojan horse' antibiotics, especially relevant to chronic respiratory infection, which may lead to a curable disease. An antibiotic conjugated to endogenous siderophores of *B. cenocepacia* may specifically limit the growth of the bacterium. However, an antibiotic conjugated to a xenosiderophore of *B. cenocepacia* could suggest an inhibition of *B.*

cenocepacia and co-existing pathogens. This effect could thereby allow a combination therapy against CF pathogens in a multiple infection.

Another aim of this study was to characterise the receptors (TBDRs) that are involved in uptake of the *B. cenocepacia* xenosiderophores. *B. cenocepacia* possesses specific outer membrane receptors for each endogenous siderophore and it also encodes additional TBDRs of unknown function (Butt and Thomas, 2017). This may allow them access to additional iron sources in an environment populated by other species of microbes. This study was designed to find out which of additional TBDRs are involved in xenosiderophore utilisation in *B. cenocepacia*. Also, from bioinformatics analysis, one of the TBDR gene loci in *B. cenocepacia* has been predicted to be involved in the haem uptake system. Although most investigations in this study will focus on identifying and characterising the TBDRs involved in iron acquisition, the TBDR for transporting haem will also be investigated.

Gram-negative bacteria require a TonB system for ferric-siderophore transport. Many bacteria contain a single type of this TonB-ExbB-ExbD system that fulfils the uptake role of ferric siderophores, haem and vitamin B_{12}, as TonB interacts with multiple TBDRs. A mutational analysis carried out on *B. cenocepacia* identified a TonB system (TonB1-ExbB1-ExbD1) required for uptake of the endogenous siderophores pyochelin and ornibactin (Asghar, 2003). A subsequent bioinformatic analysis of the genome sequence of *B. cenocepacia* has revealed another two *tonB-exbB-exbD*-homologous gene clusters (M. Thomas, unpublished observations). It is therefore possible that the other TonB system are involved in the uptake of xenosiderophores.

Bioinformatics analysis will also be performed to investigate the inner membrane transporters for identified xenosiderophores. This will be done through investigations of the cytoplasmic membrane iron-related ABC transport systems and permeases.

1.8 Simplified aims of study

1. To identify additional putative iron transport systems using bioinformatics.
2. To investigate the siderophore piracy behaviour of *B. cenocepacia* by exploring the xenosiderophores that the bacterium can exploit.
3. To characterise the receptors for the xenosiderophores that *B. cenocepacia* can utilise and investigate a TBDR for haem.
4. To identify the cytoplasmic transporters for the xenosiderophores.
5. To determine the function of the TonB1 complex in xenosiderophore transport.

Chapter 2

Materials and Methods

2.1 Bacterial strains

Bacterial strains used in this study were grown at 37 ^{o}C except for *Bacillus megaterium*, *Burkholderia phymatum, Burkholderia terrae* and some of the *Pseudomonas* strains (i.e *P. fluorescens*) which were grown at 26-28 ^{o}C. *Burkholderia* strains were maintained on minimal salts agar (M9) containing 0.5% glucose (Section 2.4.1.3) at room temperature except for *B. terrae* which was maintained on R2A agar. Other strains were maintained on LB and kept at 4°C for storage. For long term storage, bacteria were frozen at -80 ^{o}C in 15 % glycerol. Bacterial strains used in this study are listed in Table 2.1.

2.2 Plasmid vectors

Plasmids used as vectors in this study are listed in Table 2.2.

2.3 Primers

Primers (Eurogentec) used in this study are listed in Table 2.3. For cloning purposes, sequences specifying a G.C clamp and one or more restriction enzyme sites were added to the 5' end.

2.4 Bacteriological techniques

2.4.1 Bacteriological media

All sterilised media were made fresh prior to use. Autoclaving time was mostly carried out for 15-20 min at 121 °C. After pouring plates, the agar was left to solidify and dried in a 42 °C incubator.

2.4.1.1 Lysogeny broth (LB) and agar

LB broth was prepared in 200 ml of pure water with the addition of 2 g of tryptone (Oxoid), 1 g of yeast extract (BD), 2 g of NaCl (Fisher Chemicals) and the addition of 3 g of agar (VWR Chemicals) for LB agar preparation and autoclaved.

2.4.1.2 Lennox agar

Lennox agar was prepared as for LB agar with half the amount of NaCl.

2.4.1.3 Minimal salts (M9-glucose) medium and agar

M9 broth was prepared in 180 ml of pure water with 1 g of anhydrous glucose (VWR Chemicals) and was autoclaved and cooled to ~ 50 °C. 20 ml of sterilised 10x M9 salts were then added to make up the volume to 200 ml with addition of 200 µl of filter sterilised 1 M $MgSO_4$ and 200 µl of filter sterilised 0.1 M $CaCl_2$ which were added after cooling. For M9-glucose agar preparation, an additional 3 g of agar were added prior to autoclaving.

Table 2.1 Bacterial strains used in this study

Bacterial strain	Genotype/description	Source/reference
Burkholderia cenocepacia		
715j	CF isolate, prototroph (Orb^+ Pch^+)	(Darling et al., 1998)
715jΔpobA	715j containing in-frame deletion within *pobA* gene (Orb^- Pch^-)	This study
715jΔpobAΔfptA	715jΔ*pobA* containing in-frame deletion in *fptA* gene (Orb^- Pch^-)	This study
AHA9	715j-*exbB1*::mini-Tn5CmlacZYA (Orb^-Pch^-)	(Asghar, 2003)
AHA27	715j-*pobA*::mini-Tn5CmlacZYA (Orb^-Pch^-)	(Asghar et al., 2011)
AHA27-BCAL0116::Tp	AHA27 containing Tp^R cassette inserted in BCAL0116 (Orb^-Pch^-)	(Sofoluwe and Thomas, unpublished)
AHA27-BCAL1345::Tp	AHA27 containing Tp^R cassette inserted in BCAL1345 (Orb^-Pch^-)	(Sofoluwe and Thomas, unpublished)
AHA27-BCAL1371::Tp	AHA27 containing Tp^R cassette inserted in BCAL1371 (Orb^-Pch^-)	(Sofoluwe and Thomas, unpublished)
AHA27-BCAL1709::Tp	AHA27 containing Tp^R cassette inserted in BCAL1709 (Orb^-Pch^-)	(Sofoluwe and Thomas, unpublished)
AHA27-BCAM0491::Tp	AHA27 containing Tp^R cassette inserted in BCAM0491 (Orb^-Pch^-)	Sofoluwe and Thomas, unpublished
AHA27-BCAM0499::Tp	AHA27 containing Tp^R cassette inserted in BCAM0499 (Orb^-Pch^-)	(Sofoluwe and Thomas, unpublished)
AHA27-BCAM1187::Tp	AHA27 containing Tp^R cassette inserted in BCAM1187 (Orb^-Pch^-)	(Sofoluwe and Thomas, unpublished)
AHA27-BCAM2439::Tp	AHA27 containing Tp^R cassette inserted in BCAM2439 (Orb^-Pch^-)	(Sofoluwe and Thomas, unpublished)
H111-orbS::Tp	H111 containing Tp^R cassette inserted within *orbS* gene (Orb^- Pch^+)	(Agnoli et al., 2019)
H111ΔorbS	H111 containing in-frame deletion within *orbS* gene (Orb^- Pch^+)	(Butt and Thomas, unpublished)
H111ΔfptAΔhuvA	H111 containing in-frame deletion within *huvA* and BCAM2224 gene locus	This study
H111Δfpt-orbA::TpTer	H111 containing in-frame deletion within *fptA* gene with Tp^R cassette inserted in *orbA* gene (Orb^-Pch^-)	This study
H111ΔhuvAΔfptA-orbA::TpTer	H111 containing in-frame deletion within *huvA* and *fptA* gene locus with Tp^R cassette inserted in *orbA* gene (Orb^-Pch^+)	This study

H111ΔpobA	H111 containing in-frame deletion within *pobA* gene (Orb^- Pch^-)	This study
H111ΔpobAΔfptA	H111ΔpobA containing in-frame deletion within *fptA* gene locus	This study
H111ΔpobAΔhuvA	H111ΔpobA containing in-frame deletion within BCAM2626 gene locus	This study
H111ΔpobA-BCAL0116::TpTer	H111ΔpobA containing Tp^R cassette inserted in BCAL0116 (Orb^-Pch^-)	This study
H111ΔpobA-orbA::TpTer	H111ΔpobA containing Tp^R cassette inserted in BCAL1700 (Orb^-Pch^-)	This study
H111ΔpobAΔBCAL0117	H111ΔpobA containing in-frame deletion within BCAL0117 gene locus	This study
H111ΔpobAΔBCAL2281	H111ΔpobA containing in-frame deletion within BCAL2281 gene locus (Orb^-Pch^-)	This study
H111ΔpobAΔBCAL2281-BCAL0116::TpTer	H111ΔpobAΔBCAL2281 containing Tp^R cassette inserted in BCAL0116 (Orb^-Pch^-)	This study
H111ΔpobAΔBCAM2007	H111ΔpobA containing in-frame deletion within BCAM2007 gene locus	This study
H111ΔpobA-BCAM1187::TpTer	H111ΔpobA containing Tp^R cassette inserted in BCAM1187 (Orb^-Pch^-)	This study
H111ΔpobA-BCAM0491::TpTer	H111ΔpobA containing Tp^R cassette inserted in BCAM0491 (Orb^-Pch^-)	This study
H111ΔpobAΔBCAM2007-BCAM1187::TpTer	H111ΔpobAΔBCAM2007 containing Tp^R cassette inserted in BCAL1187 (Orb^-Pch^-)	This study
H111ΔpobAΔBCAM2007-*orbA*::TpTer	H111ΔpobAΔBCAM2007 containing Tp^R cassette inserted in BCAL1700 (Orb^-Pch^-)	This study
H111ΔpobA-BCAL1709::TpTer	H111ΔpobA containing Tp^R cassette inserted in BCAL1709 (Orb^-Pch^-)	This study
H111ΔpobA-BCAM0491::TpTer-BCAL1345::Cm	H111ΔpobA containing Tp^R cassette inserted in BCAM0491 and Cm^R cassette inserted in BCAL1345 (Orb^-Pch^-)	This study
H111ΔpobA-BCAL1709::TpTer-BCAM0499::Cm	H111ΔpobA containing Tp^R cassette inserted in BCAL1709 and Cm^R cassette inserted in BCAM0499 (Orb^-Pch^-)	This study
H111ΔpobA-BCAL1371::TpTer	H111Δ*pobA* containing Tp^R cassette inserted in BCAL1371 and (Orb^-Pch^-)	(Aljadani, 2018)
H111ΔpobA-BCAL1371::TpTer-BCAM2439::Cm	H111Δ*pobA* containing Tp^R cassette inserted in BCAL1371 and Cm^R cassette inserted in BCAM2439 (Orb^-Pch^-)	(Aljadani, 2018)
H111ΔC3	H111 cured of chromosome 3 ($C3^-$ Orb^+ Pch^+)	(Agnoli et al., 2012)

H111ΔC3ΔpobA	H111ΔC3 containing in-frame deletion within *pobA* (Orb$^-$ Pch$^-$)	This study
H111ΔC3ΔpobAΔfptA	H111ΔC3ΔpobA containing in-frame deletion within *fptA* gene	This study
H111ΔC3ΔpobA-orbA::TpTer	H111ΔC3ΔpobA containing Tp^R cassette inserted in BCAL1700 (Orb$^-$Pch$^-$)	This study
H111ΔC3ΔpobA-BCAL1709::TpTer	H111 ΔC3ΔpobA containing Tp^R cassette inserted in BCAL1709 (Orb$^-$Pch$^-$)	This study
H111ΔC3ΔpobA-BCAL1371::TpTer	H111ΔC3ΔpobA containing Tp^R cassette inserted in BCAL1371 (Orb$^-$Pch$^-$)	This study
H111ΔC3ΔpobA-BCAL0499::Cm	H111ΔC3ΔpobA containing Cm^R cassette inserted in BCAM0499 (Orb$^-$Pch$^-$)	This study
H111ΔC3ΔpobA-BCAM2439::Cm	H111ΔC3ΔpobA containing Cm^R cassette inserted in BCAM2439 (Orb$^-$Pch$^-$)	This study
H111ΔC3ΔpobA -BCAL1709::TpTer-BCAM0499::Cm	H111ΔC3ΔpobA containing Tp^R cassette inserted in BCAL1709 and Cm^R cassette inserted in BCAM0499 (Orb$^-$Pch$^-$)	This study
Burkholderia thailandensis		
E264	Prototroph; environmental isolate (Mba$^+$ Pch$^+$)	(Brett et al., 1998)
E264 pchE:Tet	E264 containing *pchE*:Tet allele (Mba$^+$ Pch$^-$) Tet^R	(Franke et al., 2013)
E264 mbaB::Tet^a	E264 containing *mbaB*:Tet allele (Mba$^+$ Pch$^-$) Tet^R	(Franke et al., 2013)
E264 pchE::Km mbaB::Tet^a	E264 containing *pchE*::Km *mbaB*::Tet allele (Mba$^-$ Pch$^-$) Km^R Tet^R	(Franke et al., 2013)
Burkholderia ambifaria		
AMMD	Prototroph, rhizophere of pea isolate	(Coenye et al., 2001a)
Burkholderia phymatum		
STM815	Prototroph, root nodule isolate	(Vandamme et al., 2002)
STM815-*phmA*::Tp	STM815 containing *phmA*::Tp allele (Phm$^-$)	This study
Burkholderia terrae		
BS001	Prototroph, sandy soil isolate underneath fungal fruiting bodies	(Nazir et al., 2012)
BS001-*phmA*::Tp	BS001 containing *phmA*::Tp allele (Phm$^-$)	This study
Pseudomonas aeruginosa		
PAO1	Prototroph, wildtype isolate (PvdI$^+$ Pch$^+$)	(Stover et al., 2000)
PAO1 pch$^-$ pvd$^-$	PAO1 containing deletion of entire *pch* gene cluster (PvdI$^-$ Pch$^-$)	(Ankenbauer et al., 1985)
PAO1Δpch	PAO1 containing deletion of entire *pch* gene cluster (PvdI$^+$ Pch$^-$)	(Ankenbauer et al., 1988)

W15 Dec8	Prototroph, wildtype isolate (PvdII$^+$ Pch$^+$)	(Meyer, unpublished)
W15Aug24	Prototroph, wildtype isolate (PvdIII$^+$ Pch$^+$)	(Pirnay et al., 2005)
Pseudomonas fluorescens		
ATCC 17400	Prototroph, environmental isolate	(Gaballa et al., 1996)
5F1	ATCC 17400 containing Tn5 insertion in *pvd* locus (Pvd$^-$, Qbn$^-$ tQbn$^+$)	(Barry and Challis, 2009)
ATCC17571	wildtype isolate (PflW$^+$ Pch$^+$)	(Elomari et al., 1996)
LMG 5848-pvd::TnModOTc #1	*P. fluorescens* containing TnModOTc insertion in *pvd* locus (Pvd$^-$, Ocn+)	(Meyer, unpublished)
Pseudomonas protegens		
Pf-5 ΔpvdD	Pf-5 containing partial deletion of *pvdD* gene (Pvd$^-$ ePch$^+$)	(Cornelis, unpublished)
Pf-5 ΔpchEF	Pf-5 containing deletion of *pchEF* genes (Pvd$^-$ ePch$^+$)	(Cornelis, unpublished)
Pseudomonas chlororaphis		
ATCC17813 1D1	*P. chlororaphis* ATCC17813 containing Tn5 insertion in pvd locus (Km^R) (Pvd$^-$ Pdm$^+$)	(Cornelis, unpublished)
Escherichia coli		
JM83	F$^-$ *ara* Δ(*lac-proAB*) *rpsL* (Sm^R) *ϕ80dlacZ* Δ*M15*	(Yanisch-Perron et al., 1985)
SM10 (λpir)	*thi-1 thr leu tonA lacY supE recA RP4-2-Tc::Mu* λpir Km^R	(Simon et al., 1983)
CC118 (λpir)	*araD139 Δ(ara-leu)7697 ΔlacX74 galE galK phoA20 thi-1 rpsE rpoB* (Rf^R) a*rgE*(*am*) *recA*l λpir	(Herrero et al., 1990)
S17-1 (λpir)	*recA, thi, pro, hsdR$^-$M$^+$RP4:* 2-Tc:Mu: Km Tn7 λpir Tp^R Sm^R	(Simon et al., 1983)
AN90	K-12 without *thi leuB proC trpE lacY mtl xyl rpsL azi fhuA tsx supA recA thi entD*	(Cox et al., 1970)
MC1061	*hsdR araD139* Δ(*ara-leu*)*7697 ΔlacX74 galU galK rpsL* (Sm^R)	(Casadaban and Cohen, 1980)
WW3352	F$^-$ *leu$^-$47 lac-3350 galK2 galT22 (tonB-trp)39 rpsL179* (Sm^R) *IN*(rrnD-rrnE)1	*E. coli* Genetic Stock Centre (5390)
ED8659	*trpAC9 supE supF hsdR$^-$*M$^+$S$^+$ *met trpR tonB*	(Borck et al., 1976)
JC28	W3110, Δ*fecABCD*E, Δ*zupT*, Δ*mntH*, Δ*entC*, Δ*feoABC*	(Cao et al., 2007)
GM48	F$^-$ *thr leu thi lacY galK galT ara fhuA tsx dam dcm glnV44*	(Marinus, 1973)
Serratia marcescens Db10	Drosophila flies isolate, non-pigmented	(Flyg et al., 1980)
Cupriavidus metallidurans 31A	Metal factory isolate	(Schmidt et al., 1991)
Bacillus subtilis 168	Tryptophan-requiring auxotroph	(Zeigler et al., 2008)
Bacillus megaterium	Wildtype. Schizokinen producer	(Thomas, unpublished)

Acinetobacter baylyi ADP1	Unencapsulated mutant derived from soil isolate	(Vaneechoutte et al., 2006)

[a]These mutants were designated as mbaA in the paper (Franke et al., 2013), but in fact they are mbaB mutants.

Abbreviations used: Rf^R, rifampicin resistant; Sm^R, streptomycin resistant; Tp^R, trimethoprim resistant; Tet^R, tetracycline resistant; Km^R, kanamycin resistant; Gm^R, gentamycin resistant; Pch, pyochelin phenotype; Orb, ornibactin phenotype; Pvd, pyoverdine phenotype; Mba, malleobactin phenotype; Pdm, pseudomonine phenotype; ePch, enantio-pyochelin phenotype; Ocn, ornicorrugatin phenotype; PflW, pyoverdine unique to ATCC17571; Qbn, quinolobactin phenotype; tQbn, thioquinolobactin phenotype and Phm, phymabactin phenotype.

Table 2.2 Plasmids used in this study

Plasmid	Description	Source/reference
Vectors		
pEX18Tp-*pheS*	Gene replacement vector based on counter selection *phe*S (Tp^R)	(Barrett et al., 2008)
pEX18TpTer-*pheS*	Gene replacement vector based on *phe*S rrnBT1T2 (Tp^R)	(Spiewak, 2015)
pEXTpTer-*pheS*-Cm-SceI	pEX18TpTer-pheS derivative containing *cat* gene and *I-SceI* recognition site (Tp^R, Cm^R)	(Spiewak, 2015)
pBBR1MCS	Mobilisable BHR cloning vector $IncP^-$ and ColE1-compatible, *lacZα* MCS (Cm^R)	(Agnoli et al., 2012)
pBBR1MCS-2	Mobilisable BHR cloning vector $IncP^-$ and ColE1-compatible (Km^R)	(Huber et al., 2001)
pBluescriptII KS (+)	General *E. coli* loning vector, ColE1-derived phagemid, *lacZα* MCS (Amp^R)	(Alting-Mees and Short, 1989)
pSRKKm	pBBR1MCS-2 derivative; with a P_{lac} promoter, *lacIq*,*lacZa*$^+$Δ*lacZ*α (Km^R)	(Khan et al., 2008)
pSHAFT2	Mobilisable suicide vector derived from pUT, oriR6K (Amp^R Cm^R)	(Shastri et al., 2017)
pDAI-SceI-*pheS*	Cloning vector based on *pheS* and *I-SceI* endonuclease (Tet^R)	(Fazli et al., 2015)
pDAI-SceI-*pheS*-Kmfor	Cloning vector based on *pheS* and *I-Sce* (Tet^R, Km^R)	(Butt and Thomas, unpublished)
p34E-TpTer	p34E derivative containing TpTer StuI fragment of pUC19-TpTer at *Eco*RI site (Amp^R, Tp^R)	(Shastri, 2011)
p34E-Cm2	p34E derivative containing *cat* gene with synthetic promoter at *Eco*RI site. (Amp^R, Cm^R)	(Shastri, 2011)
Vector derivatives		
pEX18Tp-*pheS*-*pobA*	pEX18Tp-*pheS* containing *B. cenocepacia pobA* gene	(Sofoluwe and Thomas, unpublished)
pEX18Tp-*pheS*-Δ*pobA*	pEX18Tp-*pheS*-*pobA* with in-frame deletion within *pobA* gene	(Sofoluwe and Thomas, unpublished)
pEX18TpTer-*pheS*-Δ*pobA*	pEX18TpTer-*pheS* containing ΔpobA DNA fragment from pEX18Tp-*pheS*-Δ*pobA*	This study
pEX18TpTer-*pheS*-*fptA*	pEX18TpTer-pheS containing entire *B. cenocepacia fptA* gene	This study
pEX18TpTer-*pheS*-Δ*fptA*	pEX18TpTer-*pheS* containing in-frame deletion within *fptA* gene	This study
pEX18TpTer-*pheS*-BCAL2281	pEX18TpTer-pheS-BCAL2281 containing *B. cenocepacia* BCAL2281 gene	This study
pEX18TpTer-*pheS*-ΔBCAL2281	pEX18TpTer-*pheS* containing in-frame deletion within BCAL2281 gene	This study
pEX18TpTer-*pheS*-Cm-SceI-*huvA*	pEX18TpTer-*pheS*-Cm-*SceI* containing *B. cenocepacia huvA* gene	This study
pEX18TpTer-*pheS*-Cm-SceI-Δ*huvA*	pEX18TpTer-*pheS*-Cm-*SceI*-*huvA* containing in-frame deletion within *huvA*	This study

pEX18TpTer-*pheS*-Cm-SceI-BCAL0117	pEX18TpTer-*pheS*-Cm-SceI containing *B. cenocepacia* BCAL0117 gene	This study
pEX18TpTer-pheS-Cm-SceI-ΔBCAL0117	pEX18TpTer-*pheS*-Cm-SceI-BCAL0117 containing in-frame deletion within BCAL0117 gene	This study
pEX18TpTer-*pheS*-Cm-SceI-ΔBCAM2007	pEX18TpTer-*pheS*-Cm-SceI containing the BCAM2007 gene with an in-frame deletion	This study
pBBR1-*fptA*	pBBR1MCS carrying *B. cenocepacia fptA* gene	This study
pBBR1-*orbA*	pBBR1MCS carrying a segment of the *B. cenocepacia* BCAL1700 gene	This study
pBBR1-*orbA*::TpTer	pBBR1-BCAL1700 with TpTer cassette inserted in *Bam*HI site of *orbA*	This study
pBBR2-BCAM2626	pBBR1-2 carrying *B. cenocepacia* BCAM2626 gene	This study
pBBR2-ΔBCAM2626	pBBR2-BCAM2626 containing in-frame deletion within BCAM2626 gene	This study
pSHAFT2-o*rbA*::TpTer	pSHAFT2-BCAL1700 with TpTer cassette inserted in *Bam*HI site of *orbA*	This study
pSHAFT2-OM13	pSHAFT2 containing *orbI*::mini-Tn5Tp	((Tyrrell et al., 2015)
pSHAFTGFP-BCAL1371::TpTer	pSHAFTGFP-BCAL1371 with TpTer cassette inserted in BCAL1371	(Sofoluwe and Thomas, unpublished)
pSHAFTGFP-BCAM1187::TpTer	pSHAFTGFP-BCAM1187 with TpTer cassette inserted in BCAM1187	(Sofoluwe and Thomas, unpublished)
pSHAFTGFP-BCAL0116::TpTer	pSHAFTGFP-BCAL0116 with TpTer cassette inserted in BCAL0116	(Sofoluwe and Thomas, unpublished)
pSHAFTGFP-BCAL1709::TpTer	pSHAFTGFP-BCAL1709 with TpTer cassette inserted in BCAL1709	(Sofoluwe and Thomas, unpublished)
pSHAFTGFP-BCAM0491::TpTer	pSHAFTGFP-BCAM0491 with TpTer cassette inserted in BCAM0491	(Sofoluwe and Thomas, unpublished)
pSHAFTGFP-BCAM0499	pSHAFTGFP containing a whole of the BCAM0499 gene	(Sofoluwe and Thomas, unpublished)
pSHAFTGFP-BCAM0499::Cm	pSHAFTGFP-BCAM0499 with Cm^R cassette inserted in BCAM0499	This study
pSHAFTGFP-BCAM2439::Cm	pSHAFTGFP-BCAM2439 with Cm^R cassette inserted in BCAM2439	(Aljadani, 2018)
pSHAFTGFP-BCAL1345	pSHAFTGFP containing a whole of the BCAL1345 gene	(Sofoluwe and Thomas, unpublished)
pSHAFTGFP-BCAL1345::Cm	pSHAFTGFP-BCAL1345 with Cm^R cassette inserted in BCAL1345	This study
pBBR-BCAM2626	pBBR1MCS carrying the entire BCAM2626	This study
pBBR1-BCAM2007	pBBR1MCS carrying the entire BCAM2007	This study
pSRKKm-*fmtA*	pSRKKm carrying the entire BTHI_I2415	This study
pSRKKm-BCAL0116	pSRKKm carrying the entire BCAL0116	This study
pSRKKm-*orbA*	pSRKKm carrying the entire BCAL1700	This study
pSRKKm-BCAL2281	pSRKKm carrying the entire BCAL2281	This study
pSRKKm-BCAL0117	pSRKKm carrying the entire BCAL0117 *B*	This study

Abbreviations used within this table: Amp^R, encodes ampicillin resistance; Cm^R, encodes chloramphenicol resistance; Km^R, encodes kanamycin resistance; Tp^R, encodes trimethoprim resistance; Tet^R, encodes tetracycline.

Table 2.3 Oligonucleotides used in this study

Primer	Oligonucleotide[a] (5' → 3')	Restriction sites present
BCAL0116forfull	gcgcggatccg**TAA**ccttgtacgcggcatggaat	*Bam*HI
BCAL0116revfull	gcgcaagcttgggaaaatcccgaggccatt	*Hin*dIII
BCAL0117for	gcgcggatccg**TAA** gcgcggtgctcgacatcaaa	*Bam*HI
BCAL0117for2	gcgcggatccgcgagtaaaaatgcgagtaag	*Bam*HI
BCAL0117rev2	gcgcgtcgacacttgccccgcggtcc**TTA**t	*Sal*I
BCAL0117rev3	gcgcgaattcatcgagaaattgctggagaa	*Eco*RI
BCAL1700for	gcgcggtaccaagcttagatctatcatcgacgtgcacaccaa	*Bgl*II, *Hin*dIII, *Kpn*I
BCAL1700rev	gcgctctagacatggatgcgtcgtggaaaa	*Xba*I
BCAL1700fullfor	gcgctctagag**TAA**gtcgctcgaaaacgggatcg	*Xba*I
BCAL1700fullrev	gcgcaagcttcatggatgcgtcgtggaaaa	*Hin*dIII
BCAL2281for	gcgcaagcttgttccttttgaagagtgcgg	*Hin*dIII
BCAL2281rev	gcgcggtacctccgttcttcacgcaactga	*Kpn*I
BCAM2007for	gcgctctagacggcagcatcaacctgatca	*Xba*I
BCAM2007rev	gcgccaattgaacacctgccactgcttcgt	*Mfe*I
BCAM2007full3for	gcgcggtaccg**TAA**ataattcccgccggcgtgca	*Acc*65I, *Kpn*I
BCAM2007full4rev	gcgcctctagacttcagcgatacggcctcca	*Xba*I
BCAM2007SOEfor	gcgcgaattctacagcgtctcgacgttctg	*Eco*R1
BCAM2007SOErev	gcgcaagcttcagccgcgcatagttgaact	*Hin*dIII
BCAM2224for	gcgcctcgagaagcttcgggaacctgagagatcgat	*Hin*dIII, *Xho*I,
BCAM2224rev	gcgctctagaagccggacgccatcagaatt	*Xba*I
BTHI2415for2	gcgctctagag**TAA**ccgctttgcaacttggagca	*Xba*I
BTHI2415rev	gcgcaagcttccgcccatgggatgatgaaa	*Hin*dIII
HuvAfor	gcgcggtacccgtctggcgtccttgtattg	*Kpn*I
HuvArev	gcgctctagatcctcgaacatcgccggaaa	*Xba*I
BCAM2007SOEmutfor	tgaagctcggcaagttcaccaagagcgaactgcgcgacaa	-
BCAM2007SOEmutrev	ttgtcgcgcagttcgctcttggtgaacttgccgagcttca	-
M13for	gtaaaacgacggccagt	-
M13for (-20)	tgtaaaacgacggccagt	-
M13for2	aaggcgattaagttgggt	-
M13BACTHrev	gtgtggaattgtgagcggat	-
M13rev	caggaaacagctatgac	-
pEX18Tpfor	gaagccagttaccttcgga	-
pEX18Tprev	ttgtcggtgaacgctctcct	-
pUTcatrev	aacggttgtggacaacaagc	-
catendout	gatgtgtgataacatactga	-
GFPstartout	attatttctacaggggaagg	-
FlrAforout	tccgatcatggcttccatcc	-
FlrArevout	cgcagcatgtccttgcgata	-
HuvAforout	gtttctcgagacttcccccg	-
HuvArevout	cttttcgtggacggccgtgt	-
HuvAmidfor	taacctgaaaagctggcgca	-
mbaBscrnfor	cggcgatcatttcttcgaac	-
mbaBscrnrev	cgacacgatgtgatgaacga	-
OrbIfor	gaccgatacgatgctgaagc	-
OrbIrev	cagatgcgcatgaatccgct	-
pchEscrnfor	gccctcgaacgacctataca	-
pchEscrnrev	gtcgcaccacaattcgatcc	-
pobAfor4	gcgccatcgaacgtgcatgt	-
pobArev3	gaatgcggcgtgacgaccaa	-

BCAL0116forout	gttctcgacgaccatcgtca	-
BCAL0116revout	gttcgctgcgttcgcgtatt	-
BCAL0116midpsrkfor	gacgtacaacgacggcaaca	-
BCAL0116midpsrkrev	tagacatcgttcacgcggct	-
BCAL0117forout	tgcgcggccgtgatgttgag	-
BCAL0117revout	gtcgatgccgtcgcacgctt	-
BCAL0117midfor	taacctgaaaagctggcgca	-
BCAL1187forout	catggaaagcggtgttgcac	-
BCAL1187revout	ccgaatccgacacgagatag	-
BCAL1345forout	gatcacgtttccgttcgaca	-
BCAL1345revout	gtctggttgaatgcgtcgta	-
BCAL1700forout	gtcgatccgtacatgatcga	-
BCAL1700revout	cgactggatgtagacgagat	-
BCAL1709forout	cggaaaacttcggacatgtg	-
BCAL1709revout	gcgaggtcagaacttgtatg	-
BCAL2281forout2	caggatcagcgcaaaggcga	-
BCAL2281revout	ggtgtgcgtgtactacatcg	-
BCAL2281psrkfor2	ccgacgtgctcgacaacgat	-
BCAL2281psrkrev2	ttcgtcgccggatcggtgta	-
BCAM0491forout	gtcgaccacatcgacgtgtt	-
BCAM0491revout	gaagcgccagcttatccaca	-
BCAM0499forout	cgttcacgatgaaactccac	-
BCAM0499revout	ttgacgttcgacgacgtgta	-
BCAM2007for2out	gagatcaccaagggttccga	-
BCAM2007revout	gcgcagttcgctcttcatgt	-
BCAM2224outfor	gcgtgaatgcggtacgaggt	-
BCAM2224outrev	gtaatgacgggccagcgtga	-
BCAM2224pBBfor2	tacgaggatcgccacttctt	-
BCAM2224pBBrev2	ttcacgtagtagcagctcgg	-
BCAM2439forout	tcgatccaaccgtcggctat	-
BCAM2439revout	gcgcttgtcgatctggtaca	-
Midpsrk1700for	aacacgatcaacctcgcgag	-
Midpsrk1700rev	caatcgccactacatcagcg	-

[a]Restriction sites used for cloning are underlined.
Stops codon for *lacZ* promoter are written in bold CAPITAL letters.

M9 salts solution (10X)

M9 salts (10X) consisted of: 60 g Na_2HPO_4 (anhydrous), 30 g KH_2PO_4 (anhydrous), 5 g NaCl and 10 g NH_4Cl dissolved in 1000 ml pure water and autoclaved.

2.4.1.3.1 Minimal salts-casamino acids ((M9-glucose (CAA)) medium and agar

M9-glucose-CAA agar was made up the same way as M9-glucose medium but 0.2 g (0.1 %) of CAA were added along with 1 g glucose. CAA was either added from a sterile stock solution or added and autoclaved with the agar.

For transformation of *E. coli* cells with pEX18Tp-*pheS* derivatives, glucose was omitted, and 1 ml of 50% glycerol (final concentration of 0.5%), 50 µl of 1% freshly prepared thiamine (final concentration of 0.0005%), 200 µl of 20 mg ml^{-1} X-gal (final concentration of 40 µg ml^{-1}), 10 µl of 1 M IPTG (final concentration of 100 µM) and 100 µl of 25mg ml^{-1} trimethroprim in DMSO (final concentration 25 µg ml^{-1}) were added to the medium after autoclaving and cooling. This medium helps to select pEX18Tp-*pheS* and pEX18TpTer transformants at 30 ^{o}C and is not a standard transformation medium.

M9-glucose-CAA medium was also used to stimulate production of siderophores in *B. cenocepacia* mutant strains, in which case filtered casamino acid solution was added to M9-glucose liquid medium to make a final concentration of 0.1%.

2.4.1.3.2 Minimal salts-chlorophenylalanine ((M9-glucose (cPhe)) agar

M9-glucose agar with a final concentration of 0.1 % chlorophenylalanine (cPhe) was prepared by adding 1 g glucose and 200 mg cPhe (Acros Organics) to 180 ml pure water. This was shaken on an orbital shaker for ~2 hours for the cPhe to completely dissolve. 3 g of highly purified agar (Oxoid) was then added and the solution was autoclaved for 15 to 20 min. Upon cooling, 20 ml of 10x M9 salts was added; with 200 µl of 1 M filter sterilised $MgSO_4$ and 200 µl of 0.1 M of filter sterilised $CaCl_2$.

2.4.1.4 Iso–Sensitest (IST) broth and agar

For preparation of 100 ml broth, 2.34 g of IST powder (Oxoid) was added to 100 ml of pure water and autoclaved. An additional 1.5 g of agar was added prior to autoclaving for IST agar preparation.

2.4.1.5 Chrome azurol S (CAS) agar

CAS agar was prepared with a mixture of 90 ml Y minimal agar and 10 ml of CAS mix (see below), which were prepared and autoclaved separately (Schwyn and Neilands, 1987). Following cooling to ~45 °C, the mixtures were mixed slowly and swirled until homogenous.

Y minimal agar

The agar was prepared by dissolving of 0.169 g of sodium glutamate (Sigma), 0.3 g Tris base (Fisher Scientific), 0.1 ml of $MgSO_4.7H_2O$ (10 % w/v), 0.1 ml of $CaCl_2.6H_2O$ (22 % w/v) and 0.1 ml of $K_2HPO_4.3H_2O$ (22 % w/v) in 50 ml pure water. The pH was adjusted to 6.8 and 1.5 g agar were then added to the medium prior to autoclaving.

CAS mix

To prepare 100 ml CAS mix, 10 ml of 1 mM $FeCl_3.6H_2O$ (dissolved in dH_2O) and 60.5 mg of CAS powder were dissolved in 50 ml of pure water giving a final volume of 60 ml. 72.9 mg of hexadecyltrimethylammonium bromide (HDTMA) was dissolved in 40 ml pure water and both solutions were mixed with constant stirring giving a total of 100 ml CAS mix solution. This dark purple solution was autoclaved and stored at room temperature in the dark. Mixing 10 ml of this solution with 90 ml Y minimal agar would give a final concentration of 10 µM $FeCl_3$. To prepare CAS agar with high iron content, 10 ml of 6 mM $FeCl_3.6H_2O$ (dissolved in 10 mM HCl) were used making a 60 µM $FeCl_3$ deep blue CAS mix solution.

2.4.1.6 King's B broth and agar

For 400 ml of King's B medium preparation, 8 g of proteose peptone were mixed with 4 ml glycerol in 396 ml water on a magnetic stirrer and adjusted to pH 7.2. The 400 ml mixure were then autoclaved. 6 g of agar powder were added for agar preparation.

2.4.1.6.1 Modified Kings B (MKB) broth and agar

MKB medium was used for initiation of siderophore production in *Pseudomonas* spp. For 400 ml of MKB broth preparation, 2 g of proteose peptone, 2.4 ml of 1 M $MgSO_4.7H_2O$, 2 ml of 1 M K_2HPO_4 and 800 ul of glycerol were added to 400 ml pure water and the pH was adjusted to 7.2. The mixture was then autoclaved. 6 g of agar powder was added for MKB agar preparation.

2.4.1.7 Casamino acids liquid media

Casamino acids medium was used for initiation of siderophore production in *Pseudomonas* spp. Casamino acids liquid medium was prepared by dissolving 0.5 g casamino acids to 100 ml pure water. After autoclaving and cooling, 500 µl of filter sterilised 1 M K_2HPO_4 and 100 µl of 1M $MgSO_4.7H_2O$ were added.

2.4.1.8 R2A broth and agar

R2A medium was used for maintenance of the *Burkholderia* spp., *B. phymatum* and *B. terrae*. For 1 litre of R2A broth, 0.5 g of each yeast extract, proteose peptone no. 3, casamino acids, glucose, starch and sodium pyruvate with 0.3 g of dipotassium phosphate and 0.05 g of magnesium sulphate were dissolved in 1 litre pure water and autoclaved. 15 g of agar powder was added for R2A agar preparation.

2.4.2 Media supplements/solutions preparation

Stock solutions of media supplements were made up as described below. They were incorporated into media after autoclaving and cooling. Solutions prepared were used in selected experiments.

2,2'-bipyridyl

2,2'-bipyridyl was dissolved in absolute ethanol to 0.1 M and stored at –20 °C.

5-bromo-4-chloro-3-indolyl-β-D-galactoside (X-gal)

X-gal was dissolved to 20 mg ml^{-1} in DMSO, and stored at –20 °C.

Casamino acids (CAA)

Stock solution of casamino acids (10 %) was prepared by addition of 2 g casamino acids (Difco) to 20 ml pure water and filter-sterilised.

Diethylenetriamine pentaacetic acid (DTPA)

A 19.7 mg of DTPA were dissolved in 170 µl of 1 M NaOH and was made up to 5 ml solution with pure water. The pH of the solution (0.01 M) was checked and filter-sterilised.

Ethylenediaminedi (o-hydroxyphenylacetic) acid (EDDHA)

Stock solution of 0.1 M EDDHA (Sigma) was prepared by dissolving 180 mg of EDDHA in 5 ml of 1 M NaOH. This was filter sterilised and stored at 4 ˚C.

$FeCl_3$

$FeCl_3$ was dissolved in 10 mM HCl to a concentration of 0.1 M. It was then filter sterilised and stored at room temperature in the dark.

Glycerol solution

Glycerol was added to pure water to a final concentration of 50 % and autoclaved.

Haemin solution

Haemin was dissolved in 0.1 M NaOH at a final concentration of 10 mg ml^{-1} and stored at 4 ˚C.

Isopropyl β-D-thiogalactoside (IPTG)

1 M IPTG (Melford) was prepared by dissolving 2.38 g IPTG in 10 ml of pure water, and was filter sterilised and stored at –20 °C.

Sodium hydroxide (NaOH)

Stock solution of 0.1 M NaOH was prepared by dissolving 0.4 g of NaOH in 100 ml pure water.

TAE buffer (50x)

For preparation of 50x TAE buffer, 242 g of Tris base were mixed with 57.1 ml of glacial acetic acid and 37.2 g of disodium EDTA dihydrate in water. The pH was adjusted to 8.0 and the final volume adjusted to 1 litre. For 1x TAE buffer preparation, 20 ml of 50x TAE buffer were made up to 1 L with ultrapure water.

Tris-EDTA (TE) buffer

Tris-EDTA (TE) buffer was prepared by mixing 10 ml of 1 M Tris-HCl (pH 7.5), 2 ml of 500 mM EDTA (pH 8.0) and 88 ml of ultrapure H_2O.

Antibiotics stocks

Final concentration of antibiotic used was as below unless otherwise stated.

Table 2.4 Antibiotics used for bacterial selection

			E. coli	*B. cenocepacia*
Antibiotic	**Stock concentration**	**Solvent**	**Final concentration**	
Ampicillin (Amp)	100 mg ml^{-1}	pure water	100 µg ml^{-1}	N/A
Tetracycline (Tn)	10 mg ml^{-1}	50 % ethanol	10 µg ml^{-1}	125 µg ml^{-1}
Streptomycin (Sm)	75 mg ml^{-1}	pure water	75 µg ml^{-1}	N/A
Kanamycin (Km)	50 mg ml^{-1}	pure water	25 µg ml^{-1}	50 µg ml^{-1}
Trimethoprim (Tp)	25 mg ml^{-1}	DMSO	25 µg ml^{-1}	25 µg ml^{-1}
Chloramphenicol	25 mg ml^{-1}	100 % ethanol	25 µg ml^{-1}	50 µg ml^{-1}

2.4.3 Maintenance of bacterial strains

Burkholderia strains were maintained in long term storage at – 80 °C as 50 % glycerol stocks and in short term 1-2 months storage at room temperature on M9-glucose agar plates. *Burkholderia* strains maintained on M9-glucose (CAA) were stored for less than 1 month. Agar plates were sealed with Parafilm for storage and were restreaked periodically for healthy cell maintenance. Other bacterial strains used in this study were maintained in long term storage at – 80 °C as glycerol stocks and in short term 1-2 months storage at 4 °C on LB agar plates.

2.4.3.1 Glycerol stocks

Bacteria harbouring plasmids were cultured in media containing the appropriate antibiotic for plasmid maintenance. The overnight cultures (700 µl) were aliquoted in cryovials and mixed with 300 µl of sterile 50 % glycerol solution to give a final concentration of ~15% glycerol. Alternatively, several loopful of pure bacterial colonies from an agar plate culture were transferred into a 700 of µl sterile medium and vortexed prior to the addition of 300 µl sterile 50 % glycerol solution. The cryovials were vortexed several times for homogenous mixing. The mixture was then stored frozen at -80 °C.

2.4.4: Techniques for plasmid DNA transfer

2.4.4.1 Transformation of *E. coli* cells

2.4.4.1.1 Preparation of competent cells for transformation: Hanahan's method

The method of Hanahan et al (1995) was used to transform *E. coli* cells with plasmid DNA. A single isolated colony of the *E. coli* strain was inoculated in 2 ml LB broth with appropriate antibiotics and was incubated at 37 °C overnight with shaking. 500 µl of the overnight culture were then transferred into 50 ml LB broth in a 250 ml flask. The culture was incubated at 37 °C with shaking for 2 hr to allow the *E. coli* to enter into log phase (optical density (OD_{600}) of 0.3 – 0.6). An OD_{600} of 0.5 is the optimum value. After 2 hr, the culture was chilled on ice for 15 min to prevent further growth and was then centrifuged at 4000 rpm for 10 min at 4 °C in a refrigerated bench top centrifuge (Beckman Coulter). The supernatant was discarded and the cell pellet was then resuspended by gentle pipetting in 16 ml of cold RF1 solution and was left on ice for 30 min. The solution was centrifuged again at 4000 rpm for 10 min at 4 °C and the resulting cell pellet was resuspended in 4 ml RF2. 300 µl aliquots were transferred to 1.5 ml microcentrifuge tubes and immediately stored frozen at -80 °C.

RF1 solution

RF1 solution preparation involved dissolving 7.46 g KCl, 9.90 g $MnCl_2.4H_2O$, 2.94 g potassium acetate, 1.50 g $CaCl_2.2H_2O$ and 150 ml glycerol in 750 ml of pure water. The resultant solution was adjusted to pH 5.8 using 0.2 M acetic acid and made up to 1 L with pure water. The solution was filter sterilised through a 0.22 µm membrane and stored at 4 ˚C.

RF2 solution

RF2 solution comprised of a mixture of 0.2 ml solution A and 9.8 ml of solution B and was freshly mixed prior to use. Solution A consisted of 0.5 M MOPS (pH 6.8) while solution B consisted of 10 mM KCl, 75 mM $CaCl_2.2H_2O$ and 15% glycerol. Both solution A and B were made up to 1L in pure water, was filter-sterilised and stored at 4 °C.

2.4.4.1.2 Transformation of *E. coli* strains with plasmid DNA

Competent cells were thawed from -80 °C storage and chilled on ice. Competent cells (100 µl) were added to 0.5-1 µl of plasmid DNA and chilled on ice for 30 min, during which time the mixture was agitated with an occasional flick. A cell control without DNA was also prepared. After 30 min, the mixtures were heat shocked at 42 °C for 2.5 min to allow transformation of plasmid DNA and chilled again on ice for 5 min.

1 ml of a suitable medium for the cells was then added and incubated for 1 hr at 37 °C or at any temperature suitable for the specific cells to allow expression of the antibiotic resistance genes carried by the plasmid. After 1 hr incubation, 100 ul of the culture were pipetted on a selective medium agar plate with appropriate antibiotics and incubated at 30 °or 37 °C overnight. The remainder of the culture was kept at 4 °C for storage or otherwise discarded. For ligation purposes, 5-15 µl of ligation products were added to competent cells.

2.4.4.2 Conjugation of plasmid DNA into *B. cenocepacia*

The plasmid DNA was initially transformed into the *E. coli* donor strain and purified on a selective medium. The donor strain harbouring the plasmid with an origin of transfer (*oriT*) was then inoculated and cultured overnight in 4 ml broth medium at 37 °C. The *B. cenocepacia* recipient strains were also grown overnight at 37 °C in 4 ml LB. The following day, the cultures were transferred into a 1 ml microcentrifuge tube and were centrifuged at 13,000 rpm for 5 min. The supernatants were discarded and the pellets were resuspended in 100 µl of 0.85 % sterile saline. Conjugation was performed on an LB agar plate overlaid with a 0.45 µm nitrocellulose membrane filter (Millipore).

Both 25 µl of donor strain in sterile saline and 25 µl of recipient strain in sterile saline were pipetted and spread onto the same membrane using a sterile pipette tip. Control plates consisted of mixtures of sterile saline and either donor or recipient strains. Conjugation plates were inverted and incubated at 37 °C for 8-16 hrs. The following day, the nitrocellulose filter from each plate was transferred with sterile forceps into 3 ml of sterile saline in universal tubes and was vortexed to resuspend the cells. For allelic replacement approaches, the undiluted bacterial suspensions (100 µl) were pipetted onto M9-glucose agar plates supplemented with appropriate antibiotics and were spread with an alcohol-flamed glass spreader. Diluted bacterial suspensions were used for introducing complementation plasmids into *Burkholderia* cells. Plates were then incubated at 37 °C for ~42 hr.

2.4.4.3 Chromosomal mutagenesis of *B. cenocepacia*

Chromosomal mutagenesis in this study was carried out using two approaches, either the generation of unmarked mutants or antibiotic-resistance cassette marked mutants. For the generation of the former, the pEX18 derivatives: pEX18TpTer-*pheS,* pEX18TpTer-*pheS*-SceI and pEX18TpTer-*pheS*-Cm-SceI were used. For the generation of marked-mutants, pSHAFT2 and pSHAFT-GFP plasmids were used. Plasmids were introduced into *Burkholderia* spp. as described in Section 2.4.5.2 and selection of exconjugants and subsequent screening for mutants is described in the results chapter.

2.5: Techniques for DNA purification and analysis

2.5.1: PCR techniques

For DNA amplification purposes prior to cloning, a high-fidelity proof reading DNA polymerase was used, either KOD Hot Start polymerase or Q5 High-fidelity DNA polymerase. If diagnostic PCR was to be carried out, DreamTaq or GoTaq were used. DMSO was included in the PCR reaction for *B. cenocepacia* template having GC rich DNA to increase primer specificity and to improve amplification. DNA polymerase was added last and reagents were kept on ice to prevent premature extension. Templates were either from bacterial cells obtained colony picking or bacterial cell lysate prepared by boiling a colony suspended in the buffer for 10 minutes. Colony picking was usually used for diagnostic PCR when screening recombinants or newly constructed plasmid clones.

PCR components included DNA polymerase enzyme, Mg^{2+} ions, dNTPs, forward and reverse primers, high GC enhancers or DMSO, DNA template and nuclease-free water at amounts according to the manufacturer's instructions (Promega/NEB). Table 2.5 shows the components added to a 0.5 ml PCR tube for one reaction using GoTaq G2 Flexi DNA polymerase.

Table 2.5 Components for GoTaq G2 Flexi DNA polymerase

Reagents	Volume added per reaction (µl)	Final Concentration
5x buffer	5	1x
$MgCl_2$ (25.0 mM)	2	1.0 – 4.0 mM
dNTP Mix[a]	0.5	0.2 mM of each dNTP
10 µM forward primer	1.5	0.1-1.0 µM
10 µM reverse primer	1.5	0.1-1.0 µM
TAQ DNA polymerase (Promega)	0.125	1.25 U
H_2O	13.125	-
DMSO	1.25	-
DNA template	colony	<0.5 µG/50 µl
Total	25	-

[a]dNTP Mix contains the sodium salts of dATP, dCTP, dGTP and dTTP, each at a concentration of 0.2 mM in water. The total concentration of nucleotides is 10 mM.

2.5.1.1 PCR regime

Most PCRs were performed using a T100 Thermo Cycler (Biorad) according to the following PCR Regime.

Initial denaturation (95 °C)	4 minutes	
Denaturation (95 °C)	30 seconds	30 cycles.
Annealing temperature	30 seconds	
Extension (72 °C)	1 minute	

Annealing temperature was determined in accordance to the length and GC content of the primers by the NEB online Tm calculator or by manual calculation as shown below

$[(A+T) \times 2] + [(G+C) \times 4] - 5\ °C$

Elongation time was determined by the length of the gene being amplified, where to polymerise 1000 bp of DNA, 60 s was used using DreamTaq and GoTaq DNA polymerases and 30 s using KOD and Q5 DNA polymerases.

2.5.2 Genomic DNA template preparation

2.5.2.1 Colony picking

Well separated colonies were picked using sterilised wooden toothpick and scraped inside the bottom of the 0.5 ml PCR tube.

2.5.2.2 Boiled lysate

To prepare crude chromosomal DNA, 200 µl TE buffer were inoculated with a bacterial colony. The cells were resuspended by vortexing and boiled for 10 min followed by centrifugation at 13,000 rpm for pelleting cell debris. The supernatants were transferred to a clean microcentrifuge tube and cell pellets were discarded.

2.5.3 Purification of plasmid DNA

Single colonies were inoculated into appropriate media and antibiotic and incubated overnight. The bacterial cultures were then centrifuged for 5 min at 14,000 rpm in a microcentrifuge tube. The harvested pellet was resuspended in 250 µl chilled RNAse solution followed by the addition of 250 µl Lysis solution. The tube was inverted several times for a viscous solution to be formed. 350 µl Neutralisation solution was added and the tube was inverted several times until white precipitate was formed. The microcentrifuge tube was then centrifuged for 5 min at 13,500 rpm and the supernatant solution containing plasmid DNA was transferred into a spin column. 500 µl of binding buffer (PB) was added to the spin column which was centrifuged for 1 min to enhance binding of DNA into the column. The flow through was discarded, and 500 µl of washing solution was added to the column before centrifuging for 1 minute to wash the column and remove unbound material. Washing solution was added twice and the flow through discarded. The last centrifugation was performed without any solution to completely remove residual washing solution. The spin column was then transferred to a clean microcentrifuge tube and 20-35 µl elution buffer was added. The column was incubated with the elution buffer for 2 min and was centrifuged for another 2 min to elute the plasmid DNA into the microcentrifuge tube. Solutions stated above were added chronologically according to the manufacturer's instruction (Miniprep Kit Thermo Scientific) with modifications by the addition of PB buffer.

2.5.4 Purification of DNA fragments

Following PCR amplifications of genomic DNA and restriction digestions, DNA fragments were purified using GeneJet PCR purification kit (Thermo Scientific) according to manufacturer's instructions. Reaction mixtures containing DNA were mixed with binding buffer which promotes DNA binding to the silica membrane present in spin column filters. Impurities were removed using wash buffers containing ethanol and purified DNA was eluted from the spin column filters with an elution buffer.

2.5.5 Restriction digestion techniques

Plasmid DNA was subjected to restriction digestion in a volume of 50 µl in a 1.5 ml microcentrifuge tube according to the following procedure. Amount of plasmid DNA and ultrapure H_2O added was dependent on the concentration of plasmid DNA. The amount of plasmid DNA to be digested was determined based on its concentration when electrophoresed in an agarose gel. Plasmid DNA restriction digestions were incubated at room temperature for 2 h or 15 min for fast digest enzymes. Following digestion, the enzyme was inactivated, and buffer components removed using the PCR Purification Kit (Thermo Scientific). Where double digestions were conducted, appropriate buffers were selected which provided optimum efficiency of both enzymes. Digested DNA was then analysed by gel electrophoresis for diagnostic purposes.

Table 2.6 Components of restriction digestion

Reaction components	Volume (µl)
Plasmid DNA	To be determined
Appropriate buffer for enzyme	5.0
BSA (10 µg $µl^{-1}$) (Promega/New England Biolabs)	0.5
Sterile H_2O	TBD
Restriction enzyme (10 U $µl^{-1}$) (Promega/New England Biolabs)	1.0
Total	50

2.5.6 DNA ligation techniques

Restriction digestion fragments were ligated using T4 DNA ligase (1 U $µl^{-1}$) (Promega) and buffer as follows. Components of ligation were mixed in a 10-30 µl reaction mixture in a microcentrifuge tube. Ligase buffer was added as 1/10 of the total reaction mixture. The insert:vector volume ratio was adjusted according to the insert and vector concentrations. Two control reactions were also performed in which the ligation control was comprised of vector with ligase enzyme without the DNA fragment to be cloned while the vector control did not contain either the ligase enzyme or the DNA fragment. The ligation mixture was left at room temperature overnight and was transformed into *E. coli* competent cells the following day.

Successful ligation was initially determined by colour screening of colonies on selective medium containing X-gal (40 µg ml^{-1}) and IPTG (100 µM) for pEX18, pBBR1MCS, pBBR1MCS-2, pSRKKm, pBluescript derivatives and then by gel electrophoresis analysis of plasmid minipreps or was screened by diagnostic PCR. Selected colonies having the desired plasmid were prepared by miniprep (Thermo Scientific) and were sequenced to ensure no PCR-induced errors were present in the cloned DNA fragments.

Table 2.7 Components for a typical ligation (1:1)

Components	Ligation	Ligation Control	Vector Control
H_2O (µl)	0.0	4.0	5.0
Ligase Buffer (µl)	1.0	1.0	1.0
Cut plasmid (µl)	4.0	4.0	4.0
Cut DNA fragment (µl)	4.0	-	-
T4 DNA ligase (µl)	1.0	1.0	-
Total volume (µl)	10	10	10

2.5.7 Agarose gel DNA electrophoresis

Agarose gel was prepared by boiling 0.5 – 0.8 g agarose powder (Fisher Scientific) in 50 ml 1x TAE in a microwave oven. The amount of agarose used depended on the size of DNA fragments to be analysed. Any reduction in volume of boiled gel solution was replaced by addition of ultrapure H_2O. The gel was poured into a gel tray with a comb (Biorad). Alternatively, gel stain (Midori stain or Gel Red) was added to the boiled gel solution before pouring. Agarose gel was left to set at room temperature for 1 hr before placing the gel tray in a Biorad gel tank filled with 1x TAE buffer.

The gel comb was removed and 5 µl of DNA sample mixed with 1 µl of 6x loading dye was pipetted into the wells. Linear or supercoiled DNA ladders were added to allow approximation of DNA fragment/plasmid sizes. Samples were electrophoresed at 100-120 V according to the size of the gel tank, with a current of 400 mA, for approximately 60-75 min. Gels with added gel stain were then visualised on a UV transilluminator (U:Genius). Alternatively, gels were soaked in 5 µg ml^{-1} of ethidium bromide (EtBr) for 15-45 min prior to visualisation to allow intercalation of the EtBr into the DNA within the gel.

2.5.8 DNA gel extraction

The DNA fragment was gel-purified using a GeneJet Thermo Scientific or Qiagen gel-extraction kit according to manufacturer's instructions. Desired DNA fragments present with other fragments in an agarose gel following electrophoresis were purified by gel extraction. The electrophoresis gel was visualised under UV light and the desired DNA fragment was cut from the gel with a scalpel. Gel slices containing the desired DNA fragment were placed in pre-weighed empty microcentrifuge tube and weighed. Solubilisation buffer (Qiagen) twice the weight of the gel was added, and the mixture kept at 50 ^{o}C for 10 min, with occasional vortexing to allow the gel to dissolve.

The gel solution was applied to a spin column to allow binding of the DNA to the silica membrane of the column and washed with ethanol-based washing buffer. Purified DNA was then eluted with an elution buffer and subjected to agarose gel electrophoresis for diagnostic purposes.

2.5.9 DNA Sequencing

The integrity of cloned DNA was confirmed by Sanger DNA sequencing carried out by the Medical School Genetic Core Sequencing Facility at the University of Sheffield. Appropriate vector primers were used to perform sequencing as follows: M13 for and M13 rev primers were used for reading DNA inserted into the multiple cloning site (MCS) of the plasmids pBBR1MCS-1, pBBR1MCS-2 and pSRKKm. M13 for and M13 BACTH rev primers was used for pEX18 plasmids while catendout and PUTcatrev primers were used for pSHAFT derivatives.

2.6 Xenosiderophore utilisation bioassay

Xenosiderophore utilisation bioassays were performed on bacteria growing in both solid and liquid media.

2.6.1 Disc diffusion assay

Siderophores used were either purified products (Table 2.8) or present in bacterial supernatants. To acquire siderophores from culture supernatants, bacterial strains were cultured in 2 ml of appropriate medium at 37 °C for 48 hr. The 2 ml bacterial culture was then centrifuged at 4500 rpm for 10 min and the supernatant was filter sterilised using a 0.45 µM filter. Sterilised supernatants in amounts of 30-100 µl were spotted onto sterilised filter discs (Whatman, 5-10 mm) and air-dried. Purified siderophores were dissolved in a suitable solvent and were spotted onto the sterilised filter disc in amounts of 10-20 µl. All siderophores used in this study were dissolved in HPLC-graded pure water in a stock concentration of 5 mM except for the catecholate siderophores which were dissolved in DMSO and yersiniabactin (50 % methanol solution) at the same concentration. To perform the assay, bacterial test strains, commonly the *B. cenocepacia pobA* mutant derivatives, were cultured in 2 ml LB broth overnight at 37 °C on a shaker.

The following day, 100 µl of the culture was transferred to 3 ml of 0.65 % LB agar maintained at 42 °C and then overlaid as a thin layer onto an LB agar plate supplemented with EDDHA at a final concentration of 40 µM unless otherwise stated. Filter discs impregnated with siderophores or supernatants were then aseptically placed onto the solidified bacterial overlay with alcohol-sterilised forceps and the plates incubated inverted at 37 °C for 48 hr. Bacterial growth around the filter disc suggests siderophore utilisation. Images were captured using Olympus ED 60 mm fr.8 Macro.

Table 2.8 Sources of Purified Siderophores used

Siderophore	Source
Aerobactin	EMC collection
Alcaligin	Gift from T. Brickman
Arthrobactin	EMC collection
Azotochelin	Gift from A. Duhme-Klair
Bacillibactin	EMC collection
Cepabactin	Gift from G. Mislin
DHBS dimer	EMC collection
DHBS monomer	EMC collection
DHBS trimer	EMC collection
Enterobactin	EMC collection
Ferrichrome	Sigma-Aldrich
Ferricrocin	Gift from A. Duhme-Klair
Ferrioxamine B	Sigma-Aldrich
Nicotianamine	Santa Cruz Biotechnology
PVD I, II, III	Gifts from P. Cornelis
Rhizoferrin	EMC collection
Rhodotorulic acid	EMC collection
Schizokinen	EMC collection
Triacetylfusarinine C	EMC collection
Vibriobactin	EMC collection
Yersiniabactin	EMC collection

2.6.2 Liquid growth stimulation bioassay

Xenosiderophore utilisation in liquid culture was performed by growing cultures in an iron-restricted environment using a hydrophilic iron chelator, DTPA. A single colony of each *Burkholderia* strain to be tested was cultured as an inoculum for 24-48 hr in M9-glucose (CAA) medium supplemented with antibiotics where appropriate. Liquid cultures (50 ml) were prepared in 250 ml plastic flasks consisting of 50 ml M9-glucose (CAA) medium and 0.1 mM DTPA. 500 µl of filter-sterilised CAA from a 10 % stock solution and 500 µl of 0.1 µM stock DTPA solution were added to each flask.

Inoculums were added to the culture to an initial optical density (OD) at 600 nm of 0.010 to 0.011 absorbance reading (approximately 1: 250 dilution of the overnight culture), equating to approximately 8.0×10^6 CFU ml^{-1}. Siderophore solutions (10 µM) or haemin were added to each culture unless otherwise stated. Cultures were incubated at 37 °C on a shaker and bacterial growth was measured by monitoring OD_{600} at 1 hr intervals up to 10 hrs by a spectrophotometer (Pharmacia LKB- Ultraspec III).

2.7 HPLC purification and liquid chromatography mass spectrometry (LC-MS) analysis

Bacterial culture supernatants were filter-sterilised and analysed by high performance liquid chromatography (HPLC) (XBridge-18 Column). Purified siderophore samples were obtained by preparative HPLC by using a gradient of solvents (water, acetonitrile, trifluoroacetic acid) at appropriate mixture percentages and wavelength for obtaining high peaks. The fractions were checked for purity by analytical HPLC and were collected at desired peaks.

Collected fractions were concentrated in a concentrator (Eppendorf - concentrator 5301) placed in a fume hood for 4-6 hrs. Samples were resuspended in 50 µl HPLC-graded pure water and were directly infused into the mass spectrometer (Waters, LCT classic mass spectrometer). Infusion was performed using a syringe pump at 20 µl min^{-1} by both negative and positive electrospray ionisation (ESI) at a capillary voltage of 3000v and with a sample cone of 30v. HPLC purification and LC-MS analysis were carried out by the Centre of Chemical Instrumentation and Analytical Services (CCIAS), Department of Chemistry, University of Sheffield.

2.8 Statistical analyses

Differences between growth rates in liquid growth assay were evaluated by using paired one-tailed Student t-tests. Values of $p<0.05$ were considered as statistically significant. All experiments were replicated at least three times and results were displayed as mean values with ± SEM. Data were analysed using GraphPad Prism 7 and presented using line charts. Growth rates were determined by plotting optical density values at 600 nm (y-axis) against time in hours (x-axis).

Chapter 3

In silico genome mining of iron uptake pathways in *B. cenocepacia*

3.1 Rationale

The past decade has seen developments in the investigation of iron uptake pathways in many bacteria, particularly the common enteric bacteria, *E. coli* and the respiratory pathogen, *P. aeruginosa.* Given that exploitation of the knowledge in these pathways could facilitate drug development for the control of pathogens, extensive studies have been conducted in this subject. In this study, iron acquisition pathways of a respiratory pathogen, *B. cenocepacia* is investigated.

The *B. cenocepacia* ET12 lineage is highly transmissible and has known to cause an epidemic which leads to high mortality among infected CF patients (LiPuma, 2010). Although the genome sequence of strain J2315 from the ET12 lineage has been determined, it is not easy to maintain this strain in the laboratory context. Another CF sputum isolate, *B. cenocepacia* H111, is closely related to the ET12 lineage and is genotypically comparable to strain J2315. It has, however, a smaller chromosomes 1 and 2, and a larger chromosome 3 (pC3 replicon) (Carlier et al., 2014). In contrast to the virulent ET12 strains, strain H111 does not show acute symptoms upon infection and is more sensitive to antibiotics. H111 strain is known to be easily maintained and cultivated under laboratory conditions. It also has a published gene-protein sequence annotation (Carlier et al., 2014). As it is flexible to genetic manipulations, strain H111, was selected for this study.

The genome of *B. cenocepacia* H111 was subjected to a bioinformatic analysis to identify genes encoding proteins involved in ferric iron uptake pathways (i.e siderophore-mediated transport). As the first step in these pathways involves transport through the OM, as in other Gram-negative bacteria, the analyses included the TBDRs and the proteins constituting in the TonB complex(es) in addition to the inner membrane transporters. The focus of the work described in this chapter, however, emphasises on the TBDRs of *B. cenocepacia* as this is the main theme of the work described in this thesis.

3.2 Identification of putative TBDRs in *B. cenocepacia*

To identify the putative TBDRs in *B. cenocepacia*, two characterised TBDRs in *P. aeruginosa* PAO1 were initially considered as queries for searching for TBDRs in the *B. cenocepacia* protein database via BLASTP analysis. The decision of choosing the TBDRs in *P. aeruginosa* was based on previous observations that *B. cenocepacia* 715j was shown to utilise the siderophores, ferrichrome and ferrioxamine B by a disc diffusion assay (Paleja, Sofoluwe and Thomas, unpublished observations). The ability of this strain to utilise these xenosiderophores indicates the likely occurrence of more than two TBDRs in this species, as two TBDRs are known to be present that are specific for endogenous siderophores produced by *B. cenocepacia*, ornibactin and pyochelin.

The TBDRs for the siderophores ferrichrome and ferrioxamine B in *B. cenocepacia* were hypothesised to be similar to the corresponding receptors found in *P. aeruginosa* as this bacterium can also utilise both as xenosiderophores. The amino acid sequence of the mature part (the region C-terminal to the signal peptide) of the two receptors from *P. aeruginosa* PAO1 for ferrioxamine B, PA2466, (FoxA), and ferrichrome, PA0470 (FiuA) (Hannauer et al., 2010b), were used as queries in BLASTP searches for similar proteins in *B. cenocepacia* J2315. TBDRs were initially probed in strain J2315 due to its recognised gene locus designations. To ensure that all putative TBDRs present in strain J2315 were identified, a few of the most poorly matching TBDRs in *B. cenocepacia* J2315 were used as a query in successive BLASTP searches until no more TBDRs were detected. The full list of putative TBDRs present in strain J2315 is shown in Table 3.1.

The TBDRs encoded by *B. cenocepacia* H111 were then identified via BLASTP searches at Burkholderia.com using the amino acid sequence of each TBDR found in *B. cenocepacia* J2315 as a query. The TBDRs identified in strain H111 are shown in Table 3.1 alongside the corresponding TBDRs from J2315. *B. cenocepacia* H111 is designated in three successive locus tags, and the most recent is used in this study. For the strain J2315, an old locus tag was used from two successive designations as it is familiar to workers in the field.

The number of amino acid residues and the length of the coding region of the TBDR gene loci are identical in both strains. Most TBDRs are encoded by the middle chromosome of the two strains, with 9 TBDRs encoded by the large chromosome, 13 in the middle chromosome and 2 in the megaplasmid pC3 replicon. Twenty-two (22) intact TBDRs were identified in strain J2315. Orthologues of all these TBDRs were present in strain H111. H111 encoded two additional TBDR genes which were present as pseudogenes in J2315. The two TBDR genes in chromosome 1 and 2 of J2315 are therefore likely to be non-functional. Thus, 22 functional TBDR-encoding genes were identified in *B. cenocepacia* J2315 and 24 in the H111 strain. The proteome of strain H111 possesses orthologues of all 22 TBDRs present in J2315, with the two additional TBDRs, I35_RS08490 and I35_RS19580 ('BCAL1783' and BCAM0706, respectively). The orthologous TBDRs in the two strains show an identity of nearly 100% and their genes are located at the corresponding genomic loci in all cases.

Strain J2315 encodes truncated versions of the two TBDRs that are encoded by strain H111. I35_RS19580 is annotated as BCAM0706 in J2315 and is a pseudogene having a frameshift mutation at codon 66 of its coding sequence. Accordingly, the I35_RS19580 gene product is not orthologous to the BCAM0706 gene product. The other additional TBDR found in H111 (I35_RS08490) is expected to be encoded between BCAL1782 and BCAL1785 in J2315 and is annotated as a pseudogene in the NCBI database.

However, the inactivated gene that corresponds to I35_RS08490 in strain J2315 was not given a gene locus designation in the NCBI resource. For convenience, it is referred to as 'BCAL1783' henceforth. The gene product of 'BCAL1783' is not orthologous to the I35_RS19580 protein due to an internal nonsense mutation at codon 677 of its coding sequence (Burkholderia.com).

The list of potential TBDRs identified in *B. cenocepacia* includes BCAL1700 that transports the endogenous siderophore ornibactin (Sokol et al., 2000). TBDR BCAL1700 has the highest similarity bit score to both FoxA and FiuA amino acid sequences. However, the BCAL1700 TBDR has been demonstrated to be the ornibactin receptor (OrbA) (Sokol et al., 2000). This observation is surprising as, unlike ferrichrome and ferrioxamine B, ornibactin does not contain three hydroxamate bidentate groups.

BCAM2224, which is encoded in the pyochelin gene cluster in *B. cenocepacia* J2315, exhibits high amino acid sequence homology to the product of the gene locus PA4221, the pyochelin receptor, FptA, in *P. aeruginosa* PAO1*,* and is therefore very likely to be involved in pyochelin transport. The putative TBDRs also includes metal chelate receptors. This is not surprising as TBDRs are known to be involved in transporting other compounds including vitamin B_{12} (cobalamin) and haem. The BCAM2626 gene is annotated as encoding a haem receptor based on the homology with other haem receptors (HuvA) but its function has not been demonstrated. The BCAM1593 gene is annotated to encode a vitamin B_{12} receptor (Burkholderia.com), giving a protein homology of 28 % to the TBDR BtuB of *E. coli* K-12 (P06129) (Figure 3.1). The putative TBDR PA1271 is a putative BtuB in *P. aeruginosa* PAO1 and gives and percentage identity of 29 % to BtuB in *E. coli*. BCAM0948 has a homology of 58 % with a *P. aeruginosa* PAO1 TBDR (OprC, PA3790) which is proposed to bind to a copper chelate (Yoneyama and Nakae, 1996; Hartney et al., 2011) (Figure 3.2). Likewise, the TBDR BCAS0360 is predicted to be similar to CntO, the product of the PA4837 gene locus in *P. aeruginosa* PAO1 that is involved in zinc transport (Lhospice et al., 2017; Mastropasqua et al., 2017). The amino acid sequence of CntO, or presently named as pseudopaline displays an identity of 41 % to BCAS0360 (Figure 3.3). Additionally, another predicted zinc receptor in *B. cenocepacia* is BCAM1571 protein which gives a 57 % homology to the product of the PA0781 gene locus in *P. aeruginosa* PAOI (ZnuD) (Figure 3.4) (Pederick et al., 2015). The BCAM2007 gene has a sequence identity to PiuA (PA4514) with a 48 % identity (Figure 3.5) while both BCAL1345 and BCAM0491 genes are seen to be similar to the product of PA2911 by an identity of 43 % (Figure 3.6). The products of these genes have yet to be fully characterised in *P. aeruginosa* PAO1 although the PA2911 has also been proposed as a zincophore (Llamas et al., 2006; Van Delden et al., 2013; Pederick et al., 2015).

Conserved domains within the putative TBDR proteins were identified according to protein sequence analysis and classification (InterProScan) (Jones et al., 2014). Interpro identifies homologous protein superfamilies and classifies them into families and also identifies the presence of conserved domains.

The TBDR-like β-barrel superfamily domains (IPR036942 and IPR000531) were identified in the amino acid sequences of all 24 putative TBDRs in H111. Domains involved in substrate binding, i.e, the homologous plug domain (IPR012910 and IPR037066) were also identified in all TBDRs with one exception. The exception is the BCAM0564, which is not listed as comprising the domain IPR0307066, although its conserved sequences is aligned with other putative TBDRS (Figure 3.5 and 3.6). A domain characteristic of the TBDRs for siderophore utilisation (IPR010105) was identified in sixteen of the 24 putative TBDRs, including three which were identified as catecholate siderophore receptors (IPR030148): BCAM0499, BCAM1187 and BCAM2007 and another three being identified as hydroxamate receptors (IPR030149): BCAL0116, BCAM2281 and BCAM0706 (I35_RS19580). The eight putative TBDRs that do not possess the IPR010105 domain are BCAL1777, BCAL3001, BCAM0564, BCAM0948, BCAM1571, BCAM1593, BCAM2367 and 'BCAL1783' (I35_RS08490). As expected, BCAM2626 was defined as having the haem receptor homologous domain (IPR010949 and IPR011276) and one putative TBDR (BCAM0948) was indicated as exhibiting the copper receptor domain (IPR010100), consistent with its high degree of similarity to the *P. aeruginosa* copper chelate TBDR, OprC (See Table 3.2).

The TBDRs found in each of the two *B. cenocepacia* strains were then aligned and conserved amino acids among the TBDRs were identified (Figures 3.7 and 3.8). To perform the alignment, the signal sequence of each TBDR was identified using SignalBLAST and the mature processed protein sequences were used to construct the alignment. Due to one putative TBDR (BCAL1371/I35_RS06295) that possesses a long N-terminal extension that signals to an anti-sigma factor, the mature proteins were aligned beginning with their conserved TonB boxes. TonB boxes were identified by a conserved sequence at the N-terminal region of the aligned protein sequences (Peacock et al., 2005). The alignment of the putative TBDRs demonstrated that various regions within the TBDRs are highly conserved, particularly the β-barrel comprising the β-strands region and the receptor plug site (Figures 3.7 and 3.8). These conserved features of TBDRs were separated by long regions of weak or negligible conservation which may contribute to differences in protein length of the putative TBDRs.

3.3 Phylogenetic analysis of putative TBDRs

To investigate the relationships between the TBDRs, phylogenetic analysis of the candidates in both strains were performed by two statistical methods, the unweighted pair group method with arithmetic mean (UPGMA) and the maximum likelihood (ML) method. Both analyses show that several TBDR amino acid sequences are more closely related than others (Figures 3.9, 3.10, 3.11 and 3.12). This may suggest a certain degree of redundancy in function in some cases. For example, the well characterised TBDR in *B. cenocepacia*, OrbA (Sokol et al., 2000) (I35_RS08065 in H111), is very closely related to BCAS0333 (I35_RS31745 in H111) in both phylogenetic trees, although the function of BCAS0333 has not been determined.

Table 3.1 List of putative TBDRs present in *B. cenocepacia* J2315 and H111 strains

	J2315 TBDRs[a,b]	chromosome	Amino acid residues	Similarity bit score to PA2466	Similarity bit score to PA0470	H111 TBDRs[b]	chromosome	Amino acid residues	% match between J2315 and H111
1	BCAL0116	1	707	255	182	I35_RS00620	1	707	99.7
2	BCAL1345	1	736	398	235	I35_RS06170	1	736	99.3
3	BCAL1371	1	839	589	347	I35_RS06295	1	839	98.8
4	BCAL1700	1	755	960	856	I35_RS08065	1	755	99.6
5	BCAL1709	1	712	351	219	I35_RS08115	1	712	99.7
6	BCAL1777	1	906	89		I35_RS08460	1	906	99.9
7	'BCAL1783'[c]	1				I35_RS08490	1	941	
8	BCAL2281	1	726	170	182	I35_RS11045	1	726	99.0
9	BCAL3001	1	787	131	134	I35_RS04375	1	787	100.0
10	BCAM0491	2	707	222	226	I35_RS18505	2	707	98.4
11	BCAM0499	2	732	471	279	I35_RS18545	2	732	99.6
12	BCAM0564	2	788	147	143	I35_RS18860	2	788	99.6
13	BCAM0706[d]	2		231	284	I35_RS19580	2	743	
14	BCAM0948	2	688	96	91	I35_RS20820	2	688	99.9
15	BCAM1187	2	739	232	245	I35_RS21645	2	739	100.0
16	BCAM1571	2	694	100		I35_RS23575	2	694	100.0
17	BCAM1593[e]	2	642	124	187	I35_RS23700	2	642	99.7
18	BCAM2007	2	747	226	218	I35_RS25625	2	747	99.7
19	BCAM2224	2	727	442	291	I35_RS26975	2	727	99.7
20	BCAM2367	2	777	129	72	I35_RS27690	2	777	99.2
21	BCAM2439	2	722	454	272	I35_RS28095	2	722	99.6
22	BCAM2626[f]	2	757	129	116	I35_RS29035	2	757	99.5
23	BCAS0333	3	724	922	837	I35_RS31745	3	724	99.7
24	BCAS0360	3	701	515	413	I35_RS31880	3	701	98.6

[a]Ranked in order of gene locus location in chromosomes. [b]Corresponding J2315 and H111 TBDRs are shown in the same rows.
[c]Not annotated in J2315 although pseudogene is present. [d]Indicates gene disruption. BCAM0706 is likely to be non-functional as encoded protein is truncated.
[e]Function based on high similarity to *Escherichia coli* BtuB, vitamin B12 receptor; [f]Function based on high similarity to *Vibrio anguillarum* HuvA, haem receptor.
Grey-shaded boxes are no hits found by query. Table includes similarity score towards *P. aeruginosa* hydroxamate receptors, FoxA (PA2466) and FiuA (PA0470).
The number of amino acid residues in each TBDR protein is stated.

Table 3.2 Identification of conserved domains in putative TBDRs present in *B. cenocepacia* J2315 and H111 strains

	J2315 TBDRs	H111 TBDRs	IPR036942	IPR000531	IPR037066	IPR012910	IPR010105	IPR030149	IPR030148	IPR010949	IPR011276	IPR010100
1	BCAL0116	I35_RS00620	•	•	•	•	•	•				
2	BCAL1345	I35_RS06170	•	•	•	•	•					
3	BCAL1371	I35_RS06295	•	•	•	•	•					
4	BCAL1700	I35_RS08065	•	•	•	•	•					
5	BCAL1709	I35_RS08115	•	•	•	•	•					
6	BCAL1777	I35_RS08460	•	•	•	•						
7	ʻBCAL1783ʼ	I35_RS08490	•	•	•	•						
8	BCAL2281	I35_RS11045	•	•	•	•	•	•				
9	BCAL3001	I35_RS04375	•	•	•	•						
10	BCAM0491	I35_RS18505	•	•	•	•	•					
11	BCAM0499	I35_RS18545	•	•	•	•	•		•			
12	BCAM0564	I35_RS18860	•	•		•						
13	BCAM0706	I35_RS19580	•	•	•	•	•	•				
14	BCAM0948	I35_RS20820	•	•	•	•						•
15	BCAM1187	I35_RS21645	•	•	•	•			•			
16	BCAM1571	I35_RS23575	•	•	•	•						
17	BCAM1593	I35_RS23700	•	•	•	•						
18	BCAM2007	I35_RS25625	•	•	•	•			•			
19	BCAM2224	I35_RS26975	•	•	•	•	•					
20	BCAM2367	I35_RS27690	•	•	•	•						
21	BCAM2439	I35_RS28095	•	•	•	•	•					
22	BCAM2626	I35_RS29035	•	•	•	•	•			•	•	
23	BCAS0333	I35_RS31745	•	•	•	•	•					
24	BCAS0360	I35_RS31880	•	•	•	•	•					

Inter Pro member database
IPR036942: TBDR-like, β-barrel domain superfamily
IPR000531: TBDR-like, β-barrel
IPR037066: TBDR (plug domain superfamily)
IPR012910: TBDR (plug domain)
IPR010105: TBDR (siderophore)
IPR030149: TBDR FcuA/FatA (hydroxamate)
IPR030148: TBDR FiuA (catecholate)
IPR010949: TBDR (haem/ transferrin/lactoferrin)
IPR011276: TBDR (haem/haemoglobin)
IPR010100: TBDR (copper)

```
BtuB                  1   MIKKASLLTACSVT----AFSAWAQDTSPD-------------TLVVTANRFEQPRSTVL
BCAM1593              1   -MNLRHLLATSAATALLSPLAHAAGDTAPAQPAGPAEGADLPTISVTDTRELPESFDRRY

BtuB                 44   APTTVVTRQDIDRWQS--TSVNDVLRRLPGVDITQNGGSGQLSSIFIRGINASHVLVLID
BCAM1593             60   ASTQVLTRDDIDRLSPADPSITQALATLPGVTVTQNGGPGSSASVSIRGSSASQVAVFID

BtuB                102   GVRLNLAGVSGSADLSQFPIALVQRVEYIRGPRSAVYGSDAIGGVVNIITTRDEPGTE-I
BCAM1593            120   GIRIGSP-TTGIAPWADLPTDAFERVEVISGPAAASFGNNAMGGVVQLFTRRAAQQPNQT

BtuB                161   SAGWGSNSYQNYDVS--TQQQLGDKTRVTLLGDYAHTHGYDVVAYGNTGTQAQT-----D
BCAM1593            179   TVSFGGGTNKTFDTRFRTSGTVPSTGPLAALGGLTYSLG--LHDYNTAGIDATRPFFYGH

BtuB                214   NDG---FLSKTLYGALEHNFTDAWSGFVRGYGYDNRTNYDAYYSPGSPLLDTRKLYSQSW
BCAM1593            237   EDGRNPYHAQDLDARL-GYARDNWSISTF----------AL-YHRSDL----------SY

BtuB                271   DAGLRYNGELIKSQLITSYS----HSKDYNYDPHYGRYDSS-------ATL--DEYKQYT
BCAM1593            275   DN-SGYANRELDHQLTTGVAFHLDITPDTQFDQSFGYANDRQFIYADNPALATDQINSQR

BtuB                318   VQWANN-VIVGHGS--IG--------AGVDWQKQTTTPGTGYVEDGYDQRNTGI-YLTGL
BCAM1593            334   ISTSTSLTHQAHGFHLFGLPLSGESKLAYDFTREQAFLP-VDIPGGVPTRNDSAFSLHQS

BtuB                366   QQVGDFTFEGAARSDDNSQFGRHGTWQTSAGWEFIEGYRFIASYGTSYKAPNLGQL-YGF
BCAM1593            393   ATLGSVTMFVAGRHEIV-AGQAVNTGNAALSWAITPVYTARVSYGNAFRLPTFNDLYYPG

BtuB                425   YGNPNLDPEKSKQWEGAFECLTAGVNWRISGYRNDVSDLIDYDDHTLKYYNEGKARIKGV
BCAM1593            452   YGNPSLSPERSTSVEAALDANTAYGTFTAAIYDTRVNNLIAYNPATFSPMNIGRSIIRGI

BtuB                485   EATANFDTGPLIH-TVSYDYVDARNAITDTPLLRRAKQQVKYQLD--WQLY---DFDWGI
BCAM1593            512   DLSYKGTIGRSIPVSIAVGILNPQDETNQTWLSRRPRQTVSLNVDHTWDELKLHALSTGA

BtuB                539   TYQYLGTRYDKDYSSYPYQTVKMGGVSLWDLAVAYPVTSHLTVRGKIANLFDKDYETVYG
BCAM1593            572   SLLYGGSTFDDPA-----NRQYLASYLTVSLRASYRINSHLTVSASLSNLFDRQYMTAYG

BtuB                599   YQTAGREYTLSGSYTF
BCAM1593            627   YNTLGRTAFGKVSYTF
```

Figure 3.1: Alignment of *E.coli* BtuB and the putative *B. cenocepacia* TBDR, BCAM1593/I35_RS23700
Amino acid sequences of BtuB from *E.coli* K-12 (P06129) were aligned with the putative TBDR, BCAM1593/I35_RS23700 from *B. cenocepacia* H111 by ClustalW and identical or similar amino acids were highlighted using BOXSHADE. White font with black shading indicates identical residue (28 %) at the corresponding position in both sequences and white font with grey shading indicates similar residues at the corresponding position in both sequences. Protein designations are indicated on the left.

```
BCAM0948      1   ----MTNFQLRAPRASRNARARPLPRMLKLTVPALAVGALAASAAAAEIAPAAGATAN--
OprC          1   MEKRMSTQQRAAGNACPTAAFSFDPARLAQRRRWAGAFAALCGLALSPGALLAEEHSQHQ

BCAM0948     55   DAAMLLPPVEVVAAPLSTPLVVVTDPKAPRQPLPASDGADYLKTIPGFTSIRSGGINGDP
OprC         61   DHAVELAPSVVTGVAQSSPLTIVTNPKEPRQPVPASDGADYLKTIPGFAVIRNGGSNGDP

BCAM0948    115   VLRGMFGSRLNILANGMPTLGACPNRMDAPTSYIAPESYDKVTVVKGPQTVLYGPGASAG
OprC        121   VLRGMFGSRLNILTNGGMMLGACPNRMDAPTSYISPETYDKLTVIKGPQTVLWGPGASAG

BCAM0948    175   TVLFERVTPREERPGMRFEGSLVGGSFGRNDQNIDLTAGTPDVYGRVTANHAHSQDYQDG
OprC        181   TILFEREPERFGELGSRVNASLLAGSNGRFDKVLDAAAGNRLGYLRFTGNHAQSDDYEDG

BCAM0948    235   NGNTVPSQWDKWNADAALGWTPDDHTRVELTAGTGDGYARYAGRGMDGAHFRRETFGLSF
OprC        241   AGNTVPSRWKKWNGDVAVGWTPDEDTLIELTAGKGDGEARYAGRGMDGSQFKRESLGLRF

BCAM0948    295   DKRHLGDVLDRIEARVYYNEADHVMDNYTLRQPDPASSMPMRMAADVRRRTVGARAAATF
OprC        301   VKSNVSDVLEKVEAQVYYNYADHIMDNFRLRTPDPSSMMPMPMASQVDRRTLGGRLAATW

BCAM0948    355   REGDDFKLVTGVDAQSNRLDSRSS------MGQQNYRDQPWDAQATMWNAGVFSELTWYA
OprC        361   RW-DDFKLVTGVDAMRNEHRARGSKYDMMTDYYTDADQFPWSKDAVFHNYGAFGELTWFA

BCAM0948    409   SDVSRVIGGARVDYASARDKRAMKRG--MMMSKPNPTFDDDRTKVLPSGFVRYERDLASL
OprC        420   AERDRLIGGLRLDRASVKDYRQTLKSGHMGHAMANPTANDTRADTLPSGFVRYEHDLADS

BCAM0948    467   PVTWYAGIGHAERYPDYWELFSATRGPTGSVNAFSAVRPEKTTQLDIGAQYKSDRFDAWV
OprC        480   PTTLYAGLGHAERFPDYWELFSPKRGPNGSVNAFDKIKPEKTTQLDFGLQYNGDKLQAWA

BCAM0948    527   SAYAGYVQDFILFDYATGMMGPITQATNVNAQIMGGEAGVSWRPVAPLRVETSLAYAWGR
OprC        540   SGYVGVVQDFILFSYREGMMGSSTQATNVDARIMGGELGASYQLTGNWKTDASLAYAWGK

BCAM0948    587   NVASGDPLPQMPPLEARIGLEYTRGAWSAGGLWRIVASQHRYALNEGNVVGKDFGPSAGF
OprC        600   NSSDDRALPQIPPLEARFGLTYEEGDWSAGSLWRVVAPQNRIARDQGNVVGKDFDKSAGF

BCAM0948    647   GVLSLHTQYNVSKTVQISVGVDNVLNKAYTEHLNLAGNAGFGYPANAPVMEPGRTAWVRV
OprC        660   GVFSLNGAYRVTRNVKLSAGVDNLFDKDYTEHLNKAGDAGFGFSANETVPEPGRTFWTKV

BCAM0948    707   SAKL
OprC        720   DFSF
```

Figure 3.2: Alignment of OprC of *P. aeruginosa* and the putative *B. cenocepacia* TBDR, BCAM0948/I35_RS20820

Amino acid sequences of OprC from *P. aeruginosa* PA3790 were aligned with the putative TBDR, BCAM0948/I35_RS20820 from *B. cenocepacia* H111 by ClustalW and identical or similar amino acids were highlighted using BOXSHADE. White font with black shading indicates identical residue (58 %) at the corresponding position in both sequences and white font with grey shading indicates similar residues at the corresponding position in both sequences. Protein designations are indicated on the left.

```
BCAS0360    1 MSRRNWAAAPMAIVVGTTGMGSAD---------AQETALPTIEISAQRA---TAPFRTRE
PA4837      1 ------MRVSVSLVLG-VGLGCSSPALWAETESPAELEVLTVTAEAERAEGPVQGYRANR

BCAS0360   49 STSATRSEADVMEIPFAWSSVDTKLIQTVAATRGDDLYDWVAGVSRQNNFGGLW-DNYAV
PA4837     54 TASATRTDTRIEDIPQALSVVPRQVLDDLDSARIERALDFAGGVSRQNNFGGLTMFEYNV

BCAS0360  108 RGFAGDGNTSGTDYLVNGFSWNRGMSVPRDIVNLERMEVLKGPASALYGRGDPGGIISYT
PA4837    114 RGFTT------SEFYRDGFSANRGYMNAPDSATIERVEILKGPASSLYGRGDPGGTVNLV

BCAS0360  168 TKQPQFARATTVGVSAGSYGALRQTLDTTGPVTQ--SLAYRFVAMNENNGSFRDTVSSKR
PA4837    168 TKKPQAERFARLHASAGSWDRYRSTLDLNTPLDEEGDLLYRMNLAVEDSKGFRDYADGQR

BCAS0360  226 YLFSPSFTWDIGADTTLHYEFESARQRAPLDRGVLAVNGQLGVIPASRFLGEPRDGDYDV
PA4837    228 LLVAPSISWQLDPDTSLLVEAEVVRNRQVFDRGTVAPHNHLGSLPRSRFFGEPDDGKIDN

BCAS0360  286 RNTGHQFTLEHRIDSAWSINAGVAQRKTDLSGRSSEAFALQPDGRTLWRRYRQVAFHSND
PA4837    288 NNETLQATLRHHFNEQWSLRLASHYKHGHLDGYASENSSLAADGYSLRREYRYRDFEWHD

BCAS0360  346 LQGRLETAGSFRTGGIGHTLVMGVDAYRFNYDQFVTRSTPTAAAPYAIDIFDPVYGQPAP
PA4837    348 SITQLDLLGDLHTGSIRHQLLMGLEYERYHNDELILRSIPS-RNPYAIDIRRPVYGQPKP

BCAS0360  406 TPRTATNLLERDDGQGVYAQDTLAFGPHWKILAGLRWDRFHQSIDN------RLKGVTTS
PA4837    407 PFGRDDRNHEEVDAMAINLQDQIEFSEKWRGLLGVRFDRYRQDMNATRLNNGRFRETSSQ

BCAS0360  460 QLQTALSPRIGVVYEMSPAWSFYANTAYSFRPNNGADINGRAFDPEKGHGYEAGAKWAG-
PA4837    467 QTQRAATPRIGVLYQATPEVGLFANASKSFKPNGGTDMAGKAFDPEEGRGYEAGVKLDLL

BCAS0360  519 -ARSLTTVSAFYVTKRNVLTADPANAGFSRAAGEVRSRGIEFEWSGDLGHGLRGLANLAY
PA4837    527 DGRLGMTLAAFHLKKKNVLTADPSNPGYQQTAGEARSQGFDLQFSGQLTEQLRLIGAYAY

BCAS0360  578 VDAEVTRDAVLASGARLVDVPRLSGSALLMYETTLPFADKAGAGAGVIYVGRRAGNIANT
PA4837    587 IDAEVTKDENIARGSRLLNVPKHSGSLMGVYEFREGWLHGADAGAAVNYVGERAGDSS--

BCAS0360  638 QDGFELPAYATVQLNGYLQVNKHLRASVVLNNLFNRTTYVSSYNSLWVTPGAPRSLFASL
PA4837    645 DSGFELPAYTTVDLLARYPLASNATLGVNVNNLFDRRYYERSYNNVWVAPGEPRNLTMSL

BCAS0360  698 AYSF
PA4837    705 TLNY
```

Figure 3.3: Alignment of CntO and the putative TBDR, BCAS0360/I35_RS31880
Amino acid sequences of CntO (PA4837) from *P.* aeruginosa PAOI were aligned with the putative TBDR, BCAS0360/I35_RS31880 from *B. cenocepacia* H111 by ClustalW and identical or similar amino acids were highlighted using BOXSHADE. White font with black shading indicates identical residue (41 %) at the corresponding position in both sequences and white font with grey shading indicates similar residues at the corresponding position in both sequences. Protein designations are indicated on the left.

```
PA0781      1 MSSSGLFPSRPLWPLTPLALACLIV----SGETLGADGRPS----ELPSQVITANPLGNE
BCAM1571    1 ---MRDLPRLPLRPLSSLSLMLFAAVAHAQTDAPGASGTPANASAPLAPIFVTANPLGDT

PA0781     53 SPATPSSVLEGDELTLRQKGSLGETLNGLPGVSSTYFGPGASRPVIRGMDGDRIRLLRNG
BCAM1571   58 ELIAPLVQLSGDALTRRQADSLGETLNGLPGVSTTTYGPMVGRPIIRGMDGDRIRLLQNG

PA0781    113 VGALDASSLSYDHAVPEDPNSVERLEVVRGPAALLYGGNAIGGVVNSFDNRIPSEPVDGI
BCAM1571  118 VAAYDASSLSYDHAVPQDPLSIERVEIVRGPAALLYGGNAVGGVVNIIDNRIPREAIQGV

PA0781    173 HGSGELRYGGADTTRSRSGALEAGDGNFALHVDAASREFNDVRIPGYAHSSRQRQIDGDT
BCAM1571  178 TGALDARYGGANSVRAGAAQVEGGNGRFAFHVDAFDRETSKLRIPGYARSSQQRAIDGPD

PA0781    233 G---KHRVQNSDGRQDGGAVGGSYHWEHGYAGLSYSGYDSNYGSPAEDDVRLKMQQDRYA
BCAM1571  238 TPQPEGNVPNSDGRVHGGAVGASYTWADGFAGLSYSGYESNYGSVAESDVRLRMRQERLA

PA0781    290 FASEIRDLEGPFTSLKLDAAYTKYEHKEIEDGETGTTFKNEGYEGRIEARHRPLGPLNGV
BCAM1571  298 LASEVRNLSGPFTTLKFDFAYTDYRHKEIDNGETATTFRNRGYEARIEARHRKIGPFEGA

PA0781    350 VGAQFANSRFSALGEEAFVPHTETDSAALFALEEWKLSDRLDLSFGARLEHTRVDPDAKG
BCAM1571  358 IGVQFGQNTFSALGDEMLVPSTRTNSVALFGLEEWQVVPALKLSLGGRFEHVKVDPDPAG

PA0781    410 NERFAENDGSQSFTTGSLSTGAVYKLTPIWSLAATLSYTERAPTFYELYANGPHAATGTY
BCAM1571  418 VEKFAGAQ-PRDFNAGSLSAGALFTLTPVWSIAANVAYTERAPTFYELYSNGPHDATGQF

PA0781    470 EVGDADADKEKAVSTDLALRFDNGVHKGSVGVFYSRFSNYIGLLASGRHRNEEGEVVAAG
BCAM1571  477 LIGNPNASKEKAVSTDLSLRYASGPNRGSVGVFYNRFSNYLTEYNIGRVVDDDGEPVAPG

PA0781    530 DDEALPEYIYSGVRADFYGVEAQDRIHLLESPYGNFDLELSGDYTRAKNKDTGEPLPRIA
BCAM1571  537 TDGSLNEAIYRGVRAEFYGIELDGKWRAFSRRGHTVDLELTADYTHARNVDTGQPLPRIA

PA0781    590 PLRLNTALIWELQQWQARVDVEHAASQHRVPEEELSTDGYTILGASLGYNFDLGESRWLA
BCAM1571  597 PLRATLAADYGYGPEGARAQVTHAWSQHRVPDDDFSTDGYTSLGVMLTYKFRVGPTHWLA

PA0781    650 FVKGTNLTNQTVRYASSILRDRVPAAGRGIEAGVKVAF
BCAM1571  657 YLRGDNLTNQEIRYSISVVRGFAPQGGRSVMAGLRTTF
```

Figure 3.4: Alignment of ZnuD and the putative TBDR, BCAM1571/I35_RS23575
Amino acid sequences of ZnuD (PA0781) from *P.* aeruginosa PAOI were aligned with the putative TBDR, BCAM1571/I35_RS23575 from *B. cenocepacia* H111 by ClustalW and identical or similar amino acids were highlighted using BOXSHADE. White font with black shading indicates identical residue (57 %) at the corresponding position in both sequences and white font with grey shading indicates similar residues at the corresponding position in both sequences. Protein designations are indicated on the left.

```
PA4514      1 MSRQSTDTAVSSQRLLASAIGVA-ITAIAAPQAAQADEAGQKKTDKDRVLSLDAATIVGE
BCAM2007    1 MKSRPDELKLGKFTTLCSVLAASPAFADGTPPAAPASTEG------------HLAPIEIQ

PA4514     60 QQDETTYNVDRSASKKYTAPLLDTPKTVTVIPQQVIKDTGALTLADALRTTPGITFGAGE
BCAM2007   49 GKTEHSYKADFSASAKETAPLVDTPKSVTVIPQELIQSSGAATLTEALRTVPGITFGAGE

PA4514    120 GGNPAGDRPFIRGFNAESDTFLDGMRDVASQTREVFNVEQIEVSKGPGSAYTGAGSTGGS
BCAM2007  109 GGNPLGDRPFIRGYDTQGSMFVDGMRDTGATTREIFNTERVEITKGSDGAYGGRGGAGGS

PA4514    180 LNLISKTAKQDNFTDAGFTWGSDQTRRTTLDVNRMIGDNAAFRLNLMKHDAHVAGRDEVS
BCAM2007  169 INLITKAPHLGTTAAASAGLGIDRYRRFTADGNWQFADHAAFRLNLMSHNNDVAGRDAVN

PA4514    240 VSRWGVAPTVTFGFDTPTRATLSYYHLSTDDMPDYGLPLTNVNRS---KANPSKPASVDR
BCAM2007  229 NERWGVAPSIAFGLGTSTRVTASYYHLQTDDMPDGGIPYFYTTSNKPANVDTIYPAPVDR

PA4514    297 DNFYGLKDRDYRKSTTDSGTFRIEHDLNDNLTLSNSTRLVRTTLDYIVSNPDDSRGNVAN
BCAM2007  289 HNFYGLIDRDFRKTTSDISTIKIEHDITPNLTVRNTTRYTESTQDYIWTQPDDSQGNVVN

PA4514    357 GYVYRSAKSRNSISKGWVNQTDLKANFETGFIKHTLVTGLEFSYEDVHNRPYAITSGGGA
BCAM2007  349 GKVWRRNNNRNSSINSLANLTILFGEFRTGPFKHSFTTGIELSREWGKRDSYTVATDKG-

PA4514    417 GNTCNAR--LLASGDCTSLNRPTPGDNWTGSITDGLAYTDTDTKTSAAYVFDTLKLSEQW
BCAM2007  408 -TICQKGIGAPSGYNCTSLWSPNPNDPWAGSITRNNDYAHARTTTKSIYGFDTIEITPRW

PA4514    475 ELNLGLRYDDFDTKSSGYQTAGRNGPAGYFKRENNSHFWNYQTGLVYKPAPNGSIYLAWS
BCAM2007  467 QVNAGVRVDDYSTRFTDTKAN---GGKTY---TRDDTLFNWQAGLVFKPAQNGSIYASYA

PA4514    535 TSSNPTGETGGEGQADI---------SVGNNGLDPERNRNLELGTKWAFFDDALSLNAAL
BCAM2007  521 TSSTPAGMLLGEGSETQSLTPGRGGVGPNADQLSPEKNRSIELGTKWNVLNDKLSLTAAL

PA4514    586 FRTDKTNARVASPDVSTLQVLDGEQRVQGVELGFNGKLTEKWKVFGGYTYLDSEIRKSTV
BCAM2007  581 FQIDTTNARVTLPNNQ--YAVVGNKRVQGLELGLAGQVTKQWQVFGGYTYVKSELRDNGK

PA4514    646 -KSDEGNKMPQTAQNNFTLWITYDLLQNFTIGGGTTYVDKQYGNTANSTYIPSYWRYDAM
BCAM2007  639 DTANNGNRFPNTPKHSLIMWSNYDVTPKFTVGGGAFYMSEVFGDPANLRAVPSYWRFDAM

PA4514    705 ASYKVSKNVDLQLNVQNLTDKRYFDQVYSTHMAHVAPGRTALLGVNFHF
BCAM2007  699 AQYRINKKLDLQLNVNNLFNRTYFDQAYPAHYASIAPGRSAFVTLNARY
```

Figure 3.5: Alignment of PiuA and the putative TBDR, BCAM2007/I35_RS25625

Amino acid sequences of PiuA (PA4514) from *P.* aeruginosa PAOI were aligned with the putative TBDR, BCAM2007/I35_RS25625 from *B. cenocepacia* H111 by ClustalW and identical or similar amino acids were highlighted using BOXSHADE. White font with black shading indicates identical residue (48 %) at the corresponding position in both sequences and white font with grey shading indicates similar residues at the corresponding position in both sequences. Protein designations are indicated on the left.

```
PA2911      1 ----------------MPRFS-----RLRTEPFA--LGLSTSLLLVPPALAET-------
BCAL1345    1 MTRTGHTPARGERRHAAPRRNTGAWRARAARSCTTLLGCA----MATTGALAADAAASAP
BCAM0491    1 -------------------------------MKFKSMLPAAVLAALSPAGQAHAQE---RG

PA2911     31 -EEAALALPSQLVSVRQDPAELDHIDLATPVSAGSRLGLSALDTPASTSSISGEEVRRRN
BCAL1345   57 DDRHALPAINVTAS------SASADPLTQPLETGSRLGLASLDTPASVETVTADTIEARG
BCAM0491   28 VDGAGATLAPILVD------AQKAPALTQPLDTGSHLGLSPLETPASVEQINRATLDTRG

PA2911     90 NPSVQAAVTRSPGISFIGTPGDGGTGLSARGFSGHASVMQLFDGTRLYTGMGTVNFPSDP
BCAL1345  111 DRTVLDAVTRTAGFASAIAPGTGGTALSVRGFSGQESVMTLLDGVRLMPAAGTITFPFDT
BCAM0491   82 DNSIIDAVSRAAGISASPHPGNGNSELAARGFVGASSVTQLYDGMRPYGAIG-VTFPFDT

PA2911    150 WMVERIDVTRGPASVLYGEGATGAVINVVPKKPFAGEIRNHLRLGYGSYDNRQLALDSGG
BCAL1345  171 WSVARIEVTRGPASVLYGEGAIGGGVNVVPKRPQRTR-ETTLQVGVGPDGAKRFAFDTTG
BCAM0491  141 WSVDHIDVTRGPASVIYGEGAIGGVVNIVPKKPTRTPIRNELQVGGGTEGTARAAFGSGG

PA2911    210 SLTDSLSYRLNLNQQQSHGWIDRGDSRNLGISAALRWQASDDLAFTLAHDYGDQEPMNDF
BCAL1345  230 ALGPRLSYRFYASDARANGLAERADTHTTAIGGALTFDVSPRLTLTLDYDYGRQMPATYY
BCAM0491  201 AINDKLSYRFDVSGNRSSNWVDRGDSRNLSVSGALRYDVTPDLYVTASYAQGFMHPMQYF

PA2911    270 GTPLVGGKYHKRLREKNYNVRNDVQRYNDQWTRLTSDWSLSDSVTASNQLYYIKARRHWR
BCAL1345  290 GVPAPNGVLDPSLRKLNYTVGDATISYYDQWTRLSASYRPIAGVTIDNQLYYLTSNRHWR
BCAM0491  261 GVPLVDGARDRALDKKNYNVGDADIAFRDSWATVSANWQPSDALNVTSTLYRMKSNRHWK

PA2911    330 NAETYEWDVPREELLRRDYLRISHEQEQIGDRQTFAFQHALFGLDSRTLVGAEYNRIRFR
BCAL1345  350 NAESYVLDSATARVTRGDYLDIGHHQRQIGDRLSARFDGMLFGRANRFVVGTEFSQTTFS
BCAM0491  321 DAEYYTYLPSSAQARRSSYTEIFHDQEQYGNVTTATVGSALFGMRNTFSAGVEFNHTTFQ

PA2911    390 LSNNSPYTDVGGDYIDPWHPAPGYFESRSPYRPHSRSQTRTFALFAENRLQLNERLSLVT
BCAL1345  410 GTNNSPYG--GETTVPVHGFDPGVFTSPDPTVPQFSTRARQAAVFAENRLEVLPRLAWVS
BCAM0491  381 HDNNSPYA--GTSTVDPFNVDPGSFLNTAGTFPKYRSQSNQYALFAENRLEITPRWSVIG

PA2911    450 GVRRDQNHIDRDDLRAGTRSDRSLQGGNWRAGLVFALTPELSLYGQYSTSEDGVSNLITL
BCAL1345  468 GLRYDHIAFSREQAATGAGFDKRFANIGWRTGFVFDLAPMFSAYAQYTTGAEGVGSLVTL
BCAM0491  439 GLRYDHASVNRDDLVNGGAFTKVFANTGWRLGTVYDVRPGLAVYGQYSVAADPVSSLLSL

PA2911    510 NAAQQQMDLTHSKQTEVGLKQLFPDGRGEWTLAAYHIVKKKLLSANPLPPHDAQQVGQQS
BCAL1345  528 SASQMNDRLATGAQWEAGLKQTLLDGRAYWTVAVYDITKRNLLSTDPFNPALRQQVGRQS
BCAM0491  499 NASKANFTLATGRQIEIGVKQSFLDGKAEWTLAAYRIVKRNLLLADPVNPNQSIQVGQQS

PA2911    570 SDGLEASLELNLAQDWRLSANAALVRAEYDDFDETIDGQTYSRNGNRPRNVPRRTANLWL
BCAL1345  588 SRGVELTGGARLPHGWTIDANVALLRARYDAFNQTVGGATVSRAGNVPSGVPQQTANLWV
BCAM0491  559 SRGLEATVGAEIAKDWRVDANVSILRAKYDDFQQSSGGTTVSRAGNVPVSVPQRLANLWI

PA2911    630 DKSFAETLRVGAGLRYVDRRYADAANQASLPGYTVVDANLGWRVRPDLTLGLELYNLFDR
BCAL1345  648 GWAFAERWQANAGVRYVGATYGDDANRVQVPSYTVFDASLRWQPTSRTELALYLRNLANR
BCAM0491  619 SWRFAPDWTGIAGVKYVGKRFADTANQLVMPSYTTVDLGLAWKPRKDTTITARAYNVFNR

PA2911    690 QYALADNNNGQQWIVGQPRSFNVTADFSF
BCAL1345  708 TYAVTTSNGGEQWLLGPSRSAELVATMRF
BCAM0491  679 RYVQSAYYNETQYLLGNDRRVEVLANYRF
```

Figure 3.6: Alignment of PA2911 and the putative TBDRs, BCAL1345/I35_RS06170 and BCAM0491/I35_RS06170

Amino acid sequences of (PA2911) from *P.* aeruginosa PAOI were aligned with the putative TBDR, BCAL1345/I35_RS06170 and BCAM0491/I35_RS06170 from *B. cenocepacia* H111 by ClustalW and identical or similar amino acids were highlighted using BOXSHADE. White font with black shading indicates identical residue (43 %) at the corresponding position in both sequences and white font with grey shading indicates similar residues at the corresponding position in both sequences. Protein designations are indicated on the left.

```
BCAM0948    1 LPPVEVVAA---------PLSTP----------LVVVT--DPKAPRQPL-----PASDG
BCAM1571    1 LAPIFVTAN---------PLGDT----------ELIAP--TVQLSGDALTR--RQADSL
BCAL1777    1 LDKFEVTGS--AAGGQTVKK---------LIRTSDKVGHTEVQVITAKEIQQ--SGYTTV
BCAM0564    1 LGTVTVTA--RGAAARETN--------ARRRKESIQDVPVAVTALSGDAIRN--NELRVI
BCAL3001    1 LSAVSVTAASATPAGD---T--------AQRQPVDPDTPAVVTSITREQIDA--HTNVIT
BCAM2367    1 LPAVVVVGT--T--------------PLPGIGTPISKVPANVQTVRAAELDA--QHRAIL
BCAM1593    1 LPTISVTDT--RHLPES-----------------FDRRYASTQVLTRDDLDRLSPADPSI
BCAM2626    1 LDPVTVTATAAASTRGDAAL---------RTATAASRTAASVSVITDEDLEA--QQATNI
BCAL0116    1 LPALNITAA--HDSPQ---HITDTISTGALGTRRQLDTPFSTTIVTSEELEA--RQPYKL
BCAL2281    1 LPGDL--AP--TYAGG---QVARGADFGVLGRQKASDVPFSMTTYISKLIED--QQARIL
BCAM2224    1 LKAIAVNAS--RSVAD----DP-SVATVGKMSLAIREIPQSVSVTIRERIDQ--QNLFSL
BCAM0491    1 LA--PILVD--AQKAP---AITQPLDTGSHLGLSPLETPASVEQINRATLDT--RGDNSI
BCAL1345    1 LPAINVTAS--SASAD---PITQPLETGSRLGLASLDTPASVETVTADTIEA--RGDRTV
BCAL1371    1 LPTINVRSS--ALRAESY-RAPKEAG-VLRSDIPLLDTAQAVNIVPAQVLRD--QRPRNL
BCAM2439    1 LPAINVSAS--AAVDPTVGYQPRTTSIAGGDDRAIKEIPQSVAVVSSSVMQD--QQARSL
BCAS0333    1 LPPIDVRG---PADASSVGLVARRTVTGTKTDTPIDEIPQTINIVTAQQIEM--TGAADL
BCAL1700    1 LPAITVNAA--SAGDGTVGLVAKRSTTGTKTDTPISEIPQTINVVTAQQIEM--TGATDV
BCAM1187    1 LPTIAVQSS--ALSDM----QVKRS-PSYKFTAPLLDTPRSVTVIPEQLIKE--KNVTSF
BCAM2007    1 LAPIEIQGK--TEHSY----KADFS-ASAKFTAPIVDTPKSVTVIPQELIQS--SGAAIL
BCAM0360    1 LPTIEISAQ--RATAP---FRTRESTSATRSEADVMEIPFAVSSVDTKLIQT--VAATRG
BCAM0499    1 LPAISVNAA--AEHGS---YDGGHSRAATKTDMSIMDVPQTVNVVPHAVIED--QNATSL
BCAL1709    1 LPAVEVRSR--RHPND---PRAESVSTATRTASDPRDVPQTIDSVSVEETLS--YGGRIL

BCAM0948   34 ADYLK-TIPGFISIRS------------GGTNGDPVLRGMFGSR------------LNIL
BCAM1571   37 GETLN-GIPGVSTTTY------------GPMVGRPIIRGMDGDR------------IRIL
BCAL1777   56 ADFLRSTSANSASSWG-----QTTMNSSAPGGAGMAURGLSEKY------------TLVL
BCAM0564   57 NDVTK-YVPNFIGQST-----------EGRERPRWFLRGVGSND----PSDLSLSPIGVY
BCAL3001   55 EDALK-YAPNLMVRKR----------YIGDRNSIFAGRDFNELQ----SAR-----GLVY
BCAM2367   43 ADFFAANLPSVTISDA----------QGNPYQADVNYRGFAASPLLGTPQG-----LSVF
BCAM1593   42 TQALA-TIPGVTVTQN----------GGPGSSASVSIRGSSASQ------------VAVF
BCAM2626   59 KDALR-YEPGITVRRTAYRPGSAALGGGRDGDSSINIRGLEGNR------------VLLM
BCAL0116   54 GDVFA-NDASVSDNSG----------AYSAWASYMTVRGMQLDW------Q-----NGYK
BCAL2281   52 ADVLD-NDPAVRSASG-----------YGNFSQVFVIRGFALAG------D------DVS
BCAM2224   52 DEVMQ-QSAGVTVQPY-----------VLL-TTAYFVRGFKVDS--------------FE
BCAM0491   52 IDAVS-RAAGISASPH-----------PGNGNSELAARGFVGAS------S-----VTQL
BCAL1345   54 LDAVT-RTAGFASAIA-----------PGTGGTALSVRGFSGQE------S-----VMTL
BCAL1371   55 DDALG-NVSGITQGNT----------LAGTQDT-IMKRGFGGNR------D-----GSIM
BCAM2439   57 DDVLG-NISGVTQTNT----------LGGTRDA-FIKRGFGSNN------D-----GSVL
BCAS0333   56 NQALR-YVPGFATFGA-----------DSRTDWYAALRGFTPT---------------LY
BCAL1700   57 NAALR-YVPGFSSYGS-----------DNRSDWYAALRGFTPT---------------AY
BCAM1187   52 ADALR-SVPGITFLGG-------DAAANPSADR-PVIRGFESRN-------------SIF
BCAM2007   52 TEALR-TVPGITFGAG-------E-GGNPLGDR-PFIRGYDTQG-------------SVF
BCAM0360   54 DDLYD-WVAGVSRQNN----------FGGLWDN-YAVRGFAGDG---NTSG-----TDYL
BCAM0499   54 QDALR-NVPGVGFSV-----------GDGQRDQ-ITIRGFNSIT-------------DQY
BCAL1709   54 ADALA-GVPGVSNT------------SDTRFDS-FRIRGFSSAG-------------DIL

BCAM0948   69 ANGMPTLGACPNR----MDAPTSYIAPESYDNVTVVKGPQTVLYGPGAS----AGTVLFE
BCAM1571   72 QNGVAAYDASSLS----YDHA-VPQDPLSIERVEIVRGPAALLYGGNAV----GGVVNT-
BCAL1777   99 VDGQRVANYAQSVNFTDTFFDVNAIPLNMVERVEIVKTGAVSVYGSDAI----AGVVNII
BCAM0564  101 FDDVYINSVFGQ-----------GFPLFDLDHIEVLRGPQGTLNGKNTV----GGALSIT
BCAL3001   95 ADGVLLSNLLGSSYA--YPPRWSLIPPDDIARVDVLYGPFSALYPGNSI----GSTVLIT
BCAM2367   88 VDGVRVNEPFGD------VVNWDILPMQAIDRVQLIPGSNP-VYGLNTL----GGAIAIT
BCAM1593   79 IDGIRIGSPTTG------IAPWADLPTDAFERVEVISGPAAASFGNNAM----GGVVQLF
BCAM2626  106 EDGIRLPNAFSFGPL--EAGRGDYADLDTLKRIEILRGPASALYGSDGL----TGAVNFI
BCAL0116   92 IDGLPFVTY------------GITMPYEQLDRVEILKGLGGFLYGFVTP----GGVVNYV
BCAL2281   88 LNGLYGVTP------------RQLVQTDAVERVVVEKGANAFLNGASPNGSAVGGGVNIQ
BCAM2224   85 FDGVPVVIG-DMA--------SAPQDISVYERVEILRGANGILHGSGNP----AATVNLV
BCAM0491   89 YDGMRPYGAIG-V--------TFPFDTWSVDHIDVLRGPASVIYGPGAI----GGVVNIV
BCAL1345   91 LDGVRLMPAAGTI--------TFPFDTWSVARIEVLRGPASVLYGPGAI----GGGVNVV
BCAL1371   92 QNGMPLVQG--------------RAFNAATDSVEVLKGPTSLLYGLMDP----GGVVNVV
BCAM2439   94 VDGVRTPVL---------------HSYLATIDRVEVLKGPASLLYGMQDP----GGVINLV
BCAS0333   89 VDGLPAPNTAVIA--------NWRVDPYTIDSIAVLRGPTSVLYGAGEP----GAIVDAH
BCAL1700   90 VNGLQVPNTINLA--------SWRVDPYMIDSISVLRGPTSVLYGAGDP----GAIIDVH
BCAM1187   90 VDGMR--DS---G--------LQNRETFAVEQISVIKGPDSVYAGRGSV----GGSIDIV
BCAM2007   89 VDGMR--DT---G--------ATTREIFNTERVEIIKGSDGAYGGRGGA----GGSINLI
BCAM0360   94 VNGFSWNRG---M--------SVPRDTVNLERMEVLKGPASALYGRGDP----GGIISYT
BCAM0499   88 VDGIR--DD---A--------LYYRDLSNVDRVEVLKGPAAVLYGRGSA----GGIVNRV
BCAL1709   87 LDGMR--DD---A--------QYVRSLGNIERVEVLKGPAAALYGRGSG----GGVINRI
```

```
BCAM0948  121 RVTERFERPGMRFEG------SLVGGSFGR------NDQNIDLTAGTPDVYG---RVTAN
BCAM1571  122 -IDNRIPREAIQGVT------GALDARYGG------AN---SVRAGAAQVEG---GNGRF
BCAL1777  155 TKKNFQGL---QIDG------QLGKA--QH--PGD-GQGNFSVLAGFGD-----LNSDRF
BCAM0564  146 SQKETFDV---SGYG------KIGLGQYNS------RLAEAAIGGPIG-------KNDVL
BCAL3001  149 TTREEQLEA--SLST-QFFTQ--------RYHDG--YGFADSLGGNHQT-ARIANRVGRF
BCAM2367  137 TKNGRSNP---GGEA------EVSGGSWGR------KTASVEQGGTIG---------SNL
BCAM1593  129 TPRAAQQPN--QTTV------SFGGGINKTFDTRFRTSGTVPSTGPLA-------ALGGL
BCAM2626  160 TKDERDLLS--VYNKPYYFSFRPSYDSTDR-----SIGATVSAAGGNDRVQGMIIADGRR
BCAL0116  136 TKQEGAEP---VRSV------DIGYRSTNV------WTEHVDLGQRFG-------PDHMF
BCAL2281  136 LKHADDKP---LTRV------TVDGATSGS------LGTHVDLGRRFG-------SEGQF
BCAM2224  132 RKRPQYQF---SAHA------TASVGSWDR------YRAEADIGGPIN-------AAGTV
BCAM0491  136 PKKETRTPI--RNEL------QVGGGIEGT------ARAAFGSGGAIN---------DKL
BCAL1345  139 PKREQRTR---ETTL------QVGVGPDGA------KRFAFDTTGALG---------PRL
BCAL1371  134 TKQPQLVR---YNAI------SLGASIFGHGKN--GGSATFDSTGPVG--------DSRL
BCAM2439  136 TKKPEDTF---GGSI------SAS----RTSHR--GSNAQFDLTGPLGR--PGQVAGGTL
BCAS0333  137 TKLADGER---VREA------GVQIGNDAR------KQAMLDVGDRLD-------PDGRY
BCAL1700  138 TKLADGER---VREA------GVQIGNYAR------KQFMIDVGDKLD-------PDGKY
BCAM1187  133 TKTPQNDN---FINS------SIGFGIDGY------KRATVDANRKIN---------DTT
BCAM2007  132 TKAPHLGT---TAAA------SAGLGIDRY------RRFTADGNWQFA---------DHA
BCAM0360  139 TKQEQFAR---ATTV------GVSAGSYGA------LRQTLDTTGPVT---------QSL
BCAM0499  131 LKRPQANP---VNDV------GVTLGIRGE------RRGEFDLGWNPN---------DAA
BCAL1709  130 TKQPLPEN---FGHV------SATTGSYGR------LGASVDLNRMIS---------SAW

BCAM0948  166 HAHSQDYQDGNG--NTVPSQWDKW---------NADAALGWT----PDDHIRVEL-----
BCAM1571  163 AEHVDAFDRETS--KLRIPGYARSSQQRAIDGPDTPQPEGNV----PNSDGRVHGGAVGA
BCAL1777  196 NVTAAAS-------YVRDSGS-----TLGDRDMTSAQDFTQY-----PGGLAAPLGPNQQ
BCAM0564  184 AARVSVYHENAD--SEYTNTV-----QQGRFGGFHDNAVREQVLAVPTSDTDFLFNIHG-
BCAL3001  195 WPALSLDRLENN----------------GQPMQYASPASAYN----PRLGAAVPVTGAA-
BCAM2367  173 DYYATANVANDG--GWADHN--------ASRVRQAFGKDRYT-----DADTTLSIAAGGA
BCAM1593  174 TYSIGLHDYNTA-----------------------------------GIDATRPFFYGHE
BCAM2626  213 CHEVDTRGGNNTASTLRTTSN-----PQDVYSESILGKDVLT----PTTRDTIKFTAETV
BCAL0116  174 CARLNATHEEGK--TYNDG---------NIRRDSVSLALQAN----LTRDLSVSFGALYQ
BCAL2281  174 CVRVNQSISGGD--TAVDD---------ERRRSNVTAVSLDW----RGDTLRLSGDFLYQ
BCAM2224  170 RSRLVAAYEDRH--FEYDHA--------KQDTRSIYSVTEVD----VTRDTLLTFGAQYQ
BCAM0491  173 SYRFDVSGNRSS--NWVDRG--------DSRNLSVSGAIRYD----VTPDLYVTASYAQG
BCAL1345  175 SYRFYASDARAN--GLAERA--------DTHTTAIGGALTFD----VSPRLTLTLDYDYG
BCAL1371  175 AYRLIVDQSSEQ--YWRNFG--------EYRQTFVAPSLAWY-----GRDTQVAVSYQYR
BCAM2439  179 AERLTGEYDTSR--YWRSFG--------RERNALIAPALSWH-----DANTSIDVSYQYV
BCAS0333  175 AYRFVGVARDGN--AVTGPN--------GDRRVALAPSFRWR----PNADTSLTFSATFL
BCAL1700  176 AYRFVGVARDGN--ALTGPN--------NDQRVALAPSFRWR----PDADTSLTLSATYL
BCAM1187  169 AVRLNVMGHDAN-QAGRNDV--------YNKRWGVAPSIVFG----LNTPTTVTVSYYHM
BCAM2007  168 AERLNLMSHNND-VAGRDAV--------NNERWGVAPSIAFG----LGTSTRVTASYYHL
BCAM0360  175 AYRFVAMNENNG--SERDTV--------SSKRYLFSPSFTWD----IGADTTLHYEFESA
BCAM0499  167 RERITGAAENSN--SERDRF--------QLNRQATAPSAQFK----LDRDTVLNVEFDYL
BCAL1709  166 SMRLNAGREHAG--SERDHV--------DGTRQFVAPSIKWH----DARRS-WLLQFEYD

BCAM0948  206 TAG-----------------------------TGDGVARYAGRGMD-------------
BCAM1571  217 SYT-----------------------------WADGDAGLSYSGYESN-YGSVAES--D
BCAL1777  239 SYWSLADGSRVPLSPC---PPGSKTSATN-------CTYNPA-------ASTSLVPSTTR
BCAM0564  236 --RNYTGGG-NAWHAEG---AGRGG------T-NQFGFVGSS------------DPYTVS
BCAL3001  234 -----TDIG----------PNGKPRT-----------IVGAQTIERT-----EQLNETVR
BCAM2367  218 DNTLSGTQT-IPRSF---------LD-------NRKQAYTYPDRNRN-----SAGYLTLS
BCAM1593  199 DGRN-------PYHAQ-----------------DLDARIG--------YARDNWSISTFA
BCAM2626  264 QRRVSTD-----------------VLS----AI-NAPTTIGLTTH-------DRLERNRFS
BCAL0116  219 DRRT--TGQ-TPSIFTG----SYPGGALPATISGGSTNLGGKDQ----YLNTNLQLYTAG
BCAL2281  219 RQRI--DNG-RPIVLVS----GSPLPAVPSATHN----YAQPWS----FSELEDTVGIVR
BCAM2224  216 TTSSVPDMSGVPMARD-----GSSL-----GL-SRSTFLDTAWGRFNW----DTTRAFAS
BCAM0491  219 FMHPMQYFG-VPLVDGARDRALDKKN----------YNVGDADIAFR----DSWATV--S
BCAL1345  221 RQMPATYYG-VPAPNGVLDPSLRKLN----------YTVGDATISYY----DQWTRL--S
BCAL1371  220 KFHSPFDRGTALDPRT-----NAPLD-----I-PARRRIDEPFN----NMDGESHLAQLS
BCAM2439  224 DYTMPFDRGTVLVNG-------RPDD-----A-LRYRRYEEAWS----QSSGIQETLRTR
BCAS0333  221 QDSGDISSNFIPASGT-------VLPNPNGRL-SQDLYMGDPSFNDYRK--KQWS-LGYA
BCAL1700  222 QDWGDISSNFIPAQGT-------VLPNPNGQI-NKDIYEGDGNFNYYRK--KQWS-IGYQ
BCAM1187  216 NSYDMPDFS-VPFRAS---------GGTPVPT-DRGQFFGLNTRDYR-Y--GQTDTGEIR
BCAM2007  215 QTDDMPDGG-IPYFYTTSNKPANVDTIYPAPV-DRHNFYGLIDRDFR-K--TTSDISTIK
BCAM0360  221 RQRAPLDRG-VLAVNGQ-----------LGVI-PASRFLGEPRDGDY---DVRNTGHQFT
BCAM0499  213 HDRRTSDQG-IPAYR------GRPVD-----V-PINTYYGSADGGNSSYNDISAKSATVS
BCAL1709  211 TYRRVPDRG-VPAPVAAVDAAGKPLAFSLPSA-PRATFFGAAGRDTIRDETMNWRS---V
```

```
BCAM0948  223 -GAHF-------------------RRETFGLSFDK-------------------------
BCAM1571  244 VRLRM-------------------RQERLALASEV-------------------------
BCAL1777  282 LNAKVRATFKIDDNTQAYAGFWVSRDETVQLQGPASISSTTNVYNPSTGSVSPLPRTVPV
BCAM0564  271 LNAPS--------------------------SDHIS------------------------
BCAL3001  263 MGYAF--------------------------TDHVD------------------------
BCAM2367  256 GERFF--------------------------GEH--------------------------
BCAM1593  227 LYHRS----DLSYDNSGYAN----RELDHQLTTGVA------------------------
BCAM2626  296 VDYDF--------------------------RDDAL------------------------
BCAL0116  268 LQYQL--------------------------ALD--------------------------
BCAL2281  264 AEYDF--------------------------LPA--------------------------
BCAM2224  261 VEQKL--------------------------GAG--------------------------
BCAM0491  262 ANWQP--------------------------SDA--------------------------
BCAL1345  264 ASYRP--------------------------TAG--------------------------
BCAL1371  265 VDHQF--------------------------NAD--------------------------
BCAM2439  267 IEHRF--------------------------SDA--------------------------
BCAS0333  270 LEHRV--------------------------NAI--------------------------
BCAL1700  271 FERNL--------------------------TPA--------------------------
BCAM1187  262 VEHKL--------------------------NDT--------------------------
BCAM2007  270 IEHDI--------------------------TPN--------------------------
BCAM0360  265 LEHRI--------------------------DSA--------------------------
BCAM0499  260 LDHRF--------------------------NDS--------------------------
BCAL1709  266 FTHAL--------------------------DGD--------------------------

BCAM0948  238 ----------------------------------RHLGDVLD-------RIEARVYYNEA
BCAM1571  260 ----------------------------------RNLSGPFT-------TLKFDFAYTD-
BCAL1777  342 SNPYNPFGVPTAINLTFPGNVVGADTVSTFWMANTGVKGSFDTGRFGAWDWSADYGHSQS
BCAM0564  281 ----------------------TWGTSLTAHW------------------RINPAVSLTSI
BCAL3001  273 ----------------------ATLT-LGHWENHY--------------RQHGETFLRDA
BCAM2367  264 ------------------------------V-----------------ELSGNAYYRHL
BCAM1593  255 ----------------------FHLDITPDT------------------QFDQSFGYAND
BCAM2626  306 ----------------------R-------WFQ----------------TAHVQFYYQDA
BCAL0116  276 ------------------------------W-----------------QLDVAYSYSKA
BCAL2281  272 ------------------------------W-----------------TAYVSA----G
BCAM2224  269 ------------------------------W-----------------KAKVSGEYQSV
BCAM0491  270 -----------------------------L-----------------NVTSTLYRMKS
BCAL1345  272 ------------------------------V-----------------TIDNQLYYLTS
BCAL1371  273 ------------------------------W-----------------SAHVGYSYNRE
BCAM2439  275 ------------------------------W-----------------RVRATYGYGRD
BCAS0333  278 ------------------------------W-----------------TLRQDVRYSHL
BCAL1700  279 ------------------------------W-----------------TFRQNTRLMHL
BCAM1187  270 ------------------------------W-----------------KLKNTTM----
BCAM2007  278 -----------------------------L-----------------TVRNTTR----
BCAM0360  273 ------------------------------W-----------------SINAGVAQRKT
BCAM0499  268 ------------------------------L-----------------SFHGAIR----
BCAL1709  274 ------------------------------W-----------------ELRHTLGVLDL

BCAM0948  257 D-----------------------------HVMDNYTLR--QPDPASSMPMRMA------
BCAM1571  278 -----------------------------------YRHK--EIDNGET-----A------
BCAL1777  402 TVDTTYRNRINVAGLENMLANGTYN----------------FSNPAATPNGLNGVFTDD
BCAM0564  302 T----------------------AFE----GLHRWYQDDEDYSPVDAARSHDRLSS-----
BCAL3001  296 TGNPVYGGNVSIGGQNMTVAPNAFAPQRGDQENWLYALG-LNGRL--DSGWRLSGVVSAY
BCAM2367  276 R--------------------NTNT--SSNNNTDYGS---VDEDG--AIDTVQ-G----S
BCAM1593  275 ------------------------------RQFIYA---DNPAL--ATDQINS------
BCAM2626  321 ------------------------------KQDQYA---FETRG--KLP--------SR
BCAL0116  288 T-----------------------R--RRNESTLYLQDA--A-GN--YTDSRYVGM----
BCAL2281  280 A-----------------------R--HTNEHGDYYTPT-YSSSG--TTGSRLSVP----
BCAM2224  281 R--------------------SDLK--YAG----SFG-A-IDPAT--GAGGRLTG-----
BCAM0491  282 N---------------------------RHWKDAEYYT---YLPSS--AQARRSS------
BCAL1345  284 N---------------------------RHWRNAESYV---LDSAT--ARVTRGD------
BCAL1371  285 T-----------------------YD--ANQL----RTTG-VDPVK--GTMTRSN------
BCAM2439  287 R-----------------------YD--QFIT----RATA-FNSRT--GALTRSS------
BCAS0333  290 S----------------------------LDDATVFGNG-LAPRS--TT----NMMRFAG
BCAL1700  291 S----------------------------LDNASVFANG-FAGDS--LT----DVSRWAG
BCAM1187  278 ---------------------------FGRSTLDYVA---TNPQI--LASNPNMLG--LQ
BCAM2007  286 ---------------------------YTESTQDYIW---TQPDD--SQGNVVNGKVWRR
BCAM0360  285 ------------------------D--LSGRSSEAFA---LQPDG--RTLWR-------R
BCAM0499  276 ----------------------AYD--FSLERKNYVT---YEPIK--TAAHPV---VTLD
BCAL1709  286 R--------------------STFD--NTYVTQSYVA---KPRDY--RHVQRA---RYLQ
```

```
BCAM0948  280 ------------------ADVRRRTVGARAAATFRF--GD-DFK-FV--TGVDAQSNRLD
BCAM1571  290 ------------------TTFRNRGYEARIEARHRK--IG-PFE-GA--IGVQFGQNTF-
BCAL1777  445 DQ--QA-------------ISKVDSVTAKASTSNLFTLPGGPVG-IG--LGTEFRHESST
BCAM0564  332 ------------------------R------QFSQEFRLESPQNDRLSWIVGTHLFTEQLA
BCAL3001  353 DVSRDVLRAASTVQGGAGTLFQGDGTGWRTLDLKAEAPEVKGHT-FT--FGYHYDNYFLR
BCAM2367  304 NA--QST-------------IVTDSYGGSVQLTRLGKLGGMANR-LV--AGVSADVANSS
BCAM1593  293 --------------------QRISTSTSLTHQAHGFHLFGLPLS-GESKLAYDFTREQA-
BCAM2626  337 SR--DNQ-------------YKERTFGGAAFAESGFATGPLAHK-LL--VGLDGSLSRVT
BCAL0116  314 --------------------EDHRFSQWRAMVECKVRTGPFSHQ-IV--LGASWQKQAND
BCAL2281  308 --------------------HKEDAQSAEAGVRGRFTTGPVSHF-VT--AGASFIRIDSQ
BCAM2224  306 -A--AYQ-------------FSSYSRSLDANVQGPVHAFGLTHD-LL--FGVTYANSSSG
BCAM0491  305 YT--EIF-------------HDQEQYGNVTTATVGSALFGMRNT-FS--AGVEFNHTTFQ
BCAL1345  307 YL--DIG-------------HHQRQIGDRLSARFDGMLFGRANR-FV--VGTEFSQTTFS
BCAL1371  308 DA--THG-------------SLSTDSYGIGYVTGKLSLAGMRHD-VQ--VGFDTEYRRIY
BCAM2439  310 DA--NLG-------------RNDSDQIATLGLLGNVTLAGMQHA-IY--VGGEYERQRSF
BCAS0333  315 LF--QLN-------------YSRLDIDN--HAQARFGTGPLEHT-LL--FGAQFDRQTTT
BCAL1700  316 LF--QMN-------------YSRFDIDN--NLEGRFATGPLQHT-LL--LGFQYNRQTAT
BCAM1187  304 AK--SGK-------------YALNGFSNQTEVTGSASLFGMKHT-MT--AGVEFSHEQAR
BCAM2007  314 NN--NRN-------------SSINSLANLTELFGEFRTGPFKHS-FT--TGIELSREWGK
BCAM0360  307 YR--QVA-------------FHSNDLQGRLETAGSFRTGGIGHT-LV--MGVDAYRFNYD
BCAM0499  304 QS--TRQ-------------RTDHGIDGLFELTQKTSLFGMRHE-LL--YGLELSQQQK-
BCAL1709  316 D-------------------MTQLNVQTGVELGGKVATGPALHH-LL--FGIEYGWQKR-

BCAM0948  316 SR-SSM-GQ----------------QNY-----------RDQP---------------WD
BCAM1571  325 ---SAL-GD----------------EML-----------V--------------------
BCAL1777  487 IN-----------------------PQTLAS-QGV--SAP-------------A--NVQT
BCAM0564  363 EQ-----GA-------GGGLPGSPSPAYYH---------------------------LTD
BCAL3001  410 NV---------------TYNTADW-------------------------LAGPTTSLASV
BCAM2367  346 YV--ASSQDASFTDARAAIGIGDFV------------------------------PQTS
BCAM1593  331 -----------------------FLPVDIP--GGV--PTR--------------------
BCAM2626  379 NLRD---GT---------------VPGVGE-------AFPNK----------------AF
BCAL0116  351 --YSANSVF----VPLGAGNLYAPNPYRYESPHGF--IQ--------------Y--RTSE
BCAL2281  345 SAYTMSNAF--------PTTLYDPAPVASP-PTAY--AG--------------GDMNDPG
BCAM2224  347 QMTAPLLGD----VAGTPVNVYRWNPSSVPEPG-I----------------GP---YQQS
BCAM0491  347 HD-NNS-PY----AGTSTVDPFNVDPGSFLN------TAGTF----------------PK
BCAL1345  349 GT-NNS-PY----GGETTVPVHGFDPGVFTS------PDPTV----------------PQ
BCAL1371  350 RK-DMLRQA----V---KTPFSYVDPVYGLLPPSS-TVSA----------------SDSD
BCAM2439  352 RG-DTIRGK----A---TTGFNLYDPVYGLLAPGG-VPNP----------------KQSD
BCAS0333  355 NS-VWLALA----P-----SLDLYHPVYRPVTAAI--------------FSGPTSLGHVD
BCAL1700  356 DS-EWLAAA----P-----TLNLYNPVYTPVTMGV--------------FSDPDATSRTN
BCAM1187  346 YE-GYLVSD----SAGNNIRSNSPCAVVGNCTPLAGGWNPNMPWTGSIVLNGDKGFPGAT
BCAM2007  356 RD-SYTVAT----DKGTICQKGIGAPSGYNCTSLW-SPNPNDPWAGSITRNNDYA-----
BCAM0360  349 QF-VTRSTP----TAAAPYAIDIFDPVYG-----Q-PAPTPRTA--------------TN
BCAM0499  345 -F-DTIYSV----TKVATYDLFNPQPVVL-----PGVPGGTRAK--------------TN
BCAL1709  353 -T-PALWQA----DAA-PVPVTGPDRFAL-----VGST--PRPY--------------AM

BCAM0948  332 AQATMWNAGVFSELTWYA-SDVSRVIGGARVDYASARDKR--AMKRG--MMMSKP-----
BCAM1571  334 PSIRTNSVALFGLEEWQV-VPALKLSLGGRFEHVK-----------------VDP-----
BCAL1777  506 VEGSRNVAAAFYQVDIPI-LRNLTFTQAGRYDHYSDF-----------------------
BCAM0564  384 LTQHTQSAALFGSVKYRF-TDRENYTGGLRYTIERKTINLTGL-QDTGNVTFSDPNSWWS
BCAL3001  430 YRGDTRTQALFGQDAWRF-APGWLATLGLRYERWDAYGGALGNAKGT-LGYADRS-----
BCAM2367  373 AKIRNANVGVYLSDALSL-TPHWTLTLSGRYDWSKARIGDESGVQ-P-LLDGSHV-----
BCAM1593  344 ---NDSAFSIHQSATLGS---VTMFVAG-RHEIV----------A-G--QAV--------
BCAM2626  398 PDIDYTLFGAFVQDQIGY--GRLLVTPGLRFDTYRLSPTENDPLF-T-GKAVSTS-----
BCAL0116  387 IV----QKSLFASDTVQL-TERWSVLAGVRYMNYAQRAFQASG-A-E--DPGYRQ-----
BCAL2281  380 TVIKTWLRSIAVSDTLGFLDDRVLFTIGARRQSISVDNFDYTG-A-V--TNTY-S-----
BCAM2224  383 QQNDISQKGVYGLGRLKL-AEPLTIVLGGRMSWWNQDSL----------GAHYNT-----
BCAM0491  379 YRSQSNQYALFAENRLEI-TPRWSVIGGLRYDHASVNR-DDLV-N-G--GAFTKV-----
BCAL1345  381 FSIRARQAAVFAENRLEV-LPRLAWVSGLRYDHIAFSR-EQAA-T-G--AGFDKR-----
BCAL1371  385 QTDTLHDASAFFQDTVHL-TDKWIVSGGIRYITYNQVAGRGRP-F-T--ANTDLS-----
BCAM2439  387 SRSVVHAYSTIVQDSVKI-TDRLTAVGGLRWENWQQESGMGRP-F-V--FADRSR-----
BCAS0333  391 QYIAMNAFGVYAQDQIRW--RRWTITLGGREDVVNARF-DDRS-A-G--THVQQD-----
BCAL1700  392 TYITMNTFGLYAQDQIKW--NRWTITLGGREDWVNMRQ-DDRA-A-G--TSTKAD-----
BCAM1187  401 TNIRTDTVSAYIFDTVKL-SERWQFNTGLRFDRYDTTG---KQ-A-G-VADLSNT-----
BCAM2007  405 -HARTTTKSIYGFDTIEI-TPRWQVNAGVRVDDYSTRFTDTKA-N-G-GKTYTRD-----
BCAM0360  384 LLERDDGQGVYAQDTLAF-GPHWKILAGLRWDRFHQSI-DNRL-K-G--VTTSQL-----
BCAM0499  380 ASIVVGLAGVYAQDLISL-TEHWKVLAGLRFDYLNQIRHDYTS-S-N--VNLDRT-----
BCAL1709  385 NRHRVSDYALFAQDRVDL-GRAWKILGGLRAERFDVDS-TNAL-N-G--LHARRT-----
```

```
BCAM0948  382 -----NPT----FDDDRTKVLPSGEVRYERDLASLPVTWY--AGICHAERYPDYWELFSA
BCAM1571  371 -----DPAGVEKFAGAQPRDFNAGSLS-AGALFTLTPVWSIAANVAYTERAPTFYELYSN
BCAL1777  542 ----------------------GGAFSPSFALRIQPVQMLTTYASYSRGFRAPTLVENSQA
BCAM0564  442 PSSVSSPLAVS--AQQHQTNTWRAPTWDLTPEYALSSNVRAYFRYTRGFRSGGYNGNAY-
BCAL3001  483 ----------------------ANALSPKVALQTDATEVWRFRLSFATGTRFPTVGELFQG
BCAM2367  425 ----------------------FSRENPAVGLNTNPVPGLTAYATYNEGMRSPTAIELACA
BCAM1593  376 -------------------------NTGNAALSWAITPVYTARVSYCNAFRLPTFNDLY--
BCAM2626  449 ----------------------ANELSPRVAVLYEITPAVIPYVQYAHGFRAPTPDQVNSS
BCAL0116  433 ----------------------NGVVTPTFAVMEKLAPTTTAYASYAESLEPGSRVNDV--
BCAL2281  430 ----------------------NAITTPVFGLWVKPWRNVSIFANRSEALAQGEIAPNT--
BCAM2224  427 ----------------------GHQFTPYGGLIWDFARDWSWYASYAEVFQPQTKSMWG--
BCAM0491  428 ----------------------FANTGWRLGTVYDVRPGLAVYCQYSVAADPVSSLLSLNA
BCAL1345  430 ----------------------FANIGWRTGFVFDIAPMFSAYAQYTTGAEGVGSLVTLSA
BCAL1371  435 ----------------------GSKWLPRAGVVYKWTDSFSLYCSYSQSLKPSSSIAPMTG
BCAM2439  437 ----------------------GSVWLPQFGLAYALTPALTAYANVSRSFKPNVASN----
BCAS0333  439 ----------------------VSAFSGRVGLTYRGDAGWSPYVSYSTSFDPVIGVRMF-G
BCAL1700  440 ----------------------VTAFTGRVGLTYQGDYGLSPYISYSTSFNPLIGVNLL-G
BCAM1187  449 ----------------------SNLFSYQFGLVFKPVTNVSLYASYCTSSNPPGSNG-GLG
BCAM2007  455 ----------------------DTLFNWQAGLVFKPAQNGSIYASYATSSTPAGMLL-GEG
BCAM0360  433 ----------------------QTALSPRIGVVYEMSPAWSFYANTAYSFRPNNGAD----
BCAM0499  430 ----------------------DHAWSPRVGLIYEPLDWLTLYCSFSQSFSPLADTLISSG
BCAL1709  434 ----------------------TTAWSPRLGVVWSPVGAHSLYASYSKNFAPVGGDLIGIT

BCAM0948  431 TRG---------------PTGSVNAFSAVRPE----KTTQLDIGAQYKSDRF----DAWV
BCAM1571  425 G-----------------PHDATGQFLIGNPNASKEKAVSTDLSLRYASGPNRGSWGVFY
BCAL1777  581 VYLSHQNLVDPNDPSGVPTKHFTTEQVAGNPNLQPEHTKNYNIGFQLSPDA-M--TDIGA
BCAM0564  499 -------------------------TQSTVSTVSPEYLSDYEVGIKSEWFDKR--LIVNA
BCAL3001  522 ------TI-------------SNNAIVNNNPNLRPEKAIDWDFTAERDVGV----GVVRA
BCAM2367  464 DPAA--PC-------------SLPNDFIADPPLEEVISKTEEAGMFGRIG-AA--TTWSA
BCAM1593  410 ------YP------------------GYGNPSLSPERSTSVEAALDANTA--Y--GTFLA
BCAM2626  488 ----FSNP-------------VYGYTSIGNPNLKPETSDTFEAGLFGKAGTGYGIVRYSA
BCAL0116  470 -------------------------YANAGQVLKPLRSKQYEIGLKSER--AR--WSATA
BCAL2281  467 -------------------------ARNAGQALSPYRSKQYEAGVFYDT--DQ--YGASL
BCAM2224  464 ------------------------------GGILTPVKGRTYETGVKGELAGGK--LNVSL
BCAM0491  467 ----------------------------SKANFTLATGRQIEIGVKQSFLDGK--AEWTL
BCAL1345  469 ----------------------------SQMNDRLATGAQWEAGLKQTLLDGR--AYWTV
BCAL1371  474 --------------------------YIIDGATPPEEATAWEVGGKLDLA-GG--TTGTL
BCAM2439  472 -----------------------------VAAPLAPEYGRVLEAGLKFSLK-PA--TTGTL
BCAS0333  477 ------------------------------GGLPKPTRGAQTEVGLFWQPPGRN--LMLNA
BCAL1700  478 ------------------------------GGLPQPTRGKQIEAGLFWQPPGKN--LMLNA
BCAM1187  487 GGTDQ---------------------ITATNQDLAPERARNIEIGAKWDVLQDQ--LSLTS
BCAM2007  493 SETQSLTP-------------GRGGVGPNADQLSPEKNRSIELGTKWNVLNDK--LSLTA
BCAM0360  468 ---------------------------INGRAFDPEKGHGYEAGAK--WAGAR--SLTTV
BCAM0499  469 -------------------------AFSNGAALAPQKTTAYEVGSFFDLG-GK--ATASV
BCAL1709  473 -PD------------------------ARGNANDLGPQYTRQYEIGVKSDWRDGA-LSTTL

BCAM0948  468 SAYAGYVQDFILF---DYA---TGMM--GPTT---------QATN-VNAQIMGGEAGVSW
BCAM1571  468 NRFSNYLTEYNTGRVVDDD---GEPV--APGTDGSL--NEAIYRG-VRAEFYGIELDGKW
BCAL1777  638 AFYKVRIDGVIGTDDPNAVLVANDPSRVVRNADGSVRYLVQHFVNLGALDTDGFDLNFRK
BCAM0564  532 SVFHYDYRDIQVFA--------LAPN-------PFGGPPVSTLSWAGQGRADGFELELKA
BCAL3001  559 SVFQSDLRDSIYSQ----------TT-------ASGATTVTNISNVDRVRVRGVELAFSG
BCAM2367  506 AAYRTTLTDDIQFI--------SSPA-------SA----QGYFRVVGDTRRQGIELAGRT
BCAM1593  442 AIYDTRVNNLIA----------YNPA-------T------FSPMNIGRSHIRGIDLSYKG
BCAM2626  531 AAFTGRYRNFISRTTIAGS---GRPV-------DPF---VFQYVNFADARIHGLEGRAEW
BCAL0116  501 ALFRIERSAEYA----------NAA--------N-------VYVQDGESIIQGIEVGARA
BCAL2281  498 ALFQIEKPMAYT----------DPAT-------N-------LFGADGTQRHRGIET---A
BCAM2224  493 AAFRIDLDNNPQ----------VDLA-------HPCAGPSCYYVNGGSVRSQGFEFEANG
BCAM0491  497 AAYRIVKRNLIT----------ADPV-------NP-----NQSIQVGQQSSRGIEATVGA
BCAL1345  499 AVYDITKRNLIS----------TDPF-------NP-----ALRQQVGRQSSRGVELTGGA
BCAL1371  505 ALFNIDKKNVIV----------SQYN-------DA-TK-LTDWRTSGKARSRGVELDVSG
BCAM2439  501 AVYQIDKRNVAV----------TVDD-------I--------TSTIGTARSRGIELDVAG
BCAS0333  506 AVYQIDQTNVVT----------PTPV-------NLDPT-ATTSVQTGKVRSRGIELSAVG
BCAL1700  507 AIYQINQTNGIT----------PALP-------SQDPG-GTKSVQSGEVRSRGIELSATG
BCAM1187  525 ALFQTEKTNARV----------SDGL-------G-------HTVNAGKQRVRGFEFGFAG
BCAM2007  538 ALFQIDTTNARV----------TLPN-------N-------QYAMVGNKRVQGIELGLAG
BCAM0360  497 SAFYVTKRNVIT----------ADPA-------NA-----GFSRAAGEVRSRGIEFEWSG
BCAM0499  501 ALFDMRQTNQQI----------GDPA-------NP-----GYALPIGTQHVRGMELGFTG
BCAL1709  508 ALFQLDLYNRRI----------ADPV-------RP-----GFFDLTGLERNRGIELGVAG
```

```
BCAM0948  510 RPVA----PLRVETSLAYAWGRNVASG---------------------DPLPQMPPLEAR
BCAM1571  520 RAFSRRGHTVDLELTADYTHARNVDTG---------------------QPLPRIAPLRAT
BCAL1777  698 ARRTKYG-TFTLAGDWTYVWHF-----KLHSPGTAPQDFAGNNLALLQPFGASNPRWKGN
BCAM0564  577 QPVNSLY-LFA---NLGMLNTRYTEFR--------------NVPTAVGNSFARSPHTTLN
BCAL3001  602 ENVGLRG-LNL-DANVSASNAQILADA-------ANPA-------YVGSRFPRIPRMRAN
BCAM2367  547 RVGPL-G-VGL---SYSYVDATYRSSWTEHSPANSTAGANGNVTVKPGDRIPGIPAHTVK
BCAM1593  479 TIGRSTP-VSI---AVGILNPQDETNQ---------------------TWLSRRPRQTVS
BCAM2626  578 VVPNGIT-LKT---AMAFTKGSTQNDG------------------AASQPLNTVNPFSAV
BCAL0116  536 KFGAHWN-AGV---DAMLLDAW--YAN-------------G--IGNHGNRVAGAPRFVLA
BCAL2281  531 VYGEPWK-GVRLIAGATYLDATLQNTA-------------G--GTNDGHRPIGVPSFLLN
BCAM2224  536 RITPWWS-VWA---SYTYDTMRYADNL---------ANAGS-------FAPLLNPRHLFR
BCAM0491  535 EIAKDWR-VDA---NVSILRAKYDDFQ---------QSSGGTTVSRAGNVPVSVPQRLAN
BCAL1345  537 RLPHGWT-IDA---NVALLRARYDAFN---------QTVGGATVSRAGNVPSGVPQQTAN
BCAL1371  546 KLGERVN-VIA---SYAYIDAKTTEDP----------LYAG-------NQLWNVARHTAS
BCAM2439  536 QITRHLS-VIG---SYAYTNANDRDS--------------N-------TPLVNVARHTGS
BCAS0333  548 KVTRELS-IVA---SYLYQDVKNVQAN---------DASLN-----HWPVSVPLPRQMAS
BCAL1700  549 KVTPNLS-VVA---SYVYQDVKVIQAN---------DVSLN-----NWPVDIPRPRQMAS
BCAM1187  561 NLTQKWH-VFG---GYSYLNAITTDAG---------PGSPG----ASGLPMVMVPKHNFT
BCAM2007  574 QVTKQWQ-VFG---GYTYMKSELRDNG---------KDTA-----NNGNRFPNTPKHSLT
BCAM0360  535 DIGHGLR-GLA---NLAYVDAEVTRDA---------VLASG-------ARLVDVPRLSGS
BCAM0499  539 EIAPKWS-VYA---GYAYLNGTVDGSA---------QSTAAG-LAVSSNTPGLMPRHSAN
BCAL1709  546 RLTGDWF-VRG---GIGWQHARVVDAE---------PKYAG-------KRSAGVSASNGS

BCAM0948  545 IGLEYTRGA------WSAGGLWRIVASQHRYALNEGNVVGKDFGPSAGFGVLSLHTQYNV
BCAM1571  559 LAADYGYGP------FGARAQVTHAWSQHRVPD-------DDFS-TDGYTSLGVMLTYKF
BCAL1777  752 TSWSWDYR------QLTTTLTWQYTGPYTNAVAA--EFGDGGTGSVASYSQFNLMFNYRG
BCAM0564  619 AGVDYRVPVSFG--TLTAGGDVNYRSREYFSATR--QTMPQL--WQGGYTVLNAHVSYTT
BCAL3001  646 LLASYRFDEHWL-----ASVGVRYSGRQYNTL-DNSDVNPDVYGGTSSFTVVDLKARYRF
BCAM2367  602 LRIDYAATPAWD-----IGANVTWRGGVYARGDENNGDVN---GRLAGYVLVDLDMRYRI
BCAM1593  514 LNVDHTWDELKL-HALSTGASLLYGGSTFD------DPANRQ--YLASYLTVSLRASYRI
BCAM2626  616 FGVRYEPTERWF-----VQTDLLHQPAKRDKDVDKSDCSNKACFTPPSSFVVDLRGGYRF
BCAL0116  575 GDLGYAVPGV---PGLTLGVDAKFTGATPL------RAAGGL--DAPGFLVVNAGARYLT
BCAL2281  575 AGAEYDVPML---RGLTLTARWIHTGPQYL------DVANTM--SIQAWDRFDLGARYAT
BCAM2224  576 LWTNYDLP--WQERRWSIGGGVQVQSSYSA-------QANGVTMSQGGYALASVRLGYRY
BCAM0491  582 LWISWRFAPDWT-----GIAGVKYVGKRFA------DTANQL--VMPSYTTVDLGLAWKP
BCAL1345  584 LWVGWAFAERWQ-----ANAGVRYVGATYG------DDANRV--QVPSYTVFDASLRWQP
BCAL1371  585 FAAVYDFGTVAGGDDLRLGADVRYVGARPG------DSANSF--TLPSYVLADAFATYDT
BCAM2439  571 LFAVYDTAIANLPGRWRFGGGARLVGARSG------DTANRF--TLPGYVSVDAFAAYET
BCAS0333  590 MWADWTWHTGAL-AGVGVGGGVRYQSASAG------APDNSL--TVPSATLYDLAIHY-D
BCAL1700  591 LWTDWTWHTGPL-AGFGLGGGIRYQSASAG------AADNSL--TVSSVTLFDAGVHY-D
BCAM1187  604 LWTSYDVMPKLT-----LGAGATVMSKTYAS---V-SPTVKK--WTPGYARFDAAATWRV
BCAM2007  616 MWSNYDVTPKFT-----VGGGAFYMSEVFGD------PANLR--AVPSYWRFDAMAQYRI
BCAM0360  575 ALLMYETTLPFA-DKAGAGAGVIYVGRRAGN---TANTQDGF--ELPAYATVQLNGYLQV
BCAM0499  585 LWLKRELPYGFY-----AAAGMQTQSARYT------SASDLV--TLPSFTVFNLGAGY-R
BCAL1709  586 LFVSHAPLRGFF-----AELGVVYEGARYA------DRDNLL--ELPAYLRWDGKAGY-R

BCAM0948  599 --SKTVQIS-VGVDNVLNKAYTEHLNLA---------GNAGFGYPANAPVME-PGRTAWV
BCAM1571  605 RVGPTHWLAYLRGDNLTNQEIRY--STS---------VVRGFAPQGGRSVMA-GLRTTF-
BCAL1777  804 ---FKHWTIYGGTINLFDKKPPFDVEWQ----AVP--DITGY----DQSLYTNLGRFFQV
BCAM0564  673 --PNQKYIVTGYVTNLTNKVYKKLELLP---------------SYGAYPVLYGDPRTVGI
BCAL3001  700 ---DRHWTASAGIDNLTDRRYYTFHPYP--------------------------GRTFYG
BCAM2367  654 ---TKRFEVFASVTNLLDKRYASFGALGQNFFNGPNHTFDGARPVNEQFVGPGAPRGAWV
BCAM1593  565 ---NSHLTVSASLSNLFDRQYMTAYG----------------------YNTLGRTA--FG
BCAM2626  671 ---NKHVSATIGLRNLFDRKYWNWSDVR---------GIAADSQVLDAYSSP--GRTVAV
BCAL0116  624 RVGRHDVTLRASIDNVLNRRYWEYQYA--------------------DYVKPGDPRTVSL
BCAL2281  624 DVFGKKTTFRATVRSVANKSYWSSTIG--------------------GYLTQGDPRSVWL
BCAM2224  627 ---DKHWSAALNVNNLFDRHYYLSLSQP------------------GWNNRYGEPRNVML
BCAM0491  629 ---RKDTTITARAYNVFNRRYVQSAYYN------------------ETQYLLGNDRRVEV
BCAL1345  631 ---TSRTELALYLRNLANRTYAVTTSNG------------------GEQWLLGPSRSAEL
BCAL1371  637 RIGKQKLSFQLNVKNLFNRTYYPSSAN------------------RYFVAVGDARQVAL
BCAM2439  623 TIGKFPTRFQLNVKNLLDKTYYPSSNN------------------NLIVAVGEPRLVTL
BCAS0333  640 ---LPRWRFAVNVANLFDRRYVSGCQS------------------YAVCVFGNERTVLA
BCAL1700  641 ---TRNWRFAVNGTNLFNRHYISGCQS------------------TNVCIFGTDRTVIA
BCAM1187  653 ---NKTMDVQLNVQNLFDKQYYASAYPI------------------YATWAPGRSAMVTL
BCAM2007  663 ---NKKLDLQLNVNNLFNRTYFDQAYPA-----------------HYASTAPGRSAFVTL
BCAM0360  629 ---NKHLRASVLNNLFNRTTYVSSY-------------------NSLWVTPGAPRSIFA
BCAM0499  631 ---SKKVDVTLTLDNLFDRRYFIAAHGN-----------------ADLYNMPGDPRTLTA
BCAL1709  632 ---TRDLEVTLAAVNLADRDYYANATGL-----------------AQI--VPGAPRTFTL
```

```
BCAM0948  646 RVSAKL-
BCAM1571      -------
BCAL1777  851 GATYRF-
BCAM0564  716 TLTAKI-
BCAL3001  731 ELKWSL-
BCAM2367  711 GVRYAWD
BCAM1593  598 KVSYTF-
BCAM2626  717 SMKVDF-
BCAL0116  664 SAKIDF-
BCAL2281  664 SMTTDF-
BCAM2224  666 TVRGQF-
BCAM0491  668 LANYRF-
BCAL1345  670 VATMRF-
BCAL1371  678 LTTLQF-
BCAM2439  664 TTTVSF-
BCAS0333  678 SAKYSW-
BCAL1700  679 TAKYNW-
BCAM1187  692 NFYQ---
BCAM2007  703 NARY---
BCAM0360  667 SLAYSF-
BCAM0499  671 TVKWHM-
BCAL1709  670 TAAYKF-
```

Figure 3.7: Alignment of putative TBDRs in *B. cenocepacia* J2315

Amino acid sequences of putative TBDRs from *B. cenocepacia* J2315 were aligned by Clustal Omega and identical or similar amino acids were highlighted using BOXSHADE. White font with black shading indicates identical residue at the corresponding position in ~50% of sequences and white font with grey shading indicates similar residues at the corresponding position in ~50% of sequences. The gene locus designations are indicated on the left. Red box indicates the location of the TonB box conserved region. Blue box indicates the location of the receptor plug domain.

```
I35_RS20820    1 LPPVEVVAA-TAPAAG--ATANDAAM----------LPPVEVVAAPLSTPLVVVT-----
I35_RS23575    1 LAPIFVTANDAPGASG--TPANASAP--------------------PLGDTELIAP----
I35_RS08460    1 LDKFEVTCS-EQACSTTAAAPAPASGTAAGGQTVKK---------LIRTSDKV-------
I35_RS08490    1 LIRQADKVT-GASASGAAAEATPAAPGANGQGKVTQIKRFEVTCS---------------
I35_RS18860    1 LGTVTVTAR-RCAAA-----------------RETN-------------FRKESIQDVP-----
I35_RS04375    1 LSAVSVTAQ--ASAT-------PAGD-----T-------------RQPV-DPDTP-----
I35_RS29035    1 LDPVTVTAT-AAAST-------RGDA-----A-----DPVTVTATRTATAASRTA-----
I35_RS23700    1 LPTISVTDT-LAHAAGDTAPAQPAGP-----A------EGAD---------RHLPESFDR
I35_RS27690    1 LPAVVVVCT-QPADGGTIAPAEPPAV-----V---------TPLPGIGTPLSKVP-----
I35_RS11045    1 LPSINVTCA-AEPLPGDLAPTYAGGQ----------VARGADFCVLGRQKASDVP-----
I35_RS00620    1 LPALNITAA-HDSPQ----------H----------LTDTISTCALGTRRQLDTP-----
I35_RS19580    1 LPAITVSCE-RCHPL----------R----------AREA-SVAGLDDAPLRDTP-----
I35_RS26975    1 LKAIAVNAS-RSVAD---------------------DP-SVATVGRMSLALREIP-----
I35_RS06170    1 LPAINVTAS-SASAD----------P----------LTQPLETCSRLGLASLDTP-----
I35_RS18505    1 LAPI--RVD-AQKAP----------A----------LTQPLDTCSRLGLSPLETP-----
I35_RS06295    1 LPTINVRSS-ALRAE-------SY-R----------APKEAG-VLRSDIPLLDTA-----
I35_RS28095    1 LPAINVSAS-AAVDP-------TVGY----------QPRTTSIAGGDDRALKEIP-----
I35_RS08065    1 LPAITVNAA-SAGDG-------TVGL----------VAKRSTTGTKTDTPLNEIP-----
I35_RS31745    1 LPPIDVRC--PADAS-------SVGL----------VARRTVTGTKTDTPIDEIP-----
I35_RS21645    1 LPTIAVQSS-ALSDM---------------------QVKRS-PSYRFTAPLLDTP-----
I35_RS25625    1 LAPIEIQCK-TEHSY---------------------KADFS-ASAKFTAPLVDTP-----
I35_RS31880    1 LPTIEISAQ-RATAP----------F----------RTRESTSATESEADVMEIP-----
I35_RS08115    1 LPAVEVRSR-RHPND----------P----------RAESVSTATETASDPRDVP-----
I35_RS18545    1 LPAISVNAA-AEHAS----------Y----------DGGHSRATKTDMSLMDVP-----

I35_RS20820   43 ----DPKAPRQPL-----PASDGADYLK-TIPGFTSIRS-----------G-GTNGDPVL
I35_RS23575   44 ----TVQLSGDATRR--QADSLGETLN-GLPGVSTTTY-----------G-PMVGRPII
I35_RS08460   52 GHTEVQVTTAKEIQQS--GYTTVADFLRSTSANSASSWGQ-TTMNSSA----PGGAGMAL
I35_RS08490   53 GFNQVQTVTSKDIENS--GQTSVADYLRSTSANSASSWSE-GSTNSFA----PGGAGIAL
I35_RS18860   38 --VAVAALSGDAIRNN--ELRVLNDVTK-YVPNFIGQSTE----------G-RERPRWFL
I35_RS04375   36 --AVVTSITREQIDAH--TNVITEDALK-YAPNIMVRKRYIGDRNSIF-AGRDF------
I35_RS29035   39 --ASVSVITDEDLEEQ--QATNIKDALR-YEPGITVRRTAYRPGSAALGGGRDGDSSINI
I35_RS23700   49 RYASTQVITRDDLDRLSPADPSITQALA-TQPGVTVAQN----------GGPGSSASVSI
I35_RS27690   50 --ANVQTVRAAELDAQ--HRAHIADFFAANLPSVTISDA---------QGNPY-QADVNY
I35_RS11045   45 --FSMTTYTSKLIEDQ--QARHIADVLD-NDPAVRSAS-----------GYGNFSQVFVI
I35_RS00620   35 --FSTTIVTSEELEAR--QPYKLGDVFA-NDASVSDNSG----------AYSAWASYMTV
I35_RS19580   34 --ASVNVITRALIDDQ--QAKRLSDVVR-NDASVVNDYA----------PVGY-FEGFAI
I35_RS26975   33 --QSVSVTTRERIDQQ--NLFSLDDVMQ-QSAGVTVQPY-----------VLL-TTAYFV
I35_RS06170   35 --ASVETVTADTIEAR--GDRTVLDAVT-RTAGFASAIA-----------PGTGGTALSV
I35_RS18505   33 --ASVEQINRATLDTR--GANSIIDAVS-RAAGISASPH----------PGNGNSELAA
I35_RS06295   36 --QAVNIVPAQVLRDQ--RPRNLDDALG-NVSGITQGNT----------LAGTQDT-IMK
I35_RS28095   38 --QSVAVVSSSVVQDQ--QARSLDDVLG-NISGVTQTNT----------LGGTRDA-FIK
I35_RS08065   38 --QTINVVTAQQIEMT--GATDVNAALR-YVPGFSSYGS-----------DNRSDWYAAL
I35_RS31745   37 --QTINIVTAQQIEMT--GAADLNQALR-YVPGFATFGA-----------DSRTDWYAAL
I35_RS21645   33 --RSVTVIPEQLIKEK--NVTSFADALR-SVPGITFLGGD-------AAANPSADR-PVI
I35_RS25625   33 --KSVTVIPQELIQSS--GAAILTEALR-TVPGITFGAGE--------GGNPLGDR-PFI
I35_RS31880   35 --FAVSSVDTKLIQTV--AATRGDDLYD-WVAGVSRQNN----------FGGLWDN-YAV
I35_RS08115   35 --QTIDSVSVEETLSY--GGRILADALA-GVPGVSNT-----------SDTRFDS-FRI
I35_RS18545   35 --QTVNVVPHAVIEDQ--NATSLQDALR-NVPGVGFSV-----------GDGQRDQ-ITI

I35_RS20820   81 RGMFGS--------RLNILANGVPTLGACPNR----MDAPTSYIAPESYDKVTVVKGPQT
I35_RS23575   85 RGMDGD--------RIRLLQNGVAAYDASSLS----YDHA-VPQDPLSIERVEIVRGPAA
I35_RS08460  105 RGLSEK--------YTLVLVDGRVANYAQSVNFTDTFFDVNAIPLNMVERVEIVKTGAV
I35_RS08490  106 RGLSEK--------YTLVLIDGRVSPYAFAVNGSDQFFDLNTLPLNIIDRIEIVKTGAV
I35_RS18860   82 RGVGSNDPSDLSLSPIGVYFDDVYINSVF-----------GQGFPLFDLDHIEVLKGPQG
I35_RS04375   84 NELQSA--------RGLVYADGVLLSNLLGSSYA--YPPRWSLIPPDDIARVDVLYGPFS
I35_RS29035   94 RGLEGN--------RVLLMEDGIRLPNAFSFGPL--EAGRGDYADLDTLKRIEILRGPAS
I35_RS23700   98 RGSSAS--------QVAVFIDGIRLGSPTTGI------APWADLPTDAFERVEVISGPAA
I35_RS27690   96 RGFTASPLL-GTPQGVSVFVDGVRVNEPFGDV------VNWDILPMQAIDRVQLIPGSNP
I35_RS11045   89 RGFALA----G----DDVSINGLYGVTP------------RQLVQTDAVERVDVFKGANA
I35_RS00620   80 RGMQLD----W---QNGYKIDGIPFVTY------------GITMPYEQLDRVEILKGLCG
I35_RS19580   78 RGFPVD----L---ASAIRIDGITVS-G------------EQNVPLENKERVEILKGLAG
I35_RS26975   76 RGFKVD----S------FEFDGVPVVIG-DMA--------SAPQDISVYERVEILRGANG
I35_RS06170   79 RGFSGQ----E---SVMTLIDGVRLMPAAGTI--------TFPFDTWSVARIEVLRGPAS
I35_RS18505   77 RGFVGA----S---SVTQLYDGVRPYGAIG-V--------TFPFDTWSVDHIDVLKGPAS
I35_RS06295   80 RGFGGN----R---DGSIMQNGVPLVQG--------------RAFNAATDSVEVLKGPTS
I35_RS28095   82 RGFGSN----N---DGSVLVDGVRTPVL--------------HSYLATIDRVEVLKGPAS
I35_RS08065   82 RGFTPT------------AYVNGLQVPNTINLA--------SWRVDPYMIDSISVLRGPTS
I35_RS31745   81 RGFTPT------------LYVDGLPAPNTAVIA--------NWRVDPYTIDSIAVLRGPTS
I35_RS21645   80 RGFESR----N-----SIFVDGMR--DS---G--------LQNRETFAVEQISVIKGPDS
I35_RS25625   79 RGYDTQ----G-----SMFVDGVR--DT---G--------ATTREIFNTERVEITKGSDG
I35_RS31880   79 RGFAGD----GNTSGTDYLVNGFSWNRG---M--------SVPRDTVNLERMEVLKGPAS
I35_RS08115   77 RGFSSA----G-----DLLIDGMR--DD---A--------QYVRSLGNIERVEVLKGPAA
I35_RS18545   78 RGFNSI----T-----DQYVDGIR--DD---A--------LYYRDLSNVDRVEVLKGPAA
```

```
I35_RS20820  129 VLYGPGA----SAGTVLFERVTPRFERPGMRFEGSLVGG----SFG----RNDQNIDLTA
I35_RS23575  132 LLYGGNA----VGGVVNT--IDNRIPREAIQGVTGALDA----RYG----GAN---SVRA
I35_RS08460  157 SVYGSDA----IAGVVNIITKKNFQGL---QIDGQLGKA----QHPG---DGQCNFSV-L
I35_RS08490  158 SQYGSDA----IAGVVNIITKKNFQGL---ELGGSYGGA----TNGEGG-QGTTKISI-L
I35_RS18860  131 TLWGKNT----VGGALSITSQKPTFDV---SGYGKIGLG----QYN----SRLAEAI-G
I35_RS04375  134 ALYPGNS----IGSTVLLTTRRPEQLE--ASLSTQFFTQRYHDGYGFAD-SL-------G
I35_RS29035  144 ALYGSDG----LTGAVNFITKDPRDLL--SVYNKPYYFS-FRPSYDSTDRSIGATVSAAG
I35_RS23700  144 ASFGNNA----MGGVVQLFTRRAAQQP--NQTTVSFGGG----TNK----TFDTRFRT-S
I35_RS27690  149 -VYGLNT----LGGALALTTKNGRSNP---GGEAEVSGG----SWG----RKTASVEQ-G
I35_RS11045  129 FLNGASPNGSAVGGGVNLQLKRAGDKP---LTRVTVDGA----TSG----SLGTHVDL-G
I35_RS00620  121 FLYGFVT----PGGVVNYVTKQPGAEP---VRSVDIGYR----STN----VWTEHVDL-G
I35_RS19580  118 IDSGVVA----PGGVINFVTKRSAN-----VASVTGGVD----SRG----STSAAVDL-G
I35_RS26975  117 LLHGSGN----PAATVNLVRKRPQYQF---SAHATASVG----SWD----RYRTEADI-G
I35_RS06170  124 VLYGEGA----IGGVVNVVPKRPQRTR---ETTLQVGVG----PDG----AKRFAFDT-T
I35_RS18505  121 VTYGEGA----IGGVVNIVPKKPTRTP--IRNELQVGGG----TEG----TARAAFGS-G
I35_RS06295  119 LLYGLMD----PGGVVNVVSKQPQLTR---YNAISLGAS----TFGHGKNGGSATFDS-T
I35_RS28095  121 LLYGMQD----PGGVINLVTRKPEDTF---GGSISASRT--------SHGGSNAQFDL-T
I35_RS08065  123 VLYGAGD----PGAIIDVHTKLADGER---VREAGVQIG----NYA----RKQFMIDV-G
I35_RS31745  122 VLYGAGE----PGAIVDAHTKLADGER---VREAGVQIG----NDA----RKQAMIDV-G
I35_RS21645  118 VYAGRGS----VGGSIDIVTKTPQNDN---FINSSIGFG----TDG----YKRATVDA-N
I35_RS25625  117 AYGGRGG----AGGSINLITKAPHLGT---TAAASAGLG----TDR----YRRFTADG-N
I35_RS31880  124 ALYGRGD----PGGIISYTTKQPQFAR---ATTVGVSAG----SYG----ALRQTIDT-T
I35_RS08115  115 ALYGRGS----GGGVINPITKQPLPEN---FGHVSATTG----SYG----RLGASVDL-N
I35_RS18545  116 VLYGRGS----AGGIVNRVLKRPQANP---VNDVGVTLG----IRG----ERRCEFDL-G

I35_RS20820  177 GTPDVYG---RVTANHAHSQDYQDGN-GNTV-PSQWDKW---------NADAAIGTT---
I35_RS23575  175 GAAQVEG---GNGRFAFHVDAFDRET-SKLR-IPGYARSSQQAAIDGPDTPQPEGNV---
I35_RS08460  202 AGFG---DL-NSDRFNVTAASYYRDSGSTLGD---RDMTSAQDFTQ-YP-GGIAAP---
I35_RS08490  205 GGFG---DL-NADRFNVTAALSYYKSNGISIAD---RDTTQNQNFSN-FP-GGISNQ---
I35_RS18860  175 GPIG------KNDVLAARVSVYHENA------DSFYTNTVQQGRFGG-FHDNAVRQVLA
I35_RS04375  180 GNHQTARIANRVGRFWEALSLDRLENNGQPM---QYASPASAYNPR---LGAAVPVT---
I35_RS29035  197 GNDRVQGMIIADGRRGHEVDTRGGNNTASTL-R-TTSNPQDVYSES---LLGKIVLT---
I35_RS23700  189 GTVPSTGPLAALGGLTYSLGLHDYNTAGIDATRPFFYGHEDGRNPY---HAQDIDAR---
I35_RS27690  192 GTIG--------SNLDIYATANVAND------G-GWADHNASRVRQ---AFGKLRVT---
I35_RS11045  177 RRFG------SEGQFGVRVNQSISGG------D-TAVDDERRESNV---TAVSLDVR---
I35_RS00620  165 QRFG------PDHMFGARLNATHEEG------K-TYNDGNIRRDSV---S-LAIQAN---
I35_RS19580  160 RRFG------PDHQFGFRLNAAKENM------H-SYIDGTNGRRTF---GSIAADVD---
I35_RS26975  161 GPLN------AAGTVRSRLVAAYEDR------H-FFYDHAKQDTRS---IYSVTEVD---
I35_RS06170  168 GALG--------PRLSYRFYASDARA------N-GLAERADTHTTA---IGGAITFD---
I35_RS18505  166 GAIN--------DKLSYRFDVSGNRS------S-NWVDRGDSRDLS---VSGAIRVD---
I35_RS06295  167 GPVG-------DSRLAYRLIVDQSNE------Q-YWRNFGEYRQTF---VAPSLAWY---
I35_RS28095  165 GPLGRPGQV-AGGTLAERLTGEYDTS------R-YWRSFGREENAL---IAPALSWH---
I35_RS08065  167 DKLD------PDGKYAYRFVGVARDG------N-ALTGPNNDQRVA---LAPSFRVR---
I35_RS31745  166 DRLD------PDGRYAYRFVGVARDG------N-AVTGPNGDERVA---LAPSFRVR---
I35_RS21645  162 RKIN--------DTTAVRLNVMGHDA------NQAGRNDVYNARWG---VAPSIVEG---
I35_RS25625  161 WQFA--------DHAAFRLNLMSHNN------DVAGRDAVNNERWG---VAPSLAEG---
I35_RS31880  168 GPVT--------QSLAYRFVAMNENN------G-SFRDTVSSERYL---FSPSFTVD---
I35_RS08115  159 RMLS--------SAWSMRLNAGREHA------G-SFRDHVDGTRQF---VAPSIKVH---
I35_RS18545  160 WNPN--------DAARFRVTGAAENS------N-SFRDRFQLNRQA---IAPSAQEK---

I35_RS20820  220 -PDDHTRVEL-----TAGTGD----------------------------------------
I35_RS23575  227 -PNSDGRVHGGAVGASYTWAD----------------------------------------
I35_RS08460  250 ---------LGPNQQSYWS-LADGSRVPLSPCPPGSKTS-----------ATNCTYNPAA
I35_RS08490  253 -------------SVSYWRNPATGAKVPLSPCPNGGQAVPGTSVAQVNGPGTVCANNTAY
I35_RS18860  222 VPTSDTDFLFNIHGRN-YTGGGN-----A-----------WHAEGAGRGGTNQ------F
I35_RS04375  231 -GAAT-----------------DIG--PN-----G------KP----------------R
I35_RS29035  249 -PTTRDTIKFTAETVQ-RRVSTDVL--SA-----I------NA----------------P
I35_RS23700  243 ---------IGYARDN-WS-IST-----------------------------------F
I35_RS27690  231 --DADTTISIAAGGAD-NTLTGTQT-IPR-----SFLD-------------NR------K
I35_RS11045  218 -GDT-LRISGDFLYQR-QRIDNGRPIVLV----SGSPLPAV---------PSAT-------
I35_RS00620  205 -LTRDLSVSFGALYQD-RRTTGQTPSIFTGSYPGGALPATI---------SGGS------T
I35_RS19580  201 -ISPRASIQINAEFQQ-WIQRSA-PG---YQLLGGTVVPSV---------KTTS------K
I35_RS26975  202 -VTRDTLVTFGAQYQT-TSSVPDMSGVPM---ARDG----------SSLGLSR------S
I35_RS06170  207 -VSPRLTITLDYDYGR-QMPATYYG-VPA---PNGVLDPSLRKL---------------N
I35_RS18505  205 -VTPDLYVTASYAQGF-MHPMQYFG-APL---VDGARDRALDKK---------------N
I35_RS06295  207 --GRDTQVAVSYQYRK-FHSPFDRGTALD---PRTN-----APLDI-----PA------R
I35_RS28095  211 --DANTSIDVSYQYVD-YTMPFDRGTVLV---NG-------RPDDA-----LR------Y
I35_RS08065  208 -PDADTSITLSATYLQ-DWGDISSNFLPA---QGTVLPNP-------NGQINK------D
I35_RS31745  207 -PNADTSITFSATFLQ-DSGDISSNFLPA---SGTVLPNP-------NGRLSQ------D
I35_RS21645  202 -LNTPTTVTVSYYHMN-SYDMPDFS-VPF---RAS---------GGTPVPTDR------G
I35_RS25625  201 -LGTSTRVTASYYHLQ-TDDMPDGG-IPY---FYTTSNKPANVDTIYPAPVDR------H
I35_RS31880  207 -IGADTTIHYEFESAR-QRAPLDRG-VLA---VNGQLG-----------VIPA------S
I35_RS08115  198 -DARRS-WLIQFEYDT-YRRVPDRG-MPA---PVAAVDAAGKPLAFSLPSAPR------A
I35_RS18545  199 -LDRDTVINVEFDYLH-DRRTSDQG-LPA---YRG------RPVDV-----PI------N
```

```
I35_RS20820  235 GYARYAGRGMD-----------GAHFRRETFGLSFDKR-------H---LGDVLD---RI
I35_RS23575  247 GFAGLSYSGYESNYGSVAESDVRLRMRQERLALASEVR-------N---LSGPFT---TL
I35_RS08460  289 STSLVPST------------------TRLNAKVRATFKIDDNTQ----AYAGFWV----S
I35_RS08490  300 ASSLSPWT------------------ERLSAKVHADFKITDAMQ----AFADLWE----S
I35_RS18860  259 GFVGSS----------------------DPYTVSLNAPSSDHISTWGTSLTAHWR----I
I35_RS04375  244 TIVGAQTIERT---------------EQLNETVRVGYAFTDHVDATL--TLGHWENHYRQ
I35_RS29035  278 TTLGLTTHDRL---------------ER--NRFSVDYDFRDDALRWF--QTAHVQ-----
I35_RS23700  256 ALYHRSDLSY---------------DNSGYANRELDHQLTTGVAFHL-DITPDTQ----F
I35_RS27690  263 QAYTYPDRNR---------------NSAGYLTLSGERF------------FGEHVE----L
I35_RS11045  256 HNYAQPWSFSE-L------------ED-TVGIVRAEYD------------FLPAWT----A
I35_RS00620  249 NLGGKD--QYL-N------------TNLQLYTAGLQYQ------------LAPDWQ----L
I35_RS19580  241 ALGTQPWAKPV-T------------TDALNLNARFTYQ------------FNDDWK----A
I35_RS26975  241 TFLDTAWGRFN--------------WDTTRAFASVEQK------------LGAGWK----A
I35_RS06170  246 YTVGDATISYY--------------DQWTR--LSASYR------------PTAGVT----I
I35_RS18505  244 YNVGDADIAFR--------------DSWAT--VSANWQ------------PSDALN----V
I35_RS06295  245 RRIDEPFN----NM----------DGESHLAQLSVDHQ------------FNADWS----A
I35_RS28095  247 RRYEEAWS----QS----------SGIQETLRTRLEHR------------FSDAWR----V
I35_RS08065  250 IYEGDGNFNYYRK------------KQWS-IGYQFERN------------LTPAWT----F
I35_RS31745  249 LYMGDPSFNDYRK------------KQWS-LGYALEHR------------VNAIWT----L
I35_RS21645  241 QFFGLNTRDYR-Y------------GQTDTGETRVEHK------------LNDTWK----L
I35_RS25625  249 NFYGLIDRDFR-K------------TTSDISTIKIEHD------------ITPNLT----V
I35_RS31880  244 RFLGEPRDGDY-------------DVRNTGHQFTLEHR------------IDSAWS----I
I35_RS08115  245 TFFGAAGRDTIRDE----------TMNWRS---VFTHA------------LDGDWE----L
I35_RS18545  236 AYYGSADGGNSSYN----------DISAKSATVSLDHR------------FNDSLS----F

I35_RS20820  271 EARVYYNEADH-----------------------------VMDNYT-LRQPDPASSMP--
I35_RS23575  294 KFDFAYTD-----------------------------------YR-HKEIDNCET----
I35_RS08460  323 RDETVQLQGP--------ASIS-----------------STTNV----YNPSTGSVSPLP
I35_RS08490  334 NNTTVTNNFV--------GRLG-----------------NSTQT----YDPATGGLTPIS
I35_RS18860  293 NPAVSLTSITAFEGL--------------------HRWYQDDEDYS----PVDAARSH--
I35_RS04375  287 HGETFLRDATGNPVYGGNVSIGGQNMTVAPNAFAPQRGDQENWLYALGLNGRLDSGWRLS
I35_RS29035  314 ---FYYQD-----------------------------AKQDQ--YAFETRGKLPSRSRDN
I35_RS23700  296 DQSFGYANDR-------------------------------QFIYA--DNPALATDQ---
I35_RS27690  293 SGNAYYRHLRNTNTS----------------------SNNNTDYGS--VDEDG-AIDT--
I35_RS11045  287 YVSAGARHTNE--------------------------HGDY---YTPTYSSSGTTG----
I35_RS00620  279 DVAYSYSKATR--------------------------RRNES----------------T-
I35_RS19580  273 YIAAGRSRTMI--------------------------DDNSAFAYGCSYAASCAAGATS-
I35_RS26975  272 KVSGEYQSVRSDLK---------------------------YAGSGG-AIDPATCAGGRLT
I35_RS06170  275 DNQLYYLTSN----R----------------------HWRNAESYV--LDPATARVTRG-
I35_RS18505  273 TSTLYRMKSN----R----------------------HWKDAEYYT--YLPSSAQVRRS-
I35_RS06295  276 HVGYSYNRET--YD---------------------------ANQLRTTGVDPVKCTMTRS-
I35_RS28095  278 RATYGWGRDR--YD---------------------------QFITRATAFNSRTCALTRS-
I35_RS08065  282 RQNTRLMHLS----------------------------LDNASVHANGFAGDSLT----D
I35_RS31745  281 RQDVRWSHLS----------------------------LDDATVHGNGLAPRSTT----N
I35_RS21645  273 KNTTM---------F----------------------GRSTLDYVA--TNPQILASNPNM
I35_RS25625  281 RNTTR---------Y----------------------TESTQDYIW--TQPDDSQGNVVN
I35_RS31880  276 NAGVAQRNTD----L----------------------SGRSSEAFA--LQPDGRTLWR--
I35_RS08115  277 RHTLGVLDLRSTFDN----------------------TYVTQSYVA--KPRDYRRVQRA-
I35_RS18545  271 HGAIR------AYDF----------------------SLERKNYVT--YEPIKTAAHPV-

I35_RS20820  299 --------------------MRM---------AADVRRRTVGAR-----AAATFRFGD--
I35_RS23575  313 --------------------------------ATTFRNRGYEAR-----IEARHRKIG--
I35_RS08460  354 RT--VP-VSNPY--NPFGVPTAINLTFPGNVVGADTVSTFWMAN---TGVKGSFDTGRFG
I35_RS08490  365 NL--VP-GSNPY--NPFGVPAKLVYAFPATQ-AVHTSSNFWRAA---TGVKGSFSTPRVG
I35_RS18860  327 --------------DR------------------------LSSR----QFSQEFRLESPQ
I35_RS04375  347 G------VVSAYDVSR-DVLRA--------------ASTVQGCA---GT-----------
I35_RS29035  340 Q----------Y------------------------KERAFGCA---AFAESGFATGPLA
I35_RS23700  320 -------I----NSQR------------------------ISTSTSLTHQAHGFHLFGLP
I35_RS27690  326 ----VQGSN---AQST-----I--------------VTDSYGCS---VQLTLLGKLGGVA
I35_RS11045  314 --------------SRLSVP-H--------------KEDAQSAE---AGVRGRFTTGPVS
I35_RS00620  296 --LYLQDAAGNYTDSRYVG-ME--------------DHRFSQWR---AMVEGKVRTGQFS
I35_RS19580  306 --PFFFGANGDYDVYDFRSPGE--------------YRRNDDLR---AVTTGKFATGPLR
I35_RS26975  305 GAAY------QFSSYS-----------------------RSLD---ANVQGPVHAFGLT
I35_RS06170  306 --DYLDIGH---HQRQ------------------------IGDR---LSARFDGMLFGRA
I35_RS18505  304 --SYTEIFH---DQEQ------------------------YGNV---TTATVGSALFGVR
I35_RS06295  307 ----ND-ATHGSLSTD------------------------SYCI---GYVTGKLSLAGVR
I35_RS28095  309 ----SD-ANLGRNDSD------------------------QIAT---LGLLGNVTLAGVQ
I35_RS08065  310 VSRWAGLFQMNYSRFD------------------------IDN-----NLEGRFATGPLQ
I35_RS31745  309 MMRFAGLFQLNYSRLD------------------------IDN-----HAQARFGTGPLE
I35_RS21645  300 LG--LQAKSGKYALNG------------------------FSNQ---TEVTGSASLFGVK
I35_RS25625  308 GKVWRRNNNRNSSINS------------------------LANL---TELFGEFRTGPFK
I35_RS31880  306 --RY---RQVAFHSND------------------------LQCR---LETAGSFRTGGLG
I35_RS08115  312 --RYLQD----MTQLN------------------------VQTG---VELGGKVATGPAL
I35_RS18545  300 --VTLDQSTRQRTDHG------------------------IDCL---FELTQKTSLFGVR
```

```
I35_RS20820  323 --DFKLYTGVDAQSNRLDSRSSM--------------------G----------------
I35_RS23575  334 --PFEGAIGVQFGQNTF---SAL--------------------G----------------
I35_RS08460  406 ----AWDWSADYGHSQSTVDTTYRNRINVAGLENMLANGTYNFSNPAATPNGLNGVFTDD
I35_RS08490  416 ----DWDWTASYTHSQNTVSNNYSNLINAAALENIVQNGVFNFADPSSTPNGLNGLYGST
I35_RS18860  345 NDRLSWIVGTHLFTEQL----------------AEQGAGGGLPGSP---------------
I35_RS04375  372 ------IFQGDGTGWRTLDLKAE----------APEVKGHTFTFGYH--------------
I35_RS29035  363 -HKL--LVGVDGSLSRVTNLRDG----------TVP------GVGEA--------------
I35_RS23700  345 -LSGESKLAYDFTREQAF-----------------------------------------
I35_RS27690  357 -NRL--VAGVSADVANSSYVASS-----------QDA-----SFTDA--------------
I35_RS11045  342 -HFV--TAGASFIRIDSQSAY------------TMSNAFPTTLYDP---------------
I35_RS00620  336 -HQI--VLGASWQKQANDYSANS-----------VFVPLGAGNLYAP---------------
I35_RS19580  347 -HEL--TLGVSVQRRVVHM-ADA----------VYDYVGSENVYGP---------------
I35_RS26975  332 -HDL--IFGVTYANSSSGQMTAP--------LLGDVAGTPVNVYRW---------------
I35_RS06170  334 -NRF--VVGTEFSQTTFSGT-NN--------S-PYGGETTVPVHGF---------------
I35_RS18505  332 -NTF--SAGVEFNHTTFQHD-NN--------S-PYAGTSTVDPFNV---------------
I35_RS06295  335 -HDV--QVGFDTEYRRIYRK-DM--------LRQAV---KTPFSYV---------------
I35_RS28095  337 -HAI--YVGGEYERQRSFRG-DT--------IRGKA---TTGFNLY---------------
I35_RS08065  341 -HTL--ILGFQYNRQTATDS-EW--------LAAAP-----TLNLY---------------
I35_RS31745  340 -HTL--IFGAQFDRQTTTNS-VW--------LALAP-----SLDLY---------------
I35_RS21645  331 -HTM--TAGVEFSHEQARYE-GY--------LVSDSAGNNIRSNSP---------------
I35_RS25625  341 -HSF--TTGIELSREWGKRD-SY--------TVATDKGTICQKGIG---------------
I35_RS31880  334 -HTL--VMGVDAYRFNYDQF-VT--------RSTPTAAAPYAIDIF---------------
I35_RS08115  339 -HHL--IFGIEYGWQKR--T-PA--------LWQADAA-PVPVTGP---------------
I35_RS18545  331 -HEL--LYGLELSQQQK--F-DT--------IYSVTKVATYDLFNP---------------

I35_RS20820  345 ----------------QQNYR-----------DQP-------------------------W
I35_RS23575  353 ----------------DEMLV----------------------------------------
I35_RS08460  462 DQQAISKVDSVTAKASTSNLFTLPGGPVGLGLGTEFRHESSTINPQTLASQGVSAPANVQ
I35_RS08490  472 STQAITKLDAVDATLSTPNLFTLPTGNVGLGLGTQFTHQSQYIGTGADYANGTLIQPSLQ
I35_RS18860  375 ----------------SPAYY-------------------------------------HLT
I35_RS04375  403 ----------------YDNYFL---------RNVTYN--------TADWLAGPTT-SLAS
I35_RS29035  391 ----------------FPNKAF---------PDTDYT--------L---------------
I35_RS23700  362 ----------------LPVDI----PGGVP----------------------------
I35_RS27690  385 ----------------RA-----AIGIGDF--------------------------VPQT
I35_RS11045  373 ----------------APVASPPTAYAG---GD------------------------MNDP
I35_RS00620  369 ----------------NPYRYESPHG-F---IQ------------------------Y---
I35_RS19580  379 ----------------DLTFSPSPNSPG---PS------------------------Y---
I35_RS26975  367 ----------------NPSSVPEP-GI------------------------GP----YQQ
I35_RS06170  367 ----------------DPGVFT------SPDPTV--------------------------P
I35_RS18505  365 ----------------DPGSFI------NTAGTF--------------------------P
I35_RS06295  366 ----------------DPVYGLLPPSS-TVSA--------------------------SDS
I35_RS28095  368 ----------------DPVYGLLAPGG-VPNP--------------------------KQS
I35_RS08065  370 ----------------NPVYTPVTMGV----------------------FSDPDA-TSRT
I35_RS31745  369 ----------------HPVYRPVTAAI----------------------FSGPTS-LGHV
I35_RS21645  365 ----------------CAVVGNCTPLAGGWNPNMPWT--------GSIVLNGDKG-FPGA
I35_RS25625  375 ----------------APSGYNCTSLW-SPNPNDPWA--------GSITRNNDYA-----
I35_RS31880  368 ----------------DPVYG-----Q-PAPTPRTA------------------------T
I35_RS08115  370 ----------------DRFAL-----VGST--PRPY------------------------A
I35_RS18545  363 ----------------QPVVL-----PGVPGGTRAK------------------------T

I35_RS20820  354 DAQATMWNAGVFSELTWYASDVSR-VIGGARVDYASARDKRA-MKRG--MMMSKPNP---
I35_RS23575  358 -PSTRTNSVALFGLEEWQVVPALK-LSLGGRFEHVK----------------VDPDP---
I35_RS08460  522 TVEGSRNVAAAFYQVDIPILRNLT-FTQAGRYDHYSD------------------------
I35_RS08490  532 SVNGERNVAAVYYQIDIPILKNLT-FSQSGRYDHYSD------------------------
I35_RS18860  383 DLTQHTQSAAIFGSVKYRFTDRFN-VTGGIRYTIERKTINLTGLQDTGNVTFSDPNSWWS
I35_RS04375  429 VYRGDTRTQALFGQDAWRFAPGWL-ATLGIRYERWDAYGGALGNAKGTLGYADR------
I35_RS29035  404 --------FGAFVQDQIGY-GRLL-VTPGIRIDTYRLSPTEN-DPLFTGKAVST------
I35_RS23700  372 --TRNDSAFSLHQSATL---GSVTMFVAG-RHEIV----------A---------------
I35_RS27690  398 SAKTRNANVGVYLSDALSLTPHWT-LTLSGRYDWSKARIGDE-SGVQPLLDGSH------
I35_RS11045  391 GTVTKTWLRSLAVSDTLGFLDDRVLFTLGARRQSISVDNFDY-TGAV--T-STY------
I35_RS00620  383 -RTSEIVQKSLFASDTVQLTERWS-VLAGVRYMNYAQRAFQA-SGAE--DPGYR------
I35_RS19580  394 -PRLDAWQYGVFGLDRISLGEHWQ-VLAGGRFEVLLRQRSWSS-LDGE--TT-HT------
I35_RS26975  382 SQQNDISQKGVYGLGRIKLAEPLT-LVLGGRMSWWNQDSL---------GAHYN------
I35_RS06170  380 QFSTRARQAAVFAENRLEWLPRLA-WVSGIRYDHIAFSR-EQ-AATG--AGFDK------
I35_RS18505  378 KYRSQSNQYALFAENRLEITPRWS-VIGGIRYDHASVNR-DD-LVNG--GAFTK------
I35_RS06295  384 DQTDTLHDASAFFQDTLHLTDKWI-VSGGIRYITYNQVAGRG-RPFT--ANTDL------
I35_RS28095  386 DSRSVVHAYSTIVQDSVKLTDRLT-AVGGIRYFNWQQESGMG-RPFV--FADRS------
I35_RS08065  391 NTYTTMNTFGLYAQDQIKW-NRWT-LTLGGREDWVNMRQ-DD-RAAG--TSTKA------
I35_RS31745  390 DQYTAMNAFGVYAQDQIRW-RRWT-LTLGGREDVVNARF-DD-RSAG--THVQQ------
I35_RS21645  400 TTNTRTDTVSAYIFDTVKLSERWQ-FNTGIREDRYDTTG----KQAG-VADLSN------
I35_RS25625  405 --HARTTTKSIYGFDTIELTPRWQ-VNAGIRYDDYSTRFTDT-KANG-GKTYTR------
I35_RS31880  383 NLLERDDGQGVYAQDTLAFGPHWK-ILAGIRYDRFHQSI-DN-RLKG--VTTSQ------
I35_RS08115  384 MNRHRVSDYALFAQDRVDIGRAWK-LLGGIRADRFDVDS-TN-ALNG--LHARR------
I35_RS18545  379 NASTVVGLAGVYAQDLISLTEHWK-VLAGIREDYLNQIRHDY-TSSN--VNLDR------
```

```
I35_RS20820  407 ---T------FDDDRTKVLPSGTVRYERDLASLPVTWY--AGICHAEFYPDYWELFSATR
I35_RS23575  397 ---AG--VEKFAGAQPRDFNAGSLS-AGALFTLTPVWSIAANVAYTERAPTFYELYSNG-
I35_RS08460  558 ------------------FGGAFSPSFALRGQPVQMLTTYASYSRGFRAPTLVENSQAVY
I35_RS08490  568 ------------------FGGAFSPRFALRGQPIRELTMYGSDNRGFRAPTLIENTSSRT
I35_RS18860  442 PSSVSSPLAVSAQQHQTNTWRAPTWDITPEYALSSNVRAYFRYARGFRSGGYNGNAYT--
I35_RS04375  482 ------------------SANALSPKVALQWDATEVWRFRLSFATGTRFPTVGELFQ---
I35_RS29035  447 ------------------SANELSPRVAVLYEITPAVIPYVQYAHGFRAPTPDQVNSS--
I35_RS23700  402 ------------------GQAVNTGNAALSWAITPVYTARVSYGNAFRLPTFNDLYYP--
I35_RS27690  450 ------------------VFSRFNPAVGLNWNPVPGLTAYATYNEGMRSPTAIELACADP
I35_RS11045  441 ------------------SNAITTPVFGLVVKPWRNVSIFANRSELLAQGEIAPNT----
I35_RS00620  432 ------------------QNGVVTPTFAVMFKLAPTTTAYASYAESLEPGSRVNDV----
I35_RS19580  442 ------------------DRSVFLPQVALVYKPVNVLSLYASYSKALSLGDQAPVR----
I35_RS26975  426 ------------------TGHQFTPYGGLIWDFVRDWSWYASYAEVFQPQTKSMWG----
I35_RS06170  429 ------------------RFANIGWRTGFVFDIAPTFSAYAQYTTGAEGVGSLVTLSA--
I35_RS18505  427 ------------------VFANTGWRIGTVYDVRPGLAVYGQYSVGADFVSSLLSLNA--
I35_RS06295  434 ------------------SGSKTLPRAGVVYKWTDSFSLYGSYSQSLKPSSSIAPMTG--
I35_RS28095  436 ------------------RGSVTLPQFGLAYALTPALTAYANVSRSFKPNVASN------
I35_RS08065  439 ------------------DVTAFTGRVGLTYQGDYGLSPYISYATSFNPLIGVNTL-G--
I35_RS31745  438 ------------------DVSAFSGRVGLTYRGDAGWSPYVSYSTSFDPVIGVRVF-G--
I35_RS21645  448 ------------------TSNLFSYQFGLVFKPVTNVSLYASYGTSSNPPGSNG-GLGGG
I35_RS25625  454 ------------------DDTLFNWQAGLVFKPAQNGSIYASYATSSTPAGMLL-GEGSE
I35_RS31880  432 ------------------LQTALSPRIGVVYEMSPAWSLYANTAYSFRPNNGADVG----
I35_RS08115  433 ------------------TTTAWSPRLGVVWSPVGAHSLYASYSKNEAPVGGDLIGITPD
I35_RS18545  429 ------------------TDHAWSPRVGLIYEPLDWLTLYGSFSQSFSPLADTLISSG--

I35_RS20820  456 G----------------PTGSVNAFSAVRPE----RTTQLDIGAQYKSDRF----DAWVSA
I35_RS23575  450 ----------------PHDATGQFLIGNPNASKEKAVSTDLSLRYASGPNRGSVGVFYNR
I35_RS08460  600 LSHQNLVDPNDPSGVPTKHFTTEQVAGNPNLQPEFTKNYNIGFQL---SPDAMTDIGAAF
I35_RS08490  610 YGAQGAVDSNDPNNPNAYNLVEEVQTGNSKPQPEFTKNYNIGFQL---SPTRNTDFGFDW
I35_RS18860  500 ------------------------QSTVSTVSPEYLSDYEVGIKS--EWFDKRLIVNASV
I35_RS04375  521 ---------GTIS-------NNAIVNNNPNLRPEKAIDWDFTA--ERDVGVGVVRAS--V
I35_RS29035  487 -------FSNPVY--------GYTSIGNPNLKPFTSDTFEAGLRGKAGTGYGIVRYSAAA
I35_RS23700  442 ------------------------GYGNPSLSPEFSTSVEAALDA--NT--AYGTFTAAI
I35_RS27690  492 A--------APCS-------LPNDFIADPPLEPVISKTFEAGMRG--RIG-AATTWSAAA
I35_RS11045  479 ------------------------ARNAGQALSPYFSKQYEAGVRY--DT--DKYGASLAL
I35_RS00620  470 ------------------------YANAGQVLKPLFSKQYELGIKS--ER--ARWSAIAAL
I35_RS19580  480 ------------------------ATNAYAFLPPVESHQFEVGAKY--DWL-DRLSLIAAV
I35_RS26975  464 ---------------------------GGILTPVKGRTYETGVKG--ELAGGKLNVSLAA
I35_RS06170  469 --------------------------SQMNDRLATGAQWEAGLKQ--TLLDGRAYWIVAV
I35_RS18505  467 --------------------------SKASFTLATGRQIEIGVKQ--SFLDGKAEWILAA
I35_RS06295  474 ------------------------YIIDGATPPEEATAWEVGGKL--DLA-GGMTGILAL
I35_RS28095  472 --------------------------VAAPLAPEYGRVLEAGLKF--SLK-PAITGILAV
I35_RS08065  478 ---------------------------GGLPQPTFGKQIEAGLRW--QPPGKNLMLNAAL
I35_RS31745  477 ---------------------------GGLPKPTFGVQTEAGLRW--QPPGRNLMLNAAV
I35_RS21645  489 T------DQ--------------ITATNQDLAPEFARNIEIGAKW--DVLQDQLSLISAL
I35_RS25625  495 T------QSLTPG-------RGGVGPNADQLSPEKNRSIELGTKW--NVLNDKLSLIAAL
I35_RS31880  470 ---------------------------GRAFDPEKGHGYEAGAK----WAGARWLTIVSA
I35_RS08115  475 ------------------------ARGNANDLGPQYTRQYEIGVKS--DWRDGALSTILAL
I35_RS18545  469 ------------------------AFSNGAALAPQKTTAYEVGSRF--DLG-GKATASVAL

I35_RS20820  493 YAGYVQDFILFD---------YA----TGMMGPTT-------QATN-VNAQIMGGEAGVS
I35_RS23575  494 FSNYLTEYNTGR------VVDDD----GEPVAPGTDGSLNEAIYRG-VRAEFYGIELDGK
I35_RS08460  657 YKVRIDGVIGTDDPNAVLVANDPSRVVRNADG--SVRYLV-QHFVNLGALDTDGFDLNFR
I35_RS08490  667 YKIHIDNVIGTEDIQTVIDQNDPSKVIRNPNG--TIAYVL-LPYMNLSSLDTDGFETTFR
I35_RS18860  534 FHYDYRDIQVFA------LA-------PNPFGGPP----V-STLSNAGQGRADGFELELK
I35_RS04375  561 FQSDLRDSIYSQ---------------TTASGATTV-----TNISNVDRVRVRGVELAFS
I35_RS29035  532 FTGRYRNFISRT---------------TIAGSGRPVDPFV-FQYVNFADARIHGLEGR--
I35_RS23700  474 YDTRVNNLIAY-----------------NPAT---------FSPMNIGRSHIRGIDLSYK
I35_RS27690  534 YRTTLTDDIQFI---------------SSPAS------AQ-GYGRNVGDTRRQGIELAGR
I35_RS11045  512 FQIEKPMA--Y----------------TDP--------AT-NLFGADGTQRHRGIETAVY
I35_RS00620  503 FRIERSAE--Y----------------AN---------AA-NVYVQDGESIIQGIEVGAR
I35_RS19580  514 FSISKPFQ--F----------------ADPDA--S--GTS-YTFVQRGTQRHQGIELGAA
I35_RS26975  495 FRIDLDNN--PQ---------------VDLAH--PCAGPS-CYYVNGGSVRSQGFEFEAN
I35_RS06170  501 YDITKRNL--LS---------------TDPFN--P------ALRQQVGRQSSRGVELTGG
I35_RS18505  499 YRIVKRNL--LT---------------ADPVN--P------NQSIQVGQQSSRGIEATVG
I35_RS06295  507 FNIDKKNV--LV---------------SQYND--A-TK-L-TDTRTSGKARSRGVELDVS
I35_RS28095  503 YQIDKRNV--AV---------------TVDDI-----------TSTIGTARSRGIELDVA
I35_RS08065  509 YQINQTNG--IT---------------PALPS--QDPG-G-TKSVQSGEVRSRGIELSAT
I35_RS31745  508 YQIDQTNV--VT---------------PTPVN--LDPT-A-TTSVQTGKVRSRGIELSAV
I35_RS21645  527 FQTEKTNA--RV---------------SDGLG----------HTVNAGKQRVRGFEFGFA
I35_RS25625  540 FQIDTTNA--RV---------------TLPNN----------QYAMVGNKRVQGLELGLA
I35_RS31880  499 FYVTKRNV--LT---------------ADPAN--A------GFSRAAGEVRSRGVEFEWS
I35_RS08115  510 FQLDLYNR--RI---------------ADPVR--P------GFFDLTGLERNRGIELGVA
I35_RS18545  503 FDMRQTNQ--QI---------------GDPAN--P------GYALPIGTQHVRGMELGFT
```

```
I35_RS20820  532 WRPVA----PLR-VETSLAYAWGRNVA---------------------SGDPLPQMPPLE
I35_RS23575  543 WRAFSRRGHTVD-LELTADYTHARNVD---------------------TGQPLPRIAPLR
I35_RS08460  714 KAL--RTKYGTFTLAGDWTYV----WHFK-LHSPGTAPQDFAGNNLALLQPFGASNPRWK
I35_RS08490  724 QSV--STKTGTFTLSGDWAYV----WHFK-MPVGG-ESTDFAGNNGSLNEPFGGSFPRWK
I35_RS18860  576 AQP--VNSIYLF---ANLGMLNTRYTEFR--------------NVPTAVGNSFARSPHTT
I35_RS04375  601 GENVGLRGINID---ANVSASNAQILADA--------------ANPAYVGSRFPRIPRMR
I35_RS29035  574 AEWMMPNGITLK---TAMAFTKGSTQNDG--------------A----ASQPLNTVNPFS
I35_RS23700  508 GTI--GRSTPVS---IAVGIINPQDETNQ---------------------TWLSRRPRQT
I35_RS27690  572 TRV--GP-IGVG---LSYSYWDATYRSSWIEHSPANSTADANGNVTVKPGDRIPGIPAHT
I35_RS11045  545 GEP--WKGVRII---AGATYIDATLQNTA---------G------GTNDGHRPIGVPSFL
I35_RS00620  535 AKF--GAHWNAG-----VDAWLLDAWYAN---------G------IGNHGNRVAGAPRFV
I35_RS19580  551 GRV--TERIGLT---ASVAIRARAVDSG---------S------PAYEGHQIINVPALR
I35_RS26975  535 GRI--TPWWSVW---ASYTYDTMRYADNL---------ANAGS-------FAPLLNPRHL
I35_RS06170  536 ARL--PHGWTID---ANVALLRARYDAFN---------QTVGGATVSRAGNVPSGVPQQT
I35_RS18505  534 AEI--AKDWRVD---ANVSILRAKYDDFQ---------QSSGGTTVSRAGNVPVSVPQRL
I35_RS06295  545 GKL--GERVNVI---ASYAYIDAKTTED----------PLYAG-------NQLWNVARHT
I35_RS28095  535 GQI--TRHISVI---GSYAYTNANDRDS--------------N-------TPLVNVARHT
I35_RS08065  548 GKV--TPNISVV---ASYVYQDVKVIQAN---------DVSLN-----NWPVDIPRPRQM
I35_RS31745  547 GKV--TREISIV---ASYLYQDVKNVQAN---------DASLN-----HWPVSVPLPRQM
I35_RS21645  560 GNL--TQKWHVF---GGYSYINAITTDAG---------PGSPG----ASGLPMVMVPKHN
I35_RS25625  573 GQI--TKQWQVF---GGYTYMKSELRDNG---------KDTA-----NNGNRFPNTPKHS
I35_RS31880  534 GDL--GHGTRGL---ANLAYVDAEVTRDA---------VLTPG-------SRLVDVPRLS
I35_RS08115  545 GRL--TGDWFVR---GGIGWQHARVVDAE---------PKYAG-------KRSAGVSASN
I35_RS18545  538 GEI--APKWSVY---AGYAYINGTVDGSA---------QSTAAG-LAVSSNTPGLMPRHS

I35_RS20820  566 ARIGLEYTRGA-WS-----AGGLWRIVASQHRYALNEGNVVGKDFGPSAGFGYLSLHTQY
I35_RS23575  581 ATLAADYGYGP-FG-----ARAQVTHAWSQHRVPD-------DDFS-TDGYTSLGWMLTY
I35_RS08460  767 GNTSWSWDYRQ-LT-----TTLTWQYTGPYTNAV-AAEF-GDGGTGSVASYSQFNLMFNY
I35_RS08490  776 GNTSINNNYHNQWN-----ATLTWMFTGPYSQAI-LSPGQYPNMQDSVASYSQFNLMVSY
I35_RS18860  617 LNAGVDYRVPVSFG--TLTAGGDVNYRSREYFSATR--QTMPQL--WQGGYTVLNAHVSY
I35_RS04375  644 ANLLASYRFDEHWL-----ASVGVRYSGRQ-YNTLDNSDVNPDVYGGTSSFTVVDLKARY
I35_RS29035  613 AVFGWRYEPTERWF-----VQTDLLFQAAKRDKDVDKSDCSNKACFTPPSSFVVDLRGGY
I35_RS23700  542 VSLNVDHTWDELKL-HALSTGASLLYGGSTFD------DPANRQ--YLASYLTVSLRASY
I35_RS27690  626 VKLRLDYAATPAWD-----IGANVTWRGGVYARG---DENNGDVNGRLAGYVLVDLDMRY
I35_RS11045  585 LNAGAEYDVPML---RGLTLTARWIHTGPQYL------DVANTV--SLQAWDRFDLGARY
I35_RS00620  573 LAGDLGYAVPGV---PGLTLGVDAKFTGATPL------RAAGGL--DAPGTLVVNAGARY
I35_RS19580  591 ASLYADYAVPGV---AGLNVLGGVEYSAARNA------NEEGTA--RVPSWFVFNLGARY
I35_RS26975  574 FRLWTNYDLP--WQERRWSIGGGVQVQSSYSA-------QANGVTMSQGGYALASVRLGY
I35_RS06170  582 ANLWVGVAFAERWQ-----ANAGVRYVGATYG------DDANRV--QVPSYTVFDASLRW
I35_RS18505  580 ANLWISVRFAPDWT-----GIAGVKYVGKRFA------DTANQL--VMPSYTTVDLGLAW
I35_RS06295  583 ASFAAVYDFGTVAAGDDLRLGADVRYVGARPG------DSANSF--TLPSYVLADAFATY
I35_RS28095  569 GSLFAVYDTAIANLPGRWRFGGGARLVGARSG------DTANSF--TLPGYVSVDAFAAY
I35_RS08065  589 ASLWTDVTWHTGPL-AGFGLGGGIRYQSASAG------AADNSL--TVSSVTLFDAGVHY
I35_RS31745  588 ASMWADVTWHTGAL-AGVGVGGGVRYQSASAG------APDNSL--TVPSATLYDLAIHY
I35_RS21645  602 FTLWTSYDVMPKLT-----LGAGATVMSKTYASV----SPTVKK--WTPGYARFDAAATW
I35_RS25625  614 LTMWSNYDVTPKFT-----VGGGAFYMSEVFGD------PANLR--AVPSYWRFDAMAQY
I35_RS31880  573 GSALLMYETTLPFA-DKAGAGAGVIYVGRRAGNT---ANTQDGF--DLPAYATVQLNGYL
I35_RS08115  584 GSLFVSHAPLRGFF-----AELGVVYEGARYA------DRDNLL--ELPAYLRWDGKAGY
I35_RS18545  583 ANLWLKRELPYGFY-----AAAGMQFQSARYT------SASDLV--TLPSFTYFNLGAGY

I35_RS20820  620 NV--SKTVQIS-VGVDNVLNKAYTEHLNLAGN-------AGFGY-PANAPVMEPGRTAWV
I35_RS23575  627 KFRVGPTFWLAYLRGDNLTNQEIRY--STSVV-------RGFAP-QGGRSVMAGLRTTF-
I35_RS08460  819 RG---FKHWTTYGGITNLFDKKPPFDVEW----QAVPDITGYDQ----SLYTNLG--RFF
I35_RS08490  830 TG---FKHWTTYAGIDNIFNRAPPFDPVY----MNASYQTGYDT----SLYTYVG--RFA
I35_RS18860  671 TT--PNQKYIVTGYVTNLINKVYKKLELLP----------SY-----GAYPVLYGDPRTV
I35_RS04375  698 RF---DRHWTASAGIDNLTDRRYYTFHPYPGR-------TFYGE--LKWSL---------
I35_RS29035  668 RF---NKHVSATIGIRNLFDRKYWNWSDVRGI-------AADSQ--VLDAYSSPGR--TV
I35_RS23700  593 RI---NSHLTVSASLSNLFDRQYMTAY----------------------GYNTLGRTAFG
I35_RS27690  678 RI---TKRFEVFASVTNLLDKRYASFGALGQNFFNGPNHTFDGARPVNEQFVGPGAPRGA
I35_RS11045  634 ATDVFGKKTTFRATVRNVANKSYWSS--------------------TIGGYLTQGDPRSV
I35_RS00620  622 LTRVGRHDVTLRASIDNVLNRRYWEY------------------QYADYVKPGDPRTV
I35_RS19580  640 TTKIGGHRTVLRVSVDNLFNKFYWRDAGEQ----------------QGDAYLFPGAPRTA
I35_RS26975  625 RY---DKHWSAALNVNNLFDRHYYLSLSQP------------------GWNNRYGEPRNV
I35_RS06170  629 QP---TSHTELALYLRNLANRTYAVTTSNG------------------GEQWLLGPSRSA
I35_RS18505  627 KP---RKDTTITARAYNVFNRRYVQSAYYN------------------ETQYLLGNDRRF
I35_RS06295  635 DTRIGKQHLSFQLNVKNLFNRTYYPSSAN-------------------RYFVAVGDARQV
I35_RS28095  621 ETTIGKFPTRFQLNVKNLLDKTYYPSSNN-------------------NLIVAVGEPRLV
I35_RS08065  640 -D---TRNWRFAVNGTNLFNRHYISGCQS-------------------MNVCIFGTDRTV
I35_RS31745  639 -D---LPHWRFAVNVANLFDRRYVSGCQS-------------------YAVCVFGNERTV
I35_RS21645  651 RV---NKTMDVQLNVQNLFDKQYYASAYPI------------------YATWAPGRSAMV
I35_RS25625  661 RI---NKKLDLQLNVNNLFNRTYFDQAYPA-----------------HYASIAPGRSAFV
I35_RS31880  627 QV---NKHLRASVVLNNLFNRTTYVSSY-------------------NSLWVTPGAPRSL
I35_RS08115  631 -R---TRDLEVTLAAVNLADRDYYANATGL-----------------AQI--VPGAPRTF
I35_RS18545  630 -R---SKKVDVTLTLDNLFDRRYFIAAHGN-----------------ADLYNMPGDPRTL
```

```
I35_RS20820  669 RVSAKL---
I35_RS23575      ---------
I35_RS08460  866 QVGATYRF-
I35_RS08490  877 QVGATYKF-
I35_RS18860  714 GITLTAKI-
I35_RS04375      ---------
I35_RS29035  714 AVSMKVDF-
I35_RS23700  628 --KVSYTF-
I35_RS27690  735 WVGVRYAWD
I35_RS11045  674 WLSMTTDF-
I35_RS00620  662 SLSAKIDF-
I35_RS19580  684 RVSLTYDF-
I35_RS26975  664 MLTVRGQF-
I35_RS06170  668 ELVATMRF-
I35_RS18505  666 ELLANYRF-
I35_RS06295  676 SLLTTLQF-
I35_RS28095  662 TLTTTVSF-
I35_RS08065  677 IATAKYNW-
I35_RS31745  676 LASAKYSW-
I35_RS21645  690 TLNFYQ---
I35_RS25625  701 TLNARY---
I35_RS31880  665 FASLAYSF-
I35_RS08115  668 TLTAAYKF-
I35_RS18545  669 TATVKWHM-
```

Figure 3.8: Alignment of putative TBDRs in *B. cenocepacia* H111

Amino acid sequences of putative TBDRs from *B. cenocepacia* H111 were aligned by Clustal Omega and identical or similar amino acids were highlighted using BOXSHADE. White font with black shading indicates identical residue at the corresponding position in ~50% of sequences and white font with grey shading indicates similar residues at the corresponding position in ~50% of sequences. The gene locus designations are indicated on the left. Red box indicates the location of the TonB box conserved region. Blue box indicates the location of the receptor plug domain.

Based on the UPGMA tree topology, the top part of the tree between BCAL1700 (I35_RS08065 in H111) and BCAM2224 is hypothesised in this study as ferric siderophore TBDRs because both of them correspond to known ferric siderophore receptors (Figures 3.9 and 3.11). Furthermore, a BLASTP analysis of the *B. cenocepacia* protein database using PA2398 (FpvA) of *P. aeruginosa* PAO1 as the query, which is involved in transporting the ferric-pyoverdine siderophore complex (Poole et al., 1993), identifies the TBDR BCAL1371 (I35_RS06295 in H111) as the best match, which is found in the upper part of the phylogenetic tree. Additionally, TBDRs predicted to be involved in siderophore transport by Interpro analysis are mostly found in the upper part of the phylogenetic tree. Therefore, this suggests that TBDRs in the lower half of the tree may not be involved in siderophore uptake and are most probably associated with transport of other metals such as copper and zinc and also of compounds such as vitamin B_{12}, as mentioned in Section 3.2. Alternatively, it may be possible that the TBDRs in this part of tree transports more than one metal including iron. It is also noteworthy that the predicted haem TBDR (BCAM2626) is located in the lower part of the tree.

Identical pairs of closely related TBDRs observed with the two methods include BCAL1700/BCAS0333, BCAM1187/BCAM2007, BCAL1345/BCAM0491, BCAL0116/BCAL2281 and BCAL1777/'BCAL1783' (I35_RS08490). Most pairs are distinguished by both methods, however, BCAM1187/BCAM2007 and BCAL0116/BCAL2281 pairs are not observed with the ML approach for strain H111 (Figure 3.10 and 3.12). TBDRs other than the above mentioned, are seen quite scattered or distal to each other. It can be concluded that the two statistical methods performed in this study showed sensitivity of the putative TBDRs to methodological variants. The tree topology for strain H111 is slightly distinct to the strain J2315 for both methods. This may be due to amino acid variants between the strains. Nonetheless, the bootstrap values of 70-90 presented at nodes of the ML trees show the reliability of the analysis.

Comparing the two approaches, the UPGMA algorithm shows stronger similarity to the Interpro analysis discussed in Section 3.2. The clusters observed in the UPGMA tree topology can relatively be divided into two parts, the upper and lower, whereby putative TBDRs which are predicted to transport siderophores by the InterPro analysis are clustered in the upper part and TBDRs which have other functions are mostly clustered in the lower part of the tree. The ML tree topology of the putative TBDRs was more scattered, although similar TBDR pairs observed in the UPGMA analysis were identified. Nonetheless, the numerical evidence of bootstrap values may increase the reliability of the ML phylogenetic analysis.

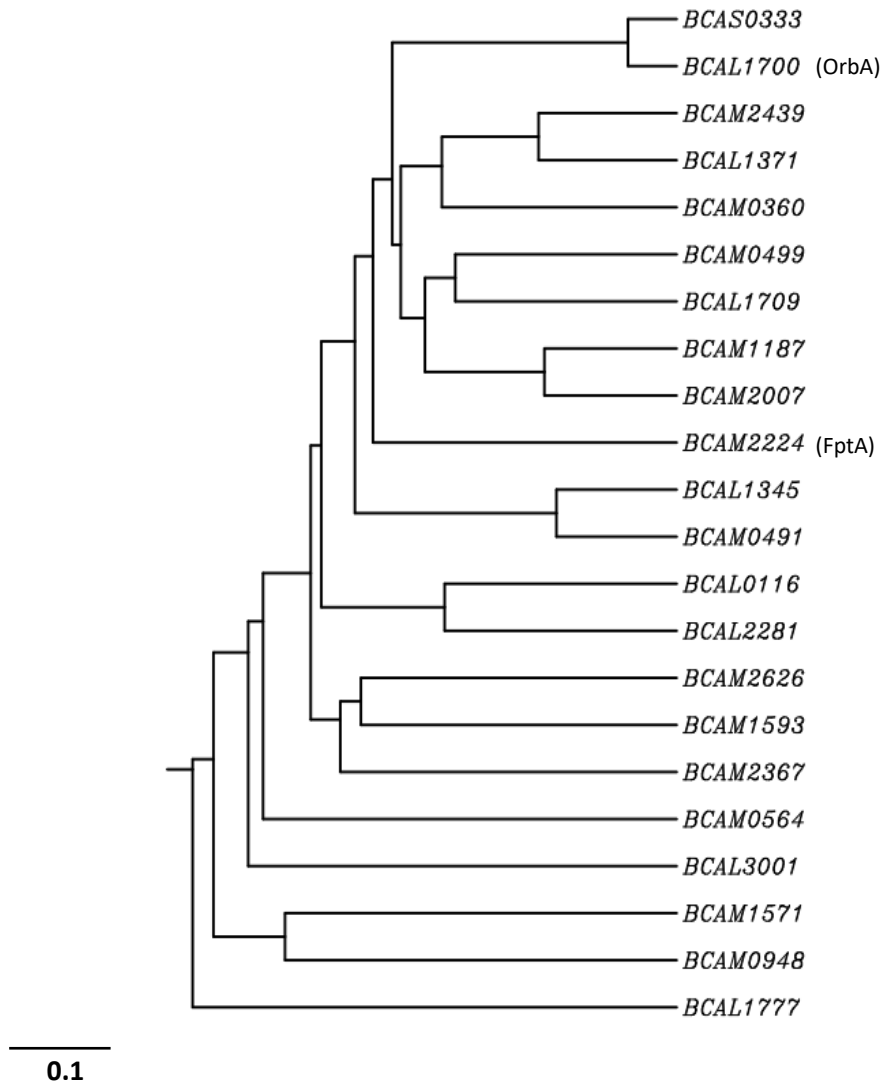

Figure 3.9: Rooted UPGMA phylogenetic tree of TBDRs from *B. cenocepacia* J2315
Rooted UPGMA tree with branch length depicting the relationship of TBDRs from *B. cenocepacia* J2315. Alignments of the TBDR amino acid sequences and phylogenetic tree were constructed by ClustalW.

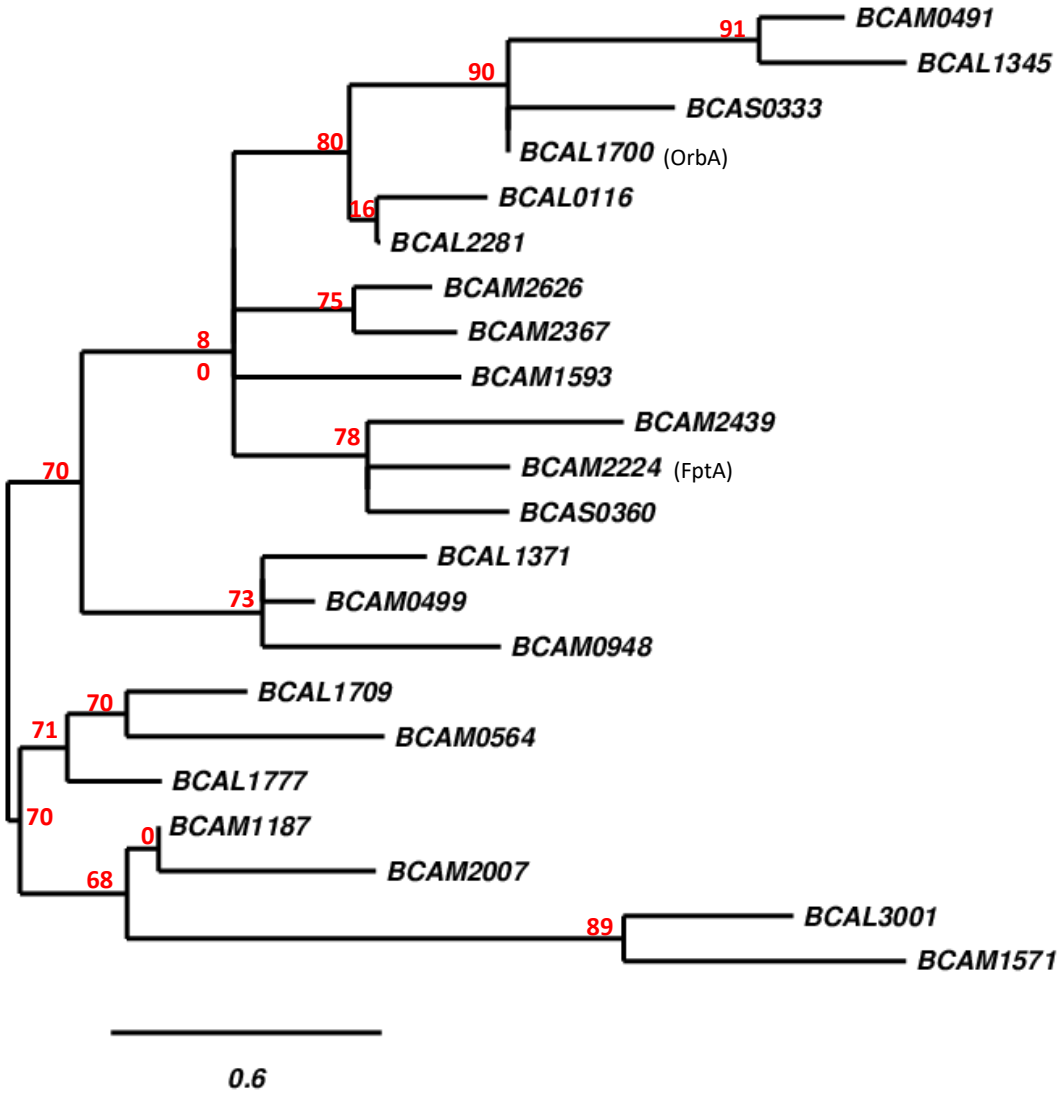

Figure 3.10: Maximum likelihood phylogenetic tree of TBDRs from *B. cenocepacia* J2315
ML bootstrap percentages are indicated at the nodes. Scale bar shows amino acid substitutions per site (in 100 amino acid residues, 60 % is similar in identity). Alignments of the TBDR amino acid sequences and phylogram constructed by Phylogeny.fr.

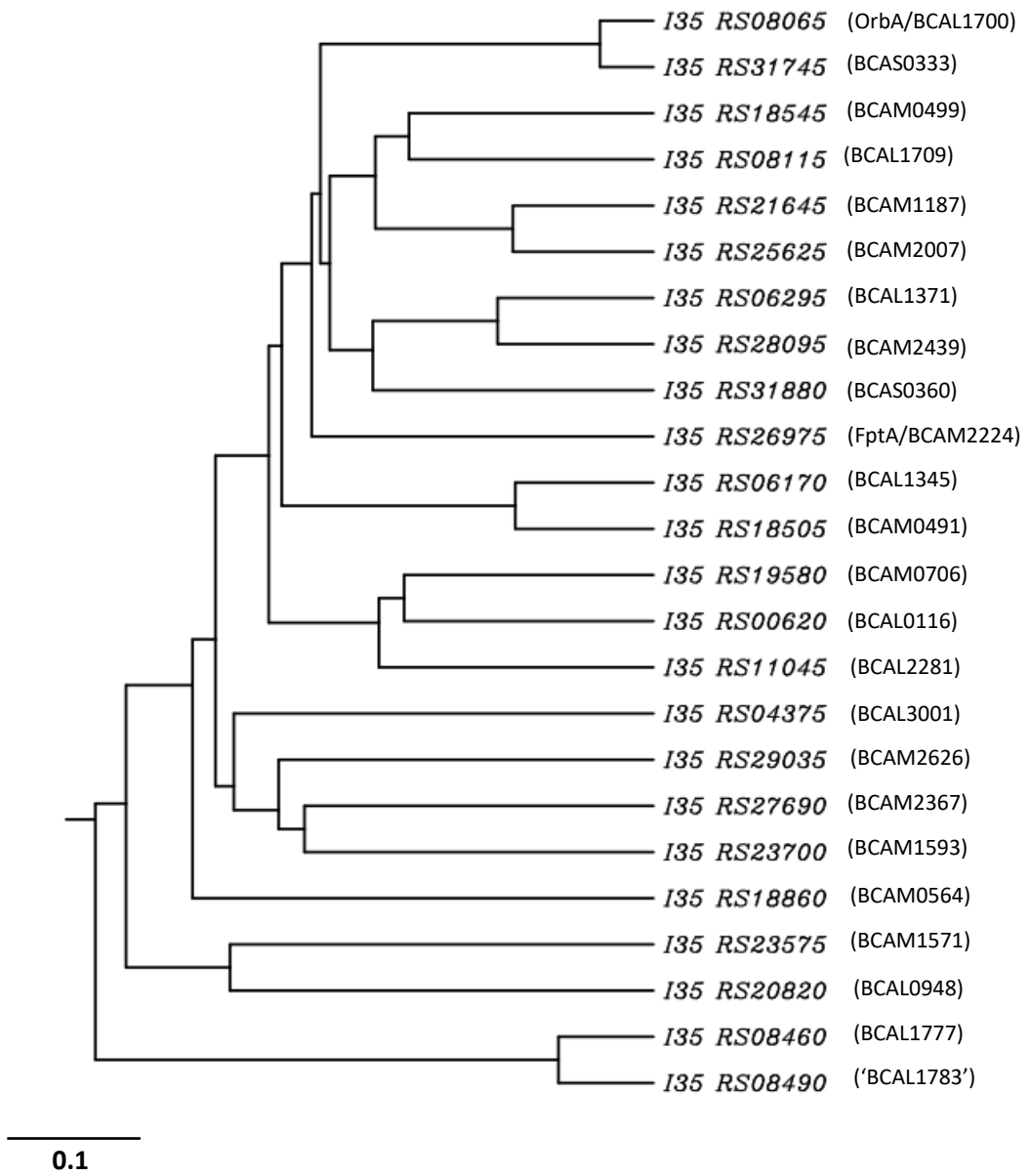

Figure 3.11: Rooted UPGMA phylogenetic tree of TBDRs from *B. cenocepacia* H111
Rooted UPGMA tree with branch length depicting the relationship of TBDRs from *B. cenocepacia* H111. Alignments of the TBDR amino acid sequences and phylogenetic tree were constructed by ClustalW.

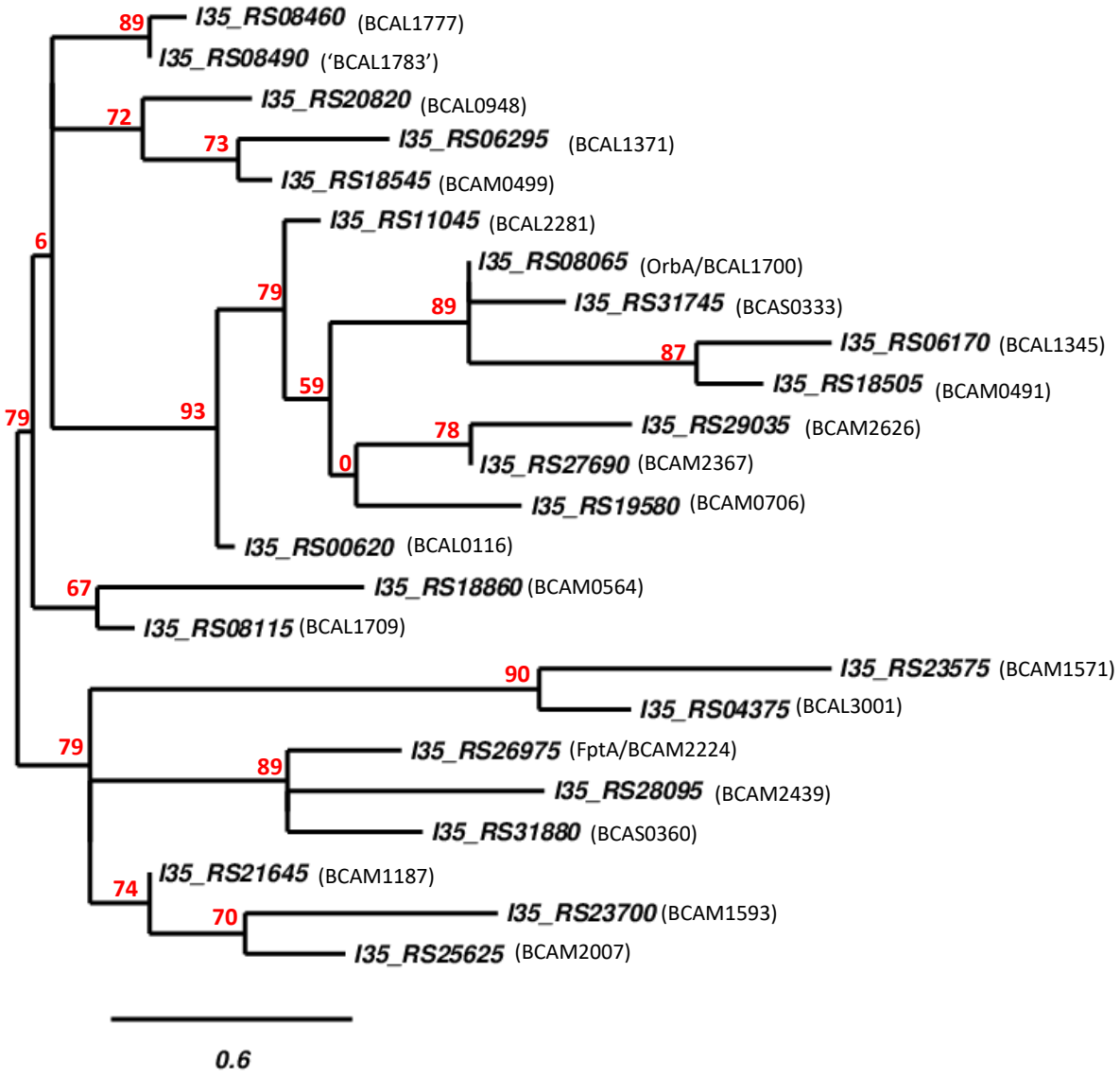

Figure 3.12: Maximum likelihood phylogenetic tree of TBDRs from *B. cenocepacia* H111
ML bootstrap percentages are indicated at the nodes. Scale bar shows amino acid substitutions per site (in 100 amino acid residues, 60 % is similar in identity). Alignments of the TBDR amino acid sequences and phylogram were constructed by Phylogeny.fr.

3.4 Genomic context of TBDR genes

The nature of the genes located in the neighbourhood of each TBDR gene was then analysed to obtain additional clues as to the possible role of each TBDR. In some cases, genes related to siderophores such as the siderophore biosynthetic enzymes, potential siderophore transporters, transcriptional regulators, iron-starvation sigma factors and alternative TonB complexes were found located upstream and downstream of the putative TBDR genes.

The TBDR for the endogenous siderophore, ornibactin, OrbA (BCAL1700) is found in the vicinity of a biosynthetic enzyme cluster, including the NRPSs, which has been shown to be required for ornibactin biosynthesis (Agnoli et al., 2006). Likewise, the pyochelin TBDR, FptA, (BCAM2224) is in close proximity to genes encoding homologous of the pyochelin biosynthetic enzymes in *P. aeruginosa* as well as iron uptake proteins and a ABC transport system, BCAM2225-BCAM2227 (Thomas, 2007). Based on the gene loci arrangements, almost all of the putative TBDR genes are observed to be near to genes encoding many types of transporters including MFS (small solute) transporters. In fact, nearly 50 % of the putative TBDR genes are near to an ABC transporter gene, i.e. BCAM1345, BCAM1777, BCAM0948, BCAM1571, BCAM2007, BCAM2224, BCAM2626, BCAS0333, BCAS0360, ('BCAL1783') I35_RS08490 and (BCAM0706) I35_RS19580. The BCAL1345, 'BCAL1783' (I35_RS08490), BCAM2224 and BCAM2007 genes are located next to genes predicted to encode ABC transporters involved in iron uptake. These TBDR genes are also observed to be adjacent to genes encoding iron-dependent enzymes or iron uptake proteins. Several other ABC transporters may not be involved in iron uptake. The BCAM1777 and BCAM0706 (I35_RS19580) genes are located next to genes encoding efflux system transporters and the latter is also located near to genes encoding porins predicted to transport other metals such as cadmium and zinc. Additionally, the BCAS0360 gene is seen to be located next to genes predicted to encode a xylose transport system. BCAM2626 is predicted to be near to genes encoding an ABC transporter involved in haem transport. BCAM0948 and BCAM1571 are observed to be located near to genes encoding an ABC transport system of unknown function.

The BCAL0116, BCAL2281 and BCAM0491 genes are each observed to be located next to a gene encoding a cytoplasmic membrane protein, predicted to be a single subunit permease. Furthermore, BCAL2281 together with another two putative TBDR genes, 'BCAL1783' (I35_RS08490) and BCAM0564 are located near to gene clusters encoding TonB systems. BCAL2281 is close by to *tonB1*, 'BCAL1783' (I35_RS08490) is close to the predicted *tonB2* and BCAM0564 is very near to genes encoding the TonB3 complex (see Section 3.6 for more details on these systems).

Many regulatory genes are also located near to these putative TBDR genes. The putative TBDR gene BCAL1371 is located downstream of a pair of genes encoding an iron-starvation sigma factor and an anti-sigma factor. BCAL3001, BCAM1187 and BCAM1593 are noted in clusters of genes encoding enzymes such as hydrolases and reductases. Three pairs of TBDR genes are seen to be nearby to each other: BCAL1700 and BCAL1709, BCAL1777 and 'BCAL1783', and BCAM0491 and BCAM0499 (see Figure 3.13).

Siderophore biosynthetic enzymes found adjacent to specific TBDRs, in this case ornibactin and pyochelin, include monooxygenases, NRPSs, aminotransferases, reductases and dehydrogenases. Most cytoplasmic membrane transporters for ferric siderophores involve single subunit permeases or ABC transporters. Most putative TBDR genes in the *B. cenocepacia* genome are therefore shown to be present in clusters with these transporter genes in addition to other transport proteins such as RND, MFS, symporters and porins. Transcriptional regulators were also shown to be near the TBDR genes which include LysR, GntR and AraC. Genes unrelated to iron acquisition that are observed close to TBDR genes include flagella synthesis, trehalose synthesis, quinone synthesis, chemotaxis receptor and ribosomes synthesis. In addition, BCAL1709 and BCAM2367 were identified in gene clusters of cobalamin and quinone biosynthesis clusters.

3.5 Investigation of putative TBDRs in other *Burkholderia* species

The existence of putative TBDRs in other *Burkholderia* species (Bcc, *Burkholderia pseudomallei* group and *xenovorans* group) were also identified using BLASTP searches using the putative TBDRs of strain J2315 and H111 as queries (Burkholderia.com) (Table 3.3). Representative strains from *Burkholderia* species were selected: *B. cenocepacia* K56-2 (ET12 lineage as with the J2315 strain*), B. cepacia* ATCC25416, *B. ambifaria* AMMD, *B. multivorans* ATCC17616 and *B. vietnamiensis* LMG10929 are from the Bcc whilst *B. pseudomallei* K96243 and *B. thailandensis* E264 are from the *Burkholderia pseudomallei* group. In addition, representatives from the *xenovorans* group, recently annotated as *Paraburkholderias*, *B. phymatum* STM815 and *B. terrae* BS001, were selected. *B. cenocepacia*, *B. cepacia*, *B. ambifaria, B. multivorans*, *B. vietnamiensis* and *B. pseudomallei* are commonly associated with infections in humans, unlike *B. thailandensis*, *B. phymatum (Paraburkholderia phymatum)* and *B. terrae (Paraburkholderia terrae)*.

In some cases, the genes encoding TBDR orthologues in different species were recognised as being located on a different chromosome. For example, the BCAS0360 gene in *B. cenocepacia* J2315 strain is located on chromosome 3 while its orthologue in *B. ambifaria* AMMD, CH72_RS24835, is located on chromosome 2 (it lacks a third chromosome). The identification of TBDR orthologues in other species and other *Burkholderia* groups potentially allow prediction of specific receptors which are responsible for the utilisation of a specific siderophore by a strain or species.

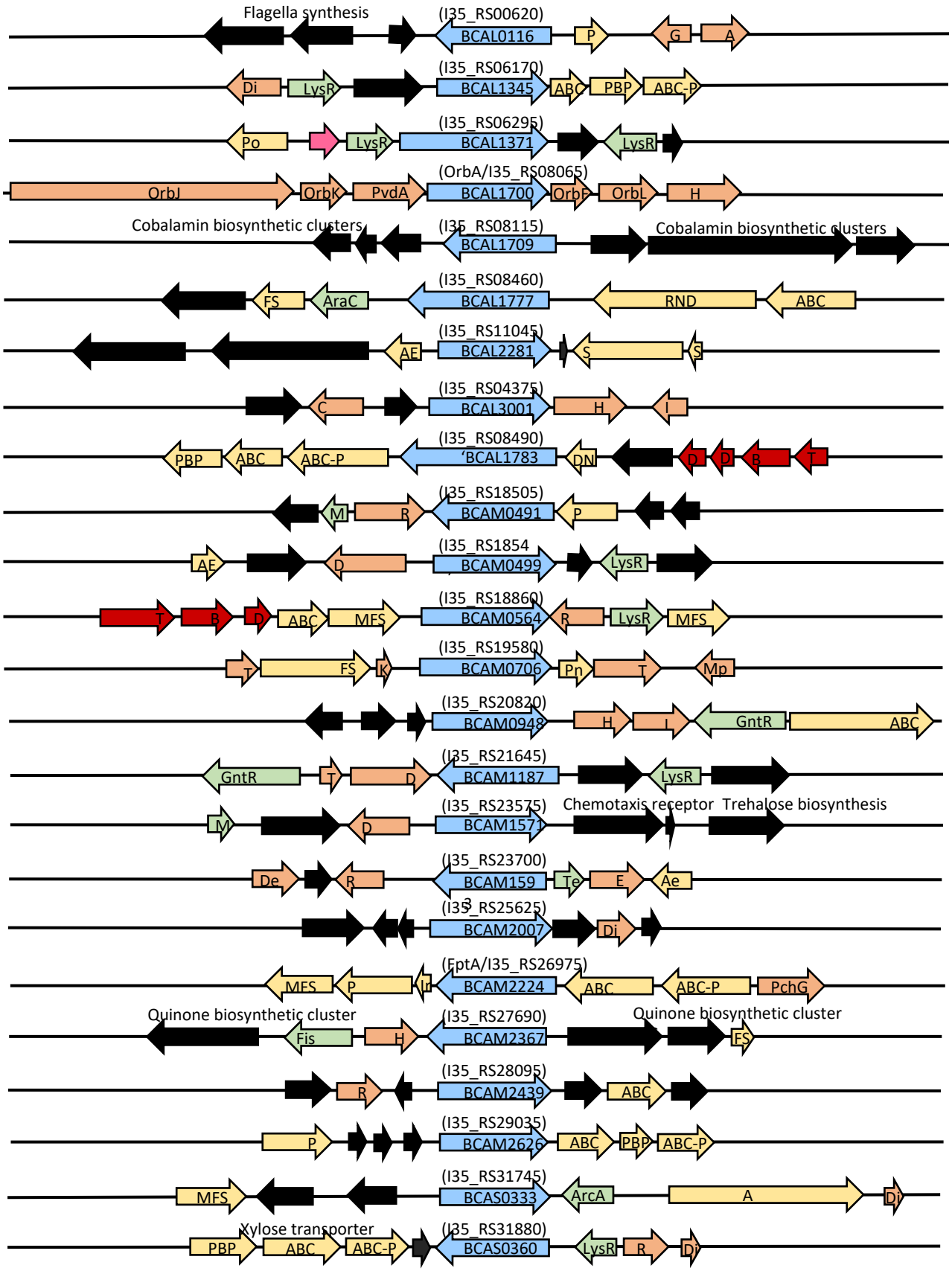
Flagella synthesis
(I35_RS00620)
BCAL0116
P
G
A
(I35_RS06170)
Di
LysR
BCAL1345
ABC
PBP
ABC-P
(I35_RS06295)
Po
LysR
BCAL1371
LysR
(OrbA/I35_RS08065)
OrbJ
OrbK
PvdA
BCAL1700
OrbF
OrbL
H
Cobalamin biosynthetic clusters
(I35_RS08115)
BCAL1709
Cobalamin biosynthetic clusters
(I35_RS08460)
FS
AraC
BCAL1777
RND
ABC
(I35_RS11045)
AE
BCAL2281
S
S
(I35_RS04375)
C
BCAL3001
H
I
(I35_RS08490)
PBP
ABC
ABC-P
'BCAL1783
DN
D
D
B
T
(I35_RS18505)
M
R
BCAM0491
P
(I35_RS1854
AE
D
BCAM0499
LysR
(I35_RS18860)
T
B
D
ABC
MFS
BCAM0564
R
LysR
MFS
(I35_RS19580)
T
FS
K
BCAM0706
Pn
T
Mp
(I35_RS20820)
BCAM0948
H
I
GntR
ABC
(I35_RS21645)
GntR
T
D
BCAM1187
LysR
(I35_RS23575)
Chemotaxis receptor
Trehalose biosynthesis
M
D
BCAM1571
(I35_RS23700)
De
R
BCAM159
Te
E
Ae
(I35_RS25625)
BCAM2007
Di
(FptA/I35_RS26975)
MFS
P
BCAM2224
ABC
ABC-P
PchG
Quinone biosynthetic cluster
(I35_RS27690)
Quinone biosynthetic cluster
Fis
H
BCAM2367
FS
(I35_RS28095)
R
BCAM2439
ABC
(I35_RS29035)
P
BCAM2626
ABC
PBP
ABC-P
(I35_RS31745)
MFS
BCAS0333
ArcA
A
Di
Xylose transporter
(I35_RS31880)
PBP
ABC
ABC-P
BCAS0360
LysR
R
Di

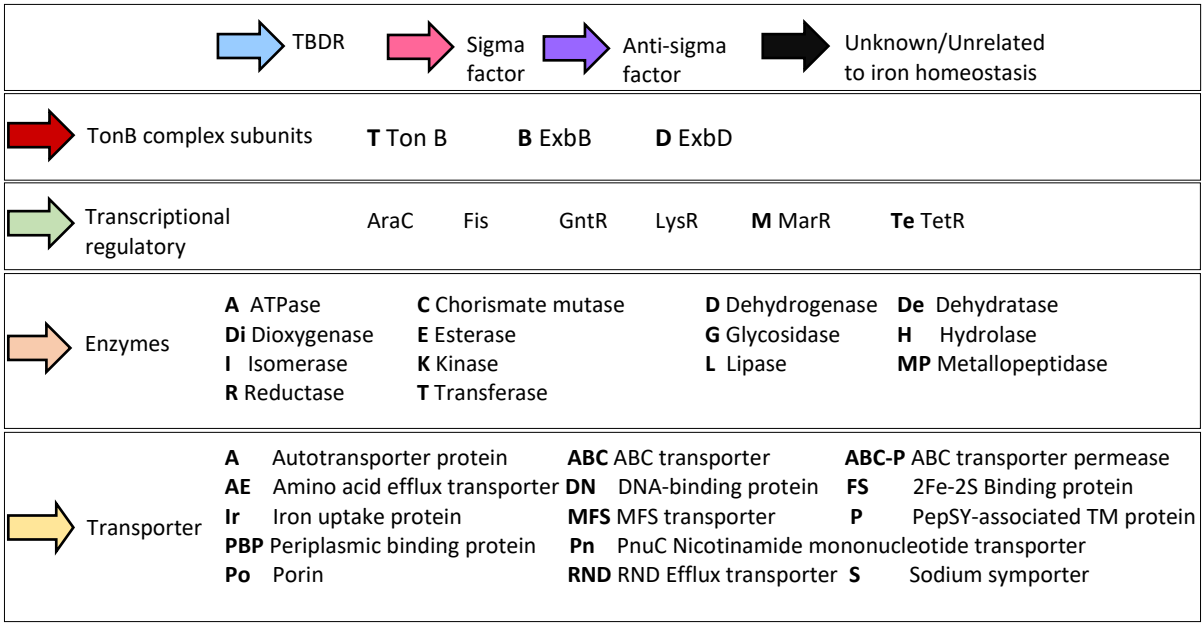

Figure 3.13: Gene organisations of all TBDR gene loci in *B. cenocepacia* H111
Diagram of the putative TBDR genetic arrangements. Arrows indicate genes and the direction of transcription. The colour scheme key and annotations represent the predicted function of the gene products. TBDR genes are annotated using J2315 strain nomenclature.

Table 3.3 List of putative TBDRs in representative *Burkholderia* species from the Bcc, *Pseudomallei* and *Xenovorans* group (*Paraburkholderia*) arranged according to bioinformatic homology. The colour code indicates the location of the TBDR gene loci on the chromosome

	Burkholderia cepacia complex group							Pseudomallei group		Xenovorans group	
	B. cenocepacia J2315	*B. cenocepacia* H111	*B. cenocepacia* K56-2[b]	*B. cepacia* ATCC25416	*B. ambifaria* AMMD	*B. multivorans* ATCC17616	*B. vietnamiensis* LMG 10929	*B. pseudomallei* K96243	*B. thailandensis* E264	*B. terrae* BS001[b]	*B. phymatum* STM815
1	BCAL0116	I35_RS00620	WQ49_RS13430	APZ15_RS04770							
2	BCAL1345	I35_RS06170	WQ49_RS33030	APZ15_RS10485				AQ15_RS24435	BTH_I1412		
3	BCAL1371	I35_RS06295	WQ49_RS32900	APZ15_RS10615		Bmul_1933		AQ15_RS00105		WQE_RS17305	
4	BCAL1700	I35_RS08065	WQ49_RS31235	APZ15_RS12790	CH72_RS16445	Bmul_1594	AK36_RS21110	AQ15_RS29965	BTH_I2415	WQE_RS26070	
5	BCAL1709	I35_RS08115	WQ49_RS31190								
6	BCAL1777	I35_RS08460	WQ49_RS30830								
7	BCAL2281	I35_RS11045	WQ49_RS28195			Bmul_1088				WQE_RS49780	
8	BCAL3001	I35_RS04375	WQ49_RS02420	APZ15_RS08735	CH72_RS03570	Bmul_2388	AK36_RS24350	AQ15_RS25330	BTH_I1598	WQE_RS04670	
9	[a]`BCAL1783’	I35_RS08490	WQ49_RS30800								
10	BCAM0491	I35_RS18505	WQ49_RS18990	APZ15_RS27215							
11	BCAM0499	I35_RS18545	WQ49_RS18955	APZ15_RS27265					BTH_II1381		
12	BCAM0564	I35_RS18860	WQ49_RS18630	APZ15_RS21665							
13	[a]BCAM0706	I35_RS19580	[a]WQ49_RS 17910	APZ15_RS20880	CH72_RS27210	Bmul_5036	AK36_RS08050				
14	BCAM0948	I35_RS20820	WQ49_RS16725	APZ15_RS19710	CH72_RS16770	Bmul_4669	AK36_RS07150		BTH_II0638		
15	BCAM1187	I35_RS21645	WQ49_RS15545	APZ15_RS18790			AK36_RS06495				
16	BCAM1571	I35_RS23575	WQ49_RS03530		CH72_RS19595		AK36_RS04500	AQ15_RS04615	BTH_II0527		
17	BCAM1593	I35_RS23700	WQ49_RS03655	APZ15_RS31265	CH72_RS19670	Bmul_4173	AK36_RS04460	AQ15_RS15520	BTH_I0834		
18	BCAM2007	I35_RS25625	WQ49_RS05705	APZ15_RS28835	CH72_RS21160	Bmul_3795		AQ15_RS01070	BTH_II1203		
19	BCAM2224	I35_RS26975	WQ49_RS06780	APZ15_RS27935				AQ15_RS10670	BTH_II1823		
20	BCAM2367	I35_RS27690	WQ49_RS07515	APZ15_RS22220		Bmul_5971	AK36_RS29780			WQE_RS01370	
21	BCAM2439	I35_RS28095	WQ49_RS07915	APZ15_RS22715	CH72_RS23175		AK36_RS01485				
22	BCAM2626	I35_RS29035	WQ49_RS22525	APZ15_RS23630	CH72_RS24060	Bmul_3338		AQ15_RS08765	BTH_II2139		
23	BCAS0333	I35_RS31745	WQ49_RS09600	APZ15_RS35470	CH72_RS29030						
24	BCAS0360	I35_RS31880	WQ49_RS09465	APZ15_RS34675	CH72_RS24835	Bmul_3200					
25					CH72_RS09095	Bmul_2944					
26					CH72_RS22580	Bmul_3574				WQE_RS29345	Bphy_5373
27					CH72_RS15720						
28					CH72_RS25455						
29				APZ15_RS30000							
30				APZ15_RS37495							
31				APZ15_RS37180							

32											Bphy_5030
33										WQE_RS17290	Bphy_6693
34										WQE_RS32240	
35										WQE_RS00050	
36										WQE_RS22845	

[b] Gene locus on contigs Chromosome 1 Chromosome 2 Chromosome 3 None [a] truncated protein

For instance, identification of the homologues of BCAL1700 protein (OrbA) in related species such as *B. cepacia, B. ambifaria, B. multivorans, B. vietnamenesis* (in the Bcc group) (APZ15_RS12790, Bmul_1594, CH72_RS16445 and AK36_RS21110, respectively) and also *B. pseudomallei, B. thailandensis* and *B. terrae* (AQ15_RS29965 BTH_I2415 and WQE_RS26070, respectively) suggest that these species possess an ability to utilise ornibactin or ornibactin-like siderophores as an iron chelator.

Correspondingly, *B. cenocepacia*, *B. ambifaria*, *B. multivorans, B. cepacia* and *B. vietnamiesis* (all in the Bcc group) are reported to produce the siderophore ornibactin. Besides, all species from the Bcc group are predicted to produce ornibactin (Butt and Thomas, 2017). Outside the Bcc group, *B. thailandensis* and *B. terrae* were also recently reported to synthesise ornibactin-like siderophores, proposed as malleobactin and phymabactin, respectively (Franke et al., 2015; Esmaeel et al., 2016; Butt and Thomas, 2017). Similarly, a gene that is highly homologous to BCAM2224, coding for the pyochelin receptor in *B. cenocepacia,* is also possessed by *B. cepacia*, *B. pseudomallei and B. thailandensis*, all of which are pyochelin producers.

B. cenocepacia H111 possesses the highest number of TBDR proteins across the species, followed by the other two *B. cenocepacia* strains (K56-2 and J2315) which also have 24, but these include a couple of truncated proteins. The TBDR protein, WQ49_RS 17910 is predicted to be non-functional in strain K56-2 just as with the corresponding protein BCAM0706 in J2315. And another pseudogene 'BCAL1783', is just found in strain J2315 but remain intact in both H111 and K56-2 strain (WQ49_RS 30800).

Other species possess less than 24 TBDRs, whereby *B. cepacia* has 22 intact TBDRs, *B. ambifaria* possesses fifteen TBDRs, *B. multivorans* has thirteen, *B. thailandensis* and *B. terrae* have ten, followed by *B. vietnamiensis* and *B. pseudomallei* both having nine TBDRs. The symbiotic bacteria, *B. phymatum* has the lowest number of TBDRs at three. As mentioned earlier, the majority of the TBDRs are found encoded on chromosome 2 across the species with all TBDR genes in *B. phymatum* found in the equivalent chromosome.

As described, the TBDR BCAL1700 (OrbA) was observed to be highly conserved across the species, as well as BCAL3001 and BCAM1593, a predicted TBDR for transporting vitamin B_{12}. The species from the xenovorans group, however, do not possess the TBDR BCAM1593. Furthermore, TBDR homologues of *B. cenocepacia* are mostly found from the *Burkholderia* assemblage (Bcc and Pseudomallei) as compared to the *Paraburkholderias* (Xenovorans).

B. cepacia, *B. ambifaria*, *B. multivorans*, *B. terrae* and *B. phymatum* seem to possess unique TBDRs which are not found in *B. cenocepacia*. *B. cepacia* and *B. terrae* each possess three unique TBDRs. The latter

species additionally possesses another two TBDRs (WQE_RS17290 and WQE_RS29345) that are not present in *B. cenocepacia*, but are highly similar to TBDRs in one or more species.

These TBDRs, however, are not found to be closely matched to any TBDRs of known functions. *B. ambifaria* possesses four TBDRs that are not present in the B*. cenocepacia* strain, whereby two are homologous to TBDRs in other species and two being unique to *B. ambifaria* among the species analysed here, CH_RS15720 and CH_RS25455. The two homologous ones (CH72_RS09095 and CH72_RS22580) are highly homologous to *B. multivorans* Bmul_2944 and Bmul_3574, respectively.

Interestingly, two TBDR proteins from the xenovorans group, WQE_RS29345 and Bphy_5373 from *B. terrae* and *B. phymatum*, respectively, are homologous to the aforementioned TBDRs found in *B. ambifaria* (CH72_RS22580) and *B. multivorans* (Bmul_3574). These species are therefore likely to utilise similar siderophores based on their sharing of orthologous TBDRs. Another TBDR in *B. phymatum* (Bphy_6693) is only similar to a TBDR in *B. terrae* (WQE_RS17290), while another is unique to the species (Bphy_5030). Both *B. terrae* and *B. phymatum* are in the same xenovorans group, and having orthologous TBDRs would be expected. However, only two TBDRs are found to be highly similar between these species. Whilst both are nitrogen fixers, *B. phymatum* is usually found in the nodules of legumes while the ecological niche of *B. terrae* is generally the soil (Yang et al., 2006; Elliott et al., 2007). In addition, *B. vietnamiensis*, which also fixes nitrogen in selected strains do not possess these two similar TBDRs (Menard et al., 2007).

B. ambifaria is known to produce two endogenous siderophores, ornibactin and cepaciachelin (Barelmann et al., 1996). The ornibactin TBDR orthologue *in B. ambifaria* is likely to be CH72_RS16445. The cepaciachelin biosynthesis and transport gene cluster that includes the gene encoding the putative cepaciachelin TBDR, CpcG , is documented to be present in chromosome 1 of this species. This gene cluster however, is reportedly not found in *B. multivorans* ATCC17616, thereby suggesting that this species does not produce cepaciachelin (Esmaeel et al., 2016; Butt and Thomas, 2017). As mentioned*, B. ambifaria* possess two TBDRs that are only found in the genome of the species (CH72_RS15720 and CH72_RS25455). As cepaciachelin biosynthetic cluster is unique to *B. ambifaria*, the TBDR CH72_RS15720 present in chromosome 1 is highly likely to be a cepaciachelin TBDR as compared to another, also present in chromosome 1 but is homologous to *B. multivorans* (CH_RS09095). The other unique TBDR, CH72_RS25455 is present in chromosome 2 of the *B. ambifaria* genome.

3.6 Identification of TonB systems in *B. cenocepacia*

Previous research has established that the transport of iron complexes through the TBDR is supported by the energy transduced by the TonB complex. The function of TonB complex is suggested to be transient

whereby it can facilitate multiple transport cycles by serially interacting with multiple TBDRs (Noinaj et al., 2010).

To date, the TonB complex in *B. cenocepacia* J2315 and H111 (BCAL2291-BCAL2293/I35_RS11100-I35_RS11110) consisting of the *tonB*, *exbB* and *exbD* genes is known to be required for utilisation of ferric-ornibactin and ferric-pyochelin complexes (Thomas, 2007). Bioinformatic searches in this study, via BLASTP revealed the existence of another two TonB complex gene loci (Figure 3.14). Due to the presence of these additional systems, the originally reported system is from here on referred to as the TonB1 system. One of the two newly identified putative *tonB* loci, encoding the TonB2 complex is found in the large chromosome of *B. cenocepacia* (BCAL1787-BCAL1790/I35_RS08505-I35_RS08515) and is comprised of two homologues of *exbD* (*exbD2a* and *exbD2b*). Another putative TonB system, the TonB3 is encoded by chromosome 2 (BCAM0559-BCAM0561/I35_RS18835–I35_RS18845). The function of these additional putative complexes, however, has not been investigated.

To investigate the potential function of the putative TonB systems, the genetic context of all three systems were evaluated. Upstream and downstream of the *tonB1* operon are genes involved in iron homeostasis. The upstream of the operon is adjacent to the *hemP* genes, reported to be involved in regulating the haem uptake operon followed by *ftrABCD,* the operon involved in the alternative iron uptake system in *B. cenocepacia*, FtrABCD (Sato et al., 2017). Downstream of *tonB1* operon are near to the *bfd* and *bfn* genes, coding for bacterial ferredoxin and ferritin, respectively.

The putative *tonB2* genes are in proximity to putative TBDR genes, BCAL1777 (I35_RS08460) (genes not shown) and 'BCAL1783' (I35_RS08490) (dysfunctional in J2315) and the yejABC transport system. The Yej system comprising the *yejABEF* operon transports the bacteriocin, MicrocinC rendering *B. cenocepacia* susceptible to this antibacterial agent. An efflux transporter system was identified next to the Yej system predicted as a drug efflux pump. Furthermore, a magnesium transporter gene is found upstream to the gene encoding the TonB2 system. Given that the TBDR 'BCAL1783' (I35_RS08490) is not predicted as a TBDR for transporting ferric siderophores, it is likely that the TonB2 system is involved in transporting compounds or metals other than iron, i.e. magnesium. Similarly, the TonB3 system is in close proximity to another putative TBDR, BCAM0564, which is also unlikely to be a ferric siderophore TBDR based on the InterPro analyses (Table 3.2). Furthermore, the TonB3 complex is located within clusters of transporters including an ABC transporter. This ABC transport system is adjacent to a putative nitrate utilisation cluster and maybe involved in transporting nitrates (Moir and Wood, 2001). Regardless of the clues as to the function of these alternative TonB2 and TonB3 systems from the nearby genes, it is still possible that these systems take part in transporting iron siderophore complexes.

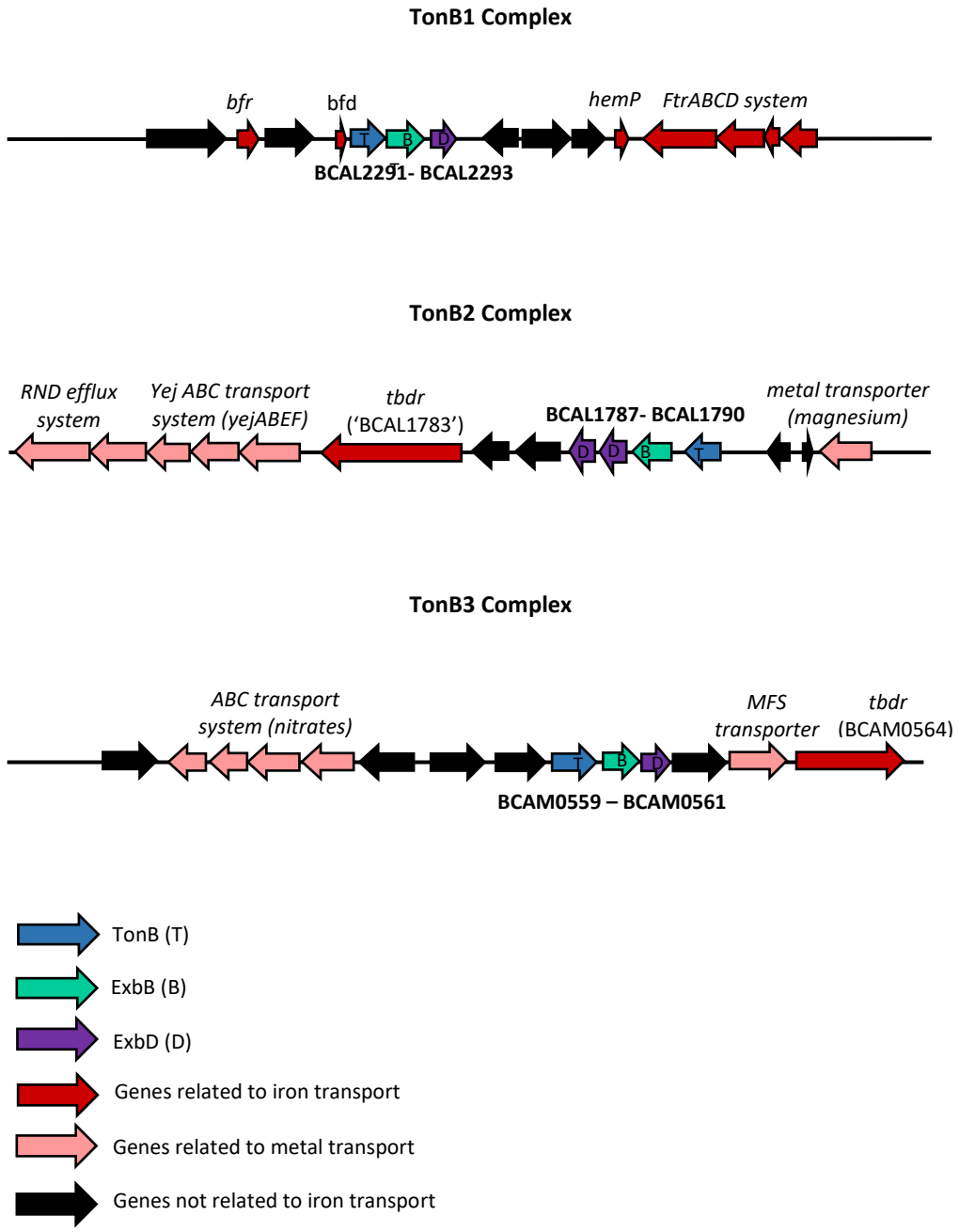

Figure 3.14: Genomic context of TonB complexes in *B. cenocepacia*
Gene arrangements of TonB complex gene loci of *B. cenocepacia* J2315 and H111. Colour code is as shown in the key.

3.7 Bioinformatic Identification of putative cytoplasmic membrane transport systems for metal chelates in *B. cenocepacia.*

To investigate the mechanisms by which iron or other metals are transported into the cytosol, putative cytoplasmic membrane transporters of *B. cenocepacia* H111 were identified by similar bioinformatic approaches to those used for identifying the putative TBDRs and *tonB* operons present in the strain. Ferric siderophores or other metal chelators have been reported to be transported across the cytoplasmic membrane via a permease or ABC multi-subunit transporters.

Agnoli and colleagues (2006) proposed that the endogenous siderophore ornibactin is transported through an ABC transporter composed of OrbB, OrbC and OrbD (Agnoli et al., 2006). Ferric-pyochelin was reported to be transported by a single subunit permease, FptX, in *P. aeruginosa* PAO1 (Cunrath et al., 2015) and possibly FptX also transports ferric-pyochelin in the Bcc members (Butt and Thomas, 2017). In addition, the xenosiderophores, ferrichrome and ferrioxamine B are also reported to be transported by likely single permeases, FiuB and FoxB, respectively in *P. aeruginosa* PAO1 (Cuív et al., 2007; Hannauer et al., 2010b).

To predict additional permeases in *B. cenocepacia,* four known ferric-siderophore cytoplasmic membrane transporters found in *B. cenocepacia* and *P. aeruginosa* were selected as queries in these searches. The proposed single subunit permease for pyochelin transport in *P. aeruginosa*, FptX (PA4218) along with FiuB (PA0476) and FoxB (PA2465) were used as queries in a BLASTP search at Sanger.ac.uk. The permease component of the ABC transporter for ornibactin in *B. cenocepacia,* OrbD (BCAL1692/I35_RS08025), was also used as a query to probe for other putative ABC transporters for iron-siderophore uptake using the same search method. As FptX and FiuB are confirmed as single subunit permeases and OrbD is a permease within an ABC transporter, both types of cytoplasmic transporters were included in the search. Additionally, a search was performed using 'iron' as a query via the NCBI database, to ensure that all possible iron-related cytoplasmic membrane transporters were identified.

The putative cytoplasmic membrane transporters for iron-siderophore complexes that were identified are listed in Table 3.4. Since permeases are usually observed to be non-specific and generally promiscuous (Cuív et al., 2008), only eleven putative single subunit permeases and six permeases predicted to be components of ABC transporters were identified in this search. The former includes BCAL0606, BCAL0117, BCAL1220, BCAL1418, BCAL2042, BCAM1135, BCAM1152, BCAM1616, BCAM2221, BCAS0478 and BCAS0732 while the latter involves 1 two subunit transporters which are BCAL1846-BCAL1847, 4 three subunit transporters which are BCAL1090-BCAL1092, BCAL1346-BCAL1348, BCAL2664-BCAL2666 and

BCAM1377-BCAM1379 and 1 four subunit transporters BCAM2627-BCAM2630. The four subunit members are predicted to be the haem uptake gene cluster.

With regard to the single subunit permeases, BCAM2221 is found in the pyochelin (Pch) cluster and may pose the best candidate for a pyochelin inner membrane transporter in *B. cenocepacia*. BCAL0117 is seen adjacent to a putative TBDR in *B. cenocepacia*, BCAL0116 and is a very close match to FoxB. The putative single subunit permease genes BCAL1220, BCAM1135, BCAS0478 and BCAS0732 are found next or near to a porin outer membrane gene. BCAM1135 and BCAS0732 are predicted as permeases for nucleobases such as uracil and thymine. BCAS0478 is located in an efflux transport system gene cluster and may be involved in this system.

Although the FptX, FiuB and FoxB queries are all most likely single subunit permeases, and would be predicted to detect single subunit permeases, they do not identify the same set of transporters (Table 3.4). Besides being solute specific, distinguishable permeases obtained may be due to the ligand specificities for transporting different ferric siderophores into the cytoplasm. Although in some cases, overlapping ligand specificities have been described (Cuív et al., 2007).

ABC transport systems are commonly comprised of three protein members, the periplasmic binding protein, PBP, the inner membrane permease and the ATPase. Within the list of the putative iron-related ABC transporters, four gene clusters encoded systems comprised of the common three protein members (BCAL1090-BCAL1092, BCAL1346-BCAL1348, BCAL2664-BCAL2666 and BCAM1377-BCAM1379) and as mentioned, another is comprised of two (BCAL1846-BCAL1847), while the predicted haem cluster consist of four members (BCAM2627-BCAM2630). The BCAL1346-BCAL1348 cluster, is found next to the putative TBDR gene, BCAL1345. The BCAM2629-BCAM2630 cluster is predicted to be involved in haem uptake due to its proximity to BCAM2626, a TBDR predicted to transport haem *in B. cenocepacia* (see Chapter 7). Despite being listed as iron-related permeases, some of these putative ABC permeases may be involved in transporting substances other than iron. The putative ABC importer BCAL2664-BCAL2666 is likely to be involved in the transport of cobalamin as it is found in the cobalamin utilisation (vitamin B_{12}) cluster while BCAM1377-BCAM1379 is found in the zinc exploitation cluster.

Table 3.4 Putative cytoplasmic membrane transporters for iron in *B. cenocepacia* J2315 and H111

Query[a]			
FiuB *P.aeruginosa*	FoxB *P. aeruginosa*	FptX *B. cenocepacia*	OrbD *B. cenocepacia*
BCAL0606/ I35_RS15305	BCAL0117/ I35_RS00625	BCAL1418/ I35_RS06540	BCAL1090-BCAL1092/ I35_RS05415- I35_RS05417
BCAL1220/ I35_RS05620		BCAM1152/ I35_RS21470	BCAL1346-BCAL1348/ I35_RS06183- I35_RS06185
BCAL2042/ I35_RS09810		BCAM1616/ I35_RS23815	BCAL1846-BCAL1847/ I35_RS08805- I35_RS08806
BCAM1135/ I35_RS21385		BCAM2221/ I35_RS26960	BCAL2664-BCAL2666/ I35_RS12639- I35_RS12641
BCAS0732/ I35_RS34255		BCAS0478/ I35_RS32615	BCAM1377-BCAM1379/ I35_RS22595- I35_RS22597
			BCAM2627-BCAM2630/ I35_RS29050- I35_RS29051

[a] Type of queries used in BLASTP analysis.

3.8 Discussion

Burkholderia species, particularly the Bcc members have increasingly been a concern in making the polymicrobial respiratory infections in CF patients more complex and difficult to treat. Exploring how these pathogens secure a competitive advantage in CF patients through iron uptake pathways would improve ways of controlling or eradicating exacerbations and mortality caused by their infections.

The majority of bacterial pathogens utilise xenosiderophores and it is likely *Burkholderia* spp. have a similar advantage. In the case of *B. cenocepacia*, the 24 gene-encoding putative TBDRs in its genome currently appear to be the highest number of TBDRs possessed by a Bcc member. The abundance of these TBDRs could indicate the ability of *B. cenocepacia* to utilise a broad spectrum of exogenous siderophores. This trait may accentuate its capacity to compete with other microorganisms or other Bcc members in polymicrobial infections by having enhanced access to iron sources. The putative TBDRs were verified for the existence of their prominent domain by considering the homologous superfamily, then a characteristic domain and specific attributes which are categorised in a family by *in silico* analysis (InterPro). All the putative TBDRs lack an N-terminal signalling domain for communicating with an anti-sigma factor except for one, the TBDR BCAL1371.

To determine whether the TBDRs were related to each other, the TBDRs were analysed phylogenetically by two methods to add reliability to the statistical analyses of the constructed phylogenetic tree. The UPGMA algorithm is commonly used and is suitable for analyses of gene families while the maximum likelihood method is more applicable to studying phylogenetic relationships among different species. These methods generally gave the same conclusion regarding the redundancy and TBDR pairing found among the TBDRs. The pairing observed in the phylogenetic tree may represent transportation of similar substrates, as proposed by Mirus et al. (2009), which stated that most TBDR clusters are grouped by substrates rather than taxonomical features.

The genomic context of the TBDRs reveals that most of the TBDR encoding-genes are located in the middle chromosome. This is consistent with the role of the middle and small chromosomes as accessory chromosomes that carry non-essential genes (Higgins et al., 2017). The TBDR for the primary endogenous siderophore, ornibactin, found in chromosome 1 indicates its importance as a primary iron transporter. The gene encoding the TBDR for pyochelin, the secondary endogenous siderophore produced, is found in chromosome 2, suggesting a lesser importance. However, there are eight genes found in the large chromosome that encode TBDRs of unknown function. The proximity of TBDR loci to genes encoding proteins related to iron processes is supporting evidence for the function of TBDRs likely to be involved in iron uptake mechanisms.

The orthologues of putative TBDRs found in other *Burkholderia* spp. suggests that several TBDRs are likely to recognise similar substrates to competing *Burkholderia* species in the lungs of CF patients or other environments. The ability to utilise siderophores produced by other strains would enhance the competitive behaviour or survival of *B. cenocepacia* in these milieus.

The number of putative TBDRs far exceeds the number of the TonB systems in the genome due to the highly redundant nature of the TonB system. Two additional TonB systems found in the *B. cenocepacia* genome suggests that several of these TBDRs use an alternative TonB complex for transport of iron or other metal-containing compounds.

Based on these searches, it is expected that *Burkholderia* spp. is able to utilise an array of xenosiderophores via different TBDRs to survive and thrive under various microbial surroundings. This possibility requires further investigations by mutagenesis analysis with highly predicted TBDR candidates. In conclusion, the bioinformatic analyses in this chapter may provide additional support for further characterisation of proteins involved in the exploitation of exogenous siderophores in the iron uptake pathways in *B. cenocepacia*.

Chapter 4

Utilisation of hydroxamate xenosiderophores by *B. cenocepacia*

4.1 Rationale

Hydroxamate-type siderophores are among the most common secondary metabolites secreted by bacteria and fungi. Almost all soil fungi produce siderophores with hydroxamate moieties (Trivedi et al., 2016) and given that *B. cenocepacia* occupies a versatile niche as a pathogen and in environments such as soil, it is a highly likely that this bacterium can utilise many types of hydroxamate siderophore for survival. Different types of hydroxamate siderophores of both bacterial and fungal origin were screened in this study to investigate the types of hydroxamates that *B. cenocepacia* could benefit from (Figure 4.1). Another aim in this chapter was to identify the transport system required for utilisation of these siderophores.

To investigate the ability of *B. cenocepacia* H111 to utilise xenosiderophores, production of endogenous siderophores in the bacterium was inactivated prior to siderophore utilisation screening. As *B. cenocepacia* H111 secretes two types of siderophores by NRPS-dependent pathways, pyochelin and ornibactin, the *pobA* gene, was inactivated. The *pobA* gene encodes an Sfp-type phosphopantetheinyl transferase, an enzyme responsible for the activation of NRPSs involved in the production of both endogenous siderophores in *B. cenocepacia* (Asghar et al., 2011). Previous inactivation of the *pobA* gene with a transposon resulted in the mutant being unable to produce its own siderophores (AHA27), thereby making it useful for screening xenosiderophore utilisation. However, it was decided to make a markerless *pobA* mutant that would facilitate subsequent introduction of additional TBDR null alleles and to allow for introduction of plasmids for genetic complementation. Therefore, a markerless, *B. cenocepacia* H111 Δ*pobA* mutant was generated along with a *B. cenocepacia* H111 Δ*pobA* mutant lacking chromosome C3 (i.e. pC3), H111ΔpC3ΔpobA. In addition, a markerless *pobA* null allele was also introduced into strain 715j for further investigations.

4.2 Construction and characterisation of markerless *B. cenocepacia* Δ*pobA* mutants

4.2.1 Allelic replacement using pEX18TpTer-*pheS*

Construction of a markerless mutant was initially attempted using the suicide plasmid pEX18Tp-*pheS*-Δ*pobA* (Sofoluwe and Thomas, unpublished results). The vector pEX18Tp-*pheS* contains the trimethoprim-resistance gene to select for plasmid integration into the genome and the counter-selectable mutated *pheS* gene. The *pheS* gene encodes the α-subunit of phenylalanyl tRNA synthase of *B. pseudomallei* which charges tRNA with phenyalanine. However, the mutant form of the enzyme encoded by pEX18Tp-*pheS* can also charge the tRNA with the toxic phenylalanine analogue, chlorophenylalanine (cPhe). The gene acts as a counter-selectable marker and was inserted into the pEX18Tp plasmid for performing chromosomal mutagenesis via allelic replacement with *Burkholderia* species (Barrett et al., 2008).

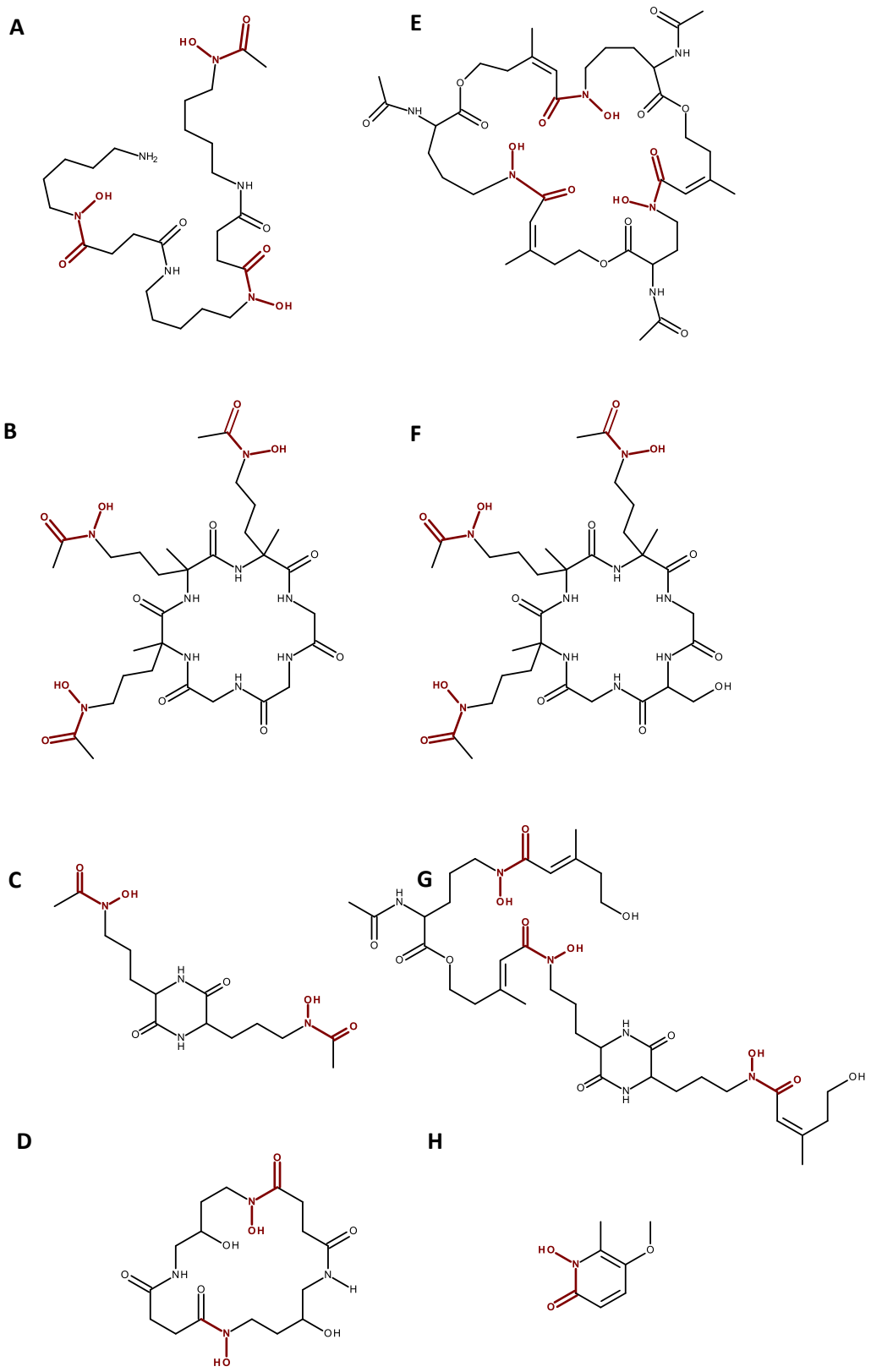

Figure 4.1: Molecular structures of hydroxamate siderophores investigated in this study
(A) ferrioxamine B, (B) ferrichrome, (C) rhodotorulic acid, (D) alcaligin, (E) triacetylfusarinine C, (F) ferricrocin, (G) coprogen, (H) cepabactin. Hydroxamate ligands are depicted in red. Chemical structures were drawn using Accelrys Draw 4.2.

However, integration of the plasmid, pEX18Tp-*pheS*-Δ*pobA,* into the *B. cenocepacia* genome could not be selected, presumably due to poor expression of the trimethoprim antibiotic resistance gene (Sofoluwe and Thomas, unpublished results). Therefore, it was hypothesised that this may due to a strong *pheS* gene promoter (P_{S12}) in the plasmid which inhibited the expression of the convergently orientated trimethoprim resistance gene, making it poorly expressed. Due to this fact, an approach was taken where the trimethoprim gene (*dfrB2*) in pEX18Tp-*pheS* was turned around into a reversed position to avoid the effect of the P_{S12} promoter. A strong transcription terminator, rrnBT1T2, was inserted downstream of the inverted trimethoprim resistance cassette to avoid interrupting the function of the origin of replication (*oriV*) by strong readthrough transcription (Dix et al., 2018). The resulting pEX18TpTer-*pheS* construct (4219 bp) showed the ability of the trimethoprim resistance gene to be expressed as a positive selection marker and was used for experiments in this study.

4.2.2 Construction of pEX18TpTer-*pheS*-Δ*pobA*

The *pobA* gene (BCAL2248), together with flanking genomic sequences, was previously introduced into the plasmid pEX18Tp-*pheS* and an in-frame deletion was introduced into *pobA* by two restriction sites of *Sac*II sites within the gene, forming the pEX18Tp-*pheS*-Δ*pobA* construct (Sofoluwe and Thomas, unpublished results). The plasmid pEX18TpTer-*pheS*-Δ*pobA* was constructed by transferring the Δ*pobA* allele from pEX18Tp-*pheS*-Δ*pobA* to pEX18TpTer-*pheS.* To do this, pEX18Tp-*pheS*-Δ*pobA* was restriction digested with *Hin*dIII and *Bam*HI enzymes to release the 1.6 kb Δ*pobA* insert and subjected to agarose gel electrophoresis (Section 2.5.7). The released insert was then cut from the gel, purified and ligated into pEX18TpTer-*pheS* cut with the same enzymes, and the ligation reaction products were transformed into the *lacZ*ΔM15 strain JM83. Transformants were selected via a white-blue colony screen. Plasmids prepared from white colonies were analysed by gel electrophoresis to ensure the resulting plasmid construct bore a size of 5.8 kb (Figure 4.2). Plasmids of the expected size were then confirmed by DNA sequencing to ensure correct insertion of the inactivated *pobA* gene using combination primers M13 and M13revBATCH. The desired plasmid was named pEX18TpTer-*pheS*-Δ*pobA.*

4.2.3 Construction of *B. cenocepacia* Δ*pobA* mutants

pEX18TpTer-*pheS*-Δ*pobA* was then introduced via transformation into an *E. coli* donor host suitable for conjugation procedure with *B. cenocepacia*, i.e. SM10(λpir). The donor possesses the ability to allow biparental conjugal transfer of plasmid DNA to Gram-negative bacteria via the RP4-derived transfer genes integrated in its chromosome (Simon et al., 1983). SM10(λpir) harbouring the plasmid was conjugated with three *B. cenocepacia* strains H111, 715j and H111ΔpC3. pEX18 derivatives cannot replicate in *B. cenocepacia.* However, in a small percentage of exconjugants, the vector integrates into the host genome via homologous DNA sequences flanking the mutation site.

There can either be a single crossover event which results in the integration of the entire plasmid into the genome (merodiploid formation), or there can be a double crossover event resulting in an exchange of the native DNA sequence with the mutated sequence, thus resulting in the replacement of the wild type allele in the *B. cenocepacia* genome by the mutant allele. However, the latter are not obtainable in a single step as there is no selection. To isolate the desired mutant, a two-step procedure is required that involves isolation of merodiploids (plasmid integrants) in the first step.

To isolate merodiploids that have resulted from a single homologous recombination, the ex-conjugants were selected on M9-glucose medium containing trimethoprim (25 µg ml^{-1}). Several small colonies from the conjugation plates were purified by two rounds of streaking on the same medium. Single colonies were then PCR screened using vector-specific primers to ensure that the constructed suicide plasmid had been integrated into the recipient genome (Figure 4.3).

In a single crossover recombination event during the construction of the *B. cenocepacia* Δ*pobA* mutant, the whole plasmid is integrated into the *B. cenocepacia* chromosome, making the recipient trimethoprim resistant and p-chlorophenyalanine (cPhe) sensitive. The chromosomally integrated *pheS* gene allows cPhe, a toxic derivative of phenyalanine, to be incorporated into the amino acid sequence of growing polypeptides instead of the usual phenylalanine, and this makes some of the proteins in the cell non-functional and hinders cell growth, resulting in cell mortality. Studies show that strains having the mutant *pheS* gene are completely killed in the presence of 0.1% cPhe (Barrett et al., 2008; Fazli et al., 2015). The mutant *pheS* gene thus acts as a counter selective marker to allow selection for a second crossover recombination that leads to excision of the plasmid. Vector excision can leave only the wild type or mutant gene on the chromosome. Therefore, the target recombinants are trimethoprim-sensitive and cPhe resistant, where the cPhe would not be incorporated in the polypeptide chains and the recombinants can be selected on M9-glucose agar supplemented with 0.1% cPhe.

Colonies containing the desired plasmid integrated into the *B. cenocepacia* genome were streaked on M9-glucose counter-selective agar plates containing 0.1 % cPhe (Section 2.4.1.3) and incubated at 37 °C for 48-72 hr to select for colonies in which the plasmid had been excised from the genome by a second recombination step. Following incubation, 50 small colonies were patched on M9-glucose agar plates containing 0.1 % cPhe and were incubated for 48 hr at 37 °C. Grown patched colonies were then repatched on M9 agar plates with trimethoprim (25 µg ml^{-1}) to identify the plasmid-less recombinant colonies (they do not grow on this medium). Trimethoprim-sensitive strains were selected from the M9-glucose cPhe plates lacking trimethoprim and purified on the same medium. Well separated colonies of the cPhe-resistant recombinants were then checked by PCR to see whether they carry the wild type or mutant *pobA* gene using `outside primers' (*pobA*for4 and *pobA*rev3) that anneal to genomic sequences flanking the *pobA* gene but outside the region contained in the pEX18TpTer-*pheS*-Δ*pobA* plasmid.

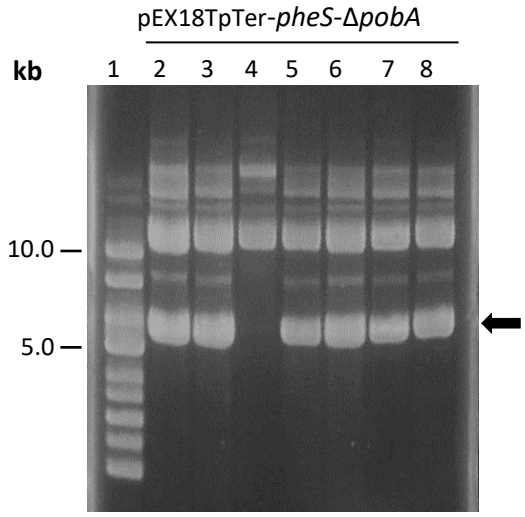

Figure 4.2: Gel electrophoresis of putative pEX18TpTer-*pheS*-Δ*pobA* plasmid clones
Lane 1, Supercoiled DNA ladder (New England Biolabs); lanes 2-8, plasmids corresponding in size to pEX18TpTer-*pheS*-Δ*pobA* (5819 bp), as indicated by arrow (the plasmid in lane 4 is present mainly in the dimer form). pEX18TpTer-pheS-ΔpobA was restriction digested and ligated with Δ*pobA* DNA fragment.

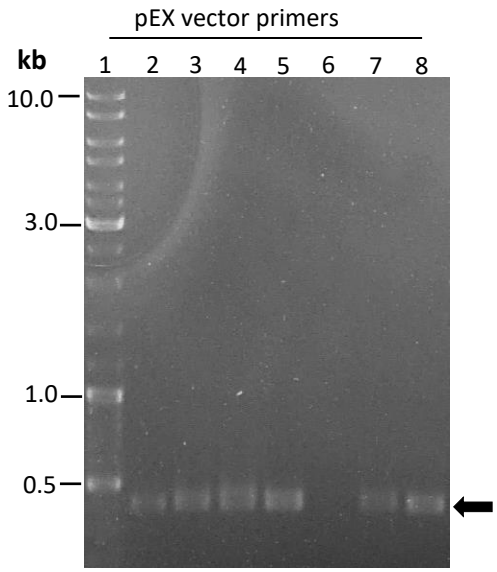

Figure 4.3: Integration of pEX18TpTer-*pheS*-Δ*pobA* into the *B. cenocepacia*
pEX18TpTer-pheS-Δ*pobA* genome integration screening in H111 and H111ΔpC3 strains using primer combination pEX18Tpfor and pEX18Tprev at an annealing temperature of 52°C giving rise to a 397 bp amplicon, as indicated by the arrow. Lane 1, Linear DNA ladder (Thermo Scientific); lanes 2-5, H111 containing pEX18TpTer-*pheS*-Δ*pobA* candidates*;* lane 6, wildtype H111; lanes 7-8, H111ΔpC3 containing pEX18TpTer-*pheS-ΔpobA* candidates.

Wild type *pobA* gave a PCR product of 2.2 kb while a Δ*pobA* mutant was detected by the presence of a DNA fragment with a size of 1.6 kb (Figure 4.4). Simplified construction of the Δ*pobA* mutant is illustrated in Figure 4.5.

4.2.4 Phenotypic analysis of *B. cenocepacia* Δ*pobA* mutants

The phenotypes of the Δ*pobA* mutants were confirmed by streaking them on CAS agar. Bacterial strains able to secrete siderophores form halos on the CAS agar (Schwyn and Neilands, 1987). Observations from the CAS agar showed the constructed mutant derivatives do not form halos which confirmed the previously observed phenotype characteristic of the *pobA* mutant (Figure 4.6A and B) (Asghar et al., 2011).

Additionally, the effect of iron-starvation was tested on growth of the Δ*pobA* strains by overlaying the mutants on iron-limited agar containing the iron chelator EDDHA (40-200 µM) and growing them in a liquid medium supplemented with DTPA, which also acts as an iron-chelator. Overlaid *B. cenocepacia* wildtype on LB medium containing EDDHA allowed full lawn growth, whereas no lawn was produced by the *pobA* mutants, indicating the inability of the latter to grow in iron-limited medium (result not shown). To grow the mutants in liquid medium, optimisation for the specified amount of the iron chelator used was investigated.

4.2.4.1 Optimisation of liquid growth stimulation assay

To establish the optimum conditions for this analysis, H111ΔpobA was grown in iron-deficient medium containing variable amounts of the hydrophilic iron chelator, diethylenetriaminepentaacetic acid (DTPA/DETAPAC), while iron (III) chloride ($FeCl_3$) was used to achieve high-iron conditions in culture. As EDDHA is not efficient in hydrophilic conditions, DTPA was used to form an iron-restriction setting for liquid growth stimulation assays in this study. DTPA only chelates extracellular Fe^{3+} and does not enter bacterial cells and chelate the Fe^{2+} in the cell. It is structurally a stronger pentadentate chelator than the Fe^{2+} scavenger, 2,2' bipyridyl (Figure 4.7). DTPA can be toxic to bacteria at certain concentrations and is efficient at <pH 8.0. Therefore, the optimum concentration must be determined empirically for each bacterial species and each medium. Optimisation was performed to determine the maximum concentration of DTPA to effect iron starvation in WT *B. cenocepacia* while not affecting its growth. This DTPA concentration will allow *B. cenocepacia* H111 WT to grow at optimum level while maintaining its ability to produce siderophores. The iron restricted conditions will therefore impede the growth of *pobA* mutant.

B. cenocepacia H111 WT was grown in medium containing a wide range of DTPA concentrations (0, 1, 2, 5, 10, 20 and 30 µM) to establish the maximum concentration that allows optimal H111 growth. Based on a set of preliminary growth curves (n=1), a DTPA concentration of 1 µM allowed near to optimal growth (result not shown).

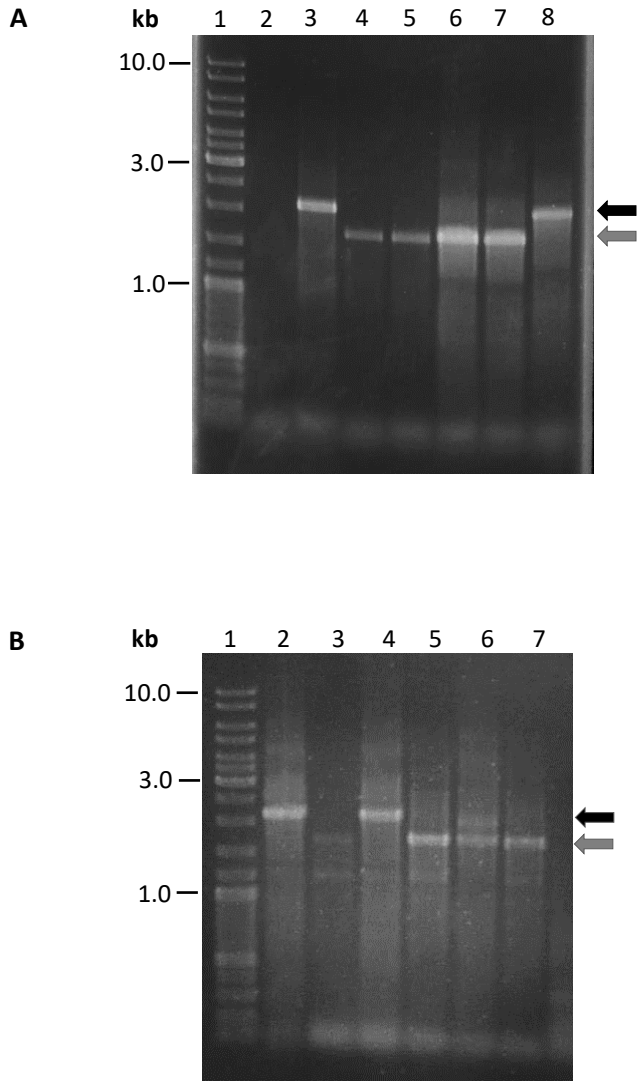

Figure 4.4: PCR screening candidate of *B. cenocepacia* Δ*pobA* mutants
(A) Colony PCR screening of H111Δ*pobA* candidates with pobAfor4 and pobArev3 at an annealing temperature of 60 °C: Lane 1, Linear DNA ladder; lane 2, negative control (no DNA); Lane 3, H111 wild type; lanes 4-7, H111Δ*pobA* candidates; lane 8, H111Δ*pobA* candidate retaining wild type gene upon plasmid excision. (B) Screening of H111ΔC3Δ*pobA* candidates: Lane 1, Linear DNA ladder; lane 2, H111ΔpC3; lanes 3-7 except lane 4, H111ΔC3Δ*pobA* candidates; Lane 4, H111ΔC3Δ*pobA* candidate retaining wildtype gene upon plasmid excision. Black arrow indicates expected size of amplicon from wild type and grey arrow indicates, amplicon corresponding to Δ*pobA* mutant.

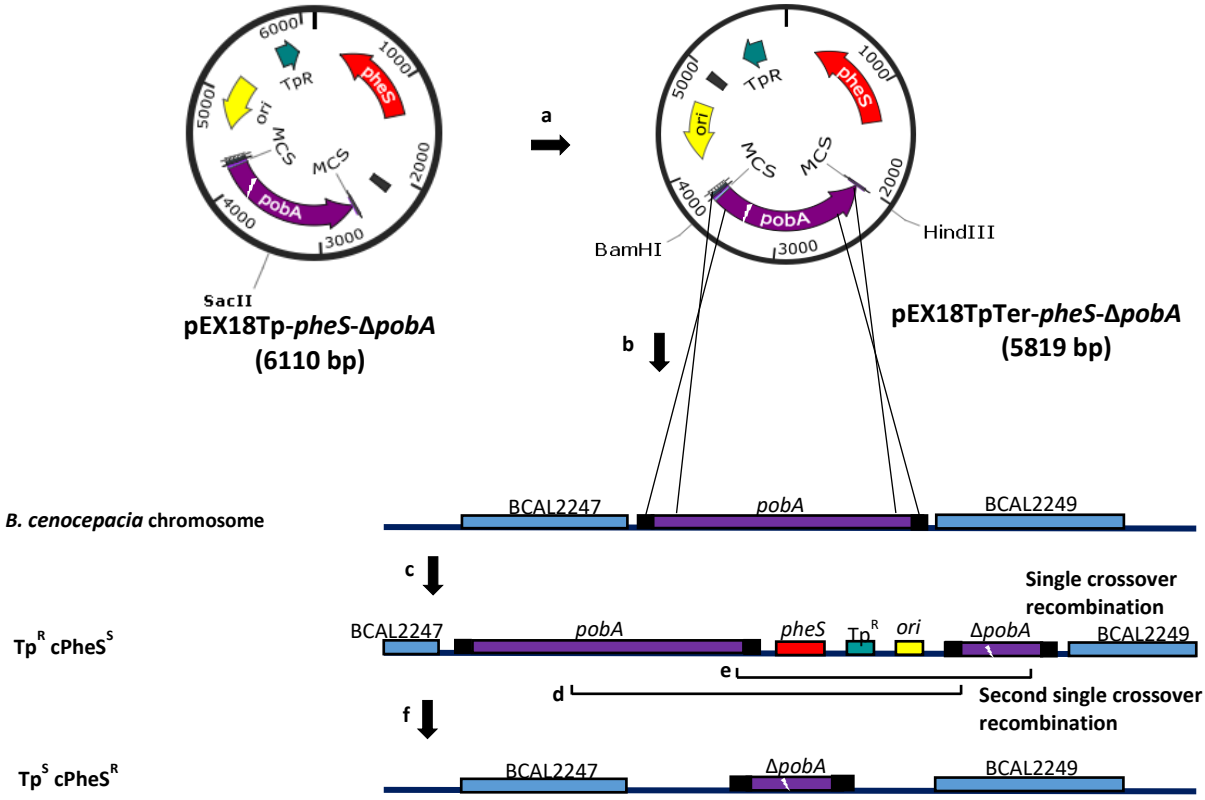

Figure 4.5: Construction of pEX18TpTer-*pheS*-Δ*pobA* and mechanism of allelic replacement in *B. cenocepacia*

(a) *Hin*dIII-*Bam*HI Δ*pobA* fragment was transferred from pEX18Tp-*pheS*-Δ*pobA* to pEX18TpTer-*pheS*. (b) and (c) Single crossover recombination of Δ*pobA* carried on plasmid with chromosomal wild type *pobA* gene after conjugal plasmid transfer allows integration of plasmid into chromosome. (d) Second single crossover within chromosome excising plasmid and retaining wild type characteristic. (e) Second single crossover excising plasmid and forming mutant Δ*pobA* strain. (f) *B. cenocepacia* Δ*pob*A mutant having trimethoprim-sensitive and cPhe-resistant characteristic. Plasmids are depicted using SnapGene.

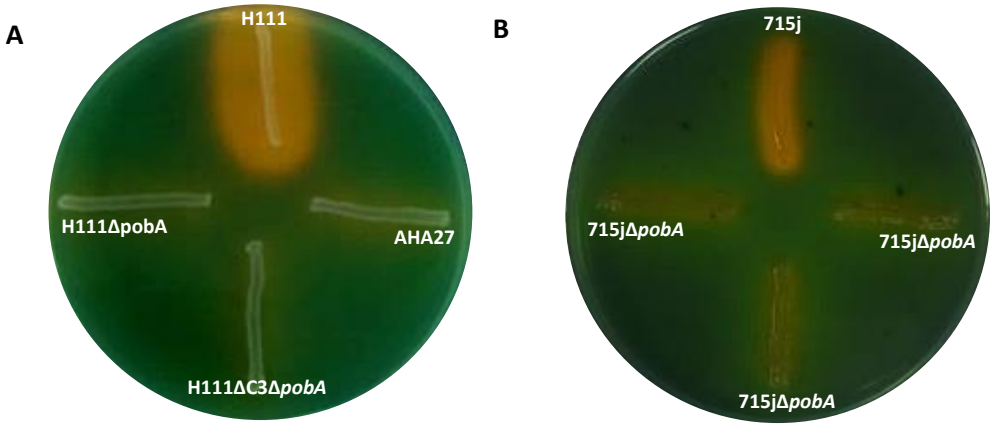

Figure 4.6: Phenotypic confirmation of the *B. cenocepacia* siderophore-deficient *pobA* mutant
(A) and (B) CAS analysis of siderophore production by the wild type and siderophore-deficient mutant derivatives of H111pobA, H111ΔC3ΔpobA and 715jΔpobA with AHA27 as a control.

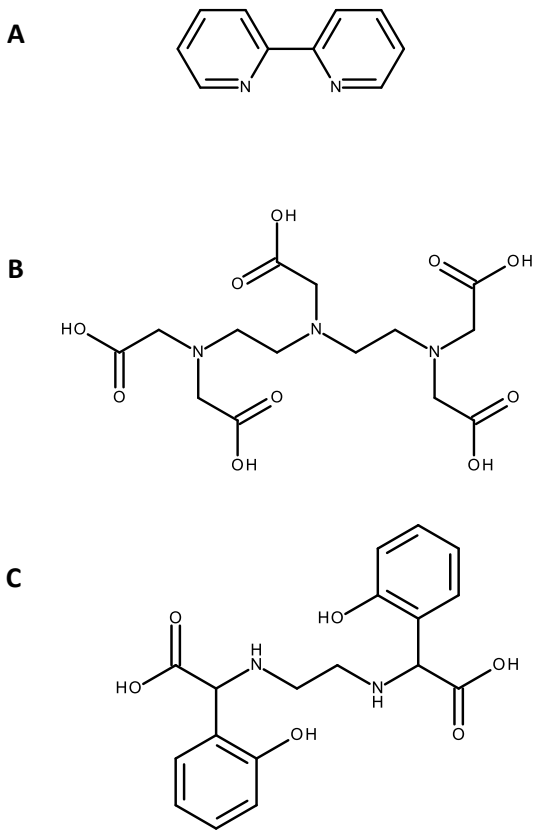

Figure 4.7: Iron chelators
Chemical structures of (A) 2,2'-bipyridyl, (B) DTPA, and (C) EDDHA. Chemical structures were drawn using Accelrys Draw 4.2.

Subsequent optimisation was performed using a smaller range of DTPA concentrations that was close to 1 µM (0, 0.25, 0.5, 1 µM) to obtain a refined DTPA optimal concentration. The growth curves (n=3) in this range of DTPA concentrations (0, 0.25, 0.5, 1 µM) showed a slight difference in growth rate across this range, with 1 µM giving rise to a slightly lower growth rate (Figure 4.8A). The concentration of 1 µM of DTPA was selected to examine its effect on the growth of the H111ΔpobA mutant. Based on a preliminary growth curve (n=1), the H111 *pobA* mutant showed a very slow growth rate under these conditions (Figure 4.8B) which supported significant growth of the wildtype, thereby approving the phenotype of the *pobA* mutant.

Although growth inhibition was expected for the *pobA* mutant in the DTPA-supplemented liquid assay, the very slow growth observed may due to the involvement of other iron acquisition systems unrelated to siderophores such as the FtrABCD system. The H111 WT strain and the *pobA* mutant grown in iron-replete conditions (50 µM $FeCl_3$) (n=3) showed comparable growth, suggesting the ability of the *pobA* mutants to acquire iron by existing mechanisms other than by utilising endogenous siderophores (Figure 4.8C).

4.3 Identification of hydroxamate xenosiderophores utilised by *B. cenocepacia*

Xenosiderophore utilisation screenings were conducted using the disc diffusion bioassay by scoring the ability of an exogenous siderophore to facilitate the growth of the *B. cenocepacia* siderophore-deficient strain, H111ΔpobA, on iron-limited medium (Section 2.6). The *in vitro* iron-limiting environment was created by the addition of the ferric iron chelator EDDHA to the agar and was overlaid with soft agar seeded with the *pobA* mutant. Filter discs that were impregnated with siderophore solutions were applied to the surface of the overlay and the appearance (or not) of halos of growth of the *pobA* mutant around the filter discs was observed.

4.3.1 Screening of hydroxamate xenosiderophore utilisation by disc diffusion assays

The growth medium used for screening by the disc diffusion bioassay was initially supplemented with 200 µM of the iron chelator, EDDHA. A disc impregnated with triacetylfusarinine C (TAFC) was shown to promote very limited growth of H111ΔpobA around the disc (not apparent in photographic images), whereas the disc impregnated with an equivalent amount of ferrichrome gave a broader and significant zone of growth (Figure 4.9A). This may indicate that the medium is suitable for detecting xenosiderophores that are very efficiently utilised by *B. cenocepacia* such as ferrioxamine B but is less suitable for siderophores that are used less efficiently. Therefore, a medium that would allow identification of weaker or less efficiently used siderophores was sought.

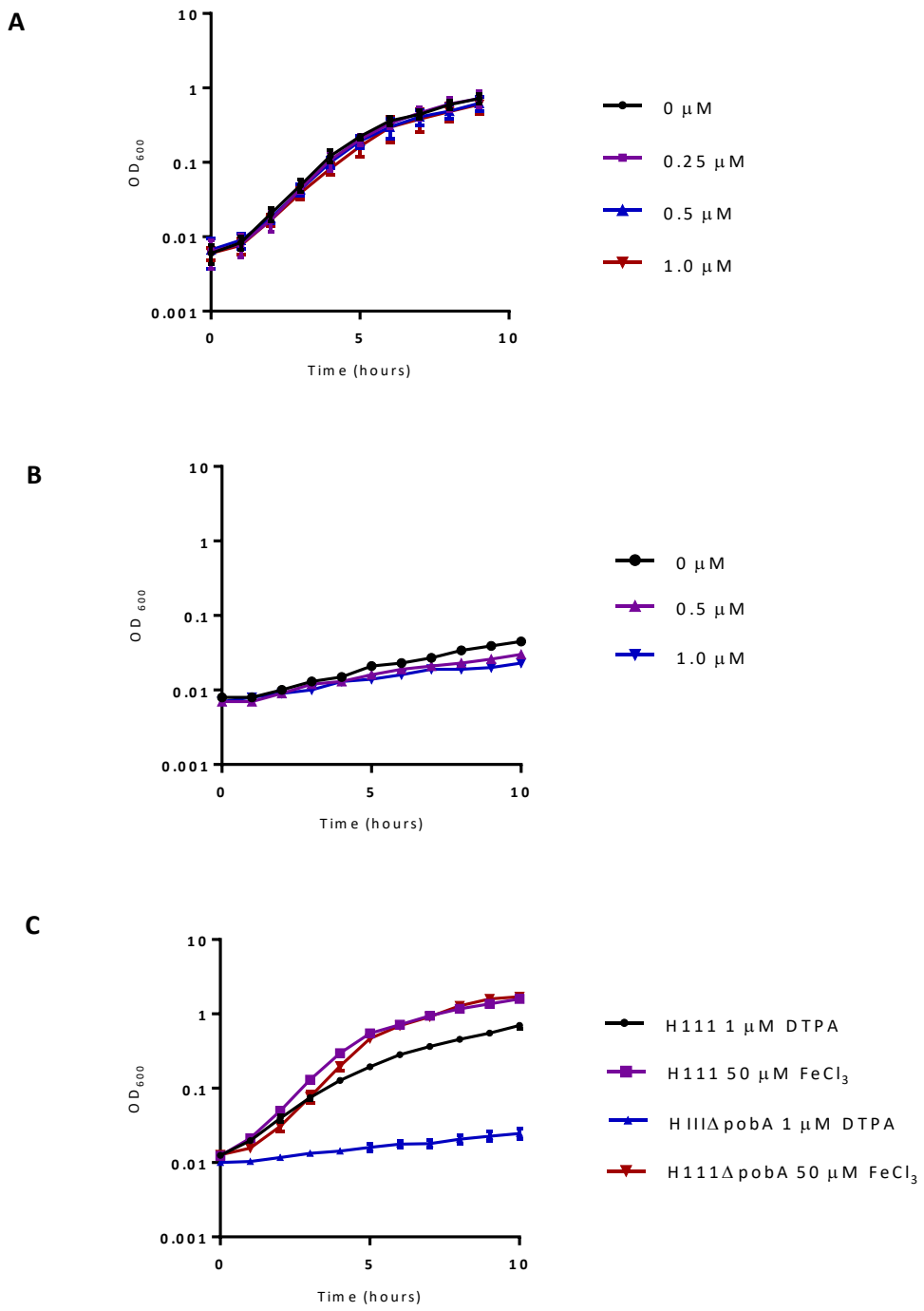

Figure 4.8: Optimisation of DTPA concentrations for establishing iron starvation conditions for *B. cenocepacia* in liquid culture

Growth of H111 and H111ΔpobA in the presence of different DTPA concentrations was monitored in M9-glucose CAA broth for optimisation purposes. Absorbance was measured every hour at OD_{600} for 10 hours. The data represent three experiments. (A) Growth curves of H111 at DTPA concentration of 0 to 1 µM (n=3). (B) Growth curve of H111ΔpobA at DTPA concentrations of 0 to 1 µM (n=1). (C) Growth curves of H111 and H111ΔpobA at selected optimal DTPA concentration of 1 µM as compared to iron-replete conditions at 50 µM $FeCl_3$ (n=3). Error bars represent the ±SEM.

To get a significant observation for TAFC utilisation, the ability of H111ΔpobA to utilise this xenosiderophore was reassayed using lower concentrations of EDDHA (0, 20, 40, 80, 160 and 200 µM) and compared with ferrichrome. A lawn of growth of H111ΔpobA was observed on agar containing 0 µM EDDHA as expected and weak growth was observed in the presence of 200 µM EDDHA. Based on the result of this experiment, an EDDHA concentration of 40 µM was selected for subsequent disc-diffusion bioassays as it showed dense and significant growth of H111ΔpobA around the filter discs impregnated with TAFC. While obtaining a reasonable EDDHA concentration for subsequent bioassay, it was also demonstrated that TAFC can be utilised by *B. cenocepacia* (Figure 4.9A).

The siderophore utilisation phenotype of H111ΔpobA, H111ΔC3ΔpobA and 715jΔpobA were compared to an available *B. cenocepacia* mutant with a marked inactivated *pobA* gene, AHA27 (715j-*pobA*::mini-Tn*5*CmlacZYA) (Asghar et al., 2011). Two hydroxamate xenosiderophores, ferrichrome and ferrioxamine B, were used in these assays as they had been previously observed to promote growth of AHA27 in the disc diffusion assay (Sofoluwe, Paleja and Thomas, unpublished results). The siderophore utilisation bioassay confirmed the *pobA* mutant can be used to identify xenosiderophores as it displayed the same phenotype as the mutant AHA27 by showing growth around the filter discs impregnated with the siderophores ferrichrome shown previously and ferrioxamine B (Figure 4.9B).

Sodium citrate, a weak siderophore that is utilised by some bacteria (e.g. *E. coli* and *Pseudomonas* species), was used as a negative control as it has been shown not to be used for iron uptake by *B. cenocepacia* (Thomas, unpublished results). Alternatively, HPLC grade water was used. AHA27 was not used for further investigation in this study.

Subsequent xenosiderophore utilisation bioassays were performed with an EDDHA concentration of 40 µM which showed growth of H111ΔpobA around filter discs impregnated with the iron-free hydroxamate siderophores alcaligin, rhodotorulic acid, cepabactin, ferrichrome, and ferrioxamine B, and the iron-complexed form of ferricrocin. The growth of H111ΔpobA promoted by alcaligin, cepabactin and rhodotorulic acid are shown in Figure 4.10A-C. Coprogen did not promote growth of *B. cenocepacia* H111. To confirm the inability of H111ΔpobA to utilise coprogen, a siderophore-deficient strain of *P. aeruginosa* was used as a positive control as it has been shown to utilise coprogen (Meyer, 1992). As expected, *P. aeruginosa* was shown to utilise coprogen under these conditions (Figure 4.10C). Utilisation of hydroxamate siderophores were reevaluated in broth culture in subsequent experiments.

4.3.2 Utilisation of hydroxamate siderophores by *B. cenocepacia* in liquid medium

The effect of hydroxamate siderophores on the growth of *B. cenocepacia* was analysed in liquid stimulation assays for further confirmation of their utilisation (Section 2.6.2).

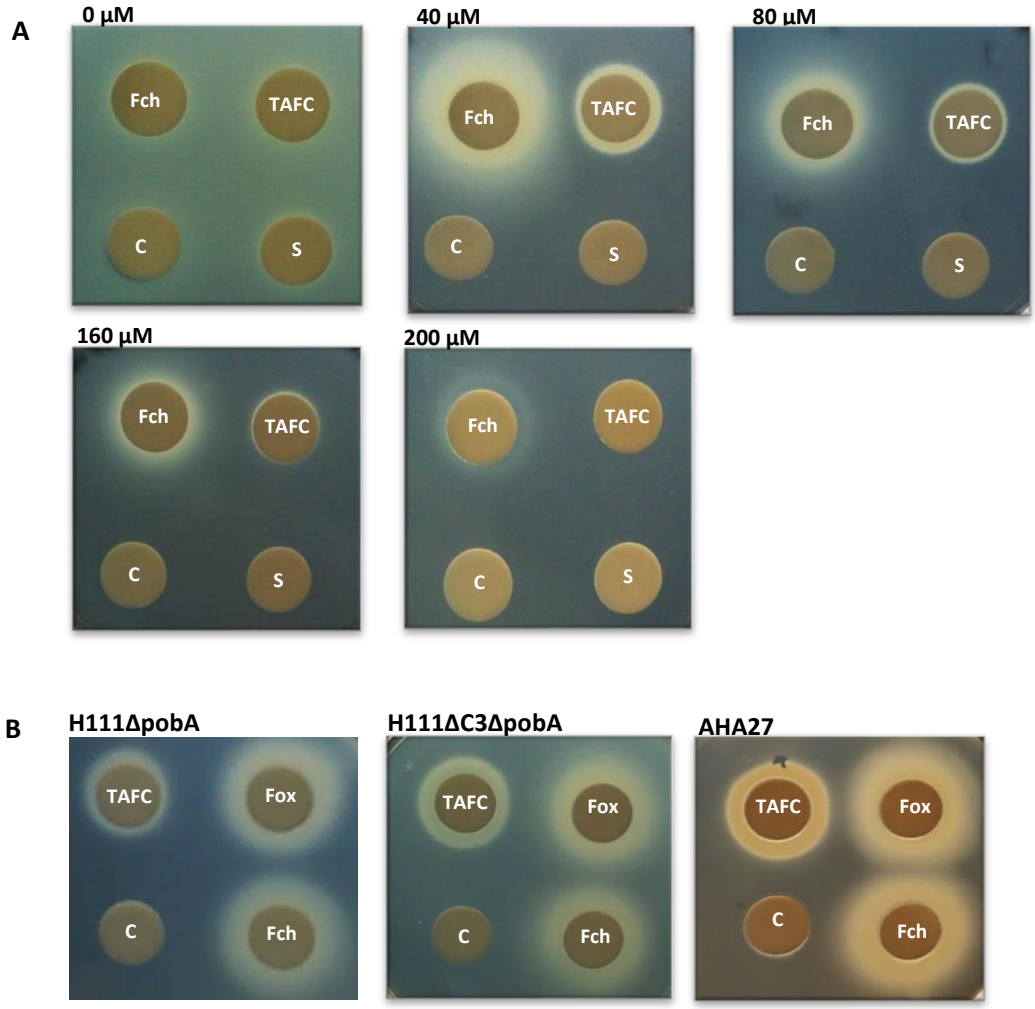

Figure 4.9: Growth promotion of H111ΔpobA by ferrichrome, ferrioxamine B, and TAFC under iron limiting conditions

Experiments were carried out using the disc diffusion assay. (A) Comparison of H111ΔpobA growth with filter discs supplemented with xenosiderophores in the presence of different EDDHA concentrations. Filter discs for each bioassay plate were impregnated with 20 µl of 1 mM purified siderophore, ferrichrome (Fch); triacetylfusarinine (TAFC) with dH_2O (C) and 5 mM sodium citrate (S) as controls. Final EDDHA concentration in agar is indicated on top of each bioassay plate. (B) Disc diffusion assay of *pobA* mutants with TAFC. Ferrichrome and ferrioxamine B were used as controls. Filter discs for each bioassay plate were impregnated with 20 µl of 1 mM purified siderophore, ferrichrome (Fch); triacetylfusarinine (TAFC); Ferrioxamine B (Fox). Control, 20 µl of 5mM sodium citrate. Final EDDHA concentration in agar in B is 40 µM.

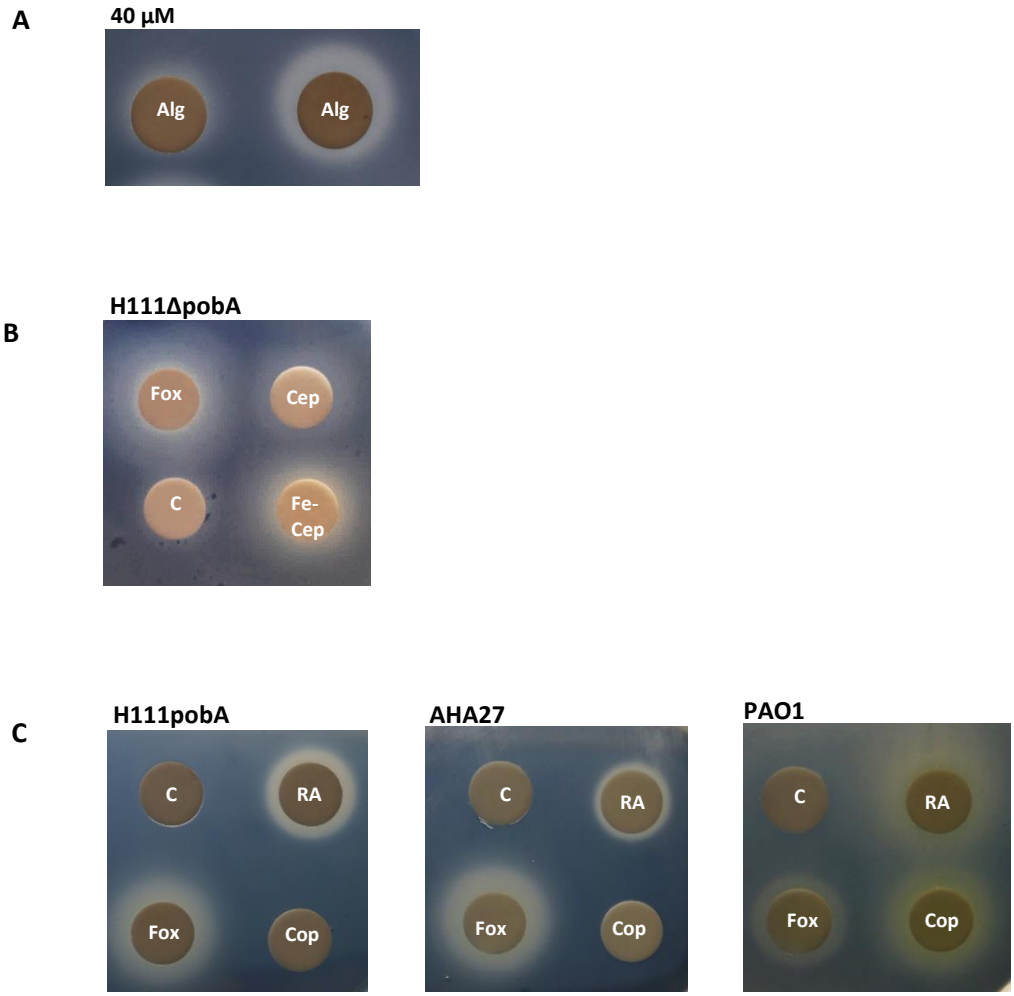

Figure 4.10: Analysis of alcaligin, cepabactin, coprogen and rhodotorulic acid utilisation by *B. cenocepacia* using the disc diffusion assay

(A) Growth of H111ΔpobA with filter discs impregnated with 10 µl of 1 mM (left hand disc) and 5 mM (right hand disc) alcaligin (Alg). (B) Utilisation of cepabactin as a xenosiderophore with ferrioxamine B as control. Filter discs were impregnated with ferrichrome B (Fox) (1 mM, 10 µl); cepabactin (Cep) (1mM, 20 µl); Fe-cepabactin (Fe-Cep) (1 mM, 20 µl); dH_2O (C) (20 µl). (C) Screening of rhodotorulic acid (RA) and coprogen (Cop) as xenosiderophores for *B. cenocepacia* with *P. aeruginosa* PAO1 Pvd^- Pch^- as control. Filter discs are impregnated with rhodotorulic acid (RA) (1 mM, 40 µl); ferrioxamine B (Fox) (1 mM, 15 µl); coprogen (Cop) (1 mM, 100 µl) and dH_2O ('C') (100 µl). Final EDDHA concentration in agar in A - B is 40 µM.

A DTPA concentration of 1 µM was used with addition of the hydroxamate xenosiderophores to H111ΔpobA growing in iron starvation conditions (Section 4.2.4.1). Establishment of these conditions allowed determination of the effect of adding exogenous xenosiderophores to H111ΔpobA growing under iron-limiting conditions.

4.3.2.1 Growth stimulation assay of the hydroxamate siderophores in liquid medium

B. cenocepacia H111ΔpobA was grown in iron-limiting medium supplemented with the hydroxamate siderophores alcaligin, cepabactin, ferrichrome, ferrioxamine B, TAF and rhodotorulic acid at 10 µM. The primary endogenous siderophore of *B. cenocepacia*, ornibactin, was used as a positive control. Addition of the xenosiderophores promoted growth of the *pobA* mutant with varying efficiency (Figure 4.11). The ferrichrome and ferrioxamine B-stimulated growth rates were shown to be similar to the ornibactin-stimulated rate but reached a slightly higher final optical density (Figure 4.11A and B). Ferrioxamine B appears to be slightly more efficient at removing Fe^{3+} from the DTPA than the endogenous siderophore, ornibactin.

The *pobA* mutant supplemented with TAFC showed a lower growth rate than when supplemented with ornibactin but achieved the same final optical density (Figure 4.11C). Alcaligin and rhodotorulic acid-supplemented cultures demonstrated a lower growth rate than with ornibactin (Figure 4.11D and E). This may due to the tetradentate nature of the siderophores, although alcaligin allowed the mutant to grow to a similar final optical density as the ornibactin-supplemented culture. A higher concentration of these siderophores may increase the growth rate of the *pobA* mutant to an optimal level.

Similarly, as cepabactin is a bidentate siderophore, the concentration of this siderophore is increased three-fold, so that the concentration of the bidentate ligands was the same as present in the ornibactin-supplemented culture, allowed growth rate of the *pobA* mutant to be identical to that of ornibactin (Figure 4.11F). These results confirmed that these siderophores may be utilised as iron sources by *B. cenocepacia* growing in iron-limiting conditions. A summary of the hydroxamate siderophore utilisation results is shown in Table 4.1**.**

4.4 Identification of a specific TBDR for hydroxamate xenosiderophores

Having identified a number of hydroxamate siderophores that *B. cenocepacia* can use, the TBDR(s) involved in transporting them into the periplasm was investigated. Previously, eight *B. cenocepacia* mutants were constructed harbouring trimethoprim-resistance cassette insertions in TBDR gene loci in strain AHA27. These loci correspond to the 715j orthologues of BCAL0116, BCAL1345, BCAL1371, BCAL1709, BCAM0491, BCAM0499, BCAM1187 and BCAM2439 in strain J2315.

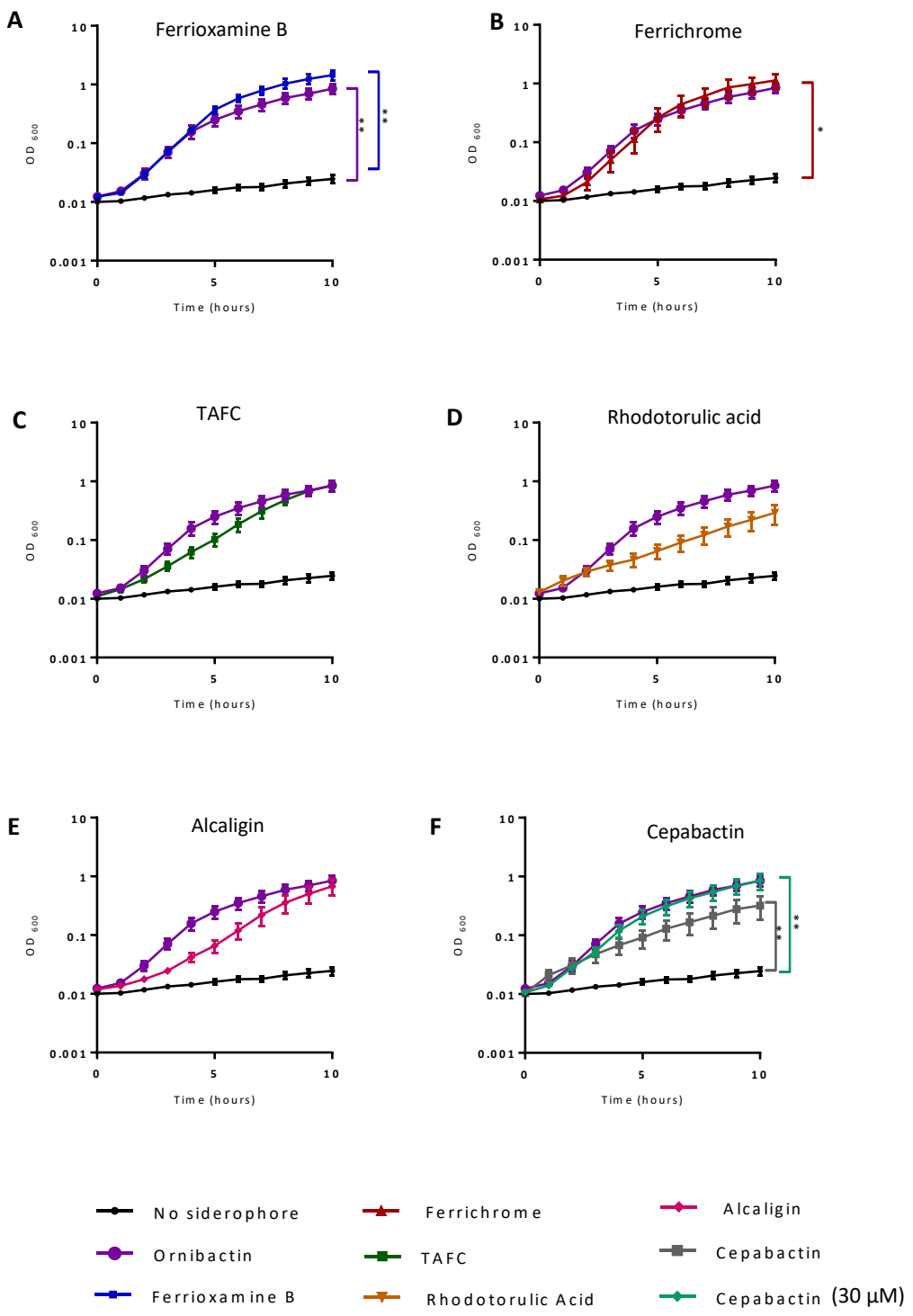

Figure 4.11: Growth curves of *B. cenocepacia* H111ΔpobA mutant in iron-depleted medium supplemented with different xenosiderophores

B. cenocepacia H111ΔpobA was grown at 37 °C in M9-glucose CAA medium supplemented with 10 µM of (A) ferrioxamine B, (B) ferrichrome, (C) TAFC, (D) rhodotorulic acid, (E) alcaligin, and (F) cepabactin. All graphs show a growth curve without siderophores as a negative control and with ornibactin-supplementation as a positive control. Siderophores were included in the medium at 10 µM except where indicated. These data represent three independent experiments (n=3). Error bars represent the mean ±SEM. Significance of siderophore-supplemented compared to unsupplemented growth rate is shown in (A), (B) and (F). *p<0.05, **p<0.01.

Table 4.1 Ability of hydroxamate siderophores to promote growth of *B. cenocepacia*[a] under iron restriction conditions[b]

	Hydroxamate[c] siderophores	Growth in presence of siderophore	Degree of growth with 200 µM EDDHA	Diameter of growth with 40 µM EDDHA
	Bidentate			
1.	Cepabactin	Yes	-	++
	Tetradentate			
2.	Alcaligin	Yes	Not tested	++
3.	Rhodotorulic acid	Yes	Not tested	+
	Hexadentate			
4.	Triacetylfusarinine	Yes	+	++
5.	Ferrioxamine B[d]	Yes	+++	++++
6.	Ferrichrome[d]	Yes	+++	++++
7.	Ferricrocin	Yes	Not tested	++++
8.	Coprogen	No	Not tested	-

Symbols and abbreviations used within this table: ++++, ±5 cm; +++, ±4 cm; ++, ±3 cm; +, ±2 cm.
[a]Strain H111ΔpobA was used.
[b]Disc diffusion assay with 1 cm filters.
[c]All are desferri forms except ferricrocin.
[d]Used as control siderophores.

The mutants were tested for their ability to utilise ferrichrome and ferrioxamine B. It was shown that inactivation of BCAL0116 prevented utilisation of ferrioxamine B but still allowed ferrichrome utilisation. There was no effect on ferrichrome utilisation following inactivation of each of the other TBDR genes (Sofoluwe and Thomas, unpublished results).

For subsequent experiments, the BCAL0116 gene was inactivated in the H111ΔpobA strain, thereby generating H111ΔpobA-BCAL0116:TpTer. Although the orthologue of BCAL0116 in strain H111 is annotated as I35_RS00620, for consistency the mutant will be designated as H111ΔpobA-BCAL0116::TpTer throughout this thesis. Also, the gene locus tags of *B. cenocepacia* J2315 will be applied to orthologous genes in other *B. cenocepacia* strains.

4.4.1 Generation of H111ΔpobA-BCAL0116::TpTer

Construction of H111ΔpobA-BCAL0116::TpTer was undertaken by using the R6K-based suicide plasmid, pSHAFT-GFP (Shastri et al., 2017). The plasmid contains a gene encoding the fluorescent marker GFP which allows for screening of recombinants via a fluorogenic approach. A previously constructed plasmid, pSHAFT-GFP-BCAL0116::TpTer, which contains the BCAL0116 gene with a trimethoprim-resistance cassette insertion (Sofoluwe and Thomas, unpublished results) was used to generate the mutant. pSHAFT-GFP-BCAL0116::TpTer was transformed into the *E. coli* donor strain SM10(λpir) and then introduced into H111ΔpobA by conjugation. H111ΔpobA ex-conjugants were selected on M9-glucose CAA minimal media containing tetracycline (10 µg ml^{-1}) and trimethoprim (25 µg ml^{-1}). The addition of casamino acids allows for faster growth of *Burkholderia* mutants in the minimal medium. Casamino acids would allow the growth of auxotrophic SM10(λpir) colonies but they are inhibited by tetracycline.

Approximately 50 ex-conjugant colonies were patched onto the selection medium and onto IST agar containing trimethoprim (25 µg ml^{-1}), concurrently. *B. cenocepacia* recombinants in which the plasmid containing the *gfp* gene has integrated into the genome produces weakly fluorescent colonies due to single gene expression. However, the colonies are highly distinguishable on IST plates under a UV transilluminator. Non-fluorescent colonies, indicating a second single crossover recombination event resulting in excision of the integrated plasmid, were identified. Non-fluorescent colonies were purified from the duplicate patches on the M9-glucose (CAA) plates and then screened by PCR using outside primers BCAL0116forout and BCAL0116revout to identify the presence of the BCAL0116::TpTer allele. The presence of the inactivated gene gave rise to a PCR product with a size of approximately 2.4 kb, whereas a ~1.5 kb product was generated for the wild type BCAL0116 gene (Figure 4.12). Generation of H111ΔpobA-BCAL0116::TpTer offers the possibility of introducing a second null allele and/or complementing plasmid.

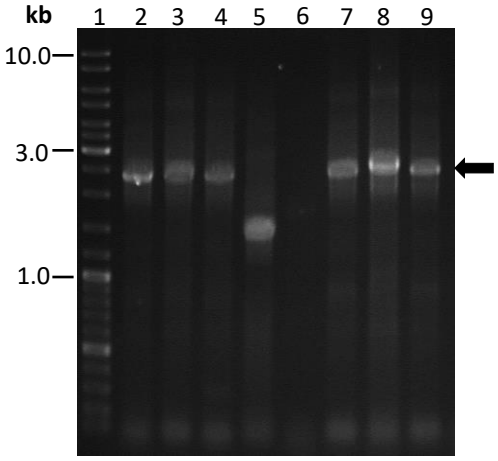

Figure 4.12: PCR screening of candidate H111ΔpobA-BCAL0116::TpTer mutants
Colony PCR screening of insertion of TpTer cassette into BCAL0116 gene locus in H111ΔpobA-BCAL0116::TpTer candidates using primer combination, BCAL0116forout and BCAL0116revout at an annealing temperature 60 °C. Reaction products were analysed by agarose gel electrophoresis. Lane 1, linear DNA ladder; lanes 2-3 and lanes 7-9, H111ΔpobA-BCAL0116::TpTer candidates giving rise to ~2.4 kb amplicon indicating the presence of the BCAL0116::TpTer allele; lane 4, AHA27-BCAL0116::TpTer as a positive control; lane 5, H111 wild type giving rise to ~1.5 kb; lane 6, H111ΔpobA-BCAL0116::TpTer candidate which failed to produce a PCR product. Amplification of BCAL0116:: TpTer is indicated by an arrow.

4.4.2 Analysis of the role of the BCAL0116 TBDR in utilisation of hydroxamate siderophores.

Disc-diffusion bioassays showed that H111ΔpobA-BCAL0116::TpTer did not exhibit growth around the discs impregnated with iron-free ferrioxamine B (as shown previously for AHA27-BCAL0116::TpTer) nor with TAFC, rhodotorulic acid and alcaligin. However, growth was observed around the filter impregnated with iron-free ferrichrome and cepabactin. H111ΔpobA was used as a control and showed growth around all the filter discs impregnated with all the hydroxamate siderophores tested (Figure 4.13A-C). This indicates that the product of the gene locus BCAL0116 is responsible for transporting a variety of hydroxamate siderophores in the form of ferric siderophore complexes. This observation strongly indicates that the BCAL0116 gene locus (or I35_RS00620 in H111) encodes the sole TBDR for some but not all the hydroxamate siderophores. In this instance, ferrioxamine B, TAFC, rhodotorulic acid and alcaligin.

While these hydroxamate siderophores use the BCAL0116 TBDR for their transport, this does not seem to be the case for cepabactin, ferrichrome and possibly ferricrocin as these siderophores still promote growth of the H111ΔpobA BCAL0116 knockout mutant. Two hypotheses may be proposed to explain this observation: cepabactin, ferrichrome and ferricrocin transport may require a different TBDR or the transport of these siderophores involves more than one TBDR including BCAL0116. According to both hypotheses, one or more TBDRs other than BCAL0116 exists in *B. cenocepacia* for the uptake of cepabactin and/or ferrichrome-like siderophores. In this case, ferrichrome and ferricrocin are very similar to each other as both are in the same ferrichrome-type group (Heymann, 2000), while cepabactin is relatively different such that the hydroxamate group in the siderophore is present on a pyridine ring, resembling a catecholate or a hydroxypyridonate ligand.

4.4.3 Bioinformatic search of an additional hydroxamate TBDR

As it was postulated that there may be another TBDR involved in transporting the hydroxamate siderophores, the putative TBDRs obtained by bioinformatic analysis in Chapter 3 were analysed to find a possible candidate as a second hydroxamate transporter. The constructed phylogenetic tree of both *B. cenocepacia* J2315 and H111 TBDRs revealed that the TBDR BCAL0116 is closely-related to the BCAL2281 receptor (or I35_RS11045 in H111). Both gene loci were paired in the phylogenetic trees (Section 3.2). In view of this, BCAL2281 was hypothesised to be another hydroxamate siderophore TBDR that may transport ferrichrome. Therefore, the next aim was to construct a BCAL2281 knockout mutant and to screen it for utilisation of cepabactin and ferrichromes (ferrichrome and ferricrocin). To investigate the BCAL2281 gene locus, inactivation of the respective gene was performed in H111ΔpobA.

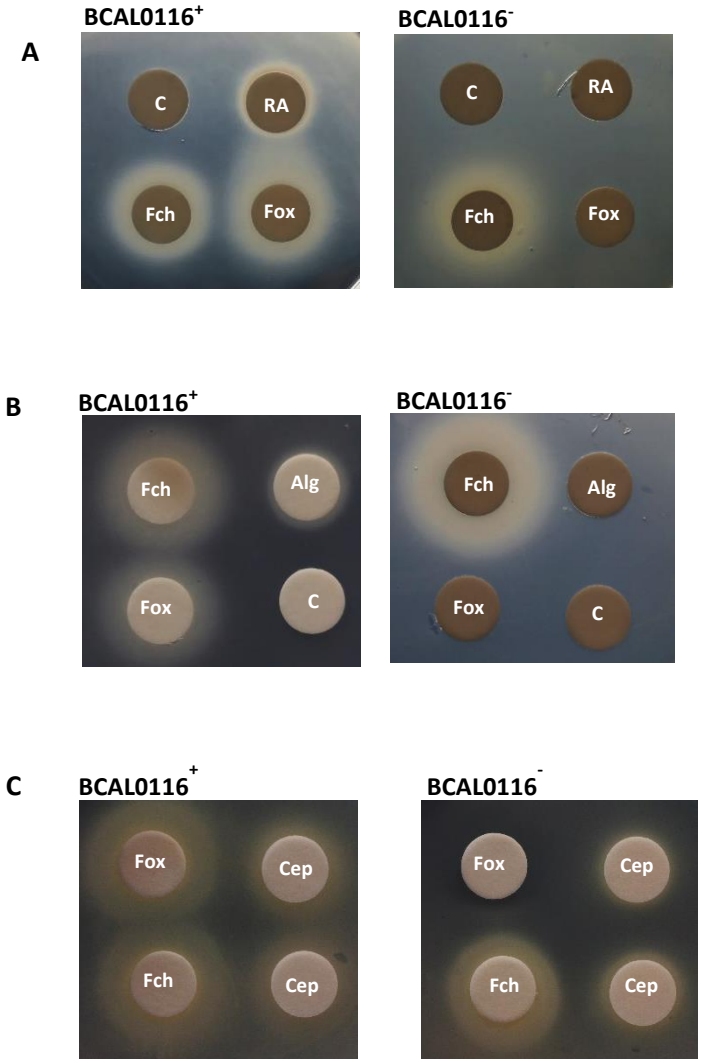

Figure 4.13: Screening of hydroxamate siderophore utilisation by *B. cenocepacia* TBDR mutants
(A) Effect of inactivation of BCAL0116 on rhodotorulic acid (RA), ferrioxamine B (Fox) and ferrichrome (Fch) utilisation by *B. cenocepacia*. dH_2O ('C') serves as negative control. (B) Effect of inactivation of BCAL0116 on alcaligin utilisation. (C) Effect of inactivation of BCAL0116 on cepabactin utilisation. *B. cenocepacia* mutants used are stated on top of figures. All mutants used are derivatives of the siderophore-deficient H111 pobA$^-$ strain. Filter disc for each bioassay plate was spotted with purified siderophore: Ferrichrome (Fch) (1 mM, 10-20 µl); ferrioxamine B (Fox) (1 mM, 10-20 µl); rhodotorulic acid (RA) (5 mM, 20 µl); alcaligin (Alg) (5 mM, 10-20 µl); cepabactin (Cep) (5 mM 20 µl); dH_2O ('C') (10-20 µl). Final EDDHA concentration in agar are 40 µM. H111ΔpobA is annotated as BCAL0116$^+$ and H111ΔpobA-BCAL0116::TpTer is annotated as BCAL0116$^-$.

4.4.4 Analysis of the role of the BCAL2281 TBDR in utilisation of hydroxamate siderophores

As a first step in the generation of a *B. cenocepacia* H111ΔpobAΔBCAL2281 mutant, the BCAL2281 gene was cloned into a suicide vector and an in-frame deletion was introduced as described below.

4.4.4.1 Construction of pEX18TpTer-*pheS*-BCAL2281 and pEX18TpTer-*pheS*-ΔBCAL2281

The BCAL2281 gene and flanking DNA was amplified as a 2936 kb fragment by PCR using Q5 high-fidelity DNA polymerase with primer combination BCAL2281for and BCAL2281rev, cut with restriction enzymes *Acc*65I and *Hin*dIII sequentially and ligated into *Acc*65I-*Hin*dIII digested pEX18TpTer-*pheS.* The ligation products were used to transform *E. coli* JM83 and white colonies were selected on IST agar plates containing trimethoprim (25 µg ml^{-1}), X-gal and IPTG, and purified on the same medium. Constructed plasmids were analysed by gel electrophoresis for identification of plasmids with a size of 7.2 kb (Figure 4.14). A candidate pEX18TpTer-*pheS*-BCAL2281 plasmid with the expected size was confirmed by DNA sequencing and the inserted gene aligned with the H111 BCAL2281 nucleotide sequence.

Inactivation of BCAL2281 in pEX18TpTer-*pheS* by in-frame deletion was carried out by restriction digestion with *Sna*BI and *Zra*I, releasing a 981 bp fragment of the BCAL2281 gene. Religated products were transformed into JM83 *E. coli* cells and transformants selected on IST agar containing trimethoprim (25 µg ml^{-1}). Constructed plasmid DNA was analysed by gel electrophoresis to identify pEX18TpTer-*pheS*-ΔBCAL2281 (~6.2 kb) (Figure 4.12). Confirmation of deletion was performed by DNA sequencing. Illustration of the construction of pEX18TpTer-pheS-ΔBCAL2281 is depicted in Figure 4.15.

The plasmid pEX18TpTer-*pheS*-ΔBCAL2281 was then transformed into the conjugal donor strain SM10(λpir) (Section 2.4.4.1). H111ΔpobA containing the ΔBCAL2281 allele was constructed by two-step allelic replacement method as described previously (Section 4.2.3). Following cPhe counter selection, trimethoprim-sensitive colonies were selected and purified for PCR screening with the 'outside primers', BCAL2281forout, and BCAL2281revout for confirmation of ΔBCAL2281 exchange for the wild type allele. PCR products were analysed by electrophoresis: the wild type gave a PCR product size of 2993 bp and the mutant, H111ΔpobAΔBCAL2281 expected DNA fragment size was 2012 bp (result not shown).

4.4.4.2 Screening of cepabactin and ferrichrome utilisation by H111ΔpobAΔBCAL2281

The constructed mutant was used to investigate BCAL2281 as the TBDR for cepabactin and the ferrichromes. H111ΔpobAΔBCAL2281 was screened for cepabactin and the ferrichromes utilisation by disc diffusion bioassay with H111ΔpobA as a positive control. However, a halo of growth of H111ΔpobAΔBCAL2281 was still seen around the filter disc impregnated with these siderophores indicating that BCAL2281 may not act as the cepabactin and the ferrichromes receptor or BCAL0116 and BCAL2281 are both involved in siderophore transport.

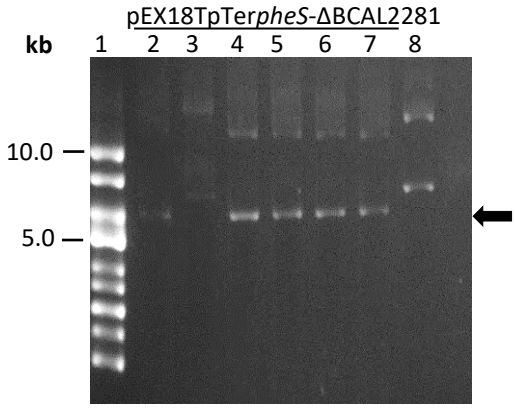

Figure 4.14: Gel electrophoresis of candidate H111ΔpobAΔBCAL2281 plasmids
Screening of candidate pEX18TpTer-*pheS*-ΔBCAL2281 plasmids by agarose gel electrophoresis: Lane 1, supercoiled DNA ladder; lanes 2-7, putative pEX18TpTer-*pheS*-ΔBCAL2281 candidates (plasmids in lanes 2 and 4-7 are the expected plasmid size of ~6.2 kb, indicated by an arrow); lane 8, pEX18TpTer-*pheS*-BCAL2281 acts as control with a plasmid size of 7.2 kb.

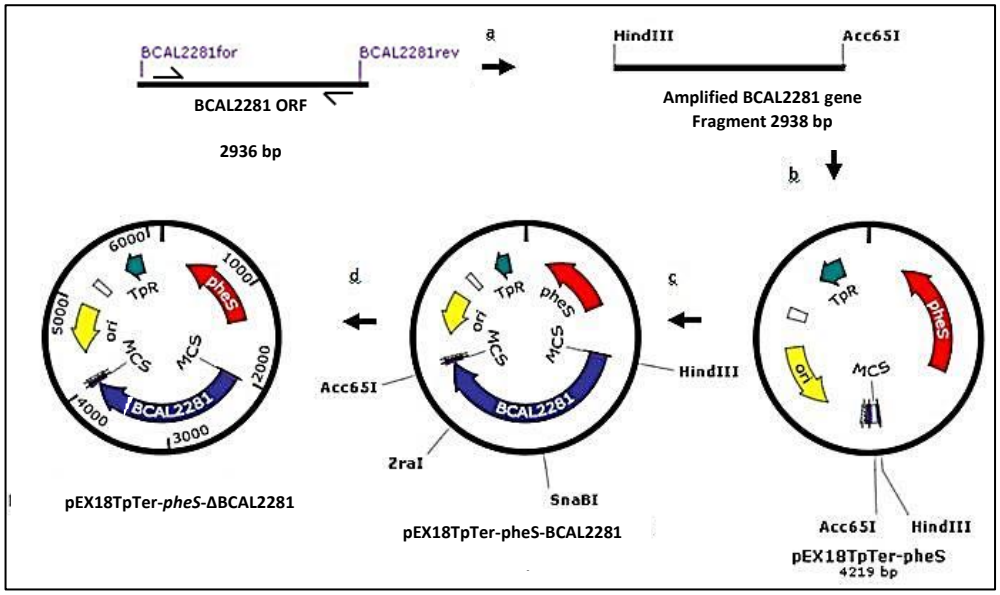

Figure 4.15: Construction of pEX18TpTer-*pheS*-ΔBCAL2281
a. A 2936 bp DNA fragment containing the BCAL2281 gene was PCR amplified with primer combination BCAL2281for and BCAL22814rev and was restriction digested with *Hin*dIII and *Acc*65I b. The cut fragment was ligated into pEX18TpTer-*pheS* cut with the same enzymes. d. In-frame deletion was performed on the BCAL2281 gene in pEX18pTer-*pheS*-BCAL2281 by cleavage with *Zra*I and *Sna*BI releasing a 981 bp *Zra*I-*Sna*BI fragment followed by self-ligation to generate pEX18TpTer-*pheS*-ΔBCAL2281. Illustration is depicted using SnapGene.

Growth of H111ΔpobAΔBCAL2281 promoted by the ferrichromes, ferrichrome and ferricrocin is shown in Figure 4.16A and B. To investigate between these two possibilities, the H111ΔpobA strain with both TBDRs knocked-out, H111ΔpobAΔBCAL2281-BCAL0116::TpTer, was constructed. This was performed by introducing pSHAFT-GFP-BCAL0116::TpTer into H111ΔpobAΔBCAL2281 by conjugation as previously described (Section 4.4.1).

4.4.4.3 Screening of cepabactin and ferrichrome utilisation by the H111ΔpobAΔBCAL2281-BCAL0116::TpTer mutant

Cepabactin and ferrichrome utilisation by H111ΔpobAΔBCAL2281-BCAL0116::TpTer were performed using the disc diffusion assay and compared to that of H111ΔpobA, H111ΔpobAΔBCAL2281 and H111ΔpobA-BCAL0116::TpTer. Cepabactin, ferrichrome and ferricrocin solution were spotted on separate filter discs and growth around the discs was observed after 24-48 hr incubation. The results showed the presence of growth of H111ΔpobA, H111ΔpobAΔBCAL2281 and H111ΔpobA-BCAL0116::TpTer around the discs containing all three siderophores. Cepabactin was seen to allow growth of the double mutant receptor, H111ΔpobAΔBCAL2281-BCAL0116::TpTer, including the single TBDR mutants (results not shown). In contrast, no growth of the double receptor mutant was observed with the ferrichromes, demonstrating the use of two receptors in *B. cenocepacia* for the transport of ferrichromes as iron sources (Figure 4.16A and B). As a zone of growth of the double mutant, BCAL0116 and BCAL2281 was observed with the filter disc spotted with cepabactin, the TBDR responsible for cepabactin transport was not further investigated. Complementation analyses of the siderophore transport defects of the BCAL0116 and BCAL2281 mutants are described in subsequent sections.

4.5 Complementation of the BCAL0116 and BCAL2281 TBDR mutants

To confirm that the phenotypes of the BCAL0116 and BCAL2281 mutants are the results of their inactivation rather than a polar effect of gene disruption, complementation tests were performed. These entailed introduction of a wild type gene copy cloned in an expression vector into the respective mutants to demonstrate restoration of the wild type phenotype.

The expression vector pSRKKm was used to construct the complementation plasmids, pSRKKm-BCAL0116 and pSRKKm-BCAL2281. The plasmid pSRKKm originates from the broad host-range pBBR1MCS vector family and was chosen due to its tightly regulated promoter activity. The *lac* operon promoter present in this plasmid can be controlled by varying the concentration of an inducer, in this case the isopropyl-β-D-thiogalactopyranoside (IPTG) (Khan et al., 2008).

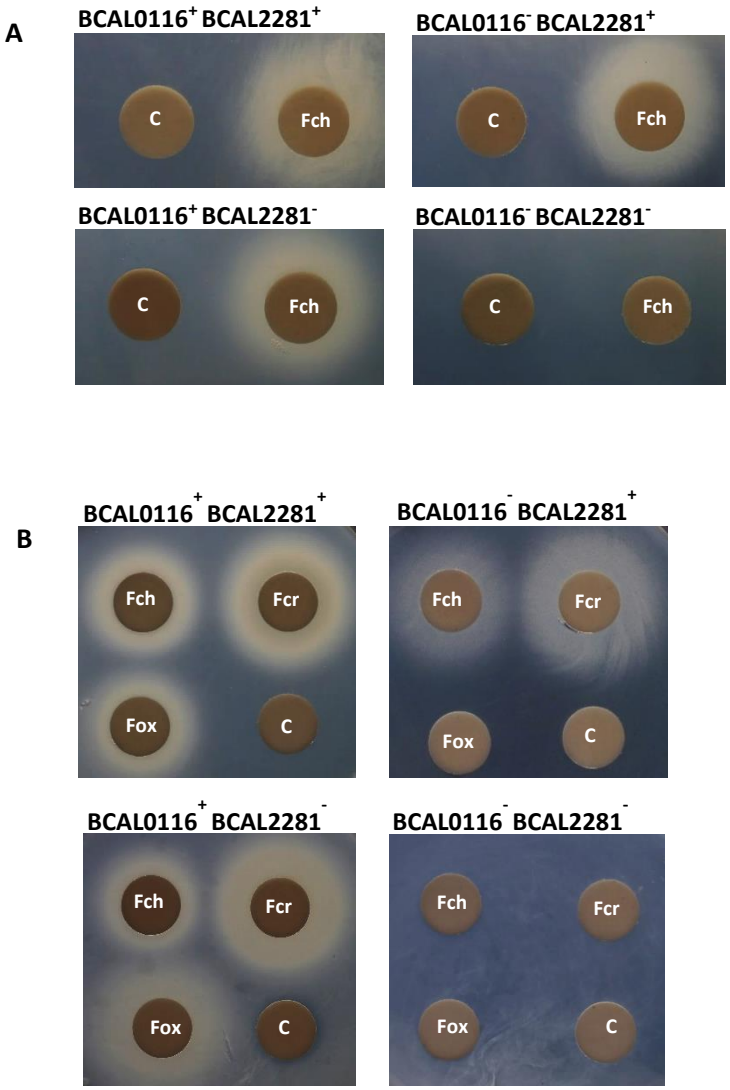

Figure 4.16: Screening of hydroxamate siderophore utilisation by *B. cenocepacia* TBDR mutants
Utilisation of hydroxamate siderophores was tested using single (H111ΔpobA-BCAL0116::TpTer and H111ΔpobAΔBCAL2281) and double TBDR mutants (H111ΔpobAΔBCAL2281-BCAL0116::TpTer). H111ΔpobA strain was used as a positive control. Hydroxamate siderophores used are (A) ferrichrome. (B) ferrichrome, ferricrocin and ferrioxamine B. *B. cenocepacia* mutants used are stated on top of figures. All mutants used are derivatives of the siderophore-deficient, H111ΔpobA strain. Filter disc for each bioassay plate was spotted with purified siderophore: Ferrichrome (Fch) (1 mM, 10-15 µl); ferrioxamine B (Fox) (1 mM, 10 µl); ferricrocin (Fcr) (1 mM, 10µl); dH_2O ('C') (10-15 µl). Final EDDHA concentration in agar was 40 µM.

4.5.1 Construction of complementation plasmids, pSRKKm-BCAL0116 and pSRKKm-BCAL2281

The BCAL0116 gene was amplified using the primers BCAL0116forfull and BCAL0116revfull (Figure 4.17A). The 2319 bp amplicon was restriction digested with *Hin*dIII and *Bam*HI, and ligated into pSRKKm which was cut with the same restriction endonucleases. Ligated products were transformed into competent *E. coli* MC1061 cells which does not permit blue/white colony screening. Therefore, transformants were PCR-screened using the insert primers, BCAL0116forfull and BCAL0116revfull. Alternatively, host strain JM83 was used in combination with the white-blue X-gal screen and selection was performed using LB agar containing kanamycin (50 µg ml^{-1}), X-gal and IPTG. Colonies giving rise to a PCR fragment size of 2319 bp with the insert primers (Figure 4.17B) were cultured for plasmid preparation. The candidate pSRKKm-BCAL0116 plasmids were analysed by agarose gel electrophoresis for size confirmation of 8075 bp (result not shown). The inserts in the prepared plasmids were sequenced with pSRKKm backbone primers, M13For and M13Rev and aligned by Clustal Omega with the BCAL0116 sequence to confirm insertion of the BCAL0116 gene into pSRKKm without mutations. Since the BCAL0116 gene is a large DNA fragment, additional primers were used to sequence the middle region of the gene. Diagrammatic representation of pSRKKm-BCAL0116 construction is illustrated in Figure 4.18.

To construct pSRKKm-BCAL2281 (8667 bp), the same PCR product used to generate pEX18TpTer-pheS-BCAL2281 (Section 4.4.4.1) containing the entire BCAL2281 ORF and flanking DNA sequences was restriction digested by *Hin*dIII and *Acc*651, and was ligated between the same restriction sites of pSRKKm. Kanamycin-resistant transformants were selected in strain JM83 as previously described (Section 4.5.1). Transformants were PCR screened with primers BCAL2281for and BCAL2281rev for confirmation (results not shown). Prepared plasmids of positive candidates were sequenced using M13For and M13Rev for confirming integrity of cloned DNA.

4.5.2 Complementation analysis of hydroxamate siderophore TBDR mutants using disc diffusion assay

Plasmids pSRKKm, pSRKKm-BCAL0116 and pSRKKm-BCAL2281 were introduced into *E. coli* S17-1(λpir) by transformation. As with SM10 (λpir), S17-1(λpir) has the RP4 conjugation machinery which promotes plasmid transfer (Simon et al., 1983). Conjugation was performed between the transformed *E. coli* S17-1(λ pir) strain containing pSRKKm only and containing the pSRKKm-BCAL0116 with both the BCAL0116 knockout mutant, H111ΔpobA-BCAL0116::TpTer, and the double TBDR mutant, H111ΔpobAΔBCAL2281-BCAL0116::TpTer. The exconjugant *B. cenocepacia* colonies were selected on Lennox agar plates containing kanamycin (100 µg ml^{-1}) and tetracycline (10 µg ml^{-1}).

Similarly, conjugation was performed between the transformed *E. coli* S17-1(λ pir) strains containing pSRKKm only and containing the pSRKKm-BCAL2281 with the BCAL2281 knockout mutant, H111ΔpobAΔBCAL2281, and the double TBDR mutant, H111ΔpobAΔBCAL2281-BCAL0116::TpTer.

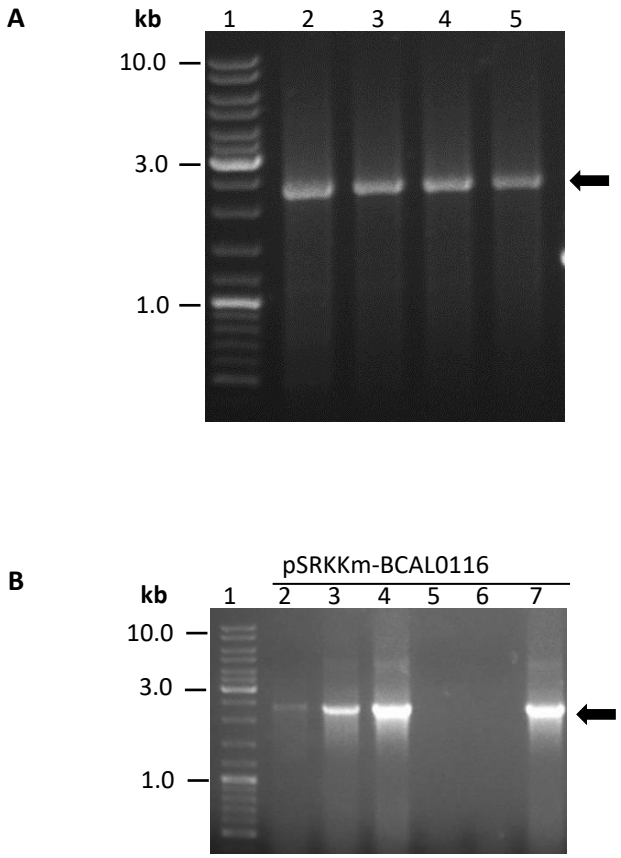

Figure 4.17: Gel electrophoresis analysis of BCAL0116 amplification for construction of pSRKKm-BCAL0116 complementation plasmid

A) Amplification of BCAL0116 gene from H111 for construction of pSRKKm-BCAL0116. Lane 1, Linear DNA ladder; lanes 2-5, amplified gene fragment giving a size of 2319 bp using primer combination BCAL0116forfull and BCAL0116revfull at a gradient annealing temperature of 57, 59, 61 and 63 °C indicated by arrow. (B) Colony PCR of MC1061 containing candidate pSRKKm-BCAL0116 plasmids using primer combination BCAL0116forfull and BCAL0116revfull at annealing temperature 57 °C: Lane 1, Linear DNA ladder; lane 2, wild type H111; lanes 3 - 7, MC1061 containing pSRKKm-BCAL0116 candidates (plasmids in lane 3,4 and 7 give rise to a 2319 bp amplicon as expected, indicated by an arrow).

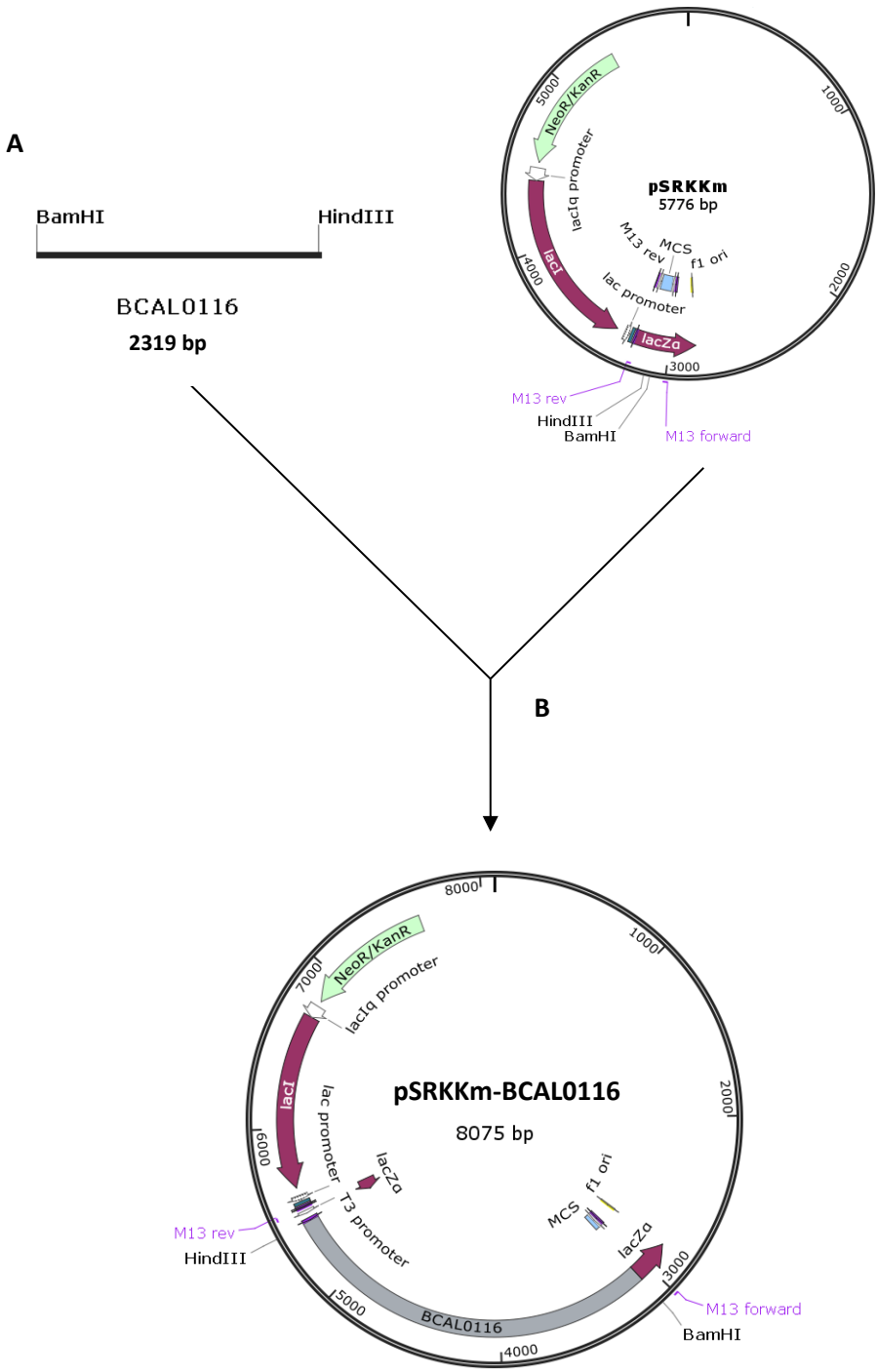

Figure 4.18: Diagrammatic representation of the construction of complementation plasmid pSRKKm-BCAL0116

(A) The full BCAL0116 gene (amplified with BCAL0116fullfor and BCAL0116fullrev) was digested with *Bam*HI and *Hin*dIII, giving rise to a 2319 bp fragment. (B) The DNA fragment was inserted into the same restriction sites in pSRKKm, forming pSRKKm-BCAL0116 with a size of 8075 bp. Plasmids are depicted using SnapGene.

The exconjugant *B. cenocepacia* colonies were selected on the same medium as for the pSRKKm-BCAL0116. pSRKKm was also introduced into BCAL0116, BCAL2281 and BCAL0116-BCAL2281 mutants. A medium with a lower salt concentration (Lennox agar) than is present in LB has been observed to be more efficient for selecting kanamycin-resistance in *Burkholderia* (Spiewak and Thomas, unpublished observations).

Several colonies from each conjugation were selected for PCR screening using the vector primer M13for and M13rev. The presence of pSRKKm-BCAL0116 in the mutants was detected by the presence of a 2528 bp DNA fragment, whereas the empty vector gave rise to a DNA fragment of 229 bp. Similarly, the mutants harbouring the complementation plasmid pSRKKm-BCAL2281 and the empty vector, pSRKKm, were PCR screened with the same primers at an annealing temperature of 51 °C giving fragments of sizes 3121 bp and 229 bp, respectively (results not shown).

For complementation analysis of the BCAL0116 mutant, which is involved in uptake of all the hydroxamate xenosiderophores reported in this study except for cepabactin and the ferrichromes, H111ΔpobA-BCAL0116::TpTer containing the complementation plasmid pSRKKm-BCAL0116 or the empty vector, pSRKKm, were used. The analysis performed with the disc diffusion assay demonstrated growth promotion of the mutant containing pSRKKm-BCAL0116 by the siderophores, alcaligin, ferrioxamine B, rhodotorulic acid and TAFC (Figure 4.19A). These observations verified that BCAL0116 is the sole TBDR responsible for the utilisation of the tested hydroxamate siderophores and supports the hypothesis that it serves to transport these siderophores into the periplasm of *B. cenocepacia* H111.

H111ΔpobAΔBCAL2281-BCAL0116::TpTer containing either of the complementation plasmids pSRKKm-BCAL0116 and pSRKKm-BCAL2281 were analysed. H111ΔpobAΔBCAL2281-BCAL0116::TpTer containing the empty vector, pSRKKm, was used as a control. The disc diffusion assay performed with discs impregnated with ferrichrome demonstrated growth of H111ΔpobAΔBCAL2281-BCAL0116::TpTer containing the pSRKKm-BCAL0116 plasmid around the disc, indicating the restoration of the BCAL0116 phenotype. Promotion of growth was also observed with the mutant containing the pSRKKm-BCAL2281 plasmid, verifying that both TBDRs are involved in ferrichrome utilisation and supports the hypothesis that these proteins serve to transport ferrichromes across the outer membrane (Figure 4.19B).

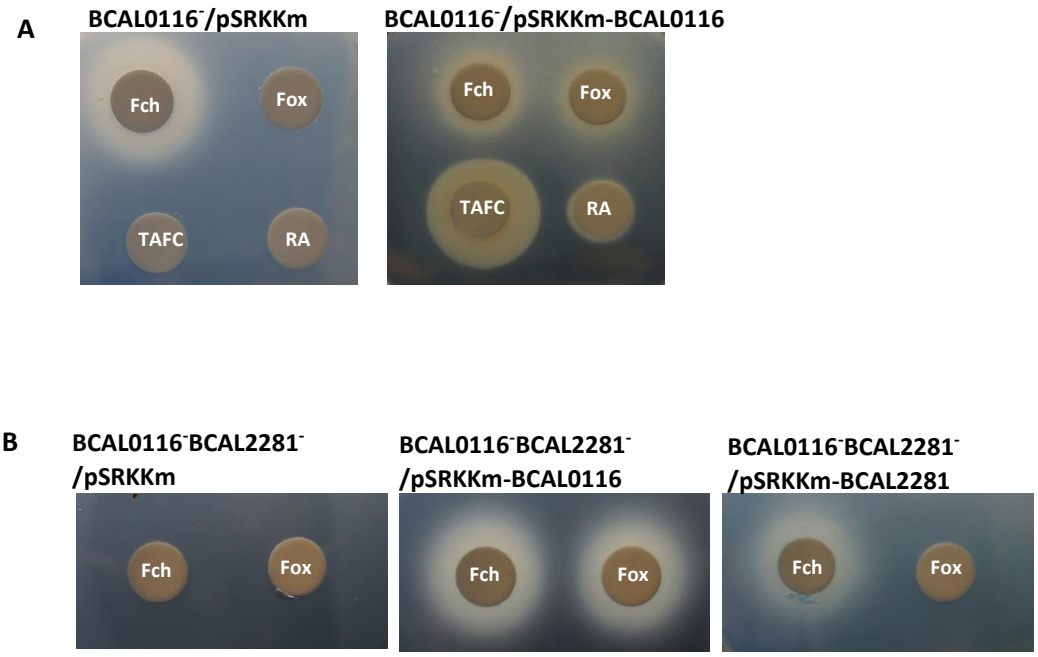

Figure 4.19: Complementation analysis of the BCAL0116 and BCAL2281 TBDR mutants using the disc diffusion assay

(A) Restoration of hydroxamate siderophore utilisation of the BCAL0116 mutant H111ΔpobA-BCAL0116::TpTer by the complementation plasmid, pSRKKm-BCAL0116 in the presence of the hydroxamate siderophores, ferrioxamine B, rhodotorulic acid and triacetylfusarinine C. (B) Complementation of TBDR double mutant H111ΔpobAΔBCAL2281-BCAL0116::TpTer by complementing plasmids, pSRKKm-BCAL2281 and pSRKKm-BCAL0116. Filter discs were spotted with purified siderophore; ferrichrome (Fch) (1 mM, 10 µl); ferrioxamine B (Fox) (1 mM, 10 µl); triacetylfusarinine (TAFC) (1 mM, 10 µl); rhodotorulic acid (RA) (5 mM, 20 µl). Final EDDHA concentration in agar was 40 µM.

4.5.3 Effect of inactivation of BCAL0116 and BCAL2281 on growth of *B. cenocepacia* promoted by hydroxamate siderophores in liquid medium

To support the conclusion based on disc diffusion assays that BCAL0116 represents the TBDR for certain hydroxamate xenosiderophores (in this case, alcaligin, ferrioxamine B, TAFC and rhodotorulic acid), the effect of ferrioxamine B on the growth of the TBDR mutant H111ΔpobA-BCAL0116::TpTer in iron-depleted liquid medium was monitored. Ferrioxamine B was used to represent the hydroxamate xenosiderophores. Growth curves (n=3) of the TBDR mutant in the presence of ferrioxamine B were comparable to those of the *pobA* mutant without supplementation with siderophores, indicating that ferrioxamine B was not transported into the intracellular compartment of this strain, thereby confirming the role of the BCAL0116 protein in utilisation of this siderophore (Figure 4.20A).

To investigate the role of the BCAL2281 TBDR in ferrichrome utilisation in liquid medium, ferrichrome was added to iron-limited culture of the H111ΔpobA-BCAL0116::TpTer, H111ΔpobAΔBCAL2281 and H111ΔpobAΔBCAL2281-BCAL0116::TpTer mutants. Comparison of the two single TBDR mutant growth curves (n=3) demonstrated that H111ΔpobA-BCAL0116::TpTer grew at a lower rate than the H111ΔpobAΔBCAL2281 mutant (Figure 4.21A). This may suggest that TBDR BCAL0116 is more efficient in transporting ferrichrome than the TBDR BCAL2281. However, the different efficiency displayed may also be due to differences in the level of expression of the TBDRs rather than their affinity for the siderophores. Growth curves (n=3) of the double TBDR mutant showed no growth promotion with the addition of ferrichrome, indicating that ferrichrome was not used when the two TBDR gene loci were disrupted.

To reconfirm that, BCAL0116 and BCAL2281 are not involved in cepabactin utilisation, the BCAL0116-BCAL2281 double TBDR mutant was grown in iron-limited medium supplemented with and without cepabactin. The growth rate of the double mutant was similar to the rate of H111ΔpobA growing in cepabactin supplemented medium, indicating no or little involvement of these two TBDRs. Promotion of growth of the BCAL0116-BCAL2281 mutant in cepabactin supplemented medium verified that cepabactin is transported into the cytosol of *B. cenocepacia* using an alternative TBDR. Without supplementation by cepabactin, the growth rate of the BCAL0116-BCAL2281 mutant was similar to that of H111ΔpobA in the absence of siderophores, demonstrating limited growth (Figure 4.20B).

4.5.4 Complementation analysis of the hydroxamate siderophore TBDR mutants using the liquid growth stimulation assay

Complementation analyses of the hydroxamate siderophore TBDR mutants by the specified TBDRs were performed in broth culture for further confirmation. The phenotype of the single BCAL0116 TBDR mutant containing the complementation plasmid pSRKKm-BCAL0116 was tested by performing growth curves using ferrioxamine B. The empty vector was used as a negative control.

The BCAL0116 mutant was partially complemented by pSRKKm-BCAL0116 as growth of the complemented strain in the presence of ferrioxamine B was at a lower rate than the growth of *B. cenocepacia* H111ΔpobA supplemented with the same siderophore (Figure 4.20A). A possible explanation for these results may be a lack of adequate expression of the BCAL0116 gene locus by the pSRKKm plasmid promoter. As expression of genes cloned in pSRKKm can be controlled through the activity of the *lacZ* promoter, the expression can be increased by a higher concentration of IPTG. A moderate IPTG concentration was used in this study (1 mM) to avoid too high expression of the TBDRs. TBDRs are β-barrel outer membrane proteins (OMPs) and higher expression may disrupt the *B. cenocepacia* cell membrane and cause lysis of the cell.

Complementation analysis of the BCAL0116, BCAL2281 and BCAL0116-BCAL2281 mutants for ferrichrome utilisation were performed using the complementation plasmids pSRKKm-BCAL0116 and pSRKKm-BCAL2281. Empty vectors were used as negative controls. As shown in Figure 4.21B and C, the growth rates of the single TBDR mutants containing their respective complementation plasmids were nearly similar to those of the H111ΔpobA strain, showing near to full efficacy of both complementation plasmids. However, a slightly lower growth rate of the individual BCAL0116 and BCAL2281 mutants containing their corresponding complementation plasmids implies a partial complementation (Figure 4.21D). Both pSRKKm-BCAL0116 and pSRKKm-BCAL2281 allowed growth of the double TBDR mutant at a similar rate to the H111ΔpobA strain (Figure 4.21D). This denotes full phenotype restoration of the BCAL2281-BCAL0116 mutant with either plasmid. A summary of the utilisation of the hydroxamate siderophores in the complementation analyses are presented in Table 4.2.

4.6 Role of the TonB1 system in utilisation of hydroxamate siderophores

Bioinformatic analysis revealed that there are two other TonB complexes in *B. cenocepacia* besides the TonB1 system that is required for ornibactin and pyochelin uptake (Section 3.6). The siderophores, enterobactin and anguibactin, have been reported to be transported by the facilitation of an alternative TonB2 system in a fish pathogen, *Vibrio anguillarium* (Li and Ma, 2017). Therefore, it is possible that the alternative TonB complexes present in *B. cenocepacia* are utilised for xenosiderophore transport. To further investigate whether the xenosiderophores are transported by the TonB1 complex, a *B. cenocepacia* 715j *exbB1* mutant, AHA9, was used to perform the hydroxamate siderophore utilisation bioassay. The *exbB1* gene encodes a component in the main TonB1 complex (Asghar, 2003).

4.6.1 Effect of an *exbB1* null allele on the ability of *B. cenocepacia* to utilise hydroxamate siderophores

Although the *exbB1* mutant, AHA9, can produce endogenous siderophores, it cannot utilise them (Asghar, 2003). Therefore, this strain does not grow on iron-depleted medium or in the disc diffusion assay.

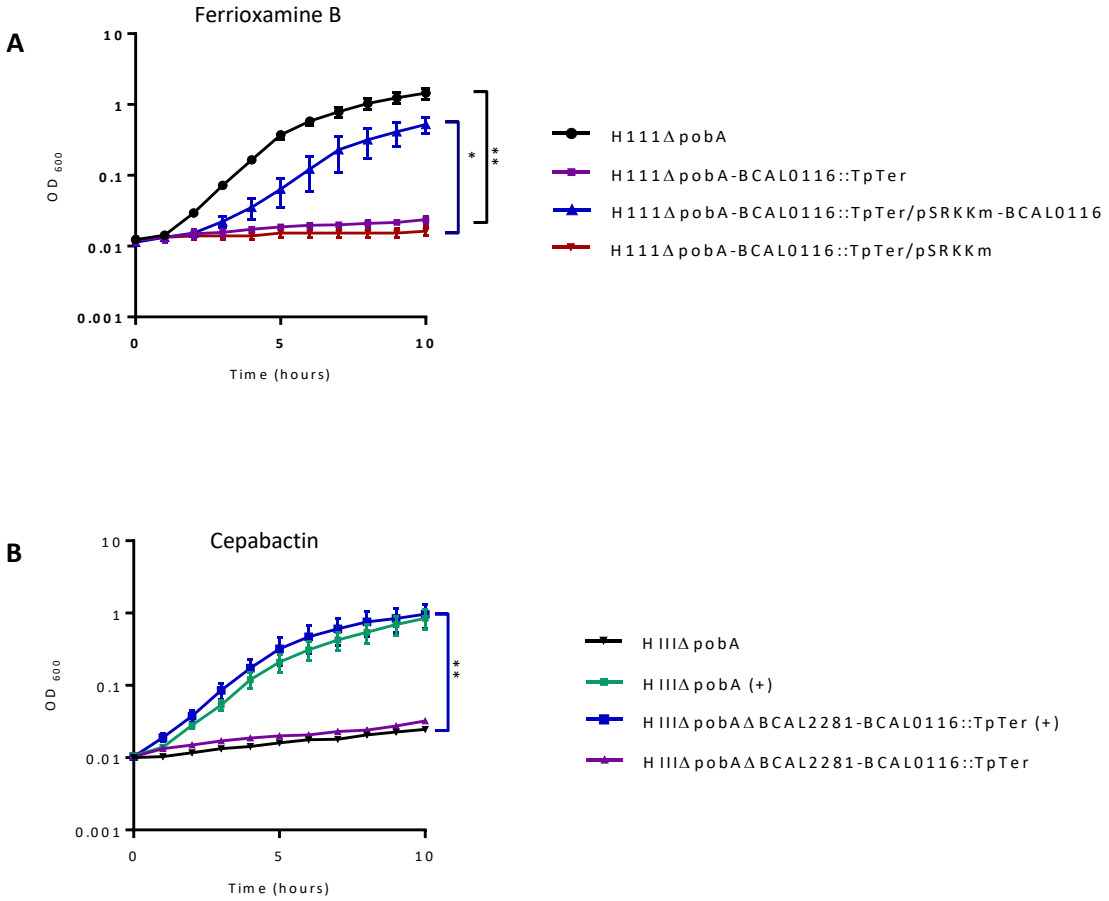

Figure 4.20: Growth curves of *B. cenocepacia* H111 hydroxamate siderophore TBDR mutants in the presence and absence of ferrioxamine B and cepabactin in iron depleted medium and complementation analysis for ferrioxamine B

(A) Growth of the single BCAL0116 TBDR mutant in iron-depleted M9-glucose CAA medium supplemented with 10 µM of ferrioxamine B and complementation of the BCAL0116 gene by pSRKKm-BCAL0116. 5 mM IPTG was included in the medium for strains containing pSRKKm plasmid derivatives. (B) Growth of the double TBDR mutant in the presence (+) and absence of 30 µM cepabactin. These data are representatives of three independent experiments (n=3). Error bars represent the ±SEM. *p<0.05, **p<0.01.

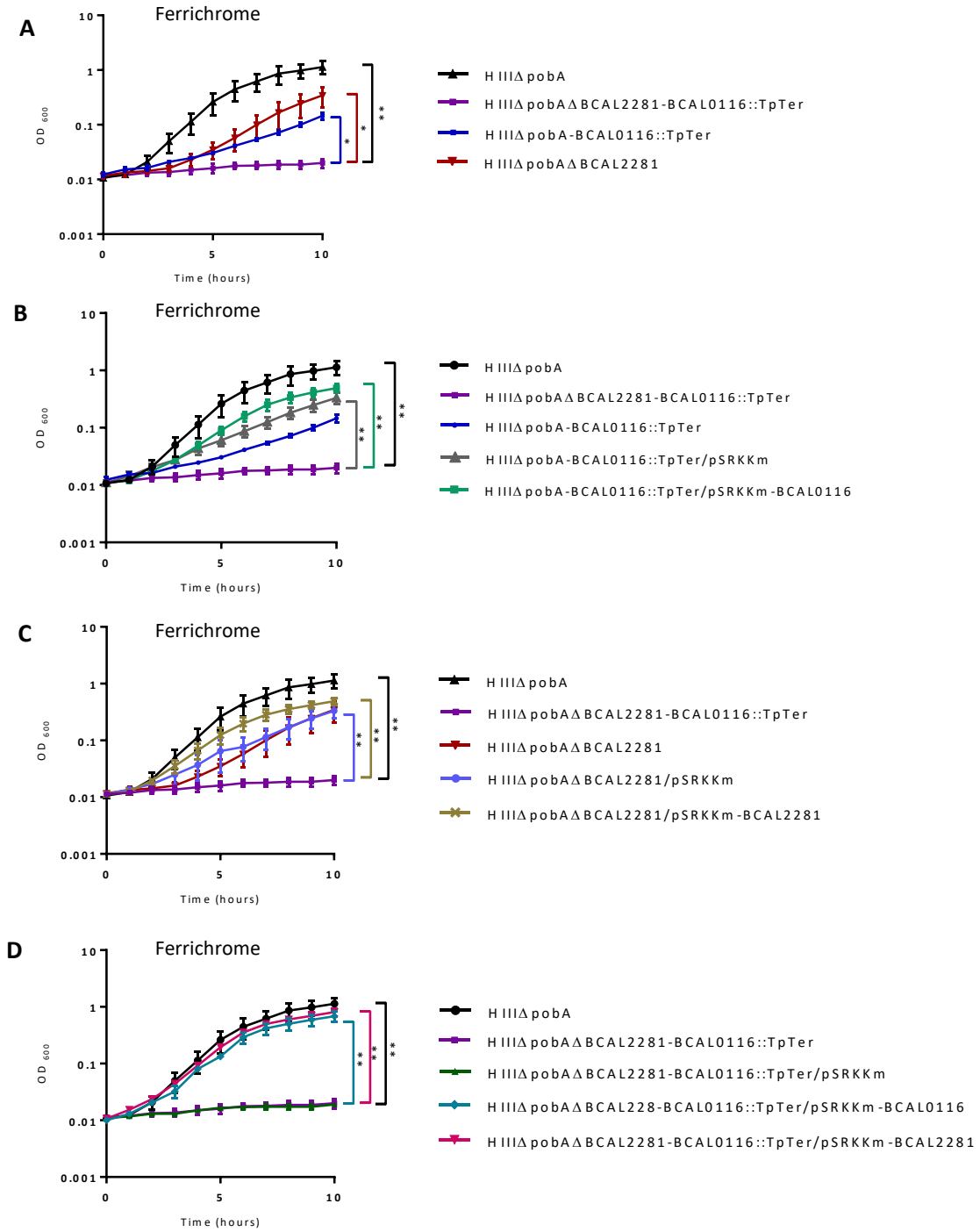

Figure 4.21: Effect of inactivation of the BCAL0116 and BCAL2281 TBDRs on ferrichrome-stimulated growth of *B. cenocepacia* in iron-limited broth culture

(A) Growth of BCAL0116, BCAL2281 and BCAL0116-BCAL2281 TBDR mutants in the presence of ferrichrome. (B) Growth curve of the BCAL0116 TBDR mutant containing the BCAL0116 complementation plasmid and the corresponding empty vector in the presence of ferrichrome. (C) Growth curves of the BCAL2281 TBDR mutant containing the BCAL2281 complementation plasmid and the corresponding empty vector in the presence of ferrichrome. (D) Growth curves of the BCAL0116-BCAL2281 double TBDR mutant containing individual BCAL0116 and BCAL2281 complementation plasmids in the presence of ferrichrome. Cultures were grown in M9-glucose (CAA) medium with 10 µM ferrichrome at 37 °C. 5 mM IPTG and kanamycin (50 µg ml^{-1}) was included in the medium for strains carrying pSRKKm plasmid. Exception of 1 mM IPTG was added for H111ΔpobABCAL2281-BCAL0116::TpTer/pSRKKm-BCAL0116. These data are representatives of three independent experiments (n=3). Error bars represent the ±SEM. *p<0.05, **p<0.01.

Table 4.2 Analysis of the role of BCAL0116 and BCAL2281 in siderophore utilisation by disc diffusion assay

Strains	Ferrichrome	Ferrioxamine B	Cepabactin	Ornibactin
H111ΔpobA	+	+	+	+
H111ΔpobA-BCAL0116:TpTer	+	-	+	+
H111ΔpobA-BCAL0116:TpTer/pSRKKm	+	-	+	+
H111ΔpobA-BCAL0116:TpTer/pSRKKm-BCAL0116	+	+	+	+
H111ΔpobAΔBCAL2281	+	+	+	+
H111ΔpobAΔBCAL2281/pSRKKm	+	+	+	+
H111ΔpobAΔBCAL2281-BCAL0116::TpTer	-	-	+	+
H111ΔpobAΔBCAL2281-BCAL0116::TpTer /pSRKKm	-	-	+	+
H111ΔpobAΔBCAL2281-BCAL0116::TpTer /pSRKKm-BCAL0116	+	+	+	+
H111ΔpobAΔBCAL2281-BCAL0116::TpTer /pSRKKm-BCAL2281	+	-	+	+

Filter discs individually spotted with the hydroxamate siderophores, ferrichrome, ferrioxamine B, TAFC, alcaligin and rhodotorulic acid were placed onto a soft agar overlay seeded with *B. cenocepacia* AHA9 as previously described (Section 4.3.2). None of the hydroxamate xenosiderophores tested promoted growth of the AHA9 mutant indicating that their transport requires the main TonB1 complex (results not shown). TonB1-independent TBDR substrates were not used as controls in this experiment as there are no *B. cenocepacia* xenosiderophores reported to use an alternative TonB complex.

4.7 Identification of the inner membrane transport system for hydroxamate siderophore uptake

Bioinformatic analysis revealed several identifiable inner membrane transport systems in *B. cenocepacia* which may be involved in siderophore uptake (Section 3.7). One of these is BCAL0117/I35_RS00625, a cytoplasmic membrane protein encoded adjacent to the gene encoding the hydroxamate TBDR, BCAL0116/I35_RS00620 (Figure 3.13). BCAL0117 was predicted to have the highest homology to FoxB of *P. aeruginosa.* Likewise*,* the gene encoding FoxB (PA2465) is found adjacent to the gene-encoding the ferrioxamine B TBDR, FoxA (PA2466) in *P. aeruginosa.* Cuiv et al. (2007) suggested that *P. aeruginosa* FoxB functions as an inner membrane transporter for the hydroxamate siderophores, ferrioxamine B and ferrichrome, and additionally the mixed-type citrate-hydroxamate siderophore, schizokinen. However, FoxB has not been shown to be the sole inner membrane transporter for hydroxamate siderophores in *P. aeruginosa* (Cuív et al., 2007), as a *P. aeruginosa foxB* mutant was not constructed and analysed.

As a gene-encoding FoxB-like protein in *B. cenocepacia* (BCAL0117/I35_RS00627) is located next to a gene-encoding a FoxA-like TBDR for hydroxamate siderophores (BCAL0116), the cytoplasmic membrane protein BCAL0117/I35_RS00627 was therefore chosen for analysis as a hydroxamate siderophore transporter from among other predicted cytoplasmic membrane transporters of siderophores (Table 3.4). To investigate the involvement of this protein in hydroxamate siderophore transport, the BCAL0117 gene was inactivated in *B. cenocepacia* H111 by allelic replacement and screened for hydroxamate xenosiderophore utilisation.

4.7.1 Construction of pEX18TpTer-*pheS*-Cm-SceI-ΔBCAL0117

To introduce a mutant allele at the BCAL0117 gene locus, DNA containing the entire BCAL0117 gene was PCR amplified (Figure 4.22A) using primer combination BCAL0117for2 and BCAL0117rev3. The amplicon was cloned between the *Bam*HI and *Eco*RI restriction sites of the allelic replacement vector pEX18TpTer-*pheS*-Cm-SceI. The insertion of the BCAL0117 gene and its flanking DNA into this plasmid was confirmed by analysing plasmid DNA derived from white colonies of JM83 *E. coli* cells by gel electrophoresis. Sequencing analysis of the newly generated plasmid, pEX18TpTer-*pheS*-Cm-SceI-BCAL0117, was performed for verification using the vector primers M13for and M13revBACTH. The plasmid was transformed into GM48 *E. coli* cells to prepare DNA without DAM methylation at the *Nru*I restriction site.

An in-frame deletion was then introduced into BCAL0117 by digestion with *Nru*I followed by self-ligation, resulting in deletion of 879 bp and which left a 1056 bp mutated BCAL0117 null allele on the plasmid, giving rise to pEX18TpTer-*pheS*-Cm-SceI-ΔBCAL0117. The deletion was confirmed by gel electrophoresis analysis (Figure 4.22B) and sequencing using the vector primers.

The suicide plasmid used in this construction is a modified version of a plasmid used previously in this study, pEX18TpTer-*pheS* (Section 4.2). pEX18TpTer-*pheS*-Cm-SceI is enhanced by the addition of an additional counter-selectable marker, an 18 bp I-SceI yeast endonuclease recognition site, and a chloramphenicol-resistance cassette. Although the mutant *pheS* gene does act as a counter-selectable marker, it has been observed to be less efficient due to single-copy expression once the plasmid has integrated into the chromosome (M. Thomas, unpublished observations). The addition of the I-SceI site was demonstrated to increase the chance of selecting the second homologous recombination event in a merodiploid by assistance of another plasmid, pDAI-SceI-*pheS*. pDAI-SceI-*pheS* encodes the endonuclease enzyme I-SceI which generates a double stranded DNA break at the I-SceI recognition site of the chromosomally integrated suicide plasmid. This is lethal to the host cell but a second recombination event occurring between homologous sequence present on the integrated plasmid and the host chromosome rescues the host and results in loss of the plasmid (Fazli et al., 2015). Use of the additional counter-selectable marker, I-SceI requires a slightly different procedure than only using the *pheS* selection for the generation of mutants and will be described in the next section.

4.7.2 Generation of a *B. cenocepacia* ΔBCAL0117 mutant

The pEX18TpTer-*pheS*-Cm-SceI-ΔBCAL0117 plasmid was transformed into *E. coli* S17-1(λpir) from where it was conjugated to the siderophore-deficient *B. cenocepacia* mutant, H111ΔpobA. The exconjugants were spread on the selection medium M9-glucose containing trimethoprim (25 µg ml^{-1}). Alternatively, the exconjugants can be spread onto LB agar supplemented with chloramphenicol (50 µg ml^{-1}). The addition of a chloramphenicol-resistance cassette to the vector can speed the selection process. Single crossover recombinants resulting in integrated pEX18TpTer-*pheS*-Cm-SceI-ΔBCAL0117 were selected and purified on the same conjugation selection medium. Plasmid integration into the *B. cenocepacia* strains was confirmed by PCR screen using the vector primers, pEX18TpFor and pEX18TpRev (Figure 4.23A).

Confirmed merodiploid colonies were then purified and cultured in LB medium containing chloramphenicol (50 µg ml^{-1}) and conjugated with *E. coli* S17-1(λpir) containing the plasmid pDAI-SceI-*pheS* to promote a second homologous recombination and resolve the merodiploid state. The *I-SceI* gene in pDAI-SceI-*pheS* encodes an endonuclease enzyme that cuts DNA at the I-SceI recognition site of the co-integrants. Ex-conjugants were plated on Lennox agar supplemented with tetracycline (125 µg ml^{-1}) to select the H111ΔpobA containing pDAI-SceI-*pheS* and with ampicillin (100 µg ml^{-1}) to inhibit donor growth.

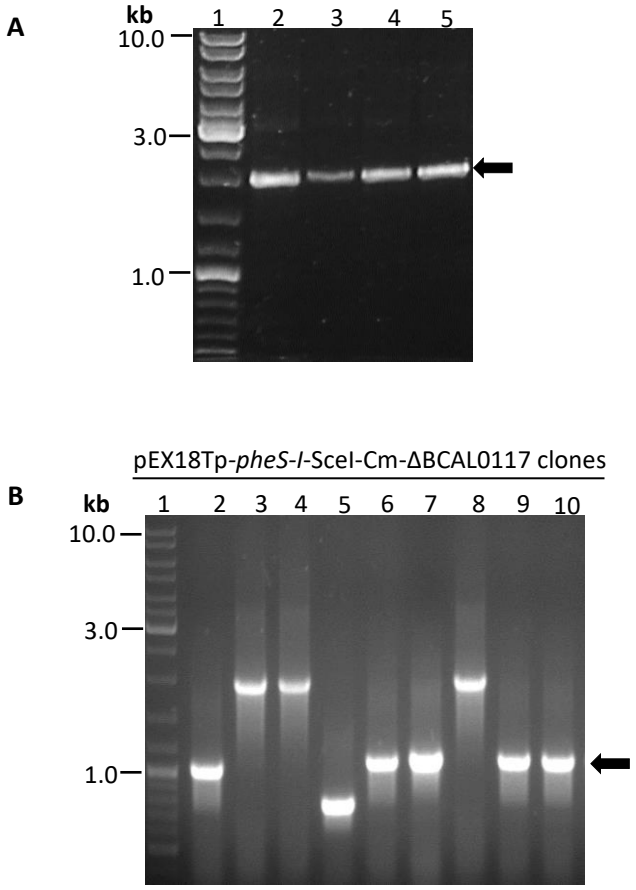

Figure 4.22: Amplification of BCAL0117/I35_RS00625 and generation of pEX18TpTer-*pheS*-Cm-SceI-ΔBCAL0117

(A) Gene amplification of BCAL0117/I35_RS00625 using Q5 HotStart High Fidelity DNA polymerase *B. cenocepacia* ΔBCAL0117 for mutant generation: Lane 1, Linear DNA ladder, lanes 2-5, amplification using primer combination BCAL0117for2 and BCAL0117rev3 at a gradient annealing temperature of 49, 51, 53 and 55 °C giving rise to a 1956 bp fragment, indicated by a black arrow. (B) PCR confirmation of introduction of an 879 bp deletion into the BCAL0117 gene cloned in pEX18TpTer-*pheS*-Cm-*SceI* using primer combination BCAL0117for2 and BCAL0117rev3 at an annealing temperature of 55 °C. Lane 1, Linear DNA ladder; lanes 2, 6, 7, 9 and 10 contain plasmids corresponding in size to pEX18TpTer-*pheS*-Cm-*SceI*-ΔBCAL0117 based on the size of the amplicon (1077 bp) and are indicated by an arrow.

Fifty colonies from the conjugation plate were patched in duplicate on the same conjugation selection medium, on LB containing chloramphenicol (50 µg ml^{-1}) and on IST containing trimethoprim (25 µg ml^{-1}), and were incubated overnight. Colonies that were sensitive to chloramphenicol and trimethoprim were selected from the tetracycline plates and PCR-screened with the primers (BCAL0117forout and BCAL0117revout) that anneal to sequences flanking the BCAL0117 gene locus.

Candidates generating a smaller fragment size (1218 bp) from the BCAL0117 gene were identified by agarose gel electrophoresis analysis. To cure mutant candidate of the pDAI-SceI-*pheS* plasmid, it was cultured in 2 ml LB broth overnight and cells were collected by centrifugation. The pellet was washed with 2 ml of 0.85 % saline twice before resuspension in 1 ml saline. The bacterial suspension (100 µl) was spread on M9-glucose agar containing 0.1 % p-chlorophenyalanine. The *pheS* gene on the pDAI-SceI-*pheS* plasmid in the mutant candidates is present in a multicopy and the candidates retaining this plasmid would be killed, thereby allowing the target mutants that have been cured of the plasmid to grow. Consequently, colonies growing on the plates were mutants that have lost the pDAI-SceI-*pheS* plasmid. The mutant candidates were streaked on three agar plates containing antibiotics, tetracycline, trimethoprim, chloramphenicol to confirm sensitivity due to the curing of both the pEX18TpTer-*pheS*-Cm-SceI-BCAL0117 and pDAI-SceI-*pheS* plasmids. *B. cenocepacia* H111ΔpobAΔBCAL0117 was reconfirmed by PCR using the BCAL0117 'outside primers' (Figure 4.23B).

4.7.3 Screening of hydroxamate siderophore utilisation by H111ΔpobAΔBCAL0117

H111ΔpobAΔBCAL0117 was overlaid on LB agar containing 40 µM EDDHA and filter discs impregnated with the hydroxamate xenosiderophores were placed on the overlay. None of the hydroxamate siderophores promoted growth of the BCAL0117 knockout mutant apart from alcaligin and cepabactin, confirming the role of BCAL0117 in utilising most hydroxamate siderophores which is consistent with the hypothesis that this protein translocates hydroxamate siderophores across the cytoplasmic membrane of *B. cenocepacia* (Figure 4.24A and B). In this regard, alcaligin and cepabactin are likely to be transported by one or more alternative inner membrane transporters. Other putative cytoplasmic membrane transporters, however, were not analysed in this study.

4.7.4 Complementation of the ΔBCAL0117 mutant

To confirm the role of in hydroxamate siderophore utilisation, a complementation experiment was performed using the BCAL0117 mutant. To do this, a complementation plasmid was constructed using the pSRKKm plasmid vector. The pSRKKm plasmid was selected in this analysis due to its low expression of cloned genes. In this case, high expression of membrane protein may lead to destabilisation of the cytoplasmic membrane which could cause cell rupture and would lower the chance of cloning the BCAL0117 wild type allele.

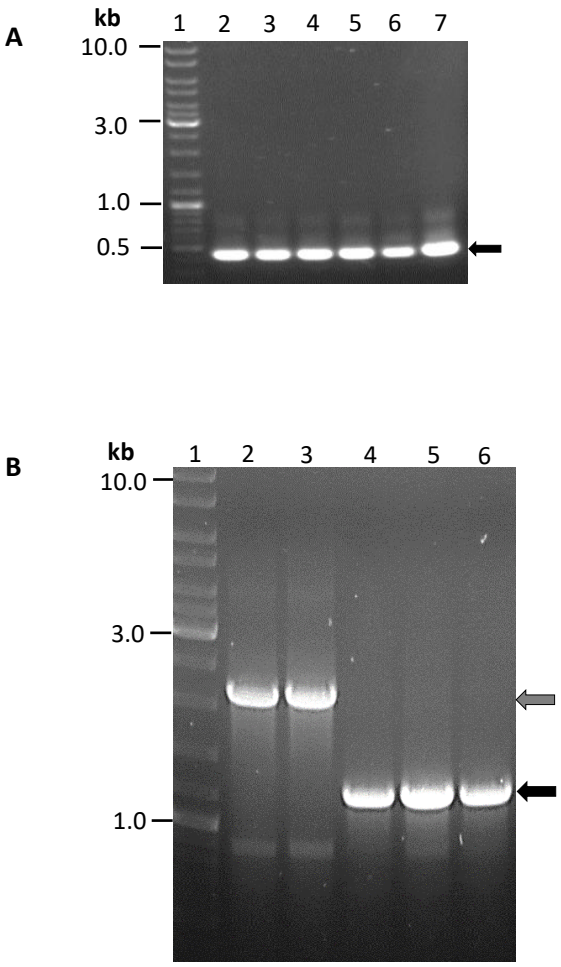

Figure 4.23: Construction of *B. cenocepacia* Δ*pobA*ΔBCAL0117
(A) PCR screening of pEX18Tp-*pheS*-Cm-*SceI*-ΔBCAL0117 integration into the H111ΔpobA genome using primer combination pEX18Tpfor and pEX18Tprev at an annealing temperature of 52°C. PCR products were analysed by agarose gel electrophoresis. Lanes 1, Linear DNA ladder; lanes 2-6, H111ΔpobA candidates containing integrated pEX18Tp-*pheS*-Cm-*SceI*-ΔBCAL0117 giving rise to a 397 bp vector DNA fragment (arrow) (B) Screening of H111ΔpobAΔBCAL0117 candidates following curing of pDAI-*SceI*-*pheS* using primers flanking the BCAL0117 gene, BCAL0117forout and BCAL0117revout at an annealing temperature of 61 °C. WT BCAL0117 gene gives rise to a 2149 bp product (grey arrow) whereas the ΔBCAL0117 mutant results in a product of ~1200 bp (black arrow). Lane 1, Linear DNA ladder; lanes 2-3, negative control-H111 wild type; lanes 3-5, H111ΔpobAΔBCAL0117 candidates.

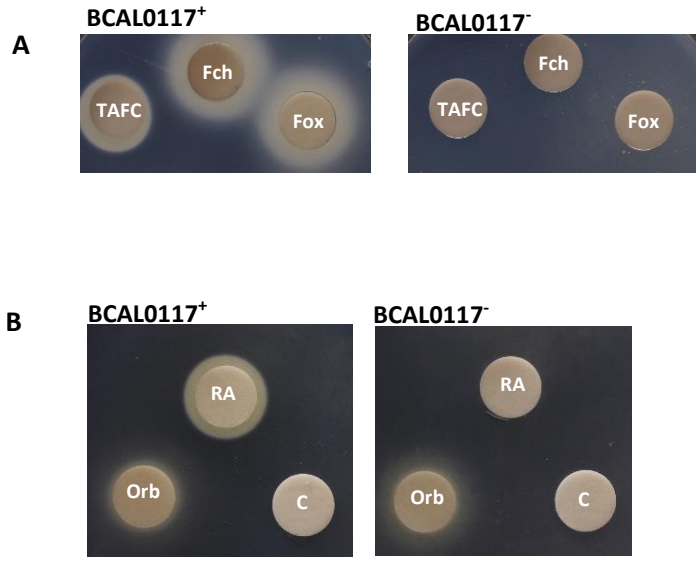

Figure 4.24: Effect of inactivation of the BCAL0117 gene on hydroxamate siderophore utilisation by *B. cenocepacia* H111

(A) Utilisation of ferrichrome, ferioxamine B and by H111ΔpobA (left hand panel). Transportation of hydroxamate siderophores is compromised in the H111ΔpobAΔBCAL0117 mutant (right hand panel). (B) Utilisation of rhodotorulic acid by H111ΔpobA mutant (left hand panel). Transportation of rhodotorulic acid is compromised in the H111ΔpobAΔBCAL0117 mutant (right hand panel). Ornibactin is used as positive control and dH_2O as a negative control. Filter disc for each bioassay plate was spotted with purified siderophore: ferrioxamine B (Fox); ferrichrome (Fch); triacetylfusarinine C (TAFC); rhodotorulic acid (RA); dH_2O as negative control ('C'), ornibactin (Orb) as positive control. Final EDDHA concentration in agar is 40 µM.

4.7.4.1 Construction of pSRKKm-BCAL0117

A DNA fragment containing the BCAL0117 gene and lacking a functional promoter sequence was amplified using combination primers BCAL0117for BCAL0117rev2. The 1348 bp DNA fragment was ligated into pSRKKm between the *Bam*HI and *Sal*I restriction sites (Figure 4.25A). Ligated products were transformed into *E. coli* JM83 cells and identification of transformants containing recombinant plasmids by blue-white screening was performed as previously described (Section 4.2.2). Positive clones of pSRKKm-BCAL0117 were confirmed by electrophoresis analysis which showed a plasmid by the size of 7065 bp (Figure 4.25B). DNA sequencing using the primers M13for and M13rev showed insertion of the BCAL0117 gene with no mutations.

4.7.4.2 Complementation of H111ΔpobAΔBCAL0117 by pSRKKm-BCAL0117

The pSRKKm-BCAL0117 plasmid and the empty vector, pSRKKm, were transformed into competent *E. coli*, S17-1(λpir) cells prior to conjugation with the H111ΔpobAΔBCAL0117 mutant. Exconjugants were spread onto Lennox agar supplemented with kanamycin (100 µg ml^{-1}) and tetracycline (10 µg ml^{-1}). H111ΔpobAΔBCAL0117 colonies containing pSRKKm-BCAL0117 were maintained on M9-glucose containing kanamycin (50 µg ml^{-1}) and were confirmed by colony PCR as previously described (Section 4.5.1).

Complementation analysis was performed with the disc diffusion bioassay using an iron-restricted LB agar containing 40 µM EDDHA and 5 mM IPTG. IPTG supplementation allows the *lac* promoter to initiate transcription of the BCAL0117 gene in the pSRKKm plasmid. The hydroxamate siderophores were individually applied to filter discs and laid on the overlay seeded with the H111ΔpobAΔBCAL0117 mutant containing the complementation plasmid, pSRKKm-BCAL0117 and the empty vector. The bioassay showed that the hydroxamate siderophores promoted growth of the mutant containing the complementation plasmid and not with the empty vector (Figure 4.26A and B). This confirmed that the defect in hydroxamate siderophore utilisation was due to the BCAL0117 cytoplasmic membrane protein.

4.7.5 Liquid growth stimulation assay of the ΔBCAL0117 mutant and its complementation

The ability of the BCAL0117 mutant to utilise hydroxamate siderophores was investigated using the liquid growth stimulation assay as previously described. Broth cultures were supplemented with ferrioxamine B and ferrichrome, as representatives of hydroxamate xenosiderophores. Growth of H111ΔpobAΔBCAL0117 in iron-limited medium was demonstrated to be significantly limited ($p<0.01$) regardless of ferrioxamine B or ferrichrome addition to the medium, consistent with the role of BCAL0117 in the utilisation of these hydroxamate xenosiderophores (Figure 4.27A and B).

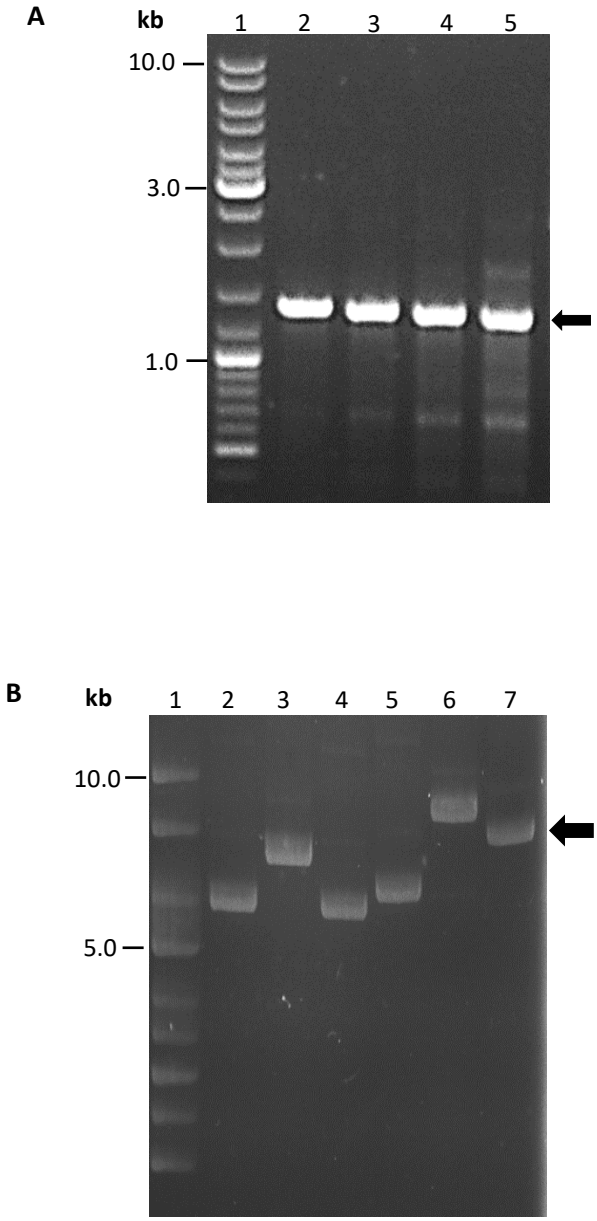

Figure 4.25: Construction of pSRKKm-BCAL0117
(A) Amplification of BCAL0117/I35_RS00625 for construction of complementation plasmid pSRKKm-BCAL0117: Lane 1, Linear DNA ladder, lanes 2-5, amplification using primer combination of BCAL0117for and BCAL0117rev2 at a gradient annealing temperature of 57, 59, 61 and 63 °C giving rise to a 1324 bp fragment indicated by an arrow. (B) PCR screening of pSRKKm-BCAL0117 plasmid candidates. Lane 1, Supercoiled DNA ladder; lane 3, JM83 containing putative pSRKKm-BCAL0117 clones with expected plasmid size of 7065 bp; lane 2 and 4-7, candidate plasmids not showing expected size of pSRKKm-BCAL0117.

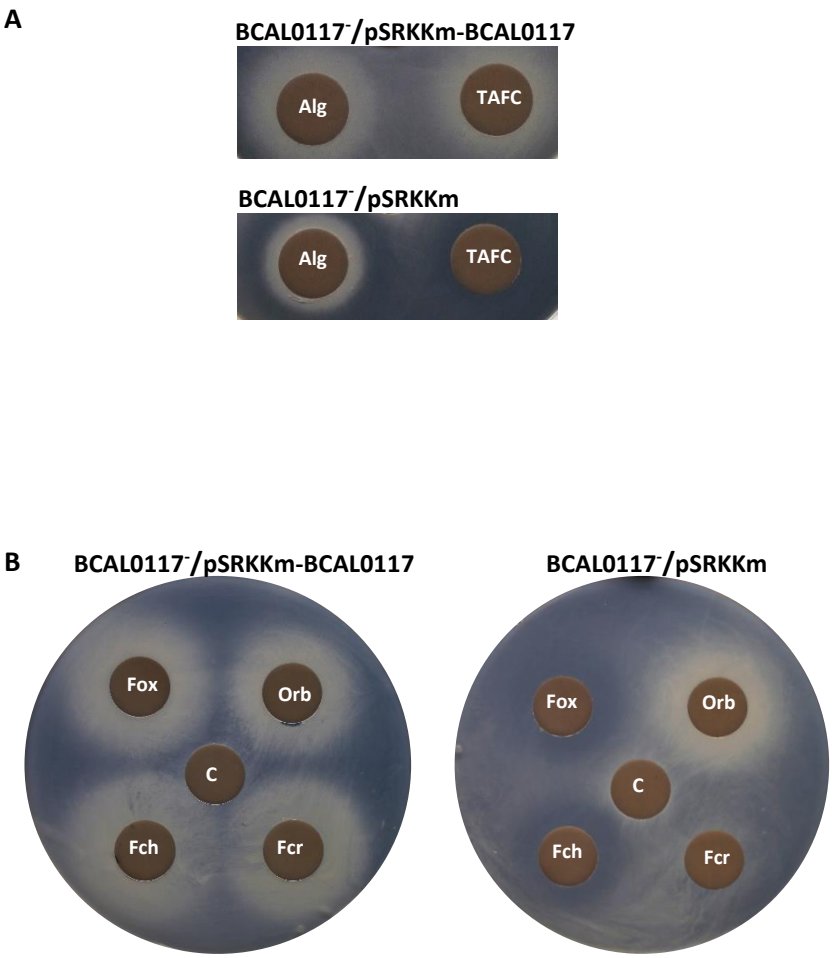

Figure 4.26: Complementation analysis of a *B. cenocepacia* BCAL0117 mutant for hydroxamate siderophore utilisation

(A) The function of BCAL0117/I35_RS00625 for TAFC utilisation is restored with the complementation plasmid pSRKKm-BCAL0117 in the H111ΔpobAΔBCAL0117 mutant. Utilisation of alcaligin occurs with the empty vector, pSRKKm, in H111ΔpobAΔBCAL0117. (B) Functional complementation of BCAL0117/I35_RS00625 for the utilisation of ferrichrome, ferrioxamine B and ferricrocin with the complementation plasmid pSRKKm-BCAL0117 in the H111ΔpobAΔBCAL0117 mutant. There is no promotion of growth with the the empty vector, pSRKKm, in H111ΔpobAΔBCAL0117. Filter disc for each bioassay plate was spotted with purified siderophore: ferrioxamine B (Fox); ferrichrome (Fch); Fe-ferricrocin (Fcr); alcaligin (Alg); triacetylfusarinine C (TAFC); dH_2O as negative control ('C'; ornibactin (Orb) as positive control. Final EDDHA concentration in agar is 40 µM.

Complementation of the BCAL0117 mutant phenotype in the presence of ferrioxamine B was conducted using the same approach. H111ΔpobAΔBCAL0117 containing the complementation plasmid pSRKKm-BCAL0117 and with the empty vector, pSRKKm, were grown in iron-deficient medium. As observed with the disc diffusion assay, the presence of wild type copies of BCAL0117 promoted growth of the BCAL0117 mutant in medium containing ferrioxamine B. The growth rate was comparable to but less than that of H111ΔpobA with a significance value of $p<0.05$ in contrast to the growth rate of H111ΔpobA which gave a significance value of $p<0.01$ when compared to growth in medium lacking ferrioxamine B. The lower growth rate of the mutant containing pSRKKm-BCAL0117 compared to H111ΔpobA is likely due to the sub-optimum expression of BCAL0117 by the *lac* promoter on pSRKKm (Figure 4.27B). These data demonstrate the restoration of the wildtype phenotype to the BCAL0117 mutant thereby confirming the role of BCAL0117 in hydroxamate siderophore utilisation. Analysis of the role of BCAL0117 and its complementation is summarised in Table 4.3.

4.8 Albomycin sensitivity assay of *B. cenocepacia* H111

Albomycin is a naturally occurring sideromycin whereby an antibiotic is attached to a siderophore moiety resembling ferrichrome and is observed to be transported through the ferric hydroxamate transport system in some bacteria. This naturally-conjugated antibiotic targets and inhibits seryl-tRNA synthetases and is reported to be effective in killing a broad spectrum of Gram-positive and Gram-negative pathogens due to the widespread existence of ferrichrome receptors (Pramanik et al., 2007).

Once transported into the cytoplasm of bacterial cells, albomycin undergoes hydrolysis by bacterial peptidases thereby activating the seryl-tRNA synthetase inhibitor (Hartmann et al., 1979; Braun et al., 1983; Stefanska et al., 2000). Albomycin transport by the ferrichrome transport system has been studied in most detail in *E. coli* K-12. Albomycin is highly effective against *S. pneumoniae* and has been used as an antibiotic in human in the Soviet Union in the past (Pramanik and Braun, 2006). The effect of albomycin on *B. cepacia* has been examined and the bacterium was shown to be resistant to albomycin (Pramanik et al., 2007). The effect of albomycin on *B. cenocepacia* was investigated in this study to verify whether it gives a similar effect as with *B. cepacia*. As *B. cenocepacia* has a highly functional ferrichrome transport system and mutants in this system are now available, albomycin was tested to determine whether it can be conveyed through this system and impair *B. cenocepacia* H111 growth.

4.8.1 Screening of *B. cenocepacia* H111 for albomycin sensitivity

Filter discs impregnated with albomycin were placed on an overlay seeded with H111ΔpobA and the H111 wild type strain, on M9-glucose agar supplemented with CAA. This iron-limited medium was employed to initiate the expression of the transporters responsible for ferrichrome uptake. *E. coli* JM83 was used a positive control as *E. coli* is known to be sensitive to albomycin.

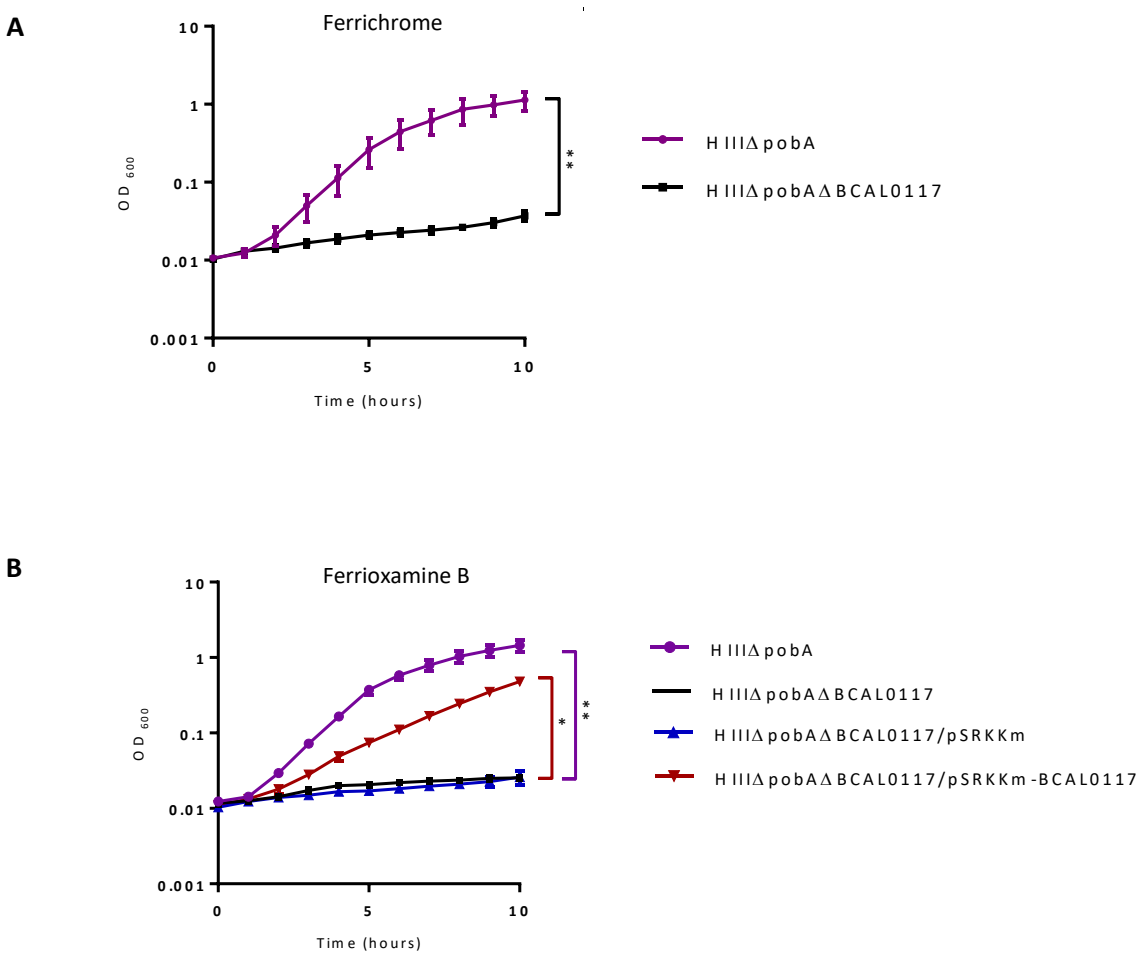

Figure 4.27: Growth of *B. cenocepacia* H111ΔpobAΔBCAL0117 in iron-depleted medium supplemented with ferrichrome and ferrioxamine B

(A) Growth of the BCAL0117 mutant in M9-glucose CAA supplemented with ferrichrome and (B) ferrioxamine B compared to that of the parent strain harbouring the WT BCAL0117 gene. Growth of the BCAL0117 mutant containing the complementation plasmid pSRKKm-BCAL0117 or the empty vector in medium supplemented with ferrioxamine B and 5 mM IPTG was also analysed. These data are representative of a minimum of three independent experiments (n=3). Error bars represent the ±SEM *$p<0.05$, **$p<0.01$.

Table 4.3 Analysis of the role of BCAL0117 in hydroxamate siderophore utilisation[a] (disc diffusion assay)

Strains	Ferrichromes	Ferrioxamine B	RA	TAFC	Alcaligin	Cepabactin	Ornibactin
H111ΔpobA	+	+	+	+	+	+	+
H111ΔpobAΔBCAL0117	-	-	-	-	+	+	+
H111ΔpobAΔBCAL0117/pSRKKm	-	-	-	-	+	+	+
H111ΔpobAΔBCAL0117/pSRKKm-BCAL0117	+	+	+	+	+	+	+

[a]Based on results of disc diffusion assay

As shown in Figure 4.28A-C, growth inhibition of *E. coli* cells was exerted by the albomycin but H111 cells were observed to be relatively resistant to the siderophore-antibiotic conjugate.

4.9 Discussion

This chapter described experiments that were designed to investigate on the ability of *B. cenocepacia* to utilise hydroxamate siderophores as a source of iron for survival in iron starvation conditions. The study includes investigation of the putative transporters and energy transducers involved in hydroxamate siderophore utilisation which focused on the initial and crucial receptor located in the outer membrane, the TBDR.

4.9.1 Utilisation of hydroxamates as *B. cenocepacia* xenosiderophores

This study demonstrated the ability of *B. cenocepacia* to exploit hydroxamate siderophores. So far, most hydroxamates which were demonstrated to sequester iron for *B. cenocepacia* (ferrichromes, fusarinines, rhodotorulic acid) are from the common structural families of fungal hydroxamate siderophores (Winkelmann, 2002). An exception was coprogen which was not observed to partake in iron sequestration by *B. cenocepacia*. These siderophores can be produced by more than one fungal species (Table 4.4) and several are known to be pathogenic to humans, predominantly in immunocompromised individuals. The ability of *B. cenocepacia* to utilise these siderophores may be due to the different niches that *B. cenocepacia* can adapt to in the environment, as it can exist in soil as a saprotroph and may co-exist with these fungi. *B. cenocepacia* may take up iron via the siderophores secreted by these fungi as one of its strategies to survive in soil.

Ferrichromes were the first siderophores to be isolated from *Ustilago sphaerogena* (smut/rust fungus) and were initially observed to act as a growth factor for other microorganisms (Emery, 1971). Both *Ustilago* species mentioned in Table 4.4, produce mostly ferrichrome and ferrichrome A, are involved in causing plant diseases, especially in maize (Heymann et al., 2000). Similarly, *Neurospora crassa* (red bread mould) and *Aspergillus quadricinctus* are not hazardous to humans. On the other hand, the ferrichrome producer, *Penicilium chrysogenum*, also called *Penicilium notatum,* is a rare opportunistic pathogenic of humans. This pathogen is reported to cause systemic mycosis and pulmonary infections (Geltner et al., 2013; Shokouhi et al., 2016).

Ferricrocin is typically secreted by the ubiquitous saprophytic fungus *Aspergillus*, notably *Aspergillus fumigatus*, *Aspergillus nidulans* and *Aspergillus viridinutans*. Ferricrocin is commonly produced as an intracellular siderophore which accumulates and stores iron in the hyphae and conidia of *A. fumigatus* and *A. nidulans* (Wallner et al., 2009), although a trace amount of the siderophore has been detected extracellularly.

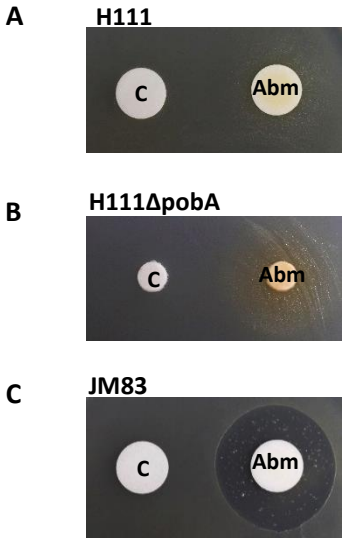

Figure 4.28: Albomycin sensitivity assay
Filter discs loaded with albomycin (5mM, 10 µl) or its solvent, dH_2O, were placed on M9-glucose CAA agar plates seeded with (A) *B. cenocepacia* H111 (B) *B. cenocepacia* H111ΔpobA or (B) *E. coli* JM83.

Table 4.4 Producers of hydroxamate xenosiderophores utilised by *B. cenocepacia* H111

Siderophores	Species	References
Fungal origin		
Ferrichromes		
Ferrichrome	*Aspergillus quadricinctus* *Penicilium chrsyogenum* *Neurospora crassa* *Ustilago maydis* *Ustilago sphaerogena*	(Siegmund et al., 1991)
Ferricrocin	*Aspergillus fumigatus* *Aspergilus nidulans* *Aspergillus viridinutans* *Fusarium culmorum* *Fusarium graminearum* *Fusarium oxysporum* *Neurospora crassa*	(Oide et al., 2015)
Fusarinines		
Triacetylfusarinine C	*Aspergillus nidulans* *Aspergillus fumigatus* *Fusarium graminearum* *Penicilium chrsyogenum*	(Schrettl et al., 2007)
Rhodotorulic acid		
Rhodotorulic acid	*Rhodotorula glutinis* *Rhodotorula mucilaginosa* *Rhodotorula pilimanae*	(Andersen et al., 2003)
Bacterial origin		
Ferrioxamines		
Ferrioxamine B	*Streptomyces coelicolor* *Streptomyces pilosus* *Streptomyces viridosporus*	(Imbert et al., 1995) (Patel et al., 2010)
Alcaligin		
Alcaligin	*Achromobacter denitrificans* *Achromobacter xylosoxidans* *Bordetella bronchiseptica* *Bordetella pertussis* *Bordetella parapertussis*	(Nishio and Ishida, 1990) (Moore et al., 1995) (Coenye et al., 2003)
Cepabactin		
Cepabactin	*Burkholderia cepacia*	(Meyer et al., 1989)

Likewise, ferricrocin can also be found in hyphal and conidial iron stores in *N. crassa* (Matzanke et al., 1988). *A. viridinutans* is phylogenetically distinct from *A. fumigatus* but secretes ferricrocin as a metabolic product (Fiedler, 1981).

Aspergillus species are commonly pathogenic to plants, animals and are known to be the most common air-borne fungal pathogen of humans, causing aspergillosis, an invasive systemic and pulmonary infection (Tekaia and Latgé, 2005). This infection most commonly occurs in immunocompromised individuals including patients suffering from chronic granulomatous disease and cystic fibrosis (CF) (Henriet et al., 2012). Ferricrocin is therefore reported to be involved in the virulence of these species among other siderophores produced by the pathogen (Wallner et al., 2009).

Other ferricrocin producers are members of the *Fusarium* genus. *F. graminearium* and *F. culmorum* are plant pathogens causing blight diseases in cereal grains and grasses. *F. solani F. oxysporum* and *F. fujikuroi* are mostly associated with infection in immunocompromised humans, animals and plants. *F. oxysporum* is documented the second most prevalent cause of infection (~20 %) by members of this genus after *F. solani* (~50 %). Among diseases reported by this species are keratitis, onychomycosis, sinusitis, pneumonia and infections of lung transplants (Nucci and Anaissie, 2007; Carneiro et al., 2011). Moreover, *Fusarium spp.* are the second most common cause of fungal infection after *Aspergillus* (Al-Hatmi et al., 2018). Both *Aspergillus* (*A. fumigatus* and *A. nidulans*) and *Fusarium* species produce ferricrocin as an intracellular siderophore and secrete triacetylfusarinine C as an extracellular siderophore (Schrettl et al., 2007; Oide et al., 2015). Due to this, ferricrocin and triacetylfusarinine C have recently been characterised as biomarkers of aspergillosis infection in patients (Luptáková et al., 2017).

N,N',N''-triacetylfusarinine C (TAFC), also named triacetylfusigen, is a typical hydroxamate fungal siderophore and is considered to be one of the most stable (Hossain et al., 1980). Due to this, it has the ability to extract iron from other siderophores in its environment (Adjimani and Emery, 1987). TAFC is secreted by many pathogenic fungal species including several *Aspergillus* species, *Fusarium* species and the *Penicillium* genus (Heymann et al., 1999). *P. chrysogenum* secretes TAFC as well as ferrichrome.

Rhodotorulic acid is mainly produced by *Rhodotorula* species and related yeasts of the phylum *Basidiomycete*s (Atkin et al., 1970). This soil inhabitant species is an emerging opportunistic pathogen of immunocompromised patients. Among related diseases caused by these pathogens are systemic fungaemia and pulmonary infections. Pathogenicity of *Rhodotorula* species is recently reported to be clinically relevant due to having a multiresistant profile (Falces-Romero et al., 2018).

Ferrioxamine B is produced by the filamentous bacteria of the genus *Streptomyces,* which belongs to the phylum *Actinobacteria*. Streptomyces species are commonly utilised to produce antibiotics, antifungals

and antiparasitic compounds for treating microbial infections. Despite this, the species are also involved in lung and bloodstream infections, causing pneumonia and pulmonary diseases, although rarely. *Streptomyces* spp. produces many types of ferrioxamines which exist in linear (A, B, C, D1 and G) and cyclic (D2 and E) forms. Ferrioxamine B is the most thoroughly studied member of the ferrioxamine family. Invasive human disease due to *Streptomyces* species is most often due to *S. griseus* and *S. somaliensis* (McNeil and Brown, 1994), with the former producing ferrioxamine E. Likewise, the ferrioxamine B producers, *S. coelicolor* and *S. viridosporus* listed in (Table 4.4), are also involved in producing ferrioxamine E (Imbert et al., 1995; Patel et al., 2010). These species are commonly found in soil and rotting vegetation and have a role in decomposition, which is similar to the ecosystem of fungi. *B. cenocepacia* may have the ability to utilise ferrioxamine E, due to its similarity in structure to ferrioxamine B. However, ferrioxamine B possess a linear structure whereas ferrioxamine E is a cyclic hydroxamate with an extra acetyl group (Figure 4.29). Investigations into the utilisation of ferrioxamine E, however, were not conducted in this study. Clinical infections from sole ferrioxamine B producers (such as *S. pilosus*) are rarely reported, though reports of *Streptomyces* infections are not always species specific (Dunne et al., 1998). Besides, ferrioxamine B, commonly referred as desferal, has been used in medical applications for treating iron toxicity and iron overload diseases such as thalassaemia (Hajigholami et al., 2018).

The macrocyclic siderophore alcaligin is produced by the bacterial species *Bordetella* and *Achromobacter*. This siderophore acts to remove iron from lactoferrin and transferrin during infection (Moore et al., 1995). Members of the genus *Bordetella* are in the family *Alcaligenaceae* and are taxonomically related to *Achromobacter* and *Alcaligenes* species. Hence it may not be surprising for the two genera to produce identical siderophores (Musser et al., 1987). The *Bordetella* species includes *B. bronchiseptica*, *B. pertussis* and *B. parapertussis*, among others. *B. bronchiseptica* and *B. pertussis* are well known to produce the siderophore alcaligin while the other, *B. parapertussis,* is reported to possess the alcaligin siderophore gene cluster (Kang et al., 1996; Parkhill et al., 2003). *Achromobacter* species reported to produce alcaligin are *A. xylosoxidans* and *A. denitrificans*. Both species are previously named as *Alcaligenes xylosoxidans* and *Alcaligenes denitrificans* (or *Achromobacter xylosoxidans* subsp. *xylosoxidans* and *Achromobacter xylosoxidans* subsp. *Denitrificans,* respectively) (Coenye et al., 2003).

Most *Bordetella* species are obligate respiratory pathogens and survive in human respiratory tracts. *B. bronchiseptica* exists as commensal floras in humans and is able to cause opportunistic infections when its host is in an immunocompromised state (Matto and Cherry, 2005). *B. bronchiseptica* is commonly associated with infections causing kennel coughs in canines, felines, swine and laboratory animals (Hou et al., 1996). Cases of chronic respiratory infections in humans have also been progressively documented (Clements et al., 2018). While *B. pertussis* is a strict human pathogen, *B. parapertussis* may cause disease in human and animals, particularly sheep and swine.

Both pathogens can cause an acute respiratory disease termed whooping cough (or 'pertussis'), sometimes associated with pneumonia. These pathogens can survive intracellularly in respiratory epithelium (Lamberti et al., 2013), and may co-exist with other respiratory bacterial pathogens (Wagner et al., 2018; Luis et al., 2018).

Both *Achromobacter denitrificans* and *A. xylosoxidans* have been reported as emerging pathogens in immunocompromised patients and are frequently isolated from cystic fibrosis and pneumonia patients (Awadh et al., 2017; Kumar et al., 2006). Traditionally an aquatic microorganism and non-infectious to humans, these opportunistic pathogens, particularly *A. xylosoxidans,* have been considered as multi-resistant strains and co-exist in infections with *P. aeruginosa, Klebsiella pneumoniae* and the Bcc members (Rajan and Saiman, 2002).

Cepabactin, is a cyclic hydroxamate siderophore reported in the supernatants of *B. cepacia* (Section 1.6) (Meyer et al., 1989). Since *B. cepacia* is a Bcc member, it is perhaps not surprising that another Bcc member, *B. cenocepacia* in this context, is able to adapt to utilise this siderophore. *B. cepacia* is a common pathogen which causes pneumonia in patients with lung disorders and is often reported to co-exist with other bacterial species in polymicrobial infections of the lung, although it is less prevalent than *B.* cenocepacia (Chaparro et al., 2001). The role of cepabactin in the virulence of *B. cepacia*, however, has not been elucidated (Butt and Thomas, 2017).

The hydroxamate siderophores tested in this study represent three classes in terms of their denticity: the trihydroxamates, dihydroxamates and a monohydroxamate. The trihydroxamates include the ferrichromes, coprogen, TAFC and ferrioxamine B. While ferrioxamine B is a linear trihydroxamate, others contain a heterocyclic ring. Ferrichromes and coprogen are considered as a semi-cyclic by structure because the hydroxamate groups are connected to the rings by the alkyl side chains and TAFC is classified as macrocyclic. The ferrichromes, ferricrocin and ferrichrome differ only by the addition of a hydroxymethyl group in ferricrocin (Figure 4.1). The ability of *B. cenocepacia* to utilise both types is explicable.

Trihydroxamate siderophores exhibit three asymmetrical bidentate ligands which form a hexadentate coordination with Fe(III) for iron chelation. This is the strongest coordination for a siderophore as it requires only one molecule of siderophore to complete the octet level of Fe(III). This coordination level usually acts as a high affinity chelator, able to sequester iron at lower concentrations. Their asymmetrical nature allows them to exist in many geometrical and optical isomers with very little energy differences resulting in no preference for a specific isomer (Dhungana et al., 2001).

Coprogen is unusual in not being identified as a xenosiderophore utilised by *B. cenocepacia*. It has a similar basic structure to that of rhodotorulic acid but with a larger molecular weight (Figure 4.1). The larger size of the coprogen molecule could be a reason why it cannot be utilised by *B. cenocepacia*.

Rhodotorulic acid and alcaligin are dihydroxamates, rhodotorulic acid is semi-cyclic while alcaligin is macrocyclic. Due to the tetradentate nature of these hydroxamates, the affinity of iron for these siderophores has been observed to be slightly lower than with the trihydroxamates as there are only two hydroxamate groups available to form a complex with iron (Hou et al., 1996). Therefore, to achieve an octahedral complex, the iron atom can be coordinated by two molecules of the tetradentate siderophores (Barclay et al., 1984). Nevertheless, alcaligin has been observed to demonstrate a higher affinity in this study as compared to rhodotorulic acid even though both are tetradentate siderophores.

Cepabactin is a heterocyclic monohydroxamate and three molecules are required to form the ferric-cepabactin complex (Figure 4.30). This study therefore demonstrates the capability of *B. cenocepacia* to utilise all three types of hydroxamate structure, tri-, di- and mono-hydroxamates as iron carriers. Two TBDRs encoded in the large chromosome of *B. cenocepacia* were shown to have a role in transporting the hydroxamate siderophores. One TBDR (BCAL0116) recognises alcaligin, ferrichrome, ferricrocin, ferrioxamine B, TAFC and rhodotorulic acid which are the tri- and dihydroxamates while the other (BCAL2281) only recognises the ferrichromes, which are also trihydroxamates.

Taken together, a mixed microbial community is common in infections of CF patients where extensive microbial interaction occurs among pathogenic bacteria and fungi in the respiratory tract of such patients (Moree et al., 2012). Considering xenosiderophores used by *B. cenocepacia*, this bacterium may benefit from a polymicrobial infection involving co-colonisers that potentially include: *P. chrysogenum, A. fumigatus*, *A. nidulans, A. viridinutans, F. oxysporum, R. glutinis, R. mucilaginosa, R. pilimanae, S. coelicolor, S. viridosporus, B. bronchiseptica*, *B. pertussis, B. parapertussis*, *A. denitrificans, A. xylosoxidans, B. cepacia* and including *P. aeruginosa,* the major pathogen in respiratory tract infections of chronic lung disorder patients. These pathogens may compete with each other for iron and this study showed *B. cenocepacia* is able to sequester iron by appropriating the siderophores secreted by these pathogens.

Relating to this observation, there would be a possibility of treating the highly resistant *B. cenocepacia* and other pathogens concurrently present in a polymicrobial chronic respiratory infection in CF patients via the targeted drug delivery of the `Trojan horse' approach (Schalk, 2018). The possibility of co-treatment arises when the hydroxamate siderophore conjugated to an antibiotic is transported through the similar TBDR orthologues in other pathogens. Likewise, there is a likely option of treating infections caused by a broad range of hydroxamate producer pathogens.

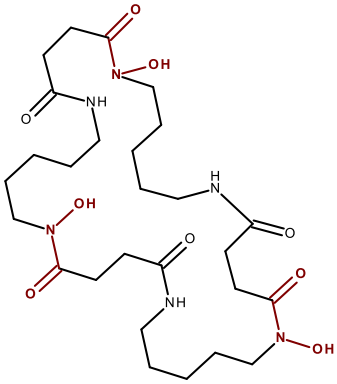

Figure 4.29: Molecular structure of ferrioxamine E
Molecular structure of the cyclic hydroxamate ferrioxamine E. Hydroxamate ligands are depicted in red. Chemical structure is drawn using Accelrys Draw 4.2.

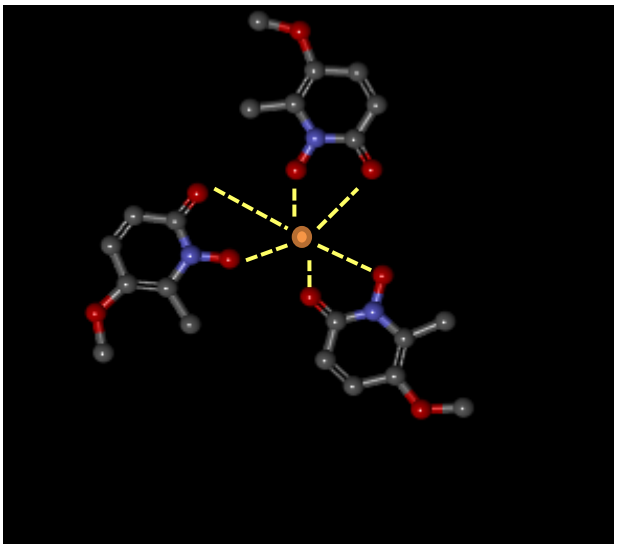

Figure 4.30: Ball and stick model of iron-hydroxamate xenosiderophore complex utilised by *B. cenocepacia* H111
Three molecules of cepabactin are required form an octahedral complex with one ferric iron atom. Chemical structures were drawn using ChemDraw 4.2. Colour code: C gray, O red, N blue and Fe orange.

4.9.2 TBDRs for hydroxamate xenosiderophore utilisation

Experimental investigations in this study strongly suggest the BCAL0116/I35_RS00620 protein to be a hydroxamate transporter in *B. cenocepacia.* BCAL0116 was demonstrated to be the sole outer membrane transporter for the hydroxamate siderophore ferrioxamine B, triacetylfusarinine C, rhodotorulic acid and alcaligin but not for the ferrichromes or cepabactin. The growth promotion by the ferrioxamine B-iron complex in *B. cenocepacia* via BCAL0116 was more efficient than that of the other hydroxamate-iron complexes investigated. According to BLASTP, homology of the BCAL0116-encoded receptor closely resembles the TBDR encoded by the gene locus PA2466, the primary receptor for ferrioxamine B uptake and a secondary ferrichrome receptor in the outer membrane of *Pseudomonas* species referred to as FoxA (Elomari et al., 1996; Llamas et al., 2006; Hannauer et al., 2010a). In this study, we showed that BCAL0116 was also able to function in ferrichrome utilisation, but it was not the only TBDR for ferrichrome.

The BCAL0116 TBDR, is also phylogenetically related to the BCAL2281-encoded receptor (Section 3.3). It was demonstrated that the gene locus BCAL2281 encodes the other ferrichrome TBDR, additional to BCAL0116. Therefore, two receptors are involved in transporting ferrichromes. The similar amino acid sequence of both *B. cenocepacia* hydroxamate TBDRs are illustrated in Figure 4.31.

FoxA of *P. aeruginosa* (PA2466) has similarly been reported to act as an additional secondary receptor for ferrichrome along with FiuA (PA0470) (Llamas et al., 2006; Hannauer et al., 2010a). Co-operating TBDRs (PfeA and PirA) for enterobactin utilisation have been demonstrated by Ghysels and colleagues, where only a double *pfeA pirA* mutant is unable to take up chelated enterobactin (Ghysels et al., 2005). There is therefore a precedent for a siderophore to be recognised by more than one TBDR.

Both TBDRs (BCAL0116 and BCAL2281) were demonstrated to transport hydroxamate siderophores, however, they did not display as transporters for cepabactin. The transport of cepabactin, therefore, is hypothesised to involve another unidentified hydroxamate TBDR or more than two TBDRs are responsible for the transport of the rare siderophore. The likely TBDR was the putative TBDR BCAM0706 (I35_RS19580) as this TBDR was predicted to be a hydroxamate siderophore by the InterPro analysis. However, this was not further investigated. Taken together, the hydroxamate TBDRs could be employed in transporting a hydroxamate-antibiotic conjugate across the *B. cenocepacia* outer membrane.

4.9.3 Role of the TonB1 complex in hydroxamate xenosiderophore transport

Inactivation of ExbB in the TonB1 system prevented growth of *B. cenocepacia* 715j supplemented with hydroxamate xenosiderophores in iron-limited conditions. This demonstrated a functional TonB1 system is required to facilitate the transport of such siderophores in addition to both endogenous siderophores, ornibactin and pyochelin.

```
I35_RS00620    1 LPALNITAAHDS-PQ---------HLTDTISTGALGTRRQLDTPFSTTIVTSEELEARQP
I35_RS11045    1 LPSINVTGAAEPLPGDLAPTYAGGQVARGADFGVLGRQKASDVPFSMTTYTSKLIEDQQA

I35_RS00620   51 YKLGDVFANDASVSDNSGAYSAWASYMTVRGMQLDWQNGYKIDGLPFVTYGITMPYEQLD
I35_RS11045   61 RTLADVLDNDPAVRSASG-YGNFSQVFVIRGFALAGD-DVSLNGLYGVTPRQLVQTDAVE

I35_RS00620  111 RVELLKGLGGFLYGFVTP----GGVVNYVTKQPGAEPVRSVDIGYRSTNVWTEHVDLGQR
I35_RS11045  119 RVDVFKGANAFLNGASPNGSAVGGGVNLQLKRAGDKPLTRVTVDGATSGSLGTHVDLGRR

I35_RS00620  167 FGPDHMFGARLNATHEEGKTYNDGNIRRDSVSLALQANLTRDLSVSFGALYQDRRTTGQT
I35_RS11045  179 FGSEGQFGVRVNQSISGGDTAVDDERRRSNVTAVSLDWRGDTLRLSGDFLYQRQRIDNGR

I35_RS00620  227 PSIFTGSYPGGALPATISGGSTNLGGKDQYLNTNLQLYTAGLQYQLAPDWQLDVAYSYSK
I35_RS11045  239 PIVLVSGSPLPAVPSATH----NYAQPWSESELEDTVGIVRAEYDFLPAWTAYVSAGA--

I35_RS00620  287 ATRRRNESTLYLQDA-AG-NYTDSRYVGMEDHRFSQWRAMVEGKVRTGQFSHQIVLGASW
I35_RS11045  293 --RHTNEHGDYYTPTYSSSGTTGSRLSVPHKEDAQSAEAGVRGRFTTGPVSHFVTAGASF

I35_RS00620  345 QKQAND--YSANSVFVPLGAGNLYAPNPYRYESPHGFIQY--RTSEIV----QKSLFASD
I35_RS11045  351 IRIDSQSAYTMSNAF----PTTLYDPAPVASP-PTAYAGGDMNDPGTVTKTWLRSIAVSD

I35_RS00620  397 TVQL-TERWSVLAGVRYMNYAQRAFQASGAEDPGYRQNGVVTPTFAVMFKLAPTTTAYAS
I35_RS11045  406 TLGFLDDRVLFTLGARRQSISVDNFDYTGAVTSTY-SNAITTPVFGLVVKPWRNVSIFAN

I35_RS00620  456 YAESLEPGSRVNDVYANAGQVLKPLRSKQYELGIKSFRARWSATAALFRIERSAEYANAA
I35_RS11045  465 RSEALAQGEIAPNTARNAGQALSPYRSKQYEAGVRYDTDKYGASLALFQIEKPMAYTDPA

I35_RS00620  516 -NVYVQDGESIIQGIEVGARAKFGAHWNAGV---DAMLLDAW--YANGIGNHGNRVAGAP
I35_RS11045  525 TNLFGADGTQRHRGIET---AVYGEPWKGVRLIAGATYLDATLQNTAGGTNDGHRPIGVP

I35_RS00620  570 RFVLAGDLGYAVPGVPGLTLGVDAKFTGATPLRAAGGLDAPGFLVVNAGARYLTRVGRHD
I35_RS11045  582 SFILNAGAEYDVPMLRGLTLTARWIHTGPQYLDVANTMSIQAWDRFDLGARYATDVFGKK

I35_RS00620  630 VTLRASIDNVLNRRYWEYQYADYVKPGDPRTVSLSAKIDF
I35_RS11045  642 TTFRATVRNVANKSYWSSTIGGYLTQGDPRSVWLSMTTDF
```

Figure 4.31: Amino acid sequence alignment of BCAL0116/I35_RS00620 and BCAL2281/I35_RS11045 from *B. cenocepacia* H111

Amino acid sequences of the mature form of the hydroxamate siderophore TBDRs were aligned by Clustal Omega and conserved amino acids were highlighted by BOXSHADE. Amino acids shown in white font with black shading indicates identical residue at the corresponding position in both sequences and white font with grey shading indicates similar residues at the corresponding position in both sequences. The amino acid sequences of both TBDRs showed 30 % identity. The H111 gene locus designations are indicated on the left. The TonB boxes are highlighted in faint blue, the plug domains are highlighted in faint lilac and beta-barrel domains are in green. Domains are emphasised according to Inter Pro analysis.

This may also indicate that the predicted alternative TonB2 and TonB3 systems may not be involved in siderophore transport as in *Vibrio* species (Kustusch et al., 2012). However, as some bacterial pathogens such as *Photobacterium* species use more than one TonB system for siderophore transport (Naka et al., 2005), there is a possibility that *Burkholderia* species can utilise an alternative TonB system for iron transport with other unidentified xenosiderophores. For the moment, the function of the alternative TonB systems remains to be elucidated.

4.9.4 Identification of a putative inner membrane transporter for hydroxamate siderophores in *B. cenocepacia*

The prediction that the BCAL0117/I35_RS00625 gene locus encodes a protein involved in hydroxamate siderophore uptake is supported in this study. A siderophore-deficient mutant with an inactivated BCAL0117 gene locus did not permit growth in iron starvation medium in the presence of most of the hydroxamate siderophores tested (ferrichrome, ferrioxamine B, rhodotorulic acid and TAFC) by disc diffusion assay. Complementation of the mutants with pSRKKm-BCAL0117 confirmed that the protein functions in hydroxamate siderophore utilisation. The two hydroxamate siderophores, alcaligin and cepabactin, however, do not show any dependence on the function of BCAL0117 in terms of utilisation via the disc diffusion assay. Nevertheless, by projecting the ability to allow utilisation and transport of different types of the hydroxamate siderophores, the BCAL0117 can be deduced as possessing a promiscuous nature in siderophore piracy, specifically for the hydroxamate siderophores.

The BCAL0117 encoded protein (411 amino acids) is predicted to be localised in the inner membrane (Burkholderia.com) and its similarity to FoxB of *P. aeruginosa* made it a prime candidate for testing as a cytoplasmic membrane transporter of hydroxamate siderophores. FoxB and its orthologues are mostly observed to be encoded next to a TBDR gene (Benson et al., 2005; Cuív et al., 2006) and the BCAL0117/I35_RS00625 gene locus is divergently located next to the previously reported hydroxamate siderophore receptor gene (BCAL0116/I35_RS00620).

Having similar features to that of FoxB (PA2465) in *P. aeruginosa* PAO1, the BCAL0117 protein is predicted to possess four transmembrane segments with high probability as determined by TMHMM analysis. The number of transmembrane segments is the same as that of *P. aeruginosa* FoxB using the equivalent analysis (Figure 4.32). However, Cuiv and colleagues have previously predicted eight transmembrane segments in FoxB (Cuív et al., 2007). The database of protein analysis (Pfam) predicted the BCAL0117 protein to have two conserved PepSY-associated transmembrane helices (PepSY_TM).

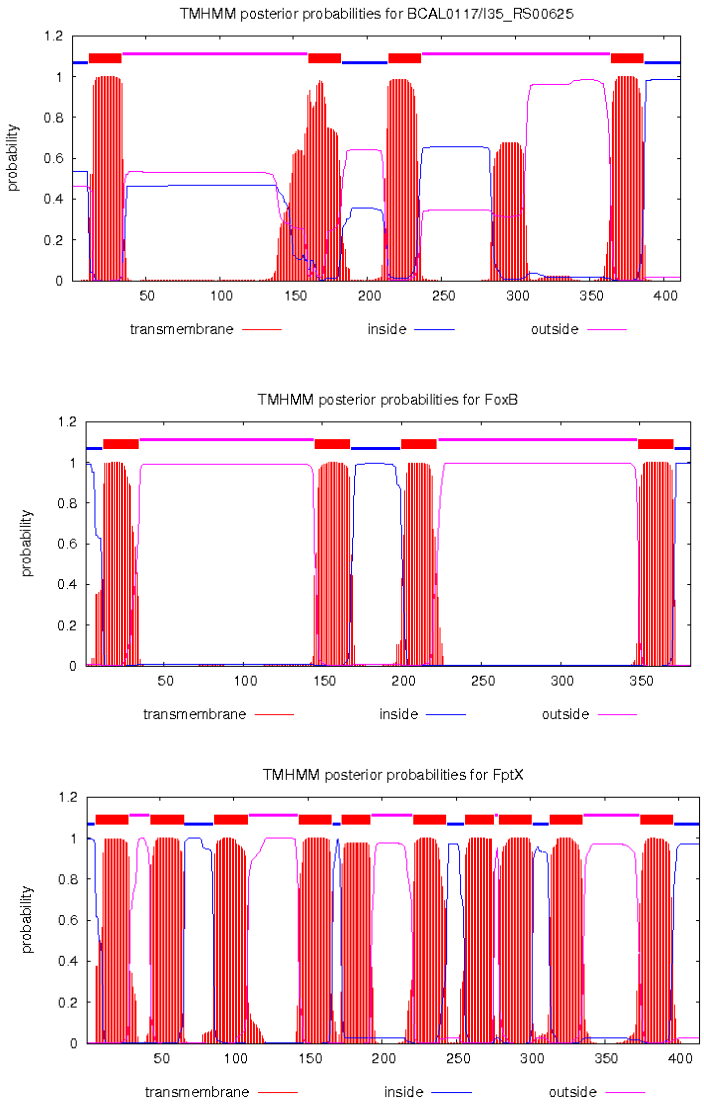

Figure 4.32: Prediction of transmembrane helices in BCAL0117/I35_RS00625 and related inner membrane proteins

Number of transmembrane segments in BCAL0117/I35_RS00625 compared to *P. aeruginosa* FoxB and FptX. Segments were predicted by TMHMM analysis.

A PepSY domain is associated with peptidases generally involved in regulation of protease activity and hence BCAL0117 is predicted as peptidase by Burkholderia.com. PepSY_TM helices are associated with several roles such as secretion, supporting the PepSY domain to the cell exterior and localising the same domain to the inner membrane (Yeats et al., 2004). The function of the PepSY_TM helices in the BCAL0117 protein however remains to be elucidated.

A BLASTP analysis of BCAL0117 amino acid sequence gives a homology of 39 % to *P. aeruginosa* FoxB (Burkholderia.com and NCBI) (Figure 4.33). FoxB (PA2465) is reported to have a redundant function for siderophore transport in *P. aeruginosa* (Cuív et al., 2006). The observation that the BCAL0117 allele prevents growth of H111ΔpobA in conditions of iron deficiency despite supplementation of the medium with some type of hydroxamate siderophores in both the disc diffusion and liquid promotion assays suggests that BCAL0117 acts as the only inner membrane transport system for these siderophores.

It seems therefore that the BCAL0117 protein has a similar function to FoxB required for ferrioxamine B transport in *P. aeruginosa* PAO1 (Cuív et al., 2007). The alignment of the predicted inner membrane proteins, BCAL0117 and FoxB showed acceptable homology, in contrast to the pyochelin cytoplasmic membrane permease, FptX (Figure 4.33). The FptX amino acid sequence showed a 20 % homology with BCAL0117. Moreover, FptX has a higher number of predicted transmembrane segments (10) with one predicted PepSY_TM (PF13000). The orthologue of FptX in *B. cenocepacia* is predicted to be BCAM2221 (Thomas, 2007), although, this function has not been demonstrated. In addition, another cytoplasmic membrane permease, FiuB (PA0476) (Hannauer et al., 2010a), responsible in ferrichrome transport in *P. aeruginosa* PAO1 showed a much lower sequence identity (17 %) to BCAL0117.

Taken together, it remains to be elucidated whether the BCAL0117 protein functions in iron transport as a single subunit permease or a permease subunit in an ABC transport complex or in the release of iron from siderophores. In addition, the potential inner membrane transporters for the two hydroxamate siderophores that are still utilised by a strain containing an inactivated BCAL0117 TBDR, i.e. alcaligin and cepabactin, are most likely be among the putative inner membrane transporters listed in Table 3.4.

4.9.5 Albomycin toxicity study

The sensitivity screening of *B. cenocepacia* H111 towards albomycin failed to show a bactericidal effect to the bacterium. Although *B. cenocepacia* can utilise ferrichrome and other hydroxamate siderophores and the ferrichrome transport system has been characterised, it can be concluded from the observations that *B. cenocepacia* H111 has very slight sensitivity to albomycin or none at all.

```
FptX        1 ------------------------------------------------------------
FoxB        1 ----MRPVLVLLHRYVGLATALFLFLAGLTGSLLAFHHEIDEWLNPGFYAVGEGGERLSP
BCAL0117    1 MNAFLRPFLVRLHRWFGLAIALFLFVAGLTGALLAWDHELDAALNPDFYTARSGAAPLAP

FptX        1 -----MLELYRHRRLVITLALLYLSQGIPIGLAMDALPTLLRQDGAP-------------
FoxB       57 GSLVQRVESRYPRQLVWYM-EYPEAGGHPALL-----ATVPREAGAK-----VEHDVFYL
BCAL0117   61 LELAARIEAADPRVLVTYL-PLAIEPGHTLQA-----GVMPRTDPATGQPYALGFSQIAV

FptX       43 ------------LQALAFLPLVGLPWVVKFLWAPWVDNHWSRRLGRRRSWIIPMOCM--V
FoxB      106 DPVSGEEVGKRLWAACCFQPANLVPWVLEFHHNLTLPG----NW---GLYIMGGVAMFWF
BCAL0117  115 DPATGAVQGRREWGAPSLARLDLMPFIYRLHYSLFLPVYGGVNF---GFWVMGVVGIVWA

FptX       89 LACLLGLA----------------------------TLGLGVASAGWAVGLLALASLASA
FoxB      159 LDCFVGAWLTLPRGRPFWSKWTTAWKI-KRGNAYRFNFDLHRAGGLWIWLLLAPVALSSV
BCAL0117  172 IDSLIALVLAFPNLKS----WRKSFAFRVRRGGYPLVFDLHRSGGVWVWGLLLVVAITSI

FptX      121 TQDIATDGMAAEHFSGELLAKVNAVQIAGVMIGFFGGGAGSLILAGHFGQRTAFLVMACV
FoxB      218 ALNLP-------------------------------------------------SQVFK
BCAL0117  228 SMNLA-------------------------------------------------VPVVR

FptX      181 PLASLCCVLAL-GRGDPHELPPAPAAKASLLRFLRRPLAPSLLALALLSAMTAVSGFGLS
FoxB      228 PLVSLFSPIEPSVYEARGRLPREQLGETRLDYDRTFQLAS-------------VEA----
BCAL0117  238 PLVSLVSPLAETPYTNPEEFPPAPPGSQILPRERIVEIAR-------------SAG----

FptX      240 KLYLSDAGWALQDIGRLGMSGGL---VTVFLGCGGGAWLVRRIGLWRGFALGVVLAGCSA
FoxB      271 ----ARLGIA-EPIGELYYSFEY-----NFFGAGF--------------GDHDDPMGKSW
BCAL0117  281 ----RDAGIA-APPGALLPAPGVNAYAVGFFTPGN--------------DHGDVGLGNAW

FptX      297 LLWYLQAGRWLALSEGLAWTCVLIGSLATGITSVAILTAAMRFAGQGGQAGTDVTAVQST
FoxB      307 LFFHGSDGRLLGQE----------------------------VAGQGS------------
BCAL0117  322 LYWNAVTGKPVAAQ----------------------------VPGRGS------------

FptX      357 RDLGEMLASSFLVSLTAQIGYAGGFLTG----SALAVLALLLALR-------LQAGEGRG
FoxB      327 --WGERF-------YRLQVPLHGGRIAGLPGRIAIAALGLAIAGLSLTGVYIWWKRRAR
BCAL0117  342 --AGDLF-------MQAQFPLHSGRIAGVAGRVAVSVLGIVIAMLSVTGVCIWWKKRGAR

FptX      406 EWKGRAEEA----------
FoxB      378 HWNGR--------------
BCAL0117  393 GRAARSARPAVPASSRAAR
```

Figure 4.33: Alignment of BCAL0117/I35_RS00625 with related inner membrane transport proteins
Amino acid sequence of BCAL0117/I35_RS00625 from *B. cenocepacia* H111 was aligned with those of FptX and FoxB from *P. aeruginosa* PAO1. Sequences were aligned by Clustal Omega and identical or similar amino acids were highlighted by BOXSHADE. White font with black shading indicates identical residue at the corresponding position in two or more sequences and white font with grey shading indicates similar residues at the corresponding position in two or more sequences. Transmembrane domains of FoxB in both *P. aeruginosa* and *B. cenocepacia* are highlighted in blue boxes.

This is in line with the observation demonstrated by Pramanik and coworkers that *B. cepacia* is resistant to albomycin, as mentioned previously (Pramanik et al., 2007). Since *B. cenocepacia* possesses a ferrichrome transport system, albomycin is hypothesised to be transported by the same system, but it was not demonstrated. It has been observed that *Bradyrhizobium japonicum* allows the transport of ferrichrome and albomycin only into the periplasm of the cell. Albomycin is not able to kill the bacterium due to a lack of an inner membrane transport system for albomycin.

Introduction of a plasmid containing a gene expressing the inner membrane transporter of *E. coli* into *B. japonicum* renders the bacterium vulnerable to albomycin (Chatterjee and O'Brian, 2018). This situation may occur in *B. cenocepacia*, i.e. *B. cenocepacia* may not possess an inner membrane transport system for albomycin as in *B. japonicum.* The BCAL0117 protein was demonstrated to allow utilisation of ferrichrome and was predicted to be the inner membrane transport for ferrichrome. However, the transport protein may not be involved in transporting albomycin, thereby exhibiting a degree of non-promiscuity.

To investigate whether BCAL0116/BCAL2281 TBDR(s) is/are involved in albomycin transport and that BCAL0117 is unable to transport albomycin, further experimentation is suggested in which the plasmid containing the gene expressing the inner membrane transporter of *E. coli* is introduced into the *B. cenocepacia* mutant lacking the BCAL0117 protein, H111ΔpobAΔBCAL0117. Sensitivity of the mutant with the plasmid to albomycin may lead to several hypotheses. It may imply that BCAL0117 does not transport albomycin but transports the hydroxamate siderophores (ferrichrome) or that the BCAL0117 protein is not involved in transporting hydroxamate siderophores into the cytoplasm and may have some other function in hydroxamate siderophore utilisation. Alternatively, there is also a possibility that albomycin cannot be activated due to *B. cenocepacia* lacking the peptidase N enzyme responsible for generating an active antibiotic or that the antibiotic is unable to inhibit the specific target site in *B. cenocepacia*. In addition, *B. cenocepacia* could also possess the ability to detoxify albomycin by modifying or exporting the antibiotic by efflux pumps, making the bacterium resistant to the antibiotic. The reason for the insensitivity of *B. cenocepacia* to albomycin therefore remains to be elucidated.

Chapter 5

Utilisation of catecholate siderophores by *B. cenocepacia*

5.1 Rationale

There is a relatively small body of literature concerned with catecholate siderophores that can be utilised by *Burkholderia* species. Even fungi are known to produce only a couple of catecholate siderophores, i.e. pistillarin (Capon et al., 2007; Haas, 2014). Species of the genus *Burkholderia,* particularly *B. ambifaria,* are known to secrete a catecholate siderophore termed cepaciachelin, in culture supernatant besides producing another non-catecholate siderophore, ornibactin (Barelmann et al., 1996). Other species of Bcc are predicted to produce cepaciachelin, but not *B. cenocepacia* (Butt and Thomas, 2017). Given that *B. ambifaria* is in the same group as *B. cenocepacia*, a Bcc member, it is hypothesised that *B. cenocepacia* may be able to utilise certain catecholate siderophores including cepaciachelin. Therefore, the uptake by *B. cenocepacia* of several siderophores that use this ligand to chelate ferric iron was investigated.

Catecholate siderophores, as in other types of siderophores, exist in linear and cyclic forms and may contain one or more catechol ligands. A related ligand consisting of a hydroxyl group on one carbon atom and a double bonded oxygen on the adjacent carbon atom of a pyridine ring is described as a hydroxypyridone. A hydroxypyridone may act like a bidentate catecholate ligand. Some mixed ligand siderophores include catechols with other ligands and their structures are described in the next chapter. This chapter reports investigations with catecholate siderophores in their pure form and present in supernatants of bacteria reported to produce siderophores having the catechol ligand. The siderophores screened were azotochelin, vibriobactin, enterobactin, bacillibactin and the linear analogue of enterobactin, the 2,3-dihydroxybenzoyl-L-serine (DHBS) trimer along with the DHBS monomer and dimer (Figure 5.1). Azotochelin is a siderophore produced by *Azotobacter vinelandii* while vibriobactin is secreted by *Vibrio cholerae*. Enterobactin and bacillibactin are secreted by *Escherichia coli* and *Bacillus subtilis,* respectively. Bacterial supernatants examined included those from *Acinetobacter baylyi*, *B. ambifaria*, *E. coli, B. subtilis* and *Serratia marcescens*. Additional work described in this chapter includes analysis of the TBDRs and the TonB1 complex in the transport of catecholate siderophores.

5.2 Screening of the utilisation of catecholate siderophores present in bacterial supernatants

Most of the bacteria used for obtaining siderophores from bacterial broth culture supernatants were wild type strains that usually produce only one siderophore or mutants which are described to produce only a single siderophore. In some cases, bacterial supernatants used in this study included more than one siderophore which will be discussed in more detail later in this section.

5.2.1 Screening of fimsbactin utilisation by *B. cenocepacia* using *A. baylyi* culture supernatants

A. baylyi ADP1 is reported to produce the siderophores fimsbactin A-F, whereby fimsbactin D and E are dicatecholate siderophores (Figure 5.1A and B) and the others are catecholate-hydroxamate siderophores. This strain also produces an unidentified siderophore (Proschak et al., 2013).

Supernatant of *A. baylyi* was tested for its ability to support growth of *B. cenocepacia* H111ΔpobA under iron limiting conditions using disc diffusion assay and also concurrently with *P. aeruginosa* PAO1 Pvd$^-$ Pch$^-$ The culture supernatants were shown to permit growth of the *P. aeruginosa* mutant (Figure 5.2A), indicating that *A. baylyi* supernatants contained at least one siderophore. However, the *A. baylyi* bacterial supernatant was unable to elicit growth of H111ΔpobA. Promotion of growth of *P. aeruginosa* may be due to one or more of the fimsbactin and /or the uncharacterised siderophore produced by *A. baylyi.*

5.2.2 Screening of enterobactin utilisation by *B. cenocepacia* using *E. coli* culture supernatants

E. coli is known to produce up to four different types of siderophores: aerobactin, enterobactin, salmochelin and yersiniabactin (Grass, 2006). To investigate the ability of *B. cenocepacia* to utilise enterobactin (Figure 5.1C), several mutant *E. coli* strains were used: JM83, AN90, WW3352, ED8659 and JC28. JM83 produces enterobactin whereas AN90 and JC28 do not. WW3352 and ED8659 are *tonB* mutants and therefore hyperproduces enterobactin (Table 2.1).

Supernatants of *E. coli* strains JM83, ED8659, AN90 and WW3352 were screened using *P. aeruginosa* PAO1 for satisfactory siderophore production as the latter is known to utilise enterobactin as a xenosiderophore (Poole et al., 1990). Based on this screening and due to obvious growth promotion elicited by the supernatant of WW3352 mutant (Figure 5.2B), this strain was used for screening the ability of *B. cenocepacia* to use enterobactin while the AN90 mutant strain was used as a negative control since it did not promote growth of *P. aeruginosa*. Correspondingly, AN90 is an *entD* mutant where the gene responsible to produce enterobactin was knocked out. However, disc diffusion bioassay of H111ΔpobA using the supernatants of AN90 showed some observable growth around the filter disc (result not shown). This may due to the production of the enterobactin precursor, 2,3-dihydroxybenzoate (DHBA), in its supernatant as DHBA has been reported to act as a weak siderophore in some bacteria (Hantke, 1990). Enterobactin biosynthetic pathway is shown in Figure 5.3.

To avoid growth due to the presence of DHBA, an alternative *E. coli* mutant, JC28, was subsequently used as a negative control. JC28 is an *entC* mutant which is blocked for the initial conversion of chorismate to isochorismate (Figure 5.3). The strain does not secrete DHBA, nor does it produce a yellow halo on CAS agar. Production of a yellow halo on CAS agar by WW3352 strain confirmed the presence of enterobactin in its supernatant (Figure 5.2C). A disc diffusion bioassay in which WW3352 and JC28 culture supernatants were applied to filter discs suggested that H111ΔpobA can use enterobactin as an iron chelator (Figure 5.2C). Following this observation, purified enterobactin was used to further investigate the ability of *B. cenocepacia* to sequester iron using this siderophore (Section 5.3.3).

5.2.3 Screening of siderophore utilisation by *B. cenocepacia* using *B. subtilis* bacterial supernatants

B. subtilis is known to secrete a siderophore with three catecholate groups called bacillibactin (Figure 5.1D). Bacillibactin is structurally similar to enterobactin but the trilactone ring is composed of three threonine residues rather than serine and is connected to the catechol group by glycine linkers (May et al., 2000). Disc diffusion assays using the supernatants of *B. subtilis* showed a slight growth of *B. cenocepacia* H111ΔpobA and H111ΔC3ΔpobA around the filter. Similarly, *P. aeruginosa* PAO1 pch$^-$pvd$^-$ elicited a halo of growth indicating that the supernatants contained siderophores (Figure 5.2D). However, a control strain that does not produce bacillibactin was not tested. Pure bacillibactin was therefore used to verify this observation (Section 5.3.3).

5.2.4 Screening of siderophore utilisation by *B. cenocepacia* using *B. ambifaria* bacterial supernatants

B. ambifaria is reported to produce two types of siderophore, ornibactin as a primary siderophore and cepaciachelin as a secondary (Barelmann et al., 1996). Cepaciachelin is a catecholate siderophore and therefore it was decided to test the ability of *B. cenocepacia* to utilise this siderophore (Figure 5.1E). *B. ambifaria* AMMD was grown in M9-glucose at 37 °C for 48 hrs. Filter-sterilised culture supernatants of *B. ambifaria* were tested using the disc diffusion assay and were shown to promote growth of H111ΔpobA (result not shown). As H111ΔpobA can use ornibactin, further investigations were performed to determine the cause of the growth promotion. The ability of a *B. ambifaria* culture supernatant to stimulate growth of a *B. cenocepacia* inactivated ornibactin TBDR mutant, H111ΔpobA-orbA::TpTer (Chapter 6), was tested. The *orbA* knock-out mutant cannot transport ornibactin and any growth observed with the culture supernatant of *B. ambifaria* is therefore likely to be due to the secondary siderophore produced. The disc diffusion assay showed that *B. ambifaria* culture supernatant still elicited growth of the *orbA* mutant, suggesting the ability of *B. cenocepacia* H111 to utilise cepaciachelin. Liquid growth stimulation assay of *B. cenocepacia* H111 using cepaciachelin was not performed due to the unavailability of purified cepaciachelin.

5.2.5 *B. cenocepacia* utilisation of siderophores present in *S. marcescens* Db10 culture supernatants

S. marcescens is known to produce the dicatecholate siderophore serratiochelin and the monocatecholate chrysobactin (Seyedsayamdost et al., 2012). To screen for utilisation of these catecholate siderophores, *S. marcescens* Db10 was grown at 37 °C for 48 hrs in four different conditions: LB and M9-glucose, with and without 2,2'-bipyridyl to determine the medium that allows maximum production of siderophores. The filter-sterilised culture supernatants all conferred growth on H111ΔpobA, H111ΔC3ΔpobA and *P. aeruginosa* PAO1 pch$^-$ pvd$^-$ in disc diffusion assays. Obvious growth was seen with supernatants conditioned in iron-restricted conditions (Figure 5.4A and B). As no reports have been published on the siderophores produced by *S. marcescens* Db10 strain, it was decided to analyse the culture supernatants of this strain to try and identify the siderophores potentially involved.

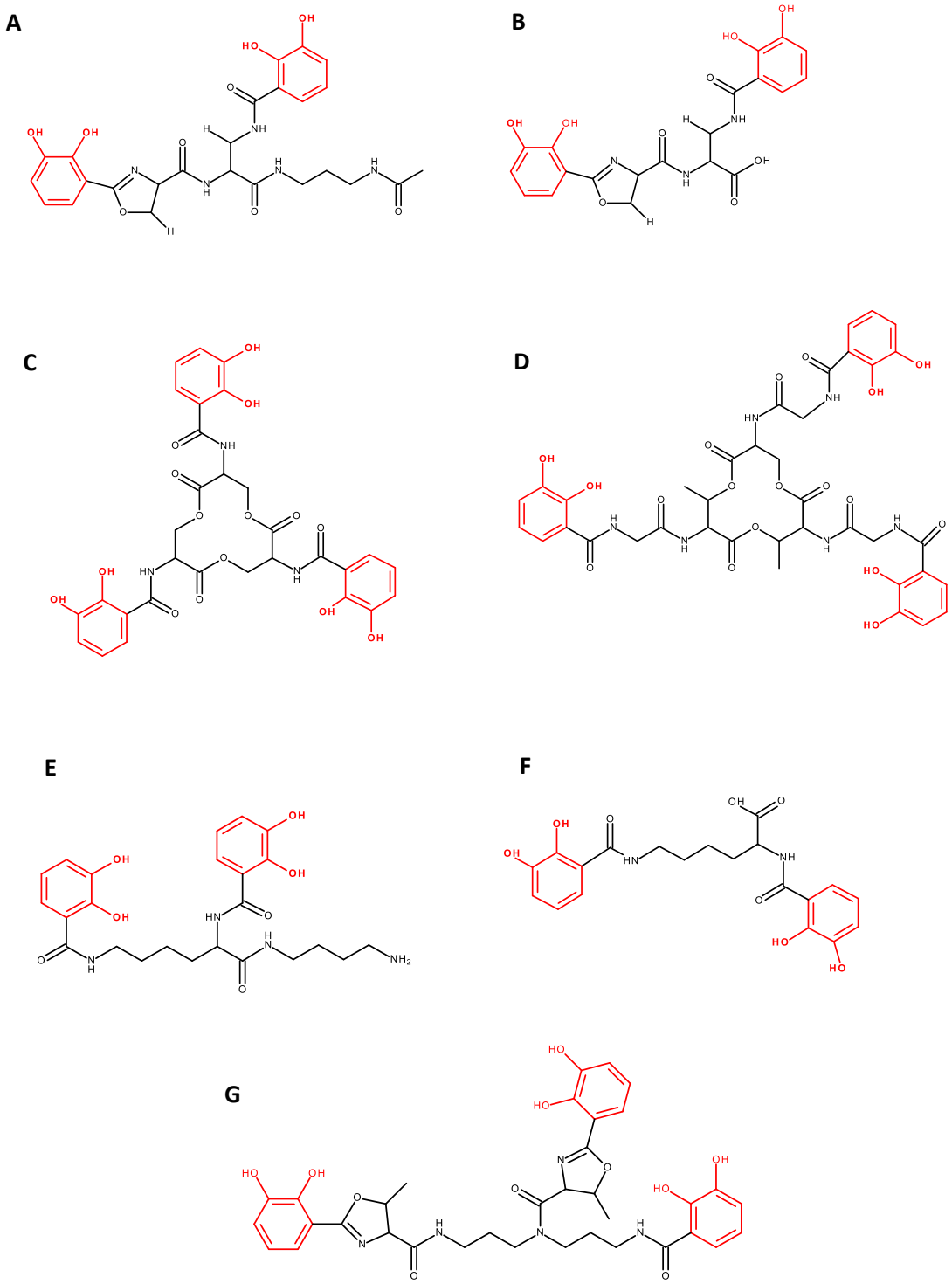

Figure 5.1: Molecular structures of some catecholate siderophores screened for utilisation by *B. cenocepacia*

(A) Fimsbactin D, (B) fimsbactin E, (C) enterobactin, (D) bacillibactin, (E) cepaciachelin, (F) azotochelin and (G) vibriobactin. The catecholate ligand is depicted in red. Structures were drawn using Accelrys 4.2.

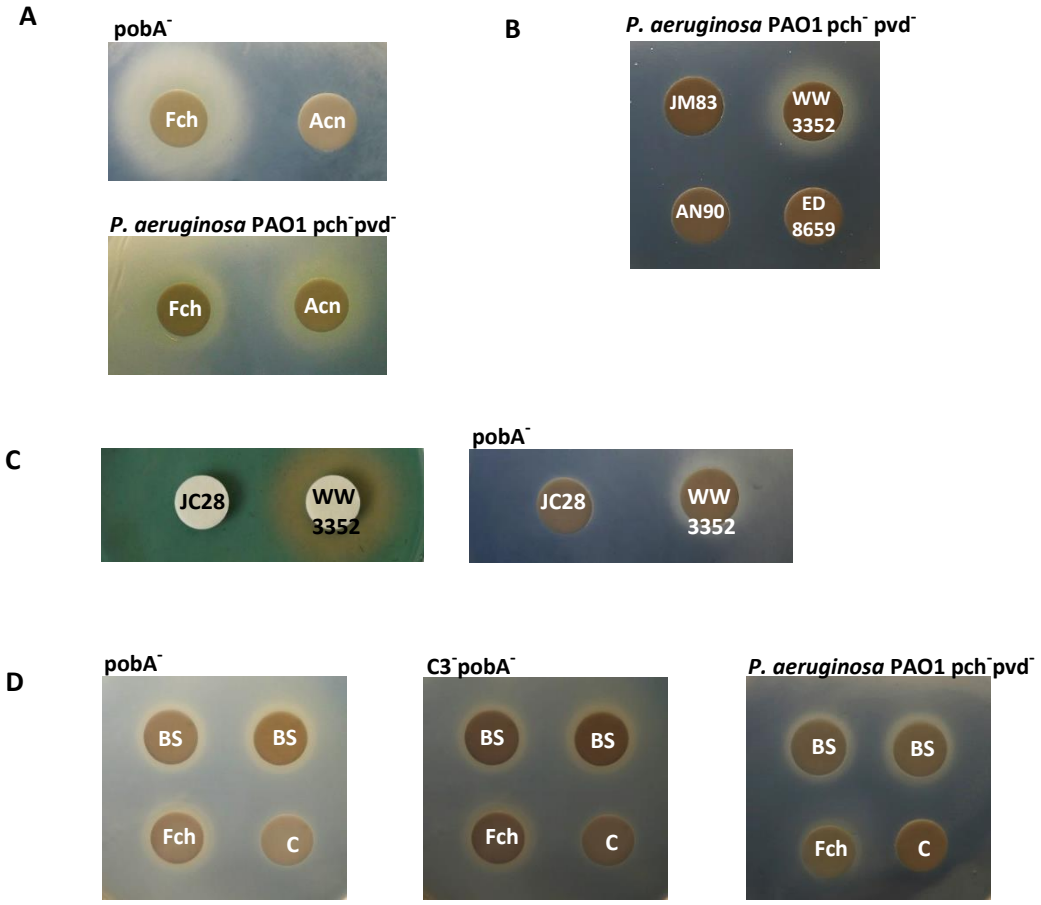

Figure 5.2: Screening of catecholate siderophore using disc diffusion assays
(A) Analysis of utilisation of *A. baylyi* siderophores by *B. cenocepacia* H111ΔpobA and *P. aeruginosa* PAO1 pch$^-$ pvd$^-$ using *A. baylyi* culture supernatants. (B) Growth promotion of *P. aeruginosa* PAO1 pch$^-$ pvd$^-$ by supernatant of the *E. coli* mutant, WW3352. (C) Left: Yellow zone around a filter disc containing WW3352 culture supernatant on CAS agar caused by enterobactin. Right: Promotion of growth of H111ΔpobA by the supernatant of WW3352 in comparison to the supernatant of the *E. coli entC* mutant, JC28. (D) Screening of siderophore utilisation by H111ΔpobA, H111ΔC3ΔpobA and *P. aeruginosa* PAO1 pch$^-$ pvd$^-$ by the presence of growth around filters to which *B. subtilis* culture supernatants were added. Filter discs were impregnated with Fch, ferrichrome (1 mM, 10-20 µl); BS, *B. subtilis* supernatant (100 µl), Acn, *A. baylyi* supernatant (100 µl), and C, growth medium (100 µl). *E. coli* culture supernatants (JM83, WW3352, ED8659, AN90 and JC28) used were 100 µl. Final EDDHA concentration in agar is 40 µM.

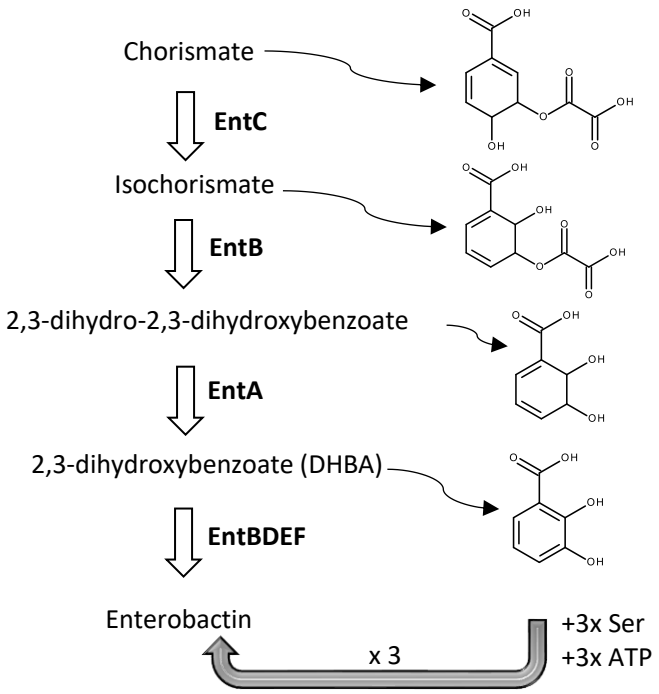

Figure 5.3: Enterobactin biosynthesis pathway
Simplified biosynthetic pathway of enterobactin in *E. coli* based on Raymond et al., 2003. The enzymes included in each step of the pathway are shown in bold font.
[metabolic conversion]

5.2.5.1 Analysis of siderophores produced by *S. marcescens* Db10

Serratia sp. V4 is reported to produce the siderophores serratiochelin (A, B and C), chrysobactin and yersiniabactin (Seyedsayamdost et al., 2012) (Figure 5.5). To investigate whether the Db10 strain produces similar siderophores, fresh culture supernatants of the Db10 strain grown in M9-glucose (with and without 2,2'-bipyridyl) were subjected to preparative high-performance liquid chromatography (HPLC) for mass spectroscopy detection.

The analysis was performed with a solvent mobile phase of 5 to 20 % acetonitrile in 0.1 % aqueous trifluoroacetic acid (TFA) over 15 mins and increasing to 80 % acetonitrile after 16 mins. As the structures of the expected siderophores from the Db10 strain possess a benzene ring, peaks were monitored at a wavelength of 240 nm, a wavelength suitable for detecting such compounds. Three major peaks were detected from the HPLC separation chromatogram of both conditioned media and collected for liquid chromatography mass spectrometry (LC-MS) analysis. Fractions of supernatants from M9-glucose were collected at retention times of 3.0, 8.0 and 9.0 minutes and annotated as 6, 7 and 8 whereas those arising from cultures grown in medium containing 2,2'-bipyridyl were collected at retention times of 8.0, 9.0 and 10.0 minutes, with the annotation A, B and S. These major peaks were designated according to their sequence of elution from the column ans size of peaks (Figure 5.6).

Eluted fractions from A, B and S were applied to filters in the disc diffusion assay. Assays for activity from these fractions were all shown to promote growth of H111ΔpobA. The fractions from A, S, 6 and 8 led to significant growth of H111ΔpobA while fractions B and 7 elicited less growth (Figure 5.4C and D). The fractions were tested with the CAS assay to screen for the presence of siderophores. The CAS assay elicits a change in colour whereby siderophores with a hydroxamate moiety would change the solution from the original yellow to violet, hydroxycarboxylate turns orange and catecholate turns the solution pink (Neilands, 1981). The purified fractions changed the solution from yellow to dark pink indicating the presence of siderophores with a catecholate moiety. Ferrioxamine B, ornibactin and enterobactin were used as controls (results not shown).

The HPLC fractions derived from both spent culture supernatants (M9-glucose and M9-glucose with 2,2'-bipyridyl) were then screened by direct fusion LC-MS. The molecular weight of the predicted siderophores are: serratiochelin A and B (448), serratiochelin C (430), chrysobactin (369) and yersiniabactin (481). The LC-MS profile data were screened for compounds with molecular weights consistent with these siderophores. Serratiochelin A is documented as an unstable compound and will exist interchangeably with serratiochelin B, while serratiochelin C is a degradation product of the A and B forms (Seyedsayamdost et al., 2012).

LC-MS profile of culture supernatants from *S. marcescens* Db10 grown in M9-glucose showed the presence of a compound with mass-to-charge ratio (m/z) 370 that matches the expected size of chrysobactin as well as serratiochelin A, and B (both m/z 447), C (m/z 431) and yersiniabactin (m/z 481). Fraction 6 and 7 showed major peaks of chrysobactin (370) and yersiniabactin (481), respectively, whereas fraction 8 showed many peaks of serratiochelins A, B and C (Figure 5.7).

Similarly, LC-MS profile of spent culture supernatants from the Db10 strain grown in M9-glucose containing 2,2'-bipyridyl also showed the presence of all three compounds. Fraction A showed major peaks of yersiniabactin and serratiochelin, fraction B exhibited the peak activity of mostly yersiniabactin and fraction S displayed many peaks of serratiochelins (Figure 5.8). The molecular weights of ions detected can be slightly higher or lower due to the protonation or deprotonation of the siderophores by in-source fragmentation. Many peaks of chrysobactin were observed (fraction 6) in M9-glucose medium suggesting more of this siderophore was produced. In contrast, many peaks of serratiochelins were observed (fraction A) in conditioned medium that contained 2,2'-bipyridyl, suggesting more serratiochelins were released into the medium with higher iron-restricted conditions.

Based on these m/z values, chrysobactin, yersiniabactin and serratiochelin A, B and C were likely to be produced by the Db10 strain. The LC-MS screening results suggested that promotion of growth from *S. marcesens* Db10 in the disc diffusion assay, may be due to one or more of these secreted siderophores. To partially deduce the siderophore that is responsible for growth of H111ΔpobA, one of the siderophores was used in its purified form for the disc diffusion assay, in this case yersiniabactin.

5.3 Investigation of the utilisation of purified catecholate siderophores by *B. cenocepacia*

5.3.1 Screening for the utilisation of yersiniabactin by *B. cenocepacia*

Although yersiniabactin is not a catecholate siderophore, as it was commercially available, it was used in a disc diffusion assay to shed light on the ability of *B. cenocepacia* to use catecholate siderophores produced by *S. marcescens*. A solution of commercially available purified yersiniabactin spotted onto a filter disc did not promote the growth of H111ΔpobA. This suggests that the supported growth of H111ΔpobA by *S. marcescens* culture supernatants was due to the catecholate siderophores, serratiochelin A/B and/or chrysobactin. The utilisation of each of these siderophores by *B. cenocepacia* was not further investigated as they were not available in their purified forms. Additionally, this correlates with the insignificant growth of H111ΔpobA with fraction B and fraction 7 which were mostly comprised of yersiniabactin (Figure 5.4C and D).

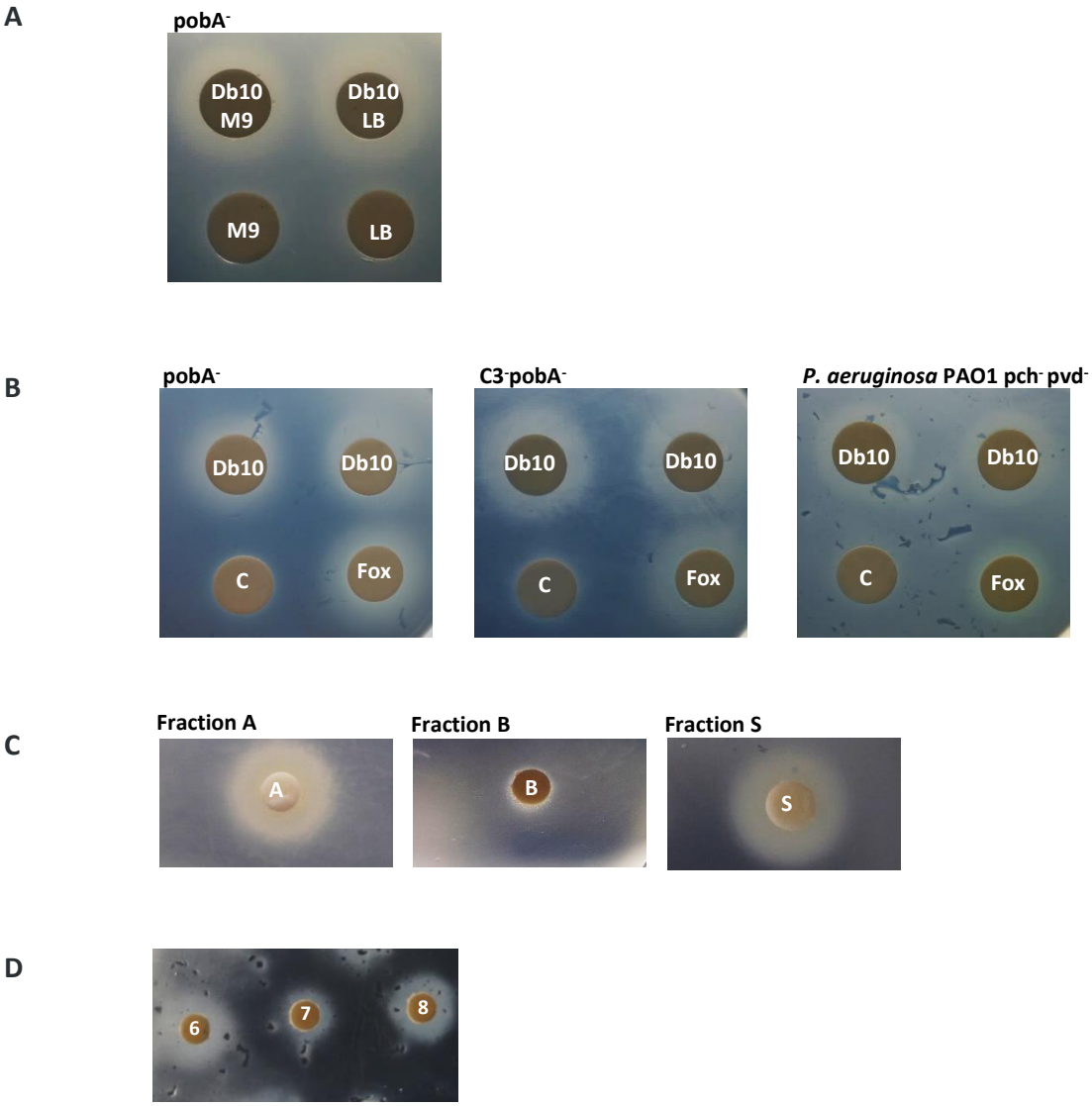

Figure 5.4: Screening of siderophore utilisation from supernatants of *S. marcescens* Db10
(A) Promotion of growth of *B. cenocepacia* on iron limited medium by culture supernatants of S. *marcescens* Db10 grown in M9-glucose or LB containing 2,2' bipyridyl exhibiting similar growth halos of H111ΔpobA with growth medium as controls. (B) Promotion of growth of H111ΔpobA, H111ΔC3ΔpobA and *P. aeruginosa* PAO1 pch$^-$ pvd$^-$ by culture supernatants of *S. marcescens* Db10 grown in LB containing 2,2'-bipyridyl. (C) Growth promotion elicited by HPLC fractions A, B and S of *S. marcescens* Db10 supernatant following growth in M9-glucose containing 2,2'-bipyridyl. (D) Growth promotion elicited by HPLC fractions 6, 7 and 8 of *S. marcescens* Db10 culture supernatant following growth in M9-glucose. Filter discs were impregnated with Fox; ferrioxamine B (1 mM, 15 µl); Db10, *S. marcescens* Db10 supernatant (100 µl); C, growth medium (100 µl). Final EDDHA concentration in agar are 40 µM.

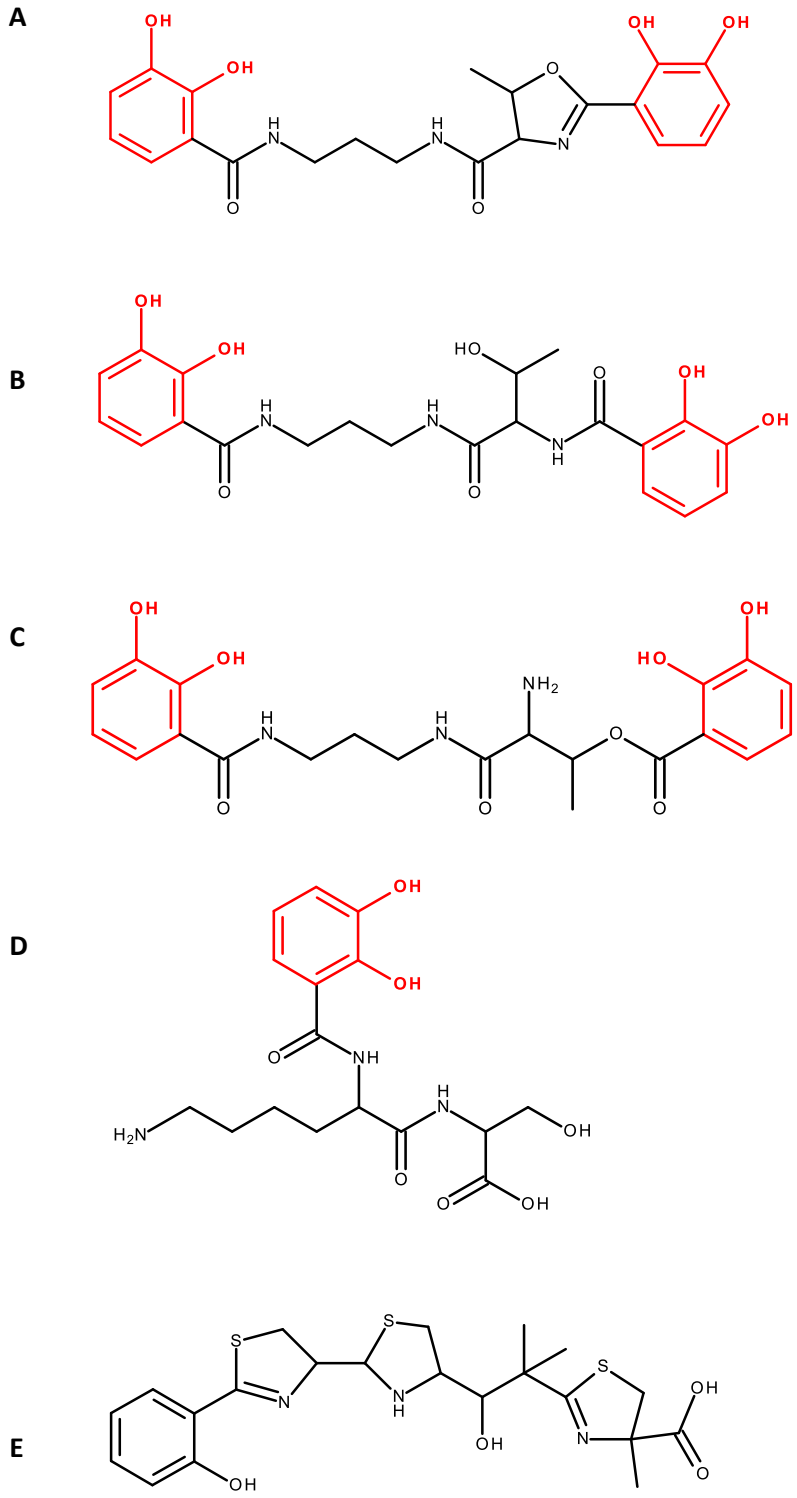

Figure 5.5: Molecular structures of siderophores detected in supernatants of *S. marcescens* Db10
(A) serratiochelin A, (B) serratiochelin B, (C) serratiochelin C, (D) chrysobactin and (E) yersiniabactin. The catecholate ligand is depicted in red. Structures were drawn using Accelrys 4.2.

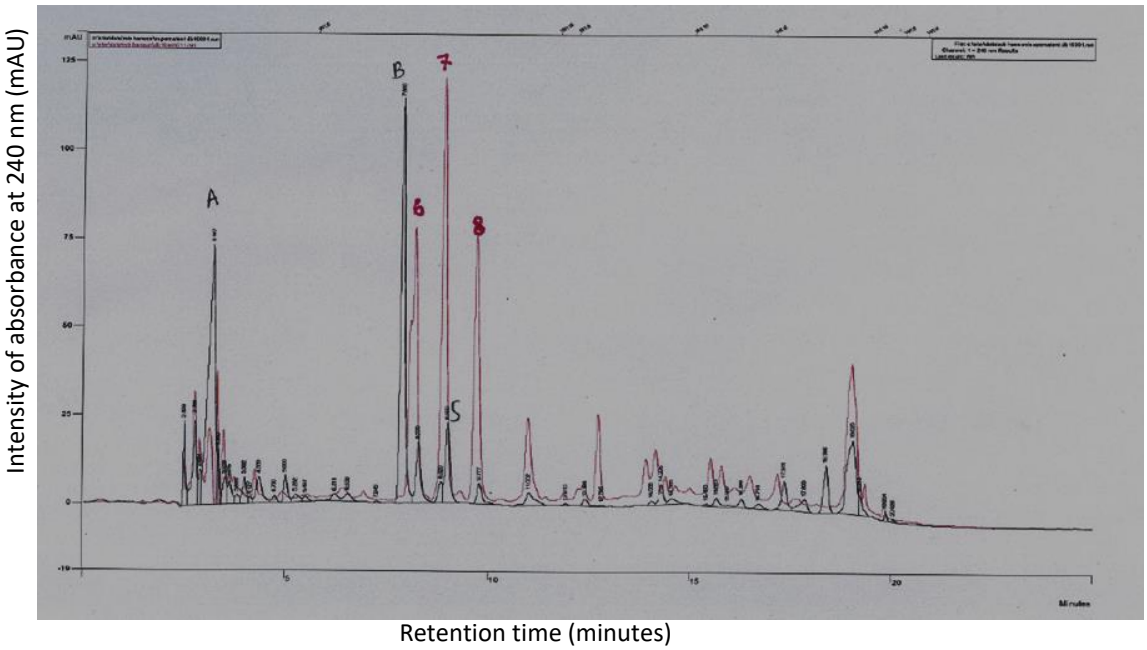

Figure 5.6: HPLC chromatogram of *S. marcescens* Db10 supernatant in iron-limiting conditions
Elution profile of the separation of compounds produced by *S. marcescens* Db10 in M9-glucose (red) and M9-glucose containing 0.2 mM 2.2'-bipyridyl (black) at an absorbance of 240 nm. Fractions of effluent were collected from major peaks of activity from the M9-glucose supernatant and are indicated as 6, 7 and 8. Fractions of effluent collected from the M9-glucose containing bipyridyl are indicated as A, B and S. Small peaks of activity are caused by impurities in the supernatant.

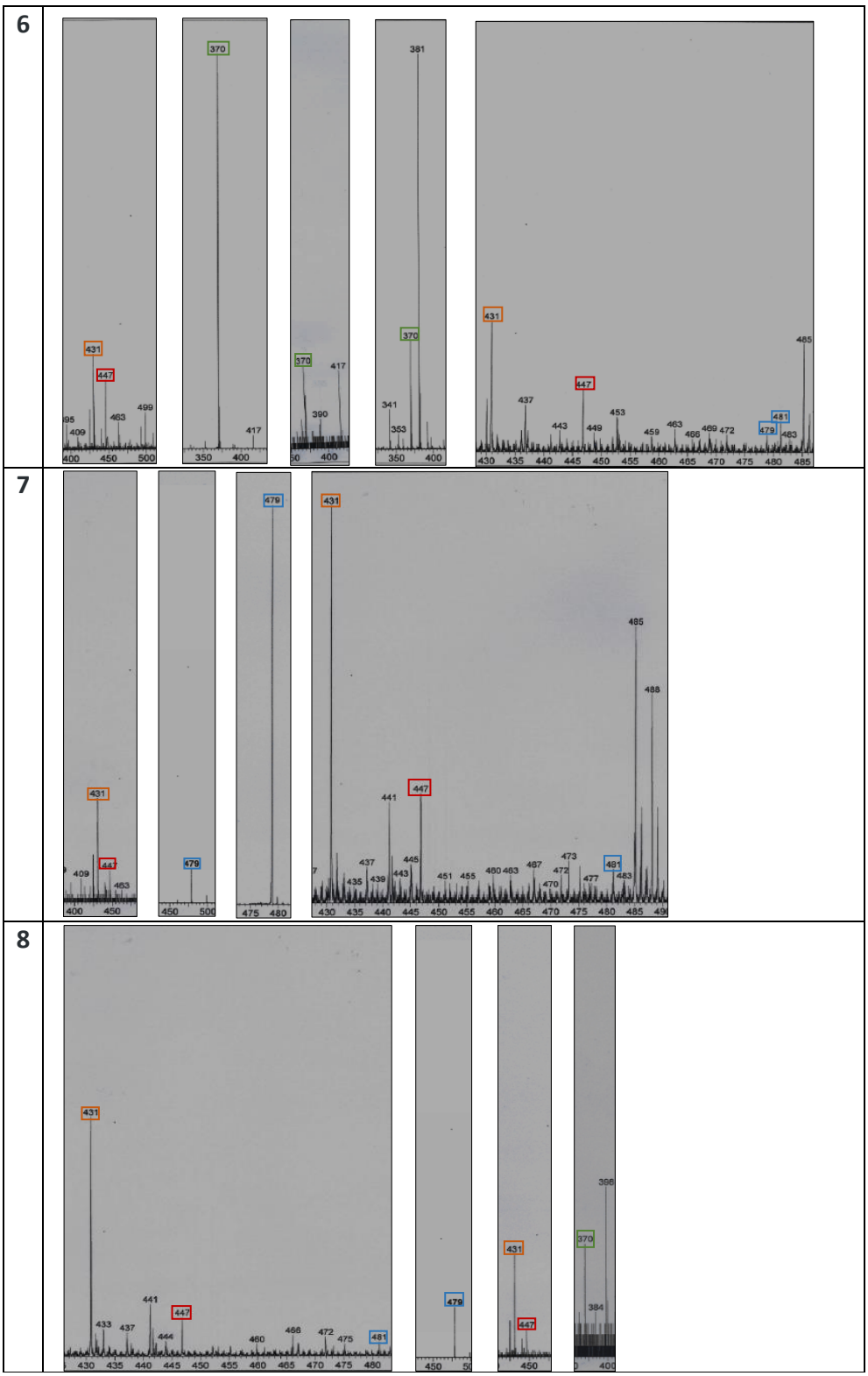

Figure 5.7: Mass spectra of compounds present in *S. marcescens* Db10 supernatant following growth in M9-glucose medium

The molecular peaks of serratiochelins are seen at m/z 431 (orange) and 447 (red), chrysobactin is seen at m/z 370 (green) and yersiniabactin is seen at m/z 479 (blue) and 481 (blue). Peak 6 showed a high peak for chrysobactin, peak 7 displayed high peaks for yersiniabactin and serratiochelin C, while peak 8 is mostly comprised of serratiochelins. The X-axis represents the mass-to-charge ratio (m/z) and the Y-axis represents the relative abundance of ions.

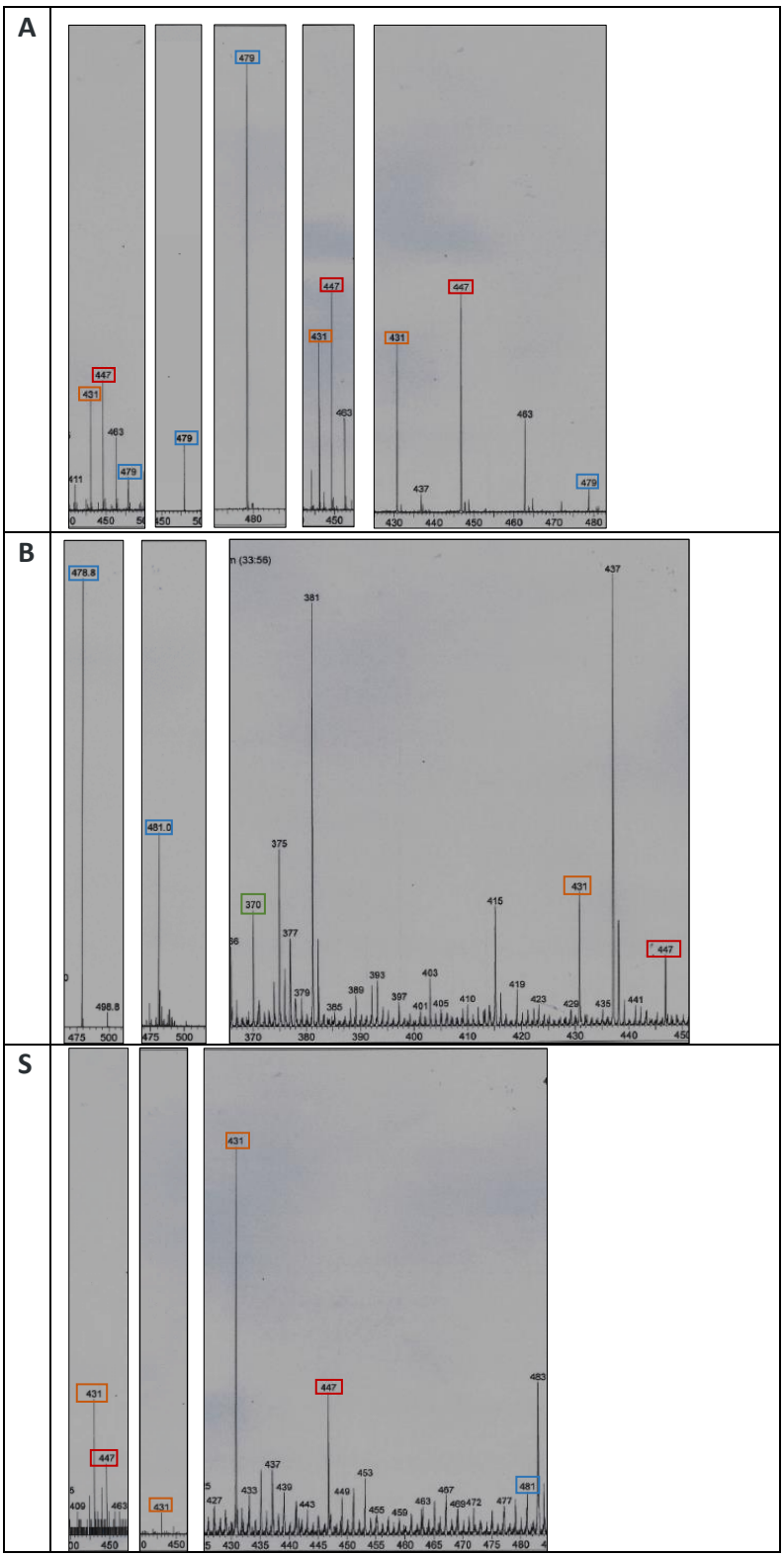

Figure 5.8: Mass spectra of compounds present in *S. marcescens* Db10 supernatant following growth in M9-glucose medium containing 2,2'-bipyridyl

The molecular peaks of serratiochelins are seen at m/z 431 (orange) and 447 (red), chrysobactin is seen at m/z 370 (green) and yersiniabactin is seen at m/z 479 and 481 (both blue). Peak A displayed peaks of yersiniabactin and serratiochelins, peak B showed mostly of yersiniabactin and peak S mostly consist of serratiochelins. The X-axis represents the mass-to-charge ratio (m/z) and the Y-axis represents the relative abundance of ions.

5.3.2 Investigation of the utilisation of azotochelin and vibriobactin by *B. cenocepacia*

Utilisation of the purified dicatecholate azotochelin and the tricatecholate vibriobactin were screened using disc diffusion assays with H111ΔpobA as previously described. This demonstrated the growth promotion of H111ΔpobA when supplemented with azotochelin but not with vibriobactin (Figure 5.9A and B), suggesting the ability of *B. cenocepacia* H111 to utilise azotochelin for iron sequestration. The utilisation of azotochelin was also assessed in the liquid growth stimulation assay which showed a significant enhancement of growth of the H111ΔpobA mutant in comparison to growth in medium without any siderophore supplementation (Figure 5.10A).

5.3.3 Analysis of purified enterobactin and bacillibactin utilisation by *B. cenocepacia*

Since the supernatants of *E. coli* and *B. subtilis*, containing enterobactin and bacillibactin, respectively, allowed growth of H111ΔpobA, the purified siderophores were tested in the disc diffusion assay. Enterobactin and bacillibactin were spotted onto filter discs and applied to an overlay of H111ΔpobA and H111ΔC3ΔpobA with *P. aeruginosa* PAO1 pch^- pvd^- serving as a control. Enterobactin elicited significant growth of all strains at 1 mM (20 and 100 µl) but with formation of a clear zone separating the halo of growth from the filter disc in the case of 100 µM (Figure 5.9C).

Enterobactin and bacillibactin are hexadentate siderophores that are categorised as high affinity siderophores due to their high binding constants for ferric iron (Loomis and Raymond, 1991). In fact, enterobactin has the highest binding constant of any siderophore (Harris et al., 1979). However, *B. cenocepacia* does not appear to utilise them efficiently based on the disc diffusion assay. To confirm the ability of *B. cenocepacia* to utilise both enterobactin and bacillibactin, liquid growth stimulation assays were performed. However, based on the assay, enterobactin did not exert a growth promotion effect on H111ΔpobA and bacillibactin had only a small growth promoting effect (Figure 5.10B).

Possibly a higher amount of these siderophores in the liquid assay would promote growth of H111ΔpobA, as seen with the disc diffusion assay. Due to this observation, it was hypothesised that enterobactin and bacillibactin were hydrolysed into linear analogues upon in contact with water in the solid and liquid growth stimulation assays, enabling the growth promotion of H111ΔpobA demonstrated in the disc diffusion assays.

5.3.4 Analysis of the ability of *B. cenocepacia* to utilise DHBS derivatives as xenosiderophores

To investigate the hypothesis mentioned above, the ability of the purified monomer, dimer and trimer of 2,3 dihydroxylbenzoylserine (DHBS), the enterobactin precursor, to support growth of H111ΔpobA under iron limiting conditions was tested using disc diffusion assay (Figure 5.9D).

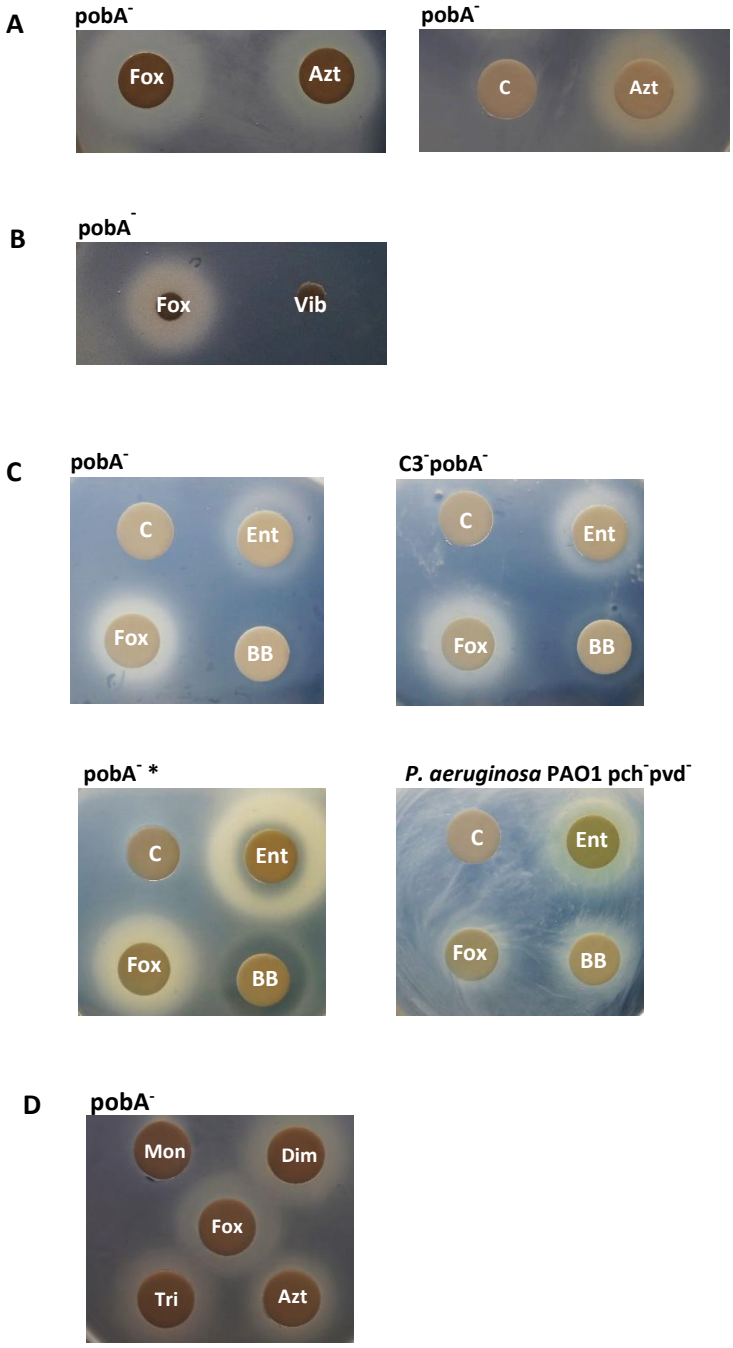

Figure 5.9: Analysis of catecholate siderophore utilisation by *B. cenocepacia* using the disc diffusion assay

(A) The growth promotion of H111ΔpobA provided by azotochelin. Ferrioxamine B (Fox) was included as a control. Right: Same assay with dH_2O as negative control. (B) Absence of growth promotion of H111ΔpobA by vibriobactin with ferrioxamine B (Fox) as positive control. (C) Zones of growth of H111ΔpobA, H111ΔC3ΔpobA and *P. aeruginosa* PAO1 pch$^-$ pvd$^-$ on iron-limiting media observed with filter containing 20 µl of 1 mM enterobactin and bacillibactin. H111ΔpobA was also tested with 100 µl 1 mM of enterobactin and bacillibactin indicated by *. (D) Utilisation of azotochelin and the DHBS derivatives by *B. cenocepacia* H111ΔpobA with ferrioxamine B as a positive control. Note that the same amount of each DHBS derivative was added to filter discs. Azt, azotochelin (1 mM, 30 µl); Vib, vibriobactin (1 mM, 10 µl); Mon, DHBS monomer (1 mM, 50µl); Dim, DHBS dimer B (1 mM, 50 µl); Tri, DHBS trimer (1 mM, 50 µl) and C, dH_2O (30 µl). Final EDDHA concentration in agar was 40 µM.

The assays with these derivatives demonstrated the ability to promote growth of H111ΔpobA, although the monomers supported weaker growth than the dimer and trimers. This may be due to the monocatecholate nature of the monomers. The ability of the DHBS derivatives to promote growth of *B. cenocepacia* under iron-limited conditions was also analysed by the liquid growth stimulation assay. All three derivatives supported growth of H111ΔpobA and led to almost the same growth rate as occurs in the presence of ornibactin, suggesting an equivalent and maximum iron transport efficiency in *B. cenocepacia* at the concentration used (Figure 5.10C). The less extensive growth of H111ΔpobA observed when supplemented with DHBS monomers in the disc diffusion assays suggests the requirement of a higher amount of the siderophore in this assay relative to the amount used in the liquid stimulation assay.

These observations are consistent with the hypothesis that enterobactin and bacillibactin are hydrolysed in the disc diffusion assay, both in their pure forms and in bacterial supernatants, producing precursor-like molecules, as has been previously reported for *E. coli* (Berner et al., 1991; Hider and Kong, 2010) and *B. subtilis* (Miethke et al., 2006). It is concluded that *B. cenocepacia* cannot utilise enterobactin and bacillibactin in their original forms at a significant rate. The promotion of growth observed in the disc diffusion assays are therefore suggested to be due to these precursors.

5.4 Identification of the TBDR for catecholate siderophore utilisation in *B. cenocepacia*

5.4.1 Screening TBDR mutants for defects in catecholate siderophore utilisation

This study has identified azotochelin, DHBS (monomer, dimer, trimer), cepaciachelin, chrysobactin and/or serratiochelins as catecholate siderophores that can be utilised by *B. cenocepacia*. The first step in identifying the TBDR responsible for transporting catecholate siderophores in *B. cenocepacia* involved screening the previously constructed mutants containing inactivated BCAL1709, BCAL1371, BCAM0491, BCAM0499, BCAM1187, BCAM0564, BCAM2439, BCAL0116 and BCAM2281 TBDR genes as well as the BCAL0116-BCAL2281 TBDR mutant. These mutants were pre-screened by PCR 'outside primers' prior to screening with the disc diffusion assay to verify their integrity (results not shown). Growth promotion, however, was still observed with all of these TBDR mutants (results not shown), indicating that these TBDRs may not be involved in transporting the catecholates.

Regarding the InterPro analysis (Section 3.2), the TBDRs which might be involved in transporting the catecholates are BCAM0499, BCAM1187 and BCAM2007. As inactivation of the BCAM0499 and BCAM1187 TBDRs did not inhibit catecholate siderophore utilisation in the disc diffusion assay, it was hypothesised that the TBDR BCAM2007 is most likely to be involved in transporting the catecholates. Therefore, the role of BCAM2007 in the uptake of catecholate siderophores BCAM2007 was investigated.

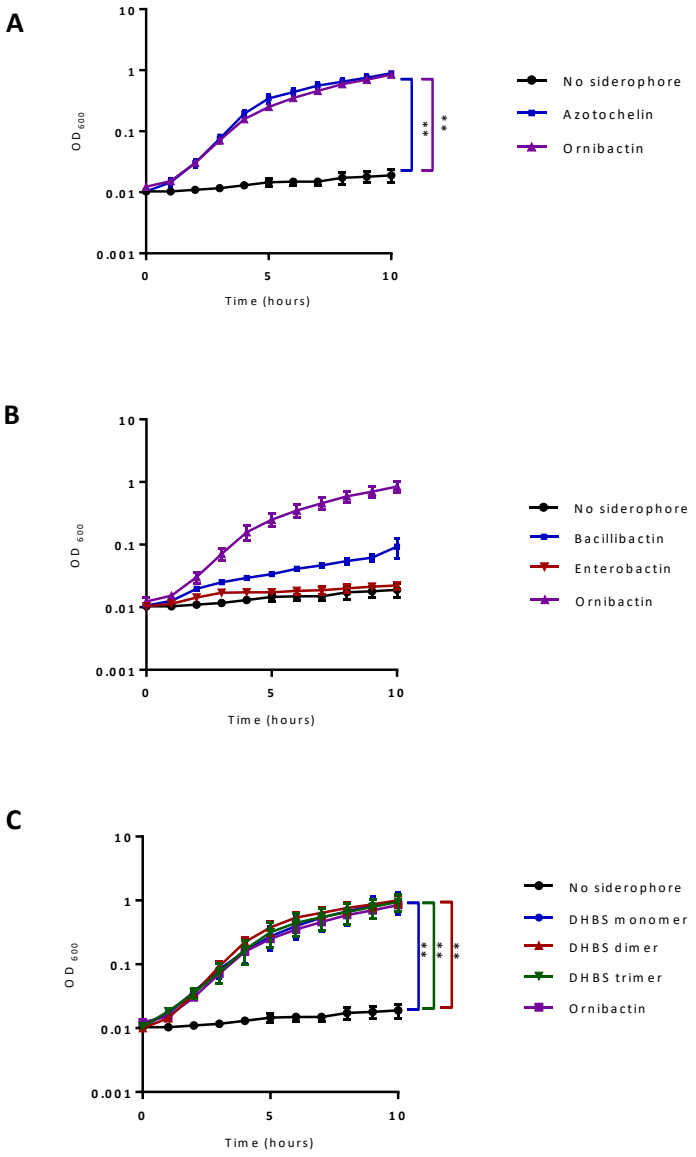

Figure 5.10: Growth curves of *B. cenocepacia* H111ΔpobA in iron-depleted medium supplemented with catecholate siderophores

(A) Growth of *B. cenocepacia* H111ΔpobA in iron-depleted M9-glucose CAA medium supplemented with 1 µM DTPA and 10 µM of (A) azotochelin, (B) enterobactin and bacillibactin, (C) DHBS derivatives (monomer, dimer and trimer) at 37 ^{o}C. Growth is compared to that of the mutant in the absence of siderophores as a negative control and in ornibactin-supplemented iron depleted media as a positive control. These data are representative of three independent experiments (n=3). Error bars represent the mean ±SEM. Significance of ornibactin-supplemented growth rate is shown in (A). *$p<0.05$, **$p<0.01$.

5.4.2 Construction of a *B. cenocepacia* BCAM2007 mutant

5.4.2.1 Construction of pEX18TpTer-*pheS*-Cm-SceI-ΔBCAM2007

To investigate the role of the BCAM2007 TBDR in catecholate siderophore utilisation, it was decided to inactivate the BCAM2007 gene in H111ΔpobA and test the ability of the resulting mutant to utilise catecholate siderophores. As a first step, the BCAM2007 gene was amplified using primer BCAM2007for and BCAM2007rev, and the amplicon was verified electrophoretically. Due to other fragments being amplified concomitantly, the BCAM2007 fragment was gel purified. However, attempts to clone the fragment into many vectors, pBBR1MCS, pBBR1MCS2, pBluescript, and the suicide plasmids, pSHAFT2 and pEX18TpTer-*pheS*-Cm-SceI, were unsuccessful. For this reason, splicing overlap extension (SOE) was employed to amplify a mutant allele and clone it directly into pEX18TpTer-*pheS*-Cm-SceI.

SOE PCR comprised of two stages. In the first stage, gene fragments flanking the BCAM2007 locus and containing the 5' and 3' ends of BCAM2007 were separately amplified and the two PCR products were used as templates for the second stage PCR. Flanking gene fragments were amplified at an annealing temperature of 57 ^{o}C by primers amplifying the region upstream of BCAM2007, BCAM2007SOEfor and BCAM2007SOEmutrev, and the region downstream, BCAM2007SOEmutfor and BCAM2007SOErev. One of each pair of primers was 'mutagenic' and would allow for introduction of an in-frame deletion into the BCAM2007 gene during the second PCR step. PCR products from the first stage were checked for their correct size electrophoretically (upstream flanking fragment size of ~720 bp and downstream fragment size of ~960 bp) and purified for the subsequent step.

In the second step, the primers BCAM2007SOEfor and BCAM2007SOErev were used at an annealing temperature of 57 ^{o}C to allow joining of the two PCR products in a 1:1 ratio. This PCR product was checked electrophoretically for the size of 1680 bp and purified. It was then restriction digested with *Eco*RI and *Hin*dIII and ligated to the same sites in pEX18TpTer-*pheS*-Cm-SceI. Ligation products were transformed as previously described (Section 4.2.2). Transformed white colonies were colony-PCR screened for an expected size of 1680 bp using the primer combination, BCAM2007SOEfor and BCAM2007SOErev (Figure 5.11A). Alternatively, the candidate pEX18TpTer-*pheS*-Cm-SceI-ΔBCAM2007 plasmids were screened electrophoretically for the expected size of ~6.6 kb. Five candidates of pEX18TpTer-*pheS*-Cm-SceI-ΔBCAM2007 were obtained and two were sequenced with primer combination, M13revBACTH and M13for2 for confirmation of an in-frame deletion. The deletion removed 615 codons of the BCAM2007 gene with 133 codons remaining.

5.4.2.2 Generation of H111ΔpobA ΔBCAM2007 by allelic replacement

Generation of H111ΔpobAΔBCAM2007 using the constructed plasmid, pEX18TpTer-*pheS*-Cm-SceI-ΔBCAM2007 involved two steps. The first step of generating a merodiploid was as previously described (Section 4.7.2). In the second step, a different plasmid was used, pDAI-SceI-*pheS*-Km(for), for resolution of the integrated suicide plasmid. This plasmid was constructed by insertion of the kanamycin-resistance from p34E-Km into the *Pst*I site of pDAI-SceI-*pheS* located upstream of the *pheS* gene (Butt and Thomas, unpublished results). Conjugation was performed between the merodiploid H111ΔpobA/pEX18TpTer-*pheS*-SceI-Cm-ΔBCAM2007 and *E. coli* S17-1 donor cells containing pDAI-SceI-*pheS*-Km(for) and ex-conjugants were selected on Lennox agar containing ampicillin (100 µg ml^{-1}) and kanamycin (100 µg ml^{-1}) after 48 hrs of incubation. Fifty colonies were patched onto the same selection medium and concurrently on M9-glucose CAA agar containing trimethoprim (25 µg ml^{-1}) to identify trimethoprim-sensitive strains. Alternatively, exconjugant colonies were concurrently patched on LB medium containing chloramphenicol (50 µg ml^{-1}) to select for chloramphenicol-sensitive strains. As sensitivity towards both trimethoprim and chloramphenicol indicates resolution of the merodiploid stage, such colonies were cPCR screened using outside primers BCAM2007Out2for and BCAM2007Out2rev. Electrophoresis analysis gave rise to an expected size of 3640 bp for the wildtype and 1616 bp for BCAM2007 mutants (Figure 5.11B). The nucleotide sequence of the shorter amplicon was determined for confirmation of mutagenesis.

Surprisingly, it was observed that growth of mutants (i.e. colony size) was slower than that of the parent H111ΔpobA strain and therefore they were grown on M9-glucose agar supplemented with CAA (0.1 %). The mutant grown in an iron limited liquid medium with supplementation by a catecholate siderophore was shown to grow at an acceptable rate and was used for subsequent experiments.

5.4.3 Analysis of catecholate siderophore utilisation by H111ΔpobAΔBCAM2007

The ability of H111ΔpobAΔBCAM2007 to utilise the catecholate siderophore azotochelin, DHBS (monomer, dimer, trimer), cepaciachelin and the siderophores secreted by *S. marcescens* Db10 (serratiochelin A/B and chrysobactin) was assessed by the disc diffusion assay as previously described. Enterobactin and bacillibactin were also included (Figure 5.12). In addition, the siderophore cepabactin, featuring hydroxypyridone characteristic by having a hydroxamate ligand on a benzene ring was also examined. Filter discs spotted with purified azotochelin did not promote growth of H111ΔpobAΔBCAM2007 in the assay (Figure 5.13A). Similarly, growth of the BCAM2007 mutant in the liquid growth assay was not stimulated when iron limited medium was supplemented with azotochelin, indicating BCAM2007 is responsible in the utilisation of this siderophore (Figure 5.12A). Growth of H111ΔpobAΔBCAM2007 in the presence of enterobactin and bacillibactin assay was almost completely abolished. However, weak growth of the mutant was still observed particularly for bacillibactin (Figure 5.12B).

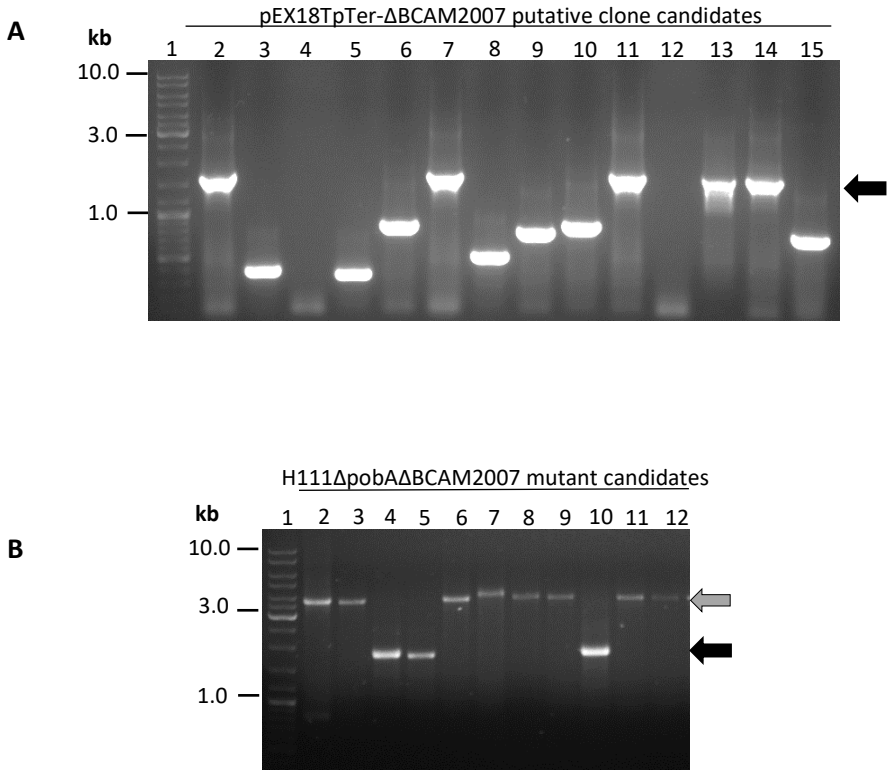

Figure 5.11: Construction of pEX18TpTer-*pheS*-Cm-SceI-ΔBCAM2007 and generation of H111ΔpobA ΔBCAM2007

(A) PCR screening of JM83 transformants containing candidate pEX18TpTer-*pheS-SceI*-Cm-ΔBCAM2007 plasmids using primer combination BCAM2007SOEfor and BCAM2007SOErev with an annealing temperature of 57°C. Positive clones gave rise to a 1.6 kb fragment as shown in lanes 2, 7, 11, 13 and 14 (black arrow). (B) H111ΔpobAΔBCAM2007 candidate mutants were screened with 'outside' primers BCAM2007Out2for and BCAM2007Out2rev using an annealing temperature of 63.5 ^{o}C, giving rise to a fragment size of 3640 bp for wildtype (grey arrow) and 1616 bp for mutants containing the ΔBCAM2007 allele. Lane 1, linear ladder; lanes, 4, 5 and 10 show mutant candidates (black arrow).

This may due to the presence of hydrolysed derivatives of both siderophores, as previously mentioned (Section 5.3.3). No promotion of growth of the ΔBCAM2007 mutant was observed in the presence of the DHBS derivatives (Figure 5.12C). However, the derivatives led to partial growth of the BCAM2007 mutant in iron-limited liquid medium (Figure 5.13B-D). This may indicate that another TBDR is involved in the transport of the DHBS derivatives.

Similarly, the ΔBCAM2007 allele caused a reduction in the ability to H111ΔpobA to utilise siderophores produced by *S. marcescens* Db10 but their utilisation was not completely abolished. As there was some growth of the ΔBCAM2007 mutant, it was not possible to conclude whether BCAM2007 is involved in utilisation of catecholate siderophores produced by *S. marcescens* (Figure 5.12D). Investigations using purified serratiochelins and chrysobactin, however were not undertaken. Growth promotion of the ΔBCAM2007 mutant was elicited in the presence of cepabactin indicating BCAM2007 may not be involved in the utilisation of cepabactin (result not shown).

5.4.4 Complementation of H111ΔpobAΔBCAM2007

To confirm the transport impediment of the catecholate siderophores was due to the inactivation of BCAM2007 and not for other reasons such as polarity effects on the downstream genes, the wild-type BCAM2007 gene was introduced into the H111ΔpobAΔBCAM2007 mutant on a plasmid.

5.4.4.1 Construction of the complementation plasmid

Attempts at cloning the BCAM2007 gene into plasmid vectors during construction of the ΔBCAM2007 allele replacement vector, as mentioned previously, encountered some setbacks. It was hypothesised that this may be due to the presence of a native promoter in the fragment being cloned. This promoter along with the promoter of the vector may cause high expression of the BCAM2007 protein which was hypothesised to cause disruption of the cell membrane, possibly leading to cell rupture, thereby obstructing cloning of the DNA fragment. To circumvent this possibility, PCR primers (BCAM2007full3for and BCAMfull4rev) were constructed which allowed for amplification of BCAM2007 by excluding the predicted native promoter sequence located 92 bp upstream of the translation start codon.

The DNA fragment encoding BCAM2007 that was amplified with these primers (~2.4 kb) was gel purified then restriction digested and ligated in parallel into broad host-range vectors, pBBRMCS-1 and pBBRMCS-2 between the *Kpn*I-*Xba*I restriction sites. Ligated products were transformed into JM83 cells as previously described. White colonies from both constructions, pBBR1-BCAM2007 and pBBR2-BCAM2007 were cPCR screened with the amplification primers (Figure 5.14A and B). The nucleotide sequence of the cloned DNA fragment in positive clones of both constructions were determined using M13for and M13rev. Sequence analysis of pBBR2-BCAM2007 (Figure 5.12B, lanes 6 and 8), however, did not show complementary amino acid alignments, suggesting unsuccessful cloning.

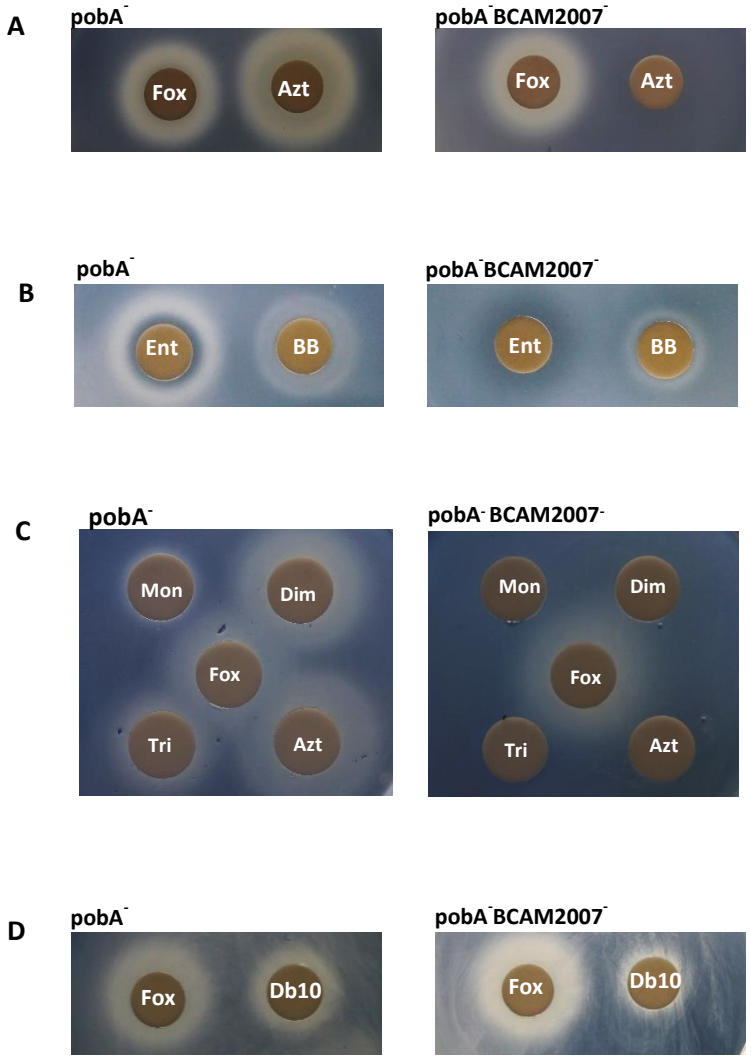

Figure 5.12: Effect of inactivation of BCAM2007 on catecholate siderophore utilisation
(A) Screening for azotochelin utilisation by H111ΔpobAΔBCAM2007 compared to H111ΔpobA. Ferrioxamine B was included as a positive control. (B) Screening for enterobactin and bacillibactin utilisation by H111ΔpobAΔBCAM2007 compared to H111ΔpobA. (C) Utilisation of DHBS derivatives by the ΔBCAM2007 mutant with ferrioxamine B and azotochelin as controls. (D) Screening for the utilisation of siderophores present in *S. marcescens* Db10 culture supernatant by H111ΔpobAΔBCAM2007 compared to H111ΔpobA with ferrioxamine B as a positive control. Filter discs were impregnated with Ent, enterobactin (1 mM, 30-100 µl); BB, bacillibactin (1 mM, 30-100 µl); Fox, ferrioxamine B (1 mM, 10-20 µl); Azt, azotochelin (1 mM, 30 µl); Mon, DHBS monomer (1 mM, 60 µl); Dim, DHBS dimer B (1 mM, 40 µl); Tri, DHBS trimer (1 mM, 20 µl) and Db10, *S. marcescens* Db10 supernatant (100 µl). Final EDDHA concentration was 40 µM.

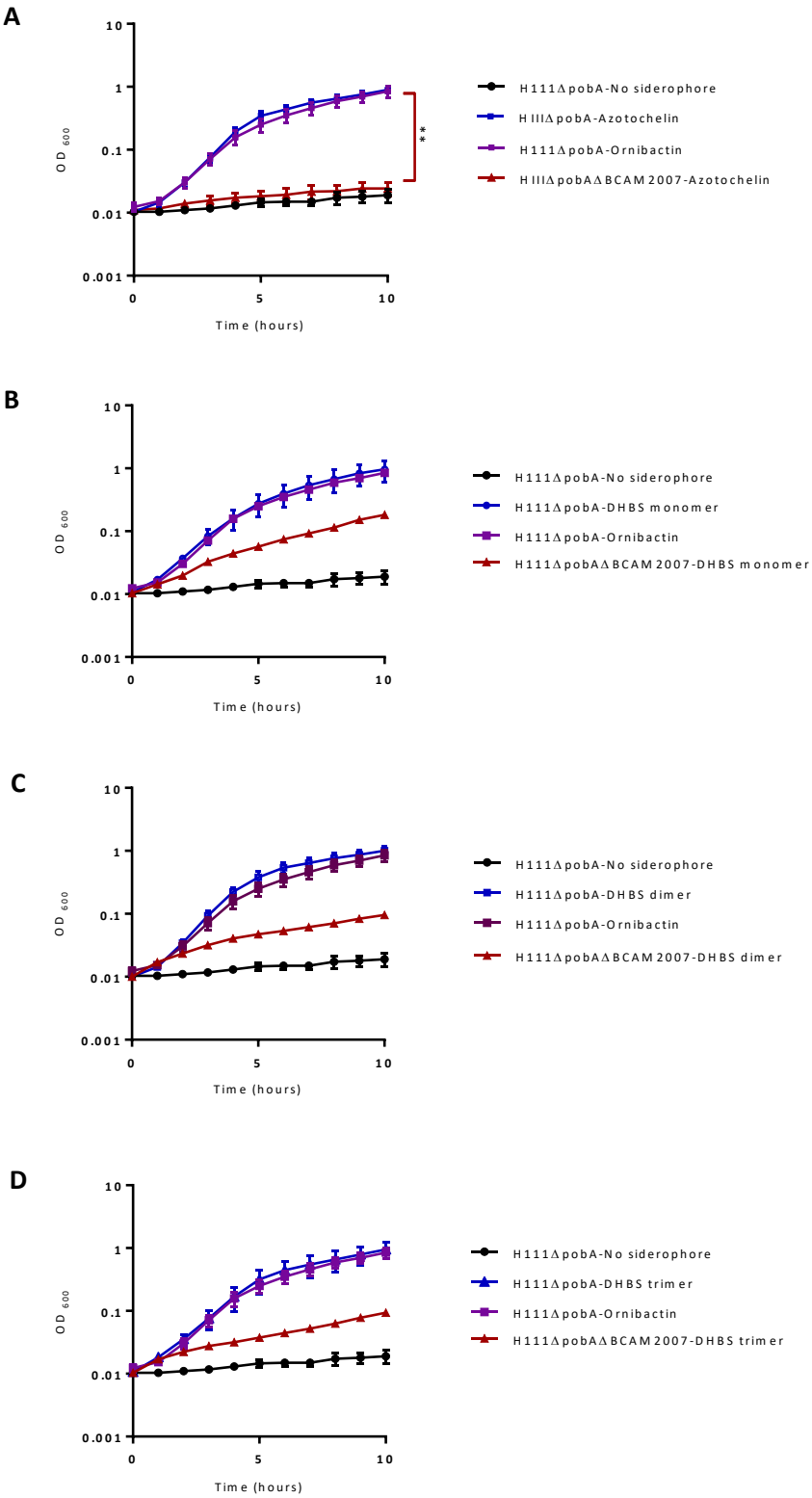

Figure 5.13: Growth curves of *B. cenocepacia* H111ΔpobAΔBCAM2007 in iron-depleted medium supplemented with azotochelin and the DHBS derivatives

The indicated bacterial strains were grown in M9-glucose CAA medium containing 1 µM DTPA at 37 ^{o}C. Medium was supplemented with 1 µm DTPA and 10 µm of the siderophore (A) Azotochelin, (B) DHBS, (C) DHBS dimer, (D) DHBS trimer. These data are representative of a minimum of three independent experiments. Error bars represent the ±SEM (n=3). *p<0.05, **p<0.01.

This may be due to the higher expression of BCAM2007 in pBBR1MCS-2 due to the promoter of the kanamycin-resistance gene. In contrast, sequencing of a candidate pBBR1-BCAM2007 plasmid (Figure 5.14A, clone from lane 6) showed the presence of the desired DNA fragment. In this case, the chloramphenicol resistance gene on the vector lacks its native promoter and so overall expression of BCAM2007 would be expected to be lower than in pBBR2-BCAM2007. This observation supports the view that only low expression levels of the BCAM2007 protein may be tolerated due to the toxicity of the membrane protein to the transformed *E. coli* JM83 cells.

5.4.4.2 Complementation of H111ΔpobAΔBCAM2007 by pBBR1MCS-BCAM2007

The constructed complementation plasmid, pBBR1-BCAM2007, and the empty vector, pBBR1MCS, were transformed into *E. coli* SM10 cells and both were conjugated into H111ΔpobAΔBCAM2007 as previously described. Exconjugants were selected on M9-glucose agar containing chloramphenicol (25 µg ml^{-1}) and purified. The generated H111ΔpobAΔBCAM2007 containing pBBR1-BCAM2007 showed better growth on this medium compared to the plasmid-less strain or the strain containing the empty vector (result not shown).

Complementation analysis was carried out by performing a disc diffusion assay with azotochelin and the trimeric DHBS derivative. The presence of pBBR1-BCAM2007 in the ΔBCAM2007 mutant led to restoration of the wild type phenotype, i.e. an ability to utilise azotochelin and DHBS trimer. In contrast, no growth of the control strain containing the empty vector was observed around filter discs impregnated with the catecholate siderophores (Figure 5.15A). Restoration of catecholate utilisation by pBBR1-BCAM2007 indicates no polarity effect of the ΔBCAM2007 lesion on downstream gene expression. The liquid growth stimulation assay was employed to test for complementation using azotochelin, and complementation of the BCAM2007 mutant by pBBR1-BCAM2007 was confirmed. The growth curve obtained in medium supplemented with azotochelin showed full restoration of the wild type ('BCAM2007-positive') phenotype (Figure 5.15B). Complementation was not performed using the DHBS derivatives due to the intermediate growth rate of the BCAM2007 mutant in the iron limited liquid assay supplemented with DHBS derivatives, as previously mentioned.

5.5 Investigation of the role of BCAM2007 in cepaciachelin utilisation

It was shown earlier that spent culture supernatants of *B. ambifaria*, which is known to produce ornibactin and cepaciachelin (Barelmann et al., 1996; Esmaeel et al., 2016), supported growth of H111ΔpobA and H111ΔpobA-orbA::TpTer under iron limited conditions in the disc diffusion assay (Section 5.2.4). This may suggest that *B. cenocepacia* can utilise cepaciachelin, unless *B. ambifaria* also produces a third siderophore.

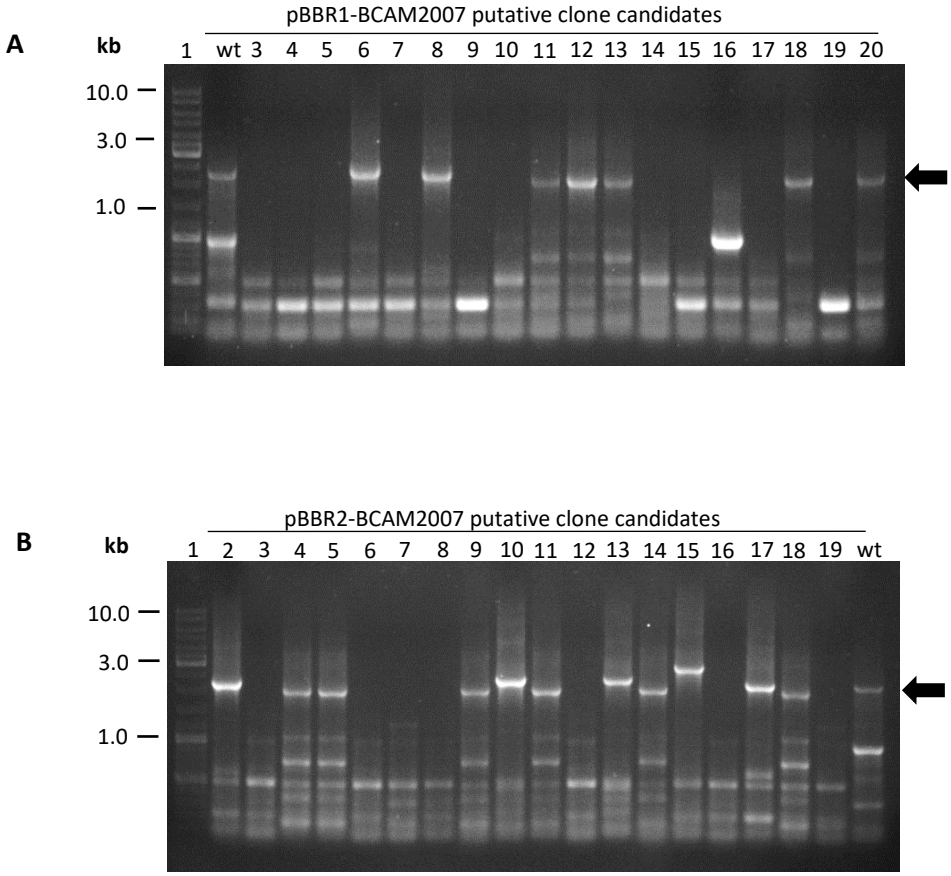

Figure 5.14: PCR screening of *E. coli* JM83 transformants containing candidate BCAM2007 complementation plasmids

(A) Putative clone candidates of pBBR1-BCAM2007 were screened using primer combination BCAM2007fullfor3 and BCAM2007fullrev4 at an annealing temperature of 59 ^{o}C. (B) Putative clone candidates of pBBR2-BCAM2007 were cPCR screened using primer combination of BCAM2007fullfor3 and BCAM2007fullrev4 at an annealing temperature of 59 ^{o}C. Products were electrophoresed in 0.8 % agarose gel. Lane 1 in A and B is the DNA linear ladder. Plasmids giving rise to an amplicon of the expected size (2.4 kb) shown by the arrow were verified by DNA sequencing.

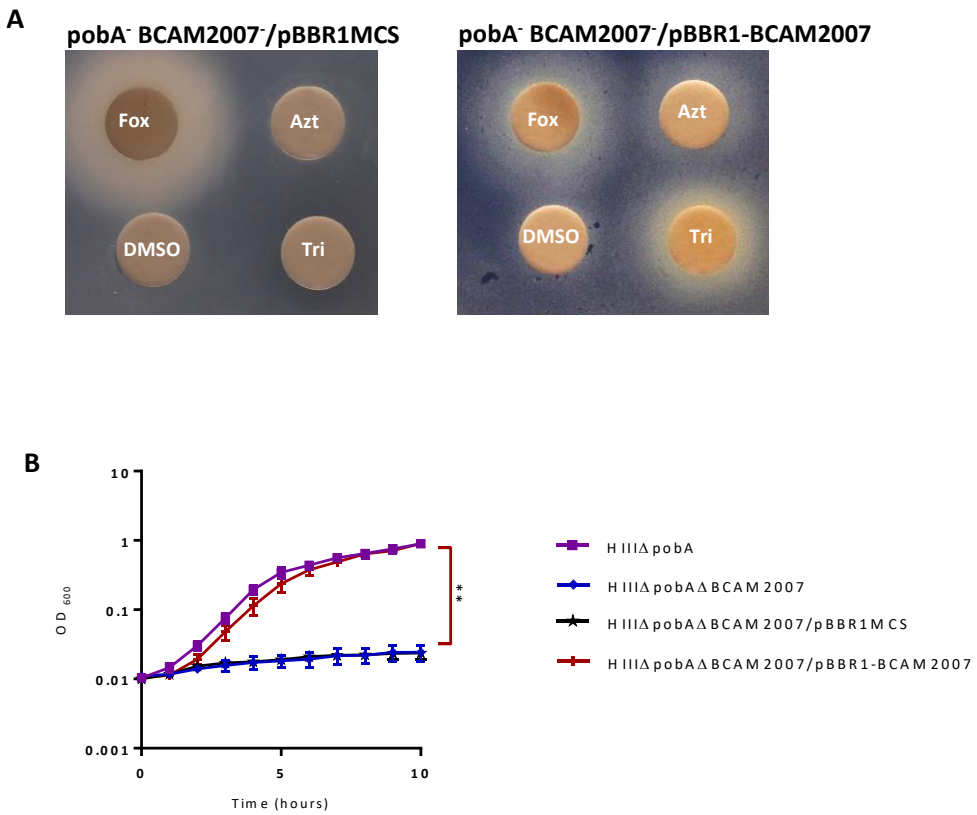

Figure 5.15: Complementation of the ΔBCAM2007 mutant for catecholate siderophore utilisation
(A) Restoration of the ability of the BCAM2007 mutant to use the catecholate siderophores using azotochelin and the DHBS trimer following introduction of pBBR1-BCAM2007. Ferrioxamine B and DMSO were included as controls. Filter discs were spotted Fox, ferrioxamine B (1 mM, 20 µl); Azt, azotochelin (1 mM, 10 µl); Tri, DHBS trimer (1 mM, 20 µl) and DMSO (20 µl). Final EDDHA concentration was 40 µM. (B) Growth curve of the BCAM2007 mutant containing pBBR1-BCAM2007 under iron-limiting conditions showing restoration of the ability to use azotochelin. These data are representative of a minimum of three independent experiments. Error bars represent the ±SEM (n=3). *$p<0.05$, **$p<0.01$.

To determine whether the siderophore that *B. cenocepacia* is able to use in addition to ornibactin is a catecholate siderophore (consistent with the use of cepaciachelin), the *orbA*::TpTer allele was introduced into H111ΔpobAΔBCAM2007. H111ΔpobAΔBCAM2007-orbA::TpTer was generated by using the constructed suicide vector, pSHAFT2-*orbA*::TpTer, as described in Section 6.4.1. PCR screening of candidate H111ΔpobAΔBCAM2007-orbA::TpTer mutants is shown in Figure 5.16.

The ability of the double TBDR mutant H111ΔpobAΔBCAM2007-orbA::TpTer to utilise siderophores produced by *B. ambifaria* was tested using the disc diffusion assay concurrently with H111ΔpobA, H111ΔpobA-orbA::TpTer and H111ΔpobAΔBCAM2007. This is because a spent culture supernatant of *B. ambifaria* was used instead of using purified cepaciachelin and therefore both ornibactin and cepaciachelin would be present. The results showed that *B. ambifaria* spent culture supernatant did not support growth of H111ΔpobAΔBCAM2007-orbA::TpTer, whereas it promoted the growth of H111ΔpobAΔBCAM2007 and, as previously shown, H111ΔpobA and H111ΔpobA-orbA::TpTer (Figure 5.17). This suggests that H111 is able to use ornibactin and one or more catecholate siderophores that depend on BCAM2007 for their uptake. In view of the fact that culture supernatant of *B. ambifaria* elicited growth of H111ΔpobA-orbA::TpTer in the disc diffusion assay, this was consistent with the presence of cepaciachelin in the supernatant. No promotion of growth was elicited by H111ΔpobAΔBCAM2007-orbA::TpTer with azotochelin as expected. Ferrioxamine B allowed growth of all the mutants and acted as a positive control for the assay.

5.6 Investigation of the role of BCAM1187 in DHBS utilisation

Due to the observation that the DHBS derivatives still allow slow growth of the TBDR mutant, H111ΔpobAΔBCAM2007, in the liquid growth stimulation assay in contrast to that with azotochelin, another putative TBDR, BCAM1187, was hypothesised to be involved in catecholate siderophore utilisation. This was based on the observation that they are closely related in the phylogenetic tree analysis (Section 3.3). Therefore, the mutants, H111ΔpobA-BCAM1187::TpTer and H111ΔpobAΔBCAM2007-BCAM1187::TpTer were generated to test this hypothesis.

5.6.1 Generation of H111ΔpobA-BCAM1187::TpTer and H111ΔpobAΔBCAM2007-BCAM1187::TpTer

These mutants were generated by introducing the previously constructed plasmid, pSHAFTGFP-BCAM1187::TpTer (Sofoluwe & Thomas, unpublished) into the mutant strains, H111ΔpobA and H111ΔpobAΔBCAM2007 by conjugation. Selection of mutant strain, H111ΔpobA BCAM1187::TpTer and H111ΔpobAΔBCAM2007-BCAM1187::TpTer was performed as described in Section 4.4.2 (Figure 5.18A and B).

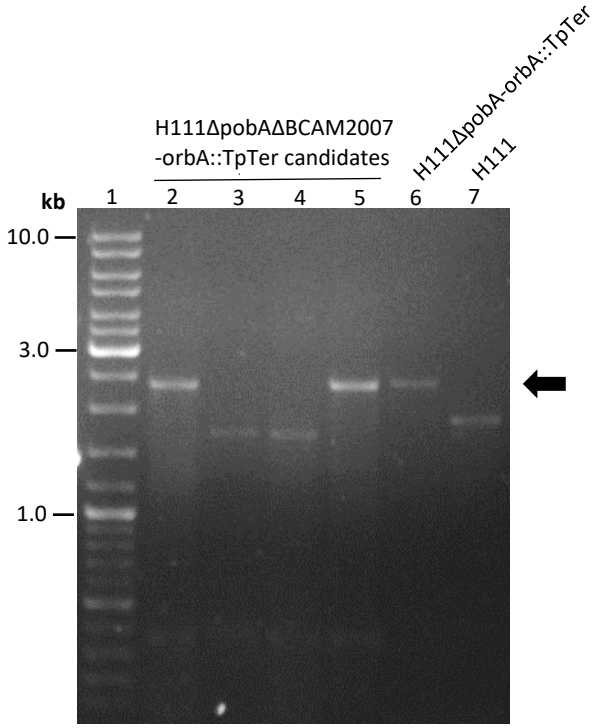

Figure 5.16: Generation of H111ΔpobAΔBCAM2007-orbA::TpTer mutants
PCR screening of candidate H111ΔpobAΔBCAM2007-orbA::TpTer mutants following allelic replacement with pSHAFT2-orbA::TpTer using 'outside primers' BCAL1700forout and BCAL1700revout flanking the *orbA* gene with an expected fragment size of 2342 bp for the *orbA*::TpTer allele (black arrow). Lane 1, linear ladder; lanes, 2 and 5 show mutant candidates; lanes 6, H111ΔpobA-orbA::TpTer as positive control; lane 7, H111 wildtype as negative control.

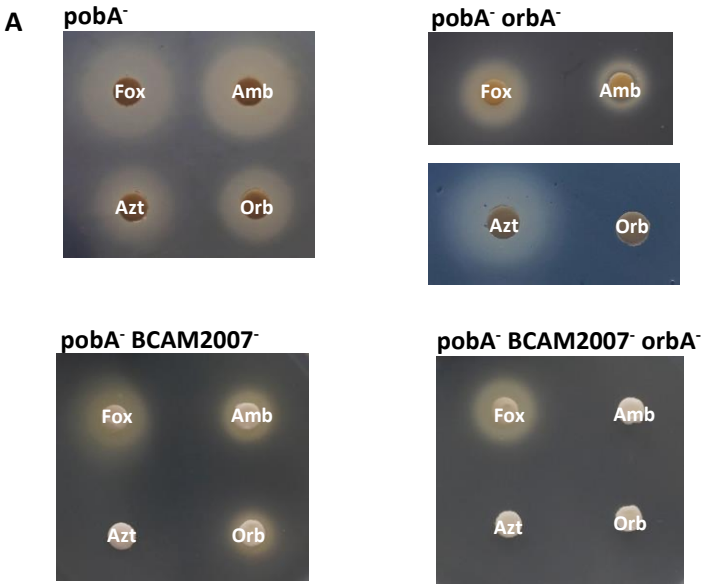

Figure 5.17: Role of BCAM2007 in cepaciachelin utilisation by *B. cenocepacia*
(A) Demonstration of the role of BCAM2007 in utilisation of cepaciachelin from the culture supernatants of *B. ambifaria* AMMD using disc diffusion assay. Filter discs were spotted with *B. ambifaria* AMMD culture supernatant (40 µl); Fox, ferrioxamine B (1 mM, 5µl); Orb, ornibactin (1 mM, 5 µl and Azt, azotochelin (1 mM, 5 µl) and placed on iron limited agar plate overlaid with H111ΔpobA, H111ΔpobA-orbA::TpTer, H111ΔpobAΔBCAM2007 and H111ΔpobAΔBCAM2007-orbA::TpTer. Final EDDHA concentration was 40 µM.

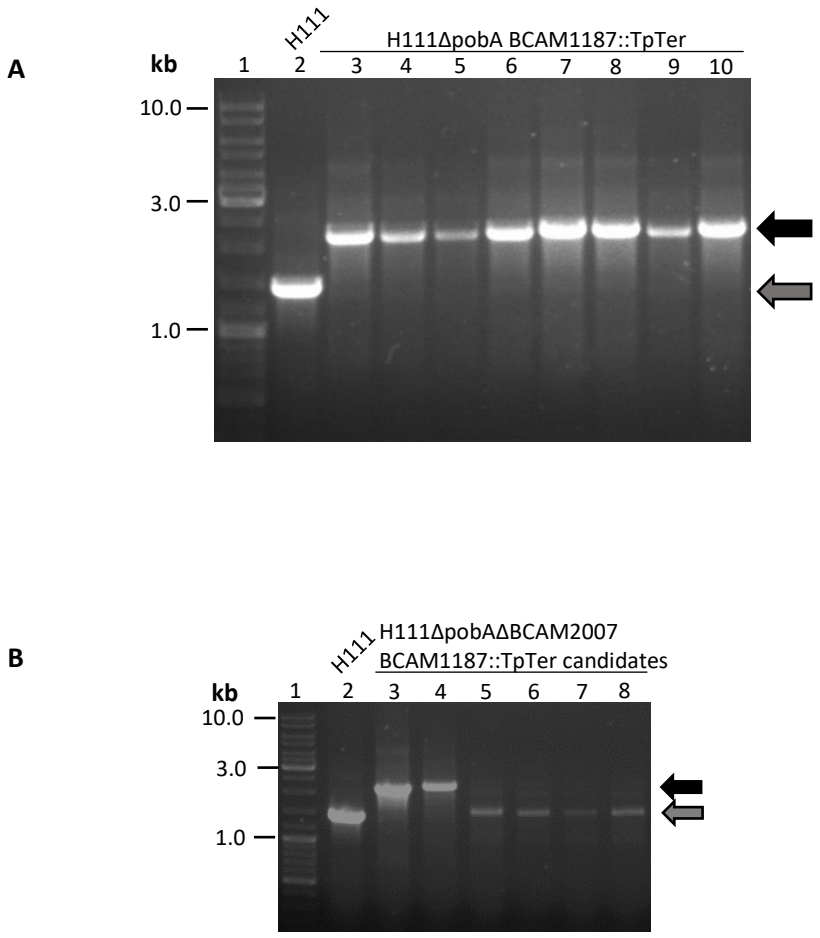

Figure 5.18: Generation of *B. cenocepacia* BCAM1187 mutants
(A) PCR screening of candidate H111ΔpobA-BCAM1187::TpTer mutants following allelic replacement with pSHAFTGFP-BCAM1187::TpTer using 'outside' primers BCAM1187forout and BCAM1187revout at an annealing temperature of 57 ^{o}C. (B) PCR screening of candidate H111ΔpobAΔBCAM2007-BCAM1187::TpTer mutants using the same set of primers at an annealing temperature of 55 ^{o}C. In A and B the expected size of the BCAM1187::TpTer amplicon (2172 bp) is indicated by a black arrow and the wild type amplicon (1426 bp) is indicated by a grey arrow.

5.6.2 Analysis of the role of BCAM1187 in disc diffusion and liquid growth stimulation assays

DHBS monomer was used as a representative siderophore in the liquid growth assay to assess the effect of inactivating BCAM1187. The growth rate of H111ΔpobAΔBCAM2007-BCAM1187::TpTer in medium supplemented with DHBS monomer, however, was almost the same as that of H111ΔpobAΔBCAM2007 (result not shown), i.e. the growth rate was less than the H111ΔpobA strain in the presence of ornibactin but greater than that of the H111ΔpobA strain in the absence of the siderophore, and may indicate that BCAM1187 is not involved in the transport of the DHBS catecholates. The reason for the slow growth of H111ΔpobAΔBCAM2007 with the DHBS derivatives therefore, remains unsolved and possibilities are discussed in Section 5.9.

5.7 Role of the *B. cenocepacia* TonB1 system in utilisation of catecholate siderophores

Hydroxamate siderophores were shown in this study to require the main TonB1 complex for their transport into the cytoplasm of *B. cenocepacia.* Catecholate xenosiderophores were tested using the same *B. cenocepacia exbB1* mutant, AHA9, to investigate whether they require the same protein complex to energise their transport.

5.7.1 Analysis of catecholate siderophores utilisation by a B. cenocepacia *exbB1* mutant

Catecholate siderophores, in this case, all the DHBS derivatives and azotochelin, were spotted on filter discs and laid individually on iron-restricted LB agar overlaid with *B. cenocepacia* AHA9. The assay demonstrated that all these catecholate siderophores also require TonB1 complex for their uptake (result not shown).

5.8 Investigation of the role of BCAL0117 in utilisation of catecholate siderophores

As mentioned in Chapter 4, most hydroxamate siderophores are transported through the cytoplasmic membrane by the BCAL0117 membrane protein. Therefore, catecholate siderophore were screened to find out whether they are also transported via the same predicted inner membrane protein. Disc diffusion assay using azotochelin as the representative catecholate siderophore showed growth promotion of H111ΔpobAΔBCAL0117 under iron limiting condition, indicating that azotochelin, and by implication the other catecholate siderophores, are not transported across the cytoplasmic membrane by the BCAL0117 protein (result not shown).

5.9 Discussion

5.9.1 Utilisation of catecholate siderophores by *B. cenocepacia*

The exogenous catecholate siderophores found to be utilised by *B. cenocepacia* in this study are azotochelin, cepaciachelin, one or more of the catecholate siderophores produced by *S. marcescens* Db10 (serratiochelin and chrysobactin) as well as the linear analogue of enterobactin (DHBS trimers) and its progenitors (the DHBS monomer and dimer). The non-utilised siderophores identified were vibriobactin, the catecholate siderophores produced by *A. baylyi* (fimsbactin), enterobactin and bacillibactin. Additionally, *P. aeruginosa*, used as a control for presence of siderophores in the culture supernatants of *A. baylyi*, *E. coli* and *B. subtilis*, may demonstrate evidence of utilisation of the fimsbactins and bacillibactin by *B. cenocepacia* and also confirmed utilisation of enterobactin by *P. aeruginosa*.

Enterobactin and bacillibactin were initially expected to be utilised by *B. cenocepacia* based on promotion of growth of the *pobA* mutant in the disc diffusion assay. However, the low growth rate of the *B. cenocepacia* siderophore-deficient mutants in the presence of enterobactin and bacillibactin in the liquid growth stimulation assay indicated that these siderophores are not utilised by *B. cenocepacia*. Moreover, the liquid growth stimulation assay clearly showed the more effective utilisation of enterobactin precursors, as compared to enterobactin.

The chirality of enterobactin is reported to be crucial for iron uptake as the enantiomer of enterobactin, D-enterobactin, is not able to be utilised by *E. coli* (Abergel et al., 2009). Utilisation of enterobactin (and bacillibactin) by *E. coli* is mediated by a cytosolic hydrolytic enzyme, an esterase referred to as Fes (BesA for bacillibactin in *B. subtilis*) (Miethke et al., 2006). This esterase hydrolyses the trilactone backbone of the siderophore into DHBS; monomer, dimer and trimers (Raymond et al., 2003). Whilst *E. coli* Fes is stereospecific in hydrolysing enterobactin, the periplasmic esterase, CEE (Cj1376), in *Campylobacter jejuni* is reported to be able to hydrolyse D-enterobactin but less efficiently than the natural enterobactin (Zamora et al., 2018). These observations demonstrate varying structure-oriented preferences in the enterobactin-iron uptake pathways.

With respect to *B. cenocepacia*, the inability to utilise enterobactin and bacillibactin demonstrated in this study are accentuated by the absence of the esterase gene in *B. cenocepacia* H111 by *in silico* analysis. This was concluded by performing a BLASTP analysis using the *E. coli* Fes protein (KO7214) and the *P. aeruginosa* PfeE esterase (PA2689) as queries (Brickman and McIntosh, 1992; Perraud et al., 2018). However, the hydrolysed products of enterobactin (and bacillibactin), appear to be utilised by *B. cenocepacia* and that Fes-related enzymes are not required in this context. These spontaneous degraded products have been reported to act as weak siderophores for *E. coli* under low iron conditions and thereby may have the ability to provide iron to other bacterial species (Hantke, 1990).

It was demonstrated in this study that DHBS and its dimer and trimer forms (Figure 5.19A-C) promote growth of H111ΔpobA at a comparable efficiency to each other. This suggests that the differences in the number of atoms or ligands, between the monocatecholate and the tricatecholate, does not markedly influence iron uptake. The growth rate of H111ΔpobA at a concentration of 10 µM of each of the DHBS derivatives implies that the rate of iron uptake achieved was similar to that stimulated by endogenous siderophores. Additionally, it has been documented that DHBS (monomer) is a faster scavenger of iron than enterobactin due to its extra carbonyl groups in the molecule, causing it to exhibit a tridentate ligand characteristic (Raines et al., 2016).

From the investigations with culture supernatants, it can be inferred that *B. cenocepacia* is able to benefit from the secretions of *E. coli* and the *Bacillus* spp., in this case, *B. subtilis,* due to the production of the siderophore biosynthetic intermediates and degradation products. It is shown from this study that *B. cenocepacia* does not use cyclic enterobactin but instead uses its linear derivatives, as demonstrated by *V. cholerae* (Wyckoff et al., 2015; Raines et al., 2016).

Iron-deficient *E. coli* culture supernatants are demonstrated to include DHBS, its dimers and trimers, as well as the enterobactin precursor, dihydroxybenzoic acid (DHBA) and also enterobactin (Furrer et al., 2002; Berner et al., 1991). Enterobactin is known to be easily hydrolysed at its ester bonds causing it to be unstable and only exist in small amounts in iron-deficient culture media. However, it remains unclear whether the presence of DHBS in cultures is due to degradation of enterobactin or as a result of its direct release as intermediates (Hider and Kong, 2010). The ability of *B. cenocepacia* to utilise DHBS monomers suggests a minimal determinant of iron transport by a catecholate and this may offer an added advantage to the fabrication of antibiotic-siderophore conjugates due to its small and easily-synthesised nature. The construction of antibiotic-siderophore conjugates in which DHBS derivatives are linked to the antibiotic ciprofloxacin has been reported by Neumann et al. (2018). However, the extent to which these conjugates are beneficial in controlling infectious disease through iron uptake pathways is still under investigation.

It was demonstrated in this study that *B. cenocepacia* cannot utilise vibrobactin. The fact that the InterPro analyses of the putative TBDRs of *B. cenocepacia* in Chapter 3 have not detected a protein similar to the TBDR ViuA (IPR030150) for the transport of vibriobactin supports this observation. Vibriobactin possess an unusual structure in which the catecholate ligands in the compound are located in a distinctive position and this may limit the degree to which it can be taken advantage of by other bacteria. Vibriobactin is produced by *Vibrio* species such as *V. cholerae*. Some *Vibrio* spp. act as intestinal pathogens (Wyckoff et al., 2001), but pneumonia-related disease caused by *V. cholerae* has also been documented (Shannon and Kimbrough, 2006).

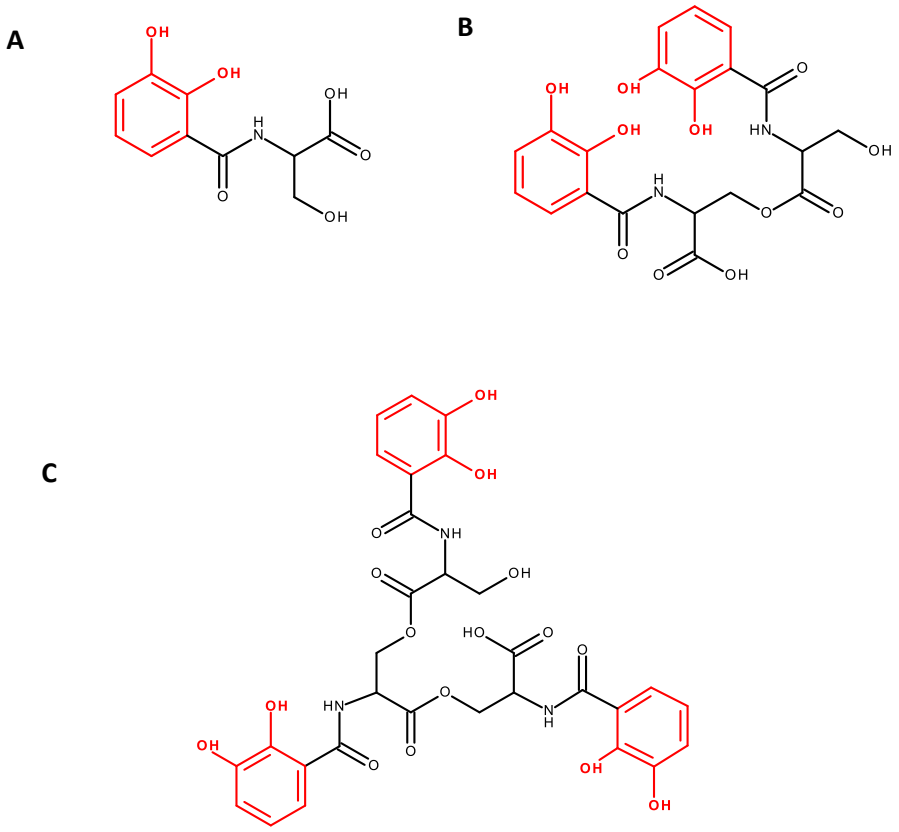

Figure 5.19: Molecular structures of the DHBS derivatives siderophores tested in this study
(A) DHBS monomer, (B) DHBS dimer and (C) DHBS trimer. Catecholate ligand are depicted in red. Structures were drawn using Accelrys 4.2.

As both *Burkholderia* and *Vibrio* spp. do not occupy the same environmental niche, it is not surprising that *B. cenocepacia* cannot utilise the triscatcholate, vibriobactin. Moreover, *V. cholerae* uses a different TBDR to transport vibriobactin (ViuA) and the linear derivatives of enterobactin (IrgA and VbtA) (Wyckoff et al., 2015). The latter is also shown to be utilised by *B. cenocepacia* in this study.

It has been reported that *A. baylyi* secretes structurally related siderophores possessing one or more catecholate groups, fimsbactin A-F, and another unidentified siderophore (Proschak et al., 2013). Among the fimsbactin derivatives, two contain only catecholate groups for iron binding: fimsbactin D and E. However, none of these siderophores i.e. including the unidentified ones, promoted growth of *B. cenocepacia* based on the disc diffusion assay. Although the specific siderophores present in the supernatants of *A. baylyi* used in this study were not determined, some siderophores were evidently present judged by promotion of growth elicited by *P. aeruginosa*. The supernatants of *A. baylyi* were screened to investigate whether a pathogenic species of the same genus, might provide an additional iron resource to *B. cenocepacia*.

The most clinically relevant among these pathogenic species, *A. baumanii,* has been reported to cause hospital-acquired pneumonia in immunocompromised patients, so may on occasion occupy a similar niche to *B. cenocepacia*. i.e. water and soil (Fournier et al., 2006). However, this study did not provide evidence to suggest that *B. cenocepacia* can utilise fimsbactin and the other unidentified siderophore. Fimsbactins, which are also produced by *A. baumanni*, as well as acinetobactin and baumannoferrin, is therefore not likely to take part in providing iron sources to *B. cenocepacia.*

Azotochelin is a biscatecholate produced by a non-pathogenic nitrogen-fixing soil bacterium, *Azotobacter vinelandii*. The Azotobacter species originates from *Pseudomonadaceae*, and posseses some traits of *P. aeruginosa* including the production of alginate, a virulence trait in the CF lungs. Azotochelin is known to have a nearly identical structure to the siderophore myxochelins. Azotochelin has a terminal carboxyl group rather than an alcohol hydroxyl present in myxochelin A or a terminal amino group exhibited by myxochelin B. It is also similar to myxochelin C, but this siderophore is a triscatecholate instead of a biscatecholate (Figure 5.20A-D). Additionally, azotochelin is also similar to the biscatecholate cepaciachelin, in which cepaciachelin possesses the same structure as azotochelin but with the terminal carboxyl group amidated with putrescine (diaminobutane) (Figure 5.20E). Cepaciachelin, demonstrated to be utilised by *B. cenocepacia* in this study, is produced by *B. ambifaria* and is predicted to be produced by several other Bcc members, i.e *B*. *metallica* and *B. multivorans,* and is proposed as a secondary siderophore after ornibactin (Barelmann et al., 1996; Butt and Thomas, 2017). Accordingly, *B. cenocepacia,* as the predominant lung pathogen, may out compete these species due to its added options of utilising cepaciachelin for iron sources.

B. multivorans, which is also categorised as the common cause of Bcc infection in the CF lungs, possesses eleven of the 22-24 TBDRs (refer Chapter 3) that *B. cenocepacia* has, which may limit the potential exogenous siderophores that it can utilise. Also, the approximate ten TBDRs that *B. multivorans* possesses may not be relevant in infection. Moreover, based on the analyses presented in Chapter 3, *B. multivorans* does not possess the TBDR for pyochelin transport, BCAM2224 (FptA). This enables *B. cenocepacia* to utilise all three siderophores, ornibactin, pyochelin and cepaciachelin whilst *B. multivorans* benefits from only two. However, the two unique and functionally unknown TBDRs found in *B. multivorans* ATCC17616 (Bmul_2944 and Bmul_3574) may give it an alternative advantage in a polymicrobial infection.

S. *marcescens* is an opportunistic pathogen that causes significant hospital-acquired diseases, including nosocomial pneumonia in CF patients (Yan et al., 2018). *S. marcescens* may also be involved in supplying additional iron resources to *B. cenocepacia*. The *S. marcescens* Db10 strain infects insects (Flyg et al., 1980), and has not been reported to act as an opportunistic pathogen in humans.The dicatecholate siderophores, serratiochelin A, B and C, were reported to exist in culture supernatants of *Serratia* sp. V4 strain, with the A and B forms as the intended products. Different forms of serratiochelin may exist interchangeably due to the instability of the compound. The structure of serratiochelin B is shown in Figure 5.20F.

Mass spectrometric characterisation of spent culture supernatants of *S. marcescens* Db10 in this study revealed identical production of siderophores relative to the *Serratia* V4 strains. Based on mass spectroscopy profiling, chrysobactin and yersiniabactin were seen as more abundant. Serratiochelin may seem to be less abundant due to its existence in different forms including in its degradation form, serratiochelin C. Nevertheless, the highest serratiochelin-based peak observed was serratiochelin C. The serratiochelin biosynthetic gene cluster was also detected in Db10 strain by performing BLASTP using the cognate genes in *Serratia sp.*V4 strains (Seyedsayamdost et al., 2012).

Chrysobactin is the only monocatecholate apart from DHBS reported in this study. It was recently reported to be produced by *S. marcescens* SM6 (Sorokina et al., 2018). The most common chrysobactin producer is the plant pathogen *Dickeya* spp. specifically, *D. dadantti* and *D. chrysanthemi*. These enterobacteria cause soft rot on a collection of host plant species (Kieu et al., 2012).

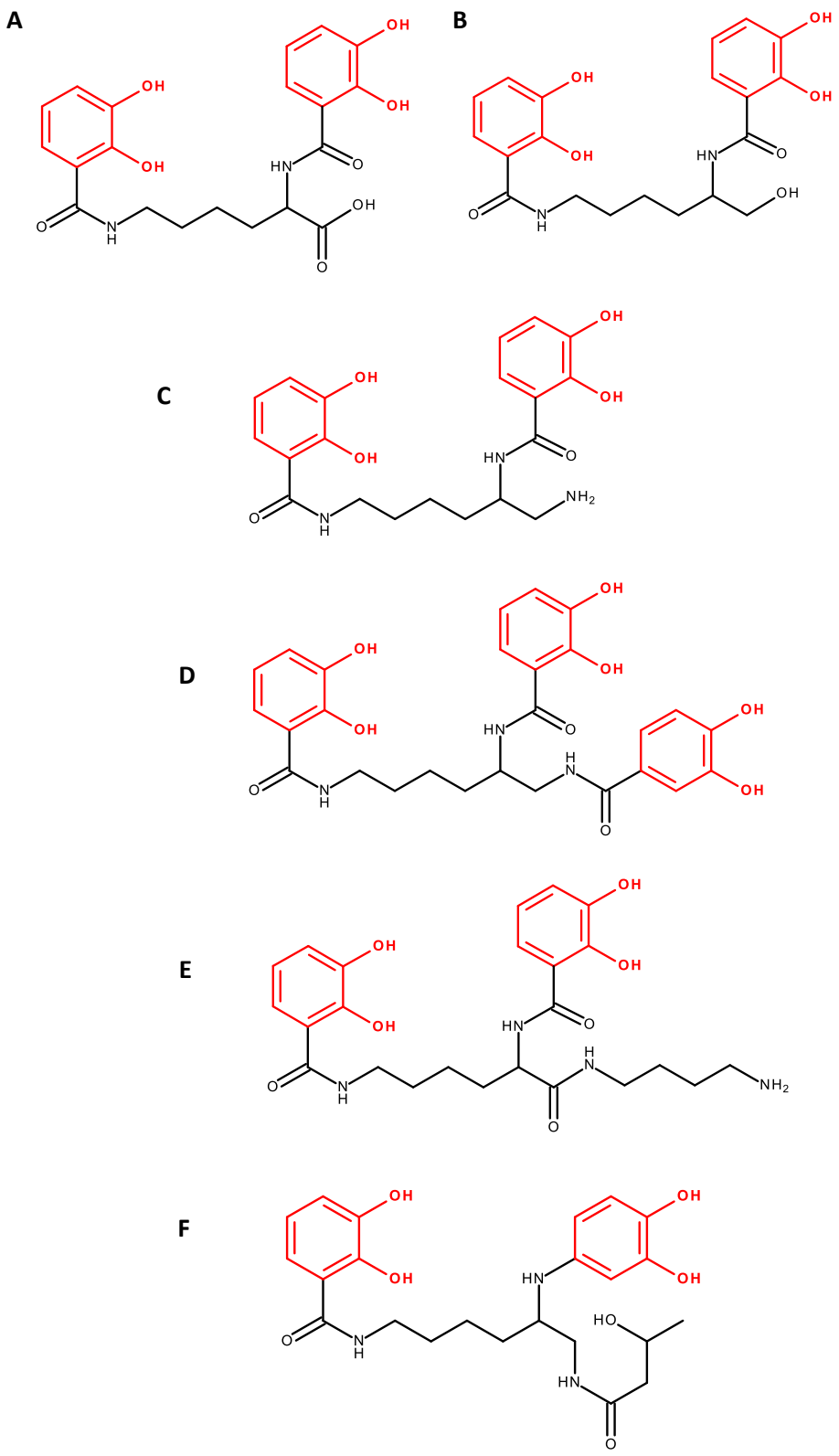

Figure 5.20: Molecular structures of bis- and tris- catecholate siderophores
(A) azotochelin, (B) myxochelin A, (C) myxochelin B, (D) myxochelin C, (E) cepaciachelin, (F) serratiochelin B. Molecular structures of A to E are bis-catecholate siderophores. The catecholate ligands are depicted in red.

5.9.2 Transport of catecholate siderophores by *B. cenocepacia*

The putative TBDR BCAM2007/I35_RS25625 was demonstrated as a receptor responsible for the transport of catecholate siderophores in this study. This observation correlates with the prediction of the InterPro analysis, which also identified another two TBDRs, BCAM1187 and BCAM0499, as potential transporters of catecholate siderophores. As BCAM1187 and BCAM2007 are closely related in phylogenetic analyses (Chapter 3), and as BCAM2007 is not wholly responsible for transport of DHBS derivatives, the function of BCAM1187 was also investigated. However, based on growth promotion assays performed in this study, the function of BCAM1187 was not elucidated. It may, however, be involved in the transport of selected catecholate siderophores to a lesser extent. The intermediate growth rate of the BCAM2007 mutant and the BCAM2007-BCAM1187 double TBDR mutant (*B. cenocepacia* Δ*pobA* background) in the presence of DHBS derivatives suggested the participation of another TBDR.

Due to the fact that BCAM0499 is also predicted to be a catecholate TBDR by InterPro analysis as previously stated, it is likely that BCAM0499 is the other predicted TBDR. Although the DHBS derivatives has shown to promote growth of the single BCAM0499 TBDR mutant in a disc diffusion assay, it would be interesting to generate a BCAM2007-BCAM0499 double mutant to verify this prediction.

P. aeruginosa is described as having two outer membrane receptors for transporting catecholate siderophores, PfeA (PA2688) and PirA (PA0931). The TBDR PfeA is reported to be the main receptor and PirA is secondary (Ghysels et al., 2005). Alignment of these TBDRs to BCAM2007 displayed sequence similarities with a homology of 20 % and 21 %, respectively. In addition, Van Delden and colleagues reported BCAM2007 to be analogous to PiuA (PA4514), a putative TBDR in *P. aeruginosa* PAO1. The organisation of the *piuA* operon also exhibits similarity to that of BCAM2007 in *B. cenocepacia* (Van Delden et al., 2013). PiuA is shown to have a higher sequence identity (47 %) to BCAM2007 (Figure 5.21A), as compared to the TBDR, PfeA and PirA. By a neighbour-joining phylogenetic analysis, it is highly likely that PiuA is an orthologue of BCAM2007 (Figure 5.21B). PiuD has also recently been demonstrated as the orthologue of PiuA found in a different strain of *P. aeruginosa,* LESB58 (Luscher et al., 2018). The crystal structure of *P. aeruginosa* PiuA has been determined (Moynié et al., 2017) and could be used to model BCAM2007 (Figure 5.22).

In *E. coli*, three TBDRs are related to catecholate transport: FepA, CirA and Fiu. Analysis of the catecholate siderophore uptake pathways in *E. coli* showed that enterobactin is transported by FepA, a TBDR encoded in the enterobactin biosynthesis cluster (McIntosh and Earhart, 1977) and to a lesser extent by Cir and Fiu (Möllmann et al., 2009). However, the enterobactin intermediate, DHBS, is primarily transported by Fiu and FepA, and less efficiently by Cir; while the enterobactin precursor, DHBA, is transported primarily by Fiu and Cir and less efficiently by FepA (Hantke, 1990).

A

```
PfeA              1 ---MSSRALPA--VPFLLLSSCLLAN---------AV--HAAG---QGDGSVIELGEQTV
PirA              1 MYPQFRRGHLA--AAVLFASSSLLGGQALAED--ERL--EELD---ERAESVVQLGDEVV
PiuA              1 ---MSRQSTDTAVSSQRLLASAIGVA-ITAIAAPQAAQADEAGQKKTDKDRVLSLDAATI
I35_RS25625       1 ---MKSRPDELKLGKFTTLCSVLAASPAFADGTPPAAPASTEG------------HLAPI

PfeA             42 VATAQEE----------------TKQAPGVSIITAEDIAKRPPSNDLSQIIRTMPGVNLT
PirA             52 LGTAEQE----------------LKQAPGVSIITAEDIRKRPPVNDLSEIIRTMPGVNLT
PiuA             57 VGEQQDETTYNVDRSASKKYTAPLLDTPKTVTVIPQQVIKDTGALTLADALRTTPGITFG
I35_RS25625     46 EIQGKTEHSYKADFSASAKFTAPLVDTPKSVTVIPQEIIQSSGAATLTEALRTVPGITFG

PfeA             86 GNSSSGQRGNNRQIDIRGMGPENTLILVDGKPVSSRNSVRYGWRGERDSRGDTNWVPADQ
PirA             96 GNSSSGQRGNNRQIDIRGMGPENTLILVDGKPVSSRNSVRYGWRGERDTRGDSNWVPPEE
PiuA            117 AGEGGNPAGD--RPFIRGFNAESDTFLDG----------------MRDVASQT--REVFN
I35_RS25625    106 AGEGGNPLGD--RPFIRGYDTQGSMFVDG----------------MRDTGATT--REIFN

PfeA            146 VERIEVIRGPAAARYGNGAAGGVVNIITKQAGAPTHGNLSVYSNFPQHKAEGASERMSFG
PirA            156 VERIEVLRGPAAARYGSGAAGGVVNIITKRPTDRLRGSMTVFTNIPESSKDGATRRANFS
PiuA            157 VEQIEVSKGPGSAYTGAGSTGGSLNLISKTAKQPNFTDAGFTW------GSDQTRRTTLD
I35_RS25625     146 TERVEITKGSDGAYGGRGGAGGSINLITKAPHLGTTAAASAGL------GTDRYRRFTAD

PfeA            206 LNGPLTINLSYRVYGNIAKTDSDDWDINAGHESNRIGKQAGTLPAGREGVRNKDIDGLLS
PirA            216 LSGPLTFALSFRAYGSANKTDSDDTDINLGHTVNPSR-----TVAGREGVRNRDLSGMLS
PiuA            211 VNRMIGDNAAFRL--------------NLM--------KHDAHVAGRDE------VSVSR
I35_RS25625     200 GNWQFADHAAFRL--------------NLM--------SHNNDVAGRDA------VNNER

PfeA            266 WRLTPEQTLEFEAGFSRQGNIYTGDTQN--------------TNSNNYVKQ---MLGH--
PirA            271 WQVTPDQVVDFEAGFSRQGNIYAGDTQN--------------NNGTANTQG-LADDGA--
PiuA            243 WGVAPTVTFGFDTPTRATLSYYHLSTDDMPDYGIPLTNVNRS---KANPSKPASVDRDNF
I35_RS25625     232 WGVAPSIAFGLGTSTRVTASYYHLQTDDMPDGGIPYFYTTSNKPANVDTIYPAPVDRHNF

PfeA            307 --ETNRMYRET------YSVTHRGEWDFG---------SSL--AYLQYEKTRNSRINEGL
PirA            314 --ETNRMYREN------YAITHNGTWSFG---------TSR--FVAQYDSTRNNRLEEGL
PiuA            300 YGLKDRDYRKSTTDSGTFRIEHDLNDNLTLSNSTRLVRTTLDYIVSNPDDSRGNVAN---
I35_RS25625     292 YGLIDRDFRKTTSDISTIKIEHDITPNLTVRNTTRYTESTQDYIWTQPDDSQGNVVN---

PfeA            348 AGGTEGIFDPNNAGFYTATLRDLTAHGEVNL----------PLHLGYEQTLTLGSEWTEQ
PirA            355 AGSVEGQIGAD-RSFSASKLENYRLSGELNL----------PLHALFEQVLTVGAEWNKE
PiuA            357 -----G------YVYRSAKSRNSTSKGWVNQTDLKANFETGFIKHTLVTGLEFSYEDVHN
I35_RS25625     349 -----G------KVWRRNNNRNSSINSLANLTELFGEFRTGPFKHSFTTGIELSREWGKR

PfeA            398 KLDDPSSNTQ---------------------NTEEGGSIPGLAGK-NRSSSSSARIFSLF
PirA            404 TLNDPSSLKQ---------------------GFVGSDSLPGTPAAGSRSPKSKAEIRALY
PiuA            406 FPYAITSGGGAGNTCNAR--LLASGDCTSLNRPTPGDNWTGSITDGLAYTDTDTKTSAAY
I35_RS25625     398 DSYTVATDKG--TICQKGIGAPSGYNCTSLWSPNPNDPWAGSITRNNDYAHARTTTKSIY

PfeA            436 AEDNIELMPGTMLTPGLRWDHHDIVGDNWSPSLNLSHALTERVT-LKAGIARAYKAPNLY
PirA            443 VEDNIELRPGTMLTPGLRLDDHSDFGDNWSPSLNASQTLGEYFT-VKAGIARAFKAPNLY
PiuA            464 VFDTTKLSEQWELNLGLRYDDFDTKSSGYQTAGRN--GPAGYFKRENNSHFWNYQTGLVY
I35_RS25625     456 GFDTIEITPRWQVNAGLRVDDYSTRFTDTKAN-----GGKTY---TRDDTLFNWQAGLVF

PfeA            495 QL--------------NPDYLLYSRGQGCYGQ--STSCYLRGNDGLKAETSVNKELGIEY
PirA            502 QS--------------NPNYLLYTRGNGCPIQTSSGGCYLVGNENLDAETSVNKELGIEF
PiuA            522 KPAPNGSIYLAWSTSSNPTGETGGEGQADI---------SVGNNGLDPERNRNLELGTKW
I35_RS25625     508 KPAQNGSIYASYATSSTPAGMLLGEGSETQSLTPGRGGVGPNADQLSPEKNRSIELGTKW
```

```
PfeA          539 S--HDGLVAGLTYFRNDYKNKIESGLSPVDHASGGKGDYANAALYQWENVPKAVVEGLEG
PirA          548 R--RDGWVAGLTYFRNDYKNKIVAPLDVMGQTGT------GNNILQWSNAKKAVVEGLEG
PiuA          573 AFFDDALSLNAALFRTDKTNARVASPDVST--------------L-QVLDGEQRVQGVEL
I35_RS25625   568 NVLNDKLSLTAALFQIDTTNARVTLPNNQ-----------------YAMVGNKRVQGLEL

PfeA          597 TLTLPLADGLKWSNNLTYMLQSK---NKETGDVLSVTPRYTLNSMLDWQATDDLS---LQ
PirA          600 NLLVPLHEDLSWSTNLTYMLQSK---DKDTGNPLSVTPEYTLNSTLDWQASERLS---TQ
PiuA          618 GFNGKLTEKWKVFGGYTYLDSEIRKSTV-KSDEGNKMPCTAQNNFTLWTTYDLLQNFTIG
I35_RS25625   611 GLAGQTTKQWQVFGGYTYMKSELRDNGKDTANNGNRFPNTPKHSLTMWSNYDVTPKFTVG

PfeA          651 ATVTWYGKQKPKKYDYHGDRVTGSANDQLSPYAIAGLGGTYRLSKNLSLGAGVDNLFDKR
PirA          654 LTSTIYGRQEPPKHGTSRNT-PVVSRKEVGTYGIWGVSAGYTFSENLSVRGGVSNLFDKR
PiuA          677 GGTTYVD----KQYGNT------ANSTYIPSYWRYDAMASYKVSKNVDLQLNVQNLTDKR
I35_RS25625   671 GGAFYMS----EVHGDP------ANLRAVPSYWRFDAMAQYRLNKKLDLQLNVNNLFNRT

PfeA          711 LFRAGNAQGVVGIDGAGAATYNRPGRTFYTSLTASF
PirA          713 LYRQGNSF------DAGAATYNRPGRAYYVSMTTSF
PiuA          727 YFDQVYSTHVAH---------VAPGRTALLGVNFHF
I35_RS25625   721 YFDQAYPAHYAS---------IAPGRSAFVTLNARY
```

B

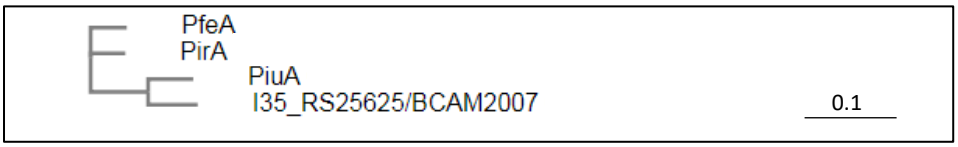

Figure 5.21: Amino acid sequence alignments and phylogenetic tree of catecholate TBDRs in *P. aeruginosa* and *B. cenocepacia*

(A) Amino acid sequence alignment of the *P. aeruginosa* catecholate TBDRs with % identity matches to BCAM2007/I35_RS25625, PfeA (20 %), PirA (21 %) and PiuA (47 %). Blue boxes depict specifically conserved sequences between PfeA and PirA and red boxes depict sequences specifically conserved between PiuA and BCAM2007/I35_RS25625. (B) Neighbour Joining phylogenetic tree construction of PfeA, PirA and PiuA of *P. aeruginosa* with BCAM2007/I35_RS25625.

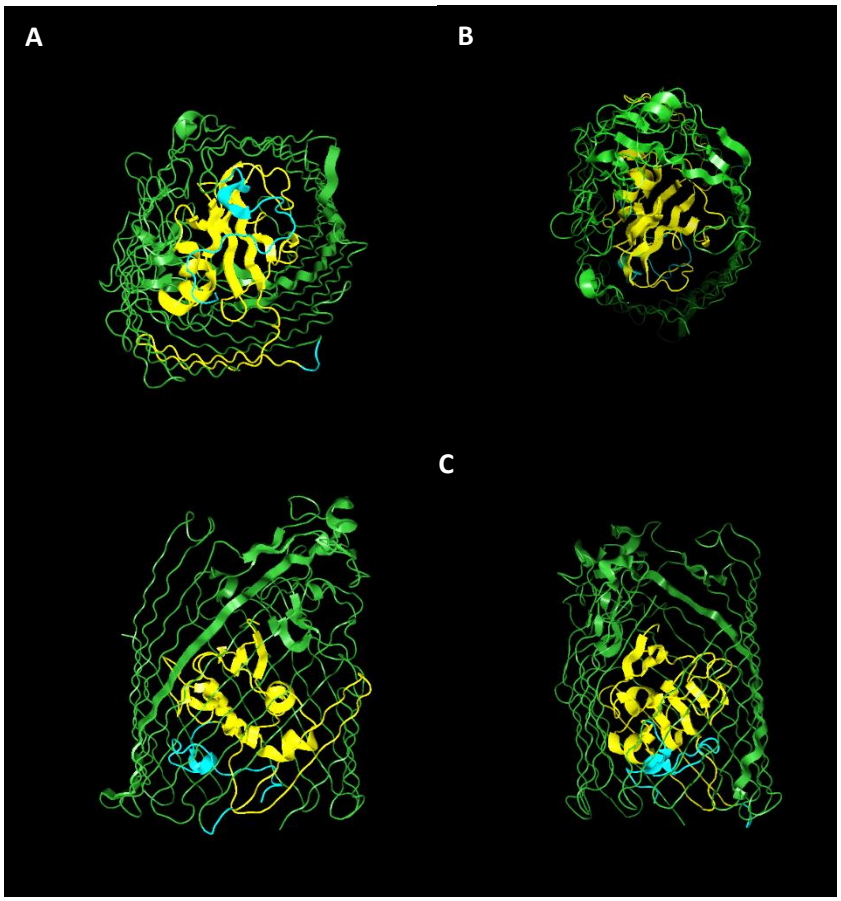

Figure 5.22: Crystal structure of PiuA of *P. aeruginosa*
Ribbon model of PiuA in *P. aeruginosa* (PDB:ID 5FOK). Green depicts β-barrel structure, yellow depicts the plug domain and blue is the N-terminal segment constituting the TonB box segment. A, view of PiuA from the periplasmic domain, B, view from extracellular domain, C, Side views of PiuA. Crystal structure was created with Swiss-model and rendered with PyMol.

Regarding these observations, it is therefore highly likely that more than one TBDR is involved in transporting catecholates in *B. cenocepacia* and that different siderophore structures are preferentially transported by specific catecholate transporters, and less preferred by other cognate transporters. In this study, it was demonstrated that azotochelin is solely transported by BCAM2007. The DHBS derivatives were also observed to be transported by BCAM2007, but with an engagement of one or more other putative catecholate TBDRs. The involvement of these putative TBDRs remains to be investigated.

The serratiochelins (A and/or B) and chrysobactin are also likely to be utilised by *B. cenocepacia* based on the promotion of growth exhibited by *S. marcescens* Db10 culture supernatants. However, it remains to be investigated whether the serratiochelins or chrysobactin is transported by BCAM2007. Also, as to whether one or both forms of serratiochelin are utilised remains to be investigated. LC/MS/MS (tandem mass spectroscopic) approach to differentiate tandem or daughter ion peaks of both forms of serratiochelin with identical molecular weights was not performed in this study. The search for the TBDR for cepabactin, having a hydroxypyridone-hydroxamate ligand, was not resolved in Chapter 4 and was investigated using the BCAM2007 TBDR mutant. However, it was demonstrated that BCAM2007 may not participate in the utilisation of cepabactin in *B. cenocepacia.*

With regard to Trojan horse applications, a siderophore with a catechol moiety conjugated to the antibiotic cephalosporin, named cefiderocol (Figure 5.23A), has recently been demonstrated to be effective against β-lactam and carbapenem resistant pathogens (Choi and McCarthy, 2018). This cephalosporin-catecholate conjugate has been shown to be transported into the bacterial cell by the monomeric catecholate TBDRs, CirA and Fiu, of *E. coli* and the TBDRs PiuA and PiuD, in *P. aeruginosa* PAO1 and LESB58, respectively (Luscher et al., 2018). Mutants in which these TBDRs are non-functional have been shown to have lowered susceptibility to cefiderocol compared to the wildtype, indicating the ability of the conjugate to exploit the bacterial iron uptake pathways (Ito et al., 2018). Ito and colleagues (2018) also demonstrated decreased MIC values for cefiderocol as compared to cephalosporins in the Bcc members, *B. cepacia* ATCC25416 and *B. multivorans* SR01869. By considering that the TBDR PiuA/PiuD/BCAM2007/I35_RS25625 is involved in transporting cefiderocol, PiuA and BCAM2007 orthologues in *B. cepacia* ATC25416 and *B. multivorans* ATCC17616 (APZ15_28835 and Bmul_3795, respectively) may almost certainly be responsible for causing the elevated sensitivity of these bacteria to the siderophore- cephalosporin conjugate. Additionally, *in silico* analysis also revealed the existence of PiuA orthologues in *B. ambifaria* AMMD, *B. pseudomallei* K96243 and *B. thailandensis* E264 (Section 3.5). It can be concluded that PiuA in *P. aeruginosa* may be an additional catecholate TBDR besides PfeA and PirA, although there are no reports about its function, since catecholate-antibiotic conjugates are shown to be transported by it.

Another two siderophore-antibiotic conjugates reported to be transported by PiuA orthologues is a monobactam (aztreonam) conjugated to a siderophore with a hydroxypyridone moiety referred to as BAL30072 and MC-1 (Figure 5.23B and C). BAL30072 and MC-1 are described as being effective against Gram-negative pathogens including *Burkholderia* spp. and *P. aeruginosa* PAO1 (Page et al., 2010; Van Delden et al., 2013). Accordingly, it is highly likely that BAL30072, MC-1 and cefiderocol are effective against *B. cenocepacia* H111 and can be transported through the BCAM2007/PiuA/I35_RS25625 TBDR. Moreover, Luscher and colleagues (2018) reported greater efficiency of PiuA in transporting the three siderophore-drug conjugates as compared to PirA in *P. aeruginosa* PAO1. The author therefore concluded that transport of the siderophores or the siderophore-antibiotic conjugates are dependent on the expression levels of the TBDRs and/or the different affinities for the transported goods (Luscher et al., 2018).

While azotochelin is a tetradentate, MC-1, cefiderocol and BAL30072 contain single bidentate hydroxypyridonate moieties (Figure 5.23). These represent the ability of PiuA/PiuD/BCAM2007 to transport both forms of denticities. Therefore, the TBDR BCAM2007 may act as a transmembrane gate for catechol-antibiotic conjugates. Additionally, according to Van Delden and colleagues (2013), the azotochelin producer, *A. vinelandii,* is reported to possess the PiuA orthologue and giving findings in this study, it is almost certainly is the TBDR responsible for transporting its own endogenous siderophore, azotochelin.

Transport of the catecholate siderophores was shown to require the TonB1 complex in this study, further supporting its role as an energy transducer for general siderophore transport. The inner membrane transporter for the catecholate siderophores was found not to be BCAL0117, which is not surprising as this protein transports hydroxamate siderophores. Siderophore ligand specificity is likely to be observed for the inner membrane transport. Based on the observation in this study that BCAM2007 is a catecholate TBDR, one or both of the cytoplasmic membrane proteins BCAM2004 and BCAM2005, encoded upstream of the catecholate transporter gene locus, maybe responsible for transporting the catecholates into the cytosol of *B. cenocepacia*.

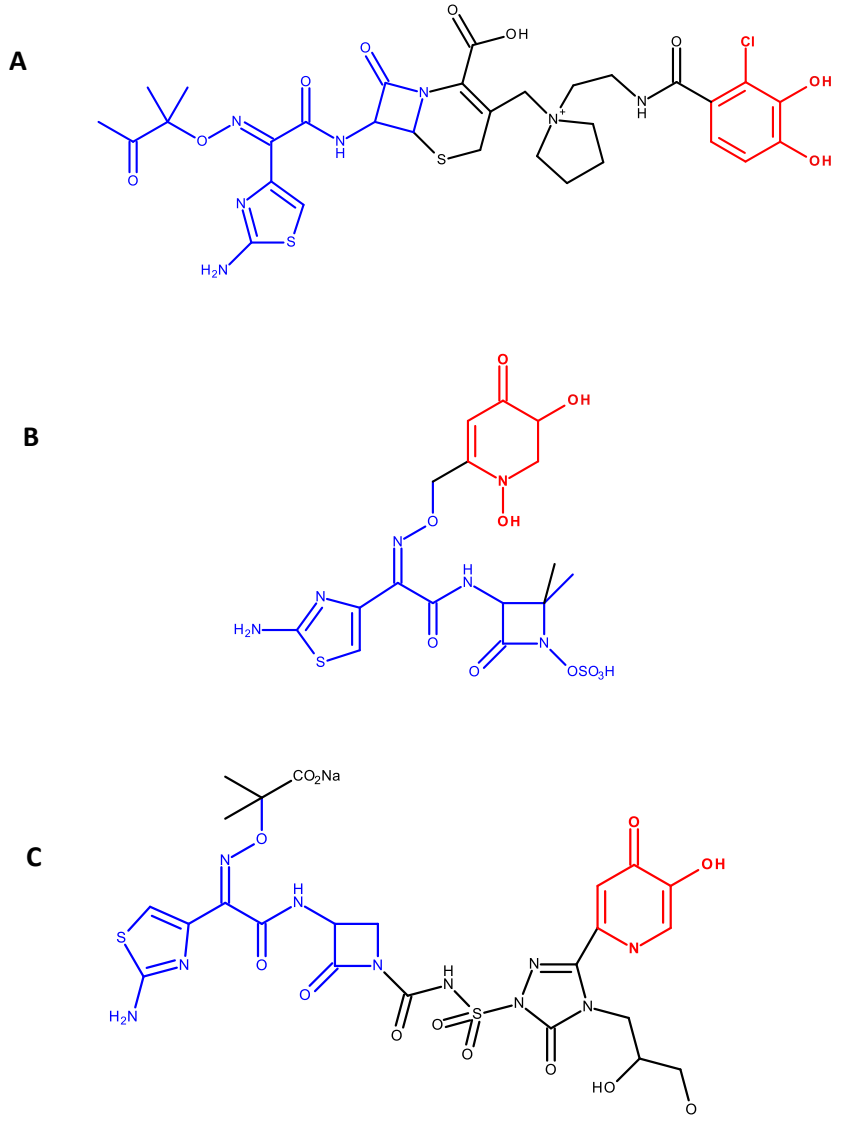

Figure 5.23: Molecular structures of catecholate/hydroxypyridone siderophore-antibiotic conjugates
(A) Cefiderocol. The mono-catecholate siderophore moiety is depicted in red. The molecule of cephalosporin is depicted in black. (B) BAL30072. (C) MC-1. The bidentate hydroxypyridone siderophore moiety is depicted in red. The region of the molecules that correspond to aztreonam is depicted in blue. Chemical structures were drawn using Accelrys Draw 4.2.

Chapter 6

Utilisation of hydroxamate-hydroxycarboxylate mixed-ligand siderophores by *B. cenocepacia*

6.1 Rationale

Another bidentate ligand commonly found in siderophores is the α-hydroxycarboxylate group. In the work described in this chapter, hydroxycarboxylate siderophores were initially tested for their utilisation by *B. cenocepacia* H111. Most hydroxycarboxylates do not exist alone and have other ligands in the same molecule (mixed type siderophores). Therefore, mixed-ligand siderophores, specifically those containing the hydroxamate-hydroxycarboxylate combinations, are also discussed in this chapter. Additionally, hydroxamate-catecholate mixed ligand siderophores were investigated along with some siderophores containing other ligands.

6.2 Screening for utilisation of hydroxcarboxylate siderophores by *B. cenocepacia*

Three siderophores containing two α-hydroxycarboxylate groups, rhizoferrin, staphyloferrin B and ornicorrugatin (Figure 6.1), were tested for their role as iron providers in *B. cenocepacia* H111. Purified rhizoferrin and the spent culture supernatants of *Cupriavidus metallidurans* 31A and *P. fluorescens* LMG5848 ΔPvd, as sources of staphyloferrin B and ornicorrugatin, respectively, were tested by disc diffusion assays with *B. cenocepacia* H111ΔpobA. Staphyloferrin B, ornicorrugatin (results not shown) and rhizoferrin obtained from respective culture supernatants were seen not to be utilised by *B. cenocepacia.* A siderophore-deficient *P. aeruginosa* was used as a control and was observed to utilise rhizoferrin as previously reported (Bano and Musarrat, 2003)(Figure 6.2). It was therefore concluded that *B. cenocepacia* is not able to utilise any of the hydroxycarboxylate siderophores tested. Therefore, siderophores containing a combination of α-hydroxycarboxylate and other ligands were screened.

6.3 Screening for utilisation of hydroxamate-hydroxycarboxylate siderophores by *B. cenocepacia*

Investigations were performed with siderophores having hydroxamate moieties in combination with an aspartate- or citrate-derived hydroxycarboxylate group. The aspartate-derived hydroxycarboxylate-dihydroxamate siderophore tested was malleobactin, a siderophore produced by *B. pseudomallei, B. mallei* and *B. thailandensis*. Malleobactin E, the active siderophore, resembles the siderophore ornibactin produced by *B. cenocepacia* and some other *Burkholderia* species (Franke et al., 2013; Franke et al., 2015). Malleobactin was not readily available commercially and the source of malleobactin E in this study was obtained from *B. thailandensis* E264, a much less virulent counterpart of *B. pseudomallei* (Haraga et al., 2008), which secretes both malleobactin and pyochelin (Brett et al., 1998). Similarly, another recently reported putative siderophore, phymabactin, that is proposed to be produced by *B. terrae* BS001 and *B. phymatum* STM815, was also investigated. The gene cluster encoding the biosynthesis of phymabactin closely resembles those responsible for malleobactin and ornibactin biosynthesis suggesting that there may be some similarity between the structure of phymabactin and those of ornibactin and malleobactin (Esmaeel et al., 2016; Butt and Thomas, 2017).

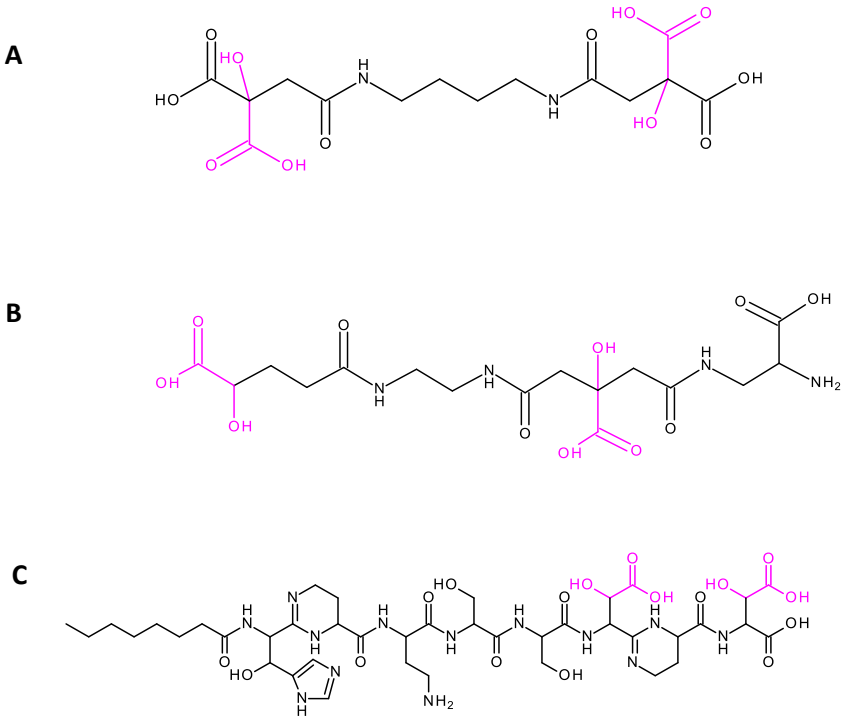

Figure 6.1: Chemical structures of the hydroxycarboxylate siderophores investigated in this study
(A) rhizoferrin, (B) staphyloferrin B and (C) ornicorrugatin. Each siderophore contains two α-hydroxycarboxylate ligands for binding ferric ion. Hydroxycarboxylate ligands are depicted in pink. Chemical structures were drawn using Accelrys Draw 4.2.

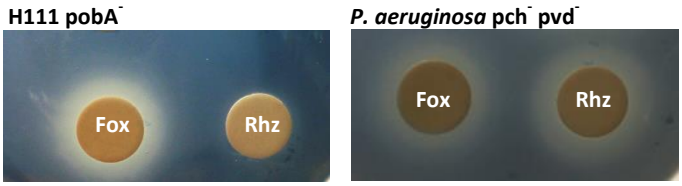

Figure 6.2: Analysis of a hydroxycarboxylate (rhizoferrin) utilisation by *B. cenocepacia* using the disc diffusion assay
Comparison of effect of rhizoferrin (1 mM 40 µl) on growth of H111ΔpobA and *P. aeruginosa* PAO1ΔPchΔPvd. Final EDDHA concentration was 40 µM.

The citrate-derived hydroxycarboxylate-hydroxamate siderophores used in this study were aerobactin, arthrobactin and schizokinen (Figure 6.3). These siderophores are structurally similar and contain a single α-hydroxycarboxylate group that is part of a citrate building block. The two terminal carboxyl groups of citrate are each connected to a hydroxamate group by alkyl linkers. Arthrobactin and aerobactin both have two additional carbon atoms in each of their alkyl chains attached to citrate compared to schizokinen, whilst aerobactin has also two additional carboxylates compared to arthrobactin. Arthrobactin used in this study was derived from *Arthrobacter pascens* and schizokinen was derived from *B. megaterium.* Both of these bacteria can be found in soil. Aerobactin was derived from *E. coli*. All three purified siderophores were obtained from a commercial source.

6.3.1 Screening for utilisation of malleobactin

Filter discs impregnated with culture supernatants from a *B. thailandensis* wild type strain elicited a faint growth of H111ΔpobA around the disc in the presence of 200 µM EDDHA in the disc diffusion assay. The siderophore utilisation assay was repeated in the presence of 40 µM EDDHA which showed a significant growth of the Δ*pobA* mutant (result not shown). As *B. thailandensis* secretes pyochelin in addition to malleobactin, the bioassay may be due to utilisation of either one of the siderophores or both.

To distinguish between these possibilities, siderophore utilisation screening of H111ΔpobA using disc diffusion bioassays were performed with the culture supernatants of *B. thailandensis* E264 and its Δ*pchE* (Pch^-Mba^+), Δ*mbaB* (Pch^+Mba^-) and Δ*pchE* Δ*mbaB* (Pch^-Mba^-) mutant derivatives having inactivated biosynthetic genes of pyochelin and malleobactin, respectively. Culture supernatant of *B. thailandensis* mutant Δ*mbaB* (*mbaB*::Tet) exhibited an unexpected observation as it did not result in growth around the filter disc as predicted. Culture supernatant of *B. thailandensis* mutant Δ*pchE* Δ*mbaB* (*pchE*::Km *mbaB*::Tet) did not give rise to growth of *B. cenocepacia* around the filter disc as expected. Bioassays carried out using culture supernatants from the wild type and the Δ*pchE* mutant (pchE::Tet) supported growth of the *pobA* mutant. As *B. cenocepacia* is a pyochelin producer, it should be able to utilise pyochelin. However, the bioassay result was not as expected when supernatant from Δ*mbaB* mutant was tested, as it should produce pyochelin only and should give growth in the bioassay (Figure 6.4).

Based on these observations, an investigation was made on the genotype and phenotype of the *B. thailandensis* wild type strain and its mutant derivatives. The integrity of *B. thailandensis* E264 and its mutant derivatives to produce or not produce siderophores was tested using the CAS agar assay (Figure 6.5). CAS agar screening of siderophore production showed formation of haloes for the *B. thailandensis* wild type and Δ*pchE* strain, and no haloes for the other two mutants, confirming that the other two mutant strains (Δ*mbaB* and Δ*pchE* Δ*mbaB*) were not producing any siderophores.

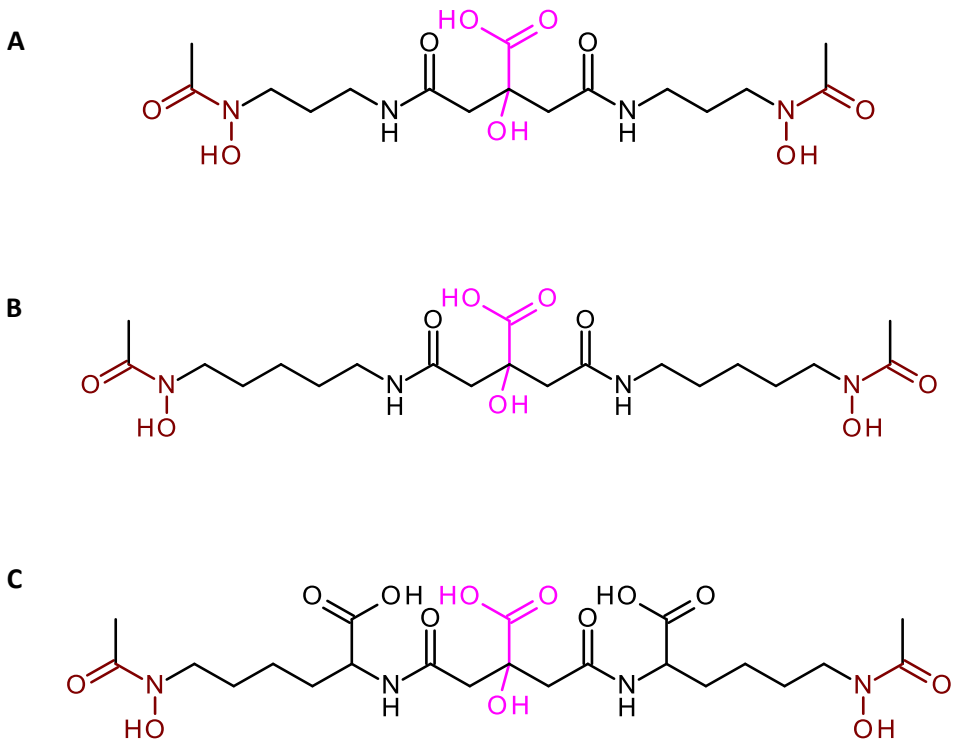

Figure 6.3: Chemical structures of citrate hydroxamate siderophores used in this investigation
(A) Schizokinen, (B) arthrobactin and (C) aerobactin. The citrate α-hydroxycarboxylate group is depicted in pink and hydroxamate groups are depicted in dark red. Chemical structures were drawn using Accelrys Draw 4.2.

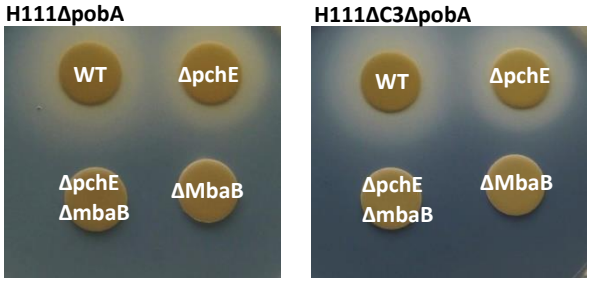

Figure 6.4: Ability of *B. thailandensis* culture supernatants to promote growth of siderophore deficient *B. cenocepacia* under iron-limiting conditions
Utilisation of siderophores in *B. thailandensis* culture supernatants by H111ΔpobA and H111ΔC3ΔpobA. Filter discs containing *B. thailandensis* culture supernatants were applied to a soft agar overlay containing the indicated *B. cenocepacia* mutants. Culture supernatants used (100 µl) were: WT, *B. thailandensis* wild type E264; ΔpchE, *B. thailandensis* mutant only producing malleobactin; ΔmbaB, *B. thailandensis* mutant only producing pyochelin and ΔpchEΔmbaB, a siderophore-deficient *B. thailandensis* mutant. Final EDDHA concentration was 40 µm.

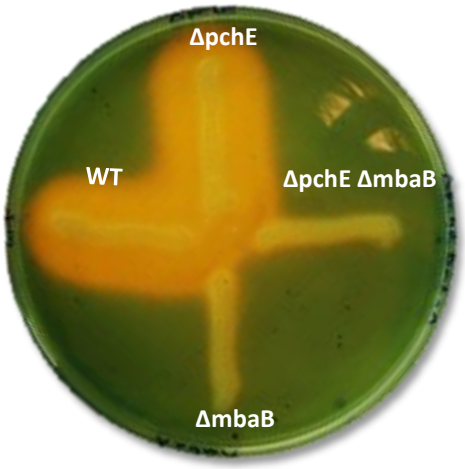

Figure 6.5: CAS agar plate of streaked *B. thailandensis* E264 and its mutant derivatives
CAS agar plate of streaked *B. thailandensis* E264 and its Δ*pchE,* Δ*mbaB* and Δ*pchE* Δ*mbaB* mutant derivatives.

Theoretically, the *B. thailandensis* Δ*mbaB* mutant should secrete the siderophore pyochelin and should therefore support growth of H111ΔpobA, but the observation was otherwise. It was unexpected that no formation of haloes was elicited by the Δ*mbaB* mutant. The integrity of the mutant was therefore investigated.

6.3.1.1 Confirming *B. thailandensis* mutant characteristics

In view that the Δ*mbaB* mutant did not appear to produce pyochelin by the CAS assay, the genotype and phenotype of the *B. thailandensis* wild type and its mutant derivatives were investigated. *B. thailandensis* and its mutant derivatives were observed under a UV transilluminator, as pyochelin is a fluorescent siderophore. The wild type *B. cenocepacia*, H111, was used as a positive control as it produces pyochelin (and ornibactin) and H111ΔpobA was used as a negative control as it does not produce pyochelin. Table 6.1 shows the degree of fluorescence observed under UV light. *B. thailandensis* Δ*mbaB* mutant did not fluoresce under UV light which was not as expected if it produces pyochelin. Other *B. thailandensis* strains exhibited expected observations under UV light.

Further investigation was performed to confirm the genotypes of the *B. thailandensis* mutant derivatives. Forward and reverse primers for the *pchE* gene were designed and the mutants were screened with *B. thailandensis* wild type as a positive control. PCR products showed a larger size of the *pchE* amplicon for all three mutants suggesting that the gene was inactivated by insertion of antibiotic resistance gene in each case (Figure 6.6A).

The *mbaB* genotype of *B. thailandensis* E264 and its mutant derivatives were then confirmed by screening using *mbaB* primers, to verify the insertion of tetracycline antibiotic cassette in the *mbaB* gene. Gel electrophoresis of diagnostic PCR showed that the tetracycline resistance cassette was inserted into the *mbaB* gene of the Δ*pchE* Δ*mbaB* mutant (Figure 6.6B). As for the Δ*mbaB* mutant strain, the PCR product was the same size as generated from the *pchE*::Km *mbaB*::Tet strain, suggesting the strain was also a *pchE*::Km *mbaB*::Tet mutant, unable to produce either malleobactin or pyochelin. The siderophore bioassay showing no growth around the supernatants derived from the Δ*mbaB* mutant is consistent with the observation that it is in fact a Δ*mbaB* Δ*pchE* double mutant (Figure 6.4). The *pchE* gene of *B. thailandensis* was inactivated by tetracycline and kanamycin antibiotic resistance cassette insertion where the *B. thailandensis* single Δ*pchE* mutant was *pchE*:Tet (tetracycline) while the Δ*pchE* Δ*mbaB* double mutant was a *pchE*::Km *mbaB*::Tet mutant strain. Following these observations, only two *B. thailandensis* mutants were used in subsequent experiments; the *pchE*::Tet and *pchE*::Km *mbaB*::Tet derivatives.

Table 6.1 Degree of fluorescence of *B. thailandensis* and its mutant derivatives under UV light

Bacterial strain	Degree of fluorescence under UV light
H111ΔpobA (negative control)	+
H111 (positive control)	++++++
B. thailandensis WT	+++
B. thailandensis Δ*pchE*	+
B. thailandensis Δ*mbaB*	+
B. thailandensis Δ*pchE*Δ*mbaB*	+

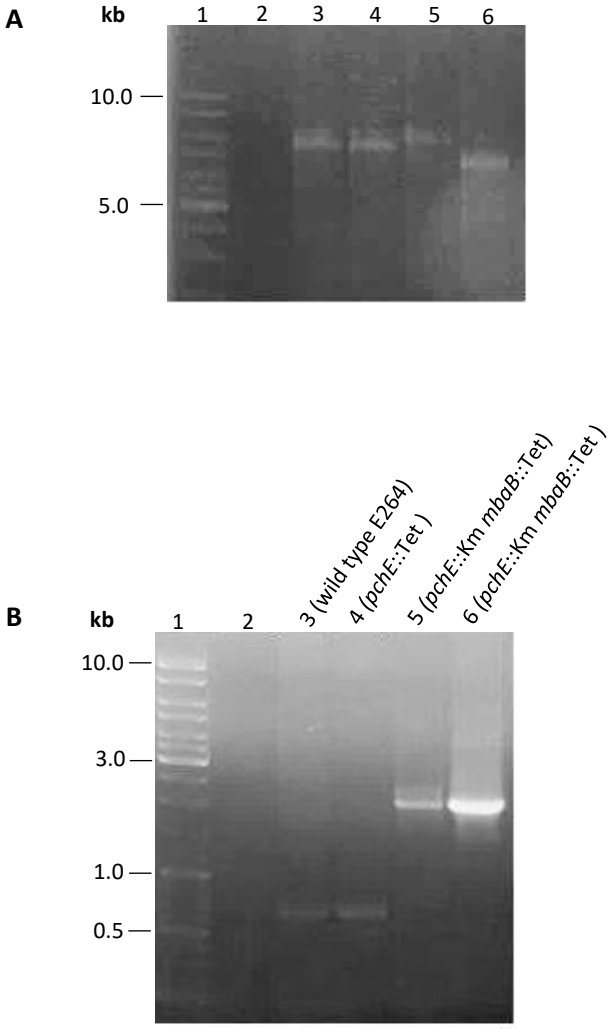

Figure 6.6: Screening *pchE* and *mbaB* alleles in *B. thailandensis* E264 wild type and mutant strains
(A) Screening of *pchE* gene for *B. thailandensis* E264 wild type and mutant strains using primer combination *pchE*scrnfor and *pchE*scrnrev at an annealing temperature of 59 °C: Lane 1, Linear DNA ladder; lane 2, negative control (no DNA template); lane 3, *pchE*::Km *mbaB*::Tet; lane 4, *pchE*::Km *mbaB*::Tet (formerly designated Δ*mbaB*); lane 5, *pchE*::Tet; lane 6, wild type E264. (B) Screening of *mbaB* gene of *B. thailandensis* E264 wild type and mutant strains using primer combination *mbaB*scrnfor and *mbaB*scrnrev at an annealing temperature of 55°C: Lane 1, Linear DNA ladder; lane 2, negative control (no DNA template); lane 3, wild type E264; lane 4, *pchE*::Tet; lane 5, *pchE*::Km *mbaB*::Tet; lane 6, *pchE*::Km *mbaB*::Tet (formerly designated as Δ*mbaB*).

Disc diffusion assay was repeated using *B. thailandensis* mutant derivatives *pchE*::Tet and *pchE*::Km *mbaB*::Tet. *B. cenocepacia* H111ΔorbS, unable to produce ornibactin, was used as a source of pyochelin. The culture supernatant of H111ΔorbS supported a small amount of growth of H111ΔpobA which indicated the presence of pyochelin and the culture supernatants of the *pchE*::Tet mutant also supported growth of Δ*pobA* mutant indicating malleobactin utilisation (Figure 6.7).

Validation on the ability of *B. cenocepacia* to utilise malleobactin was carried out to confirm the basis of growth around the filter disc with the culture supernatant of *B. thailandensis* wild type was due to utilisation of malleobactin. This was done by constructing a *B. cenocepacia* Δ*pobA* mutant that was unable to utilise pyochelin.

6.3.1.2 Generation of H111ΔpobAΔfptA

To construct a *B. cenocepacia* Δ*pobA* mutant that cannot utilise pyochelin, the gene encoding the TBDR for pyochelin, *fptA* (BCAM2224), was inactivated by introduction of an in-frame deletion. A diagrammatic representation of the construction of the Δ*fptA* mutant is shown in Figure 6.8.

In the first step, construction of pEX18TpTer-*pheS-fptA* was undertaken by amplification of a DNA fragment containing *fptA* from H111 and was confirmed by electrophoresis showing a size of 2240 bp (Figure 6.9A). The fragment was cut sequentially with *Xba*I and *Hin*dIII and was ligated into the same sites of the pEX18TpTer-*pheS* vector. Following transformation into *E. coli* JM83 cells, plasmid DNA was isolated from white colonies grown on M9-glucose (CAA) agar containing X-gal, IPTG and trimethoprim and analysed by gel electrophoresis. Plasmids having the expected size, (6415 bp), corresponding to pEX18TpTer-*pheS-fptA* were sequenced to ensure correct insertion of the *fptA* gene. An in-frame deletion was then introduced into *fptA* gene in one such plasmid by restriction digestion with *Sal*I, releasing a 915 bp DNA fragment. Religation of the plasmid was performed and it was transformed into JM83 cells. Twelve colonies were isolated and purified on M9-glucose (CAA) agar containing trimethoprim. Plasmids were prepared and analysed by gel electrophoresis (Figure 6.9B). Plasmids of the expected size of 5500 bp with an in-frame deletion of the *fptA* gene (pEX18TpTer-*pheS*-Δ*fptA*) were analysed by sequencing to confirm their integrity.

Generation of a H111ΔpobAΔfptA mutant was carried out using pEX18TpTer-*pheS*-Δ*fptA* as previously described for the generation of the Δ*pobA* and ΔBCAL2281 mutant (Section 4.2 and 4.4). Merodiploids were verified using the suicide vector primer combination pEX18Tpfor and pEX18Tprev (Figure 6.9C). H111ΔpobA recombinants that had lost the plasmid were PCR screened with the 'outside primers', BCAM2224forout and BCAM2224revout.

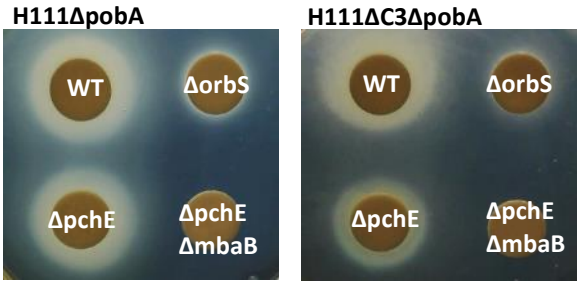

Figure 6.7: Confirmation of growth promotion of siderophore deficient *B. cenocepacia* with *B. thailandensis pchE*::tet mutant derivative under iron-limiting conditions
(A) Utilisation of siderophores in *B. thailandensis* culture supernatants by H111ΔpobA and H111ΔC3ΔpobA. Filter discs for each bioassay plate were applied to a soft agar overlay containing the indicated *B. cenocepacia* mutants. Culture supernatants used (100 µl) were: WT, *B. thailandensis* wild type E264; ΔpchE, *B. thailandensis* mutant only producing malleobactin; ΔorbS, *B. cenocepacia* mutant only producing pyochelin and ΔpchEΔmbaB, a siderophore-deficient *B. thailandensis* mutant. Final EDDHA concentration was 40 µM.

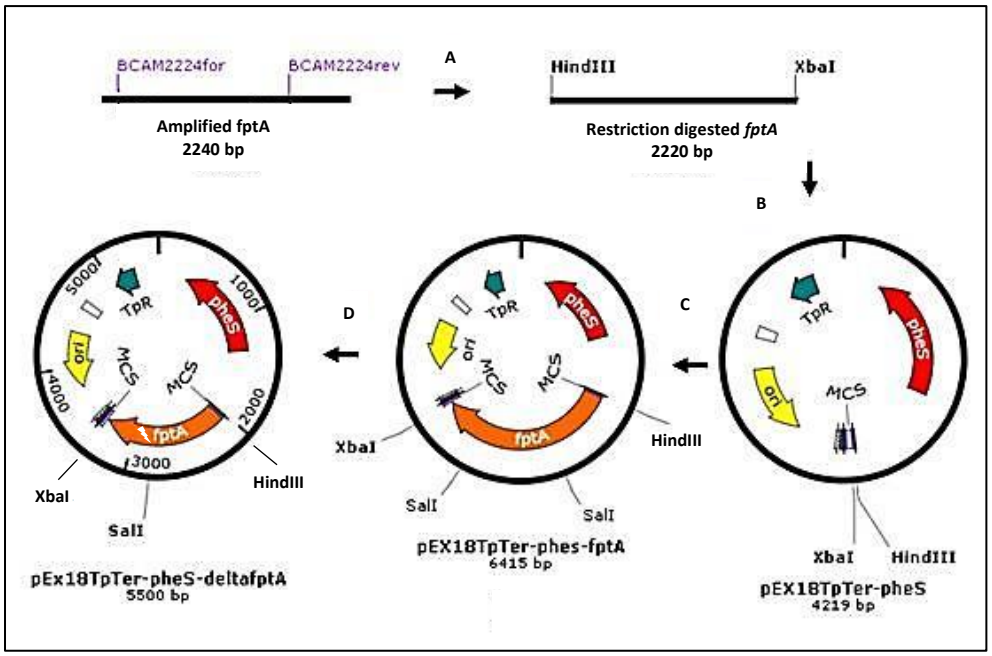

Figure 6.8: Diagram showing construction of pEX18TpTer-*pheS*-Δ*fptA*
(A) *fptA* gene (BCAM2224) was PCR amplified from H111 by restriction with primer combination BCAM2224for and BCAM2224rev forming a 2240 bp DNA fragment. (B) and (C) *fptA* DNA fragment was cut with *Hin*dIII and *Xba*I and ligated into pEX18TpTer-*pheS* to give pEX18TpTer-*pheS-fptA*. (D) An in-frame deletion was introduced into *fptA* in pEX18pTer-*pheS-fptA* by restriction with *Sal*I releasing a 915 bp *Sal*I fragment followed by self-ligation to give pEX18TpTer-*pheS*-Δ*fptA* (5500 bp).

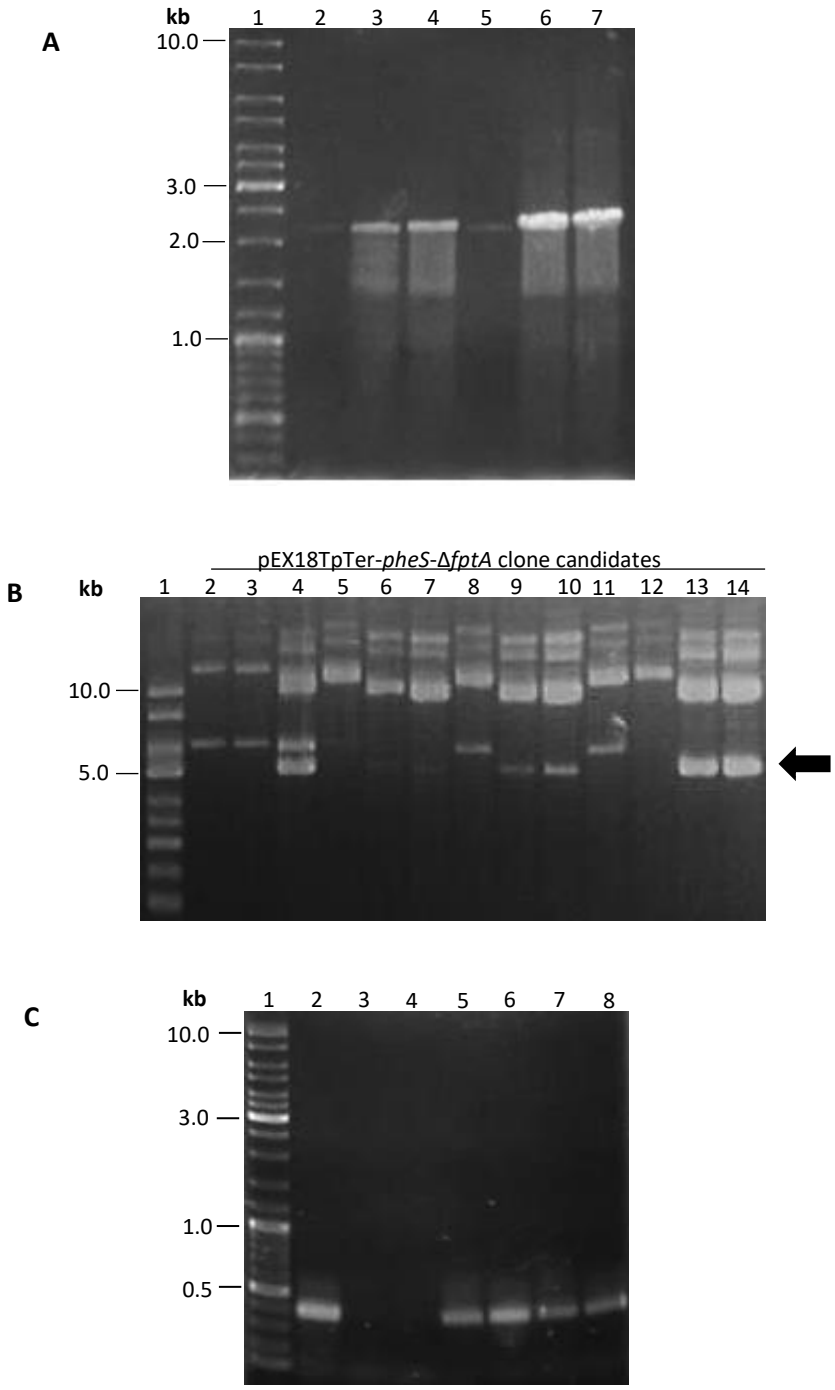

Figure 6.9: Construction of pEX18TpTer-*pheS*-Δ*fptA* and generation of H111ΔpobAΔfptA
(A) PCR amplification of a DNA fragment containing *fptA* from H111 with primer combination BCAM2224for and BCAM2224rev: Lane 1, Linear DNA ladder; lanes 2-7, PCR gradient annealing temperatures of 55, 56, 59, 64, 67 and 70 °C, respectively. (B) pEX18TpTer-*pheS*-Δ*fptA* plasmid candidates: Lane 1, Supercoiled DNA ladder; lanes 2-3, pEX18TpTer-*pheS*-*fptA*; lanes 4-14, pEX18TpTer-*pheS*-Δ*fptA* clone candidates expected size (5500 bp) are indicated with a black arrow. (C) Colony PCR of putative H111 recombinants containing integrated pEX18TpTer-*pheS*-Δ*fptA* using primer combination pEX18Tpfor and pEX18Tprev at annealing temperature 52°C: Lane 1, Linear DNA ladder; lane 2, SM10(λpir) cells containing pEX18TpTer-*pheS*-Δ*fptA*; lane 3, wild type H111; lane 4, negative control (no template); lanes 5-8, putative H111 recombinants.

Recombinants that retained the wild type *fptA* gene gave rise to an amplicon of 2315 bp while those containing the in-frame deletion of the *fptA* gene generated an amplicon of 1400 bp. H111ΔC3ΔpobAΔfptA was concomitantly generated for later experiments.

6.3.1.3 Phenotypic characterisation of H111ΔpobAΔfptA and H111ΔC3ΔpobAΔfptA

The phenotypes of H111ΔpobAΔfptA and H111ΔC3ΔpobAΔfptA were confirmed by disc diffusion bioassay in which culture supernatants of *B. cenocepacia* H111 and a H111ΔorbS, mutant only producing pyochelin, were spotted on separate filter discs. The siderophore utilisation phenotype of the Δ*fptA* mutants was compared to that of H111ΔpobA. The results demonstrated the inability of both Δ*fptA* mutants, to grow around filter discs impregnated with culture supernatant of H111ΔorbS, confirming the inability of the constructed mutants to utilise pyochelin (Figure 6.10A). As expected, growth of the Δ*fptA* mutants were observed around the disc containing culture supernatant of H111, which also produces ornibactin. Additionally, this experiment demonstrated that FptA (BCAM2224/I35_RS26975) is the sole pyochelin transporter in *B. cenocepacia* H111 as was shown in strain 715j (Visser et al., 2004).

6.3.1.4 Analysis of malleobactin utilisation by the H111ΔpobAΔfptA mutant

The culture supernatant of *B. thailandensis* containing malleobactin and pyochelin was shown to allow promotion of growth of H111ΔpobA in the disc diffusion assay. This was also the case for the *B. thailandensis* mutant derivative, the *pchE*::Tet, which only produces malleobactin. To validate that the promotion of growth was due to the presence of malleobactin, the ability of culture supernatants of *B. thailandensis* and its mutant derivatives to support growth of the pyochelin receptor mutant, H111ΔpobAΔfptA, was analysed.

Growth of the H111ΔpobAΔfptA mutant was supported by culture supernatants of the *B. thailandensis* wildtype and the *pchE*::Tet mutant but not by culture supernatants of *B. thailandensis* siderophore-deficient mutant, mbaB::Km *pchE*::Tet and *B. cenocepacia* H111ΔorbS (Figure 6.10B). These observations further support the ability of *B. cenocepacia* to utilise malleobactin in iron-limiting conditions. Investigation using purified malleobactin was not performed.

6.3.2 Analysis of the ability of *B. cenocepacia* to utilise phymabactin

6.3.2.1 Analysis of the ability of culture supernatants of *B. phymatum* and *B. terrae* to support growth of *B. cenocepacia* Δ*pobA* under iron limiting conditions

Based on bioinformatic analysis*, B. phymatum* and *B. terrae* (*Burkholderia* spp. of the xenovorans group) were predicted to synthesise a product similar to ornibactin and malleobactin, named phymabactin.

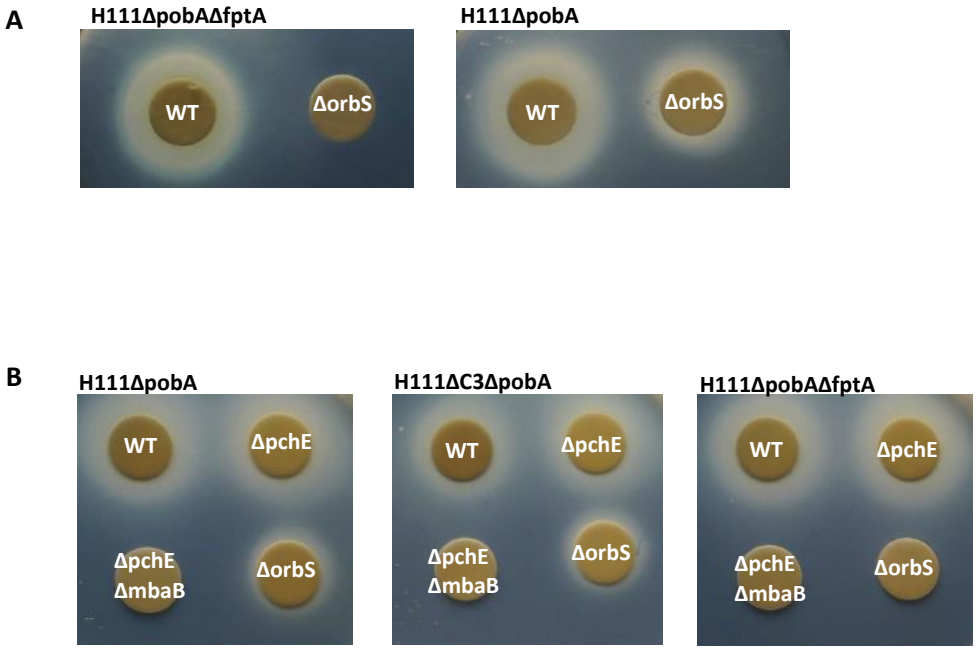

Figure 6.10: Demonstration of malleobactin utilisation by *B. cenocepacia*
(A) Phenotype confirmation of H111ΔpobAΔfptA with H111ΔpobA as a control. Filter discs for each bioassay plate contained 100 µl of culture supernatants from the indicated *B. cenocepacia* mutants. (B) Demonstration of malleobactin utilisation by H111ΔpobAΔfptA. H111ΔpobA and H111ΔC3ΔpobA were included as controls. Culture supernatants applied to filter discs (100 µl) were: WT, *B. thailandensis* wild type E264; ΔpchE, *B. thailandensis* Δ*pchE* mutant only producing malleobactin; ΔorbS, *B. cenocepacia,* mutant only producing pyochelin (H111ΔorbS); ΔpchEΔmbaB, a siderophore-deficient *B. thailandensis* mutant. Final EDDHA concentration was 40 µM.

This is due to the biosynthetic genes present in these bacteria which resembles those encoding the NRPSs involved in ornibactin and malleobactin biosynthesis. However, the structure and siderophore activity of this product has not been examined (Esmaeel et al., 2016; Butt and Thomas, 2017). In addition, BLASTP analysis was performed to investigate the production of any other siderophores produced by *B. phymatum* and *B. terrae*. BLASTP analysis using pyochelin biosynthetic NRPSs, PchE and PchF (BCAM2230 and BCAM2228), from H111 indicated that pyochelin is not produced by these species. Similarly, based on BLASTP analysis, the NRPSs for cepaciachelin (CpcC) was not encoded by the genome of these species. Based on these observations, it is likely that *B. phymatum* and *B. terrae* do not produce pyochelin or cepaciachelin as secondary siderophores.

To examine the ability of *B. cenocepacia* to utilise the siderophore produced by these species, a disc diffusion assay was performed. Zones of growth of H111ΔpobA were observed around the filter discs applied with the culture supernatants of both *B. phymatum* and *B. terrae* and a faint zone of growth was exhibited by H111ΔC3ΔpobA (Figure 6.11). Given that *B. cenocepacia* H111 was observed to utilise malleobactin and ornibactin, the zone of growth observed was predicted to be due to the putative siderophore, phymabactin. The promotion of growth by *B. phymatum* and *B. terrae* supernatants may indicate that phymabactin has a siderophore activity and this siderophore can be utilised by *B. cenocepacia*. The production of siderophores in these bacteria, however, are still under investigation but it is likely that phymabactin is a siderophore produced by *B. phymatum* and *B. terrae* and is likely to possess a molecular structure similar to ornibactin and malleobactin.

6.3.2.2 Construction of *B. phymatum* and *B. terrae* phymabactin mutants

The NRPS enzymes, PhmA and PhmB (also known as PhmI and PhmJ), for biosynthesis of phymabactin resemble OrbI and OrbJ for ornibactin biosynthesis (Esmaeel et al., 2016; Butt and Thomas, 2017). Therefore, it was hypothesised that recombination may occur between ornibactin and phymabactin biosynthetic genes in allelic replacements. By using a previously constructed plasmid, pSHAFT2-OM13 (pSHAFT2-*orbI*::mini-Tn5Tp) (M. Thomas, unpublished results), conjugations were performed between *E. coli* S17-1(λpir) cells containing the pSHAFT2-OM13 plasmid and three *Burkholderia* strains, *B. cenocepacia* H111, *B. phymatum* and *B. terrae*. As S17-1(λpir) cells are trimethoprim-resistant and the *orbI* cloned gene in pSHAFT2-OM13 contains a mini-Tn5Tp insertion, S17-1(λpir) cells harbouring the plasmid were grown in medium containing ampicillin (pSHAFT2 encodes resistance to ampicillin and chloramphenicol). Exconjugants were selected on M9-glucose agar containing trimethoprim (25 µg ml^{-1}) and were then patched on the same selection medium and incubated for 24-48 hr. Mutant candidates were then repatched on LB medium containing chloramphenicol (50 µg ml^{-1}) to select for recombinants which had lost the pSHAFT2 plasmid. Patched colonies that were chloramphenicol-sensitive were then purified and maintained on M9-glucose selection medium containing trimethoprim.

Inactivation of the *phmA* gene in *B. terrae* and *B. phymatum* and also *orbI* gene in *B. cenocepacia* was confirmed by PCR screening using primer combination, orbIfor and orbIrev (Figure 6.12). Generation of *B. phymatum* and *B. terrae phmA*::Tp mutants (STM815 phmA::Tp and BS001 phmA::Tp, respectively) is consistent with the high similarity between the phymabactin and ornibactin biosynthetic genes. *B. cenocepacia* H111-orbI::Tp was generated in parallel as a control. The production of siderophores by these mutants, was investigated by streaking the mutants on CAS assays using *B. cenocepacia* H111-orbI::Tp as a control. *B. cenocepacia* H111 elicited a yellow halo as an indication of the production of ornibactin and *B. cenocepacia* H111-orbI::Tp formed an orange halo which indicates production of pyochelin, which are expected. A high amount of pyochelin production was observed when the production of ornibactin was abolished, which suggested pyochelin as a secondary siderophore. Similarly, both mutants elicited orange haloes and the wild type strains of *B. phymatum* and *B. terrae* exhibited some yellow haloes (Figure 6.13). These observations suggested that both *B. phymatum* and *B. terrae* produce phymabactin and at least one other unidentified secondary siderophore. Further investigations on the unidentified siderophores produced by *B. phymatum* and *B. terrae* were not performed.

6.3.3 Analysis of the ability of *B. cenocepacia* to utilise schizokinen, arthrobactin and aerobactin

Culture supernatants of a sole schizokinen producer, *B. megaterium,* were initially investigated for the ability of this siderophore to allow growth of H111ΔpobA under iron-limiting conditions. As *P. aeruginosa* is documented to utilise schizokinen (Cuív et al., 2007), the siderophore-deficient *P. aeruginosa* strain was used as a positive control. Utilisation of purified schizokinen was then tested after a positive observation with the culture supernatants (Figure 6.14A and B). A high concentration of purified schizokinen (5 mM) was found to be required to allow growth of H111ΔpobA in the disc diffusion assay. Due to their similar structure to schizokinen, purified arthrobactin and aerobactin were also tested. Arthrobactin promoted a significant growth of H111ΔpobA (result not shown), while aerobactin was unable to support growth of this strain (Figure 6.14C). As H111ΔpobA was shown not able to utilise aerobactin, the siderophore activity of aerobactin was re-examined concurrently with a siderophore-deficient *P. aeruginosa*. Growth promotion was elicited by *P. aeruginosa* pch^- pvd^- as expected (Cuiv et al., 2006) and was used as a positive control in the assay (Figure 6.14C).

The effect of arthrobactin and schizokinen supplementation on the ability of H111ΔpobA to grow under iron-limited conditions was quantified by the liquid growth stimulation assay. Significant growth stimulation was observed with the addition of arthrobactin and schizokinen (Figure 6.15). The growth effect due to arthrobactin was nearly equivalent to the growth seen with addition of the endogenous siderophore ornibactin.

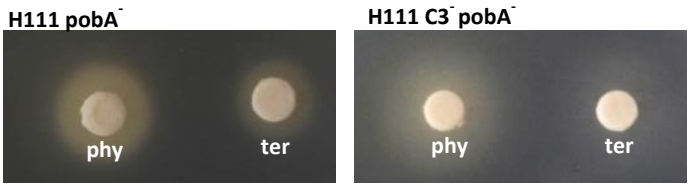

Figure 6.11: Growth stimulation of siderophore-deficient *B. cenocepacia* by *B. phymatum* and *B. terrae* under iron limiting conditions
Disc-diffusion bioassay showing growth stimulation of H111ΔpobA and H111ΔC3ΔpobA by culture supernatants of *B. phymatum* and *B. terrae* that produce phymabactin. Filter discs were impregnated with culture supernatants (100 µl) and were applied to the plate: phy, *B. phymatum;* ter, *B. terrae*;. Final EDDHA concentration was 40 µM.

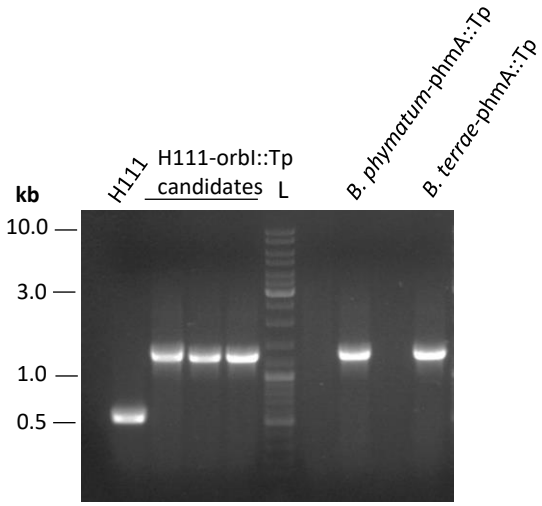

Figure 6.12: Construction of H111-orbI::Tp, and *B. phymatum* and *B. terrae phmA*::Tp mutants
Mutant candidate screening of *B. cenocepacia* H111-orbI::Tp, *B. phymatum*-phmA::Tp and *B. terrae*-phmA::Tp using primer combination OrbIfor and OrbIrev. H111 wild type was used as a negative control. Line L, Linear DNA ladder.

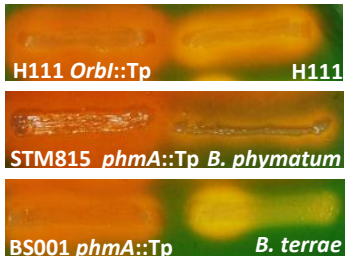

Figure 6.13: CAS agar analysis of H111-orbI::Tp, and *B. phymatum* and *B. terrae phmA*::Tp mutants
Mutant strains *B. cenocepacia* H111-orbI::Tp, *B. phymatum*-phmA::Tp and *B. terrae*-phmA::Tp were tested on CAS agar with H111-orbI::Tp as control. Orange halo growth was seen with the wild types indicating ornibactin production, while the trimethoprim-inserted mutants displayed yellow haloes, indicating production of pyochelin for *B. cenocepacia* and undetermined siderophores for *B. phymatum* and *B. terrae*. This observation suggested production of siderophores other than phymabactin in both strains.

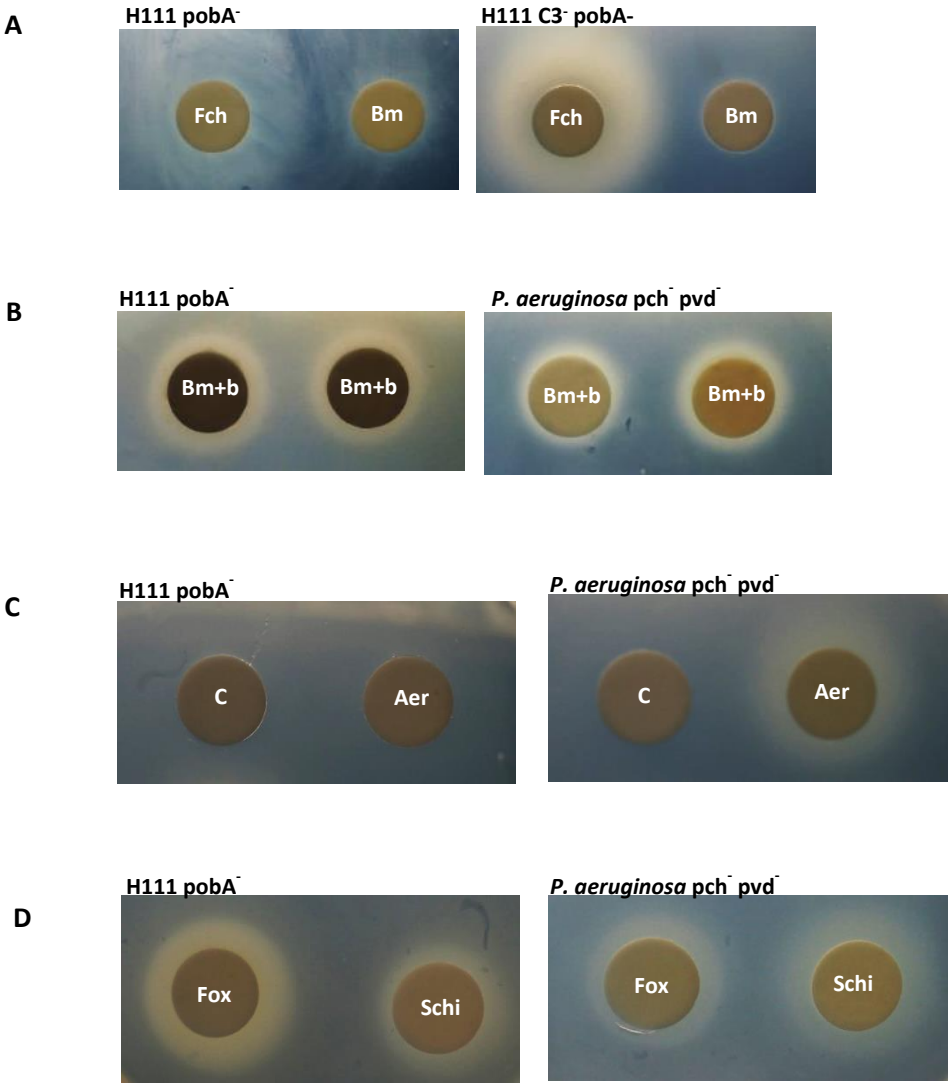

Figure 6.14: Analysis of schizokinen and aerobactin utilisation by *B. cenocepacia*
(A) Disc-diffusion bioassay showing growth stimulation of H111ΔpobA and H111ΔC3ΔpobA by culture supernatants of *B. megaterium* that produces schizokinen. Ferrichrome (1mM 15 µl) was used as a control. (B) As for (A) but *B. megaterium* was grown in the presence of 2,2'-bipyridyl. (C) Disc-diffusion bioassay of H111ΔpobA and *P. aeruginosa* PAO1 pch$^-$ pvd$^-$ using purified aerobactin. dH_2O was used as a negative control. (D) Disc-diffusion bioassay of H111ΔpobA and *P. aeruginosa* PAO1 pch$^-$ pvd$^-$ using purified schizokinen. Ferrichrome was used as a positive control. Filter discs were impregnated with culture supernatants (100 µl) or with purified siderophores (1mM 20 µl) and were applied to the plate: Bm, *B. megaterium* culture supernatants; Fch, ferrichrome; Fox, ferrioxamine B; Aer, aerobactin; Schiz, schizokinen; C, dH_2O. Final EDDHA concentration was 40 µM.

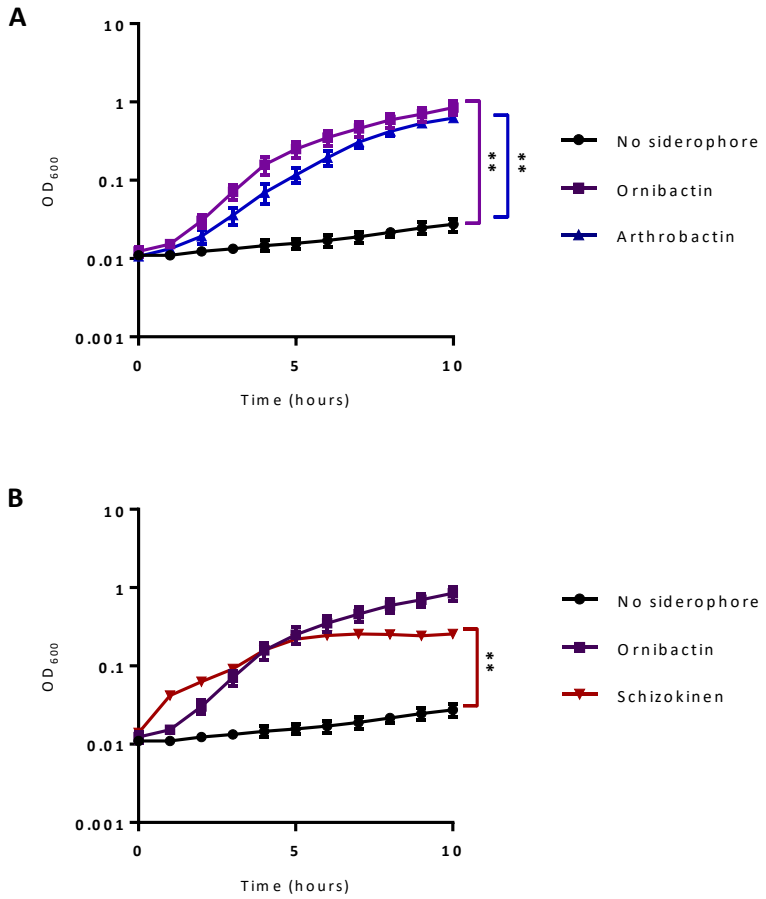

Figure 6.15: Growth curves of *B. cenocepacia* H111ΔpobA in iron-depleted medium supplemented with arthrobactin and schizokinen

B. cenocepacia H111ΔpobA was grown in M9-glucose (CAA) medium containing 1 µM DTPA at 37 °C supplemented with 10 µM of (A) arthrobactin and (B) schizokinen. Both graphs show a growth curve without siderophores as a negative control and with ornibactin-supplementation as a positive control. These data represent the means of three independent experiments (n=3). Error bars represent SEM. Significance of ornibactin-supplemented growth rate is shown in (A). *$p<0.05$, **$p<0.01$.

Schizokinen allowed faster growth of H111ΔpobA in the early part of the growth curve but this was followed by a reduced growth rate after 5 hours of incubation to a rate lower than that seen with arthrobactin-supplemented culture.

6.4 Identification of a TBDR for hydroxycarboxylate-hydroxamate siderophores

The high similarity in the molecular structures of malleobactin and ornibactin (Franke et al., 2015), suggests a similarity in the receptor used for their transport. Phymabactin may also resemble ornibactin and malleobactin due to the similarity of the NRPSs involved in their biosynthesis (Esmaeel et al., 2016; Butt and Thomas, 2017). The predicted phymabactin NRPSs in the proposed phymabactin producer, *B. phymatum*, PhmA and PhmB (Bphy_4039 and Bphy_4040) have identities of 61-63 % to the NRPSs of *B. cenocepacia* (OrbI) and *B. thailandensis* (BTH_I2418) and identities of 77 % to the other NRPSs of *B. cenocepacia* (OrbJ) and *B. thailandensis* (BTH_I2419) (Burkholderia.com). However, the molecular structure of phymabactin has not been elucidated. Nevertheless, it is likely that the *B. cenocepacia* ornibactin TBDR, BCAM1700 (OrbA), may be able to transport all three siderophores. Alternatively, BCAS0333, a highly-similar OrbA-like receptor, may be an additional TBDR for malleobactin and/or phymabactin. The TBDR for malleobactin is denoted as FmtA (BPSL1775) in *B. pseudomallei* (Alice et al., 2006) and as MbaD (BTH_I2415) in *B. thailandensis* (Franke et al., 2013). By *in silico* analysis, an ornibactin TBDR homologue (WQE_RS26070/ WP_042304263) was found encoded in a genomic DNA sequence contig of *B. terrae (Paraburkholderia terrae)*, while no ornibactin-like TBDR orthologue was found in *B. phymatum* (*Paraburkholderia phymatum*) (Section 3.5) (Butt and Thomas, 2017). As phymabactin was predicted to be produced by *B. phymatum*, the putative TBDR Bphy5373 was identified as having the highest identity of 25 % and is not present in the phymabactin (*phm*) gene cluster. All three ornibactin TBDR homologues, FmtA, MbaD and WP_042304263 showed high identities of 69 %, 70 % and 63 %, respectively to the *B. cenocepacia* OrbA except for Bphy5373 in *B. phymatum* (Figure 6.16).

B. cenocepacia chromosome 3 is predicted to encode two TBDRs, BCAS0333 and BCAS0360 (Chapter 3). Siderophore utilisation bioassays of the *B. cenocepacia pobA* mutant lacking chromosome 3, H111ΔC3ΔpobA, and unable to utilise pyochelin, H111ΔC3ΔpobAΔfptA were performed with filter discs impregnated with spent culture supernatants from *B. thailandensis* wild type and its mutant derivatives only producing malleobactin (pchE::Tet) or not producing any siderophores (pchE::Km mbaB::Tet). The assay showed the ability of H111ΔC3ΔpobA to grow around the filter disc impregnated with *B. thailandensis* wild type and the *pchE* mutant while H111ΔC3ΔpobAΔfptA growth was abolished with filter discs impregnated with culture supernatants of H111 *orbS* mutant and with the ΔpchE ΔmbaB mutant. These observations suggest that the TBDR for malleobactin may not be encoded by chromosome 3 of *B. cenocepacia* and so may not be BCAS0330 or BCAS0360 (Figure 6.3).

```
Bphy5373        1 -----------------------MYRTTPLAAAVMAAFATPLYAQTTTPATPAVQIEQAA-
WP_042304263    1 -----------------MEWVTGTQRRAIAAAASMTFLATATGHAQAQQAPDNQNSA---
OrbA            1 ---------MKKLEQKKMEWATGTRLRAIAAAASVAFGTAAAGHAYAQTAPAVNAGAAAS
FmtA            1 MMKVRPSRPLCNLEQRKMEWATSTRVRAIAAGVA-FYAAAA-GHAQAQAA---QPGADA-
MbaD            1 -----------------MEWATSTRVRAIAAAAGVAFGAAA-SHAQAQAV---RPGADA-

Bphy5373       38 -TSTSPASQPSASQPSESSVLPAVRVSGQAD--NANDFQPETSSVGAKVPTALRDIPQAA
WP_042304263   41 --------------QDKTATLPAVKVQGAAAGD-TEGFVAFRTATATKTDTPLDEVPQTV
OrbA           52 ASSAQNGATTNPSTGAQNGTLPAITVNAASAGDGTVGLVAKRSTTGTKTDTPLNEIPQTI
FmtA           55 ---RQPGG-EAKADTAAGGTLPAISVSGAAERDASVGLVARRSMTGTKTDTPIIEIPQTI
MbaD           39 ---RQPGS-QVNGDTAAGGTLPAISVSAGAERDASVGLVARRSTTGTKTDTPIVEIPQTI

Bphy5373       95 TVVPKAVLQSQAVSSFSDALRNVPGITIGAAEGGQIGNNINLRGFSARTDIYLDGFRD--
WP_042304263   86 NIVTAAQIEEQGATSINQALRYVPGFSSYGAST-RSDWYTAIRGFTP--SVFVDGLQVPN
OrbA          112 NVVTAQQIEMTGATDVNAALRYVPGFSSYGSDN-RSDWYAALRGFTP--TAYVNGLQVPN
FmtA          111 NVVTAQQIEATGATDINQAFRYIPGFSSYGSDN-RSDWYAALRGFTP--TVFVDGLQVPN
MbaD           95 NIVTAQQIEATGATDINQAFRYIPGFSTYGSDN-RSDWYAALRGFTP--TVFVDGLQVPN

Bphy5373      153 ---RGQMYRDTPNLESIDVLYGPSSLYFGRGSTGGVINQVSKEPTLRKRADVSVQAGTHD
WP_042304263  143 TINLASWRVDPYQVESITVLRGPTSVLYGQGDPGSLVDIQTKQPTAERIREIELQIGTDA
OrbA          169 TINLASWRVDPYMIDSISVLRGPTSVLYGAGDPGAIIDVHTKLADGERVREAGVQIGNYA
FmtA          168 TINLSSWRVDPYMIDSIAVLRGPTSVLYGQGDPGAIVDVQSKLANGERIRELGVQVGNYA
MbaD          152 TINLSSWRVDPYMIDSIAVLRGPTSVLYGQGDPGAIVDVQSKLANGERIREVGVQVGNYA

Bphy5373      210 RYRTTVDLDTPITDTSALRINAFGQ--SLGSSRDVKKNKDYGVAPEVKFGIGTPTEITLS
WP_042304263  203 RKQIGIDLGGKIDKDGTLTYRFVGVGRDGNMPTGPNADQRLMFAPSIKWQPTADTSLTLY
OrbA          229 RKQFMIDVGDKLDPDGKYAYRFVGVARDGNALTGPNNDQRVALAPSFRWRPDADTSLTLS
FmtA          228 RKQLMFDIGDTIGKDGTLSYRIVGVGRDGNAQTGPLADQRVSFAPSLKWQPNADTSLTLA
MbaD          212 RKQLMFDIGDKIDKDGTLSYRIVGVGRDGNAQTGPLADQRVSFAPSLKWQPNANTSLTLA

Bphy5373      268 ALIQHNRDQPDYGIPPLNGHPAPVNRGTFY--GYTDDRTIQ----DVQTLSARIKHRFNE
WP_042304263  263 ATYLRDNTDVSDNFLPASGTILPNPNGVISNDLYTGDGNFARYDKRQWSVGYQFEQRLNP
OrbA          289 ATYLQDWGDISSNFLPAQGTVLPNPNGQINKDIYEGDGNFNYYRKKQWSIGYQFERNLTP
FmtA          288 ATYLQDWGDTSSNFLPSRGTVLPNPNGTISDDLYTADANFDFYRKKQWSLGYQFEHKLNP
MbaD          272 ATYLQDWGDTSSNFLPSRGTVLPNPNGMISDDLYTADANFDFYRKKQWSIGYQFEHKLNP

Bphy5373      322 DLILRNQTQPSHYSTQARATNAASVLTGPLSTSPALTSGNFTTIDPSKLFVKLQGKDRNI
WP_042304263  323 TWTFRQNTRYMHLSLNNS-----TVYGG-----------GLDPTDPTEASLTRYAGQFQP
OrbA          349 AWTFRQNTRLMHLSLDNA-----SVFAN-----------GFAGD--SLTDVSRWAGLFQM
FmtA          348 VWTLRQNVRYMHLSLDDA-----SVYGG-----------GLDDADPTVATMTRYAGLFQF
MbaD          332 VWTFRQNVRYMHLALDDA-----SVYGG-----------GLDGADPTVATMTRYAGLFQF

Bphy5373      382 NDHSVYNSTDLEAKFNTGPLRHDVITGLDLSHETYSNQSPTATSPGMTSNTIGVVPLIDP
WP_042304263  367 NYSRFDIDNQAQAQFHTGSIEHTVLLGFEYNRQLSTDSEQLALAPSL--------NMFNP
OrbA          391 NYSRFDIDNNLEGRFATGPLQHTLLLGFQYNRQTATDSEWLAAAPTL--------NLYNP
FmtA          392 NYSRFDVDNQAQAKFTTGPLSHTLLFGFDYNRQTTTDSEWLAKGPSL--------NLYRP
MbaD          376 NYSRFDVDNQAQAKFTTGPLSHTLLFGFDYNRQTTTDSEWLAKGPGL--------NLYRP

Bphy5373      442 PYLPRPANVKEVAT----NLAESSANGVGAYVNDTVSIGQHWKVVGGVRWDRYEASIHNS
WP_042304263  419 VYVPVTSDIFSGPNSFGYSDTKTKLDSFGVYAQDQIKLTPRIVFTIGGRQDWSRNTTTNT
OrbA          443 VYTPVTMGVFSDPDATSRTNTYTTMNTFGLYAQDQIKWN-RWTLTLGGREDWVNMRQDDR
FmtA          444 VYTPIPSDIFSGPNAYPRTDTKTTLNAFGLYVQDQIKWR-RWVLTLGGRQDWTRTSQDDI
MbaD          428 VYTPIPADIFSGPNAYPRTDTKTTLNAFGLYVQDQIKWQ-RWVLTLGGRQDWTRTSQDDI

Bphy5373      498 INTPRYATQTNYFTSVRGGIIYQPADWQSYYVSYGTSFDPSLEALTLTNGQQNLPPEHNK
WP_042304263  479 VANTEQRQNDHAF-TYRVGAVYLGDYGLSPYISYATSFNPVIGVNADGT---PFQPTKGK
OrbA          502 AAGTSTKADVTAF-TGRVGLTYQGDYGLSPYISYATSFNPLIGVNLLGG--GLPQPTRGK
FmtA          503 ANAASFRQNDHAF-SGRVGLTYLGDYGLAPYLSYSTSFNPQIGLKLAGG--GLATPTKGR
MbaD          487 ANSASFKQNDHAF-SGRVGLTYLGDYGLAPYLSYSTSFNPQIGVKLAGG--GLATPTKGR
```

Figure 6.16: Alignment of OrbA TBDR in *B. cenocepacia* and the OrbA TBDR homologues

Amino acid sequences of (BCAL1700) from *B. cenocepacia* H111 were aligned with the OrbA TBDR homologue, FmtA of *B. pseudomallei*, MbaD of *B. thailandensis*, TBDR, WP_042304263 of *Paraburkholderia terrae* and Bphy5373 of *Paraburkholderia phymatum* showing percentage identities of 69 %, 70 %, 63 % and 25 %, respectively. Alignments were performed using ClustalW and identical or similar amino acids were highlighted using BOXSHADE. White font with black shading indicates identical residue at the corresponding position and white font with grey shading indicates similar residues at the corresponding position. Protein designations are indicated on the left.

Similarly, promotion of growth was also elicited by H111ΔC3ΔpobA using the culture supernatants of *B. phymatum* and *B. terrae* that produce phymabactin (Figure 6.6 and 6.7). However, it is possible that the OrbA-like receptor BCAS0333 may be able to recognise malleobactin and/or phymabactin but it is not the sole TBDR capable of transporting these siderophores. For example, OrbA may be able to transport them as discussed above.

To further test the hypothesis that OrbA is the putative malleobactin and phymabactin receptor, *orbA* knock-out mutants, H111ΔpobA-orbA::TpTer and H111ΔC3ΔpobA-orbA::TpTer were generated by allelic replacement. To do this, it was necessary to construct an appropriate allelic replacement plasmid and a complementation plasmid as described below.

6.4.1 Construction of pBBR-*orbA* and allelic replacement vector pSHAFT2-*orbA*::TpTer

Simplified diagrammatic constructions of pBBR-*orbA* and pSHAFT2-orbA::TpTer are depicted in Figures 6.17 and 6.18. The *orbA* gene (BCAL1700/I35_RS08065) was amplified by PCR using a boiled lysate of *B. cenocepacia* H111 with primer combination BCAL1700for and BCAL1700rev. PCR-amplified *orbA* gene with a size of 1780 bp (Figure 6.19A) was restriction digested with *Hin* II and *Xba*I and cloned into the same sites of pBBR1MCS forming pBBR1-*orbA* (6424 bp) (Figure 6.19B). Inactivation of the cloned *orbA* gene was performed by insertion of the TpTer cassette. The TpTer cassette was acquired from the plasmid p34E-TpTer by restriction digestion with *Bam*HI, releasing a 927 bp TpTer cassette. The cassette was ligated between the outermost of three *Bam*HI restriction sites in the *orbA* gene contained on pBBR1-*orbA,* forming pBBR-*orbA*::TpTer (6949 bp) (Figure 6.19C). Ligation products were transformed into JM83 *E. coli* cells and transformants were selected on IST medium containing trimethoprim (25 µg ml^{-1}). Six transformant colonies were patched separately on LB medium containing chloramphenicol (50 µg ml^{-1}) and LB agar containing ampicillin (100 µg ml^{-1}) to select colonies harbouring the plasmid pBBR1-*orbA*::TpTer and excluding the p34E part of the plasmid which encodes ampicillin-resistance.

The nucleotide sequence of DNA cloned into plasmids obtained from trimethoprim, chloramphenicol and ampicillin resistant colonies was determined to ensure insertion of the TpTer cassette and to determine its orientation. The orientation of the TpTer cassette in the plasmid pBBR1-*orbA*::TpTer was reconfirmed by using restriction digest method. The plasmid was restriction digested with *Bsr*GI and *Xba*I sequentially and the products were analysed by electrophoresis. The TpTer orientation diagnosis was performed by noting the different sizes of digested fragments.

The plasmid pBBR1-*orbA*::TpTer having the TpTer cassette in the same orientation as *orbA* gene was selected and was simultaneously restriction digested with *Bgl*II and *Xba*I. The products of this digestion were ligated to the plasmid pSHAFT2 digested with the same enzymes and the ligation products were transformed into *E. coli* CC118(λpir) cells.

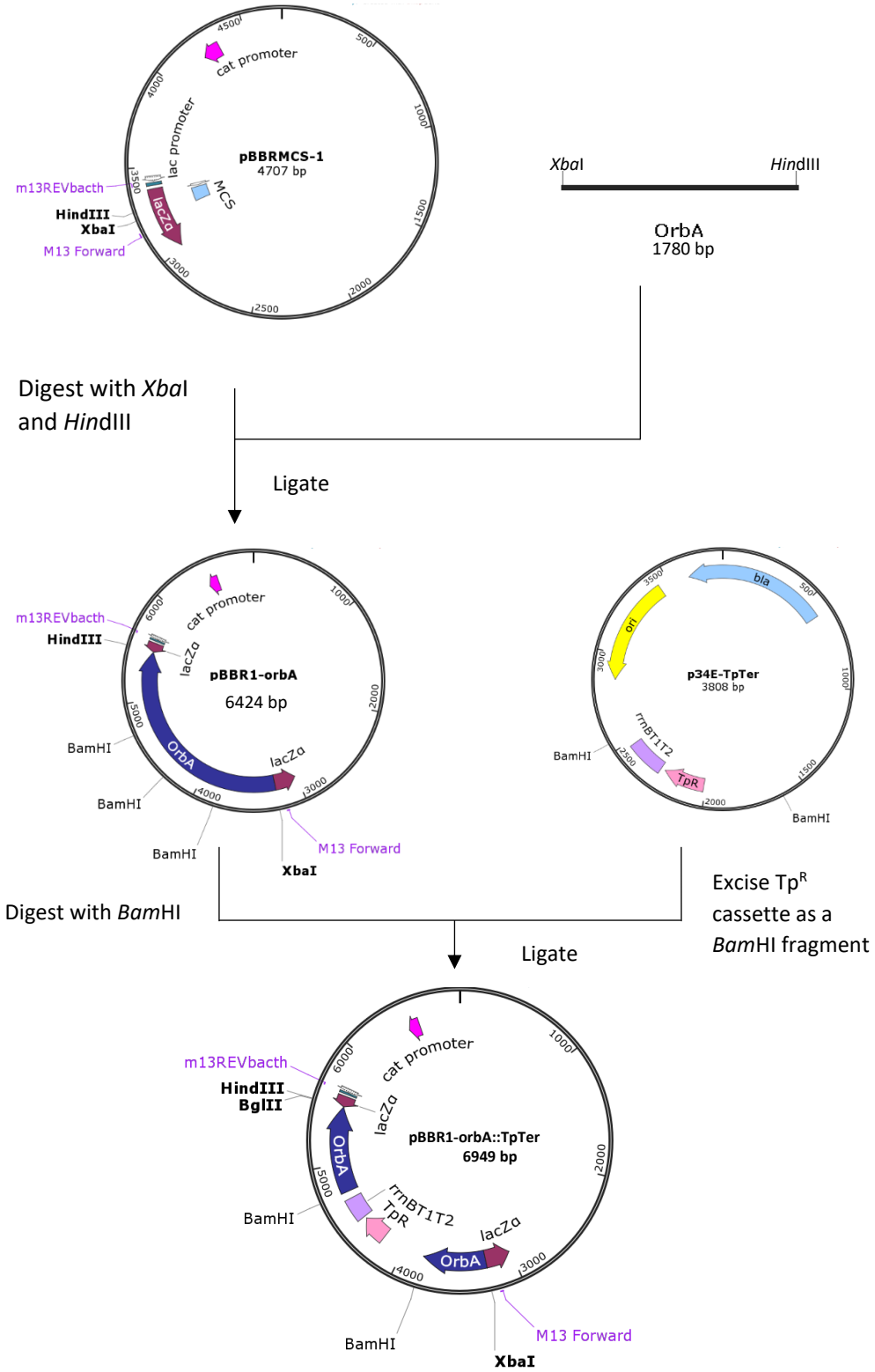

Figure 6.17: Construction of pBBR1-*orbA*::TpTer

The *orbA* gene fragment was cloned into expression vector pBBR1MCS. The trimethoprim resistance cassette (*dfr* gene) from p34E-TpTer was excised as a *Bam*HI fragment including the terminator (rrnBT1T2), and then ligated into the *Bam*HI restriction site of pBBR1-orbA, to give a pBBR1-*orbA*::TpTer with size of 6949 bp (bottom). The orientation of the trimethoprim cassette was determined by *Bsr*GI diagnostic restriction digestion. Pertinent vector features and restriction sites are indicated. Plasmid maps were depicted using SnapGene.

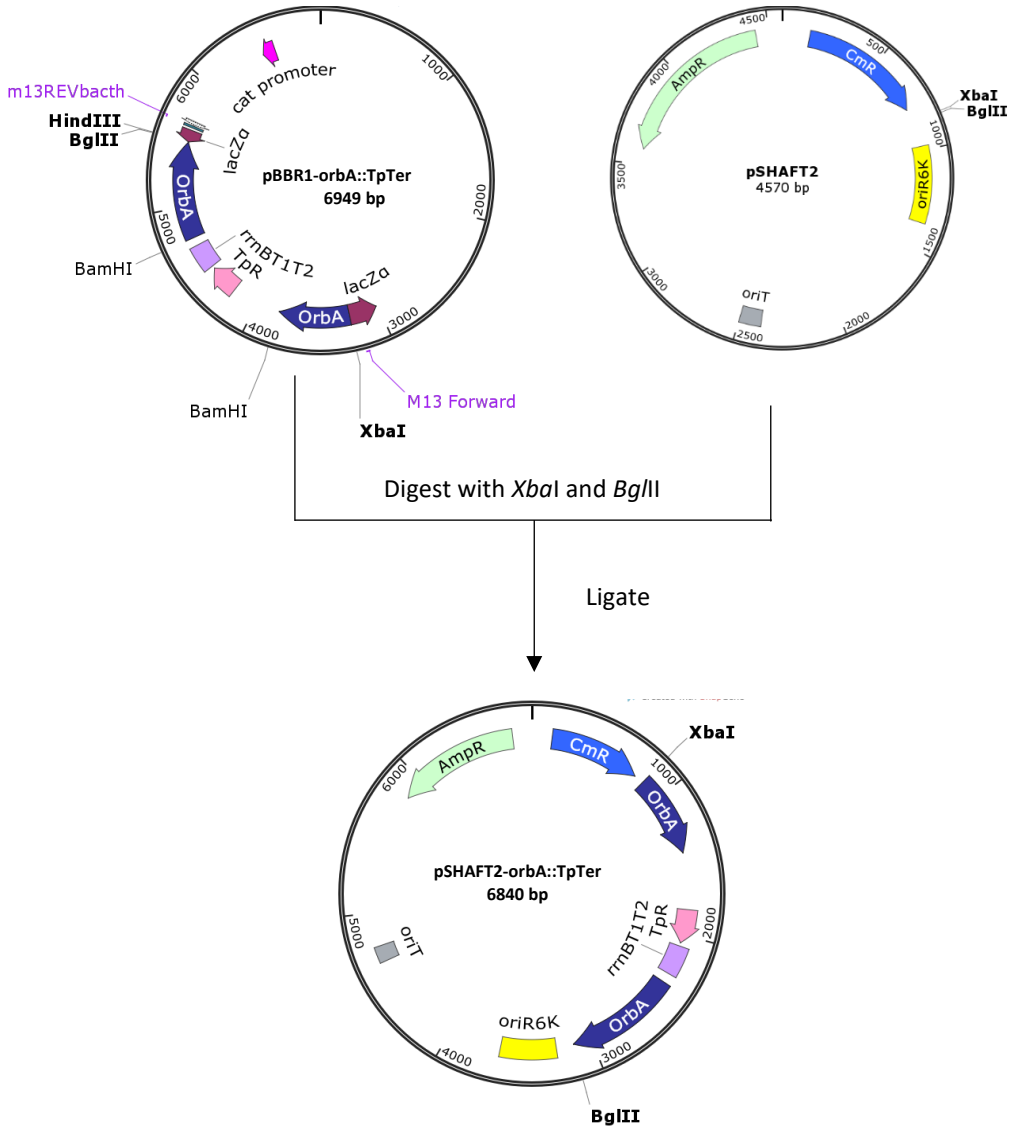

Figure 6.18: Construction of pSHAFT2-*orbA*::TpTer
The inactivated *orbA* gene was cut from pBBR1-*orbA*::TpTer and ligated into the suicide vector pSHAFT2, forming a pSHAFT2-*orbA*::TpTer (6840 bp). Pertinent vector features and restriction sites are indicated. Plasmid maps were depicted using SnapGene.

Transformed cells were selected on IST medium containing trimethoprim (25 µg ml^{-1}) and ampicillin (100 µg ml^{-1}) to select for CC118(λpir) containing the pSHAFT2-*orbA*::TpTer plasmid. Selected colonies were purified and prepared plasmid was analysed by gel electrophoresis giving a size of 6840 bp for the desired product. Confirmation of correct *orbA*::TpTer insertion in pSHAFT2 was achieved by DNA sequencing with the primers pUTcatrev and catendout.

6.4.2 Generation of H111ΔpobA-orbA::TpTer and H111ΔC3ΔpobA-orbA::TpTer

pSHAFT2-*orbA*::TpTer was introduced into the *E. coli* conjugal donor strain, SM10(λpir), and transformants were selected on IST plates containing trimethoprim (25 µg ml^{-1}). The donor strain containing pSHAFT2-*orbA*::TpTer was conjugated with *B. cenocepacia* strains H111ΔpobA and H111ΔC3ΔpobA on LB medium and the exconjugants were spread on M9-glucose agar containing 0.1 % CAA (M9-CAA, tetracycline (10 µg ml^{-1}) and trimethoprim (25 µg ml^{-1}). Approximately 50 large *Burkholderia* exconjugant colonies were patched on the same medium and separately on M9-CAA medium containing chloramphenicol (50 µg ml^{-1}). Large colonies were selected to avoid selection of spontaneous mutants. Single crossover recombination between *orbA* sequences on the chromosome and pSHAFT2-*orbA*::TpTer allows the entire plasmid to be integrated into the *B. cenocepacia* chromosome making the recombinants resistant to both trimethoprim and chloramphenicol.

A double crossover between the chromosomal *orbA* gene and the disrupted copy on the plasmid does not result in integration of the plasmid, leaving the recombinants sensitive to chloramphenicol and resistant to trimethoprim and allows selection of mutant candidates. Therefore, several mutant candidates which were sensitive to chloramphenicol were selected and purified. Candidates were screened by PCR using *orbA* 'outside primers' to confirm the allelic replacement of the wild type *orbA* gene by the constructed *orbA*::TpTer allele in H111ΔpobA and H111ΔC3ΔpobA (Figure 6.20).

6.4.3 Analysis of malleobactin utilisation by H111ΔpobA-orbA::TpTer and H111ΔC3ΔpobA-orbA::TpTer

As malleobactin structurally resembles ornibactin, the ornibactin receptor in *B. cenocepacia*, OrbA, was predicted to be the malleobactin receptor and its gene was knocked out by insertion of an antibiotic resistance cassette. The phenotype of the *orbA*::TpTer mutant was analysed with culture supernatants of *B. cenocepacia* KLF1, which only produces ornibactin, prior to analysis of the utilisation of malleobactin. The result showed that this mutant had lost ability to utilise ornibactin (Figure 6.21A). Malleobactin was obtained from the culture supernatant of the *B. thailandensis* pchE::Tet mutant, and its utilisation by the mutant H111ΔpobA-orbA::TpTer and H111ΔC3ΔpobA-orbA::TpTer was also tested. Ornibactin present in the supernatants of the *B. cenocepacia* mutant, KLF1, was included as a negative control. The siderophore bioassay showed no growth of the mutants around the filter disc impregnated with malleobactin, indicating OrbA as the TBDR for both malleobactin and ornibactin.

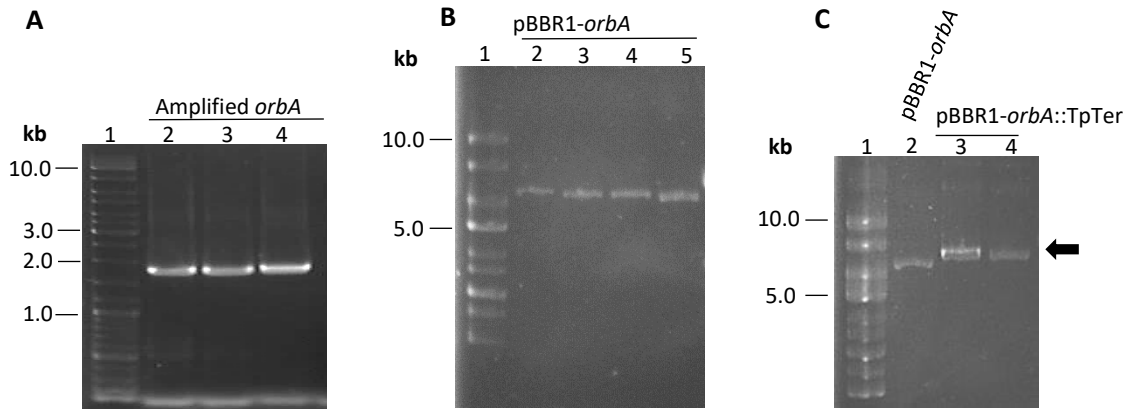

Figure 6.19: Construction of pBBR1-*orbA* and pBBR1-*orbA*::TpTer
(A) PCR amplification of *orbA* from a boiled lysate *B. cenocepacia* H111 with a gradient annealing temperature using primer combination BCAL1700for and BCAL1700rev: Lane 1, Linear DNA ladder; lanes 2-4, amplicons using annealing temperature at 61, 64 and 67 °C giving a product of 1780 bp. (B) Putative pBBR1-*orbA* clone candidates: Lane 1, Linear DNA ladder; Lanes 2-5 contain plasmids corresponding in size to pBBR-*orbA* (6424 bp). (C) Screenings of pBBR-*orbA*::TpTer candidates: Lane 1, supercoiled DNA ladder; Lane 2, pBBR-*orbA*; Lane 3-4, pBBR-*orbA*::TpTer candidate with a trimethoprim cassette insertion corresponding in size to the expected size (6949 bp) indicated by a black arrow.

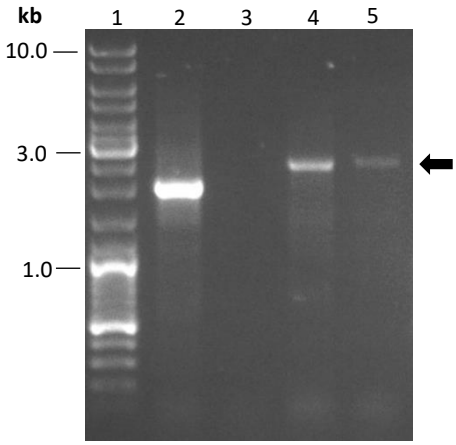

Figure 6.20: Generation of H111ΔpobA-*orbA*::TpTer
PCR 'outside primer' screenings of H111ΔpobA-*orbA*::TpTer mutant candidates using BCAL1700forout and BCAL1700revout at an annealing temperature of 59 °C: Lane 1, Linear DNA ladder; lane 2, *B. cenocepacia* H111 wildtype (1858 bp); lane 3, negative control (no template); lanes 4 and 5, H111ΔpobA-*orbA*::TpTer candidates showing an expected size of 2777 bp (indicated by a black arrow).

Growth of H111ΔC3ΔpobA, which has lost BCAS0333, was promoted by malleobactin present in the culture supernatants of the pchE::Tet mutant confirming previous observations (Section 6.4) (Figure 6.21B). In addition, the siderophore-deficient *B. thailandensis* mutant, pchE::Km mbaB::Tet was analysed for the utilisation of ornibactin and malleobactin present in the culture supernatants of the pchE::Tet mutant as a control. The mutant elicited growth in the presence of ornibactin indicating the ability of *B. thailandensis* to utilise ornibactin (Figure 6.22).

6.4.4 Screening of phymabactin utilisation by H111ΔpobA-orbA::TpTer

Although the phymabactin structure has not been determined, the siderophore is predicted to have a similar in structure to ornibactin and malleobactin, based on its NRPSs genes (Esmaeel et al., 2016; Butt and Thomas, 2017). As the culture supernatants of *B. terrae* and *B. phymatum* supported growth of H111ΔpobA under iron-limiting conditions, the supernatants were tested on H111ΔpobA-orbA::TpTer. No growth of this mutant was observed around filter discs applied with these culture supernatants (Figure 6.23). This may suggest that phymabactin is transported through the same TBDR as ornibactin.

6.5 Complementation of the *orbA* mutant

The role of OrbA in utilisation of malleobactin was validated by performing a complementation experiment with the OrbA mutant. To do this, plasmid, pSRKKm-*orbA* and pSRKKm-*fmtA* were used. The former complementation plasmid involved restoration of the ornibactin TBDR function and the latter entailed investigating the ability of the malleobactin TBDR of *B. thailandensis* E264 (FmtA, BTH_I2415) to act as an ornibactin TBDR. The full *orbA* gene was amplified (2490 bp) by the primers BCAL1700fullfor and BCAL1700fullrev and was double digested into a DNA fragment with *Xba*I and *Hin*dIII restriction ends. The cut fragment was ligated into pSRKKm plasmids having the same cut restriction sites. The constructed pSRKKm-*orbA* plasmids containing the *orbA* gene was transformed into *E. coli* S17-1(λpir) cells and were purified on LB agar containing kanamycin (25 µg ml^{-1}). The sequence of the construct was rectified by sequence analysis using the primers M13for and M13revBACTH. *E. coli* S17-1 cells containing pSRKKm-*orbA* and the empty vector, pSRKKm, were then conjugated with H111ΔpobA-orbA::TpTer. Ex-conjugants were selected on Lennox agar containing kanamycin (100 µg ml^{-1}) and tetracycline (10 µg ml^{-1}). Several colonies were screened by PCR using the vector backbone primers, M13for and M13rev, to confirm plasmid transfer (results not shown).

6.5.1 Construction of pSRKKm-*fmtA*

The *fmtA* gene from *B. thailandensis* E264 was amplified with primers BTHI2415for2 and BTHI2415rev and ligated to the *Xba*I and *Hin*dIII restriction sites of pSRKKm (Figure 6.24A). Ligated products were transformed into *E. coli* JM83 cells as previously described.

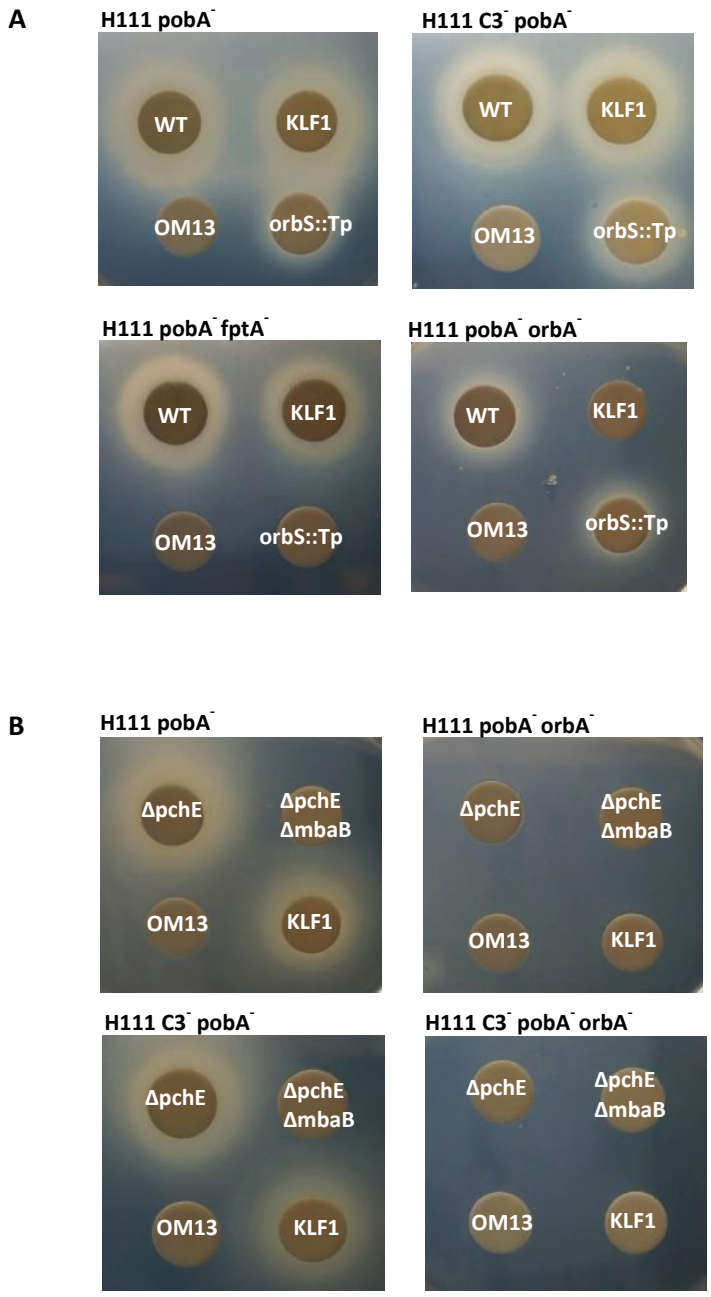

Figure 6.21: Analysis of utilisation of malleobactin by *orbA* TBDR mutant
(A) Phenotype confirmation of the *B. cenocepacia orbA* mutant, H111ΔpobA-orbA::TpTer. H111ΔpobA, H111ΔC3ΔpobA and H111ΔpobAΔfptA were included as controls. Culture supernatants applied to the filter discs contained ornibactin and pyochelin (WT H111), ornibactin (KLF1), pyochelin (H111-orbS::Tp) or no siderophores (OM13). (B) Analysis of the *B. cenocepacia* TBDR involved in malleobactin utilisation using the culture supernatants of *B. cenocepacia* and *B. thailandensis* mutants. Culture supernatants applied to the filter discs contained ornibactin, produced by *B. cenocepacia* (KLF1), malleobactin, produced by B. *thailandensis* (ΔpchE) and the negative controls for each *Burkholderia* spp. producing no siderophores (ΔpchEΔmbaB and OM13). Supernatants (100 µl) used were: WT, *B. cenocepacia* H111 wildtype; KLF1, *B. cenocepacia* mutant only producing ornibactin; orbS::Tp, H111-orbS::Tp only producing pyochelin; OM13, a siderophore-deficient *B. cenocepacia* mutant; ΔpchE, *B. thailandensis* mutant only producing malleobactin; ΔpchEΔmbaB, a siderophore-deficient *B. thailandensis* mutant. Final EDDHA concentration was 40 µM.

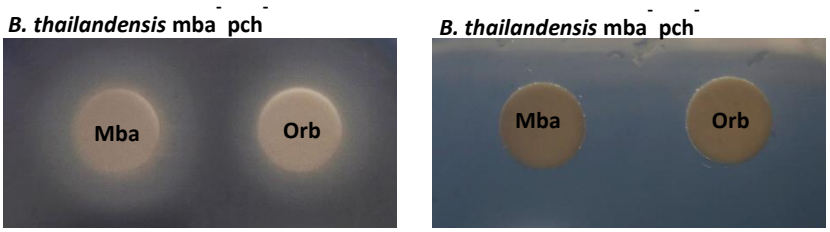

Figure 6.22: Analysis of the utilisation of ornibactin by a siderophore-deficient *B. thailandensis* mutant
Growth promotion of *B. thailandensis*, *pchE*::Km *mbaB*::Tet mutant in the presence of purified ornibactin (Orb) (1mM 10 µl). The culture supernatants of *B. thailandensis pchE:*:Tet (100 µl) containing malleobactin (Mba) was used as a positive control (left). *B. thailandensis* culture supernatants not containing malleobactin or pyochelin, *pchE*::Km *mbaB*::Tet mutant was used as a negative control and dH_2O was used as a negative control for ornibactin (right). Final EDDHA concentration was 40 µM.

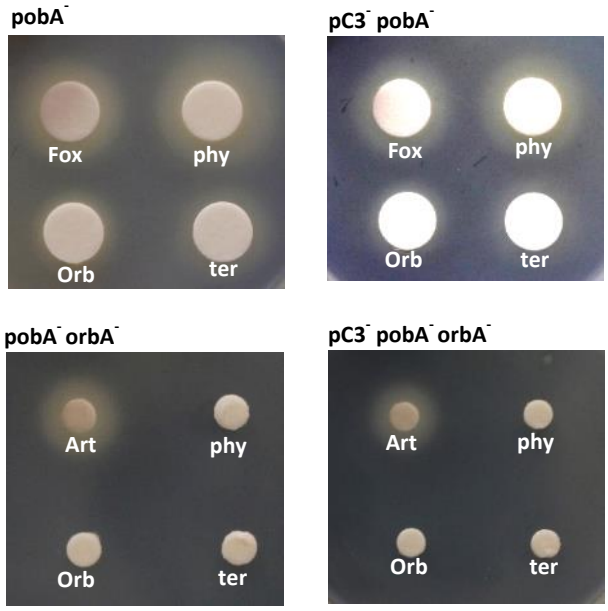

Figure 6.23: Analysis of the utilisation of phymabactin by disc diffusion assay
Growth promotion assays performed on H111ΔpobA, H111ΔC3ΔpobA, H111ΔpobA-orbA::TpTer and H111ΔC3ΔpobA-orbA::TpTer with *B. phymatum* and *B. terrae* culture supernatants. Ferrioxamine B, ornibactin and arthrobactin were used as controls. Supernatants (30-100 µl) used were from: phy, *B. phymatum* and ter, *B. terrae.* Purified siderophores used (1mM 5 µl): Orb, ornibactin; Fox, ferrioxamine B; Art, arthrobactin. Final EDDHA concentration was 40 µM.

White colonies that appeared on Lennox agar containing kanamycin (100 µg ml^{-1}), X-gal and IPTG were PCR screened with the amplification primers, and plasmids of the expected size (8045 bp) were sequenced using primers M13for and M13revBACTH (Figure 6.24B). The middle region of the gene was sequenced with primer fmtAmidfor. Two of the putative clones displayed point mutations resulting in in-frame stop codons at different positions in *fmtA* but one did not contain mutations. pSRKKm-*fmtA* and the empty vector, pSRKKm were transformed into S17-1(λpir) and then transferred to H111ΔpobA-orbA::TpTer by conjugation as previously described.

6.5.2 Complementation analysis of the malleobactin utilisation phenotype of the *B. cenocepacia orbA* mutant

H111ΔpobA-orbA::TpTer containing pSRKKm-*orbA* or pSRKKm-*fmtA* displayed growth around filter discs containing *B. thailandensis* pchE::Tet culture supernatants that contain malleobactin, and also around discs impregnated with *B. cenocepacia*, KLF1, only producing ornibactin. No growth was observed for the mutant containing the empty vector (Figure 6.25A). Zone of growth displayed by H111ΔpobA-orbA::TpTer containing pSRKKm-*fmtA,* however, was observed to be faint as compared to the *orbA*::TpTer mutant which contained the pSRKKm-*orbA* (Figure 6.25B). This observation may indicate low expression of the *B. thailandensis* genes in *B. cenocepacia* or low activity of the *lacZ* promoter on pSRKKm. Similar low efficiencies of complementation have been observed using this vector in *B. cenocepacia* (Section 4.5.4).

6.6 Screening for the TBDR for citrate-type hydroxycarboxylate-hydroxamate siderophores arthrobactin and schizokinen

As arthrobactin and schizokinen contain a single hydroxycarboxylate group and two hydroxamate groups, candidate receptors could include OrbA, the ornibactin TBDR, and the OrbA-like TBDR (BCAS0333). Therefore, H111ΔpobA, lacking pC3 and lacking both, OrbA and pC3 were tested for their ability to use these siderophores. However, growth of the *orbA*::TpTer mutant, H111ΔC3ΔpobA and H111ΔC3ΔpobA containing the *orbA*::TpTer allele under iron limiting conditions were supported by both siderophores using the disc diffusion assay (results not shown). Therefore, ten other potential single TBDR mutants (BCAL0116, BCAL1345, BCAL1371, BCAL1709, BCAL2281, BCAM0491, BCAM0499, BCAM1187, BCAM2007 and BCAM2224) were screened by disc diffusion assay using these siderophores. However, promotion of growth of these single TBDR mutants was supported by both siderophores (results not shown).

Since none of the single TBDR mutants were shown to be involved in the transport of the siderophores, strains containing double/triple mutant TBDR alleles were generated for testing by referring to the phylogenetic analysis. Combinations of double TBDR mutants included were BCAL1371^{-}BCAM2439^{-} (Aljadani and Thomas, unpublished results), BCAL0116^{-}BCAL2281^{-}, BCAM1187^{-}BCAM2007^{-}, BCAL1345^{-}BCAM0491^{-} and BCAL1709^{-}BCAM0499^{-}.

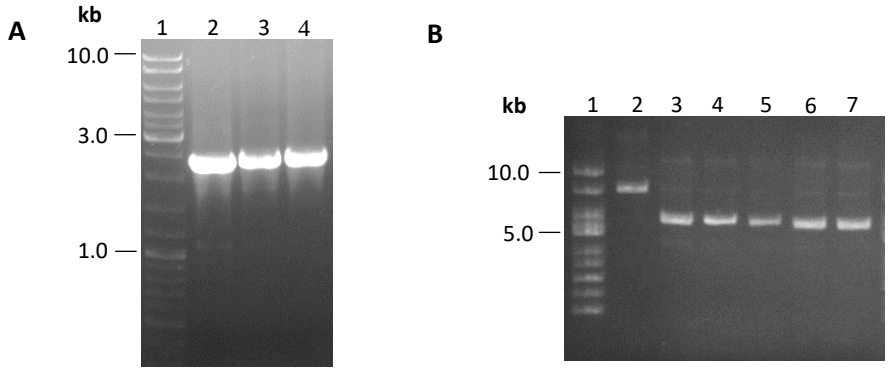

Figure 6.24: Construction of pSRKKm-*fmtA*
(A) The 2.30 kb *fmtA* DNA fragment from *B. thailandensis* E264 was amplified by cPCR with primers BTHI2415for2 and BTHI2415rev and analysed by agarose gel electrophoresis: Lane 1, Linear DNA ladder; lanes 2-4, *fmtA* PCR product generated with annealing temperatures at 55, 57 and 59 °C. (B) Gel electrophoresis of putative clone candidates of pSRKKm-*fmtA*: Lane 1, Supercoiled DNA ladder; lanes 2-7, putative clone candidates with lane 1 showing the expected plasmid size of 8045 bp.

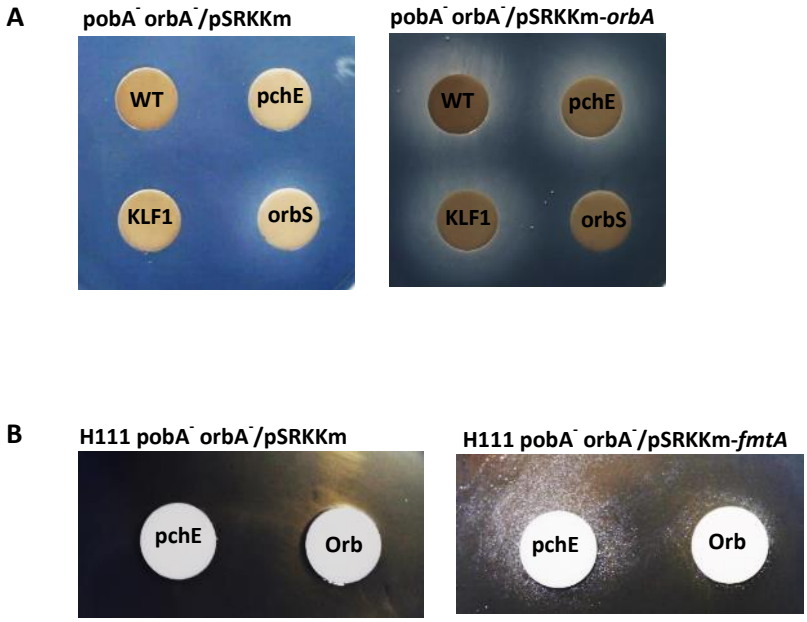

Figure 6.25: Complementation of a *B. cenocepacia orbA* mutant by *orbA* and *fmtA* in *trans*
Restoration of the ornibactin utilisation phenotype of H111ΔpobA-orbA::TpTer with complementation plasmids pSRKKm-*orbA* (A) and pSRKKm-*fmtA* (B). In both cases the corresponding empty vector was included as a control. Culture supernatants (100 µl) used were from: WT, *B. thailandensis* wildtype; KLF1, *B. cenocepacia* mutant only producing ornibactin; orbS, *B. cenocepacia* mutant, 715jΔorbS only producing pyochelin and pchE, a B. *thailandensis* mutant only producing malleobactin. Orb, purified ornibactin (1 mM 10 µl). Final EDDHA concentration was 40 µM.

The putative TBDR BCAS0360 was seen to be nearby to four putative TBDRs in the phylogenetic tree, which were BCAL1371, BCAL1709, BCAM0499 and BCAM2439. Therefore, H111ΔpobA lacking pC3 (containing the putative TBDRs BCAS0333 and BCAS0360) was used as a host to introduce mutant alleles of these TBDRs. Consequently, the additional double TBDR mutants tested, (excluding BCAS0333, in this case) were BCAM2439$^-$BCAS0360$^-$, BCAL1371$^-$BCAS0360$^-$, BCAL1709$^-$BCAS0360$^-$, BCAM0499$^-$BCAS0360$^-$ and the triple TBDR mutant tested was BCAL1371$^-$BCAM2439$^-$BCAS0360$^-$. Putative TBDRs hypothesised not to transport siderophores were not investigated (BCAL1777, BCAL3001, BCAM0564, BCAM0948, BCAM1571, BCAM1593, BCAM2367 and BCAM2626).

6.6.1 Generation of double and triple TBDR mutants

Generation of mutants was achieved by insertion of a trimethoprim or chloramphenicol-resistance cassette into the TBDR gene, which resulted in generation of the double and triple putative TBDR mutants. As the following double TBDR mutants were already available, H111ΔpobA-BCAL1371::Tp-BCAM2439::Cm (Aljadani, 2018) (Figure 6.26A and B), H111ΔpobAΔBCAL2281-BCAL0116::TpTer (Chapter 4) and H111ΔpobAΔBCAM2007-BCAM1187::TpTer (Chapter 5), the two double TBDR mutants, H111ΔpobA-BCAL1345::Cm-BCAM0491::TpTer and H111ΔpobA-BCAM0499::Cm-BCAL1709::TpTer were generated. Alleles disrupted by a trimethoprim-resistance cassette were obtained from the previously constructed plasmid pSHAFTGFP-BCAM0491::TpTer and pSHAFTGFP-BCAM1709::TpTer (Sofoluwe and Thomas, unpublished results). To disrupt TBDR genes with the chloramphenicol-resistance cassette, the cassette was obtained from plasmid p34E-Cm2 and ligated into the previously constructed plasmids pSHAFTGFP-BCAL1345 and pSHAFTGFP-BCAM0499 (Sofoluwe and Thomas, unpublished results). Previously constructed pSHAFTGFP derivatives were sequenced using the primers GFPstartout and pUTcatrev to confirm their integrity prior to use.

For the generation of H111ΔpobA-BCAM0499::Cm-BCAL1709::TpTer, pSHAFTGFP-BCAL1709::TpTer was introduced into SM10(λpir) and conjugated to H111ΔpobA. Conjugation was performed as previously described by selecting exconjugants on M9-glucose agar containing trimethoprim (Section 4.4.1). Mutant candidates with exclusion of the pSHAFTGFP plasmid were selected by picking non-fluorescent colonies which were patched concurrently on the selection medium and IST medium containing trimethoprim. Purified mutant candidates which acquired the inactivated BCAL1709 gene were screened using the outside primers BCAL1709forout and BCAL1709revout. The generated mutant, H111ΔpobA-BCAL1709::TpTer was then used for the introduction of the inactivated BCAM0499 gene. *E. coli* CC118(λpir) cells harbouring the pSHAFTGFP-BCAM0499 was grown overnight in LB medium containing ampicillin (100 µg ml^{-1}) for plasmid preparation.

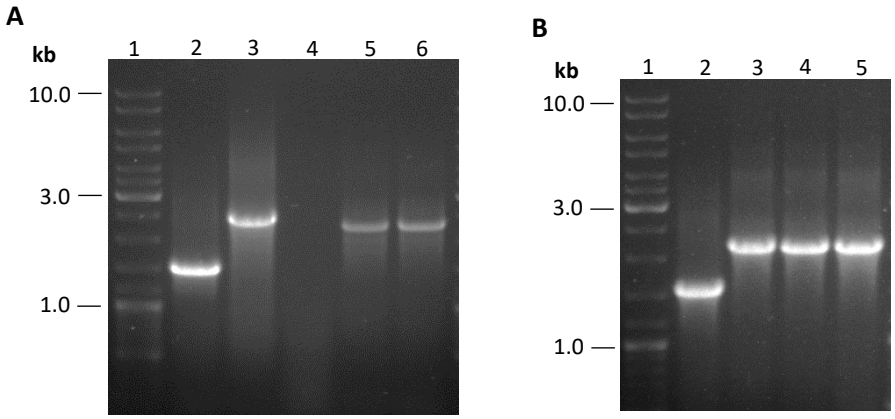

Figure 6.26: Confirmation of H111ΔpobA-BCAL1371::TpTer-BCAM2439::Cm genotype
H111ΔpobA-BCAL1371::TpTer-BCAM2439::Cm was constructed previously (Aljadani, 2018) and the integrity of the TBDR double mutant strain was confirmed by PCR screening. (A) Confirmation of the presence of the BCAM2439::Cm allele using 'outside primer' combination BCAM2439forout and BCAM2439revout at an annealing temperature of 56 °C. Lane 1, Linear DNA ladder; lane 2, H111 wildtype; lane 3, AHA27 BCAM2439::TpTer, lane 4; SM10 containing pSHAFTGFP BCAM2439::Cm as negative control; lanes 5-6, H111ΔpobA-BCAL1371::TpTer-BCAM2439::Cm. (B) Confirmation of the presence of the BCAL1371::TpTer allele using 'outside primer' combination flrAforout and flrArevout at an annealing temperature of 56 °C. Lane 1, Linear DNA ladder; lane 2, H111 wildtype; lane 3, AHA27 BCAL1371::TpTer; lanes 4-5, H111ΔpobA-BCAL1371::TpTer-BCAM2439::Cm.

The plasmids pSHAFTGFP-BCAM0499 and p34E-Cm2 were then cut at their *Eco*RI restriction sites and were analysed by agarose gel electrophoresis which gave rise to fragment sizes of 5.7 kb of cut pSHAFTGFP-BCAM0499. Cut p34E-Cm2 gave rise to two DNA fragment sizes of 2.9 kb and 0.8 kb. The chloramphenicol-resistance cassette (0.8 kb) containing *Eco*RI flanking sites was gel-purified and ligated into the *Eco*RI site located in the BCAM0499 gene in pSHAFTGFP-BCAM0499, forming pSHAFTGFP-BCAM0499::Cm with an expected size of 6.5 kb. Insertion of the chloramphenicol-resistance cassette was confirmed by sequencing using the primers, GFPstartout and pUTcatrev.

Conjugation was then employed between SM10(λpir) containing pSHAFTGFP-BCAM0499::Cm and the H111ΔpobA-BCAL1709::TpTer mutant. Exconjugants isolated from M9-glucose agar containing chloramphenicol (50 µg ml^{-1}) were then patched onto the same selection medium and IST agar containing chloramphenicol (50 µg ml^{-1}). Non-fluorescent colonies were identified and purified on the selection medium, then PCR screened using 'outside primers' BCAM0499forout and BCAM0499revout, which identified mutants with an inactivated BCAM0499 gene, H111ΔpobA-BCAL1709::TpTer-BCAM0499::Cm with a fragment size of 2.5 kb and a fragment size of 1.4 kb for H111ΔpobA-BCAL1709::TpTer (Figure 6.27A-C). H111ΔpobA-BCAM0499::Cm was generated in parallel.

For the generation of H111ΔpobA-BCAM0491::TpTer-BCAL1345::Cm, conjugation was performed between SM10(λpir) containing pSHAFTGFP-BCAM0491::TpTer and the H111ΔpobA mutant. H111ΔpobA-BCAM0491::TpTer mutants were selected as previously described and was confirmed using the outside primers BCAM0491forout and BCAM0491revout that gave rise to a 2.4 kb DNA fragment for mutants and 1.4 kb for the wildtype (Figure 6.27D). The plasmid pSHAFTGFP-BCAL1345::Cm was then constructed and introduced into H111ΔpobA-BCAM0491::TpTer. For construction of pSHAFTGFP-BCAL1345::Cm, pSHAFTGFP-BCAL1345 (5.7 kb) and p34E-Cm2 were cut with *Kpn*I and the chloramphenicol cassette released from p34E-Cm2 (0.8 kb) was gel-purified prior to ligation to pSHAFTGFP-BCAL1345.

Fluorescent CC118(λpir) colonies harbouring ligation products were selected on LB agar containing chloramphenicol (50 µg ml^{-1}). Plasmids were prepared and analysed by agarose gel electrophoresis to screen for plasmids having a size of 6.5 kb. The plasmid pSHAFTGFP-BCAL1345::Cm was sequenced for confirmation of chloramphenicol cassette insertion in the BCAL1345 gene. The plasmid was then transformed into SM10(λpir) and conjugation was performed with H111ΔpobA-BCAM0491::TpTer. Selection of mutant candidates was performed as previously described. Generation of the mutant, H111ΔpobA-BCAM0491::TpTer-BCAL1345::Cm, was confirmed by PCR screening using the outside primer BCAL1345forout and BCAL1345revout, giving rise to a fragment size of 2.2 kb for the mutants and 1.4 kb for candidates with no insertion of the chloramphenicol-resistance cassette in the BCAL1345 gene.

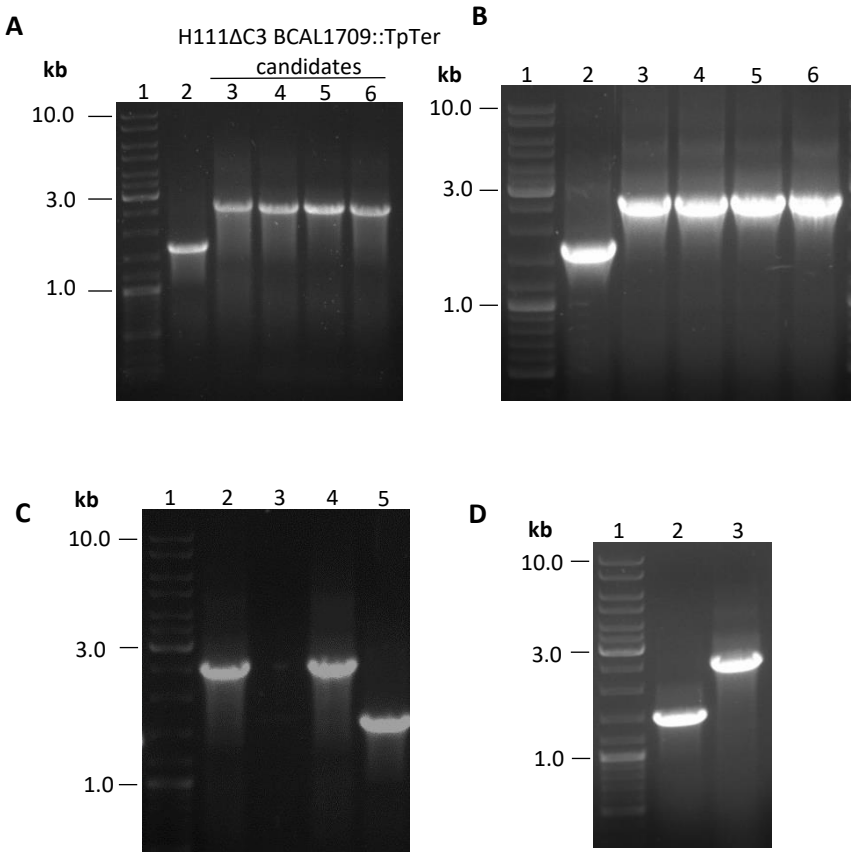

Figure 6.27: Screening of candidate H111ΔpobA-BCAL1709::TpTer, H111ΔpobA-BCAL1709::TpTer-BCAM0499::Cm, H111ΔC3ΔpobA-BCAL1709::TpTer and H111ΔpobA-BCAL0491::TpTer mutants
(A) PCR screening of H111ΔC3ΔpobA-BCAL1709::TpTer mutant candidate for trimethoprim-resistance cassette insertion in BCAL1709 gene using primer combination BCAL1709forout and BCAL1709revout with an annealing temperature of 55 °C: Lane 1, Linear DNA ladder; lane 2, H111 wildtype as negative control; lane 3, AHA27-BCAL1709::TpTer as positive control; lanes 4-6, mutant candidates of H111ΔC3ΔpobA-BCAL1709::TpTer showing insertion of the trimethoprim-resistance cassette. (B) PCR screening of H111ΔpobA-BCAL1709::TpTer mutant candidates using 'outside primer' combination BCAL1709forout and BCAL1709revout. Lane 1, Linear DNA ladder; lane 2, H111 wildtype as negative control; lane 3, AHA27 BCAL1709::TpTer as positive control; lanes 4-6, show desired mutants generating H111ΔpobA-BCAL1709::TpTer at a corresponding DNA fragment size of 2.5 kb. (C) PCR screening of H111ΔpobA BCAL1709::TpTer-BCAM0499::Cm mutant candidates using 'outside primer' combination BCAL1709forout and BCAL1709revout. Lane 1, Linear DNA ladder; lane 2, mutant candidate H111ΔpobA-BCAL1709::TpTer-BCAM0499::Cm showing trimethoprim-resistance cassette insertion in the BCAL1709 gene; lane 3, negative control (no template); lane 4, AHA27 BCAL1709::TpTer as a positive control; lane 5, H111 wildtype showing a band at a corresponding DNA fragment size of 1631 bp. (D) PCR screening of H111ΔpobA-BCAL0491::TpTer mutant candidate using primer combination BCAL0491forout and BCAL0491revout with an annealing temperature of 57 °C. Lane 1, Linear DNA ladder; lane 2, H111 wildtype as a negative control with a DNA fragment size of 1440 bp; lane 3, mutant candidate with a 927 bp trimethoprim-resistance cassette insertion in the BCAM0491 gene generating H111ΔpobA-BCAL0491::TpTer with a corresponding DNA fragment size of 2361 bp.

For the generation of H111ΔpobA TBDR mutants lacking the pC3 chromosome, pSHAFTGFP-BCAL1371::Tp (Paleja and Thomas, unpublished results), pSHAFTGFP-BCAM2439::Cm (Aljadani and Thomas, unpublished results), pSHAFTGFP-BCAL1709::TpTer (Sofoluwe and Thomas, unpublished results) and the constructed pSHAFTGFP-BCAM0499::Cm were separately transformed into the conjugal donor, SM10(λpir), and were then conjugated into H111ΔpobAΔC3. Selection media for exconjugants were based on the antibiotic cassette insertion used for inactivating the inactivated TBDR gene. Non-fluorescent mutant candidates were selected as previously described.

The mutants H111ΔC3ΔpobA-BCAL1371::Tp, H111ΔC3ΔpobA-BCAL1709::TpTer, H111ΔC3ΔpobA-BCAM2439::Cm and H111ΔC3ΔpobA-BCAM0499::Cm were identified by PCR screening using corresponding 'outside primers'. The triple TBDR mutant, H111ΔpobAΔC3-BCAL1371::Tp-BCAM2439::Cm was also generated using the same method described. The generation of this mutant involved introduction of plasmid pSHAFTGFP-BCAL1371::Tp into H111ΔC3ΔpobA-BCAM2439::Cm by conjugation (Figure 6.28).

6.6.2 Analysis on the utilisation of arthrobactin and schizokinen by *B. cenocepacia*

The ability of mutant strains harbouring two or three disrupted TBDR alleles to utilise arthrobactin and schizokinen was tested using the disc diffusion assay. These mutants are H111ΔpobAΔBCAL2281-BCAL0116::TpTer, H111ΔpobAΔBCAM2007-BCAM1187::TpTer, H111ΔpobA-BCAL1371::Tp-BCAM2439::Cm, H111ΔpobA-BCAL1709::TpTer-BCAM0499::Cm, H111ΔpobA-BCAM0491::TpTer-BCAL1345::Cm, H111ΔpobAΔC3-BCAM2439::Cm-BCAL1371::Tp, H111ΔpobAΔC3-BCAM2439::Cm, H111ΔpobAΔC3-BCAL1371::Tp, H111ΔpobAΔC3-BCAL1709::TpTer and H111ΔpobAΔC3-BCAM0499::Cm. However, growth haloes were observed in the assays using all ten mutants tested indicating another TBDR or combination of TBDRs was involved in the transport of these siderophore. Growth promotions exhibited by a single TBDR mutant, BCAM2007 and a double TBDR mutant, H111ΔpobA-BCAM0491::TpTer-BCAL1345::Cm are shown in Figure 6.29A.

Based on these observations, two other putative TBDRs only found in the H111 strain, I35_RS19580 (BCAM0706) and I35_RS08490 ('BCAL1783') were considered for arthrobactin/schizokinen transport screening. By *in silico* analysis, the TBDR gene I35_RS19580 was observed to be non-functional in *B. cenocepacia* J2315 and K56-2 strains and remain intact in 715j and H111 strains (Section 3.5). The TBDR protein I35_RS08490 is only found to be non-functional in the J2315 strain and is intact in all the three strains, H111, 715j and K56-2 (Chapter 3).

To investigate the possible role of I35_RS19580 in athrobactin utilisation, growth promotion of *B. cenocepacia* K56-2-orbI::Tp was tested under iron-limited conditions in the presence of arthrobactin.

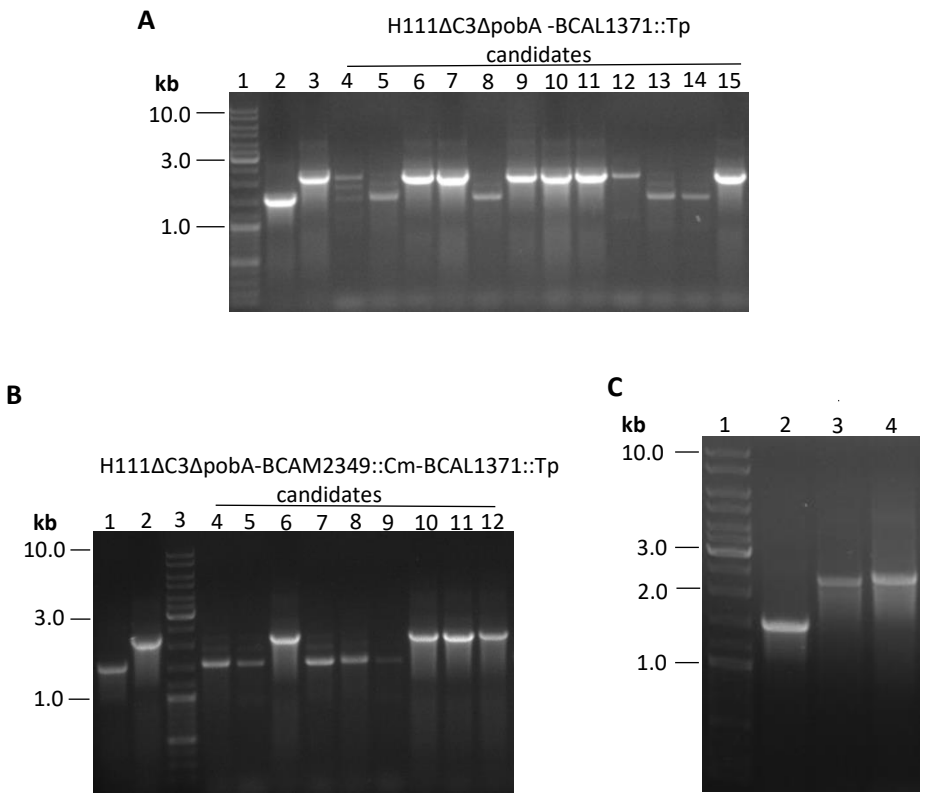

Figure 6.28: Screening of candidate *B. cenocepacia* H111ΔC3ΔpobA-BCAL1371::Tp and H111ΔC3ΔpobA-BCAM2349::Cm-BCAL1371::TpTer mutants

PCR screening of (A) H111ΔC3ΔpobA-BCAL1371::Tp and (B) H111ΔC3ΔpobA-BCAM2349::Cm-BCAL1371::Tp mutant candidate for trimethoprim-resistance cassette insertion in the BCAL1371 gene using 'outside' primer combination flrAforout and flrArevout with an annealing temperature of 57 °C. In (A) Lane 1, linear DNA ladder; lane 2, H111 wildtype as negative control; lane 3, AHA27-BCAL1371::Tp as positive control; lanes 4-15 show mutant candidates with lanes 4, 6, 7 9-12 and 15 corresponding to the desired mutants. In (B) Lane 1, H111 wildtype as negative control; lane 2, AHA27-BCAL1371::Tp as positive control; lane 3, linear DNA ladder; lanes 4-12 show mutant candidates with lanes 6 and 10-12 corresponding to the desired mutants. (C) PCR confirmation of H111ΔC3ΔpobA-BCAM2349::Cm-BCAL1371::TpTer mutant candidate for chloramphenicol-resistance cassette insertion in the BCAM2439 gene using primer combination BCAM2439forout and BCAM2439revout with an annealing temperature of 58 °C. Lane 1, Linear DNA ladder; lane 2, H111 wildtype as negative control; lane 3, H111ΔpobA-BCAM2349::Cm-BCAL1371::Tp as positive control; lane 4, H111ΔC3ΔpobA-BCAM2349::Cm-BCAL1371::Tp mutant.

Besides not having an intact I35_RS19580 TBDR protein, biosynthesis of ornibactin in *B. cenocepacia* K56-2-orbI::Tp is inhibited. Production of the secondary siderophore, pyochelin is considered negligible due to a mutation in *pchE* (Sokol et al., 1999; Shalom et al., 2007; Holden et al., 2009; Varga et al., 2013). The assay showed no growth around the filter disc impregnated with arthrobactin, suggesting that arthrobactin maybe transported via the BCAM0706 TBDR or other potential TBDRs (Figure 6.29B).

By *in silico* analysis, *B. thailandensis* was observed not to possess the BCAM0706 and 'BCAL1783' TBDRs (Section 3.5). Therefore, to re-evaluate the TBDR involved in arthrobactin transport, a siderophore-deficient *B. thailandensis* was screened using the disc diffusion assay. However, in this assay, *B. thailandensis* pchE::Tet mbaB::Km exhibited growth halos around the disc impregnated with arthrobactin (result not shown), suggesting BCAM0706 may not be the arthrobactin TBDR.

6.7 Investigation of the utilisation of catecholate-hydroxamate siderophores by *B. cenocepacia*

The pyoverdines are mixed type catecholate-hydroxamate siderophores. Many types of pyoverdine siderophores were screened for their ability to provide iron to *B. cenocepacia*: pyoverdine (I, II, III), pyoverdine ATCC17571 (PflW) and pyoverdine protegens. Pyoverdine I, II, III were provided as culture supernatants from *P. aeruginosa* PAO1 Δpch, *P. aeruginosa* W15Dec8 and *P. aeruginosa* W15Aug24, respectively. Pyoverdine PflW and pyoverdine protegens were provided from supernatants of *P. fluorescens* ATCC17571 and *P. protegens* Δepch, respectively. No growth of H111ΔpobA was elicited with filter discs impregnated with pyoverdine I, pyoverdine PflW or pyoverdine protegens (results not shown).

P. aeruginosa W15Dec8 and *P. aeruginosa* W15Aug24 are wildtypes and release two siderophores in their supernatant, pyochelin with pyoverdine II or III, respectively. H111ΔpobA exhibited growth around filter discs impregnated with these culture supernatants. Since there was a mixture of two siderophores in the tested supernatant, a pyochelin TBDR mutant H111ΔpobAΔfptA was used to re-examine the ability of these culture supernatants to support the growth of *B. cenocepacia*. However, no growth was observed around filter discs impregnated with the culture supernatants of *P. aeruginosa* W15Aug24 and W15Dec8 (result not shown) indicating an inability of *B. cenocepacia* to exploit pyoverdine II and III for iron uptake.

6.8 Investigation of utilisation of phenolate siderophores *by B. cenocepacia*

All siderophores with a phenolate moiety used for screening were obtained from culture supernatants of *Pseudomonas* spp. except for yersiniabactin and pyochelin, reported previously (Chapter 5). Both thioquinolobactin and quinolobactin were screened using culture supernatants from *P. fluorescens* ATCC17400 SF1 Δpvd, pseudomonine was from *P. chlororaphis* ATCC17813 Δpvd and enantio-pyochelin was from *P. protegens* Δpvd. None of the phenolates allowed growth of H111ΔpobA in the disc diffusion assay.

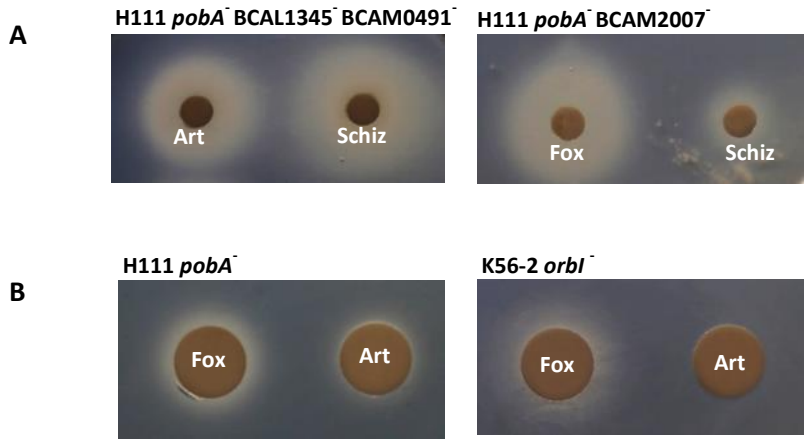

Figure 6.29: Effect of TBDR inactivation on utilisation of arthrobactin and schizokinen by *B. cenocepacia*
(A) Screening of arthrobactin (Art) and schizokinen (Schiz) utilisation using a single and double TBDR mutant, H111ΔpobAΔBCAM2007 and H111ΔpobA-BCAL1345::Cm-BCAM0491::TpTer by the disc diffusion assay. Amount of arthrobactin and schizokinen used were 1 mM 30 µl and 5 mM 30 µl, respectively. Final EDDHA concentration was 40 µM. (B) Analysis of arthrobactin utilisation by *B. cenocepacia* K56-2 *orbI*::Tp, which produces low amount of pyochelin. H111ΔpobA and ferrioxamine B (Fox) were used as controls. Amount of ferrioxamine B and arthrobactin used were 1 mM 15 µl. Final EDDHA concentration used was 200 µM to reduce growth effect of mutants due to pyochelin production.

Additionally, purified nicotianamine, a metallophore having a characteristic of a siderophore without a common ligand, was also investigated and was not shown to support growth of H111ΔpobA (Figure 6.30 and 6.31). A siderophore-deficient *P. aeruginosa* was used as a positive control for testing the activity of nicotianamine.

6.9 Role of the TonB1 system in utilisation of mixed hydroxamate-hydroxycarboxylate siderophores

The TonB1 system plays an important role in hydroxamate and catecholate siderophore transport (Chapters 4 and 5). The utilisation of the mixed hydroxamate-hydroxycarboxylate siderophores arthrobactin, schizokinen and malleobactin, by the *B. cenocepacia exbB*1 mutant, AHA9, was tested (malleobactin was provided as a culture supernatant from *B. thailandensis* E264). Purified ornibactin was included as a control. As expected, AHA9 was unable to utilise any of these siderophores (results not shown).

6.10 Investigation into the role of the BCAL0117 hydroxamate siderophore inner membrane transport system in utilisation of hydroxamate-hydroxycarboxylate mixed type siderophores

BCAL0117 has been shown to serve as the cytoplasmic membrane transport system for most of the hydroxamate siderophores utilised by *B. cenocepacia* (Section 4.9). To determine whether this system also plays a role in uptake of hydroxamate-hydroxycarboxylate siderophores, the ability of various hydroxamate-hydroxycarboxylate siderophores to support growth of the BCAL0117 mutant under iron-limiting conditions was tested. Filter discs were impregnated with ornibactin, arthrobactin, schizokinen and culture supernatant of *B. thailandensis* pchE::Tet containing malleobactin and tested by disc diffusion assay (Figure 6.32). All of these siderophores promoted growth of the mutant, indicating that transport of these siderophores does not depend on BCAL0117.

6.11 Discussion

The study findings on the utilisation of mixed-ligand siderophores by *B. cenocepacia* will be discussed as well as conclusions on additional siderophores that do not appear to deliver iron to *B. cenocepacia.*

6.11.1 Utilisation of mixed ligand siderophores containing hydroxycarboxylate groups

The siderophore malleobactin is a virulence factor of *B. pseudomallei*, a pathogenic soil bacterium able to cause a tropical infectious disease called melioidosis (White, 2003). *B. pseudomallei* has been demonstrated as a potential pathogen in CF lung disease (O'Carroll et al., 2003).

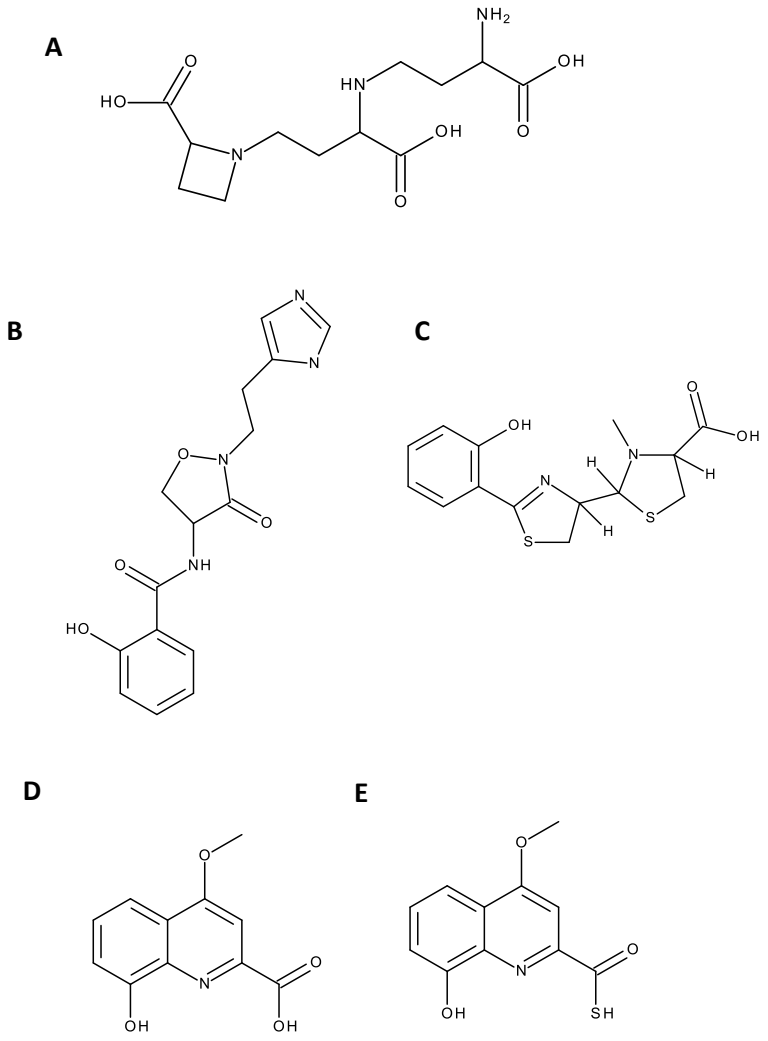

Figure 6.30: The molecular structures of some siderophores tested for utilisation by *B. cenocepacia*
(A) Nicotianamine, (B) pseudomonine, (C) enantio-pyochelin, (D) quinolobactin and (E) thioquinolobactin. Chemical structures were depicted using Accelrys Draw 4.2.

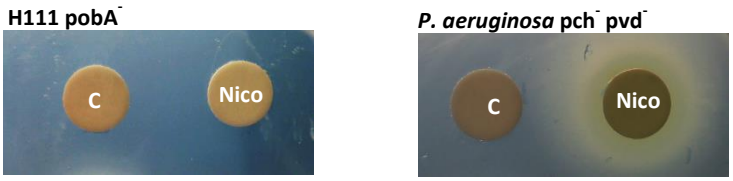

Figure 6.31: Analysis of nicotianamine utilisation by *B. cenocepacia*
Analysis on the ability of nicotianamine (1 mM 40 µl) to support growth of H111ΔpobA under iron-limiting conditions. A siderophore-deficient *P. aeruginosa* was used as a control.

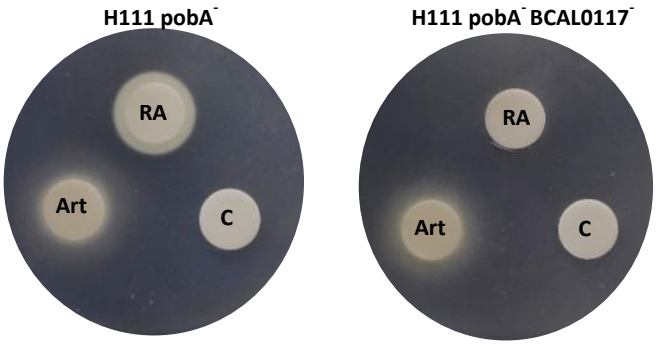

Figure 6.32: Analysis of arthrobactin utilisation by a *B. cenocepacia* BCAL0117 mutant
Analysis of arthrobactin (Art) utilisation (1mM 20 µl) using H111ΔpobAΔBCAL0117 by disc diffusion assay. H111ΔpobA was used as a control. Rhodotorulic acid (RA) (5 mM 40 µl) was used as a positive control and dH_2O (C) was used as a negative control. Final EDDHA concentration was 40 µM.

The less virulent counterpart of *B. pseudomallei*, *B. thailandensis,* also produces malleobactin (malleobactin E), has been used as a source of malleobactin in this study. Malleobactin is speculated to have a similar biosynthetic pathway and structure to ornibactin (Alice et al., 2006; Franke et al., 2013; Franke et al., 2015). Both ornibactin and malleobactin consist of a single bidentate hydroxycarboxylate and two bidentate hydroxamate groups. This allows the formation of 1:1 complexes with ferric iron with a similar binding mode in both cases (Franke et al., 2015). Utilisation of malleobactin by *B. cenocepacia* has been previously demonstrated (Sokol et al., 2000) and is confirmed in this study.

Moreover, in this study, the ornibactin TBDR, OrbA, was shown to be solely responsible for malleobactin transport in *B. cenocepacia* and likewise, the malleobactin TBDR in *B. thailandensis*, MbaD (known as FmtA in *B. pseudomallei*), was also demonstrated to be able to recognise and transport ornibactin. This is consistent with the fact that malleobactin and ornibactin have a similarity in their molecular structure. This study indicates that *B. cenocepacia* may be able to acquire iron by using malleobactin secreted by *B. pseudomallei* in a mixed infection in the lungs of CF patients. A type of malleobactin (malleobactin X) has also been reported to be secreted by *B. xenovorans* (Vargas-Straube et al., 2016; Butt and Thomas, 2017), but was not investigated in this study (Figure 6.33).

Another putative siderophore speculated to be similar to malleobactin is phymabactin. It is predicted that the product of a gene cluster present in some *Burkholderia* spp. of the *xenovorans* group such as *B. phymatum* and *B. terrae* is similar to that of malleobactin and ornibactin gene cluster (Butt and Thomas, 2017). The NRPSs encoded by this cluster in *B. phymatum* were found to be similar to those involved in ornibactin and malleobactin biosynthesis. While ornibactin and malleobactin possess the Orn-Asp-Ser-Orn backbone which is specified by the adenylation domains of the NRPSs (OrbI and Orb J), and (MbaA and MbaB), phymabactin is predicted to have an Asp-Asp-Ser-Cys backbone based on the encoded NRPSs (PhmA and PhmB) (Thomas, 2007; Esmaeel et al., 2016; Butt and Thomas, 2017) (Figure 6.34). Phymabactin utilisation was shown to require OrbA of *B. cenocepacia* in this study, as with malleobactin. However, the siderophores produced by *B. phymatum* and *B. terrae* have not been thoroughly studied and a utilisation assay using purified phymabactin should be carried out.

Utilisation of the mixed hydroxamate-hydroxycarboxylate siderophores, arthrobactin and schizokinen, where citrate donates the hydroxycarboxylate group (also called citrate-based hydroxamates), were also demonstrated in this study. Despite its structural similarity to arthrobactin and schizokinen, it was demonstrated that *B. cenocepacia* does not use aerobactin as efficiently. This may due to the presence of two additional carboxylate groups in the compound. Arthrobactin and schizokinen were hypothesised to be transported through the same TBDR due to their very similar structure.

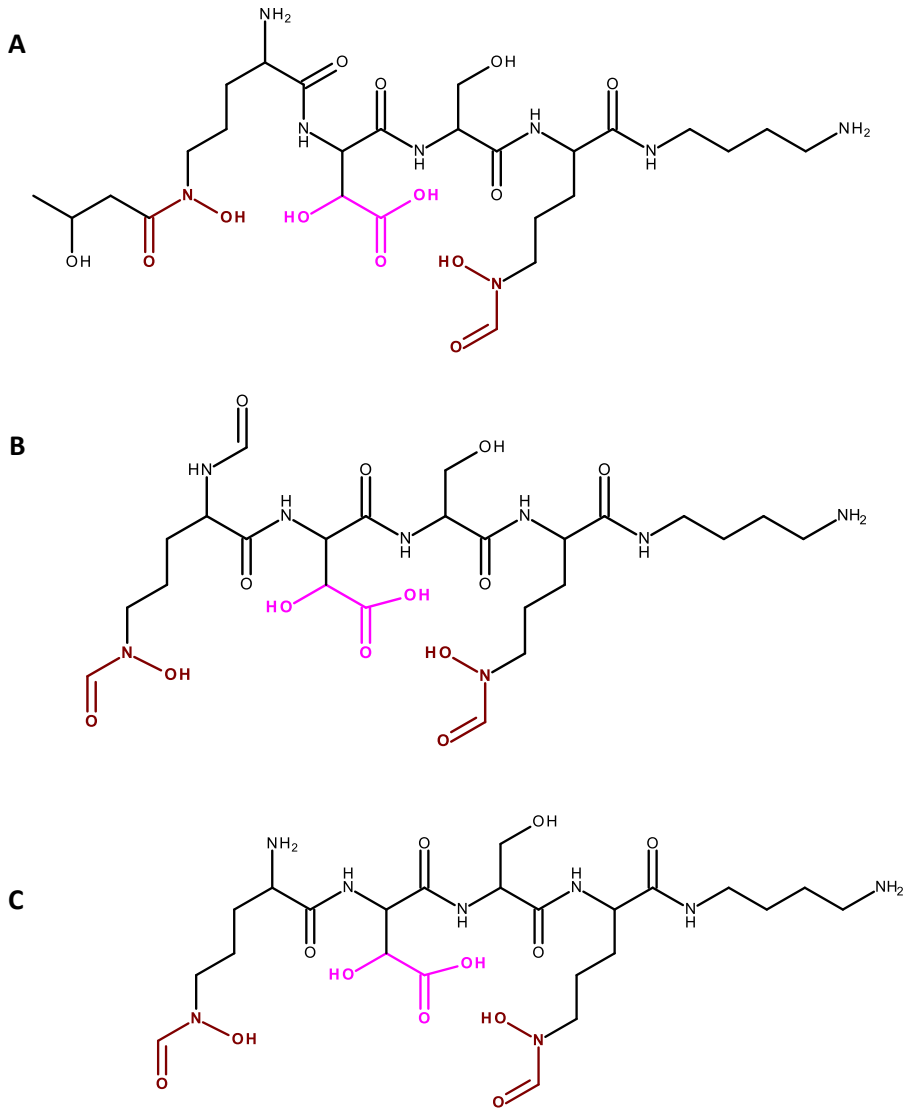

Figure 6.33: The molecular structures of malleobactin and ornibactin
(A) Ornibactin, (B) malleobactin E and (C) malleobactin X. All siderophores exhibit a single bidentate α-hydroxycarboxylate group and two bidentate hydroxamate groups. The α-hydroxycarboxylate group is depicted in pink and hydroxamate groups are depicted in dark red. Chemical structures were drawn using Accelrys Draw 4.2.

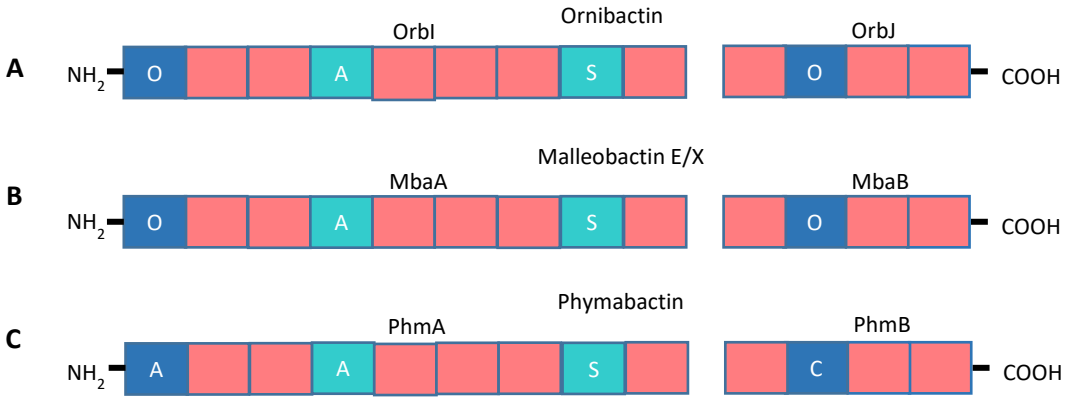

Figure 6.34: Diagrammatic representation of the predicted domain organisation of the two NRPSs encoded in the ornibactin, malleobactin and phymabactin siderophore biosynthetic gene clusters in *B. cenocepacia*, *B. thailandensis*, *B. xenovorans* and *B. phymatum*

(A) OrbI and OrbJ in *B. cenocepacia,* (B) MbaA and MbaB in *B. thailandensis* and *B. xenovorans* and (C) PhmA and PhmB in *B. phymatum*. Each NRPS is represented by two long rectangles subdivided into smaller rectangles representing domains. All domains shown in pink are identical at the corresponding position in each species except for the adenylation domains depicted in light blue. Predicted amino acid specificity is shown in each adenylation domain. Adenylation domains with predicted dissimilar amino acid are depicted in dark blue. O, L-ornithine; S, L-serine; C, cysteine.

The TBDR for these siderophores, however, does not appear to be OrbA. Similarly, it was demonstrated not to be the OrbA-like putative TBDR, BCAS0333. Due to the position of the hydroxycarboxylate moiety in the backbone of arthrobactin/schizokinen (being donated by citrate), the TBDR involved can be relatively distinct from the TBDR that recognises ornibactin-like siderophores where the latter possess the hydroxycarboxylate moiety on aspartate side chain. No TBDR candidate was identified for the utilisation of arthrobactin and schizokinen. This may indicate that the TBDR for arthrobactin/schizokinen may not be BCAM0706 (I35_RS19580) or 'BCAL1783' and is possibly among other putative TBDRs present in both the H111 strain and *B. thailandensis.*

The mutually present putative TBDRs in *B. cenocepacia* and *B. thailandensis* correspond to BCAL1345, BCAL1700 (OrbA) which is highly similar to FmtA, BCAL3001, BCAM0499, BCAM0948, BCAL1571, BCAL1593, BCAM2007, BCAM2224 (FptA) and BCAM2626 (HuvA; Chapter 7) (Section 3.5). Since BCAL1345, BCAL1700, BCAM0499, BCAM2007, BCAM2224 and BCAM2626 have been tested or characterised, TBDRs possibly involved in transporting these siderophores could be BCAL3001, BCAM0948, BCAL1571 and BCAL1593. Since BCAM0948 and BCAL1593 are likely to be the receptors for copper and vitamin B12, respectively, the two remaining TBDRs that could be investigated are BCAL3001 and BCAL1571.

These putative TBDRs (BCAL3001 and BCAM1571) are paired in the *B. cenocepacia* ML phylogenetic tree (Figure 3.10) and are found in the group of TBDRs speculated to be involved in binding or transporting other metals. Hu and Boyer (1996) demonstrated that schizokinen binds to aluminium and copper, as well as to iron, and may transport these metals through the same TBDR in *B. megaterium* (Barelmann et al., 1996). This suggests that schizokinen may act as a metallophore in *B. cenocepacia*, as with pyochelin, a lower affinity siderophore which acts as a chelator to many other metals including copper, zinc (Brandel et al., 2012a), cobalt (Kothamasi and Kothamasi, 2004), nickel and vanadium (Baysse et al., 2000; Thomas, 2007; Johnstone and Nolan, 2015). Accordingly, the TBDR for schizokinen and logically also for arthrobactin may also act as a receptor for other metallophores. Given that, BCAL3001 and BCAL1571 are both in the group speculated to be transporting additional metals, this supports the hypothesis that either one of these TBDRs is responsible for the transport of these siderophores. In addition, BCAM1571 is predicted to be a TBDR for zincophores (ZnuD) in *B. cenocepacia* (see Section 3.2).

The TBDR ChtA (PA4675) (citrate hydroxamate transporter) in *P. aeruginosa* was reported to be involved in the utilisation of citrate hydroxamate siderophores, schizokinen and aerobactin (Cuív et al., 2006). Although aerobactin has not been shown to be of benefit to *B. cenocepacia*, ChtA was used as a query for a search of the *B. cenocepacia* translated genome for a similar TBDR that may be involved in schizokinen

utilisation. The BLASTP analysis revealed four putative TBDRs with a homology between 28 to 33 %. These are BCAL1345, BCAM0491, BCAL1571 and BCAM2367.

Based on the list of mutually-existing TBDRs in *B. cenocepacia* and *B. thailandensis* (see Section 3.5 and 6.6.2), the putative TBDRs BCAL1345, BCAM0491 and BCAM2367 are not present in both pathogens and therefore were not predicted to be the TBDRs involved in the citrate hydroxamate siderophore utilisation. As a result of the analysis, the putative TBDR BCAL1571 is most likely to be the TBDR candidate for the utilisation of the siderophores, schizokinen and arthrobactin.

Additionally, a plant metallophore, nicotianamine was tested in this study. However, it did not exhibit a benefit to *B. cenocepacia* as an iron source. Moreover, as nicotianamine (or pseudopaline) commonly acts as a zincophore, this may also suggest that *B. cenocepacia* may not be able to translocate zinc ions into its cytosol as in *P. aeruginosa,* using nicotianamine (Mastropasqua et al., 2017; Lhospice et al., 2017; Gonzalez et al., 2018).

6.11.2 The role of the TonB1 system and BCAL0117 hydroxamate siderophore inner membrane transport system in utilisation of hydroxamate-hydroxycarboxylate mixed type siderophores

One of the bottlenecks of designing an efficient siderophore-antibiotic conjugate to be transported into the bacterial cytosol has been reported to be the inner membrane transport. Only a few inner membrane proteins transporting the iron-siderophore complex and their mechanisms have been studied (Schalk, 2018). In this study, the transfer of the mixed ligand siderophores across the CM was also included, as the inner membrane mechanism for the translocation of these type of siderophores has not been identified.

In contrast, the identification on the translocation of the siderophore-antibiotic conjugate via the OM has been easier. This is due to many studies on the mechanisms of transfer via the TBDR and the TonB complex (Schalk, 2018). Many translocations of iron-siderophore complexes are facilitated by a sole TonB complex as shown in *P. aeruginosa* (Cuív et al., 2006) and *Acinetobacter baumannii* (Moynié et al., 2017). Similarly, the mixed ligand siderophores have shown in this study to require the same TonB1 complex in *B. cenocepacia* as the endogenous siderophores for transport across the OM.

6.11.3 Non-utilised siderophores

This study did not identify any catecholate-hydroxamate siderophores that can be utilised by *B. cenocepacia*. The catecholate-hydroxamate siderophores tested were types of pyoverdine produced by *Pseudomonas* spp., including *P. aeruginosa*. Due to the observation that *B. cenocepacia* could not take advantage of pyoverdine this may allow *P. aeruginosa* to commonly be the dominant pathogen in the lungs of CF patients (Parkins et al., 2018).

Pyochelin, as a secondary siderophore for both pathogens, is reported to be less significant for iron uptake in both (Mahenthiralingam et al., 2000; Visser et al., 2004; Thomas, 2007). In addition, the fimsbactins consisting of catecholate and hydroxamate ligands (fimsbactin A, B, C or F) produced by *A. baylyi* ADP1 (Proschak et al., 2013) (Figure 6.35), did not support any growth of *B. cenocepacia* under iron-limiting conditions (see Section 5.8), although it remains to be confirmed that these siderophores were actually present in the culture supernatants employed in the disc diffusion assays.

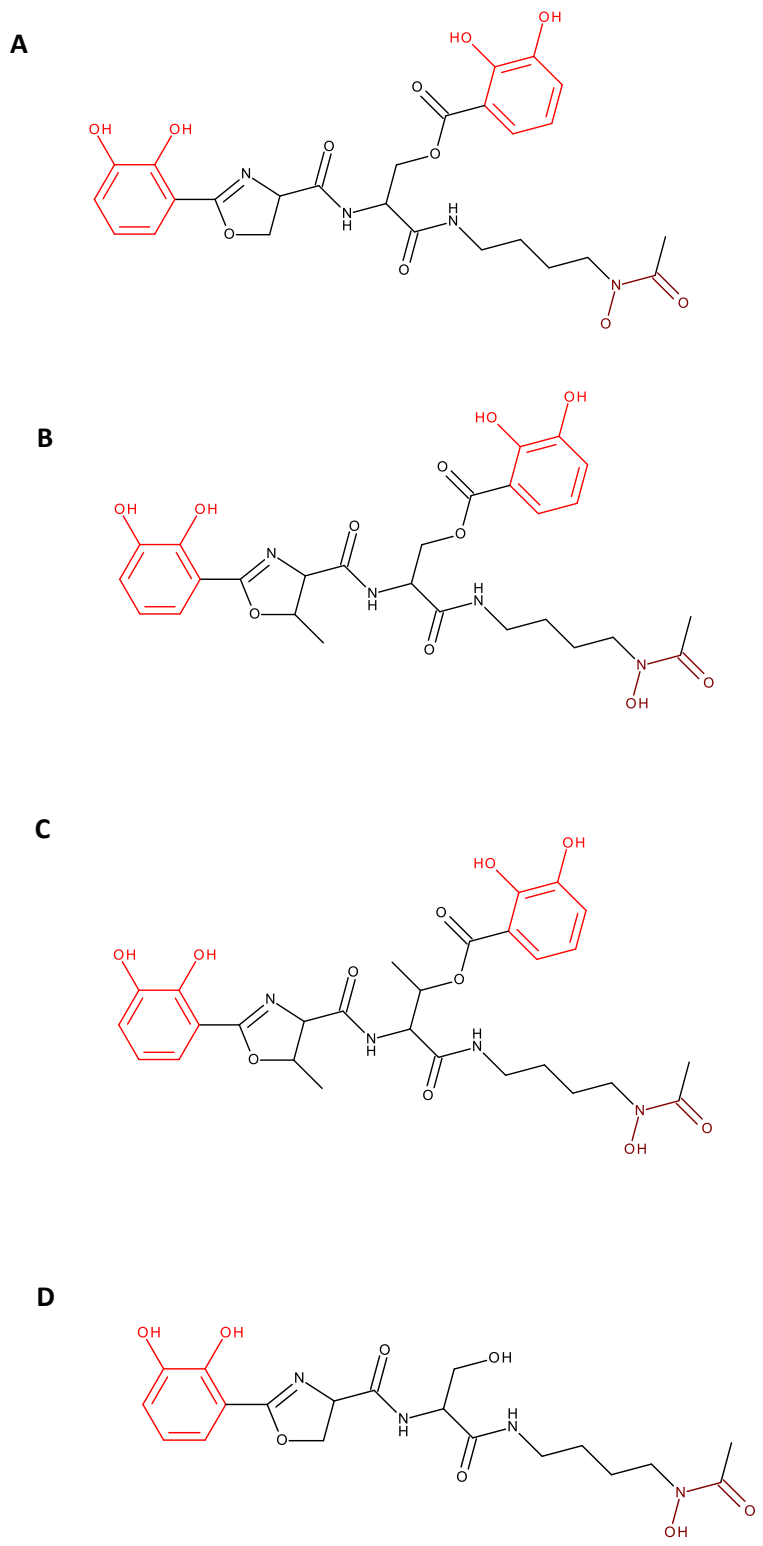

Figure 6.35: The molecular structures of the fimsbactins
(A) Fimsbactin A, (B) fimsbactin B, (C) fimsbactin C and (D) fimsbactin F. The catecholate ligands are depicted in red and the hydroxamate groups are depicted in dark red. Chemical structures were depicted using Accelrys Draw 4.2.

Chapter 7

Identification and characterisation of the *B. cenocepacia* outer membrane haem transport system

7.1 Rationale

Most of the investigations described in this thesis focus on the TBDR proteins involved in siderophore-mediated iron acquisition. In this chapter, the haem uptake system in *B. cenocepacia* was also investigated, particularly focusing on identifying and characterising the TBDR involved in binding and transporting haem. In an infection model, *B. cenocepacia* uses haem from the host to its advantage as a source iron as the haem molecule contains a single tightly bound iron atom (Figure 7.1). Haem utilisation in *B. cenocepacia* J3215 and 715j was reported by several researchers but the corresponding receptor was not identified (Whitby et al., 2006; Tyrrell et al., 2015). The work described in this chapter investigated whether the predicted haem TBDR identified in Chapter 3 can function as a haem-receptor protein and considers the growth difference between haem uptake and endogenous siderophore iron acquisition mechanisms.

From bioinformatics analysis, one of the gene loci located on the 'medium' chromosome (chromosome 2) of *B. cenocepacia* J2315, BCAM2626, is predicted to encode a TBDR protein involved in haem uptake based on amino acid sequence homology with a known TBDR for haem, BhuR/Hmu, (BPSL0244), in *B. pseudomallei* (Shalom et al., 2007; Kvitko et al., 2012; Butt and Thomas, 2017). Similarly, haem TBDR orthologues have been predicted in *B. thailandensis* E264 and *B. multivorans* (Section 3.5). BCAM2626 is located in a gene cluster along with genes encoding other components of the predicted haem uptake system that is organised similarly to the cluster in *B. pseudomallei* termed *bhuRSTUV*. *bhuS* is predicted to be involved in haem trafficking and degradation, *bhuT* is predicted to encode the PBP and *bhuUV* are ABC transporter genes where BhuU protein is an inner membrane transporter (Butt and Thomas, 2017) (Burkholderia.com) (Figure 7.2). The orthologous gene locus to BCAM2626 in the H111 strain is I35_RS29035. The 274 amino acid residues of the BCAM2626/I35_RS29035 protein of both strains are very similar with only four amino acid mismatches. In this chapter, the gene corresponding to the I35_29035 locus from H111 will be referred as BCAM2626.

7.2 Identification of the TBDR for haem utilisation

To confirm that BCAM2626 encodes the haem TBDR, the BCAM2626 gene was disrupted by introduction of an in-frame deletion. A markerless mutant was generated to facilitate subsequent investigation in characterising the haem uptake locus in *B. cenocepacia*.

7.2.1 Generation of a markerless *B. cenocepacia* H111 ΔBCAM2626 mutant

The gene BCAM2626 was amplified with the primer combination HuvAfor and HuvArev and the 2736 bp product was restriction digested with the enzymes *Xba*I and *Acc*65I. The amplicon was ligated into the expression vector pBBR1MCS-2 restricted with the same enzymes and positive clones having a plasmid size of 7770 bp were selected in JM83 and sequenced as previously described (Figure 7.3A).

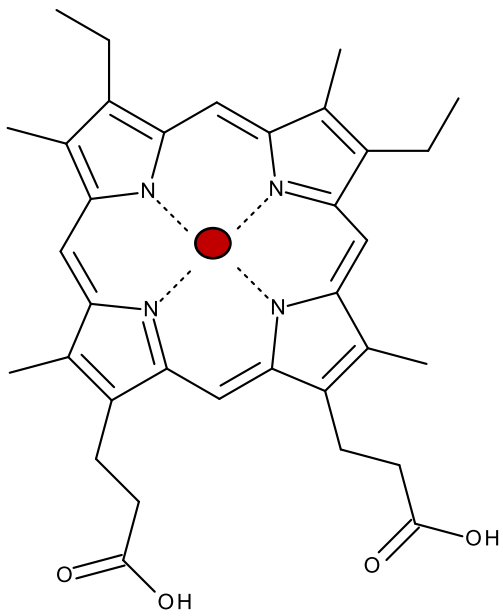

Figure 7.1: Molecular structure of haem
Molecular structure of haem in which the porphyrin ring acts as a tetradentate ligand to an iron ion. Iron is depicted in red.

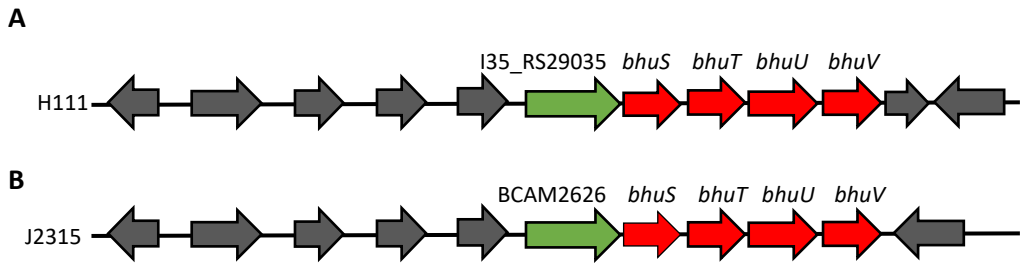

Figure 7.2: The putative haem uptake gene cluster in *B. cenocepacia.*
A schematic representation showing the putative haem uptake cluster in *B. cenocepacia* (A) J2315 and (B) H111. The putative haem TBDR gene (*bhuR*) is coloured in green. Putative genes involved in haem uptake are depicted in red. (Burkholderia.com). Unrelated genes are depicted in dark grey.

Internal deletion of BCAM2626 was performed by restriction digestion of pBBR2-BCAM2626 with *Xmn*I. The BCAM2626 gene containing two *Xmn*I sites released a 1491 bp of DNA fragment. Religation without the released *Xmn*I fragment gave rise to a plasmid of 6279 bp (pBBR2-ΔBCAM2626) following selection in JM83 (Figure 7.3B). Confirmation of the internal deletion was performed by DNA sequencing.

Prior to transfer of the BCAM2626 gene harbouring the deletion into the suicide plasmid, pEX18TpTer-*pheS*-Cm-SceI, Dam methylation of the *Xba*I restriction site in pBBR2-ΔBCAM2626 was relieved. The site was methylated at the adenine residue in a GATC motif that overlapped the *Xba*I site preventing restriction cleavage. The methylated *Xba*I site in pBBR2-ΔBCAM2626 was made available by passaging the plasmid through an *E. coli dam* methylase mutant, GM48, which released the methylation on the adenine residue and allowed restriction digestion by *Xba*I. The prepared plasmid was then restriction digested concurrently with *Xba*I and *Acc*65I and ligated to the same sites of the suicide plasmid, pEX18TpTer-*pheS*-Cm-SceI for construction of pEX18TpTer-*pheS*-Cm-SceI-ΔBCAM2626. The ligation products were transformed into *E. coli* JM83 cells as previously described. Prepared plasmids of positive clones giving a size of 6295 kb were subjected to DNA sequence analysis using the primers M13For and M13RevBACTH.

Generation of the H111ΔBCAM2626 mutant was performed following conjugal mobilisation of the plasmid into H111 and H111ΔpobA as previously described (Section 4.8). The co-integration of the pEX18TpTer-*pheS*-Cm-SceI-ΔBCAM2626 plasmid into the *B. cenocepacia* chromosome was verified by PCR and subsequent selection of mutant was performed as previously described (Section 4.7.2) (Figure 7.4A). The candidate mutants were confirmed using the BCAM2626 'outside primers' (Figure 7.4B). The wild type DNA fragment gave rise to a size of 2820 bp and the desired mutant gave rise to a size of 1320 bp.

7.3 Haem growth induction assay with *B. cenocepacia* H111ΔBCAM2626 mutant

H111ΔBCAM2626 and H111ΔpobAΔBCAM2626 overnight cultures suspended in LB agar were overlaid separately on LB agar containing 200 µM EDDHA. Filter discs impregnated with haemin in NaOH solution were placed on the overlay and the plates were incubated overnight. Filter discs impregnated with NaOH solution were used as negative controls. The haem induction assay confirmed that the gene locus BCAM2626 is the TBDR responsible for haem transport as no growth halo was seen from either mutant around filters impregnated with haemin. H111ΔpobA was used as a positive control and showed substantial growth with haemin supplementation (Figure 7.5). The gene locus BCAM2626 will henceforth be referred to as *huvA*.

7.4 Confirming the role of the gene product of BCAM2626 as the haem receptor protein

The *huvA* mutant was complemented with the *huvA* wild type gene cloned into plasmid, pBBR1MCS to confirm the role of BCAM2626 as the haem receptor gene.

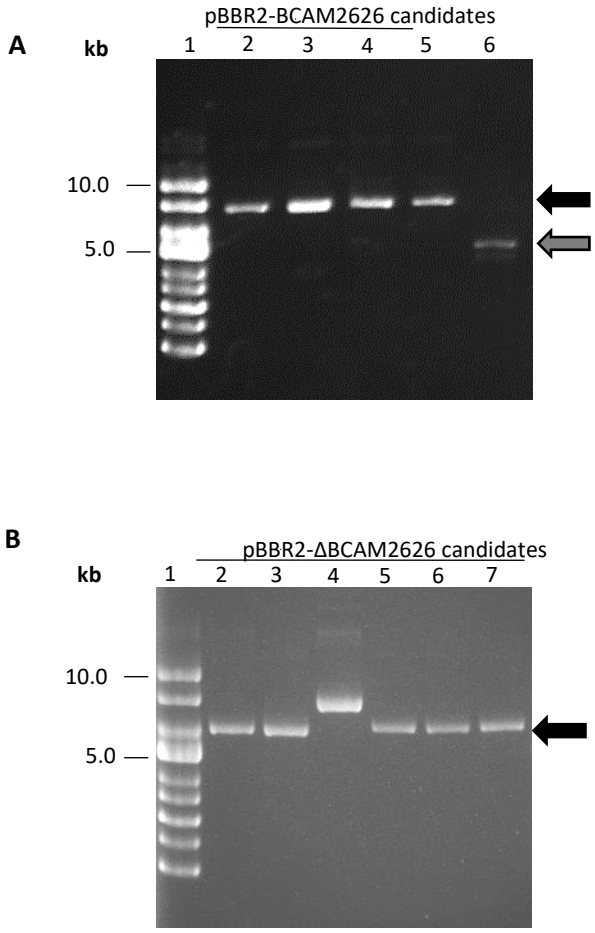

Figure 7.3: Construction of a plasmid for *B. cenocepacia* BCAM2626 mutant generation
A PCR product containing the BCAM2626 gene was ligated into pBBR1MCS-2 and an in-frame deletion was introduced into the gene prior to insertion into a suicide plasmid for mutant generation. (A) Extracted candidate pBBR2-BCAM2626 plasmids from JM83 white colony transformants were analysed by electrophoresis. Lane 1, Supercoiled DNA ladder; lanes 2-5 displayed the expected band size of pBBR2-BCAM2626 (7770 bp) indicated by a black arrow; lane 6, pBBR2 empty vector as a negative control (5144 bp) is indicated by a grey arrow. (B) pBBR2-BCAM2626 was digested with *Xmn*I and self-ligated to give rise to a 6279 bp plasmid, pBBR2-ΔBCAM2626, indicated by the arrow. Lane 1, Supercoiled DNA ladder; lanes 2-7 except lane 4 displayed the expected plasmid size of 6279 bp.

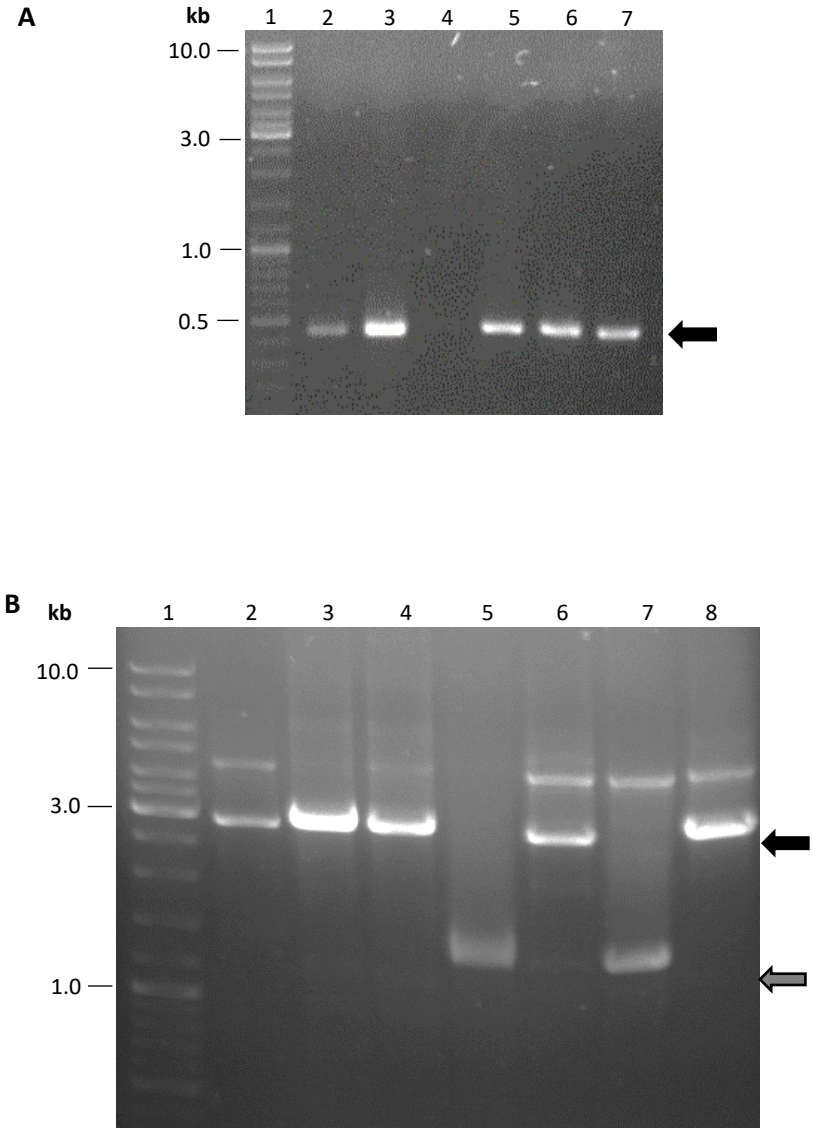

Figure 7.4: Generation of *B. cenocepacia* BCAM2626 mutant by allelic replacement
(A) Confirmation of pEX18TpTer-*pheS*-Cm-*SceI*-ΔBCAM2626 integration into the *B. cenocepacia* chromosome using the vector primer combination pEX18Tpfor and pEX18Tprev at an annealing temperature of 52 ^{o}C, giving rise to an amplicon size of 397 bp, indicated by the arrow. (B) PCR screening using primers HuvAforout and HuvArevout, which annealled to genomic sequences outside the ΔBCAM2626 fragment contained on the plasmid. Replacement of the BCAM2626 gene (2820 bp) with ΔBCAM2626 allele gave rise to a 1320 bp DNA fragment, as indicated by the grey arrow. Lane 1, Linear ladder; lane 2, H111 wildtype used as a control (black arrow); lanes 3-5, H111ΔBCAM2626 mutant candidates with lane 5 showing a band size of 1320 bp; lanes 6-8, H111ΔpobAΔhuvA mutant candidates with lane 7 showing a band size of 1320 bp. Q5 hotstart high fidelity DNA polymerase was used for amplification due to high GC content of the BCAM2626 gene.

The plasmid pBBR1MCS was used for complementation as it does not excessively express the recombinant protein, which could affect the resilience of the bacterial host.

7.4.1 Construction of pBBR1-*huvA*

The previously amplified PCR product of the *huvA* gene that was used to generate pBBR2-BCAM2626 was digested and ligated to the *Acc*65I-*Xba*I restriction sites of the pBBR1MCS plasmid vector. The ligated products were transformed as previously described (Section 4.3) and prepared plasmids were screened by gel electrophoresis. Two putative clones harbouring pBBR1-*huvA* with the expected size of 7333 bp were verified by DNA sequencing using primers M13For and M13RevBACTH (Figure 7.6).

7.4.2 Complementation of a *B. cenocepacia* haem receptor mutant

Constructed pBBR1-*huvA* and pBBR1MCS empty vector were transformed into *E. coli* SM10 and conjugated into the constructed haem receptor mutants, H111ΔhuvA and H111ΔpobAΔhuvA. Exconjugants were spread at 10^{-1} dilution on M9-glucose agar supplemented with tetracycline (10 µg ml^{-1}) and chloramphenicol (50 µg ml^{-1}) and were purified on the same medium. The presence of pBBR1-*huvA* in H111ΔhuvA and H111ΔpobAΔhuvA was verified by PCR screening using primers M13For and M13Rev. The haem growth induction assay was then performed as previously described (Section 7.3). Growth around the filter disc with haemin solution was seen with the strains containing pBBR1-huvA, indicating restoration of haem utilisation to wild type levels, but was not seen with pBBR1MCS control vector (Figure 7.7). This confirmed the essential role of the HuvA protein in the haem acquisition system.

7.5 Analysis of haem utilisation in *B. cenocepacia* by liquid growth stimulation assay

The effect of an inactivated haem transport system on growth of *B. cenocepacia* in iron depleted liquid medium was compared to that of the wild type mutants in which the inactivated endogenous siderophore transport was inactivated. To establish the effect of an inactivated *huvA* gene in combination with inactivated endogenous siderophore uptake systems in *Burkholderia* spp. on acquisition of iron, multiple TBDR mutants were generated.

7.5.1 Generation of *B. cenocepacia* H111-orbA::TpTer and H111ΔfptA TBDR mutants

Three single TBDR mutants were to be investigated: H111ΔhuvA, H111ΔfptA and H111-orbA::TpTer. H111-orbA::TpTer and H111ΔfptA were generated by using pSHAFT2-*orbA*::TpTer and pEX18TpTer-*pheS*-Δ*fptA*, as previously described (Sections 6.3.1 and 6.4.2). Candidate mutants were verified by PCR screening using the corresponding 'outside' primers.

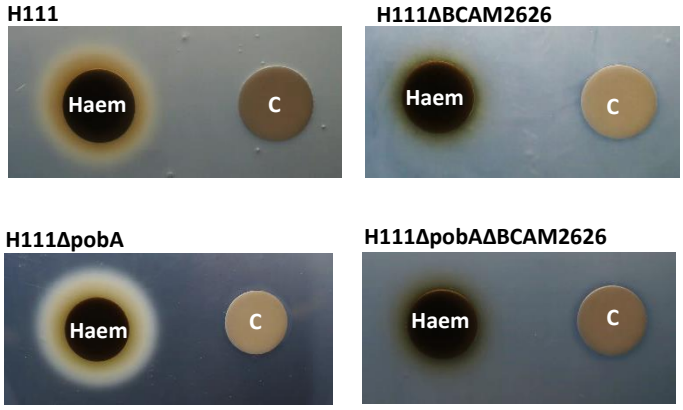

Figure 7.5: Haem growth stimulation assay of the ΔBCAM2626 mutant
Haem induction assay of the generated mutants, H111ΔBCAM2626 and H111ΔpobAΔBCAM2626. Filter discs for bioassay plates were spotted with 10 µl haemin solution 10 mg ml^{-1} on the left and the filter discs on the right act as negative controls (C) and were impregnated with 10 µl 0.1 M NaOH. Overlaid strains used for the assay are indicated above each assay image. Final EDDHA concentration used was 200 µM in each case.

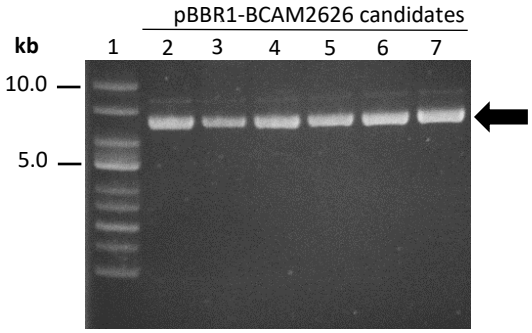

Figure 7.6: Construction of BCAM2626 complementation plasmid
A 2.7 kb DNA fragment encoding the BCAM2626 gene was ligated into pBBR1MCS and plasmids isolated form transformants were analysed by electrophoresis. Positive clones were expected to have a size of 7.8 kb, indicated by the arrow. Lane 1; Supercoiled DNA ladder; lanes 2-7, pBBR1-BCAM2626 candidates.

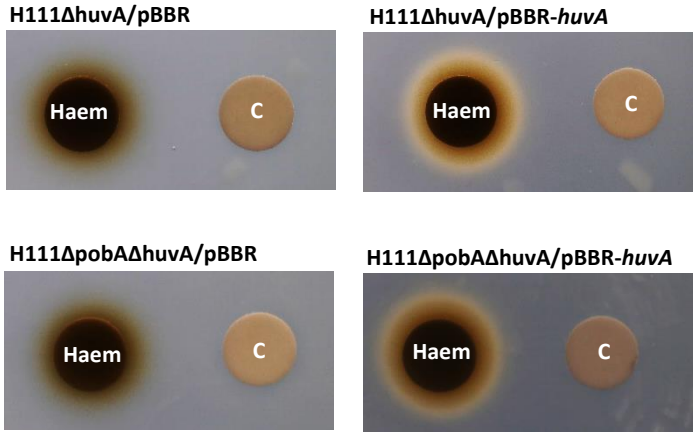

Figure 7.7: Complementation analysis of the huvA mutant phenotype
Complementation analysis showing restoration of the HuvA phenotype in mutants H111ΔhuvA and HIIIΔpobAΔhuvA. Empty vectors were used as negative controls. Filter discs for bioassay plates were spotted with haemin solution (10 mg ml^{-1}) on the left and the filter discs on the right act as negative controls and were impregnated with 0.1 M NaOH. Final EDDHA concentration used was 200 µM.

7.5.2 Generation of *B. cenocepacia* H111ΔhuvA-orbA::TpTer, H111ΔfptAΔhuvA and H111ΔfptA-orbA::TpTer mutants

To generate mutants with two disrupted TBDR alleles, both H111ΔfptA and H111ΔhuvA were conjugated with SM10(λpir) containing pSHAFT2-*orbA*::TpTer. H111ΔfptA-orbA::TpTer and H111ΔhuvA-orbA::TpTer mutants were identified among exconjugants and verified using 'outside primers' as described in Section 6.5. (Figure 7.8A).

H111ΔfptAΔhuvA was generated by a conjugation performed between H111ΔfptA and SM10(λpir) containing pEX18TpTer-*pheS*-Cm-SceI-Δ*huvA.* Mutants were obtained as previously described (Section 7.2.1) and were verified by using *huvA* 'outside' primers (Figure 7.8B).

7.5.3 Generation of a *B. cenocepacia* ΔfptAΔhuvA-orbA::TpTer triple TBDR mutant

H111ΔfptAΔhuvA-orbA::TpTer was generated by following conjugation between H111ΔfptAΔhuvA and *E.coli* SM10(λpir) containing the plasmid, pSHAFT2-orbA::TpTer as previously described (Section 6.5). Mutants were verified using 'outside' primers flanking the *orbA* gene (Figure 7.9).

7.5.4 Phenotype confirmation of mutants

The HuvA$^-$ phenotype of the generated multiple TBDR mutants (H111ΔfptAΔhuvA, H111ΔhuvA-orbA::TpTer and H111ΔfptAΔhuvA-orbA::TpTer) was confirmed by assaying their ability to utilise haemin. No zone of growth of the mutants was observed around the filter discs impregnated with haemin (Figure 7.10).

7.5.5 Growth stimulation assay of *huvA*, *orbA* and *fptA* mutants in liquid medium

The growth of the generated mutants in liquid culture was studied with and without supplementation of haemin. Optimisation of haemin concentration was performed prior to this study. A concentration of 0, 1, 2, 5, 10, 20 µM haemin was screened to identify optimal growth of H111ΔpobA in iron limited conditions. All concentrations except with no haemin were observed to produce a similar effect on the growth of H111ΔpobA (Figure 7.11A). A concentration of 2 µM haemin was selected for further analyses.

Growth curves of the mutants in iron-limiting conditions without the addition of haemin were determined over a 10-hour incubation period at 37 °C. Growth of the single TBDR mutants, H111ΔhuvA, H111ΔfptA and H111-orbA::TpTer was as expected. The growth rate of H111-orbA::TpTer was slightly lower than the growth rates of the other two mutants, particularly the null *fptA* allele mutant. The other two mutants grew at a similar rate (Figure 7.11B). Comparison of the growth curves of the TBDR double mutants, H111ΔhuvAΔfptA, H111ΔfptA-orbA::TpTer and H111ΔhuvA-orbA::TpTer showed the growth rate of H111ΔfptA-orbA::TpTer to be reduced compared to the two other mutants (Figure 7.11C).

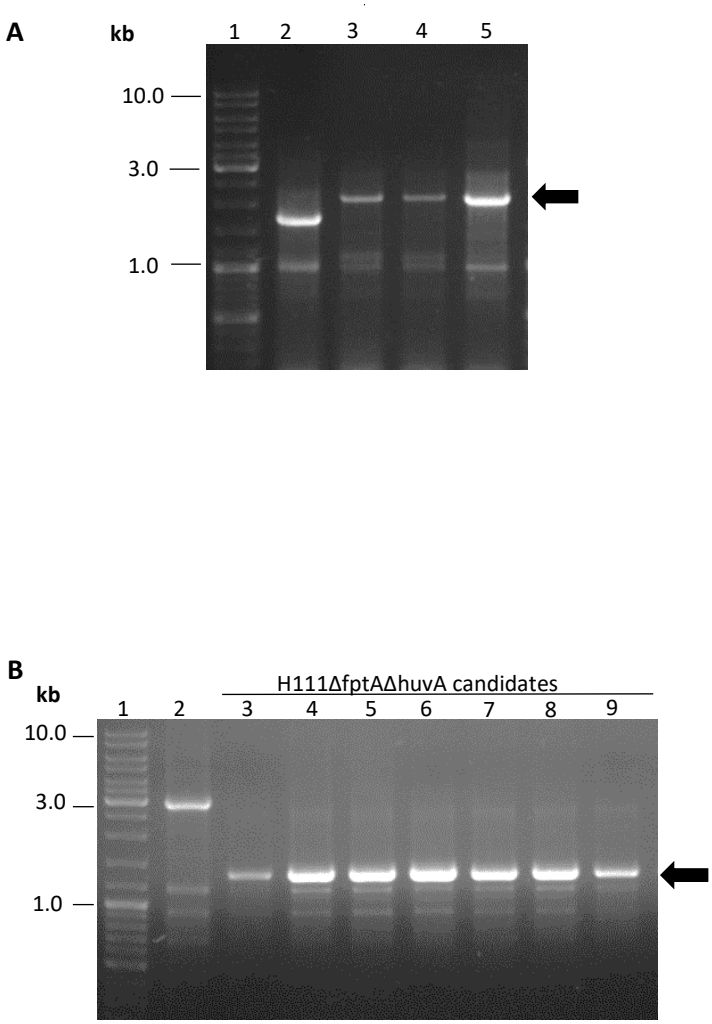

Figure 7.8: Generation of double TBDR mutants, H111ΔhuvA-orbA::TpTer and H111ΔfptAΔhuvA
(A) Screening of trimethoprim-resistance cassette insertion in the *orbA* gene of H111ΔhuvA-orbA::TpTer candidates using outside primers BCAL1700forout and BCAL1700revout. Lane 1, Linear DNA ladder; lane 2, H111 wildtype; lanes 3 and 4, H111ΔhuvA-orbA::TpTer positive candidates showing a DNA fragment band size of 2.1 kb; lane 5, H111ΔpobA-orbA::TpTer used as a positive control. The arrow shows the location of the expected PCR product. (B) PCR screening of H111ΔfptAΔhuvA candidates using combination of 'outside primers' flanking the *huvA* gene, HuvAforout and HuvArevout, at annealing temperature of 59.5 ^{o}C using Q5 hot start high fidelity DNA polymerase due to high GC content of the *huvA* gene. Lane 1, Linear ladder; lane 2, H111 wildtype; lane 3, H111ΔpobA as a negative control; lane 4, H111ΔpobAΔhuvA used as a positive control; lanes 5-9, H111ΔfptAΔhuvA positive candidates giving rise to 1.3 kb DNA fragments (arrow).

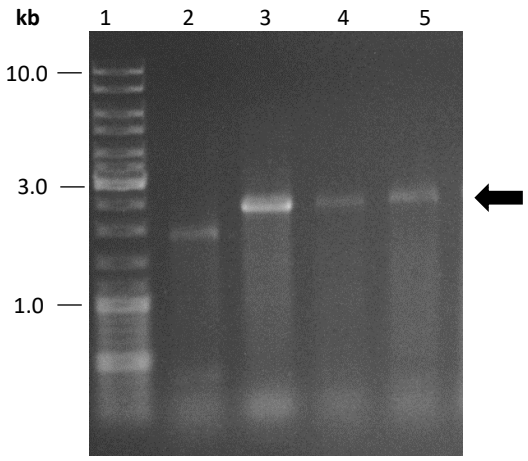

Figure 7.9: Generation of the triple TBDR mutant H111ΔhuvAΔfptA-orbA::TpTer
Screening of trimethoprim-resistance cassette insertion in the *orbA* gene of H111ΔhuvAΔfptA -orbA::TpTer candidates using 'outside' primers BCAL1700forout and BCAL1700revout. Lane 1, Linear DNA ladder; lane 2, H111 wildtype; lanes 3-5, H111ΔhuvAΔfp tA-orbA::TpTer positive candidates showing an amplicon size of 2.1 kb. The arrow shows the location of the expected PCR product.

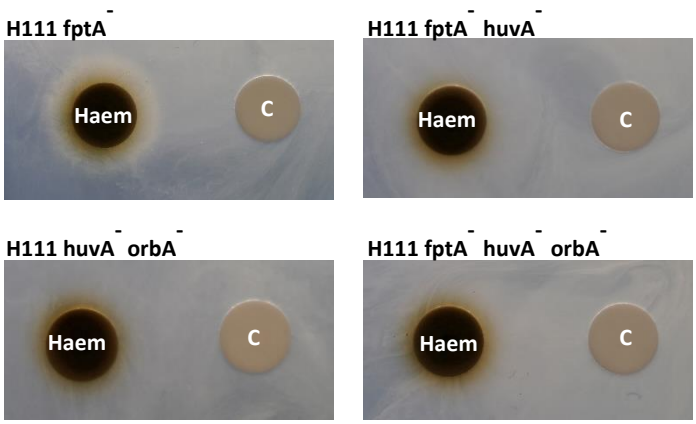

Figure 7.10: Confirmation of haem utilisation defect of H111ΔfptAΔhuvA, H111ΔhuvA-orbA::TpTer and H111ΔfptAΔhuvA-orbA::orbA::TpTer
Phenotype confirmation using disc diffusion assay showing growth promotion of H111ΔfptA by haem (positive control) (top left). No growth was observed with the H111ΔfptAΔhuvA, H111ΔhuvA-orbA::TpTer and H111ΔfptAΔhuvA-orbA::orbA::TpTer mutant (right). Filter discs were spotted with haemin solution (10 mg ml^{-1}) on the left and the filter discs on the right act as negative controls and were impregnated with 0.1 M NaOH. Final EDDHA concentration used was 200 µM.

The growth rate of the triple TBDR mutant, H111ΔfptAΔhuvA-orbA::TpTer, in the absence of haem was slightly lower than that of the H111ΔfptA-orbA::TpTer mutant and nearly as low as that of the H111ΔpobA mutant (Figure 7.11D). Addition of haemin as the sole iron source in iron-deprived conditions allowed the growth rate of the siderophore TBDR double mutant, H111ΔfptA-orbA::TpTer to increase as expected. The growth rate, however, was lower than the positive control, H111ΔpobA, in the presence of haemin (Figure 7.11E). The growth rate of the H111ΔpobA strain in the presence of haemin is identical to the growth rate of the wild type strain without haemin addition (Figure 7.11F).

7.6 Discussion

This study demonstrates that BCAM2626/I35_RS29035 is the sole haem TBDR (HuvA/BhuR/HmuR) in *B. cenocepacia*. Whilst *P. aeruginosa* possesses two TBDRs involved in haem transport, *B. cenocepacia* is served by one. The demonstration that HuvA is the sole haem uptake protein in this study correlates with the mechanism of haem uptake by the Bhu system in *B. cenocepacia* proposed by Butt and Thomas (2017). The mechanism is equivalent to the pathway for ornibactin uptake in the Bcc group as it involves the participation of the ABC transport system. The gene loci downstream of the BCAM2626 gene locus, BCAM2628-2630 (I35_RS29045-29055) were predicted to code for the ABC transport system for haem uptake in the following organisation, BhuTUV (Chapter 3). The function of this transport system, however, was not investigated in this study. A cytoplasmic protein, BhuS (BCAM2627), is predicted to be involved in haem-iron complex trafficking for degradation under iron-depleted conditions (Butt and Thomas, 2017).

The haemophore proteins that participate in an alternative haem sequestration pathway in some bacteria, such as HasA (Arnoux et al., 1999), HmuY (Smalley et al., 2011) and HusA (Gao et al., 2018a) have not been reported in *B. cenocepacia* to date. By BLASTP analysis using the *P. aeruginosa* haemophore, HasA (Haem assimilation system) (PA3407), as a query, it is predicted that haemophores are not produced by *B. cenocepacia* and therefore are not used as an alternative haem acquisition system. Some bacteria, for example *Porphyromonas gingivalis,* an anaerobic bacteria frequently found in CF lungs, are able to use the haem acquisition systems of other bacteria to meet their own haem requirements (Smalley and Olczak, 2017), and *B. cenocepacia* may have the same attributes as a survival mechanism.

7.6.1 Growth curve studies

The growth rate of the single mutant, H111-orbA::TpTer was slightly lower than the growth rates of the two other single TBDR mutants, H111ΔfptA and H111-orbA::TpTer. This may due to the strong suggestion that ornibactin is the primary siderophore for iron uptake (Visser et al., 2004), particularly in comparison to the null *fptA* allele mutant. Similarly, the growth rate of H111ΔfptA-orbA::TpTer was slightly lower than the growth rates of the other two double TBDR mutants.

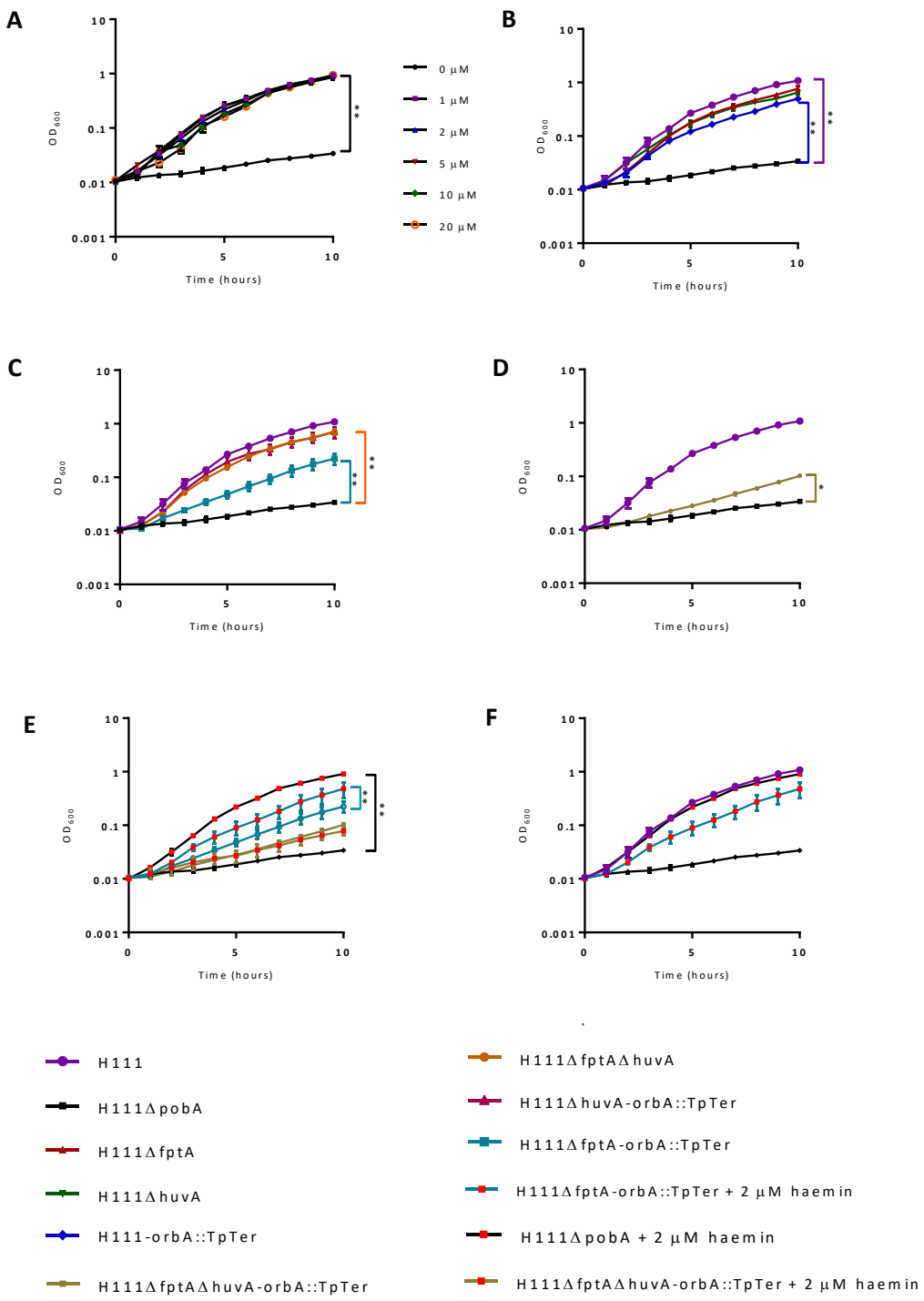

Figure 7.11: Haemin optimisation assay and growth of *huvA*, *fptA* and *orbA* single and multiple mutants with and without haemin addition in iron-limiting M9-glucose (CAA) medium containing 1 µM DTPA
(A) Effect of different haemin concentrations (0, 1, 2, 5, 10, 20 µM) on growth of H111ΔpobA showing an identical maximal growth. (B) Growth of single TBDR mutants, H111ΔhuvA, H111ΔfptA and H111-orbA::TpTer in iron-limiting conditions. (C) Growth of double TBDR mutants, H111ΔhuvAΔfptA, H111ΔfptA-orbA::TpTer and H111ΔhuvA-orbA::TpTer in iron-limiting conditions. (D) Growth of triple TBDR mutant, H111ΔhuvAΔfptA-orbA::TpTer in iron-limiting conditions. H111 and H111ΔpobA were included as controls. (E) Growth of the double siderophore TBDR mutant, H111ΔfptA-orbA::TpTer, with and without haemin (2 µM) addition. H111ΔpobA and H111ΔfptA-orbA::TpTer were included as controls. (F) Growth of H111ΔpobA and H111ΔfptA-orbA::TpTer, in the presence of haemin (2 µM). These data represent three independent experiments (n=3). Error bars represent the mean ±SEM. *p<0.05, **p<0.01.

This is expected as both the ornibactin and pyochelin TBDRs, which are the main sources of iron transport were non-functional. However, the growth rate of this mutant (H111ΔfptA-orbA::TpTer) was unexpectedly greater than that of the H111ΔpobA mutant. There are several possible explanations for this observation. A functional *pobA* gene may be required to produce factors that support alternative iron uptake (Jenul et al., 2018). A more likely possibility could be that the ornibactin or pyochelin that are being produced by the double mutant are entering the cell inefficiently.

The growth of the H111 wild type is slightly higher than the double mutants, as seen with the single TBDR mutants. The growth rates of H111ΔhuvAΔfptA and H111ΔhuvA-orbA::TpTer double TBDR mutants were similar suggesting the ability of pyochelin to deliver iron to *B. cenocepacia* with a similar efficiency to ornibactin. This observation contrasts with the growth rate differences of the single TBDR mutants where the growth rate of the H111-orbA::TpTer was slightly lower than the Δ*fptA* mutant. Inactivation of HuvA could modulate the efficiency of other TBDRs and in this case, may upregulate the production and transport of pyochelin as a survival mechanism. In *S. aureus*, the iron-siderophore synthesis is activated by a haem-responsive transcriptional regulator when haem-iron is unavailable (Farrand et al., 2013; Choby and Skaar, 2016). In this instance, a probable explanation could be that the inactivated haem TBDR may have a role in promoting the synthesis, and thereby the transport of pyochelin although the siderophore is regarded as a secondary siderophore. Visser at al. (2004) showed that pyochelin uptake system cannot compensate for inactivation of ornibactin transport but with an inactivated HuvA TBDR, the pyochelin uptake system is shown to be upregulated in this study.

As no siderophores are produced by the Δ*pobA* mutant, the growth rate of the H111ΔpobA was expected to be the lowest. A slight growth of the triple TBDR mutant may be due to limited transportation of ornibactin or pyochelin as previously mentioned. However, the difference of growth rate between the H111ΔfptA-orbA::TpTer and the H111ΔfptAΔhuvA-orbA::TpTer was quite evident and these observation may possibly show that HuvA may have an effect on the function of other TBDRs although in this case, the two TBDRs, FptA and OrbA should not function efficiently. In other words, participation of a global TBDR regulator in co-regulating the TBDR function may possibly exist.

Addition of haemin to the triple TBDR mutant did not allow the mutant to grow at a higher rate than in the absence of haemin addition, which is as expected (Figure 7.11E). Similarly, as mentioned previously, this may due to the participation of an alternative iron uptake pathways or a likely manifestation of pyochelin and ornibactin being transported inefficiently. Alternatively, this may suggest an involvement of co-regulation between the TBDR functions as mentioned, and there could be a possibility that HuvA may function better in the presence of the endogenous siderophore TBDRs, FptA and OrbA.

To compare the effect of inactivating the haem transport system in *B. cenocepacia* with inhibiting transport of endogenous siderophores, individual endogenous siderophore TBDRs were also inactivated. A mutant lacking the haem TBDR HxuC in *H. influenzae* was shown to be less virulent as compared to the wild type (Morton et al., 2009; Choby and Skaar, 2016). The comparison of growth rate of *B. cenocepacia* TBDR mutants in iron-deprived conditions *in vitro* may suggest the virulence of the pathogen *in vivo*. Moreover, this analysis validates the reliance of *B. cenocepacia* on haem and the siderophore acquisition system in iron deprived conditions.

The *B. cenocepacia pobA* mutant, H111ΔpobA, was not used in this study for generating the mutants because the synthesis of ornibactin and pyochelin in the mutant is blocked. *B. cenocepacia* strains, J2315 and 715j are able to utilise haemin as an alternative iron source in a rat infection model and it is consistent that the H111 strain may have the same ability (Whitby et al., 2006; Tyrrell et al., 2015). Both the extracellular iron transport proteins, transferrin and lactoferrin were clearly shown to be less preferred iron sources.

The mutants of *B. cenocepacia*, which do not have the ability to produce the primary siderophore ornibactin (715j-*orbI*) or lack the ability to produce both siderophores (715j-*pobA*) were demonstrated to be able to utilise haemin more efficiently than the wild type (Tyrrell et al., 2015). Therefore, it is likely that inactivation of the siderophore-mediated iron uptake pathways may boost haem utilisation and transport.

It was similarly demonstrated in this study that H111ΔpobA, which cannot produce ornibactin and pyochelin, is able to grow more efficiently with haemin supplementation as compared to H111ΔfptA-orbA::TpTer, which can make these siderophores but cannot utilise them. Therefore, there seems to be more efficient haemin utilisation with all TBDRs being intact. Conversely, without haem addition, the observation is *vice versa,* in which, the growth rate of the *B. cenocepacia* null *pobA* allele mutant is slower than the growth rate of the endogenous siderophore TBDR mutants (H111ΔfptA-orbA::TpTer). A recently reported quorum sensing signal molecule in *B. cenocepacia*, valdiazen, may have a role in the growth of the mutants used in this study, as the molecule is proposed to be involved in regulating expression of genes in metal homeostasis including the siderophore and the haem uptake system (Jenul et al., 2018). Moreover, Tyrell and coworkers' (2015) findings indicate that without siderophore-mediated iron acquisition, specifically without the existence of a dominant siderophore, *B. cenocepacia* tends to revert to an alternative iron source and consequently grows more efficiently in iron-deprived conditions. Similarly, *P. aeruginosa* reverts to haem as an iron-source in iron-limiting conditions when the dominant siderophore-mediated iron uptake pathways is compromised (Marvig et al., 2014).

Chapter 8

General discussion

8.1 Conclusion

This study shows that several siderophores that are not produced by *B. cenocepacia*, mostly those produced by soil microorganisms, are able to be utilised by *B. cenocepacia* for iron sources in iron limiting conditions and therefore can be considered as xenosiderophores for this organism (Table 8.1). Additional xenosiderophores utilised by *P. aeruginosa* were also observed (Table 8.2). The types of xenosiderophore identified provide an insight into the community interactions and competition in the normal environment of *B. cenocepacia*. Although these siderophores are able to promote growth to *B. cenocepacia* with variable efficiencies, there are also siderophores tested in this study that are not able to provide iron to *B. cenocepacia.* These may limit growth of the pathogenic *B. cenocepacia* in certain cases.

Sass and co-workers (2018) proposed that siderophores that are not able to act as a xenosiderophores to co-existing microorganisms can limit the growth of the non-producing microorganism (Sass et al., 2018). The siderophore pyoverdine produced by *P. aeruginosa* allows the pathogen to out-compete Bcc members, resulting in Bcc growth inhibition (Tyrrell et al., 2015; Leinweber et al., 2018), presumably due to the inability of Bcc to take advantage of the pyoverdine, which is also observed in this study. Pyoverdine produced by *P. aeruginosa* is also not able to act as a xenosiderophore to *A. fumigatus* in a co-existing environment as is commonly seen in the CF lung, and so may limit the growth of the fungi (Sass et al., 2018). Based on these observations, it can be deduced that co-existing microorganisms producing xenosiderophores which can be utilised by *B. cenocepacia* could enhance growth of the pathogen in CF patients, and xenosiderophores which cannot be utilised by the pathogen may limit or have no effect on growth of *B. cenocepacia.*

Burkholderia species, as with other pathogens such as *P. aeruginosa* (Hartney et al., 2011), contain many putative TBDR genes which could enable them to take advantage of a variety of xenosiderophores. Xenosiderophores appear to show substrate specificity in TBDR transport in this study as reported by many researchers, for example in *Pseudomonas* spp. (Cuív et al., 2006; Hartney et al., 2011). In this study, the utilisation of mixed ligand siderophores of the aspartate hydroxycarboxylate-hydroxamate type such as malleobactin is dependent on OrbA, the TBDR for ornibactin (Sokol et al., 2000), which also exhibits an aspartate hydroxycarboxylate-hydroxamate ligand. However, this TBDR does not appear to display redundancy in the transport of siderophores possessing the citrate hydroxycarboxylate-hydroxamate ligand such as arthrobactin, although they have similar ligand arrangments.

Five of the additional 22 putative TBDRs present in *B. cenocepacia* H111 were characterised in this study (Table 8.1). By excluding the known endogenous siderophore transporting TBDRs, the likely copper and zinc chelator TBDRs and also the vitamin B_{12} transporter, the remaining 12 TBDRs, remain to be characterised (Table 8.3). These putative TBDRs may be involved in transporting siderophores, other metal chelators or other compounds unrelated to metal transport.

Some of these putative TBDRs may be redundant in function or may transport iron and other metals, analogous to the role exhibited by FptA. Additionally, the undetermined transporters for other catecholates, cepabactin and the mixed type siderophores, arthrobactin and schizokinen, maybe amongst these uncharacterised TBDRs.

Two hydroxamate TBDRs, BCAL0116 and BCAL2281, were characterised in this study. It was shown from the *in silico* analysis of selected *Burkholderia* species that apart from *B. cenocepacia*, only *B. cepacia* possesses the TBDR BCAL0116 (Table 3.2). Similarly, only *B. multivorans* and *B. cenocepacia* possess the TBDR BCAL2281. Since the prevalent Bcc species are mostly *B. cenocepacia* and *B. multivorans*, it is likely that BCAL2281 plays a significant role in gaining benefits from the fungal-derived siderophores to provide iron sources when compared to the role of BCAL0116. Moreover, possession of hydroxamate TBDRS could benefit *B. cenocepacia*, in co-infection with *A. fumigatus,* which is the most prevalent fungus found in the CF lungs, which produces four hydroxamate siderophores (Tyrrell and Callaghan, 2016).

The catecholate TBDR, BCAM2007 is more widely distributed among the analysed *Burkholderia* species. However, only a limited number of catecholate siderophores are of fungal origin and this TBDR may be less advantageous as compared to the hydroxamate TBDRs. A number of antibiotics have been conjugated to catecholate and hydroxamate siderophores (Möllmann et al., 2009; Górska et al., 2014). These siderophore conjugates have also been shown to be efficient in gaining intracellular access and limiting growth of Bcc members. However, based on the existence of hydroxamate TBDRs in Bcc as predicted by *in silico* analysis, the hydroxamate siderophore-antibiotic conjugates may be more effective in controlling or limiting growth of *B. cenocepacia* due to its feature of possessing two hydroxamate TBDRs. In contrast, catecholate siderophore-antibiotic conjugates maybe more advantageous for the killing of Bcc members due to the more widespread occurrence of catecholate TBDRs in these species.

In *P. aeruginosa*, there are three TonB complex homologues found, and only one of these (TonB1) is indispensable for siderophore-mediated iron uptake (Zhao and Poole, 2000; Huang et al., 2004; Cuív et al., 2006). In this study, xenosiderophores with different ligands to the endogenous siderophores, are demonstrated to also require the TonB1 system. Therefore, it is likely that only the TonB1 system is required to facilitate siderophore-mediated iron uptake in *B. cenocepacia*. Moreover, the location of the genes encoding the other two putative TonB systems is not proximal to the genes expressing iron uptake systems (Chapter 3). These putative TonB system are seen near to genes expressing other metal- or compound -related proteins and may be involved in facilitating their transport.

The utilisation of most hydroxamate siderophores in *B. cenocepacia* was abolished in this study when the inner membrane protein, BCAL0117 was inactivated. It was predicted that BCAL0117 function is analogous to FoxB, present in *P. aeruginosa* (Cuív et al., 2004).

Table 8.1 Siderophores tested for utilisation by *B. cenocepacia* H111 strain

Denticity	Ligand	Siderophore[a]	TBDR
Hexadentate	Hydroxamate	Coprogen	
		Ferrichrome	BCAL0116-BCAL2281
		Ferricrocin	BCAL0116-BCAL2281
		Ferrioxamine B	BCAL0116
		TAFC	BCAL0116
	Catecholate	Bacillibactin	
		DHBS trimer	BCAM2007
		Enterobactin	
		Vibriobactin	
	Mixed type	Aerobactin	
		Arthrobactin	*
		Fimsbactin	
		Malleobactin	OrbA
		Phymabactin	OrbA[b]
		Schizokinen	*
Tetradentate	Hydroxamate	Alcaligin	BCAL0116
		Rhodotorulic acid	BCAL0116
	Catecholate	Azotochelin	BCAM2007
		Cepaciachelin	BCAM2007
		DHBS dimer	BCAM2007
		Serratiochelins	BCAM2007[b]
	Mixed type	Enantio-pyochelin	
		Nicotianamine	
		Ornicorrugatin	
		Pseudomonine	
		PVD	
		Pyochelin	FptA[c]
		Quinolobactin	
		Rhizoferrin	
		Staphyloferrin B	
		Thioquinolobactin	
		Yersiniabactin	
Bidentate	Hydroxamate	Cepabactin	*
	Catecholate	Chrysobactin	BCAM2007[b]
		DHBS monomer	BCAM2007

[a]Utilised siderophore are in shaded boxes.
[b]Requires validation using purified siderophore
[c]Demonstrated in H111 strain.
*Unidentified TBDR.

Table 8.2 Xenosiderophores utilised by *P. aeruginosa* identified or confirmed in this study[a]

		Siderophore	References
Purified siderophore		Aerobactin	(Cuív et al., 2006)
		Bacillibactin	This study
		Coprogen	(Meyer, 1992)
		Enterobactin	(Poole et al., 1990)
		Nicotianamine	(Gi et al., 2015)
		Ferrioxamine B	(Cuív et al., 2007)
		Rhizoferrin	(Bano and Musarrat, 2003)
		Rhodotorulic acid[b]	This study
		Schizokinen	(Cuív et al., 2006)
		Siderophore	References
Bacterial culture supernatants	*A. baylyi*	Fimsbactin	This study
		Unidentified	
	B. megaterium	Schizokinen	(Cuív et al., 2006)
	B. subtilis	Bacillibactin	This study
	E. coli	Enterobactin	(Poole et al., 1990) (Ghysels et al., 2005)
	S. marcescens	Chrysobactin	This study
		Serratiochelins	
		Yersiniabactin[c]	

[a]Performed by disc diffusion assay.
[b]The receptor for rhodotorulic acid is predicted to be redundant to the receptor for coprogen in *Pseudomonas* spp. (UniProt).
[c]Yersiniabactin is produced by other *Pseudomonas* spp. and may be utilised by *P. aeruginosa.*

Table 8.3 List of TBDR function in *B. cenocepacia* J2315 and H111 strains[a]

	chromosome	J2315 TBDRs[b,c]	H111 TBDRs[b]	TBDR function[d]
1	1	BCAL0116	I35_RS00620	FoxA (hydroxamate)
2	1	BCAL1345	I35_RS06170	Putative zinc chelator
3	1	BCAL1371	I35_RS06295	-
4	1	BCAL1700	I35_RS08065	OrbA (aspartate-type hydroxamate and hydroxycarboxylate)
5	1	BCAL1709	I35_RS08115	-
6	1	BCAL1777	I35_RS08460	-
7	1	'BCAL1783'[e]	I35_RS08490	-
8	1	BCAL2281	I35_RS11045	FiuA (hydroxamate)
9	1	BCAL3001	I35_RS04375	-
10	2	BCAM0491	I35_RS18505	Putative zinc chelator
11	2	BCAM0499	I35_RS18545	Putative catecholate
12	2	BCAM0564	I35_RS18860	-
13	2	BCAM0706[f]	I35_RS19580	Putative hydroxamate
14	2	BCAM0948	I35_RS20820	Putative OprC (copper chelator)
15	2	BCAM1187	I35_RS21645	Putative catecholate
16	2	BCAM1571	I35_RS23575	Putative citrate-type hydroxamate and hydroxycarboxylate Putative ZnuD (zinc chelator)
17	2	BCAM1593	I35_RS23700	Putative BtuB
18	2	BCAM2007	I35_RS25625	PiuA (catecholate)
19	2	BCAM2224	I35_RS26975	FptA
20	2	BCAM2367	I35_RS27690	-
21	2	BCAM2439	I35_RS28095	-
22	2	BCAM2626	I35_RS29035	HuvA (Haem)
23	3	BCAS0333	I35_RS31745	Putative OrbA-like Putative aspartate-type hydroxamate and hydroxycarboxylate
24	3	BCAS0360	I35_RS31880	Putative CntO (zinc chelator)

[a]Highlighted according to Inter Pro analysis.
Putative siderophore TBDRs (Pink). Other metal chelator TBDRs (Green).
[b]Ranked in order of gene locus location in chromosomes.
[c]Corresponding J2315 and H111 TBDRs are shown in the same rows.
[d]Some TBDR functions are putative.
[e]Not annotated in J2315 although pseudogene is present.
[f]Indicates gene disruption. BCAM0706 is likely to be non-functional as encoded protein is truncated.
-Non-predictive specific function

The transport of the iron complex through FoxB has not been investigated as to whether the FoxB protein is a single-subunit permease or a permease subunit in an ABC transport complex (Cuív et al., 2007). Therefore, the characterisation of BCAL0117 as to which type of permeases it imposes remains to be elucidated. The BCAL0117 protein may entirely function as the FoxB protein or it may function in a different manner.

The catecholate siderophores and the mixed type siderophores which exhibit two hydroxamate and a single hydroxycarboxylate ligand were observed to be utilised by *B. cenocepacia* with an inactivated BCAL0117 cytoplasmic membrane protein. BCAL0117 therefore does not participate in the catecholate and mixed ligand siderophore utilisation. Inner membrane siderophore transport is highly specific as shown by the pyochelin cytoplasmic membrane transporter, FptX. While pyochelin is transported by FptX (Cuív et al., 2004), enantio-pyochelin requires a PBP and an ABC transporter, FetCDE in *P. aeruginosa* (Reimmann, 2012). A similar mechanism is proposed in *B. cenocepacia* (Thomas, 2007). This inner membrane protein does not show redundancy in the utilisation of all types of xenosiderophore and is only responsible for the utilisation of most hydroxamate siderophores, as alcaligin and cepabactin are not transported. It is therefore likely that another inner membrane transport system is responsible for the transport of other hydroxamate xenosiderophores such as alcaligin. Due to fewer studies reporting on the inner membrane transport proteins for the transfer of iron-siderophore complexes into bacterial cytoplasm, designing the mechanisms of siderophore-antibiotic conjugates are suggested to allow the release of the attached antibiotics in the periplasm for transfer into the bacterial cytoplasm rather than utilising the inner membrane transport protein used for translocating iron complexes (Mislin and Schalk, 2014; Schalk, 2018).

P. aeruginosa has been reported to have three haem acquisition mechanisms, the Has, Phu and Hxu systems. The Phu system was shown to be regulated by the iron uptake regulator, Fur, while the other two systems are both dependent on the function of an ECF (extra cytoplasmic function) sigma factor (Cornelis et al., 2009). In this study, one haem acquisition system was demonstrated in *B. cenocepacia* that may resemble either the Phu system or the Hxu system which require only one TBDR, PhuR or HxuC, to transport haem and may not involve haemophores as demonstrated by the Has system. In addition, Phu system is not shown to be regulated by an ECF sigma factor and may highly resemble the haem uptake system in *B. cenocepacia* constituting the TBDR, BCAM2626, which do not posseses a long N-terminal extension for an ECF sigma factor regulation.

BCAM2626 (HuvA) is predicted by *in silico* analysis to be highly distributed among the analysed Bcc species in this study, including species from the pseudomallei group (Table 3.2). Many Bcc and the *pseudomallei* group members therefore are highly likely to benefit from haem availability in the CF lungs. The regulation

of haem acquisition system by the TBDR BCAM2626, however, remains to be investigated. Moreover, based on this study, it is likely that *B. cenocepacia* has only one haem acquisition system.

8.2 Limitations

Limitations in this study are encountered in which variation in growth haloes of bacteria in the disc diffusion assay can be observed. Bacterial growth haloes can be seen as thick growth with smaller diameters or thinner growth with larger diameters. The assay therefore may not be very precise in quantitative terms as described by Neilands (Neilands, 1984) and analysis using liquid growth stimulation is more reliable. Nevertheless, promotion of growth haloes around filter discs in the disc diffusion assay certainly indicates bacterial growth or an ability of a bacterial mutant to utilise a siderophore. Capturing images of bacterial growth in the disc diffusion assay was another limitation encountered in this study. Some bacterial growth haloes were too faint to be captured and this was also the case with some bacterial mutants containing complementation plasmids. Additionally, the colour background in the images may vary as a result of modifying exposure conditions to capture visible growth in the images.

Two receptors (BCAL0116 and BCAL2281) were involved in utilising the ferrichromes. When both receptors were present, the diameters of the zones of growth of the *pobA* mutant were observed to be small. Bigger haloes of growth were observed when one of the receptors was inactivated as in Figure 4.10 and 4.12. Human error was negligible in performing the disc diffusion assays in this study, in terms of the concentration, amount and quantity of agar used. Similarly, for the concentration, amount and quantity of bacterial culture used. Therefore, discrepancies in zones of bacterial mutant growth can be assumed as due to the mechanisms of the receptors. Moreover, the expression of the two TBDR genes (*fiuA* and *foxA*) responsible for the transport of ferrichrome in *P. aeruginosa* are regulated by a signalling cascade involving the iron-starvation ECF sigma factor, FoxI and anti-sigma factor, FoxR (Llamas et al., 2006). However, based on *the in silico* analyses in this study, the putative TBDR sequences in *B. cenocepacia* do not seem to possess the N-terminal extension characteristic of a receptor that are regulated by a sigma or anti sigma regulatory system except for BCAL1371.

8.3 Future work

The TBDR for the cyclic hydroxamate siderophore produced by *B. cepacia*, cepabactin has not been determined in this study. Cepabactin also can be categorised as a siderophore exhibiting a hydroxypyridone or catecholate characteristics but was also shown in this study, not to utilise the catecholate siderophore, TBDR BCAM2007, for its transport into *B. cenocepacia.* Similarly, the TBDR responsible for arthrobactin and schizokinen utilisation has not been identified. Other putative TBDRs could be inactivated, particularly BCAM0706 and BCAL1571, either single or in combination with other TBDRs according to the analysis discussed. For instance, BCAL0116 and BCAL2281 may cooperate with

BCAM0706 in transporting cepabactin. Although cepabactin, arthrobactin and schizokinen contain hydroxamate ligands, non-hydroxamate TBDRs may be responsible for their utilisation or may cooperate with the characterised TBDRs in this study.

The other TBDR that participates in the utilisation of DHBS derivatives was also not determined. Two TBDRs were demonstrated to transport the DHBS derivatives in *E. coli* (Fir and Cir) (Hider and Kong, 2010) and *V. cholerae* (IrgA and VctA) (Wyckoff et al., 2015). Based on the results of this study, it is likely that *B. cenocepacia* utilises at least two TBDRs in the transport of the DHBS derivatives. The predicted catecholate TBDR, BCAM0499 was not shown to be a catecholate or a sole catecholate TBDR since the BCAM0499 TBDR mutant grew in the presence of the DHBS derivatives. Whether the *B. cenocepacia* BCAM0499 single TBDR mutants promoted full growth or intermediate growth can be quantified by its growth rate using the liquid growth stimulation assay. An intermediate growth may indicate participation of BCAM0499 in the transport of DHBS derivatives.

The inner membrane transport proteins for the catecholate siderophores have not been explored in this study and the gene loci encoding inner membrane proteins adjacent to BCAM2007, i.e. BCAM2004 and BCAM2005 could be investigated using further mutagenesis studies. The inner membrane protein for malleobactin utilisation has also not been investigated in this study. The most likely transporter for malleobactin is likely to be the ABC transport system which is responsible for transporting ornibactin. A previously constructed *B. cenocepacia* sigma factor mutant that does not activate the expression of the *orbBCD* operon encoding the ABC transport system, H111-orbS::Tp could be used to investigate this mechanism. The inner membrane transport system for the many hydroxamate siderophores appears to be encoded in the vicinity of the hydroxamate TBDR identified in this study, BCAL0116. A inner membrane protein responsible for the transport of other hydroxamate xenosiderophores into the bacterial cytosol such as alcaligin may potentially be encoded near to the other hydroxamate TBDR, BCAL2281. The genes located near to BCAL2281 that are predicted to encode cytoplasmic membrane transport proteins are BCAL2280, BCAL2282 and BCAL2283 (Section 3.4). In addition , the operon for hydroxamate transport in *B. cenocepacia* can also be elucidated.

The transport of the iron-complexes via their determined TBDR proteins (BCAL0116, BCAL2281, BCAL1700, BCAM2007, BCAM2626) and inner membrane protein (BCAL0117) can be confirmed by performing iron uptake assays using radioactive ^{55}Fe coupled to the siderophores as demonstrated by Hannaeur *et al*. (2010) or coupled to haemin. Inhibition of the ^{55}Fe incorporation into a mutant with a particular inactivated transport protein, demonstrated by a limited growth rate under iron limiting conditions, can be used as a validation that the protein has a vital role in the transport of a particular siderophore. Besides, the efficiency of the two TBDRs, BCAL0116 and BCAL2281, responsible for

ferrichrome-iron complex transport can also be distinguished by these radioactive uptake assays. Ferrichrome transport in *B. cenocepacia* may have a similarity to the ferrichrome uptake pathway in *P. aeruginosa,* in which the FiuA is a primary TBDR for ferrichrome transport and FoxA is a secondary receptor (Hannauer et al., 2010a). By performing the radioactive assay, the TBDR that acts as the primary and secondary TBDRs can be determined. The transport efficiency of each xenosiderophore via its cognate TBDR can also be analysed by this approach.

The virulence of *B. cenocepacia* with and without ornibactin, pyochelin or the haem TBDRs (OrbA, FptA, BCAM2626) can be investigated using the animal infection model, *Galleria mellonella* larvae (wax moth) (Seed et al., 2008). However, haem may be present only in few cellular proteins in the larvae blood haemolymph and therefore a virulence study related to haem utilisation in the larvae may not allow high accuracy outcomes. Therefore, the role of the haem uptake system in virulence should be conducted in vertebrate animal models.

Diversity in the iron transport pathways can be observed in this study, in relation to both the outer and inner membrane transport. By far, the involvement of the energy transducer, TonB1 complex has been shown to be undistinguishable. Other iron transport-related pathways, including the release mechanism of iron from the xenosiderophores, xenosiderophore recycling (which may be applicable to ferrichrome as in *P. aeruginosa*) and regulation of iron transport proteins have not been investigated in this study. Taken together, the study of the siderophore piracy of *B. cenocepacia* remains of interest for a better understanding of the iron acquisition mechanisms in *B. cenocepacia* and as a route to the development of siderophore-related antimicrobial strategies.

Appendices

APPENDIX 1

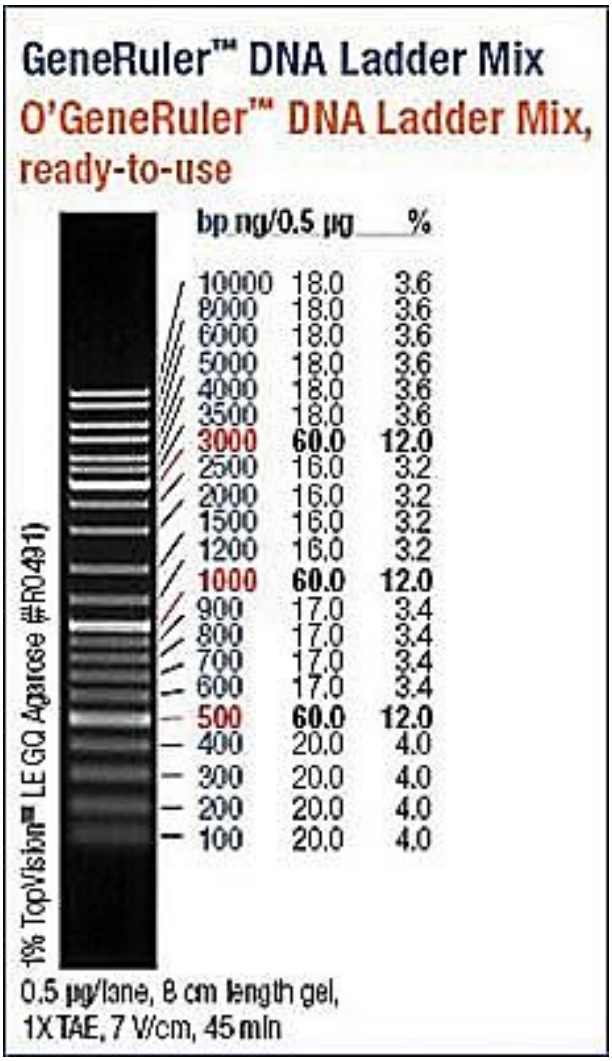

Thermo Scientific™ GeneRuler™ DNA reference band was used to quantify the size of double-stranded DNA fragments on agarose gels.

APPENDIX 2

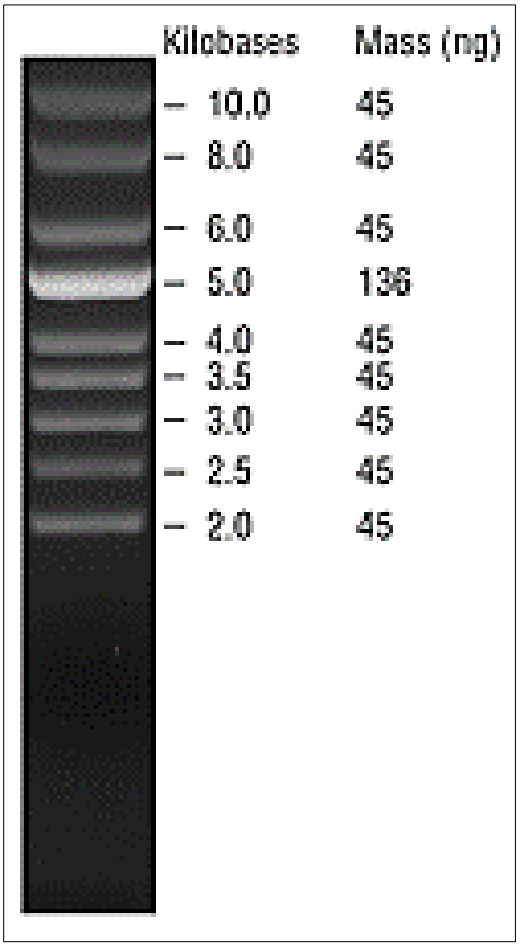

Supercoiled DNA Ladder marker (New England Biolabs) with a standard supercoiled molecular weight ranging in size from 2 to 10 kb was referred to quantify the size of supercoiled plasmids in agarose gels. The 5 kb plasmid has an increased intensity to serve as a reference band.

Bibliography

ABERGEL, R. J., WILSON, M. K., ARCENEAUX, J. E., HOETTE, T. M., STRONG, R. K., BYERS, B. R. & RAYMOND, K. N. 2006. Anthrax pathogen evades the mammalian immune system through stealth siderophore production. *Proceedings of the National Academy of Sciences,* 103**,** 18499-18503.

ABERGEL, R. J., ZAWADZKA, A. M., HOETTE, T. M. & RAYMOND, K. N. 2009. Enzymatic Hydrolysis of Trilactone Siderophores: Where Chiral Recognition Occurs in Enterobactin and Bacillibactin Iron Transport. *Journal of the American Chemical Society,* 131**,** 12682-12692.

ADHIKARI, P., BERISH, S. A., NOWALK, A. J., VERALDI, K. L., MORSE, S. A. & MIETZNER, T. A. 1996. The fbpABC locus of *Neisseria gonorrhoeae* functions in the periplasm-to-cytosol transport of iron. *Journal of Bacteriology,* 178**,** 2145-2149.

ADJIMANI, J. P. & EMERY, T. 1987. Iron uptake in *Mycelia sterilia* EP-76. *Journal of Bacteriology,* 169**,** 3664-3668.

AGNOLI, K., HALDIPURKAR, S. S., TANG, Y., BUTT, A. T. & THOMAS, M. S. 2019. Distinct Modes of Promoter Recognition by Two Iron Starvation σ Factors with Overlapping Promoter Specificities. *J of Bacteriology,* 201**,** 507-518.

AGNOLI, K., LOWE, C. A., FARMER, K. L., HUSNAIN, S. I. & THOMAS, M. S. 2006. The ornibactin biosynthesis and transport genes of *Burkholderia cenocepacia* are regulated by an extracytoplasmic function σ factor which is a part of the Fur regulon. *Journal of Bacteriology,* 188**,** 3631-3644.

AGNOLI, K., SCHWAGER, S., UEHLINGER, S., VERGUNST, A., VITERI, D., NGUYEN, D., SOKOL, P., CARLIER, A. & EBERL, L. J. M. M. 2012. Exposing the third chromosome of Burkholderia cepacia complex strains as a virulence plasmid. *Molecular Microbiology,* 83**,** 362-378.

AL-HATMI, A. M. S., BONIFAZ, A., RANQUE, S., SYBREN DE HOOG, G., VERWEIJ, P. E. & MEIS, J. F. 2018. Current antifungal treatment of fusariosis. *International Journal of Antimicrobial Agents,* 51**,** 326-332.

ALICE, A. F., LÓPEZ, C. S., LOWE, C. A., LEDESMA, M. A. & CROSA, J. H. 2006. Genetic and transcriptional analysis of the siderophore malleobactin biosynthesis and transport genes in the human pathogen *Burkholderia pseudomallei* K96243. *Journal of Bacteriology,* 188**,** 1551-1566.

ALJADANI, S. 2018. *Regulation of iron acquisition by an iron starvation sigma factor system in Burkholderia cenocepacia.* PhD thesis, University of Sheffield.

ALTING-MEES, M. & SHORT, J. 1989. pBluescript II: gene mapping vectors. *Nucleic acids research,* 17**,** 9494.

ANDERSEN, D., RENSHAW, J. C. & WIEBE, M. G. 2003. Rhodotorulic acid production by *Rhodotorula mucilaginosa*. *J Mycological research,* 107**,** 949-956.

ANDREWS, S. C., ROBINSON, A. K. & RODRÍGUEZ-QUIÑONES, F. 2003. Bacterial iron homeostasis. *FEMS Microbiology Reviews,* 27**,** 215-237.

ANKENBAUER, R., SRIYOSACHATI, S. & COX, C. D. 1985. Effects of siderophores on the growth of *Pseudomonas aeruginosa* in human serum and transferrin. *Infection and Immunity,* 49**,** 132-140.

ANKENBAUER, R. G., TOYOKUNI, T., STALEY, A., RINEHART, K. L. & COX, C. D. 1988. Synthesis and biological activity of pyochelin, a siderophore of *Pseudomonas aeruginosa*. *Journal of Bacteriology,* 170**,** 5344-5351.

ANZALDI, L. L. & SKAAR, E. P. 2010. Overcoming the heme paradox: heme toxicity and tolerance in bacterial pathogens. *Infection and Immunity,* 78**,** 4977-4989.

ARMSTRONG, S. K., BRICKMAN, T. J. & SUHADOLC, R. J. 2012. Involvement of multiple distinct *Bordetella* receptor proteins in the utilization of iron liberated from transferrin by host catecholamine stress hormones. *Molecular Microbiology,* 84**,** 446-462.

ARNOUX, P., HASER, R., IZADI, N., LECROISEY, A., DELEPIERRE, M., WANDERSMAN, C. & CZJZEK, M. 1999. The crystal structure of HasA, a hemophore secreted by *Serratia marcescens*. *Nature Structural and Molecular Biology,* 6**,** 516-520.

ASGHAR, A. H. 2003. *Identification and characterisation of genes involved in iron acquisition in Burkholderia cepacia. PhD thesis. University of Sheffield.*

ASGHAR, A. H., SHASTRI, S., DAVE, E., WOWK, I., AGNOLI, K., COOK, A. M. & THOMAS, M. S. 2011. The *pobA* gene of *Burkholderia cenocepacia* encodes a group I Sfp-type phosphopantetheinyltransferase required for biosynthesis of the siderophores ornibactin and pyochelin. *Microbiology,* 157**,** 349-361.

ATKIN, C., NEILANDS, J. & PHAFF, H. 1970. Rhodotorulic acid from species of *Leucosporidium, Rhodosporidium, Rhodotorula, Sporidiobolus*, and *Sporobolomyces*, and a new alanine-containing ferrichrome from *Cryptococcus melibiosum*. *Journal of bacteriology,* 103**,** 722-733.

AWADH, H., MANSOUR, M., AQTASH, O. & SHWEIHAT, Y. 2017. Pneumonia due to a Rare Pathogen: *Achromobacter xylosoxidans*, Subspecies *denitrificans*. *Case reports in infectious diseases,* 2017**,** 1-4.

BAGG, A. & NEILANDS, J. 1987. Molecular mechanism of regulation of siderophore-mediated iron assimilation. *Microbiological Reviews,* 51**,** 509-518.

BAKER, H. M. & BAKER, E. N. 2004. Lactoferrin and iron: structural and dynamic aspects of binding and release. *Biometals,* 17**,** 209-216.

BALDWIN, A., MAHENTHIRALINGAM, E., THICKETT, K. M., HONEYBOURNE, D., MAIDEN, M. C., GOVAN, J. R., SPEERT, D. P., LIPUMA, J. J., VANDAMME, P. & DOWSON, C. G. 2005. Multilocus sequence typing scheme that provides both species and strain differentiation for the Burkholderia cepacia complex. *Journal of clinical microbiology,* 43**,** 4665-4673.

BALLARD, R., PALLERONI, N., DOUDOROFF, M., STANIER, R. & MANDEL, M. 1970. Taxonomy of the aerobic pseudomonads: *Pseudomonas cepacia, P. marginata, P. alliicola* and *P. caryophylli*. *Microbiology,* 60**,** 199-214.

BAMFORD, S., RYLEY, H. & JACKSON, S. K. 2007. Highly purified lipopolysaccharides from Burkholderia cepacia complex clinical isolates induce inflammatory cytokine responses via TLR4-mediated MAPK signalling pathways and activation of NFκB. *Cellular Microbiology,* 9**,** 532-543.

BANO, N. & MUSARRAT, J. 2003. Characterization of a New *Pseudomonas aeruginosa* Strain NJ-15 as a Potential Biocontrol Agent. *Current Microbiology,* 46**,** 0324-0328.

BARCLAY, S. J., HUYNH, B. H. & RAYMOND, K. N. 1984. Coordination chemistry of microbial iron transport compounds. 27. Dimeric iron(III) complexes of dihydroxamate analogs of rhodotorulic acid. *Inorganic Chemistry,* 23**,** 2011-2018.

BARELMANN, I., MEYER, J. M., TARAZ, K. & BUDZIKIEWICZ, H. 1996. Cepaciachelin, a new catecholate siderophore from *Burkholderia* (*Pseudomonas*) *cepacia*. *Zeitschrift für Naturforschung C,* 51**,** 627-630.

BARRETT, A. R., KANG, Y., INAMASU, K. S., SON, M. S., VUKOVICH, J. M. & HOANG, T. T. 2008. Genetic tools for allelic replacement in *Burkholderia* species. *J Applied environmental microbiology reports,* 74**,** 4498-4508.

BARRY, S. M. & CHALLIS, G. L. 2009. Recent advances in siderophore biosynthesis. *Current Opinion in Chemical Biology,* 13**,** 205-215.

BÁUMLER, A. J. & HANTKE, K. 1992. Ferrioxamine uptake in *Yersinia enterocolitica*: characterization of the receptor protein FoxA. *Molecular Microbiology,* 6**,** 1309-1321.

BAYSSE, C., DE VOS, D., NAUDET, Y., VANDERMONDE, A., OCHSNER, U., MEYER, J.-M., BUDZIKIEWICZ, H., SCHÄFER, M., FUCHS, R. & CORNELIS, P. 2000. Vanadium interferes with siderophore-mediated iron uptake in *Pseudomonas aeruginosa*. *Microbiology,* 146**,** 2425-2434.

BEARDEN, S. W. & PERRY, R. D. 1999. The Yfe system of *Yersinia pestis* transports iron and manganese and is required for full virulence of plague. *Molecular Microbiology,* 32**,** 403-414.

BEASLEY, F. C., MAROLDA, C. L., CHEUNG, J., BUAC, S. & HEINRICHS, D. E. 2011. *Staphylococcus aureus* transporters Hts, Sir, and Sst capture iron liberated from human transferrin by Staphyloferrin A, Staphyloferrin B, and catecholamine stress hormones, respectively, and contribute to virulence. *Infection and Immunity,* 79**,** 2345-2355.

BELD, J., SONNENSCHEIN, E. C., VICKERY, C. R., NOEL, J. P. & BURKART, M. D. 2014. The phosphopantetheinyl transferases: catalysis of a post-translational modification crucial for life. *Natural product reports,* 31**,** 61-108.

BENNETT, N., MAGLIONE, P. J., WRIGHT, B. L. & ZERBE, C. 2018. Infectious Complications in Patients With Chronic Granulomatous Disease. *Journal of the Pediatric Infectious Diseases Society,* 7**,** S12-S17.

BENSON, H. P., BONCOMPAGNI, E. & GUERINOT, M. L. 2005. An iron uptake operon required for proper nodule development in the *Bradyrhizobium japonicum*-soybean symbiosis. *Molecular plant-microbe interactions,* 18**,** 950-959.

BERNER, I., GREINER, M., METZGER, J., JUNG, G. & WINKELMANN, G. 1991. Identification of enterobactin and linear dihydroxybenzoylserine compounds by HPLC and ion spray mass spectrometry (LC/MS and MS/MS). *Biology of metals,* 4**,** 113-118.

BERNIER, S. P., SON, S. & SURETTE, M. G. 2018. The Mla pathway plays an essential role in the intrinsic resistance of Burkholderia cepacia complex species to antimicrobials and host innate components. *Journal of bacteriology,* 200**,** 1-17.

BERRIATUA, E., ZILUAGA, I., MIGUEL-VIRTO, C., URIBARREN, P., JUSTE, R., LAEVENS, S., VANDAMME, P. & GOVAN, J. 2001. Outbreak of subclinical mastitis in a flock of dairy sheep associated with Burkholderia cepacia complex infection. *Journal of clinical microbiology,* 39**,** 990-994.

BLACKBURN, L., BROWNLEE, K., CONWAY, S. & DENTON, M. 2004. 'Cepacia syndrome'with *Burkholderia multivorans*, 9 years after initial colonization. *J Journal of Cystic Fibrosis,* 3**,** 133-134.

BODILIS, J., DENET, E., BROTHIER, E., GRAINDORGE, A., FAVRE-BONTÉ, S. & NAZARET, S. 2018. Comparative Genomics of Environmental and Clinical *Burkholderia cenocepacia* Strains Closely Related to the Highly Transmissible Epidemic ET12 Lineage. *Frontiers in Microbiology,* 9**,** 1-12.

BÖHNKE, R. & MATZANKE, B. 1995. The mobile ferrous iron pool in Escherichia coli is bound to a phosphorylated sugar derivative. *Biometals,* 8**,** 223-230.

BORCK, K., BEGGS, J. D., BRAMMAR, W., HOPKINS, A. & MURRAY, N. E. 1976. The construction in vitro of transducing derivatives of phage lambda. *Molecular General Genetics,* 146**,** 199-207.

BRANDEL, J., HUMBERT, N., ELHABIRI, M., SCHALK, I. J., MISLIN, G. L. & ALBRECHT-GARY, A.-M. 2012a. Pyochelin, a siderophore of Pseudomonas aeruginosa: physicochemical characterization of the iron (III), copper (II) and zinc (II) complexes. *Dalton Transactions,* 41**,** 2820-2834.

BRANDEL, J., HUMBERT, N., ELHABIRI, M., SCHALK, I. J., MISLIN, G. L. A. & ALBRECHT-GARY, A.-M. 2012b. Pyochelin, a siderophore of *Pseudomonas aeruginosa*: Physicochemical characterization of the iron(iii), copper(ii) and zinc(ii) complexes. *Dalton Transactions,* 41**,** 2820-2834.

BRAUD, A., HANNAUER, M., MISLIN, G. L. A. & SCHALK, I. J. 2009. The *Pseudomonas aeruginosa* Pyochelin-Iron Uptake Pathway and Its Metal Specificity. *Journal of Bacteriology,* 191**,** 3517-3525.

BRAUN, V., GÜNTHNER, K., HANTKE, K. & ZIMMERMANN, L. 1983. Intracellular activation of albomycin in Escherichia coli and Salmonella typhimurium. *Journal of bacteriology,* 156**,** 308-315.

BRAUN, V. & HANTKE, K. 2011. Recent insights into iron import by bacteria. *Current Opinion in Chemical Biology,* 15**,** 328-334.

BRAUN, V., PRAMANIK, A., GWINNER, T., KOBERLE, M. & BOHN, E. 2009. Sideromycins: tools and antibiotics. *Biometals,* 22**,** 3-13.

BRETT, P. J., DESHAZER, D. & WOODS, D. E. 1998. Burkholderia thailandensis sp. nov., a *Burkholderia pseudomallei*-like species. *International Journal of Systematic Bacteriology,* 48 Pt 1**,** 317-20.

BRICKMAN, T. J. & ARMSTRONG, S. K. 2012. Iron and pH-responsive FtrABCD ferrous iron utilization system of *Bordetella* species. *Molecular Microbiology,* 86**,** 580-593.

BRICKMAN, T. J. & MCINTOSH, M. A. 1992. Overexpression and purification of ferric enterobactin esterase from *Escherichia coli*. Demonstration of enzymatic hydrolysis of enterobactin and its iron complex. *Journal of Biological Chemistry,* 267**,** 12350-12355.

BRILLET, K., RUFFENACH, F., ADAMS, H., JOURNET, L., GASSER, V. R., HOEGY, F., GUILLON, L., HANNAUER, M. L., PAGE, A. & SCHALK, I. J. 2012. An ABC transporter with two periplasmic binding proteins involved in iron acquisition in *Pseudomonas aeruginosa*. *ACS chemical biology,* 7**,** 2036-2045.

BURKHOLDER, W. H. 1942. Three bacterial plant pathogens: *Phytomonas earyophylli* sp. n., *Phytomonas alliicola* sp. n., and *Phytomonas manihotis* (Arthaud-Berthet et Sondar) Viégas. *Phytopathology,* 32**,** 141-149.

BURKHOLDER, W. H. 1950. Sour skin, a bacterial rot of onion bulbs. *Phytopathology,* 40**,** 115-117.

BURONI, S., MATTHIJS, N., SPADARO, F., VAN ACKER, H., SCOFFONE, V. C., PASCA, M. R., RICCARDI, G. & COENYE, T. 2014. Differential role of RND efflux pumps in antimicrobial drug resistance of sessile and planktonic *Burkholderia cenocepacia* cells. *Antimicrobial Agents and Chemotherapy***,** 7424-7429.

BUTT, A. T. & THOMAS, M. S. 2017. Iron acquisition mechanisms and their role in the virulence of *Burkholderia* species. *J Frontiers in cellular infection microbiology,* 7**,** 1-21.

CABISCOL, E., TAMARIT, J. & ROS, J. 2000. Oxidative stress in bacteria and protein damage by reactive oxygen species. *International Microbiology,* 3**,** 3-8.

CAO, J., WOODHALL, M. R., ALVAREZ, J., CARTRON, M. L. & ANDREWS, S. C. 2007. EfeUOB (YcdNOB) is a tripartite, acid-induced and CpxAR-regulated, low-pH Fe2+ transporter that is cryptic in *Escherichia coli* K-12 but functional in *E. coli* O157: H7. *Molecular Microbiology,* 65**,** 857-875.

CAPON, R. J., STEWART, M., RATNAYAKE, R., LACEY, E. & GILL, J. H. 2007. Citromycetins and Bilains A–C: New Aromatic Polyketides and Diketopiperazines from Australian Marine-Derived and Terrestrial *Penicillium* spp. *Journal of Natural Products,* 70**,** 1746-1752.

CARLIER, A., AGNOLI, K., PESSI, G., SUPPIGER, A., JENUL, C., SCHMID, N., TÜMMLER, B., PINTO-CARBO, M. & EBERL, L. 2014. Genome sequence of B*urkholderia cenocepacia* H111, a cystic fibrosis airway isolate. *Genome announcements,* 2**,** 298-14.

CARNEIRO, H. A., COLEMAN, J. J., RESTREPO, A. & MYLONAKIS, E. 2011. *Fusarium* infection in lung transplant patients: report of 6 cases and review of the literature. *J Medicine,* 90**,** 69-80.

CARPENTER, B. M., WHITMIRE, J. M. & MERRELL, D. S. 2009. This Is Not Your Mother's Repressor: the Complex Role of Fur in Pathogenesis. *Infection and Immunity,* 77**,** 2590-2601.

CARROLL, C. S. & MOORE, M. M. 2018. Ironing out siderophore biosynthesis: a review of non-ribosomal peptide synthetase (NRPS)-independent siderophore synthetases. *Critical Reviews in Biochemistry and Molecular Biology,* 53**,** 356-381.

CARTRON, M., MADDOCKS, S., GILLINGHAM, P., CRAVEN, C. J. & ANDREWS, S. 2006. Feo – Transport of ferrous iron into bacteria. *Biometals,* 19**,** 143-157.

CASADABAN, M. J. & COHEN, S. N. 1980. Analysis of gene control signals by DNA fusion and cloning in *Escherichia coli*. *Journal of molecular biology,* 138**,** 179-207.

CAZA, M. & KRONSTAD, J. W. 2013. Shared and distinct mechanisms of iron acquisition by bacterial and fungal pathogens of humans. *Frontiers in Cellular and Infection Microbiology,* 3**,** 1-23.

CELIA, H., NOINAJ, N., ZAKHAROV, S. D., BORDIGNON, E., BOTOS, I., SANTAMARIA, M., BARNARD, T. J., CRAMER, W. A., LLOUBES, R. & BUCHANAN, S. K. 2016. Structural insight into the role of the Ton complex in energy transduction. *Nature,* 538**,** 60-77.

CENDROWSKI, S., MACARTHUR, W. & HANNA, P. 2004. *Bacillus anthracis* requires siderophore biosynthesis for growth in macrophages and mouse virulence. *Mol Microbiol,* 51**,** 407-17.

CERNAT, A., TERTIS, M., GANDOUZI, I., BAKHROUF, A., SUCIU, M. & CRISTEA, C. 2018. Electrochemical sensor for the rapid detection of P*seudomonas aeruginosa* siderophore based on a nanocomposite platform. *Electrochemistry Communications,* 88**,** 5-9.

CESCAU, S., CWERMAN, H., LETOFFE, S., DELEPELAIRE, P., WANDERSMAN, C. & BIVILLE, F. 2007. Heme acquisition by hemophores. *J Biometals,* 20**,** 603-613.

CESCUTTI, P., BOSCO, M., PICOTTI, F., IMPALLOMENI, G., LEITÃO, J. H., RICHAU, J. A. & SÁ-CORREIA, I. 2000. Structural study of the exopolysaccharide produced by a clinical isolate of *Burkholderia cepacia*. *J Biochemical biophysical research communications,* 273**,** 1088-1094.

CHALLIS, G. L. 2005. A widely distributed bacterial pathway for siderophore biosynthesis independent of nonribosomal peptide synthetases. *ChemBioChem,* 6**,** 601-611.

CHAN, C., ANDISI, V. F., NG, D., OSTAN, N., YUNKER, W. K. & SCHRYVERS, A. B. 2018. Are lactoferrin receptors in Gram-negative bacteria viable vaccine targets? *BioMetals,* 31**,** 381-398.

CHAPARRO, C., MAURER, J., GUTIERREZ, C., KRAJDEN, M., CHAN, C., WINTON, T., KESHAVJEE, S., SCAVUZZO, M., TULLIS, E. & HUTCHEON, M. 2001. Infection with *Burkholderia cepacia* in cystic fibrosis: outcome following lung transplantation. *American journal of respiratory critical care medicine,* 163**,** 43-48.

CHATTERJEE, A. & O'BRIAN, M. R. 2018. Rapid evolution of a bacterial iron acquisition system. *Molecular microbiology,* 108**,** 90-100.

CHENG, Q. & PARK, J. T. 2002. Substrate specificity of the AmpG permease required for recycling of cell wall anhydro-muropeptides. *Journal of Bacteriology,* 184**,** 6434-6436.

CHENG, S. H., GREGORY, R. J., MARSHALL, J., PAUL, S., SOUZA, D. W., WHITE, G. A., O'RIORDAN, C. R. & SMITH, A. E. 1990. Defective intracellular transport and processing of CFTR is the molecular basis of most cystic fibrosis. *Cell,* 63**,** 827-834.

CHIEN, Y.-C., LIAO, C.-H., SHENG, W.-H., CHIEN, J.-Y., HUANG, Y.-T., YU, C.-J. & HSUEH, P.-R. 2018. Clinical characteristics of bacteraemia caused by Burkholderia cepacia complex species and antimicrobial susceptibility of the isolates in a medical centre in Taiwan. *International Journal of Antimicrobial Agents,* 51**,** 357-364.

CHOBY, J. E. & SKAAR, E. P. 2016. Heme Synthesis and Acquisition in Bacterial Pathogens. *Journal of Molecular Biology,* 428**,** 3408-3428.

CHOI, J. J. & MCCARTHY, M. W. 2018. Cefiderocol: a novel siderophore cephalosporin. *Expert Opinion on Investigational Drugs,* 27**,** 193-197.

CHRISTINE C, F.-G., TAMMY M.-H, H. & MIGUEL A, V. 2002. Identification of a general secretory pathway in a human isolate of *Burkholderia vietnamiensis* (formerly B. cepacia complex genomovar V) that is required for the secretion of hemolysin and phospholipase C activities. *J Microbial pathogenesis,* 32**,** 249-254.

CHU, B. C., PEACOCK, R. S. & VOGEL, H. J. 2007. Bioinformatic analysis of the TonB protein family. *Biometals,* 20**,** 467.

CHUNG, J. W., ALTMAN, E., BEVERIDGE, T. J. & SPEERT, D. P. 2003. Colonial Morphology of Burkholderia cepacia Complex Genomovar III: Implications in Exopolysaccharide Production, Pilus Expression, and Persistence in the Mouse. *Infection and Immunity,* 71**,** 904-909.

CLARKE, T. E., BRAUN, V., WINKELMANN, G., TARI, L. W. & VOGEL, H. J. 2002. X-ray crystallographic structures of the *Escherichia coli* periplasmic protein FhuD bound to hydroxamate-type siderophores and the antibiotic albomycin. *Jounal of Biological Chemistry,* 277**,** 13966-72.

CLEMENTS, J., MCGRATH, C. & MCALLISTER, C. 2018. *Bordetella bronchiseptica* pneumonia: beware of the dog! *BMJ case reports,* 2018.

CLIFTON, M. C., CORRENT, C. & STRONG, R. K. 2009. Siderocalins: siderophore-binding proteins of the innate immune system. *Biometals,* 22**,** 557-564.

COBURN, B., WANG, P. W., CABALLERO, J. D., CLARK, S. T., BRAHMA, V., DONALDSON, S., ZHANG, Y., SURENDRA, A., GONG, Y. & TULLIS, D. E. 2015. Lung microbiota across age and disease stage in cystic fibrosis. *Scientific reports,* 5**,** 1-12.

COENYE, T., MAHENTHIRALINGAM, E., HENRY, D., LIPUMA, J. J., LAEVENS, S., GILLIS, M., SPEERT, D. P. & VANDAMME, P. 2001a. *Burkholderia ambifaria* sp. nov., a novel member of the Burkholderia cepacia complex including biocontrol and cystic fibrosis-related isolates. *International Journal of Systematic and Evolutionary Microbiology,* 51**,** 1481-1490.

COENYE, T., VANCANNEYT, M., CNOCKAERT, M. C., FALSEN, E., SWINGS, J. & VANDAMME, P. 2003. Kerstersia gyiorum gen. nov., sp. nov., a novel *Alcaligenes faecalis*-like organism isolated from human clinical samples, and reclassification of *Alcaligenes denitrificans* Rüger and Tan 1983 as *Achromobacter denitrificans* comb. nov. *International journal of systematic evolutionary microbiology,* 53**,** 1825-1831.

COENYE, T. & VANDAMME, P. 2003. Diversity and significance of *Burkholderia* species occupying diverse ecological niches. *Environmental Microbiology,* 5**,** 719-729.

COENYE, T., VANDAMME, P., GOVAN, J. R. & LIPUMA, J. J. 2001b. Taxonomy and identification of the Burkholderia cepacia complex. *Journal of clinical microbiology,* 39**,** 3427-3436.

COMPANT, S., NOWAK, J., COENYE, T., CLÉMENT, C. & BARKA, E. A. 2008. Diversity and occurrence of Burkholderia spp. in the natural environment. *FEMS Microbiology Reviews,* 32**,** 607-626.

CONWAY, B.-A. D., CHU, K. K., BYLUND, J., ALTMAN, E. & SPEERT, D. P. 2004. Production of exopolysaccharide by *Burkholderia cenocepacia* results in altered cell-surface interactions and altered bacterial clearance in mice. *Journal of Infectious Diseases,* 190**,** 957-966.

COPP, J. & NEILAN, B. 2006. The phosphopantetheinyl transferase superfamily: phylogenetic analysis and functional implications in cyanobacteria. *Applied and environmental microbiology,* 72**,** 2298-2305.

CORNELIS, P., MATTHIJS, S. & VAN OEFFELEN, L. 2009. Iron uptake regulation in *Pseudomonas aeruginosa*. *Biometals,* 22**,** 15-22.

CORNELISSEN, C. N., BISWAS, G. D., TSAI, J., PARUCHURI, D. K., THOMPSON, S. A. & SPARLING, P. F. 1992. Gonococcal transferrin-binding protein 1 is required for transferrin utilization and is homologous to TonB-dependent outer membrane receptors. *Journal of Bacteriology,* 174**,** 5788-5797.

COURTNEY, J., DUNBAR, K., MCDOWELL, A., MOORE, J., WARKE, T., STEVENSON, M. & ELBORN, J. 2004. Clinical outcome of Burkholderia cepacia complex infection in cystic fibrosis adults. *Journal of Cystic Fibrosis,* 3**,** 93-98.

COUTINHO, C., DOS SANTOS, S., MADEIRA, A., MIRA, N., MOREIRA, A. & SÁ-CORREIA, I. 2011. Long-Term Colonization of the Cystic Fibrosis Lung by Burkholderia cepacia Complex Bacteria: Epidemiology, Clonal Variation, and Genome-Wide Expression Alterations. *Frontiers in Cellular and Infection Microbiology,* 1**,** 1-11.

COX, C. D. & GRAHAM, R. 1979. Isolation of an iron-binding compound from *Pseudomonas aeruginosa*. *Journal of Bacteriology,* 137**,** 357-364.

COX, C. D., RINEHART, K. L., MOORE, M. L. & COOK, J. C. 1981. Pyochelin: novel structure of an iron-chelating growth promoter for Pseudomonas aeruginosa. *Proceedings of the National Academy of Sciences,* 78**,** 4256-4260.

COX, G., GIBSON, F., LUKE, R., NEWTON, N., O'BRIEN, I. & ROSENBERG, H. 1970. Mutations affecting iron transport in *Escherichia coli*. *Journal of bacteriology,* 104**,** 219-226.

CRICHTON, R. & BOELAERT, J. R. 2001. *Inorganic biochemistry of iron metabolism: from molecular mechanisms to clinical consequences*, John Wiley & Sons.

CROSA, J. H. & WALSH, C. T. 2002. Genetics and assembly line enzymology of siderophore biosynthesis in bacteria. *Microbiology and Molecular Biology Reviews,* 66**,** 223-249.

CUI, C., YANG, C., SONG, S., FU, S., SUN, X., YANG, L., HE, F., ZHANG, L.-H., ZHANG, Y. & DENG, Y. 2018. A novel two-component system modulates quorum sensing and pathogenicity in *Burkholderia cenocepacia*. *Molecular Microbiology,* 108**,** 32-44.

CUÍV, P. Ó., CLARKE, P., LYNCH, D. & O'CONNELL, M. 2004. Identification of rhtX and fptX, novel genes encoding proteins that show homology and function in the utilization of the siderophores rhizobactin 1021 by *Sinorhizobium meliloti* and pyochelin by *Pseudomonas aeruginosa*, respectively. *Journal of bacteriology,* 186**,** 2996-3005.

CUÍV, P. Ó., CLARKE, P. & O'CONNELL, M. 2006. Identification and characterization of an iron-regulated gene, chtA, required for the utilization of the xenosiderophores aerobactin, rhizobactin 1021 and schizokinen by *Pseudomonas aeruginosa*. *Microbiology,* 152**,** 945-954.

CUÍV, P. Ó., KEOGH, D., CLARKE, P. & O'CONNELL, M. 2007. FoxB of *Pseudomonas aeruginosa* functions in the utilization of the xenosiderophores ferrichrome, ferrioxamine B, and schizokinen: evidence for transport redundancy at the inner membrane. *Journal of bacteriology,* 189**,** 284-287.

CUÍV, P. Ó., KEOGH, D., CLARKE, P. & O'CONNELL, M. 2008. The hmuUV genes of *Sinorhizobium meliloti* 2011 encode the permease and ATPase components of an ABC transport system for the utilization of both haem and the hydroxamate siderophores, ferrichrome and ferrioxamine B. *Molecular Microbiology,* 70**,** 1261-1273.

CULLEN, L., O'CONNOR, A., MCCORMACK, S., OWENS, R. A., HOLT, G. S., COLLINS, C., CALLAGHAN, M., DOYLE, S., SMITH, D., SCHAFFER, K., FITZPATRICK, D. A. & MCCLEAN, S. 2018. The involvement of the low-oxygen-activated locus of *Burkholderia cenocepacia* in adaptation during cystic fibrosis infection. *Scientific Reports,* 8**,** 1-18.

CUNRATH, O., GASSER, V., HOEGY, F., REIMMANN, C., GUILLON, L. & SCHALK, I. J. 2015. A cell biological view of the siderophore pyochelin iron uptake pathway in P*seudomonas aeruginosa*. *Environmental microbiology reports,* 17**,** 171-185.

DARLING, P., CHAN, M., COX, A. D. & SOKOL, P. A. 1998. Siderophore production by cystic fibrosis isolates of *Burkholderia cepacia*. *Infection and Immunity,* 66**,** 874-877.

DE CARVALHO, C. C. C. R. & FERNANDES, P. 2014. Siderophores as "Trojan Horses": tackling multidrug resistance? *Frontiers in Microbiology,* 5**,** 290.

DENG, Z., WANG, Q., LIU, Z., ZHANG, M., MACHADO, A. C. D., CHIU, T.-P., FENG, C., ZHANG, Q., YU, L., QI, L., ZHENG, J., WANG, X., HUO, X., QI, X., LI, X., WU, W., ROHS, R., LI, Y. & CHEN, Z. 2015. Mechanistic insights into metal ion activation and operator recognition by the ferric uptake regulator. *Nature Communications,* 6**,** 1-12.

DHUNGANA, S., WHITE, P. S. & CRUMBLISS, A. L. 2001. Crystal structure of ferrioxamine B: a comparative analysis and implications for molecular recognition. *Journal of Biological Inorganic Chemistry,* 6**,** 810-818.

DIX, S. R., SUN, R., HARRIS, M. J., BATTERS, S. L., SEDELNIKOVA, S. E., BAKER, P. J., THOMAS, M. S. & RICE, D. W. 2018. TssA from *Aeromonas hydrophila*: expression, purification and crystallographic studies. *Acta Crystallographica Section F: Structural Biology Communications,* 74**,** 578-582.

DOBRITSA, A. P. & SAMADPOUR, M. 2016. Transfer of eleven species of the genus *Burkholderia* to the genus *Paraburkholderia* and proposal of *Caballeronia* gen. nov. to accommodate twelve species of the genera *Burkholderia* and *Paraburkholderia*. *International Journal of Systematic and Evolutionary Microbiology,* 66**,** 2836-2846.

DREVINEK, P., HOLDEN, M. T., GE, Z., JONES, A. M., KETCHELL, I., GILL, R. T. & MAHENTHIRALINGAM, E. 2008. Gene expression changes linked to antimicrobial resistance, oxidative stress, iron depletion and retained motility are observed when *Burkholderia cenocepacia* grows in cystic fibrosis sputum. *J BMC Infectious Diseases,* 8**,** 1-16.

DREVINEK, P. & MAHENTHIRALINGAM, E. 2010. *Burkholderia cenocepacia* in cystic fibrosis: epidemiology and molecular mechanisms of virulence. *Clinical Microbiology and Infection,* 16**,** 821-830.

DUNNE, E. F., BURMAN, W. J. & WILSON, M. L. 1998. *Streptomyces pneumonia* in a patient with human immunodeficiency virus infection: case report and review of the literature on invasive Streptomyces infections. *Clinical infectious diseases,* 27**,** 93-96.

DUPONT, L. 2017. Lung transplantation in cystic fibrosis patients with difficult to treat lung infections. *Current opinion in pulmonary medicine,* 23**,** 574-579.

EBERL, L. 2006. Quorum sensing in the genus *Burkholderia*. *International Journal of Medical Microbiology,* 296**,** 103-110.

EDGEWORTH, J. D., MERANTE, D., PATEL, S., YOUNG, C., JONES, P., VITHLANI, S., WYNCOLL, D., ROBERTS, P., JONES, A. & DEN NAGATA, T. 2018. Compassionate use of cefiderocol as adjunctive treatment of native aortic valve endocarditis due to XDR-*Pseudomonas aeruginosa*. *Clinical Infectious Diseases***,** 1349-1356.

ELHASSANNY, A. E., ANDERSON, E. S., MENSCHER, E. A. & ROOP, R. M. 2013. The ferrous iron transporter FtrABCD is required for the virulence of *Brucella abortus* 2308 in mice. *Molecular Microbiology,* 88**,** 1070-1082.

ELLIOTT, G. N., CHEN, W. M., CHOU, J. H., WANG, H. C., SHEU, S. Y., PERIN, L., REIS, V. M., MOULIN, L., SIMON, M. F., BONTEMPS, C., SUTHERLAND, J. M., BESSI, R., DE FARIA, S. M., TRINICK, M. J., PRESCOTT, A. R., SPRENT, J. I. & JAMES, E. K. 2007. B*urkholderia phymatum* is a highly effective nitrogen-fixing symbiont of *Mimosa* spp. and fixes nitrogen ex planta. *New Phytol,* 173**,** 168-80.

ELOMARI, M., COROLER, L., HOSTE, B., GILLIS, M., IZARD, D. & LECLERC, H. 1996. DNA relatedness among *Pseudomonas* strains isolated from natural mineral waters and proposal of *Pseudomonas veronii* sp. nov. *International Journal of Systematic Evolutionary Microbiology,* 46**,** 1138-1144.

EMERY, T. 1971. Role of ferrichrome as a ferric ionophore in *Ustilago sphaerogena*. *Biochemistry,* 10**,** 1483-1488.

ENDICOTT, N. P., LEE, E. & WENCEWICZ, T. A. 2017. Structural Basis for Xenosiderophore Utilization by the Human Pathogen *Staphylococcus aureus*. *ACS Infectious Diseases,* 3**,** 542-553.

ESCOLAR, L., PÉREZ-MARTÍN, J. & DE LORENZO, V. 1999. Opening the Iron Box: Transcriptional Metalloregulation by the Fur Protein. *Journal of Bacteriology,* 181**,** 6223-6229.

ESMAEEL, Q., PUPIN, M., KIEU, N. P., CHATAIGNÉ, G., BÉCHET, M., DERAVEL, J., KRIER, F., HÖFTE, M., JACQUES, P. & LECLÈRE, V. 2016. *Burkholderia* genome mining for nonribosomal peptide synthetases reveals a great potential for novel siderophores and lipopeptides synthesis. *MicrobiologyOpen,* 5**,** 512-526.

EXLEY, C. 2009. Darwin, natural selection and the biological essentiality of aluminium and silicon. *Trends in Biochemical Sciences,* 34**,** 589-593.

FALCES-ROMERO, I., CENDEJAS-BUENO, E., ROMERO-GÓMEZ, M. P. & GARCÍA-RODRÍGUEZ, J. 2018. Isolation of *Rhodotorula mucilaginosa* from blood cultures in a tertiary care hospital. *Mycoses,* 61**,** 35-39.

FARRAND, A. J., RENIERE, M. L., INGMER, H., FREES, D. & SKAAR, E. P. 2013. Regulation of host hemoglobin binding by the *Staphylococcus aureus* Clp proteolytic system. *Journal of bacteriology,* 195**,** 5041-5050.

FARRELL, C., RIDDELL, P., KLEINEROVA, J. & EGAN, J. Post-Transplant Cepacia Syndrome Due to B*urkholderia Contaminans*. B35. LUNG TRANSPLANT AND ILD SCIENTIFIC ABSTRACTS: DRUG INDUCED LUNG DISEASE, AUTOIMMUNE LUNG DISEASE, 2018. American Thoracic Society, A3101.

FATH, M. J. & KOLTER, R. 1993. ABC transporters: bacterial exporters. *Microbiological Reviews,* 57**,** 995-1017.

FAZLI, M., HARRISON, J. J., GAMBINO, M., GIVSKOV, M. & TOLKER-NIELSEN, T. 2015. In-frame and unmarked gene deletions in *Burkholderia cenocepacia* via an allelic exchange system compatible with gateway technology. *Applied environmental microbiology reports,* 81**,** 3623-3630.

FENTON, H. J. H. 1894. LXXIII. - Oxidation of tartaric acid in presence of iron. *Journal of the Chemical Society, Transactions,* 65**,** 899-910.

FERGUSON, A. D., BRAUN, V., FIEDLER, H. P., COULTON, J. W., DIEDERICHS, K. & WELTE, W. 2000. Crystal structure of the antibiotic albomycin in complex with the outer membrane transporter FhuA. *Protein Science,* 9**,** 956-63.

FETHERSTON, J. D., KIRILLINA, O., BOBROV, A. G., PAULLEY, J. T. & PERRY, R. D. 2010. The yersiniabactin transport system is critical for the pathogenesis of bubonic and pneumonic plague. *Infection and Immunity,* 78**,** 2045-2052.

FIEDLER, H.-P. 1981. Preparative-scale high-performance liquid chromatography of ferricrocin, a microbial product. *Journal of Chromatography A,* 209**,** 103-106.

FILLAT, M. F. 2014. The FUR (ferric uptake regulator) superfamily: diversity and versatility of key transcriptional regulators. *Archives of Biochemistry and Biophysics,* 546**,** 41-52.

FISCHBACH, M. A. & WALSH, C. T. 2009. Antibiotics for emerging pathogens. *Science (New York, N.Y.),* 325**,** 1089-1093.

FLANNAGAN, R. S. & VALVANO, M. A. 2008. *Burkholderia cenocepacia* requires RpoE for growth under stress conditions and delay of phagolysosomal fusion in macrophages. *Microbiology,* 154**,** 643-653.

FLYG, C., KENNE, K. & BOMAN, H. G. 1980. Insect pathogenic properties of *Serratia marcescens*: phage-resistant mutants with a decreased resistance to Cecropia immunity and a decreased virulence to Drosophila. *Microbiology,* 120**,** 173-181.

FODOR, A. A., KLEM, E. R., GILPIN, D. F., ELBORN, J. S., BOUCHER, R. C., TUNNEY, M. M. & WOLFGANG, M. C. 2012. The adult cystic fibrosis airway microbiota is stable over time and infection type, and highly resilient to antibiotic treatment of exacerbations. *PloS one,* 7**,** 1-15.

FONTECAVE, M., COVÈS, J. & PIERRE, J.-L. 1994. Ferric reductases or flavin reductases? *Biometals,* 7**,** 3-8.

FOURNIER, P.-E., VALLENET, D., BARBE, V., AUDIC, S., OGATA, H., POIREL, L., RICHET, H., ROBERT, C., MANGENOT, S. & ABERGEL, C. 2006. Comparative genomics of multidrug resistance in *Acinetobacter baumannii*. *PLoS genetics,* 2**,** 62-72.

FRANCIS, J., MADINAVEITIA, J., MACTURK, H. M. & SNOW, G. A. 1949. Isolation from acid-fast bacteria of a growth-factor for *Mycobacterium johnei* and of a precursor of phthiocol [14]. *Nature,* 163**,** 365-366.

FRANKE, J., ISHIDA, K. & HERTWECK, C. 2015. Plasticity of the Malleobactin Pathway and Its Impact on Siderophore Action in Human Pathogenic Bacteria. *Chemistry – A European Journal,* 21**,** 8010-8014.

FRANKE, J., ISHIDA, K., ISHIDA-ITO, M. & HERTWECK, C. 2013. Nitro versus hydroxamate in siderophores of pathogenic bacteria: effect of missing hydroxylamine protection in malleobactin biosynthesis. *Angewandte Chemie International Edition,* 52**,** 8271-8275.

FROST, F., SHAW, M. & NAZARETH, D. 2018. Antibiotic therapy for chronic infection with Burkholderia cepacia complex in people with cystic fibrosis. *Cochrane Database of Systematic Reviews***,** 1-7.

FURRER, J. L., SANDERS, D. N., HOOK-BARNARD, I. G. & MCINTOSH, M. A. 2002. Export of the siderophore enterobactin in *Escherichia coli*: involvement of a 43 kDa membrane exporter. *Molecular microbiology,* 44**,** 1225-1234.

GABALLA, A., KOEDAM, N. & CORNELIS, P. 1996. A cytochrome c biogenesis gene involved in pyoverdine production in *Pseudomonas fluorescens* ATCC 17400. *Molecular Microbiology,* 21**,** 777-785.

GANNE, G., BRILLET, K., BASTA, B., ROCHE, B., HOEGY, F., GASSER, V. & SCHALK, I. J. 2017. Iron Release from the Siderophore Pyoverdine in *Pseudomonas aeruginosa* Involves Three New Actors: FpvC, FpvG, and FpvH. *ACS Chemical Biology,* 12**,** 1056-1065.

GAO, J.-L., KWAN, A. H., YAMMINE, A., ZHOU, X., TREWHELLA, J., HUGRASS, B. M., COLLINS, D. A. T., HORNE, J., YE, P., HARTY, D., NGUYEN, K.-A., GELL, D. A. & HUNTER, N. 2018a. Structural properties of a haemophore facilitate targeted elimination of the pathogen *Porphyromonas gingivalis. Nature Communications,* 9**,** 4097.

GAO, L., GUO, Z., WANG, Y., WANG, Y., WANG, K., LI, B. & SHEN, L. 2018b. The two-operon-coded ABC transporter complex FpvWXYZCDEF is required for *Pseudomonas aeruginosa* growth and virulence under iron-limiting conditions. *The Journal of membrane biology,* 251**,** 91-104.

GARCIA-HERRERO, A., PEACOCK, R. S., HOWARD, S. P. & VOGEL, H. J. 2007. The solution structure of the periplasmic domain of the TonB system ExbD protein reveals an unexpected structural homology with siderophore-binding proteins. *Mol Microbiol,* 66**,** 872-89.

GEHRING, A. M., DEMOLL, E., FETHERSTON, J. D., MORI, I., MAYHEW, G. F., BLATTNER, F. R., WALSH, C. T. & PERRY, R. D. 1998. Iron acquisition in plague: modular logic in enzymatic biogenesis of yersiniabactin by Yersinia pestis. *Chemistry & biology,* 5**,** 573-586.

GELTNER, C., LASS-FLÖRL, C., BONATTI, H., MÜLLER, L. & STELZMÜLLER, I. 2013. Invasive pulmonary mycosis due to *Penicillium chrysogenum*: a new invasive pathogen. *Transplantation,* 95**,** e21-e23.

GERC, A. J., STANLEY-WALL, N. R. & COULTHURST, S. J. 2014. Role of the phosphopantetheinyltransferase enzyme, PswP, in the biosynthesis of antimicrobial secondary metabolites by *Serratia marcescens* Db10. *Microbiology,* 160**,** 1609-1617.

GHOSH, M., LIN, Y.-M., MILLER, P. A., MÖLLMANN, U., BOGGESS, W. C. & MILLER, M. J. 2018. Siderophore Conjugates of Daptomycin are Potent Inhibitors of Carbapenem Resistant Strains of *Acinetobacter baumannii. ACS Infectious Diseases,* 4**,** 1529-1535.

GHOSH, S., DUREJA, C., KHATRI, I., SUBRAMANIAN, S., RAYCHAUDHURI, S. & GHOSH, S. 2017. Identification of novel small RNAs in *Burkholderia cenocepacia* KC-01 expressed under iron limitation and oxidative stress conditions. *Microbiology,* 163**,** 1924-1936.

GHYSELS, B., OCHSNER, U., MÖLLMAN, U., HEINISCH, L., VASIL, M., CORNELIS, P. & MATTHIJS, S. 2005. The *Pseudomonas aeruginosa* pirA gene encodes a second receptor for ferrienterobactin and synthetic catecholate analogues. *FEMS microbiology letters,* 246**,** 167-174.

GI, M., LEE, K.-M., KIM, S. C., YOON, J.-H., YOON, S. S. & CHOI, J. Y. 2015. A novel siderophore system is essential for the growth of *Pseudomonas aeruginosa* in airway mucus. *Scientific Reports,* 5**,** 14644.

GILARDI, G. L. 1972. INfrequently encountered *pseudomonas* species causing infection in humans. *Annals of Internal Medicine,* 77**,** 211-215.

GILLIS, M., VAN VAN, T., BARDIN, R., GOOR, M., HEBBAR, P., WILLEMS, A., SEGERS, P., KERSTERS, K., HEULIN, T. & FERNANDEZ, M. P. 1995. Polyphasic taxonomy in the genus *Burkholderia* leading to an emended description of the genus and proposition of *Burkholderia vietnamiensis* sp. nov. for N2-fixing isolates from rice in Vietnam. *International Journal of Systematic Evolutionary Microbiology,* 45**,** 274-289.

GOLD, B., RODRIGUEZ, G. M., MARRAS, S. A., PENTECOST, M. & SMITH, I. 2001. The Mycobacterium tuberculosis IdeR is a dual functional regulator that controls transcription of genes involved in iron acquisition, iron storage and survival in macrophages. *Molecular microbiology,* 42**,** 851-865.

GONZALEZ, M. R., DUCRET, V., LEONI, S. & PERRON, K. 2018. *Pseudomonas aeruginosa* zinc homeostasis: Key issues for an opportunistic pathogen. *Biochimica et Biophysica Acta (BBA) - Gene Regulatory Mechanisms***,** 1-12.

GÓRSKA, A., SLODERBACH, A. & MARSZAŁŁ, M. P. 2014. Siderophore–drug complexes: potential medicinal applications of the 'Trojan horse' strategy. *Trends in Pharmacological Sciences,* 35**,** 442-449.

GOYAL, T. & ANISHETTY, S. An in silico study on molecular level interactions of host Siderocalin with siderophores from *Mycobacterium tuberculosis* and other bacterial species. BMC Infectious Diseases, 05/27 2014. BioMed Central, O15.

GRASS, G. 2006. Iron Transport in *Escherichia Coli*: All has not been said and Done. *Biometals,* 19**,** 159-172.

GRIGG, J. C., VERMEIREN, C. L., HEINRICHS, D. E. & MURPHY, M. E. 2007. Haem recognition by a *Staphylococcus aureus* NEAT domain. *Molecular microbiology,* 63**,** 139-149.

GROßE, C., SCHERER, J., KOCH, D., OTTO, M., TAUDTE, N. & GRASS, G. 2006. A new ferrous iron-uptake transporter, EfeU (YcdN), from *Escherichia coli*. *Molecular Microbiology,* 62**,** 120-131.

GUERINOT, M. L. 1994. Microbial iron transport. *Annual Review of Microbiology,* 48**,** 743-72.

HAAS, H. 2014. Fungal siderophore metabolism with a focus on *Aspergillus fumigatus*. *Natural product reports,* 31**,** 1266-1276.

HAJIGHOLAMI, A., ANSARI, H. & HONARMAND, S. 2018. Comparing the efficacy of Dexeroyx (Osveral) and Deferoxamine (Desferal) in reducing serum ferritin level in patients with thalassemia major. *Middle East Journal of Family Medicine,* 7**,** 218-222.

HANAHAN, D., JESSEE, J. & BLOOM, F. 1995. Techniques for transformation of *E. coli*. *DNA cloning,* 1**,** 1-36.

HANNAUER, M., BARDA, Y., MISLIN, G. L., SHANZER, A. & SCHALK, I. J. 2010a. The ferrichrome uptake pathway in *Pseudomonas aeruginosa* involves an iron release mechanism with acylation of the siderophore and recycling of the modified desferrichrome. *Journal of Bacteriology,* 192**,** 1212-1220.

HANNAUER, M., YETERIAN, E., MARTIN, L. W., LAMONT, I. L. & SCHALK, I. J. 2010b. An efflux pump is involved in secretion of newly synthesized siderophore by *Pseudomonas aeruginosa*. *FEBS letters,* 584**,** 4751-4755.

HANSON, M. S., PELZEL, S. E., LATIMER, J., MULLER-EBERHARD, U. & HANSEN, E. J. 1992. Identification of a genetic locus of *Haemophilus influenzae* type b necessary for the binding and utilization of heme bound to human hemopexin. *Proceedings of the National Academy of Sciences,* 89**,** 1973-1977.

HANTKE, K. 1983. Identification of an iron uptake system specific for coprogen and rhodotorulic acid in *Escherichia coli* K12. *Molecular General Genetics,* 191**,** 301-306.

HANTKE, K. 1990. Dihydroxybenzoylserine-a siderophore for E. coli. *FEMS Microbiology Letters,* 55.

HANTKE, K., NICHOLSON, G., RABSCH, W. & WINKELMANN, G. 2003. Salmochelins, siderophores of *Salmonella enterica* and uropathogenic *Escherichia coli* strains, are recognized by the outer membrane receptor IroN. *Proceedings of the National Academy of Sciences,* 100**,** 3677-3682.

HARAGA, A., WEST, T. E., BRITTNACHER, M. J., SKERRETT, S. J. & MILLER, S. I. 2008. *Burkholderia thailandensis* as a model system for the study of the virulence-associated type III secretion system of *Burkholderia pseudomallei*. *Infection immunity,* 76**,** 5402-5411.

HARRIS, W. R., CARRANO, C. J., COOPER, S. R., SOFEN, S. R., AVDEEF, A. E., MCARDLE, J. V. & RAYMOND, K. N. 1979. Coordination chemistry of microbial iron transport compounds. 19. Stability constants and electrochemical behavior of ferric enterobactin and model complexes. *Journal of the American Chemical Society,* 101**,** 6097-6104.

HARTMANN, A., FIEDLER, H. P. & BRAUN, V. 1979. Uptake and Conversion of the Antibiotic Albomycin by *Escherichia coli* K-12. *European journal of biochemistry,* 99**,** 517-524.

HARTNEY, S. L., MAZURIER, S., KIDARSA, T. A., QUECINE, M. C., LEMANCEAU, P. & LOPER, J. E. 2011. TonB-dependent outer-membrane proteins and siderophore utilization in *Pseudomonas fluorescens* Pf-5. *BioMetals,* 24**,** 193-213.

HENDERSON, R. K., FENDLER, K. & POOLMAN, B. 2019. Coupling efficiency of secondary active transporters. *Current Opinion in Biotechnology,* 58**,** 62-71.

HEO, J. & HUA, S. Z. 2009. An overview of recent strategies in pathogen sensing. *Sensors (Basel),* 9**,** 4483-4502.

HERRERO, M., DE LORENZO, V. & TIMMIS, K. N. 1990. Transposon vectors containing non-antibiotic resistance selection markers for cloning and stable chromosomal insertion of foreign genes in gram-negative bacteria. *Journal of bacteriology,* 172**,** 6557-6567.

HEYMANN, P., ERNST, J. & WINKELMANN, G. 1999. Identification of a fungal triacetylfusarinine C siderophore transport gene (TAF1) in *Saccharomyces cerevisiae* as a member of the major facilitator superfamily. *Biometals,* 12**,** 301-306.

HEYMANN, P., ERNST, J. F. & WINKELMANN, G. 2000. Identification and substrate specificity of a ferrichrome-type siderophore transporter (Arn1p) in *Saccharomyces cerevisiae*. *FEMS microbiology letters,* 186**,** 221-227.

HIDER, R. C. & KONG, X. 2010. Chemistry and biology of siderophores. *Natural Product Reports,* 27**,** 637-657.

HIDER, R. C. & KONG, X. L. 2011. Glutathione: a key component of the cytoplasmic labile iron pool. *Biometals,* 24**,** 1179-1187.

HIGGINS, S., SANCHEZ-CONTRERAS, M., GUALDI, S., PINTO-CARBÓ, M., CARLIER, A. & EBERL, L. 2017. The essential genome of *Burkholderia cenocepacia* H111. *Journal of bacteriology,* 199**,** 1-14.

HOARE, R., HARRISON, P. & HOY, T. 1975. Structure of horse-spleen apoferritin at 6 Å resolution. *Nature*.

HOLDEN, M. T., SETH-SMITH, H. M., CROSSMAN, L. C., SEBAIHIA, M., BENTLEY, S. D., CERDENO-TARRAGA, A. M., THOMSON, N. R., BASON, N., QUAIL, M. A., SHARP, S., CHEREVACH, I., CHURCHER, C., GOODHEAD, I., HAUSER, H., HOLROYD, N., MUNGALL, K., SCOTT, P., WALKER, D., WHITE, B., ROSE, H., IVERSEN, P., MIL-HOMENS, D., ROCHA, E. P., FIALHO, A. M., BALDWIN, A., DOWSON, C., BARRELL, B. G., GOVAN, J. R., VANDAMME, P., HART, C. A., MAHENTHIRALINGAM, E. & PARKHILL, J. 2009. The genome of *Burkholderia cenocepacia* J2315, an epidemic pathogen of cystic fibrosis patients. *J Bacteriology,* 191**,** 261-77.

HOLLENSTEIN, K., DAWSON, R. J. & LOCHER, K. P. 2007. Structure and mechanism of ABC transporter proteins. *Current opinion in structural biology,* 17**,** 412-418.

HONSA, E. S., FABIAN, M., CARDENAS, A. M., OLSON, J. S. & MARESSO, A. W. 2011. The five near-iron transporter (NEAT) domain anthrax hemophore, IsdX2, scavenges heme from hemoglobin and transfers heme to the surface protein IsdC. *Journal of Biological Chemistry,* 286**,** 33652-33660.

HOSSAIN, M., ENG-WILMOT, D., LOGHRY, R. & VAN DER HELM, D. 1980. Circular dichroism, crystal structure, and absolute configuration of the siderophore ferric N, N', N"-triacetylfusarinine, FeC39H57N6O15. *Journal of the American Chemical Society,* 102**,** 5766-5773.

HOU, Z., SUNDERLAND, C. J., NISHIO, T. & RAYMOND, K. N. 1996. Preorganization of Ferric Alcaligin, Fe2L3. The First Structure of a Ferric Dihydroxamate Siderophore. *Journal of the American Chemical Society,* 118**,** 5148-5149.

HU, X. & BOYER, G. L. 1996. Siderophore-Mediated Aluminum Uptake by *Bacillus megaterium* ATCC 19213. *Applied and Environmental Microbiology,* 62**,** 4044-4048.

HUANG, B., RU, K., YUAN, Z., WHITCHURCH, C. B. & MATTICK, J. S. 2004. tonB3 is required for normal twitching motility and extracellular assembly of type IV pili. *Journal of bacteriology,* 186**,** 4387-4389.

HUANG, Y. J. & LIPUMA, J. J. 2016. The microbiome in cystic fibrosis. *Clinics in chest medicine,* 37**,** 59-67.

HUBER, B., RIEDEL, K., HENTZER, M., HEYDORN, A., GOTSCHLICH, A., GIVSKOV, M., MOLIN, S. & EBERL, L. 2001. The cep quorum-sensing system of Burkholderia cepacia H111 controls biofilm formation and swarming motility. *Microbiology,* 147**,** 2517-2528.

HUNTER, R. C., ASFOUR, F., DINGEMANS, J., OSUNA, B. L., SAMAD, T., MALFROOT, A., CORNELIS, P. & NEWMAN, D. K. 2013. Ferrous Iron Is a Significant Component of Bioavailable Iron in Cystic Fibrosis Airways. *mBio,* 4**,** 1-8.

IMBERT, M., BÉCHET, M. & BLONDEAU, R. 1995. Comparison of the main siderophores produced by some species of *Streptomyces*. *Current Microbiology,* 31**,** 129-133.

ITO, A., SATO, T., OTA, M., TAKEMURA, M., NISHIKAWA, T., TOBA, S., KOHIRA, N., MIYAGAWA, S., ISHIBASHI, N., MATSUMOTO, S., NAKAMURA, R., TSUJI, M. & YAMANO, Y. 2018. In Vitro Antibacterial Properties of Cefiderocol, a Novel Siderophore Cephalosporin, against Gram-Negative Bacteria. *Antimicrobial Agents and Chemotherapy,* 62**,** 1-11.

IZADI-PRUNEYRE, N., HUCHÉ, F., LUKAT-RODGERS, G. S., LECROISEY, A., GILLI, R., RODGERS, K. R., WANDERSMAN, C. & DELEPELAIRE, P. 2006. The heme transfer from the soluble HasA hemophore to its membrane-bound receptor HasR is driven by protein-protein interaction from a high to a lower affinity binding site. *Journal of Biological Chemistry,* 281**,** 25541-25550.

JANAKIRAMAN, A. & SLAUCH, J. M. 2000. The putative iron transport system SitABCD encoded on SPI1 is required for full virulence of *Salmonella typhimurium*. *Molecular Microbiology,* 35**,** 1146-1155.

JENUL, C., SIEBER, S., DAEPPEN, C., MATHEW, A., LARDI, M., PESSI, G., HOEPFNER, D., NEUBURGER, M., LINDEN, A., GADEMANN, K. & EBERL, L. 2018. Biosynthesis of fragin is controlled by a novel quorum sensing signal. *Nature Communications,* 9**,** 1-13.

JOHNSTONE, T. C. & NOLAN, E. M. 2015. Beyond iron: non-classical biological functions of bacterial siderophores. *Dalton Transactions,* 44**,** 6320-6339.

JONES, A. M., DODD, M. E., GOVAN, J. R., BARCUS, V., DOHERTY, C. J., MORRIS, J. & WEBB, A. K. 2004. *Burkholderia cenocepacia* and *Burkholderia multivorans*: influence on survival in cystic fibrosis. *Journal of Thorax,* 59**,** 945-951.

JONES, P., BINNS, D., CHANG, H.-Y., FRASER, M., LI, W., MCANULLA, C., MCWILLIAM, H., MASLEN, J., MITCHELL, A. & NUKA, G. 2014. InterProScan 5: genome-scale protein function classification. *Bioinformatics,* 30**,** 1236-1240.

KAHLKE, T., GOESMANN, A., HJERDE, E., WILLASSEN, N. & HAUGEN, P. 2012. Unique core genomes of the bacterial family vibrionaceae: insights into niche adaptation and speciation. *BMC Genomics,* 13.

KAI, M., EFFMERT, U., BERG, G. & PIECHULLA, B. 2007. Volatiles of bacterial antagonists inhibit mycelial growth of the plant pathogen Rhizoctonia solani. *Archives of microbiology,* 187**,** 351-360.

KAMMLER, M., SCHÖN, C. & HANTKE, K. 1993. Characterization of the ferrous iron uptake system of *Escherichia coli*. *Journal of Bacteriology,* 175**,** 6212-6219.

KAMPFENKEL, K. & BRAUN, V. 1992. Membrane topology of the *Escherichia coli* ExbD protein. *Journal of Bacteriology,* 174**,** 5485-5487.

KAMPFENKEL, K. & BRAUN, V. 1993. Topology of the ExbB protein in the cytoplasmic membrane of *Escherichia coli*. *Journal of Biological Chemistry,* 268**,** 6050-6057.

KANG, H. Y., BRICKMAN, T. J., BEAUMONT, F. C. & ARMSTRONG, S. K. 1996. Identification and characterization of iron-regulated *Bordetella pertussis* alcaligin siderophore biosynthesis genes. *Journal of Bacteriology,* 178**,** 4877-4884.

KAPNADAK, S. G., HISERT, K. B., POTTINGER, P. S., LIMAYE, A. P. & AITKEN, M. L. 2016. Infection control strategies that successfully controlled an outbreak of Mycobacterium abscessus at a cystic fibrosis center. *American journal of infection control,* 44**,** 154-159.

KARUPIAH, G., HUNT, N., KING, N. & CHAUDHRI, G. 2000. NADPH oxidase, Nramp1 and nitric oxide synthase 2 in the host antimicrobial response. *Reviews in immunogenetics,* 2**,** 387-415.

KASTING, J. F. 1993. Earth's early atmosphere. *Science,* 259**,** 920-926.

KHALIL, E. A., SEGOND, D., TERPSTRA, T., ANDRÉ-LEROUX, G., KALLASSY, M., LERECLUS, D., BOU-ABDALLAH, F. & LE ROUX, C. N. 2015. Heme interplay between IlsA and IsdC, two structurally different surface proteins from *Bacillus cereus*. *Biochimica et Biophysica Acta (BBA)-General Subjects***,** 1930-1941.

KHAN, S. R., GAINES, J., ROOP, R. M. & FARRAND, S. K. 2008. Broad-Host-Range Expression Vectors with Tightly Regulated Promoters and Their Use To Examine the Influence of TraR and TraM Expression on Ti Plasmid Quorum Sensing. *Applied and Environmental Microbiology,* 74**,** 5053-5062.

KIEU, N. P., AZNAR, A., SEGOND, D., RIGAULT, M., SIMOND-CÔTE, E., KUNZ, C., SOULIE, M. C., EXPERT, D. & DELLAGI, A. 2012. Iron deficiency affects plant defence responses and confers resistance to *Dickeya dadantii* and *Botrytis cinerea*. *Molecular plant pathology,* 13**,** 816-827.

KLUMPP, C., BURGER, A., MISLIN, G. L. & ABDALLAH, M. A. 2005. From a total synthesis of cepabactin and its 3: 1 ferric complex to the isolation of a 1: 1: 1 mixed complex between iron (III), cepabactin and pyochelin. *Bioorganic & Medicinal Chemistry Letters,* 15**,** 1721-1724.

KOBAYASHI, S. D., VOYICH, J. M., BRAUGHTON, K. R., WHITNEY, A. R., NAUSEEF, W. M., MALECH, H. L. & DELEO, F. R. 2004. Gene expression profiling provides insight into the pathophysiology of chronic granulomatous disease. *The Journal of Immunology,* 172**,** 636-643.

KÖHLER, S. D., WEBER, A., HOWARD, S. P., WELTE, W. & DRESCHER, M. 2010. The proline-rich domain of TonB possesses an extended polyproline II-like conformation of sufficient length to span the periplasm of Gram-negative bacteria. *Protein Science : A Publication of the Protein Society,* 19**,** 625-630.

KONINGS, A. F., MARTIN, L. W., SHARPLES, K. J., RODDAM, L. F., LATHAM, R., REID, D. W. & LAMONT, I. L. 2013. *Pseudomonas aeruginosa* uses multiple pathways to acquire iron during chronic infection in cystic fibrosis lungs. *Infection and Immunity***,** 2697-2704.

KOOI, C., CORBETT, C. & SOKOL, P. 2005. Functional analysis of the *Burkholderia cenocepacia* ZmpA metalloprotease. *Journal of bacteriology,* 187**,** 4421-4429.

KOOI, C. & SOKOL, P. A. 2009. *Burkholderia cenocepacia* zinc metalloproteases influence resistance to antimicrobial peptides. *Microbiology,* 155**,** 2818-2825.

KOOI, C., SUBSIN, B., CHEN, R., POHORELIC, B. & SOKOL, P. A. 2006. *Burkholderia cenocepacia* ZmpB is a broad-specificity zinc metalloprotease involved in virulence. *Infect Immunology,* 74**,** 4083-4093.

KORKHOV, V. M., MIREKU, S. A. & LOCHER, K. P. 2012. Structure of AMP-PNP-bound vitamin B12 transporter BtuCD–F. *Nature,* 490**,** 367.

KOTHAMASI, D. & KOTHAMASI, S. 2004. Cobalt interference in iron-uptake could inhibit growth in *Pseudomonas aeruginosa*. *World Journal of Microbiology and Biotechnology,* 20**,** 755-758.

KREWULAK, K. D. & VOGEL, H. J. 2011. TonB or not TonB: is that the question? . *Biochemistry and Cell Biology,* 89**,** 87-97.

KUMAR, A., RAY, P., KANWAR, M., SETHI, S. & NARANG, A. 2006. Investigation of hospital-acquired infections due to *Achromobacter xylosoxidans* in a tertiary care hospital in India. *Journal of Hospital Infection,* 62**,** 248-250.

KÜMMERLI, R., JIRICNY, N., CLARKE, L., WEST, S. & GRIFFIN, A. 2009. Phenotypic plasticity of a cooperative behaviour in bacteria. *Journal of evolutionary biology,* 22**,** 589-598.

KUSTUSCH, R. J., KUEHL, C. J. & CROSA, J. H. 2012. The ttpC gene is contained in two of three TonB systems in the human pathogen Vibrio vulnificus, but only one is active in iron transport and virulence. *Journal of bacteriology,* 194**,** 3250-3259.

KVITKO, B. H., GOODYEAR, A., PROPST, K. L., DOW, S. W. & SCHWEIZER, H. P. 2012. *Burkholderia pseudomallei* known siderophores and hemin uptake are dispensable for lethal murine melioidosis. *PLoS neglected tropical diseases,* 6**,** 1-13.

LAMBERT, L. A. 2012. Molecular evolution of the transferrin family and associated receptors. *Biochimica et Biophysica Acta (BBA) - General Subjects,* 1820**,** 244-255.

LAMBERTI, Y., GORGOJO, J., MASSILLO, C., RODRIGUEZ, M. E. & DISEASE 2013. *Bordetella pertussis* entry into respiratory epithelial cells and intracellular survival. *Pathogens and Disease,* 69**,** 194-204.

LARDI, M., AGUILAR, C., PEDRIOLI, A., OMASITS, U., SUPPIGER, A., CÁRCAMO-OYARCE, G., SCHMID, N., AHRENS, C. H., EBERL, L. & PESSI, G. 2015. σ54-Dependent Response to Nitrogen Limitation and Virulence in *Burkholderia cenocepacia* Strain H111. *Applied and Environmental Microbiology,* 81**,** 4077-4089.

LARSON, J. A., HOWIE, H. L. & SO, M. 2004. *Neisseria meningitidis* accelerates ferritin degradation in host epithelial cells to yield an essential iron source. *Molecular Microbiology,* 53**,** 807-820.

LATORRE, M., QUENTI, D., TRAVISANY, D., SINGH, K. V., MURRAY, B. E., MAASS, A. & CAMBIAZO, V. 2018. The Role of Fur in the Transcriptional and Iron Homeostatic Response of *Enterococcus faecalis*. *Frontiers in microbiology,* 9**,** 1580-1580.

LEHNER, S. M., ATANASOVA, L., NEUMANN, N. K. N., KRSKA, R., LEMMENS, M., DRUZHININA, I. S. & SCHUHMACHER, R. 2013. Isotope-assisted screening for iron-containing metabolites reveals a high degree of diversity among known and unknown siderophores produced by *Trichoderma* spp. *Applied and Environmental Microbiology,* 79**,** 18-31.

LEINWEBER, A., WEIGERT, M. & KÜMMERLI, R. 2018. The bacterium *Pseudomonas aeruginosa* senses and gradually responds to inter-specific competition for iron. *Evolution***,** 1515-1528.

LEITÃO, J. H., FELICIANO, J. R., SOUSA, S. A., PITA, T. & GUERREIRO, S. I. 2017. Burkholderia cepacia Complex Infections Among Cystic Fibrosis Patients: Perspectives and Challenges. *Progress in Understanding Cystic Fibrosis.* InTech.

LÉTOFFÉ, S., GHIGO, J. M. & WANDERSMAN, C. 1994. Secretion of the *Serratia marcescens* HasA protein by an ABC transporter. *Journal of Bacteriology,* 176**,** 5372-5377.

LEWENZA, S., CONWAY, B., GREENBERG, E. & SOKOL, P. A. 1999. Quorum sensing in *Burkholderia cepacia*: identification of the LuxRI homologs CepRI. *Journal of Bacteriology,* 181**,** 748-756.

LHOSPICE, S., GOMEZ, N. O., OUERDANE, L., BRUTESCO, C., GHSSEIN, G., HAJJAR, C., LIRATNI, A., WANG, S., RICHAUD, P., BLEVES, S., BALL, G., BOREZEE-DURANT, E., LOBINSKI, R., PIGNOL, D., ARNOUX, P. & VOULHOUX, R. 2017. *Pseudomonas aeruginosa* zinc uptake in chelating environment is primarily mediated by the metallophore pseudopaline. *Sci Rep,* 7**,** 1-10.

LI, Y. & MA, Q. 2017. Iron Acquisition Strategies of *Vibrio anguillarum*. *Frontiers in cellular infection microbiology,* 7**,** 1-11.

LIMMATHUROTSAKUL, D., GOLDING, N., DANCE, D. A., MESSINA, J. P., PIGOTT, D. M., MOYES, C. L., ROLIM, D. B., BERTHERAT, E., DAY, N. P. & PEACOCK, S. J. 2016. Predicted global distribution of *Burkholderia pseudomallei* and burden of melioidosis. *Nature microbiology,* 1**,** 1-5.

LIN, H., FISCHBACH, M. A., LIU, D. R. & WALSH, C. T. 2005. In vitro characterization of salmochelin and enterobactin trilactone hydrolases IroD, IroE, and Fes. *Journal of the American Chemical Society,* 127**,** 11075-11084.

LIPUMA, J. J. 2005. Update on the Burkholderia cepacia complex. *Current Opinion in Pulmonary Medicine,* 11**,** 528-533.

LIPUMA, J. J. 2010. The changing microbial epidemiology in cystic fibrosis. *Clinical microbiology reviews,* 23**,** 299-323.

LIU, H., IBRAHIM, M., QIU, H., KAUSAR, S., ILYAS, M., CUI, Z., HUSSAIN, A., LI, B., WAHEED, A., ZHU, B. & XIE, G. 2015. Protein profiling analyses of the outer membrane of *Burkholderia cenocepacia* reveal a niche-specific proteome. *Microbial Ecology,* 69**,** 75-83.

LLAMAS, M. A., SPARRIUS, M., KLOET, R., JIMÉNEZ, C. R., VANDENBROUCKE-GRAULS, C. & BITTER, W. 2006. The heterologous siderophores ferrioxamine B and ferrichrome activate signaling pathways in *Pseudomonas aeruginosa. Journal of bacteriology,* 188**,** 1882-1891.

LOCHER, K. P., LEE, A. T. & REES, D. C. 2002. The E. coli BtuCD structure: a framework for ABC transporter architecture and mechanism. *Science,* 296**,** 1091-1098.

LOCHER, K. P., REES, B., KOEBNIK, R., MITSCHLER, A., MOULINIER, L., ROSENBUSCH, J. P. & MORAS, D. 1998. Transmembrane signaling across the ligated-gated FhuA receptor: crystal structures of free and ferrichrome-bound states reveal allosteric changes. *Cell,* 95**,** 771-778.

LOOMIS, L. D. & RAYMOND, K. N. 1991. Solution equilibria of enterobactin and metal-enterobactin complexes. *Inorganic Chemistry,* 30**,** 906-911.

LOUTET, S. A., FLANNAGAN, R. S., KOOI, C., SOKOL, P. A. & VALVANO, M. A. 2006. A complete lipopolysaccharide inner core oligosaccharide is required for resistance of *Burkholderia cenocepacia* to antimicrobial peptides and bacterial survival in vivo. *Journal of bacteriology,* 188**,** 2073-2080.

LOUTET, S. A. & VALVANO, M. A. 2010. A Decade of *Burkholderia cenocepacia* Virulence Determinant Research. 78**,** 4088-4100.

LOWE, C. A., ASGHAR, A. H., SHALOM, G., SHAW, J. G. & THOMAS, M. S. 2001. The Burkholderia cepacia *fur* gene: co-localization with omlA and absence of regulation by iron. *Microbiology,* 147**,** 1303-1314.

LUGTENBERG, B. & VAN ALPHEN, L. 1983. Molecular architecture and functioning of the outer membrane of *Escherichia coli* and other gram-negative bacteria. *Biochimica et Biophysica Acta (BBA)-Reviews on Biomembranes,* 737**,** 51-115.

LUIS, B. A. L., GUERRERO ALMEIDA, M. D. L. & RUIZ-PALACIOS, G. M. 2018. A place for *Bordetella pertussis* in PCR-based diagnosis of community-acquired pneumonia. *Infectious Diseases,* 50**,** 232-235.

LUNDRIGAN, M. & KADNER, R. 1986. Nucleotide sequence of the gene for the ferrienterochelin receptor FepA in *Escherichia coli*. Homology among outer membrane receptors that interact with TonB. *Journal of Biological Chemistry,* 261**,** 10797-10801.

LUPTÁKOVÁ, D., PLUHÁČEK, T., PETŘÍK, M., NOVÁK, J., PALYZOVÁ, A., SOKOLOVÁ, L., ŠKRÍBA, A., ŠEDIVÁ, B., LEMR, K. & HAVLÍČEK, V. 2017. Non-invasive and invasive diagnoses of aspergillosis in a rat model by mass spectrometry. *Journal of Scientific reports,* 7**,** 1-10.

LUSCHER, A., MOYNIÉ, L., SAINT AUGUSTE, P., BUMANN, D., MAZZA, L., PLETZER, D., NAISMITH, J. H. & KÖHLER, T. 2018. The TonB-receptor repertoire of *Pseudomonas aeruginosa* for the uptake of siderophore-drug conjugates. *Antimicrobial Agents and Chemotherapy***,** 1-11.

LUTTER, E., LEWENZA, S., DENNIS, J., VISSER, M. & SOKOL, P. 2001. Distribution of quorum-sensing genes in the Burkholderia cepacia complex. *Infection immunity,* 69**,** 4661-4666.

MACHUCA, A. & MILAGRES, A. M. 2003. Use of CAS-agar plate modified to study the effect of different variables on the siderophore production by Aspergillus. *Letter of Applied Microbiology,* 36**,** 177-181.

MADEMIDIS, A. & KÖSTER, W. 1998. Transport activity of FhuA, FhuC, FhuD, and FhuB derivatives in a system free of polar effects, and stoichiometry of components involved in ferrichrome uptake. *Molecular and General Genetics MGG,* 258**,** 156-165.

MAHENTHIRALINGAM, E., COENYE, T., CHUNG, J. W., SPEERT, D. P., GOVAN, J. R., TAYLOR, P. & VANDAMME, P. 2000. Diagnostically and experimentally useful panel of strains from the Burkholderia cepacia complex. *Journal of clinical microbiology,* 38**,** 910-913.

MAKI-YONEKURA, S., MATSUOKA, R., YAMASHITA, Y., SHIMIZU, H., TANAKA, M., IWABUKI, F. & YONEKURA, K. 2018. Hexameric and pentameric complexes of the ExbBD energizer in the Ton system. *eLife,* 7**,** 1-24.

MARAHIEL, M. & ESSEN, L. O. 2009. Nonribosomal peptide synthetases: mechanistic and structural aspects of essential domains. *Methods in enzymology,* 458**,** 337-351.

MARAHIEL, M. A. 2016. A structural model for multimodular NRPS assembly lines. *Natural Product Reports,* 33**,** 136-140.

MARCIANO, B. E., SPALDING, C., FITZGERALD, A., MANN, D., BROWN, T., OSGOOD, S., YOCKEY, L., DARNELL, D. N., BARNHART, L. & DAUB, J. 2014. Common severe infections in chronic granulomatous disease. *Clinical Infectious Diseases,* 60**,** 1176-1183.

MARINUS, M. G. 1973. Location of DNA methylation genes on the *Escherichia coli* K-12 genetic map. *Molecular and General Genetics* 127**,** 47-55.

MARK, M., MIRJAM, K., GLENDA, H., ALLEN, C. C., LINDA, W., DANUTA, K., PETER, J., DANIEL, G., BRIAN, G. S. & BART, J. C. 2011. *Burkholderia pseudomallei* in unchlorinated domestic bore water, Tropical Northern Australia. *Emerging Infectious Disease Journal,* 17**,** 1283-1285.

MARTINA, P., LEGUIZAMON, M., PRIETO, C. I., SOUSA, S. A., MONTANARO, P., DRAGHI, W. O., STÄMMLER, M., BETTIOL, M., DE CARVALHO, C. C. C. R., PALAU, J., FIGOLI, C., ALVAREZ, F., BENETTI, S., LEJONA, S., VESCINA, C., FERRERAS, J., LASCH, P., LAGARES, A., ZORREGUIETA, A., LEITÃO, J. H., YANTORNO, O. M. & BOSCH, A. 2018. Burkholderia puraquae sp. nov., a novel species of the Burkholderia cepacia complex isolated from hospital settings and agricultural soils. *International Journal of Systematic and Evolutionary Microbiology,* 68**,** 14-20.

MARVIG, R. L., DAMKIÆR, S., KHADEMI, S. H., MARKUSSEN, T. M., MOLIN, S. & JELSBAK, L. 2014. Within-host evolution of *Pseudomonas aeruginosa* reveals adaptation toward iron acquisition from hemoglobin. *MBio,* 5**,** 1-8.

MASTROPASQUA, M. C., D'ORAZIO, M., CERASI, M., PACELLO, F., GISMONDI, A., CANINI, A., CANUTI, L., CONSALVO, A., CIAVARDELLI, D. & CHIRULLO, B. 2017. Growth of *Pseudomonas aeruginosa* in zinc poor environments is promoted by a nicotianamine-related metallophore. *Molecular microbiology,* 106**,** 543-561.

MATHEW, A., EBERL, L. & CARLIER, A. L. 2014. A novel siderophore-independent strategy of iron uptake in the genus Burkholderia. *Molecular Microbiology,* 91**,** 805-820.

MATTO, S. & CHERRY, J. 2005. Molecular pathogenesis, epidemiology, and clinical manifestations of respiratory infections due to *Bordetella pertussis* and other *Bordetella* subspecies. *Clin Microbiol Rev,* 18**,** 326-382.

MATZANKE, B. F., ANEMÜLLER, S., SCHÜNEMANN, V., TRAUTWEIN, A. X. & HANTKE, K. 2004. FhuF, Part of a Siderophore−Reductase System. *Biochemistry,* 43**,** 1386-1392.

MATZANKE, B. F., BILL, E., TRAUTWEIN, A. X. & WINKELMANN, G. 1988. Ferricrocin functions as the main intracellular iron-storage compound in mycelia of *Neurospora crassa*. *Biology of metals,* 1**,** 18-25.

MATZANKE, B. F., BÖHNKE, R., MÖLLMANN, U., REISSBRODT, R., SCHÜNEMANN, V. & TRAUTWEIN, A. X. 1997. Iron uptake and intracellular metal transfer in mycobacteria mediated by xenosiderophores. *BioMetals,* 10**,** 193-203.

MATZANKE, B. F., BÖHNKE, R., MÖLLMANN, U., SCHÜNEMANN, V., SCHUMANN, G., TRAUTWEIN, A. X. & WINKELMANN, G. 1999. Transport and utilization of rhizoferrin bound iron in *Mycobacterium smegmatis*. *BioMetals,* 12**,** 315-321.

MAY, J. J., WENDRICH, T. M. & MARAHIEL, M. A. 2000. The dhb operon of *Bacillus subtilis* encodes the biosynthetic template for the catecholic siderophore 2, 3-dihydroxybenzoate-glycine-threonine trimeric ester bacillibactin. *Journal of Biological Chemistry***,** 7209-7217.

MCCARRON, A., DONNELLEY, M. & PARSONS, D. 2018. Airway disease phenotypes in animal models of cystic fibrosis. *Respiratory Research,* 19**,** 1-12.

MCCLEAN, S. & CALLAGHAN, M. 2009. Burkholderia cepacia complex: epithelial cell–pathogen confrontations and potential for therapeutic intervention. *Journal of Medical Microbiology,* 58**,** 1-12.

MCDOUGALL, S. & NEILANDS, J. B. 1984. Plasmid- and chromosome-coded aerobactin synthesis in enteric bacteria: insertion sequences flank operon in plasmid-mediated systems. *Journal of Bacteriology,* 159**,** 300-305.

MCINTOSH, M. A. & EARHART, C. F. 1977. Coordinate regulation by iron of the synthesis of phenolate compounds and three outer membrane proteins in *Escherichia coli*. *Journal of Bacteriology,* 131**,** 331-339.

MCLEAN, S., BOWMAN, L. A. H., SANGUINETTI, G., READ, R. C. & POOLE, R. K. 2010. Peroxynitrite Toxicity in *Escherichia coli* K12 Elicits Expression of Oxidative Stress Responses and Protein Nitration and Nitrosylation. *The Journal of Biological Chemistry,* 285**,** 20724-20731.

MCNEIL, M. M. & BROWN, J. M. 1994. The medically important aerobic actinomycetes: epidemiology and microbiology. *Clinical microbiology reviews,* 7**,** 357-417.

MENARD, A., MONNEZ, C., ESTRADA DE LOS SANTOS, P., SEGONDS, C., CABALLERO-MELLADO, J., LIPUMA, J. J., CHABANON, G. & COURNOYER, B. 2007. Selection of nitrogen-fixing deficient *Burkholderia vietnamiensis* strains by cystic fibrosis patients: involvement of nif gene deletions and auxotrophic mutations. *Environ Microbiol,* 9**,** 1176-85.

MERCHANT, A. T. & SPATAFORA, G. A. 2014. A role for the DtxR family of metalloregulators in gram-positive pathogenesis. *Molecular oral microbiology,* 29**,** 1-10.

MEYER, J.-M. 1992. Exogenous siderophore-mediated iron uptake in *Pseudomonas aeruginosa*: possible involvement of porin OprF in iron translocation. *Microbiology,* 138**,** 951-958.

MEYER, J. M., HOHNADEL, D. & HALLE, F. 1989. Cepabactin from *Pseudomonas cepacia*, a new type of siderophore. *Journal of General Microbiology,* 135**,** 1479-87.

MIETHKE, M., KLOTZ, O., LINNE, U., MAY, J. J., BECKERING, C. L. & MARAHIEL, M. A. 2006. Ferri-bacillibactin uptake and hydrolysis in *Bacillus subtilis*. *Molecular microbiology,* 61**,** 1413-1427.

MIETHKE, M. & MARAHIEL, M. A. 2007. Siderophore-based iron acquisition and pathogen control. *Microbiology and Molecular Biology Reviews,* 71**,** 413-451.

MIETHKE, M., MONTEFERRANTE, C. G., MARAHIEL, M. A. & VAN DIJL, J. M. 2013. The *Bacillus subtilis* EfeUOB transporter is essential for high-affinity acquisition of ferrous and ferric iron. *Biochimica et Biophysica Acta (BBA)-Molecular Cell Research,* 1833**,** 2267-2278.

MIL-HOMENS, D. & FIALHO, A. M. 2012. A BCAM0223 mutant of *Burkholderia cenocepacia* is deficient in hemagglutination, serum resistance, adhesion to epithelial cells and virulence. *PLoS One,* 7**,** 1-12.

MILLER, S. S. & STEINBERG, R. H. 1977. Active transport of ions across frog retinal pigment epithelium. *Experimental eye research,* 25**,** 235-248.

MIRUS, O., STRAUSS, S., NICOLAISEN, K., VON HAESELER, A. & SCHLEIFF, E. 2009. TonB-dependent transporters and their occurrence in cyanobacteria. *BMC biology,* 7**,** 1-25.

MISLIN, G. L. & SCHALK, I. J. 2014. Siderophore-dependent iron uptake systems as gates for antibiotic Trojan horse strategies against *Pseudomonas aeruginosa*. *Metallomics,* 6**,** 408-20.

MOIR, J. & WOOD, N. 2001. Nitrate and nitrite transport in bacteria. *Cellular and Molecular Life Sciences CMLS,* 58**,** 215-224.

MÖLLMANN, U., HEINISCH, L., BAUERNFEIND, A., KÖHLER, T. & ANKEL-FUCHS, D. 2009. Siderophores as drug delivery agents: application of the "Trojan Horse" strategy. *BioMetals,* 22**,** 615-624.

MOON, Y. H., TANABE, T., FUNAHASHI, T., SHIUCHI, K., NAKAO, H. & YAMAMOTO, S. 2004. Identification and characterization of two contiguous operons required for aerobactin transport and biosynthesis in *Vibrio mimicus*. *Microbiol Immunology,* 48**,** 389-98.

MOORE, C. H., FOSTER, L. A., GERBIG, D. G., DYER, D. W. & GIBSON, B. W. 1995. Identification of alcaligin as the siderophore produced by *Bordetella pertussis* and *B. bronchiseptica*. *Journal of Bacteriology,* 177**,** 1116-1118.

MOREE, W. J., PHELAN, V. V., WU, C.-H., BANDEIRA, N., CORNETT, D. S., DUGGAN, B. M. & DORRESTEIN, P. C. 2012. Interkingdom metabolic transformations captured by microbial imaging mass spectrometry. *Proceedings of the National Academy of Sciences,* 109**,** 13811-13816.

MORTON, D. J., SEALE, T. W., BAKALETZ, L. O., JURCISEK, J. A., SMITH, A., VANWAGONER, T. M., WHITBY, P. W. & STULL, T. L. 2009. The heme-binding protein (HbpA) of *Haemophilus influenzae* as a virulence determinant. *International journal of medical microbiology : IJMM,* 299**,** 479-488.

MOYNIÉ, L., LUSCHER, A., ROLO, D., PLETZER, D., TORTAJADA, A., WEINGART, H., BRAUN, Y., PAGE, M. G., NAISMITH, J. H. & KÖHLER, T. 2017. Structure and function of the PiuA and PirA siderophore-drug receptors from *Pseudomonas aeruginosa* and *Acinetobacter baumannii*. *Antimicrobial agents and chemotherapy***,** 1-14.

MULLEN, T., MARKEY, K., MURPHY, P., MCCLEAN, S. & CALLAGHAN, M. 2007. Role of lipase in Burkholderia cepacia complex (Bcc) invasion of lung epithelial cells. *European Journal of Clinical Microbiology & Infectious Diseases,* 26**,** 869-877.

MUSSER, J. M., BEMIS, D. A., ISHIKAWA, H. & SELANDER, R. K. 1987. Clonal diversity and host distribution in Bordetella bronchiseptica. *Journal of bacteriology,* 169**,** 2793-2803.

NAKA, H., HIRONO, I. & AOKI, T. 2005. Cloning and Characterization of Two Types of tonB Genes, *tonB1* and *tonB2*, and FerricUptake Regulator Gene, *fur* from Photobacterium damselae subsp. *piscicida*. *J Fish Pathology,* 40**,** 73-79.

NAKANO, M. M., CORBELL, N., BESSON, J. & ZUBER, P. 1992. Isolation and characterization of sfp: a gene that functions in the production of the lipopeptide biosurfactant, surfactin, in *Bacillus subtilis*. *Molecular and General Genetics MGG,* 232**,** 313-321.

NATHAN, D. G., BAEHNER, R. L. & WEAVER, D. K. 1969. Failure of nitro blue tetrazolium reduction in the phagocytic vacuoles of leukocytes in chronic granulomatous disease. *The Journal of clinical investigation,* 48**,** 1895-1904.

NAZIR, R., HANSEN, M. A., SØRENSEN, S. & VAN ELSAS, J. D. 2012. Draft Genome Sequence of the Soil Bacterium *Burkholderia terrae* Strain BS001, Which Interacts with Fungal Surface Structures. *Journal of Bacteriology,* 194**,** 4480-4481.

NEILANDS, J. 1984. Methodology of siderophores. *Siderophores from microorganisms and plants.* Springer.

NEILANDS, J. B. 1981. Microbial Iron Compounds. *Annual Review of Biochemistry,* 50**,** 715-731.

NEUMANN, W., SASSONE-CORSI, M., RAFFATELLU, M. & NOLAN, E. M. 2018. Esterase-Catalyzed Siderophore Hydrolysis Activates an Enterobactin–Ciprofloxacin Conjugate and Confers Targeted Antibacterial Activity. *Journal of the American Chemical Society,* 140**,** 5193-5201.

NISHIO, T. & ISHIDA, Y. 1990. Production of dihydroxamate siderophore alcaligin by *Alcaligenes xylosoxidans* subsp. *xylosoxidans*. *J Agricultural biological chemistry,* 54**,** 1837-1839.

NOINAJ, N., EASLEY, N. C., OKE, M., MIZUNO, N., GUMBART, J., BOURA, E., STEERE, A. N., ZAK, O., AISEN, P., TAJKHORSHID, E., EVANS, R. W., GORRINGE, A. R., MASON, A. B., STEVEN, A. C. & BUCHANAN, S. K. 2012. Structural basis for iron piracy by pathogenic Neisseria. *Nature,* 483**,** 53-58.

NOINAJ, N., GUILLIER, M., BARNARD, T. J. & BUCHANAN, S. K. 2010. TonB-dependent transporters: regulation, structure, and function. *Annual Review of Microbiology,* 64**,** 43-60.

NOVIKOVA, O. D. & SOLOVYEVA, T. F. 2009. Nonspecific porins of the outer membrane of Gram-negative bacteria: Structure and functions. *Biochemistry (Moscow) Supplement Series A: Membrane and Cell Biology,* 3**,** 3-15.

NUCCI, M. & ANAISSIE, E. 2007. Fusarium infections in immunocompromised patients. *Journal of Clinical microbiology reviews,* 20**,** 695-704.

O'CARROLL, M., KIDD, T., COULTER, C., SMITH, H., ROSE, B., HARBOUR, C. & BELL, S. 2003. *Burkholderia pseudomallei*: another emerging pathogen in cystic fibrosis. *Thorax,* 58**,** 1087-1091.

O'DONNELL, P. M., AVILES, H., LYTE, M. & SONNENFELD, G. 2006. Enhancement of in vitro growth of pathogenic bacteria by norepinephrine: importance of inoculum density and role of transferrin. *Applied and Environmental Microbiology,* 72**,** 5097-5099.

O'GRADY, E. P., SOKOL, P. A. & MICROBIOLOGY, I. 2011. *Burkholderia cenocepacia* differential gene expression during host–pathogen interactions and adaptation to the host environment. *Journal Frontiers in cellular,* 1**,** 1-23.

O'TOOLE, G. A. 2018. Cystic Fibrosis Airway Microbiome: Overturning the Old, Opening the Way for the New. *Journal of Bacteriology,* 200**,** 1-8.

OCHSNER, U. A., JOHNSON, Z. & VASIL, M. L. 2000. Genetics and regulation of two distinct haem-uptake systems, *phu* and *has*, in *Pseudomonas aeruginosa*. *Microbiology,* 146**,** 185-198.

OEEMIG, J. S., OLLILA, O. S. & IWAÏ, H. 2018. NMR structure of the C-terminal domain of TonB protein from *Pseudomonas aeruginosa*. *PeerJ,* 6**,** 1-19.

OIDE, S., BERTHILLER, F., WIESENBERGER, G., ADAM, G. & TURGEON, B. G. 2015. Individual and combined roles of malonichrome, ferricrocin, and TAFC siderophores in *Fusarium graminearum* pathogenic and sexual development. *Frontiers in microbiology,* 5**,** 1-15.

ONG, K. S., AW, Y. K., LEE, L. H., YULE, C. M., CHEOW, Y. L. & LEE, S. M. 2016. *Burkholderia paludis* sp. nov., an antibiotic-siderophore producing novel Burkholderia cepacia complex species, isolated from Malaysian tropical peat swamp soil. *Frontiers in microbiology,* 7**,** 2046.

ORTEGA, X., SILIPO, A., SALDÍAS, M. S., BATES, C. C., MOLINARO, A. & VALVANO, M. A. 2009. Biosynthesis and structure of the *Burkholderia cenocepacia* K56-2 lipopolysaccharide core oligosaccharide. truncation of the core oligosaccharide leads to increased binding and sensitivity to polymyxin B. *Journal of Biological Chemistry***,** 1-19.

PAGE, M. G., DANTIER, C. & DESARBRE, E. 2010. In vitro properties of BAL30072, a novel siderophore sulfactam with activity against multiresistant gram-negative bacilli. *Antimicrobial agents and chemotherapy,* 54**,** 2291-2302.

PALLERONI, N., KUNISAWA, R., CONTOPOULOU, R. & DOUDOROFF, M. 1973. Nucleic acid homologies in the genus Pseudomonas. *International Journal of Systematic and Evolutionary Microbiology,* 23**,** 333-339.

PANDAY, A., SAHOO, M. K., OSORIO, D. & BATRA, S. 2015. NADPH oxidases: an overview from structure to innate immunity-associated pathologies. *Cellular & molecular immunology,* 12**,** 5-23.

PARKE, J. L. & GURIAN-SHERMAN, D. 2001. Diversity of the Burkholderia cepacia complex and implications for risk assessment of biological control strains. *Annual Review of Phytopathology,* 39**,** 225-258.

PARKHILL, J., SEBAIHIA, M., PRESTON, A., MURPHY, L. D., THOMSON, N., HARRIS, D. E., HOLDEN, M. T., CHURCHER, C. M., BENTLEY, S. D. & MUNGALL, K. L. 2003. Comparative analysis of the genome sequences of *Bordetella pertussis*, *Bordetella parapertussis* and *Bordetella bronchiseptica*. *Nature genetics,* 35**,** 32-40.

PARKINS, M. D., SOMAYAJI, R. & WATERS, V. J. 2018. Epidemiology, Biology, and Impact of Clonal *Pseudomonas aeruginosa* Infections in Cystic Fibrosis. *Clinical Microbiology Reviews,* 31**,** 1-38.

PARTE, A. C. 2018. LPSN - List of Prokaryotic names with Standing in Nomenclature , 20 years on. *International Journal of Systematic and Evolutionary Microbiology,* 68**,** 1825-1829.

PATEL, P., SONG, L. & CHALLIS, G. L. 2010. Distinct extracytoplasmic siderophore binding proteins recognize ferrioxamines and ferricoelichelin in *Streptomyces coelicolor* A3 (2). *J Biochemistry,* 49**,** 8033-8042.

PAWELEK, P. D., CROTEAU, N., NG-THOW-HING, C., KHURSIGARA, C. M., MOISEEVA, N., ALLAIRE, M. & COULTON, J. W. 2006. Structure of TonB in complex with FhuA, E. coli outer membrane Receptor. *Science,* 312**,** 1399-1402.

PEACOCK, R. S., WELJIE, A. M., HOWARD, S. P., PRICE, F. D. & VOGEL, H. J. 2005. The solution structure of the C-terminal domain of TonB and interaction studies with TonB box peptides. *J Journal of molecular biology,* 345**,** 1185-1197.

PEDERICK, V. G., EIJKELKAMP, B. A., BEGG, S. L., WEEN, M. P., MCALLISTER, L. J., PATON, J. C. & MCDEVITT, C. A. 2015. ZnuA and zinc homeostasis in *Pseudomonas aeruginosa*. *Scientific reports,* 5**,** 1-14.

PEETERS, C., ZLOSNIK, J. E., SPILKER, T., HIRD, T. J., LIPUMA, J. J. & VANDAMME, P. 2013. *Burkholderia pseudomultivorans* sp. nov., a novel Burkholderia cepacia complex species from human respiratory samples and the rhizosphere. *System of Applied Microbiology,* 36**,** 483-489.

PERRAUD, Q., MOYNIÉ, L., GASSER, V. R., MUNIER, M., GODET, J., HOEGY, F. O., MÉLY, Y., MISLIN, G. T. L., NAISMITH, J. H. & SCHALK, I. J. 2018. A key role for the periplasmic PfeE esterase in iron acquisition via the siderophore Enterobactin in *Pseudomonas aeruginosa*. *ACS chemical biology,* 13**,** 2603-2614.

PERRY, R. D., BOBROV, A. G. & FETHERSTON, J. D. 2015. The role of transition metal transporters for iron, zinc, manganese, and copper in the pathogenesis of *Yersinia pestis*. *Metallomics*, 965-978.

PERRY, R. D. & FETHERSTON, J. D. 2011. Yersiniabactin iron uptake: mechanisms and role in *Yersinia pestis* pathogenesis. *Microbes and infection,* 13, 808-817.

PHILPOTT, C. C. 2006. Iron uptake in fungi: A system for every source. *Biochimica et Biophysica Acta (BBA) - Molecular Cell Research,* 1763, 636-645.

PIRNAY, J. P., MATTHIJS, S., COLAK, H., CHABLAIN, P., BILOCQ, F., VAN ELDERE, J., DE VOS, D., ZIZI, M., TRIEST, L. & CORNELIS, P. 2005. Global *Pseudomonas aeruginosa* biodiversity as reflected in a Belgian river. *J Environmental microbiology,* 7, 969-980.

PITA, T., FELICIANO, J. R. & LEITÃO, J. H. 2018. Small Noncoding Regulatory RNAs from *Pseudomonas aeruginosa* and Burkholderia cepacia Complex. *International journal of molecular sciences,* 19, 3759.

POOLE, K. 2007. Efflux pumps as antimicrobial resistance mechanisms. *Annals of Medicine,* 39, 162-176.

POOLE, K., HEINRICHS, D. E. & NESHAT, S. 1993. Cloning and sequence analysis of an EnvCD homologue in *Pseudomonas aeruginosa*: regulation by iron and possible involvement in the secretion of the siderophore pyoverdine. *Journal of Molecular Microbiology,* 10, 529-544.

POOLE, K., YOUNG, L. & NESHAT, S. 1990. Enterobactin-mediated iron transport in *Pseudomonas aeruginosa*. *Journal of Bacteriology,* 172, 6991-6996.

PORTSMOUTH, S., VAN VEENHUYZEN, D., ECHOLS, R., MACHIDA, M., FERREIRA, J. C. A., ARIYASU, M., TENKE, P. & DEN NAGATA, T. 2018. Cefiderocol versus imipenem-cilastatin for the treatment of complicated urinary tract infections caused by Gram-negative uropathogens: a phase 2, randomised, double-blind, non-inferiority trial. *The Lancet Infectious Diseases*, 1319-1328.

POSEY, J. E. & GHERARDINI, F. C. 2000. Lack of a role for iron in the Lyme disease pathogen. *Science,* 288, 1651-1653.

POWER, R. F., LINNANE, B., MARTIN, R., POWER, N., HARNETT, P., CASSERLY, B., O'CONNELL, N. H. & DUNNE, C. P. 2016. The first reported case of *Burkholderia contaminans* in patients with cystic fibrosis in Ireland: from the Sargasso Sea to Irish Children. *Journal BMC pulmonary medicine,* 16, 2-5.

PRABHU, M. & VALCHANOV, K. 2017. Pre-anaesthetic evaluation of the patient with end-stage lung disease. *Best Practice Journal of Research Clinical Anaesthesiology,* 31, 249-260.

PRADENAS, G., MYERS, J. & TORRES, A. 2017. Characterization of the *Burkholderia cenocepacia* TonB Mutant as a Potential Live Attenuated Vaccine. *Vaccines,* 5, 1-12.

PRAMANIK, A. & BRAUN, V. 2006. Albomycin uptake via a ferric hydroxamate transport system of *Streptococcus pneumoniae* R6. *Journal of bacteriology,* 188, 3878-3886.

PRAMANIK, A., STROEHER, U. H., KREJCI, J., STANDISH, A. J., BOHN, E., PATON, J. C., AUTENRIETH, I. B. & BRAUN, V. 2007. Albomycin is an effective antibiotic, as exemplified with *Yersinia enterocolitica* and *Streptococcus pneumoniae*. *International Journal of Medical Microbiology,* 297, 459-469.

PROSCHAK, A., LUBUTA, P., GRÜN, P., LÖHR, F., WILHARM, G., DE BERARDINIS, V. & BODE, H. B. 2013. Structure and Biosynthesis of Fimsbactins A–F, Siderophores from *Acinetobacter baumannii* and *Acinetobacter baylyi. ChemBioChem,* 14, 633-638.

PUPIN, M., ESMAEEL, Q., FLISSI, A., DUFRESNE, Y., JACQUES, P. & LECLÈRE, V. 2016. Norine: A powerful resource for novel nonribosomal peptide discovery. *Synthetic and Systems Biotechnology,* 1, 89-94.

RAINES, D. J., MOROZ, O. V., BLAGOVA, E. V., TURKENBURG, J. P., WILSON, K. S. & DUHME-KLAIR, A.-K. 2016. Bacteria in an intense competition for iron: Key component of the *Campylobacter jejuni* iron uptake system scavenges enterobactin hydrolysis product. *Proceedings of the National Academy of Sciences,* 113, 5850-5855.

RAJAN, S. & SAIMAN, L. Pulmonary infections in patients with cystic fibrosis. Seminars in respiratory infections, 2002. 47-56.

RAJASEKARAN, M. B., MITCHELL, S. A., GIBSON, T. M., HUSSAIN, R., SILIGARDI, G., ANDREWS, S. C. & WATSON, K. A. 2010a. Isolation and characterisation of EfeM, a periplasmic component of the putative EfeUOBM iron transporter of *Pseudomonas syringae* pv. *syringae*. *Biochemical and Biophysical Research Communications,* 398, 366-371.

RAJASEKARAN, M. B., NILAPWAR, S., ANDREWS, S. C. & WATSON, K. A. 2010b. EfeO-cupredoxins: Major new members of the cupredoxin superfamily with roles in bacterial iron transport. *BioMetals,* 23**,** 1-17.

RAJENDRAN, R., QUINN, R. F., MURRAY, C., MCCULLOCH, E., WILLIAMS, C. & RAMAGE, G. 2010. Efflux pumps may play a role in tigecycline resistance in *Burkholderia* species. *International Journal of Antimicrobial Agents,* 36**,** 151-154.

RAYMOND, K. N., ALLRED, B. E. & SIA, A. K. 2015. Coordination Chemistry of Microbial Iron Transport. *Accounts of chemical research,* 48**,** 2496-2505.

RAYMOND, K. N., DERTZ, E. A. & KIM, S. S. 2003. Enterobactin: an archetype for microbial iron transport. *Proceedings of the National Academy of Sciences,* 100**,** 3584-3588.

REIK, R., SPILKER, T. & LIPUMA, J. J. 2005. Distribution of Burkholderia cepacia complex species among isolates recovered from persons with or without cystic fibrosis. *Journal of Clinical Microbiology,* 43**,** 2926-2928.

REIMMANN, C. 2012. Inner-membrane transporters for the siderophores pyochelin in Pseudomonas aeruginosa and enantio-pyochelin in *Pseudomonas fluorescens* display different enantioselectivities. *Microbiology,* 158**,** 1317-1324.

RIORDAN, J. R., ROMMENS, J. M., KEREM, B., ALON, N., ROZMAHEL, R., GRZELCZAK, Z., ZIELENSKI, J., LOK, S., PLAVSIC, N., CHOU, J. L. & ET AL. 1989. Identification of the cystic fibrosis gene: cloning and characterization of complementary DNA. *Science,* 245**,** 1066-73.

RONNEBAUM, T. A. & LAMB, A. L. 2018. Nonribosomal peptides for iron acquisition: pyochelin biosynthesis as a case study. *Current Opinion in Structural Biology,* 53**,** 1-11.

RONPIRIN, C., JERSE, A. E., CORNELISSEN, C. N. & IMMUNITY 2001. Gonococcal genes encoding transferrin-binding proteins A and B are arranged in a bicistronic operon but are subject to differential expression. *J Infection,* 69**,** 6336-6347.

ROSENZWEIG, S. 2008. Inflammatory manifestations in chronic granulomatous disease (CGD). *J Journal of clinical immunology,* 28**,** 67-72.

ROSSI, M.-S., FETHERSTON, J. D., LÉTOFFÉ, S., CARNIEL, E., PERRY, R. D. & GHIGO, J.-M. 2001. Identification and characterization of the hemophore-dependent heme acquisition system of *Yersinia pestis. Infection and immunity,* 69**,** 6707-6717.

RUNYEN-JANECKY, L. J. 2013. Role and regulation of heme iron acquisition in gram-negative pathogens. *Frontiers in cellular and infection microbiology,* 3**,** 1-11.

RYAN, R. P., MCCARTHY, Y., WATT, S. A., NIEHAUS, K. & DOW, J. M. 2009. Intraspecies Signaling Involving the Diffusible Signal Factor BDSF 2-Dodecenoic Acid) Influences Virulence in *Burkholderia cenocepacia*. *Journal of Bacteriology,* 191**,** 5013-5019.

RYNDAK, M. B., WANG, S., SMITH, I. & RODRIGUEZ, G. M. 2010. The *Mycobacterium tuberculosis* High-Affinity Iron Importer, IrtA, Contains an FAD-Binding Domain. *Journal of Bacteriology,* 192**,** 861-869.

SAJJAN, S. U., CARMODY, L. A., GONZALEZ, C. F. & LIPUMA, J. J. 2008. A type IV secretion system contributes to intracellular survival and replication of *Burkholderia cenocepacia*. *Infection immunity,* 76**,** 5447-5455.

SALDÍAS, M. S., LAMOTHE, J., WU, R., VALVANO, M. A. & IMMUNITY 2008. *Burkholderia cenocepacia* requires the RpoN sigma factor for biofilm formation and intracellular trafficking within macrophages. *J Infection,* 76**,** 1059-1067.

SANDRINI, S. M., SHERGILL, R., WOODWARD, J., MURALIKUTTAN, R., HAIGH, R. D., LYTE, M. & FREESTONE, P. P. 2010. Elucidation of the mechanism by which catecholamine stress hormones liberate iron from the innate immune defense proteins transferrin and lactoferrin. *Journal of Bacteriology,* 192**,** 587-594.

SASS, A., KIEKENS, S. & COENYE, T. 2017. Identification of small RNAs abundant in *Burkholderia cenocepacia* biofilms reveal putative regulators with a potential role in carbon and iron metabolism. *Scientific Reports,* 7**,** 15665.

SASS, A. M., VAN ACKER, H., FÖRSTNER, K. U., VAN NIEUWERBURGH, F., DEFORCE, D., VOGEL, J. & COENYE, T. 2015. Genome-wide transcription start site profiling in biofilm-grown *Burkholderia cenocepacia* J2315. *BMC genomics,* 16**,** 1-15.

SASS, G., NAZIK, H., PENNER, J., SHAH, H., ANSARI, S. R., CLEMONS, K. V., GROLEAU, M.-C., DIETL, A.-M., VISCA, P. & HAAS, H. 2018. Studies of *Pseudomonas aeruginosa* mutants indicate pyoverdine as the central factor in inhibition of Aspergillus fumigatus biofilm. *Journal of bacteriology,* 200**,** 1-24.

SATO, T., NONOYAMA, S., KIMURA, A., NAGATA, Y., OHTSUBO, Y. & TSUDA, M. 2017. A Small Protein, HemP, is a Transcriptional Activator for Hemin Uptake Operon in *Burkholderia multivorans* ATCC 17616. *Applied and Environmental Microbiology***,** 1-14.

SAWANA, A., ADEOLU, M. & GUPTA, R. S. 2014. Molecular signatures and phylogenomic analysis of the genus *Burkholderia*: proposal for division of this genus into the emended genus *Burkholderia* containing pathogenic organisms and a new genus *Paraburkholderia* gen. nov. harboring environmental species. *Frontiers in Genetics,* 5**,** 1-22.

SCHALK, I. J. 2018. A Trojan-Horse Strategy Including a Bacterial Suicide Action for the Efficient Use of a Specific Gram-Positive Antibiotic on Gram-Negative Bacteria. *Journal of Medicinal Chemistry,* 61**,** 3842-3844.

SCHALK, I. J. & GUILLON, L. 2013. Fate of ferrisiderophores after import across bacterial outer membranes: different iron release strategies are observed in the cytoplasm or periplasm depending on the siderophore pathways. *Amino Acids,* 44**,** 1267-1277.

SCHAUER, K., RODIONOV, D. A. & DE REUSE, H. 2008. New substrates for TonB-dependent transport: do we only see the 'tip of the iceberg'? *Trends in Biochemical Sciences,* 33**,** 330-338.

SCHMID, N., PESSI, G., DENG, Y., AGUILAR, C., CARLIER, A. L., GRUNAU, A., OMASITS, U., ZHANG, L. H., AHRENS, C. H. & EBERL, L. 2012. The AHL- and BDSF-dependent quorum sensing systems control specific and overlapping sets of genes in *Burkholderia cenocepacia* H111. *PLoS One,* 7**,** 1-12.

SCHMIDT, T., STOPPEL, R.-D. & SCHLEGEL, H. G. 1991. High-level nickel resistance in A*lcaligenes xylosoxydans* 31A and *Alcaligenes eutrophus* KTO2. *Applied and environmental microbiology,* 57**,** 3301-3309.

SCHRETTL, M., BIGNELL, E., KRAGL, C., SABIHA, Y., LOSS, O., EISENDLE, M., WALLNER, A., ARST JR, H. N., HAYNES, K. & HAAS, H. 2007. Distinct roles for intra-and extracellular siderophores during *Aspergillus fumigatus* infection. *PLoS pathogens,* 3**,** 1195-1207.

SCHRYVERS, A. B., BONNAH, R., YU, R.-H., WONG, H. & RETZER, M. 1998. Bacterial lactoferrin receptors. *Advances in Lactoferrin Research***,** 123-133.

SCHWARTZ, C. J., GIEL, J. L., PATSCHKOWSKI, T., LUTHER, C., RUZICKA, F. J., BEINERT, H. & KILEY, P. J. 2001. IscR, an Fe-S cluster-containing transcription factor, represses expression of *Escherichia coli* genes encoding Fe-S cluster assembly proteins. *Proceedings of the National Academy of Sciences,* 98**,** 14895-14900.

SCHWARZ, S., SINGH, P., ROBERTSON, J. D., LEROUX, M., SKERRETT, S. J., GOODLETT, D. R., WEST, T. E. & MOUGOUS, J. D. 2014. VgrG-5 is a *Burkholderia* type VI secretion exported protein required for multinucleated giant cell formation and virulence. *J Infection immunity***,** 1445-1452.

SCHWYN, B. & NEILANDS, J. B. 1987. Universal chemical assay for the detection and determination of siderophores. *Anal Biochem,* 160**,** 47-56.

SCOFFONE, V. C., CHIARELLI, L. R., TRESPIDI, G., MENTASTI, M., RICCARDI, G. & BURONI, S. 2017. *Burkholderia cenocepacia* infections in cystic fibrosis patients: Drug resistance and therapeutic approaches. *Frontiers in microbiology,* 8**,** 1-13.

SEED, K. D., DENNIS, J. J. & IMMUNITY 2008. Development of *Galleria mellonella* as an alternative infection model for the Burkholderia cepacia complex. *J Infection,* 76**,** 1267-1275.

SEGAL, B. H., LETO, T. L., GALLIN, J. I., MALECH, H. L. & HOLLAND, S. M. 2000. Genetic, biochemical, and clinical features of chronic granulomatous disease. *J Medicine,* 79**,** 170-200.

SEO, S. W., KIM, D., LATIF, H., O'BRIEN, E. J., SZUBIN, R. & PALSSON, B. O. 2014. Deciphering Fur transcriptional regulatory network highlights its complex role beyond iron metabolism in *Escherichia coli*. *Nature Communication,* 5**,** 1-10.

SESTOK, A. E., LINKOUS, R. O. & SMITH, A. T. 2018. Toward a mechanistic understanding of Feo-mediated ferrous iron uptake. *Metallomics,* 10**,** 887-898.

SEYEDMOHAMMAD, S., FUENTEALBA, NATALIA A., MARRIOTT, ROBERT A. J., GOETZE, TOM A., EDWARDSON, J. M., BARRERA, NELSON P. & VENTER, H. 2016. Structural model of FeoB, the iron transporter from *Pseudomonas aeruginosa*, predicts a cysteine lined, GTP-gated pore. *J Bioscience Reports,* 36**,** 1-26.

SEYEDSAYAMDOST, M. R., CLETO, S., CARR, G., VLAMAKIS, H., JOÃO VIEIRA, M., KOLTER, R. & CLARDY, J. 2012. Mixing and Matching Siderophore Clusters: Structure and Biosynthesis of Serratiochelins from *Serratia* sp. V4. *Journal of the American Chemical Society,* 134**,** 13550-13553.

SHALOM, G., SHAW, J. G. & THOMAS, M. S. 2007. In vivo expression technology identifies a type VI secretion system locus in *Burkholderia pseudomallei* that is induced upon invasion of macrophages. *Microbiology,* 153**,** 2689-2699.

SHANNON, J. D. & KIMBROUGH, R. C. 2006. Pulmonary cholera due to infection with a non-O1 *Vibrio cholerae* strain. *Journal of clinical microbiology,* 44**,** 3459-3460.

SHASTRI, S. 2011. *Characterisation of the Type VI Secretion System of Burkholderia cenocepacia.* PhD thesis, University of Sheffield, School of Medicine and Biomedical Sciences.

SHASTRI, S., SPIEWAK, H. L., SOFOLUWE, A., EIDSVAAG, V. A., ASGHAR, A. H., PEREIRA, T., BULL, E. H., BUTT, A. T. & THOMAS, M. S. 2017. An efficient system for the generation of marked genetic mutants in members of the genus *Burkholderia*. *Plasmid,* 89**,** 49-56.

SHEA, C. M. & MCINTOSH, M. A. 1991. Nucleotide sequence and genetic organization of the ferric enterobactin transport system: homology to other peripiasmic binding protein-dependent systems in Escherichia coli. *Molecular Microbiology,* 5**,** 1415-1428.

SHELDON, J. R. & HEINRICHS, D. E. 2015. Recent developments in understanding the iron acquisition strategies of gram positive pathogens. *FEMS Microbiology Reviews***,** 592-630.

SHOKOUHI, S., TEHRANI, S. & HEMMATIAN, M. 2016. Mixed pulmonary infection with *Penicillium notatum* and *Pneumocystis jiroveci* in a patient with acute myeloid leukemia. *Tanaffos,* 15**,** 53-56.

SHUKLA, R., BILOLIKAR, A. & UDAYASRI, B. 2018. Pragya Rani. Antibiotic susceptibility pattern of Burkholderia cepacia complex from various clinical samples in a tertiary care center: A one yea r prospective study. *J Med Sci Res,* 6**,** 1-5.

SIEGMUND, K.-D., PLATTNER, H. J. & DIEKMANN, H. 1991. Purification of ferrichrome synthetase from *Aspergillus quadricinctus* and characterisation as a phosphopantetheine containing multienzyme complex. *Molecular Enzymology* 1076**,** 123-129.

SILHAVY, T. J., KAHNE, D. & WALKER, S. 2010. The bacterial cell envelope. *Cold Spring Harbor Perspectives in Biology,* 2**,** 1-17.

SILVA, I. N., PESSOA, F. D., RAMIRES, M. J., SANTOS, M. R., BECKER, J. D., COOPER, V. S. & MOREIRA, L. M. 2018. The OmpR Regulator of *Burkholderia multivorans* Controls Mucoid-to-Nonmucoid Transition and Other Cell Envelope Properties Associated with Persistence in the Cystic Fibrosis Lung. *J of Bacteriology,* 200**,** 1-22.

SILVER, L. L. 2008. Are natural products still the best source for antibacterial discovery? The bacterial entry factor. *Expert Opinion in Drug Discovery,* 3**,** 487-500.

SILVERMAN, J. M., BRUNET, Y. R., CASCALES, E. & MOUGOUS, J. D. 2012. Structure and regulation of the type VI secretion system. *Annual Review of Microbiology,* 66**,** 453-472.

SIMON, R., PRIEFER, U. & PÜHLER, A. 1983. A broad host range mobilization system for in vivo genetic engineering: transposon mutagenesis in gram negative bacteria. *Nature biotechnology,* 1**,** 784-791.

ŠMAJS, D., ŠMARDA, J. & WEINSTOCK, G. M. 2003. The *Escherichia fergusonii iucABCD iutA* genes are located within a larger chromosomal region similar to pathogenicity islands. *Folia Microbiologica,* 48**,** 139-147.

SMALL, S. K., PURI, S., SANGWAN, I. & O'BRIAN, M. R. 2009. Positive control of ferric siderophore receptor gene expression by the Irr protein in *Bradyrhizobium japonicum*. *Journal of bacteriology,* 191**,** 1361-1368.

SMALLEY, J. W., BYRNE, D. P., BIRSS, A. J., WOJTOWICZ, H., SROKA, A., POTEMPA, J. & OLCZAK, T. 2011. HmuY haemophore and gingipain proteases constitute a unique syntrophic system of haem acquisition by *Porphyromonas gingivalis*. *PLoS One,* 6**,** 1-10.

SMALLEY, J. W. & OLCZAK, T. 2017. Heme acquisition mechanisms of *Porphyromonas gingivalis* – strategies used in a polymicrobial community in a heme-limited host environment. *Molecular Oral Microbiology,* 32**,** 1-23.

SMET, B. D., MAYO, M., PEETERS, C., ZLOSNIK, J. E. A., SPILKER, T., HIRD, T. J., LIPUMA, J. J., KIDD, T. J., KAESTLI, M., GINTHER, J. L., WAGNER, D. M., KEIM, P., BELL, S. C., JACOBS, J. A., CURRIE, B. J. & VANDAMME, P. A. 2015. *Burkholderia stagnalis* sp. nov. and *Burkholderia territorii* sp. nov., two novel Burkholderia cepacia complex species from environmental and human sources. *International Journal of Systematic and Evolutionary Microbiology***,** 2265-2271.

SMITH, A. D. & WILKS, A. 2015. Differential contributions of the outer membrane receptors PhuR and HasR to heme acquisition in *Pseudomonas aeruginosa*. *Journal of Biological Chemistry,* 290**,** 7756-7766.

SOKOL, P., DARLING, P., LEWENZA, S., CORBETT, C. & KOOI, C. 2000. Identification of a siderophore receptor required for ferric ornibactin uptake in Burkholderia cepacia. *Infection and immunity,* 68**,** 6554-6560.

SOKOL, P. A. 1986. Production and utilization of pyochelin by clinical isolates of *Pseudomonas cepacia*. *Journal of Clinical Microbiology,* 23**,** 560-562.

SOKOL, P. A., DARLING, P., WOODS, D. E., MAHENTHIRALINGAM, E. & KOOI, C. 1999. Role of Ornibactin Biosynthesis in the Virulence of *Burkholderia cepacia*: Characterization of pvdA, the Gene Encoding Ornithine Oxygenase. *Infection and Immunity,* 67**,** 4443-4455.

SOROKINA, A., DASHTI, Y., KHILYAS, I., SHARIPOVA, M., BOGOMOLNAYA, L. & CHALLIS, G. Siderophores produced by *Serratia marcescens* SM6. 2018.

SOUSA, S. A., RAMOS, C. G. & LEITÃO, J. H. 2011. Burkholderia cepacia Complex: Emerging Multihost Pathogens Equipped with a Wide Range of Virulence Factors and Determinants. *International journal of microbiology,* 2011**,** 1-9.

SOUSA, S. A., ULRICH, M., BRAGONZI, A., BURKE, M., WORLITZSCH, D., LEITÃO, J. H., MEISNER, C., EBERL, L., SÁ-CORREIA, I. & DÖRING, G. 2007. Virulence of Burkholderia cepacia complex strains in gp91phox−/− mice. *Cellular microbiology,* 9**,** 2817-2825.

SPIEWAK, H. L. 2015. *Identifying novel secreted effectors of the type VI protein secretion system in Burkholderia cenocepacia.* PhD Thesis, University of Sheffield.

STEFANSKA, A. L., FULSTON, M., HOUGE-FRVDRYCH, C. S., JONES, J. J. & WARR, S. R. 2000. A Potent Seryl tRNA Synthetase Inhibitor SB-217452. *J The Journal of antibiotics,* 53**,** 1346-1353.

STEPHAN, H., FREUND, S., BECK, W., JUNG, G., MEYER, J.-M. & WINKELMANN, G. 1993. Ornibactins—a new family of siderophores from Pseudomonas. *Biometals,* 6**,** 93-100.

STITES, S. W., PLAUTZ, M. W., BAILEY, K., O'BRIEN-LADNER, A. R. & WESSELIUS, L. J. 1999. Increased concentrations of iron and isoferritins in the lower respiratory tract of patients with stable cystic fibrosis. *American Journal of Respiratory and Critical Care Medicine,* 160**,** 796-801.

STOVER, C., PHAM, X., ERWIN, A., MIZOGUCHI, S., WARRENER, P., HICKEY, M., BRINKMAN, F., HUFNAGLE, W., KOWALIK, D. & LAGROU, M. 2000. Complete genome sequence of *Pseudomonas aeruginosa* PAO1, an opportunistic pathogen. *Nature,* 406**,** 959-964.

STRANGE, H. R., ZOLA, T. A. & CORNELISSEN, C. N. 2011. The fbpABC operon is required for Ton-independent utilization of xenosiderophores by *Neisseria gonorrhoeae* strain FA19. *Infection and Immunity,* 79**,** 267-278.

SU, T., CHI, K., WANG, K., GUO, L. & HUANG, Y. 2015. Expression, purification and preliminary crystallographic analysis of a haem-utilizing protein, HutX, from *Vibrio cholerae*. *Acta Crystallographica Section F: Structural Biology Communications,* 71**,** 141-144.

SUÁREZ-MORENO, Z., CABALLERO-MELLADO, J., COUTINHO, B., MENDONÇA-PREVIATO, L., JAMES, E. & VENTURI, V. 2012. Common features of environmental and potentially beneficial plant-associated *Burkholderia*. *Microbial Ecology,* 63**,** 249-266.

SUN, J., DENG, Z. & YAN, A. 2014. Bacterial multidrug efflux pumps: mechanisms, physiology and pharmacological exploitations. *Biochemical and biophysical research communications,* 453**,** 254-267.

SUN, L., JIANG, R.-Z., STEINBACH, S., HOLMES, A., CAMPANELLI, C., FORSTNER, J., SAJJAN, U., TAN, Y., RILEY, M. & GOLDSTEIN, R. 1995. The emergence of a highly transmissible lineage of cbl+ *Pseudomonas* (*Burkholderia*) *cepacia* causing CF centre epidemics in North America and Britain. *Nature medicine,* 1**,** 661-666.

SZAMOSVÁRI, D., RÜTSCHLIN, S. & BÖTTCHER, T. 2018. From pirates and killers: does metabolite diversity drive bacterial competition? *Organic & biomolecular chemistry,* 16**,** 2814-2819.

TAKESHITA, K., MATSUURA, Y., ITOH, H., NAVARRO, R., HORI, T., SONE, T., KAMAGATA, Y., MERGAERT, P. & KIKUCHI, Y. 2015. *Burkholderia* of Plant-Beneficial Group are Symbiotically Associated with Bordered Plant Bugs (Heteroptera: Pyrrhocoroidea: Largidae). *Microbes and environments,* 30**,** 321-329.

TAMMA, P. D., FAN, Y., BERGMAN, Y., SICK-SAMUELS, A. C., HSU, A. J., TIMP, W., SIMNER, P. J., PROKESCH, B. C. & GREENBERG, D. E. 2018. Successful Treatment of Persistent Burkholderia cepacia Complex Bacteremia with Ceftazidime-Avibactam. *J Antimicrobial agents chemotherapy,* 62**,** 1-7.

TAYEB, L. A., LEFEVRE, M., PASSET, V., DIANCOURT, L., BRISSE, S. & GRIMONT, P. A. 2008. Comparative phylogenies of *Burkholderia*, *Ralstonia*, *Comamonas*, *Brevundimonas* and related organisms derived from *rpoB*, *gyrB* and *rrs* gene sequences. *Research in Microbiology,* 159**,** 169-177.

TEKAIA, F. & LATGÉ, J.-P. 2005. *Aspergillus fumigatus*: saprophyte or pathogen? *Current Opinion in Microbiology,* 8**,** 385-392.

TERI, A., SOTTOTETTI, S., BIFFI, A., GIRELLI, D., D'ACCICO, M., ARGHITTU, M., COLOMBO, C., CORTI, F., PIZZAMIGLIO, G. & CARIANI, L. 2018. Molecular typing of Burkholderia cepacia complex isolated from patients attending an Italian Cystic Fibrosis Centre. *New Microbiol,* 41**,** 141-144.

THOMAS, C. & TAMPÉ, R. 2018. Multifaceted structures and mechanisms of ABC transport systems in health and disease. *Current opinion in structural biology,* 51**,** 116-128.

THOMAS, M. S. 2007. Iron acquisition mechanisms of the Burkholderia cepacia complex. *Biometals,* 20**,** 431-452.

THOMSON, E. L. S. & DENNIS, J. J. 2012. A Burkholderia cepacia complex non-ribosomal peptide-synthesized toxin is hemolytic and required for full virulence. *Virulence,* 3**,** 286-298.

TOMICH, M., GRIFFITH, A., HERFST, C. A., BURNS, J. L. & MOHR, C. D. 2003. Attenuated virulence of a *Burkholderia cepacia* type III secretion mutant in a murine model of infection. *Infection immunity,* 71**,** 1405-1415.

TRIVEDI, H. B., VALA, A. K., DHRANGADHRIYA, J. H. & DAVE, B. P. 2016. Marine-derived Fungal Siderophores: A Perception. *Indian Journal of Geo-Marine Sciences***,** 431-439.

TSENG, C.-F., BURGER, A., MISLIN, G. A., SCHALK, I., YU, S. F., CHAN, S. & ABDALLAH, M. 2006. Bacterial siderophores: the solution stoichiometry and coordination of the Fe(III) complexes of pyochelin and related compounds. *Journal of Biological Inorganic Chemistry,* 11**,** 419-432.

TYRRELL, J. & CALLAGHAN, M. 2016. Iron acquisition in the cystic fibrosis lung and potential for novel therapeutic strategies. *J Microbiology,* 162**,** 191-205.

TYRRELL, J., WHELAN, N., WRIGHT, C., SÁ-CORREIA, I., MCCLEAN, S., THOMAS, M. & CALLAGHAN, M. 2015. Investigation of the multifaceted iron acquisition strategies of *Burkholderia cenocepacia. BioMetals,* 28**,** 367-380.

UEHLINGER, S., SCHWAGER, S., BERNIER, S. P., RIEDEL, K., NGUYEN, D. T., SOKOL, P. A. & EBERL, L. 2009. Identification of Specific and Universal Virulence Factors in *Burkholderia cenocepacia* Strains by Using Multiple Infection Hosts. *J Infection and Immunity,* 77**,** 4102-4110.

URBAN, T. A., GRIFFITH, A., TOROK, A. M., SMOLKIN, M. E., BURNS, J. L. & GOLDBERG, J. B. 2004. Contribution of *Burkholderia cenocepacia* Flagella to Infectivity and Inflammation. *Infection and Immunity,* 72**,** 5126-5134.

VALENTI, P., CATIZONE, A., PANTANELLA, F., FRIONI, A., NATALIZI, T., TENDINI, M. & BERLUTTI, F. 2011. Lactoferrin decreases inflammatory response by cystic fibrosis bronchial cells invaded with *Burkholderia cenocepacia* iron-modulated biofilm. *International journal of immunopathology and pharmacology,* 24**,** 1057-1068.

VAN ACKER, H., SASS, A., DHONDT, I., NELIS, H. J. & COENYE, T. 2014. Involvement of toxin–antitoxin modules in *Burkholderia cenocepacia* biofilm persistence. *Pathogens and Disease,* 71**,** 326-335.

VAN DALEM, A., HERPOL, M., ECHAHIDI, F., PEETERS, C., WYBO, I., DE WACHTER, E., VANDAMME, P. & PIÉRARD, D. 2018. Susceptibility of Burkholderia cepacia Complex Isolated from Cystic Fibrosis Patients to Ceftazidime-Avibactam and Ceftolozane-Tazobactam. *Antimicrobial Agents and Chemotherapy,* 62**,** 1-5.

VAN DELDEN, C., PAGE, M. G. & KÖHLER, T. 2013. Involvement of Fe-uptake systems and AmpC β-lactamase in susceptibility to the siderophore monosulfactam BAL30072 in *Pseudomonas aeruginosa. Antimicrobial agents and chemotherapy***,** 2095-2102.

VANDAMME, P., GORIS, J., CHEN, W.-M., DE VOS, P. & WILLEMS, A. 2002. *Burkholderia tuberum* sp. nov. and *Burkholderia phymatum* sp. nov., nodulate the roots of tropical legumes. *Systematic and Applied Microbiology,* 25**,** 507-512.

VANDAMME, P., HOLMES, B., COENYE, T., GORIS, J., MAHENTHIRALINGAM, E., LIPUMA, J. J. & GOVAN, J. R. 2003. *Burkholderia cenocepacia* sp. nov.—a new twist to an old story. *Research in Microbiology,* 154**,** 91-96.

VANDAMME, P., HOLMES, B., VANCANNEYT, M., COENYE, T., HOSTE, B., COOPMAN, R., REVETS, H., LAUWERS, S., GILLIS, M. & KERSTERS, K. 1997a. Occurrence of multiple genomovars of *Burkholderia cepacia* in cystic fibrosis patients and proposal of *Burkholderia multivorans* sp. nov. *International Journal of Systematic and Evolutionary Microbiology,* 47**,** 1188-1200.

VANDAMME, P., HOLMES, B., VANCANNEYT, M., COENYE, T., HOSTE, B., COOPMAN, R., REVETS, H., LAUWERS, S., GILLIS, M., KERSTERS, K. & GOVAN, J. R. W. 1997b. Occurrence of Multiple Genomovars of *Burkholderia cepacia* in Cystic Fibrosis Patients and Proposal of *Burkholderia multivorans* sp. nov. *International Journal of Systematic and Evolutionary Microbiology,* 47**,** 1188-1200.

VANDAMME, P., MAHENTHIRALINGAM, E., HOLMES, B., COENYE, T., HOSTE, B., DE VOS, P., HENRY, D. & SPEERT, D. 2000. Identification and Population Structure of *Burkholderia stabilis* sp. nov.(formerly *Burkholderia cepacia* Genomovar IV). *Journal of clinical microbiology,* 38**,** 1042-1047.

VANEECHOUTTE, M., YOUNG, D. M., ORNSTON, L. N., DE BAERE, T., NEMEC, A., VAN DER REIJDEN, T., CARR, E., TJERNBERG, I. & DIJKSHOORN, L. 2006. Naturally transformable *Acinetobacter* sp. strain ADP1 belongs to the newly described species *Acinetobacter* baylyi. *Applied environmental microbiology reports,* 72**,** 932-936.

VANLAERE, E., BALDWIN, A., GEVERS, D., HENRY, D., DE BRANDT, E., LIPUMA, J. J., MAHENTHIRALINGAM, E., SPEERT, D. P., DOWSON, C. & VANDAMME, P. 2009. Taxon K, a complex within the Burkholderia cepacia complex, comprises at least two novel species, *Burkholderia contaminans* sp. nov. and *Burkholderia lata* sp. nov. *International journal of systematic and evolutionary microbiology,* 59**,** 102-111.

VANLAERE, E., LIPUMA, J. J., BALDWIN, A., HENRY, D., DE BRANDT, E., MAHENTHIRALINGAM, E., SPEERT, D., DOWSON, C. & VANDAMME, P. 2008. *Burkholderia latens* sp. nov., *Burkholderia diffusa* sp. nov., *Burkholderia arboris* sp. nov., *Burkholderia seminalis* sp. nov. and *Burkholderia metallica* sp. nov., novel species within the Burkholderia cepacia complex. *International journal of systematic and evolutionary microbiology,* 58**,** 1580-1590.

VARGA, J. J., LOSADA, L., ZELAZNY, A. M., KIM, M., MCCORRISON, J., BRINKAC, L., SAMPAIO, E. P., GREENBERG, D. E., SINGH, I., HEINER, C., ASHBY, M., NIERMAN, W. C., HOLLAND, S. M. & GOLDBERG, J. B. 2013. Draft Genome Sequences of *Burkholderia cenocepacia* ET12 Lineage Strains K56-2 and BC7. *Genome Announcements,* 1**,** 1-2.

VARGAS-STRAUBE, M. J., CÁMARA, B., TELLO, M., MONTERO-SILVA, F., CÁRDENAS, F. & SEEGER, M. 2016. Genetic and functional analysis of the biosynthesis of a non-ribosomal peptide siderophore in *Burkholderia xenovorans* LB400. *PloS one,* 11**,** 1-23.

VELAYUDHAN, J., HUGHES, N. J., MCCOLM, A. A., BAGSHAW, J., CLAYTON, C. L., ANDREWS, S. C. & KELLY, D. J. 2000. Iron acquisition and virulence in *Helicobacter pylori:* a major role for FeoB, a high-affinity ferrous iron transporter. *Molecular Microbiology,* 37**,** 274-286.

VENTURI, V., FRISCINA, A., BERTANI, I., DEVESCOVI, G. & AGUILAR, C. 2004. Quorum sensing in the Burkholderia cepacia complex. *Research in Microbiology,* 155**,** 238-244.

VERMIS, K., COENYE, T., LIPUMA, J. J., MAHENTHIRALINGAM, E., NELIS, H. J. & VANDAMME, P. 2004. Proposal to accommodate *Burkholderia cepacia* genomovar VI as *Burkholderia dolosa* sp. nov. *International journal of systematic and evolutionary microbiology,* 54**,** 689-691.

VISCA, P., CIERVO, A., SANFILIPPO, V. & ORSI, N. 1993. Iron-regulated salicylate synthesis by *Pseudomonas* spp. *Journal of General Microbiology,* 139**,** 1995-2001.

VISCA, P., COLOTTI, G., SERINO, L., VERZILI, D., ORSI, N. & CHIANCONE, E. 1992. Metal regulation of siderophore synthesis in *Pseudomonas aeruginosa* and functional effects of siderophore-metal complexes. *Applied and environmental microbiology,* 58**,** 2886-2893.

VISCA, P., LEONI, L., WILSON, M. J. & LAMONT, I. L. 2002. Iron transport and regulation, cell signalling and genomics: lessons from *Escherichia coli* and *Pseudomonas*. *J Molecular microbiology,* 45**,** 1177-1190.

VISSER, M., MAJUMDAR, S., HANI, E. & SOKOL, P. 2004. Importance of the ornibactin and pyochelin siderophore transport systems in *Burkholderia cenocepacia* lung infections. *Infection and Immunity,* 72**,** 2850-2857.

VORONINA, O. L., KUNDA, M. S., RYZHOVA, N. N., AKSENOVA, E. I., SHARAPOVA, N. E., SEMENOV, A. N., AMELINA, E. L., CHUCHALIN, A. G. & GINTSBURG, A. L. 2018. On Burkholderiales order microorganisms and cystic fibrosis in Russia. *BMC Genomics,* 19**,** 77-90.

WAGNER, K., SPRINGER, B., IMKAMP, F., OPOTA, O., GREUB, G. & KELLER, P. M. 2018. Detection of respiratory bacterial pathogens causing atypical pneumonia by multiplex Lightmix® RT-PCR. *J International Journal of Medical Microbiology,* 308**,** 317-323.

WALLNER, A., BLATZER, M., SCHRETTL, M., SARG, B., LINDNER, H. & HAAS, H. 2009. Ferricrocin, a siderophore involved in intra-and transcellular iron distribution in *Aspergillus fumigatus*. *J Applied environmental microbiology reports,* 75**,** 4194-4196.

WANDERSMAN, C. & DELEPELAIRE, P. 2004. Bacterial iron sources: from siderophores to hemophores. *Annual Review of Microbiology,* 58**,** 611-47.

WANDERSMAN, C. & DELEPELAIRE, P. 2012. Haemophore functions revisited. *Molecular Microbiology,* 85**,** 618-631.

WEAVER, E. A., WYCKOFF, E. E., MEY, A. R., MORRISON, R. & PAYNE, S. M. 2013. FeoA and FeoC Are Essential Components of the *Vibrio cholerae* Ferrous Iron Uptake System, and FeoC Interacts with FeoB. *Journal of Bacteriology,* 195**,** 4826-4835.

WEBER, C. F. & KING, G. M. 2017. Volcanic Soils as Sources of Novel CO-Oxidizing *Paraburkholderia* and *Burkholderia*: *Paraburkholderia hiiakae* sp. nov., *Paraburkholderia metrosideri* sp. nov., *Paraburkholderia paradisi* sp. nov., *Paraburkholderia peleae* sp. nov., and *Burkholderia alpina* sp. nov. a Member of the Burkholderia cepacia Complex. *Frontiers in Microbiology,* 8**,** 1-10.

WENCEWICZ, T. A., LONG, T. E., MÖLLMANN, U. & MILLER, M. J. 2013. Trihydroxamate siderophore-fluoroquinolone conjugates are selective sideromycin antibiotics that target S*taphylococcus aureus*. *Bioconjugate Chemistry,* 24**,** 473-486.

WHITBY, P. W., VANWAGONER, T. M., SPRINGER, J. M., MORTON, D. J., SEALE, T. W. & STULL, T. L. 2006. *Burkholderia cenocepacia* utilizes ferritin as an iron source. *Journal of Medical Microbiology,* 55**,** 661-668.

WHITE, N. 2003. Melioidosis. *The Lancet,* 361**,** 1715-1722.

WILSON, M. J. & LAMONT, I. L. 2000. Characterization of an ECF sigma factor protein from *Pseudomonas aeruginosa. Biochemical and Biophysical Research Communications,* 273**,** 578-583.

WINKELMANN, G. 2002. Microbial siderophore-mediated transport. *Biochemical Society Transactions***,** 691-696.

WYCKOFF, E. E., ALLRED, B. E., RAYMOND, K. N. & PAYNE, S. M. 2015. Catechol Siderophore Transport by Vibrio cholerae. *Journal of bacteriology,* 197**,** 2840-2849.

WYCKOFF, E. E. & PAYNE, S. M. 2011. The Vibrio cholerae VctPDGC system transports catechol siderophores and a siderophore-free iron ligand. *Molecular microbiology,* 81**,** 1446-1458.

WYCKOFF, E. E., SMITH, S. L. & PAYNE, S. M. 2001. VibD and VibH are required for late steps in vibriobactin biosynthesis in Vibrio cholerae. *Journal of bacteriology,* 183**,** 1830-1834.

YABUUCHI, E., KOSAKO, Y., OYAIZU, H., YANO, I., HOTTA, H., HASHIMOTO, Y., EZAKI, T. & ARAKAWA, M. 1992. Proposal of *Burkholderia* gen. nov. and transfer of seven species of the genus *Pseudomonas* homology group II to the new genus, with the type species *Burkholderia cepacia* (Palleroni and Holmes 1981) comb. nov. *Microbiology and Immunology,* 36**,** 1251-1275.

YAN, S. T., SUN, L. C., LIAN, R., TAO, Y. K., ZHANG, H. B. & ZHANG, G. 2018. Diagnostic and predictive values of procalcitonin in bloodstream infections for nosocomial pneumonia. *Journal of critical care,* 44**,** 424-429.

YANG, H.-C., IM, W.-T., KIM, K. K., AN, D.-S. & LEE, S.-T. 2006. *Burkholderia terrae* sp. nov., isolated from a forest soil. *International journal of systematic and evolutionary microbiology,* 56**,** 453-457.

YANISCH-PERRON, C., VIEIRA, J. & MESSING, J. 1985. Improved M13 phage cloning vectors and host strains: nucleotide sequences of the M13mpl8 and pUC19 vectors. *J Gene,* 33**,** 103-119.

YEATS, C., RAWLINGS, N. D. & BATEMAN, A. 2004. The PepSY domain: a regulator of peptidase activity in the microbial environment? *J Trends in biochemical sciences,* 29**,** 169-172.

YETERIAN, E., MARTIN, L. W., LAMONT, I. L. & SCHALK, I. J. 2010. An efflux pump is required for siderophore recycling by *Pseudomonas aeruginosa*. *Environmental microbiology reports,* 2**,** 412-418.

YONEYAMA, H. & NAKAE, T. 1996. Protein C (OprC) of the outer membrane of *Pseudomonas aeruginosa* is a copper-regulated channel protein. *Microbiology,* 142**,** 2137-2144.

YUHARA, S., KOMATSU, H., GOTO, H., OHTSUBO, Y., NAGATA, Y. & TSUDA, M. 2008. Pleiotropic roles of iron-responsive transcriptional regulator Fur in *Burkholderia multivorans*. *J Microbiology,* 154**,** 1763-1774.

ZAMBOLIN, S., CLANTIN, B., CHAMI, M., HOOS, S., HAOUZ, A., VILLERET, V. & DELEPELAIRE, P. 2016. Structural basis for haem piracy from host haemopexin by *Haemophilus influenzae*. *Nature communications,* 7**,** 1-12.

ZAMORA, C. Y., MADEC, A. G., NEUMANN, W., NOLAN, E. M. & IMPERIALI, B. 2018. Design, solid-phase synthesis and evaluation of enterobactin analogs for iron delivery into the human pathogen *Campylobacter jejuni*. *Bioorganic & medicinal chemistry***,** 5314-5321.

ZEIGLER, D. R., PRÁGAI, Z., RODRIGUEZ, S., CHEVREUX, B., MUFFLER, A., ALBERT, T., BAI, R., WYSS, M. & PERKINS, J. B. 2008. The Origins of 168, W23, and Other *Bacillus subtilis* Legacy Strains. *Journal of Bacteriology,* 190**,** 6983-6995.

ZHAO, Q. & POOLE, K. 2000. A second *tonB* gene in *Pseudomonas aeruginosa* is linked to the *exbB* and *exbD* genes. *FEMS microbiology letters,* 184**,** 127-132.

ZHENG, T. & NOLAN, E. M. 2012. Siderophore-based detection of Fe (III) and microbial pathogens. *Metallomics,* 4**,** 866-880.

ZHU, M., VALDEBENITO, M., WINKELMANN, G. & HANTKE, K. 2005. Functions of the siderophore esterases IroD and IroE in iron-salmochelin utilization. *Microbiology,* 151**,** 2363-2372.

ZUGHAIER, S. M. & CORNELIS, P. 2018. The Role of Iron in Bacterial Pathogenesis. *Frontiers in cellular infection microbiology,* 8**,** 1-2.